DEPARTMENT OF HISTORY, ARCHAEOLOGY
AND CULTURAL RESOURCES MANAGEMENT

UNIVERSITY OF THE PELOPONNESE

VANESSA MUROS
(R.N. 2013401220129900 9)

THE TECHNOLOGY, TRADE, AND DEGRADATION PATHOLOGIES OF LATE BRONZE AGE VITREOUS MATERIALS IN THE EASTERN MEDITERRANEAN

DOCTORATE THESIS

ΚΑΛΑΜΑΤΑ 2021

SUPERVISING COMMITTEE:

SUPERVISOR

Professor Nikolaos Zacharias, University of the Peloponnese

MEMBERS

Professor Julian Henderson, University of Nottingham

Professor John Papadopoulos, University of California, Los Angeles

ABSTRACT

Archaeometric studies of Late Bronze Age vitreous artifacts can provide important information on the raw materials and production methods used to make these artifacts, while also offering insight into the origins of this prestige good. Although there has been an increase in the number of analyses of glass and faience finds from this period, most of the research has centered on Egypt, the Near East, and Mycenaean Greece. This thesis focuses on beads excavated from ancient Methone (northern Greece), Kefalonia (western Greece), and Lofkënd (southwestern Albania) in order to investigate the technology and origins of vitreous materials from these understudied regions. Chemical (pXRF, EPMA, LA-ICP-MS, SEM-EDS, XRD) and isotopic analysis indicates that the majority of the glass and faience beads were made at primary production sites in Egypt and the Near East. The results also revealed regional differences in bead types and glass technologies, as well as some material from different production zones.

The vitreous assemblages from Kefalonia were greatly influenced by Mycenaean sites on the mainland. However, unique relief bead types were found that had been worked using glass of Egyptian origin. The identification of mixed alkali glass provides another early example of this compositional type made at primary production centers located to the west. Ancient Methone and Lofkënd are characterized by glass assemblages with less common color palettes and production technologies. In the case of Lofkënd, the glasses analyzed point to a composition not seen in the Late Bronze Age but are comparable to low lime, natron black glasses found in Europe and the Near East from 10th-8th c. BC contexts. The Lofkënd finds point to regional innovation in glass technology and a possible new production zone that may include very early experimentation with a mineral alkali flux.

The thesis also investigates the degradation pathologies identified on the glasses and the deterioration processes they underwent in situ. The examination and analysis of the beads shows that a complex series of factors, which include the burial environment, the presence of microorganisms, and the composition of the glass, act together to impact the preservation of archaeological vitreous materials.

ACKNOWLEDGEMENTS

This thesis would not have been possible without the help and dedication of many people. I am indebted to my advisor Nikos Zacharias for his guidance, encouragement, and support throughout this research. He also arranged for permission to analyze and sample the beads from the Archaeological Museum of Argostoli and liaised with museum staff for access. I am also very grateful to my other committee members. Julian Henderson provided much needed help and guidance with the interpretation of the analytical results and the writing of the thesis. John Papadopoulos always offered his invaluable support for my research, even before agreeing to be on my committee. His encouragement to study the beads from Lofkënd got me interested in wanting to learn more about Late Bronze Age glass technology and trade. By also allowing me to study the beads from ancient Methone, he set me on the path to making this thesis possible.

I am grateful to many who granted permission for me to work on materials from their archaeological field projects or museum collections. Without providing access to these artifacts, and permission to sample them, the analysis presented in this thesis would not have taken place. John Papadopoulos, Sarah Morris, and Lorenc Bejko, co-directors of the Lofkënd Archaeological Project, for allowing me to analyze and sample the vitreous beads. Konstantinos Noulas who excavated the Late Bronze Age cemetery at ancient Methone who let me study the beads, and the Ephorate of Prehistoric and Classical Antiquities of Pieria who granted permission for the analysis. The work on those beads would also not have occurred without the support of the co-directors of the Ancient Methone Archaeological Project, John Papadopoulos, Sarah Morris, Athena Athanassiadou, and Matthaios Bessios. The Archaeological Museum of Argostoli and the Ephorate of Antiquities of Kefalonia allowed for the in situ analysis and sampling of the Kefalonian material. Many thanks as well to the museum staff that facilitated access to the material and provided much needed help during the examination and pXRF analysis of the collection.

Many scientists and specialists provided access to laboratory space and equipment, training on several analytical instruments or methods, and even ran samples for me: Rosario Esposito, Dept. of Earth, Planetary, and Space Sciences at UCLA who provided training and help with the EPMA; Austin Cole at the UC Davis Interdisciplinary Center for Plasma Mass Spectrometry for the LA-ICP-MS analysis; Justin Glessner, UC Davis Interdisciplinary Center for Plasma Mass Spectrometry who conducted the radiogenic isotopic analysis; Eleni Palamara, Laboratory of Archaeometry, University of the Peloponnese for her help with the SEM-EDS analysis of the ancient Methone beads; Alan Farahani, Dept. of Anthropology, University of Nevada, Las Vegas, for his knowledge of statistics and coding skills (and his endless patience) for the PCA; Panagiotis Karkanas and Dimitris Michailidis at the Malcolm H. Wiener Laboratory for Archaeological Science, American School of Classical Studies, Athens for lab access and use of the equipment; the UCLA/Getty Conservation Program for use of lab access, sample preparation equipment, and the pXRF; Sergey Prikhodkho and Ioanna Kakoulli, UCLA Molecular and Nano Archaeology Lab, for access to the Keyence Digital Microscope and the VP-SEM-EDS.

Much of the analysis and travel required for this research could not have occurred without funding from the John Anson Kittredge Fund, the UCLA Non-Senate Faculty Professional Development Grant, and the Malcolm H. Wiener Laboratory for Archaeological Science Fellowship, American School of Classical Studies, Athens. Portions of the examination and analysis of the vitreous beads from Lofkënd and ancient Methone took place during project field seasons where I worked as a conservator. I am grateful for the financial support provided from the Steinmetz Family Foundation

and the National Endowment of the Humanities that helped to make it possible for me to participate on those field projects and conduct my research.

The thesis was completed while I was employed full-time, and therefore am grateful to supervisors and colleagues who let me use time during the workday for analysis and writing, or allowed for deadlines or priorities to be shifted to help me finish this. Allison Lewis, Chrysanthe Pantages, and Deidre Brin read drafts of the thesis, and I thank them for taking time from their very busy lives to offer much needed edits and suggestions. A special thanks to my friends who went through the PhD process themselves and shared their own experiences, which helped alleviate a lot of stress and anxiety. To all my friends and family who supported and encouraged me during this period, thank you for believing in me, especially at times when I could not believe I can do this.

Finally, the bulk of the thesis writing took place during an unprecedented year, dealing with the impact of a global pandemic and political unrest in the US. I am grateful for the southern California weather, hiking trails, my sourdough starter Sydney, the beach, streaming services, and the voters of Georgia, all of which helped me cope with everything that was going on in the world and made things a little bit easier.

TABLE OF CONTENTS

LIST OF FIGURES

LIST OF TABLES

LIST OF ABBREVIATIONS

Abbreviations used in the text, tables, and figures

c.	Century
EDS	Energy Dispersive Spectroscopy
EH	Early Helladic
EIA	Early Iron Age
EPMA	Electron Probe Microanalysis
HMG	High Magnesium Glass
HMLK	High Magnesium Low Potassium Glass
IA	Iron
MH	Middle Helladic
LBA	Late Bronze Age
LH	Late Helladic
LMLK	Low Magnesium Low Potassium Glass
PPM	Parts Per Million
SEM	Scanning Electron Microscopy
SEM-EDS	Scanning Electron Microscopy-Energy Dispersive Spectroscopy
VP-SEM-EDS	Variable Pressure- Scanning Electron Microscopy-Energy Dispersive Spectroscopy
wt%	Weight Percent

Oxides and elements mentioned in the text, tables, and figures

Li	Lithium	Y	Yttrium	Tm	Thulium
Be	Beryllium	Zr	Zirconium	Yb	Ytterbium
B	Boron	Nb	Niobium	Hf	Hafnium
Na	Sodium	Mo	Molybdenum	Ta	Tantalum
Mg	Magnesium	Rh	Rhodium	W	Tungsten
Al	Aluminum	Pd	Palladium	Re	Rhenium
P	Phosphorus	Ag	Silver	Pt	Platinum
K	Potassium	Cd	Cadmium	Au	Gold
Ca	Calcium	In	Indium	Tl	Thallium
Sc	Scandium	Sn	Tin	Pb	Lead
Ti	Titanium	Sb	Antimony	Bi	Bismuth
V	Vanadium	Cs	Cesium	Th	Thorium
Cr	Chromium	Ba	Barium	U	Uranium
Mn	Manganese	La	Lanthanum	Al_2O_3	Alumina, Aluminum Oxide
Fe	Iron	Ce	Cerium	CaO	Lime, Calcium Oxide
Co	Cobalt	Pr	Praseodymium	CoO	Cobalt Oxide
Ni	Nickel	Nd	Neodymium	CuO	Copper Oxide
Cu	Copper	Sm	Samarium	FeO	Iron Oxide
Zn	Zinc	Eu	Europium	K_2O	Potash, Potassium Oxide
Ga	Gallium	Gd	Gadolinium	MgO	Magnesia, Magnesium Oxide
Ge	Germanium	Tb	Terbium	MnO	Manganese Oxide
As	Arsenic	Dy	Dysprosium	Na_2O	Soda, Sodium Oxide
Se	Selenium	Ho	Holmium	P_2O_5	Phosphorus Pentoxide
Rb	Rubidium	Er	Erbium	SiO_2	Silica, Silicon Dioxide
Sr	Strontium	Lu	Lutetium	TiO_2	Titania, Titanium Dioxide

1 INTRODUCTION

1.1 ORIGINS OF THE THESIS

The origins of this thesis can be traced back to the 2006 field season of the Lofkënd Archaeological Project in Albania. One of the archaeologists had block lifted the remains of a skull surrounded by some grave goods. As an archaeological conservator on the project, I excavated the block back in the lab and encountered a group of beads with extremely different states of preservation. Some of the beads had severely devitrified into flaky fragments. Another had very little surface deterioration and was in very good condition. Other beads had completely altered in color and could not initially be identified as glass. While working on this material I began to wonder why the beads looked the way they did. How could beads from the same burial context, located right next to each other, undergo such varying degrees of degradation? Was it influenced by the composition of the beads, the specific raw materials used, or their origin? This led me to begin a technical study on the Lofkënd beads looking at their chemical composition, production technology, and provenance to answer those questions. This initial project grew to incorporate the study of the technological aspects and trade of Late Bronze Age glass and faience from other regions, the results of which are presented here.

1.2 AIMS AND SCOPE OF THESIS

This research aims to contribute to our understanding of the production and origins of vitreous materials in the Eastern Mediterranean during the Late Bronze Age. Glass and faience objects from this period and region have not been as extensively studied. There could be several reasons for this. These earlier vitreous finds may not preserve as well as those from later periods, in particular those materials found in more humid burial environments, such as the Aegean (Smirniou et al. 2009). Few production sites have been discovered, which may related to preservation issues or that there were not many places making glass at this time (Shortland 2012). There could also be difficulty in accessing excavated glass collections that makes sampling and analysis impossible (Smirniou et al. 2009). All of these factors have created gaps in our knowledge of this early technology. As the number of studies on Late Bronze Age glasses has increased over the years and existing analytical techniques are refined or new ones are applied (Nikita and Henderson 2006; Walton et al. 2009; Smirniou et al. 2009; Degryse et al. 2010a), a clearer picture can emerge of how glass and faience was made, how this prestige good was used, and how it moved around the ancient world.

Several of the information gaps concerning the production of vitreous materials were addressed through the analysis of vitreous beads excavated from Late Bronze Age cemeteries at ancient Methone (Macedonia, northern Greece), the island of Kefalonia (Ionian Sea, western Greece), and Lofkënd (southwestern Albania). The glass and faience from these regions is not well understood with few archaeometric studies undertaken. There was a need for the instrumental analysis of the beads from these sites to provide information on their manufacturing technology and to add to the current body of data on archaeological glasses. The tumulus at Lofkënd was used through the 9th c. BC (Damiata and Southon 2014a) allowing the beads to serve as a diachronic study to uncover any technological changes that may be observed in the transition between the Late Bronze Age and Early Iron Age.

The sites are located in areas along trade routes used in the Late Bronze Age for the exchange of a wide range of artifact types, which includes prestige goods such as glass (Pulak 1998; Souyoudzoglou-Haywood 1999; Bejko 2002). In addition to being located along sea trade routes, ancient Methone and the sites of Kefalonia are near Mycenaean palatial centers that used, and may have worked, glass and faience (Nikita and Henderson 2006; Smirniou et al. 2009; Polikreti et al. 2011). This study also looked at the trade of these materials, and more specifically at the origins of the glass and faience artifacts uncovered at the sites to

provide information on which primary production sources they came from. This was accomplished through the use of trace element and isotopic analysis, the latter being a technique that is only newly being applied to the sourcing of glass from the Late Bronze Age (Degryse et al. 2010a; Henderson et al. 2015).

Finally, the thesis includes an investigation into the deterioration pathologies found on the archaeological beads analyzed. This portion of the project contained an additional aim which was to add to a field of study that has often focused on the corrosion and weathering of historic glasses, mainly those from the Roman and Medieval periods (Perez y Jorba et al. 1980; Krumbein et al. 1991). This part originated from the questions that arose, and the challenges presented, when trying to conserve extremely degraded vitreous materials in the field. The results of the deterioration studies can be used to aid conservators and other cultural heritage professionals in the examination and condition assessment of vitreous materials, as well as their preservation.

1.3 Outline of the Thesis

Following this introduction, Chapters 2 and 3 provide background information on the production of faience and glass during the Late Bronze Age. Chapter 2 begins with a history of vitreous materials in the Eastern Mediterranean with a brief overview of the origins of faience and glass in Egypt, the Near East, and their emergence in the Aegean. The archaeological evidence for primary glass production sites during this period is also discussed. Chapter 3 describes the raw materials used for the manufacture of faience and glass, in addition to some production methods. This chapter provides much of the background information used for the interpretation of the analytical results presented in the subsequent chapters.

Chapter 4 discusses the materials and methods used. The methods for sampling and sample preparation are described. The analytical techniques utilized for the compositional and isotopic analysis are included. The parameters used and the purpose of each technique are explained.

Chapters 5, 6, and 7 comprise the results of the analysis with a discussion of their significance interwoven into the data interpretation. Each chapter can be treated as an individual case study providing insight into the aspects of the glass industry in that particular part of the Eastern Mediterranean. Chapter 5 focuses on the examination and non-invasive analysis of beads from ancient Methone dating to the 13th c. BC. This site is located just outside the boundaries of the Mycenaean palatial centers and provides a glimpse into the types of vitreous materials, and interactions outside of these areas. Chapter 6 describes the analysis of beads from three cemeteries located on the island of Kefalonia: Mazarakata, Metaxata, and Kokkolata-Menegata. Based on associated tomb finds, the beads date from the 14th-11th c. BC, with some possibly even earlier. This collection provides an overview of the technology of vitreous materials over a broader chronological range and offers a glimpse into the glass industry in areas off the mainland, but that are still part of the Mycenaean world. The final case study is found in Chapter 7 and represents the westernmost group of beads analyzed. The beads excavated from the tumulus at Lofkënd offers some insight into the vitreous materials available to groups in this region outside of the Aegean and whether different types of vitreous materials were obtained and used. Lofkënd represents the latest group studied, ranging from the 12th-9th c. BC, or Early Iron Age. These samples encompass a period of technological change observed in other areas of the Eastern Mediterranean, Egypt and the Near East and evidence for these new glass types at Lofkënd are investigated.

Chapter 8 reviews the deterioration pathologies observed on the glasses analyzed. Through images and analytical data, it provides further information on the factors that affect the preservation of archaeological vitreous materials. The physical and compositional signs of deterioration due to the burial environment, the activity of microorganisms, and the composition of the glasses are discussed.

Chapter 9 concludes the thesis with a discussion of the three case studies, comparing and contrasting the types of vitreous materials represented, their compositions, and origins. The results are framed within the larger context of the production and trade of vitreous materials in the Late Bronze Age Eastern Mediterranean using ancient Methone, Kefalonia, and Lofkënd to highlight areas of cultural connections, technological continuity, and regional innovations or idiosyncrasies.

Four Appendices are included that contain analytical data and images of the beads and samples analyzed. Appendix A describes the workflow for the examination and analysis of the vitreous beads in addition to the results of the analysis of glass standard reference materials used for this study. In Appendix B, there are images of the ancient Methone beads and full results of the analysis conducted. Appendix C contains the same type of information for the beads from Kefalonia. The last one, Appendix D, has images and data from the Lofkënd vitreous materials.

2 PRODUCTION OF VITREOUS MATERIALS IN THE LATE BRONZE AGE

2.1 ORIGINS OF VITREOUS MATERIALS

The earliest vitreous materials appear during the 5th-early 4th millennium BC and are in the form of faience beads (Foster 1979; Bouquillon et al. 2008). They are first found in the Near East, at two sites in northern Iraq—Tepe Gawra and Tell Arpachiya. Beginning in the 4th millennium BC there was an increase in the number of sites in northern Mesopotamia where faience was found. In this period, additional object types were created which include inlays, seals, and pendants. These vitreous materials were now found in very large numbers at sites like Nineveh and Tell Brak. The geographic range of faience objects expanded late in the 4th millennium BC to southern Iraq. The artifacts here were similar to those found in the north. However, new bead forms were developed signifying that faience production was now occurring in this area as well (Foster 1979). It is during this period that faience also appears in Egypt. It is not clear if the technology was transferred from the Near East to Egypt, or if it was an independent innovation. Whether due to technology transfer or a local invention, by the end of the 4th millennium BC, faience was produced in both regions.

Glass does not appear in the archaeological record until later. Remains of glass artifacts dated as early as the 3rd millennium BC have been discovered in the Near East. A glass bead from Tell Judeideh (Syria) and a glass pin head from Nuzi (Iraq) from 2350-2150 BC are some of the earliest examples of glass discovered (Henderson 2013). Vitreous objects manufactured during this period are rare and tend to be small items of personal adornment (Moorey 1994). A small chunk of blue raw glass was excavated from Eridu (Abu Shahrein) from ca. 21st c. BC that indicated the existence of glass production in this area by this time (Henderson, 2012). It was not until the 16th c. BC, however, that significant numbers of glasses were manufactured in both the Near East and Egypt. Large numbers of beads and other small objects were initially produced, but by second half of the 16th-15th c. BC, vessels were also made. At the sites of Tell Brak (Syria) and Tell Atchana (Turkey) core formed vessels from the 15th c. and 16th c. BC respectively have been found representing some of the earliest glass vessels produced (Shortland 2012).

Despite the discovery of these early glass finds at Near Eastern sites, there is still some debate as to where glass originated. There are several reasons for this uncertainty. The number of early finds is small, and there is very little evidence for glassmaking sites in the Near East. Some of the early glass objects come from archaeological contexts that are not securely dated. Excavation at Nuzi uncovered some of the earliest glasses reported. A recent reassessment of the chronology at the site, however, may suggest they are not as old as previously thought (Shortland et al. 2018). The majority of the glasses found at Nuzi come from Stratum II, and initial dates place these pieces about 100-150 years older than the glasses found at sites in Egypt. Revised dates push the dates of some of the finds later and contemporaneous with Egyptian production sites, such as that found at Amarna (Shortland et al. 2018, 780). Some have stressed the fact that the early glasses produced in Egypt have a wider color palette using Egyptian sourced colorants, the glassworking was of higher quality, and it was being produced at a larger scale that what is seen in the Near East (Shortland et al. 2018, 781). These characteristics would have likely taken time to develop which could suggest the glass industry in Egypt could be older.

There is epigraphic evidence that may support the origin of glass in the Near East. A group of cuneiform tablets were found at the site Nineveh (Iraq) in an area designated as the Library of Ashurbanipal (Moorey 1994). The tablets date to the 7th c. BC (668-627 BC), but are copies of older tablets. Oppenheim et al. (1970) attributes the original tablets to at least the mid-2nd millennium BC, or possibly earlier to the later 3rd millennium BC. The tablets cover several technical topics including the production of glass. The texts are similar to recipes, where ingredients were listed as was the process for making blue and red glasses. The types of kilns needed is also mentioned (Shortland 2012). The tablets detailed the several different stages

involved in glassmaking with the end products of each step described. It was not clear initially if the tablets referred to the production of glass or perhaps another vitreous material such as faience. Experimental work by Brill (1970 334), who followed the recipes in the texts, produced glass which he described as being of "very good quality" showing that the tablets were indeed referring to the manufacture of glass.

Glass in Egypt that can be sourced to Egyptian raw materials does not appear until a bit later than those found in the Near East. Some of these locally produced glasses are from the reign of Thutmosis III (1479-1425 BC) (Shortland 2012). Dark blue glass from one of his tombs with a well-dated context was analyzed and found to have been made with cobalt from the Kharga Oasis in the Western Desert of Egypt. There is no evidence that cobalt was exported out of Egypt as a raw material for the manufacture of glass, therefore the cobalt glass was made locally. At this same time, there is also the evidence for the importation of glass from the Near East. An inscription found in the Hall of Annals at Karnak depicts several items being brought as tribute to King Thutmosis III after his victories in the Near East (Shortland 2012). Among the items are glass vessels and ingots. Some of the tribute or gifts may have included craftsmen who specialized in glassmaking. Additional epigraphic evidence from Amarna supports the import of Near Eastern glass as gifts during this period. A group of mid-14th c. B.C. cuneiform tablets, known as the Amarna Letters, describe the Egyptian vassal rulers in the Near East giving glass to the Egyptian king.

Recent analysis of glass found at the site of Gurob in the Fayum region of Egypt has provided archaeological evidence for the importation of Near Eastern glass (Kemp et al. 2020). During excavations in the 1920s, beads were discovered within an undisturbed tomb that contained seven women and two children. The tomb dates to the period between the reign of Amenhotep I (1525-1504 BC) and Thutmosis III (1479-1425 BC). The burial style and grave goods were described as being non-Egyptian and this, along with the proximity of the tomb to the harem palace, meant that the women were likely foreign wives of the king who were part of a diplomatic marriage. Trace element analysis of the glasses pointed to a Near Eastern source for the copper colored beads. What the Amarna Letters, the depiction in the Hall of Annals, and the beads from Gurob show is that glass was being imported into Egypt from the Near East beginning in the late 16th c.-15th c. BC and likely predates the production of glass in Egypt. These examples also demonstrate that even though glass was being produced in Egypt, especially at a large industrial scale like at Amarna, Near Eastern glass was still a desired prestige item.

2.2 Glass Production Centers in the Late Bronze Age

Early glass production centers are rare in the archaeological record and evidence for these activities has been difficult to find (Figure 2.1). This is in part due to the small number of sites that likely manufactured glass in the Late Bronze Age, but also because the identification of the remains of these activities can be challenging. The production of glass objects can be broken down into two main types of activities: glassmaking and glassworking. In glassmaking, raw materials are mixed together and heated to produce glass. The process is also known as primary production. The end product of glassmaking is to create raw glass. In glassworking, this raw glass or ingot is taken and subjected to heat again to be formed into an object, such as a bead or vessel. This is also referred to as secondary glass production.

The tools and furnaces needed for both processes can be the same or can leave similar traces in the archaeological record (Nicholson 2007; Shortland 2012). Both types of workshops could contain glass debris, crucibles, and metal rods. Poor preservation of furnaces would make it difficult to determine whether they were used for glassmaking or working. There is some evidence of possible glass workshops located in the same areas of a site where other pyrotechnologies were taking place, such as metallurgy and pottery making, or were associated with these industries (Mass et al. 2002; Shortland 2012) . Depending on what components are preserved, it may be difficult to distinguish the different industries.

There are some characteristics that are distinct to the primary and secondary production of glass. Glassworking areas can be identified by the remains of flawed or misshapen objects, as well as molds, which would not be present at a workshop that would only be making raw glass or ingots (Shortland, 2012). Glassmaking sites would have raw materials used for making glass and reaction vessels or crucibles with semi-fused glass or failed glass batches (Shortland 2012; Nicholson and Jackson 2018). Unfortunately, many of the remains that could be used to identify these activities do not preserve well in the archaeological record. If multiple activities occurred in the same workshop, determining which processes took place is challenging.

Figure 2.1. Location of some of the glass production sites discussed in the text. Map data ©2021 GeoBasis-DE/BKG (©2009) Google, Inst. Geogr. Nacional, Mapa GISrael. The sites marked with a green dot have archaeological evidence of glassmaking. The yellow dots represent sites with archaeological evidence of glassworking, but are thought to be glassmaking sites as well. The sites marked with a red dot have evidence of only glassworking.

2.2.1 Near East

No glassmaking sites have been conclusively identified in the Near East. Sites with some glass debris and ingots have been found which signify glassworking activities. Most do not have material that clearly identifies glassmaking. As mentioned, a chunk of blue glass was found at Eridu pointing to glass production in the 21st c. BC. Fragments of raw glass were found at Nuzi. One of those fragments seems to have a shape similar to the interior of a vessel indicating it is an ingot (Shortland et al. 2018). Ingots were also found at Tell Brak and at Ugarit (Syria). Although some of the sites have substantial amounts of glass artifacts and raw chunks of glass, none clearly point to the primary production of glass. As more archaeological excavations take place and the number of archaeometric studies of vitreous materials increases (Dardeniz 2018), new evidence of glassmaking activities may come to light.

2.2.1.1 Tell Atchana

Recent excavations at the site of Tell Atchana may have uncovered the first evidence for glassmaking in the Near East. Excavations began at Tell Atchana (Alalakh) in the early 20th century and some of the earliest glasses, including some of the first core formed vessels, were found (Shortland 2012). Included in the 16th c. BC materials were three pieces of raw glass, which were described as “cake ingots” (Shortland 2012, 137). The presence of ingots clearly showed that glassworking was taking place, but no evidence related to glassmaking was found at the time.

Excavations undertaken in 2011 have changed the interpretation of the glass industry at Tell Atchana. Archaeologists uncovered an area in the southern part of the tell with evidence of glass production

(Dardeniz 2018). Vitrified material in the form of glass debris, as well as faience and glass objects, were found. They were located in a workshop dating to the transition of two Late Bronze Age phases—LBA I, ca. 1500-1450 BC, and LBA II, ca. 1400-1330/1200BC. A glass ingot as well as a crucible was discovered in the workshop. The crucible contained material that was white and porous and described as "frit-like" (Dardeniz 2018, 99). Analysis of the frit-like material identified silica grains and diopside ($CaMgSi_2O_6$). Diopside crystals were found in crucibles used for adding colorants to glass at the site of Qantir (Rehren 1997) and within fragments of semi-finished and raw glass from Amarna (Smirniou and Rehren 2011). Diopside crystals, along with the presence of other crystalline materials, can indicate the partial reaction of glass raw materials in the crucible during the initial stages of glassmaking (Smirniou and Rehren 2011, 65).

Trace element and isotopic analysis of finished objects and the glass ingot shows similarities to other Near Eastern glasses. They are unlike Egyptian glasses in composition (Dardeniz, 2018). There were, however, aspects of the Tell Atchana glasses that seem to be unique to that assemblage. The samples contained high chromium, as well as higher alumina and iron, which indicated the use of sand as a silica source. This is unlike most Late Bronze Age glasses made at the time that use a purer silica source such as quartz pebbles. Pieces colored with copper were found to have higher arsenic concentrations than what is usually found in glasses from this period. The use of arsenical copper as the colorant choice was suggested, instead of a copper mineral colorant used for other Near Eastern glasses or bronze scrap like in Egypt. Although more analytical work is needed, the analytical results point to primary production taking place at Tell Atchana.

2.2.2 Egypt

The majority of information on the production of Late Bronze Age glasses comes from sites in Egypt. The large-scale glass industry that was present at some of these sites, and the better preservation, has allowed for more of the material to be discovered and studied. There are four sites in Egypt that have been identified as glassworking sites, with three having archaeological evidence of glassmaking. All of these sites date to the 14th c. BC or later and therefore could not have manufactured any of the early glass found in Egypt. Although there is evidence of glass made using local raw materials, like the cobalt colored glass from the tomb of Thutmosis III, the workshop that produced these early glasses is still unknown.

2.2.2.1 Malkata

The site of Malkata is located on the west bank of the Nile near Thebes. It was the location of the palace complex of Amenhotep III (1391-1353 BC) and is considered the earliest site of glass production in Egypt (Mass et al. 2002). The site was first excavated in 1920-1921, and it is during these campaigns sponsored by the Metropolitan Museum of Art that most of the vitreous materials were found. Glass and faience objects, glassworking debris, and faience molds were discovered in various parts of the site. Three areas contained the bulk of the finds: the South Village, the storage magazines and the Pavilion/North Village/North Palace area (Hodgkinson 2014). Correspondence and notes/publications written by the archaeologists working at Malkata describe crucibles found for glass and faience making, in addition to faience molds in the storage magazines near the South Village. Crucibles used for producing vitreous materials were excavated from the Pavilion/North Palace/North Village area. There is a third mention of glass crucibles found but the location was not specified. It is thought to possibly have been in the South Village.

Despite the fact that the archaeologists discovered crucibles with evidence of a glass industry, they did not keep any of these finds (Mass et al. 2002; Hodgkinson 2014). No glass production debris has ever been technically examined or analyzed. No furnaces that could be associated with the production of vitreous materials have been found and neither have any raw materials (Hodgkinson 2014). The physical evidence studied thus far only points to glassworking activities occurring at the site. The description of finds that include crucibles, and the identification of Egyptian cobalt as the colorant for some of the faience, has helped to support the idea of Malkata as a glassmaking site. Moreover, the fact that the glass vessels found of the site are considered to be of very high quality and show that the craftsmen had mastered the

technique, suggests that the technology had been established for a while there (Keller 1983). Others have proposed that the glass was made by foreign craftsmen from the Near East who were at Malkata (Mass et al. 2002). Since this could be the earliest site of glassmaking, it would not have allowed sufficient time for glassmaking technology to develop so quickly in Egypt. The glass would have to have been made by foreign workers. This idea could be plausible given the evidence for foreign craftsmen coming to Egypt from the Near East depicted at the Hall of Annals at Karnak.

2.2.2.2 Amarna

Tell el-Amarna was the capital of Egypt during the reign of Akhenaten (Amenhotep IV) from 1347-1332 BC (Kemp 2014). The site was quite large and contained temples, palaces, administrative buildings, industrial areas, and living quarters. Although Amarna was the capital for only a short period, the number of faience and glass finds at the site, along with the evidence of the production of vitreous materials, shows that glass production occurred on a large scale here

The first systematic excavations at Amarna were undertaken by Sir Flinders Petrie from 1891-1892 (Petrie 1894). Petrie's work primarily focused on the Central City where he investigated the Great Palace and the surrounding areas (Kemp 2014). It is in an area outside the palace where he found many broken vessels he located in "rubbish heaps" (Petrie 1894, 15). Because of their proximity to the palace, he concluded that glass was a high status material linked to the palaces and the elite.

At other locations at the site, Petrie discovered an industrial area with evidence of glass and faience production (Petrie, 1894). No workshops were found but he uncovered large amounts of debris associated with the manufacture of vitreous materials. These included fragments of ceramic vessels that contained partially fused glass he described as "fritting pans" (Petrie 1894, 26). Cylindrical jars with glass on the exterior were found. There were quartz pebbles with vitreous material on the surface, thought to line the floor of the furnace or that could also serve as the silica source for the glass. Misshapen beads, some with the wire used to make them still inside, glass drips, strips and fragments of finished objects were also discovered. He also found many molds for making faience objects. Based on his findings, Petrie concluded that glass was being both made and worked at Amarna. The archaeological evidence at that time only proved that glassworking took place without clear evidence of glassmaking, even though both activities were assumed to have taken place there.

Continued excavations at Amarna, as well as analysis of some of the finds from Petrie's excavations, have provided more evidence that glassmaking was carried out. Excavations resumed in the 1990's at the main city, an area previously identified by Petrie that housed factories that made vitreous materials (Nicholson and Hart 2007). Two kilns were found there (O45.1, Kilns 2 and 3) that were somewhat different in appearance to those previously identified at Amarna as being used for producing pottery. The mud brick walls of the kilns were much thicker. The structure's construction suggested they were built for heat retention and maximum resistance to thermal shock (Nicholson and Hart 2007, 38). Remains of glassworking debris found in that area, together with the appearance of the kilns and the large amount of slag found, could suggest these were used for making glass.

A replica of a better preserved kiln (Kiln 3) was constructed so that experiments could be conducted to determine if glass could be made in a kiln of that size and type (Nicholson and Jackson 2007). The experimental glassmaking produced two different vitreous materials. The first crucible fired produced a frit-like material with material more fully fused below. The frit material was similar to what was produced in the first stage of glassmaking if fritting was part of the process. Another crucible that was left in the kiln for a longer period produced a dark cobalt blue ingot of good quality glass.

The dark blue, experimentally produced ingot was analyzed and its composition compared to cobalt glasses from Amarna and a cobalt blue ingot from the Uluburun shipwreck known to be of Egyptian origin

(Nicholson and Jackson 2007). The analytical results were comparable, though the experimental glass did have lower concentrations of alkali and silica (Nicholson and Jackson 2007, 97, table 4.2). This slight difference in composition is attributed to the fact that the raw materials used for the experimental glass were likely not the same as those used in antiquity. This is particular true for the alkali where the experiments relied on the ash from seaweed collected from England as a substitute for a desert species of halophytic plants, though Nicholson and Jackson (2007, 84) felt that the composition was similar to *Salsola kali*, one of possible sources of plant ash for glassmaking in the Late Bronze Age. The results of these experiments do show that the kilns found at Amarna could have been used to make glass, though there is no definitive proof that they were actually used for glassmaking.

Analysis of what has been identified as semi-finished glass from Amarna has provided clearer evidence for glassmaking. Smirniou and Rehren (2011) analyzed materials from Petrie's excavations, currently housed at the Petrie Museum of Archaeology, that represented what they described as raw glass and glass waste. The raw glass appeared opaque white, porous, and frothy (Smirniou and Rehren 2011, 63). This raw glass was not completely fused and described as semi-finished glass produced as part of the glassmaking process.

Several features of this semi-finished glass helped identify it as a product of an early stage of glassmaking (Smirniou and Rehren 2011). Residual quartz grains were found within the glass matrix showing it had not been completely melted or fused. There were lime rich crystalline phases in the raw glass, such as wollastonite and diopside, which formed during the early stages of glassmaking. Finally, this raw glass had lower lime content than finished glass, something interpreted as being produced in an earlier stage of making glass. Since the glass was free of colorants this meant that uncolored glass was produced in an early stage and would later have had the mineral colorants added in a second step.

Smirniou and Rehren (2016) also examined technical ceramics excavated from Amarna that retained remnants of glass. They compared the structure of the interior surface and the glass/crucible interface to see if they could determine whether they had been used for glassmaking. They also examined vessels that were used for the experimental production of raw glass and the remelting of glass for adding the colorant. The test samples helped to establish what layers and reaction products could be produced during these manufacturing activities.

Cross-sections taken of the Amarna vessels were compared to vessels from Qantir (Egypt) that were identified for the primary production of glass during the 13th c. BC (Smirniou and Rehren 2016). Although the shape of the vessels from Amarna differed and was not the same profile as those from Qantir, the composition of the interior surface and the layers formed during firing were similar. The Amarna vessels were also lined with a lime-parting layer to separate any glass melted from the crucible walls. This was seen in the Qantir reaction vessels and crucibles. The analysis found that the layers formed within the Amarna vessel walls due to the reaction of the glass and the parting layer with the vessel wall were due to exposure to temperatures high enough for glassmaking. The similarities between the Qantir reaction vessels and the Amarna cylindrical vessels suggest they were used for making glass. No other vessel forms were found at Amarna that could have been used for different stages of glassmaking, for example one set for making semi-finished glass and others for coloring glass. This means that the different stages of glassmaking may have taken place within the same vessels.

2.2.2.3 Qantir

Qantir (Pi-Ramesse) is located at the site of an ancient harbor in the eastern Nile Delta. It was founded in the early 13th c. BC, but became the capital of Egypt under Ramesses II in the 19th Dynasty (1279-1213 BC) (Shortland 2012). The first excavations at the site in 1928 revealed evidence of pyrotechnological industries at the site. It was not until work undertaken in the 1980s that evidence of glass and faience production was found.

Three areas of the site, which date to about 1300-1270 BC, preserve evidence of workshops that could have produced vitreous materials (Shortland 2012). No furnaces dedicated to glassmaking have been uncovered, but the areas did contain technical ceramics that were utilized for the production of glass and faience, debris from these activities, and finished products (Rehren and Pusch 1997; Rehren and Pusch 2005). Despite the lack of furnaces, the technical ceramics found at Qantir have provided the largest body of evidence for Late Bronze Age glassmaking in Egypt and the processes involved in the making of glass during this period.

At Qantir, two different types of technical ceramics were found with remnants of glass or a glass-like material inside (Rehren and Pusch 1997; Rehren and Pusch 2005). The vitreous materials within the vessels are different and represent different stages of glassmaking. This shows that at Qantir, glass was made in a multi-step process rather than the glass being formed in one stage. There were specific vessel forms for each stage of glassmaking where the form played a role in the process. A group of jars, some storage jars and others identified as reused beer jars, were used for the first stage of glassmaking. These vessels were ovoid and some had a narrow neck (Rehren and Pusch 2005). They were lined with lime so that the melted glass could be easily separated from the interior surface of the vessels and removed. The vitreous material found within the jars was semi-fused glass that had been fired at a low temperature. It was white in color and porous (Smirniou and Rehren 2016). The material formed included residual quartz grains and wollastonite, both of which are characteristic of semi-fused glass. These jars are referred to as reaction vessels and were only used to produce semi-finished glass. Because glass at this stage releases gases and other compounds during initial firing, the material at the top of the batch can become frothy. The advantage of having a jar with a narrow neck could be to help keep the glassy material from being lost as it rises (Rehren and Pusch 2005).

The semi-finished glass was removed from the reaction vessel and ground (Smirniou and Rehren 2016). The glass could then be sorted and washed to remove unwanted materials (Rehren and Pusch 2005). Additional alkali would be added along with the crushed glass and mineral colorants (Smirniou and Rehren 2016). The crushed material would be put into crucibles and heated at a higher temperature to create a fully fused glass. The crucibles used for this step at Qantir were cylindrical with a flat bottom and a wide top (Rehren and Pusch 1997). They were also lined with lime like the reaction vessels. A funnel shaped piece of ceramic was found attached to the rim of one of the crucibles (Rehren and Pusch 2005, 1577, fig. 3). These were also found within the workshop areas. This funnel is thought to have been added to the rim of the crucible prior to firing to allow for more crushed glass to be added into the crucible during firing. Once the firing was complete, the completely fused glass could be removed and either worked to form an object or could be shipped elsewhere as an ingot. An ingot found from the 1928 excavations, now currently at the Egyptian Museum in Cairo, has the shape of the interior dimensions of the Qantir cylindrical vessels (Rehren and Pusch 1997). This denotes that these vessels were crucibles used to produce ingots.

The majority of the glass remains found within the crucibles at Qantir were colored red, with a smaller number blue (Rehren and Pusch 1997). The predominance of one color of glass at the site was concluded to indicate that the glassmakers at Qantir specialized in the production of a specific color of glass, something that may also have occurred at other sites. At Amarna for example, though multiple colors of glass objects and glass debris were found, dark cobalt blue is the predominant color, and therefore that site may have specialized in the production of blue glass.

Not only was Qantir unique in the color of glass it was producing, but the method of making glass might also be distinctive to the site. No other evidence of beer jars used as reaction vessels, nor the use of funnels for adding crushed glass to crucibles, has been found at other glassmaking sites in Egypt (Rehren and Pusch 2005). Because so little evidence of glassmaking has been found, it is not clear if this is truly a technical innovation at Qantir or it just seems unique due to the lack of other examples thus far because these items have not been correctly identified upon excavation or due to poor preservation.

2.2.2.4 Lisht

The site of Lisht, located south of Cairo on the left bank of the Nile, was first established in the 12th Dynasty (20th c. BC) and contained pyramid complexes with royal and elite burials (Smirniou et al. 2018). The pyramids contained the tombs of Amenemhat I, who founded the site, and his successor Senusret I. Excavations that took place in the early 20th century around the pyramid complex uncovered a later settlement and cemetery used from the Middle Kingdom (1875 BC) to the Third Intermediate Period (1069-664 BC). Located within this settlement was a technological complex that seems to have included in the production of glass (Mass et al. 2002).

The evidence of glass production consisted of glass slag, glass debris, ingots, misshapen beads, and crucibles with glass attached (Mass et al. 2002). Finished glass and faience objects were discovered as well. A mud brick structure was uncovered that was described as a glass factory (Keller 1983). The finds were sent to the Metropolitan Museum of Art, who sponsored the excavation, but little information on the archaeological context of this material was included (Smirniou et al. 2018). The technological complex was dated to 1295-1070 BC. This makes the glass produced here the latest Bronze Age glassmaking sites in Egypt discovered so far.

Most of the analysis undertaken on the vitreous material from Lisht was undertaken on the finished glass objects. The results of these studies has characterized the glasses as one of poorer quality than that produced at earlier Egyptian sites (Keller 1983). The glass of the vessels contains more air bubbles. The vessel walls are thicker than other core formed vessels found and the decoration is simpler. The colors are not as clear and seem to have a slight yellow or brown tone to them. The color palette is not considered as broad. Most of the glasses are blue in color, with opaque yellow and white the next most commonly produced colors (Smirniou et al. 2018). However, if the site specialized in the production of a specific color or set of colors of glass, then this would not necessarily point to less skilled glassmakers.

Recent work (Smirniou et al. 2018) has focused on the glass production debris and the crucibles found at the site in an effort to determine whether they represent glassmaking or glassworking. Two sets of materials were analyzed by Smirniou et al. (2018), crucibles and fragments of what could be semi-finished glass. The Lisht samples were compared to similar finds at Qantir and Amarna that had been identified as signifying glassmaking.

The crucibles from Lisht were cylindrical in shape, similar to those found at Amarna (Smirniou and Rehren 2016). They were also lined with a lime parting layer. The layers produced within the crucibles during firing and their compositions were similar to those seen in Amarna and Qantir reaction vessels and crucibles. The conclusion was that these crucibles were used for glassmaking. No ovoid shaped reaction vessels were found at Lisht like those used at Qantir. The same vessel could have been used as a reaction vessel and a coloring crucible similar to the process assumed about the Amarna crucibles.

Glass samples from Lisht, which were colored blue and white, consisted of a porous glassy material with many air bubbles and inclusions (Smirniou et al. 2018). The pieces contained residual quartz grains, semi-reacted crystals, and lime-rich phases located within areas of fully fused glass. These pieces resembled the compositions of semi-finished glass found at Amarna and Qantir and are evidence of glassmaking.

Additional compositional analyses of the semi-finished glass, the glass within the crucibles, and an ingot were conducted to look at major and minor oxides in addition to trace elements (Smirniou et al. 2018). Based on their overall composition and in particular their trace element concentrations, the Lisht glasses were made in Egypt and share similarities with glasses made at other Egyptian sites. There are some characteristics of the Lisht glasses that seem unique to the site. They have a lower lime concentration than other Egyptian glasses. This could be due to the use of a lower firing temperature, a thinner lime-parting layer used in the crucibles, or perhaps even a different plant ash used as the flux.

The colorants also distinguish the glass from Lisht (Smirniou et al. 2018). There are no cobalt blue glasses found at the site. All blue glasses were colored with copper. The opaque glasses found have very low concentrations of antimony unlike other Egyptian opaque yellow and white glasses. The low antimony content and the lack of cobalt glasses at the site may point to restricted access to these "exotic" raw materials (Smirniou et al. 2018, 514). The difficulty in obtaining access to certain raw materials and the possible lower temperature used to make the glass may explain why the Lisht glasses have been described as lower quality than glasses made at other sites like Amarna and Qantir. The fact that Lisht is not a royal site may have played a role in the access to specific raw materials. Economic reasons and control of resources by other sites may have made it difficult to procure certain components needed. The type of material found at Lisht shows that glassmaking occurred there and that sites other than those tied to royal palaces were participating in this industry.

2.2.3 Greece

Vitreous materials first emerge in the Aegean during the 3rd millennium BC with the appearance of faience objects on Minoan Crete and northern Greece (Mirtsou et al. 1996; Panagiotaki 2008). These were likely imports originating from Egypt, with some also coming from the Near East (Foster 1979). By the end of the 3rd millennium BC, faience objects were being made locally on Crete. The technology expanded to the Greek mainland by the 2nd millennium BC. At around this time, glass objects appeared in the Eastern Mediterranean and were found on sites on Crete as well as on the Greek mainland.

Many of the vitreous materials found during this period in the Aegean are small objects such as beads, plaques, and inlays. They are often associated with palatial centers or found in tombs (Eder 2015; Nightingale 2018). Due to the poor preservation of vitreous materials in Greece and the few archaeological remains of glass production, there are still many unknowns concerning the manufacture and trade of faience and glass in the region during the Late Bronze Age. An increase in the number of analytical studies of Aegean glass and faience has contributed more information on the sources of raw materials and the movement of materials throughout the eastern Mediterranean (Nikita and Henderson 2006; Smirniou et al. 2009; Walton et al. 2009; Jackson and Nicholson 2010; Triantafyllidis and Karatasios 2012).

Unlike faience production, which was manufactured on both Crete and mainland Greece, no clear evidence of glassmaking has been found in the Aegean. There does seem to be evidence of some type of glass production in Greece based on some of the archaeological remains. A unique glass object type is found at Mycenaean site, the relief bead (Nightingale 2008). These beads are thin pieces of glass formed into a plaque using a mold. They have relief decoration that can be found on one or both sides. If the decoration is only on one side, the reverse is flat. The bead can have two perforations, one at either end, or have one to hang as a pendant. The motifs found on the beads are those commonly found in Minoan and Mycenaean art and often reflect those seen in other media such as pottery, frescoes, and gold beads. The bead form becomes quite common in the 15th-14th c. BC (Panagiotaki 2008) and are found mainly in tombs. They are produced in either dark blue or lighter blue glass colored using cobalt, copper, or a mixture of both colorants. The fact that this bead type is restricted to Mycenaean contexts and is rarely found outside of Greece indicates is it made locally.

Provenance studies of Mycenaean relief beads have shown that the glass used to make them was imported into Greece. Studies of bead from the Mycenaean sites of Tiryns, Elateia, Thebes and Kazanaki have sourced the glass raw materials to the Near East and Egypt (Smirniou et al. 2009; Walton et al. 2009; Henderson et al. 2010). This means that glass was imported into Greece as ingots and then remelted or softened in workshops to be poured or pressed into molds to form the relief beads (Panagiotaki, 2008). Some of the glasses studied, such as those from Elateia, do show unusual compositions suggesting at first a possible alternative primary production source (Nikita and Henderson 2006). However, isotopic analysis of some of

these samples points to Egyptian and Near Eastern sources for the various beads found at the site, which includes relief beads (Henderson et al. 2010).

Molds for making relief beads have been found at Knossos on Crete, Mycenae and Tiryns on the Greek mainland, and Trianda on the island of Rhodes (Panagiotaki 1999; Panagiotaki et al. 2005; Panagiotaki 2008; Triantafyllidis and Karatasios 2012). One of the molds from Mycenae still had blue glass attached to it showing it clearly was used to make glass relief beads (Nightingale 2002). The discovery of molds point to workshops located at these sites. No traces of the workshops, furnaces, or crucibles have been found in association with the molds. Linear B tablets from Mycenae described craftsmen producing a material that some have translated as dark blue glass, known to have been imported to Mycenaean Greece from Egypt (Henderson et al. 2010), though others have said it could be lapis lazuli (Nightingale 2002). The tablets were found in an area with many glass finds. The texts, combined with molds found, the size of the site, and the fact that it is a palatial center, point to Mycenae likely having glass workshops.

In addition to the discovery of molds, there has also been evidence of glassworking waste, misshapen beads, and ingots at Tiryns and Trianda. Although these two sites only represent the working of glass, the archaeological evidence will be very briefly discussed below since they are the few examples that point to glass workshops in the Late Bronze Age Aegean.

2.2.3.1 Tiryns

The fortified site of Tiryns is located in the Argolid region of mainland Greece and served as a port city during the Late Bronze Age. Heinrich Schliemann conducted excavations at Tiryns in the late 19th c. AD and among his finds were the remains of glass beads, inlays, and what appears to be glass waste (Panagiotaki et al. 2005). The glass waste consists of drops of glass and strips. Damaged or misshapen objects were found. Relief beads with drips on the surface were uncovered, as well as groups of misshapen objects. No crucibles or furnaces were found at Tiryns. However, fragments of severely burnt clay were found among the glass waste. The burnt clay did not have any glass attached to it so it is likely not a crucible fragment, but is thought to be the lining of a kiln (Panagiotaki et al. 2005, 15). The glass waste, molds, and misshapen beads clearly point to glassworking taking place at the site.

Schliemann did not record the exact find spot for this material nor did he include any notes on their archaeological context (Panagiotaki et al. 2005). The location and date of this workshop is unknown. Schliemann mainly excavated in the upper citadel so it is possible that the material comes from that area. A metallurgical workshop and storerooms were located there so there is evidence that some industrial activities were taking place in that part of the site. A piece of glass of an unidentifiable shape was found in the lower citadel and Panagiotaki et al., (2005, 15) proposed this could be evidence of raw glass in an area that could have had a workshop dating to the LH IIIB period (ca. 1500-1400 BC).

Six glasses from Tiryns were analyzed and determined to have compositions similar to other LBA glasses (Panagiotaki et al. 2005). The beads were blue and included dark blue beads colored with cobalt and copper colored turquoise beads. This initial analysis conducted revealed that the Tiryns glasses shared similarities with glasses made in the Near East more so than those made in Egypt. This source attribution was confirmed through trace element analysis using LA-ICP-MS (Walton et al. 2009). Glass ingots from the Near East made their way to Tiryns, and were then softened or remelted in a workshop at the site to form relief beads and other objects.

2.2.3.2 Trianda

The island of Rhodes is in the Greek Island group of the Dodecanese located in the eastern Aegean not far from the western coast of Turkey. It was an important trade center during the Late Bronze Age (1600-1070 BC) and a link for the movement of materials from east to west (Triantafyllidis and Karatasios 2012). Vitreous materials appear on the island beginning in the LH IIIA1-IIIC period (1390-1070 BC). Glass beads

and vessels were found in the cemeteries on the island. The settlement site of Trianda also contained glass objects in addition to evidence of a possible glass workshop.

The evidence for glassworking included a stone mold for relief beads and a chunk of raw glass (Triantafyllidis and Karatasios 2012). The raw glass was found on the floor of a room dated to the LH IIIA1-IIIB1 (1390-1200 BC) and was likely a workshop. The piece of glass is covered with a layer of white corrosion, but the glass is an opaque blue. There is a smooth layer along the surface with traces of ceramic that suggests the chunk was removed from a crucible (Triantafyllidis and Karatasios 2012, 28). The composition of the raw glass was similar to Late Bronze Age plant ash glasses from the Near East. It had been colored by copper and included the opacifier, calcium antimonate. The smooth ceramic layer was highly vitrified. This could be the remains of the interaction layer between the glass and the interior walls of the crucible or reaction vessel. No further evidence for workshops was found on Rhodes, nor were other glassworking remains such as a furnace discovered. The mold and the raw glass, however, do support the existence of a workshop specializing in glassworking at Trianda.

2.2.4 Europe

Around 1200 BC, glass with a composition distinct from glasses produced in Egypt and the Near East appears in Europe (Henderson 2012). This glass was made with a different alkali that was higher in potash and lower in soda. These glasses are referred to as mixed alkali, or low magnesium high potassium (LMHK) glasses. Mixed alkali glass artifacts have been discovered at archaeological sites across Europe, from as far west as Ireland and the UK to as far east as Greece (Henderson 1988b; Henderson 1988a; Henderson et al. 2015; Nikita et al. 2017). Based on their distinct composition and geographic distribution, these glasses were produced at different glassmaking centers than those that manufactured plant ash glasses.

One of the questions surrounding LMHK vitreous materials is the location of the production sites. Like several of the sites described above in other regions of the Late Bronze Age, there if no clear evidence for the primary production of mixed alkali glasses (Henderson et al. 2015). The largest concentration of these glasses comes from the site of Frattesina in northern Italy (Henderson 1988b; Brill 1992; Santopadre and Verità 2000; Angelini et al. 2004; Angelini et al. 2005; Angelini et al. 2009; Henderson et al. 2015, p.200). Archaeological remains resulting from glassworking activities were found there. At two other sites located not too far from Frattesina, Mariconda de Rovigo and Montagnana, evidence for the working of glass was also uncovered (Towle et al. 2001; Towle 2002). The material associated with glass production from Frattesina and the results of analysis to source that material will be briefly described.

2.2.4.1 Frattesina

Frattesina is located in northern Italy, south of a branch of the Po river (Towle et al. 2001). The site consists of a large settlement that was occupied from the 12th-9th c. BC. Most of the evidence of workshops and various industrial activities were found in the west central section of the site. Imported materials such as amber, ostrich eggs, and Mycenaean pottery show the site was participating in a long distance trade network.

The glassworking remains from Frattesina consist of crucibles with colored glass attached, raw glass, glass waste, and misshapen objects (Henderson 1988b; Henderson et al. 2015). The glass ingots excavated from the site have the same shape as the crucibles found there indicating similar technical ceramics were used to produce them. Ingots of a similar shape were also found at Mariconda and Montagnana (Towle et al. 2001; Towle 2002). Translucent turquoise blue seems to be the dominant color of glass found at Frattesina (Henderson et al. 2015). Opaque red, opaque white, translucent cobalt blue and translucent green glasses are also commonly found.

Because there is no evidence of glassmaking at Frattesina and there is evidence of trade from the east, it was initially proposed that Near Eastern or Egyptian ingots could have been imported into Frattesina and then

reshaped. Radiogenic isotopic analysis undertaken on five samples, however, points to a different source of the raw materials (Henderson et al. 2015). The ratios of neodymium and strontium isotopes in the raw materials used to make the LMHK glasses were compared to those found in glasses made in the Near East, at both Tell Brak and Nuzi, as well as in Egypt. Based on results, the raw materials used for the mixed alkali glasses are distinct from those manufactured in the Near East and Egypt and were not made from ingots imported from the east.

Geological samples collected in northern Italy underwent isotopic analysis to determine whether the materials from this area could have been used to make the Frattesina glasses (Henderson et al. 2015). One Frattesina sample seems to have a radiogenic signature similar to plants selected from a volcanic rock area near Rome. Three glasses were made with a silica source that was similar to sands or quartz found around Frattesina and the coast near the mouth of the Po River. Although additional analysis is needed both on archaeological and geological samples, this initial isotopic study demonstrates that the glasses at Frattesina could have been made from raw materials obtained locally and others closer to Rome.

2.3 Trade of Vitreous Materials

Archaeological, textual, and scientific evidence shows that vitreous materials were traded across the Eastern Mediterranean. Glass and faience were moved along trade routes established for other materials via land and sea. Late Bronze Age Egyptian and Near Eastern glasses traveled farther into Europe with these vitreous materials found as far north as Denmark (Varberg et al. 2015) and as far west as Ireland (Henderson 1988b). The glass likely arrived in the area along the maritime and land based trade routes that transported Baltic amber from the north and other trade materials westward.

One of the best sources of evidence for the maritime trade of vitreous materials in the Eastern Mediterranean is the Uluburun shipwreck. The wreck of this ship was found off the coast of Kaş, in southwestern Turkey and has been dated to the late 14th c. BC (Nicholson et al. 1997). The Uluburun was carrying 17 tons of cargo that originated in different places along the Eastern Mediterranean (Pulak 2008). Among the material in the cargo hold were copper ingots from Cyprus, tin ingots from Central Asia, pithoi, Canaanite jars, amber, ivory, gold and silver, ebony, murex shells, and many more types of exotic materials. Among the remains of the ship were 175 glass ingots, most of which were dark blue and turquoise, along with one purple and amber glass ingot. Many beads were also discovered. Around 75,000 faience and 9500 glass beads were placed on board the ship, held within large storage jars or perhaps bags (Pulak 2008; Ingram 2014). Several bead types were found including Mycenaean relief beads.

There has been some discussion as to what the purpose of the Uluburun cargo was, whether it was for commercial trade or part of a gift exchange between political entities to ensure or strengthen diplomatic relations (Bachhuber 2006; Pulak 2008). The large number of prestige goods on board may point to the items being gifts, but there were also large number of utilitarian vessels that would not have been part of this type of exchange. It is possible that this vessel was involved in both types of activities. Bachhuber (2006, 359) surmises that there is evidence for the cargo being part of an elite exchange network, but there is no clear evidence of political gift exchange. Several of the items on board would have been destined for ports not connected to palatial centers.

Trace element analysis was conducted on three of the glass ingots to determine the composition and provenance in order to understand the origins and movement of the vitreous material across the eastern Mediterranean (Nicholson et al. 1997; Jackson and Nicholson 2010). Two of the glass ingots were dark cobalt blue and the third was turquoise blue colored by copper. The major, minor and trace element compositions of the ingots match those of Egyptian glasses. The size and shape of one of the cobalt ingots was similar to the interior dimension of the cylindrical vessels used at Amarna as crucibles (Nicholson et al. 1997). One of the ingots had finger grooves on the underside that match finger grooves inside one of those crucibles from

Amarna (Jackson and Nicholson 2010). There is also a fragment of a ceramic vessel still attached to one of the ingots that looks like the same material used for manufacturing the cylindrical crucibles at Amarna. This evidence clearly points to the use of the Uluburun in transporting glass ingots from Egypt to be worked elsewhere. Only three ingots were analyzed in the study by Jackson and Nicholson (2010) so the provenance of the other ingots is unknown. These may include ingots made in Near Eastern primary production areas.

Figure 2.2. Map showing the route of the Uluburun shipwreck along with the location of where some of the cargo originated. (From Pulak, 2008, p. 298, fig. 97).

Studies of the materials on board and the direction of the currents in the Eastern Mediterranean have been undertaken to identify the route of the ship, its origin, and likely destinations (Pulak 2008; Jackson and Nicholson 2010). The artifacts found that would have been used on board, such as dishes and vessels, as well as some of the personal items, indicated it originated on the Levantine coast (Pulak 2008). The stones from which the anchors were constructed come from the Carmel coast in Israel, and the pottery used aboard the ship was sourced to just north of that area. This area is the likely the starting point of its travels. Based on the cargo and the westward currents of the eastern Mediterranean, the ship would have traveled counterclockwise (Figure 2.2).

Ships like the Uluburun would have headed westward after leaving the Levantine coast and Cyprus navigating towards ports along the southern coast of the Greek mainland and Crete. They could have also traveled north into the Aegean to trade along the northern coast of Turkey, the Black Sea coast, and the northern coast of Greece. Loaded with glass ingots as well as other raw materials and finished products, either route would have taken the Uluburun, or ships like it, along the coast of the Greek mainland where it could have stopped at different ports to provide glass ingots to Mycenaean palatial centers.

Egyptian objects have been found in the Aegean and it appears that there is knowledge in Egypt of the Mycenaeans, but the Linear B texts found do not mention direct gift exchanges between Egypt and Mycenaean Greece (Bachhuber 2006). If items were not directly traded between the two regions, this means that raw glass or finished objects of Egyptian origin would have had to make its way to the Aegean along a trade route like that proposed for the Uluburun, using what some have described as “sea faring middlemen” (Walton et al. 2009, 1502). It has been suggested that for some of the Uluburun cargo, items from different areas of the eastern Mediterranean could have already been on the Levantine coast before the ship set off, arriving via some other route (Pulak 2008). Since no Egyptian glass has been found in the Near East (Walton et al. 2009, 1502), the Uluburun would have picked up the Egyptian made glass ingots after stopping in the Aegean on its route back east taking it along the northern coast of Africa (Figure 2.2).

Here it could have picked up glass from the Egyptian glassmaking centers, along with other African materials such as ebony and elephant ivory, and then continued eastward towards the Levantine coast.

The presence of two men from the Aegean onboard the Uluburun seems to strengthen the idea that the ship, and the cargo, was headed to Greece. These passengers could have been ambassadors or messengers that were part of the exchange of gifts or tribute (Pulak 2008). Pulak (2008) has argued that these men were Mycenaean based on the types of personal adornments found, such as relief bead necklaces, Mycenaean style knives and razors, and some utilitarian ware that was not imported to the Near East. Others, such as Bachhuber (2006), have cautioned against assigning an ethnicity to these two passengers based on the material culture found onboard. He instead refers to the them as "individuals of possible Aegean origin" (Bachhuber 2006, 353) that may have carried these Aegean or Mycenaean type artifacts with them.

If the ship did have an Aegean destination, one of the possible places mentioned by Pulak (2008, 300) where the cargo could have been unloaded is the port city of Tiryns. Glass ingots could have been imported to this Mycenaean site to be turned into relief beads or other glass objects and then traded elsewhere. Tiryns also could have exported the ingots themselves to other sites that were also involved in the working of glass during this period. Other suggestions for possible destinations could be the island of Rhodes or Crete. Ports in these locations would act as intermediaries to distribute the items from the Uluburun cargo across the Aegean and the broader eastern Mediterranean (Bachhuber 2006). These two areas were suggested based on the large number of exotic items discovered clearly indicating a large number of imports. Crete, and in particular the port at Kommos, has been proposed as the likely destination not only because of the very large number of foreign Late Bronze Age items found, but also its proximity to the Greek mainland, which would make it easier to distribute material to Mycenaean sites (Bachhuber 2006, 358).

Figure 2.3. Chronology of Egypt, mainland Greece and Crete taken from Jackson and Wager, 2008, p. X. There are various dates given in the literature for the start and end dates for the periods in the table. This chronology is provided to give general approximate dates for the periods mentioned in the text.

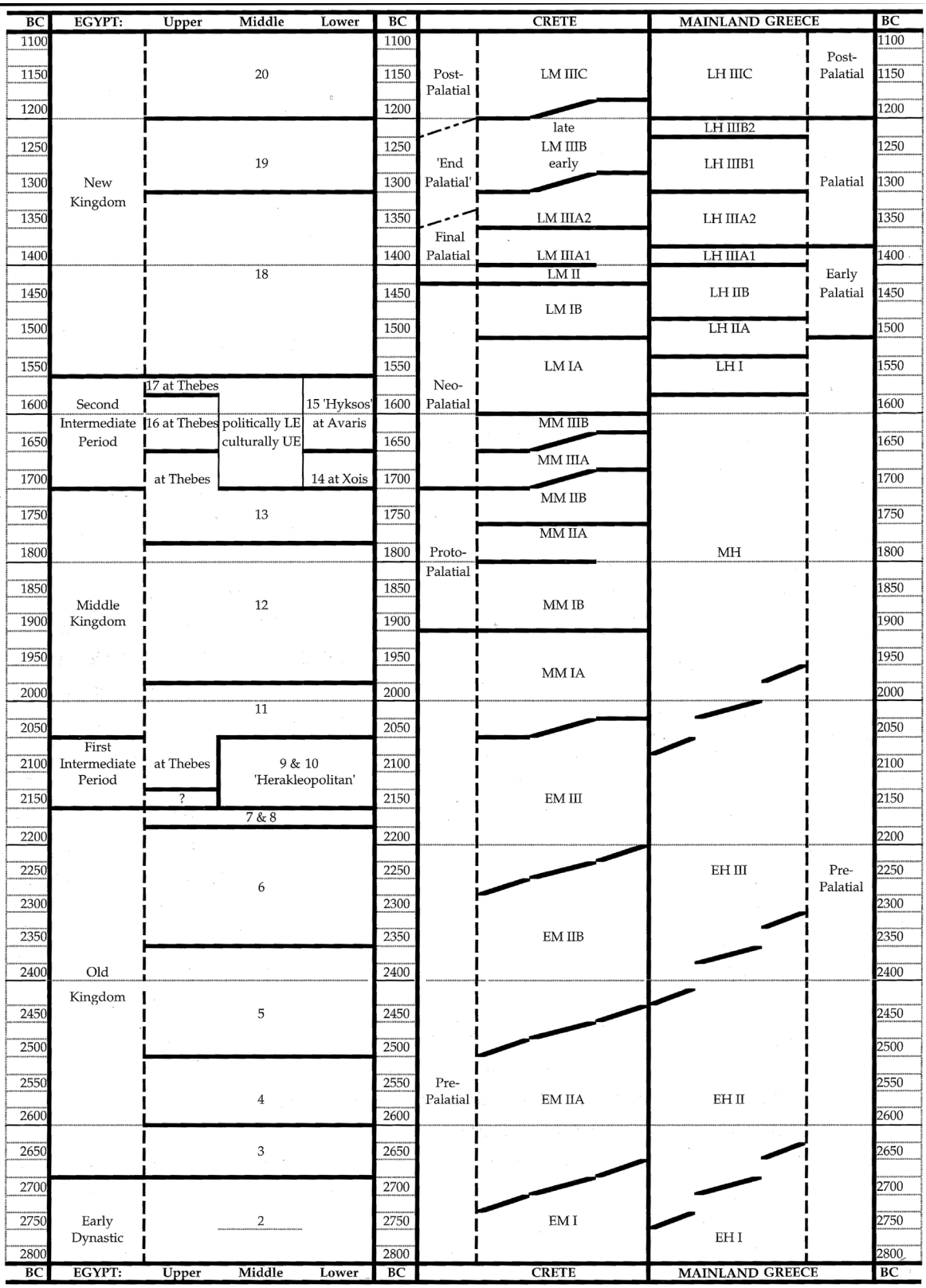

3 THE RAW MATERIALS AND TECHNOLOGY OF GLASS AND FAIENCE

3.1 GLASS

3.1.1 Silica

Glass is primarily made of silica which is the principle network former (Davison 2008). The structure is composed of one silicon atom and four oxygen atoms. Some of the oxygen atoms form bridges to silicon atoms while others form bonds to cations present in the glass. In ancient soda-lime glasses, the silica content is approximately 65-70% (Henderson 2012).

Quartz pebbles, sands from river or coastal deposits, or geological deposits can be used to produce glass (Henderson 2012). The silica source used can introduce impurities into the glass. One of the more common impurities is iron, which will produce a greenish tint in uncolored glass. Quartz pebbles are a purer source of silica, and therefore do not introduce as many impurities into the glass. Sand contains many more impurities due to the minerals it contains, such as chromite, olivine, calcite, and mica. These are introduced into the glass batch when sand is used. This silica source contains more iron, alumina, and titania than quartz pebbles. Higher concentrations of rare earth elements such as lanthanum, yttrium, and neodymium are present within sands. The composition of minerals and rare earth elements in sand is dependent on where it is found. The presence and concentrations of these elements create a chemical signature that can be used to source the silica.

Quartz pebbles are thought to be the main silica source used for Late Bronze Age glasses (Smirniou and Rehren 2011). The finds from Amarna and Qantir point to the use of crushed quartz as the source of silica used at those glassmaking sites (Shortland 2012). Unlike sand, this purer silica introduced less iron, alumina, and titania into the glasses made during this period. Later glasses tend to use sand and have higher concentrations of these three components, as well as additional impurities. The concentrations of these elements in the glass can be used to identify whether sand or pebbles were used as the silica source. Although there is evidence for the predominance of crushed quartz pebbles as the silica source, sand could still have been used. The higher levels of zirconium in Egyptian glasses could point to the use of inland sands (Henderson 2013). Higher chromium in Mesopotamian glasses could indicate the use of sands containing chromite (Shortland et al. 2007). There have also been some Mycenaean glasses

3.1.2 Alkalis and alkali earths

Silica melts at 1710°C, a temperature too high for ancient furnaces to achieve (Henderson 2012). In order to be able to melt glass, a flux is added to the glass to modify the silica network reducing the melting temperature to around 1000-1100°C, or possibly even lower (800-900°C), depending on the composition of the glass and type of flux used (Turner 1954; Turner 1956; Rehren 2000). The two alkalis commonly added as a flux in ancient glasses are soda and potash. Although the alkalis added have allowed glass to be made at a lower temperature, the network produced is not stable. Alkaline earths metals such as calcium and magnesium must be added to improve durability and make the glass less water-soluble. The double charged cations in these compounds are more tightly bound to the non-bridging oxygen atoms and strengthen the silica network (Davison 2008).

3.1.2.1 Plant ash glasses

The flux used for Late Bronze Age glasses was based on the alkalis present in plant ashes. They were used as the primary flux until the 1st millennium BC when it was replaced by the mineral evaporite natron (Henderson 2012). Natron was used until about the 8th c. AD when plant ashes were used again.

The ashes used in Late Bronze Age glasses came from burning halophytic plants that grow in soils with high salinity (Shortland 2012). These soils are high in alkalis. These are taken up by the plants and stored as salts.

These salts which are primarily soda rich salts, such as sodium carbonate, (Barkoudah and Henderson 2006), get incorporated into the glass when the ash is added to the raw materials. The plants chosen by Late Bronze Age glassmakers were not only high in soda but also had elevated potash and magnesia. These glasses are known as high magnesium glasses (HMG). The plants chosen also contained lime. This means that both the flux and network stabilizers needed entered the raw material through the plant ash alkali. Typical Late Bronze plant ash glasses have been analyzed and on average contain 15–21% soda, 1.5–4% potash, 4–9% lime, 2–8% magnesia, 0.4-2.5% alumina, and 58-68% silica (Table 3.1) (Henderson 2012; Nicholson 2007; Shortland 2012).

Work has been undertaken to try to identify which halophytic plants were used by trying to work backwards from the concentrations of the alkalis and stabilizers in the glass (Henderson 2012). This data has been combined with other types of evidence to identify plant sources. Ancient texts mentioning glassmaking have been studied to try and link the names of the plant ashes found to their modern equivalent (Oppenheim et al. 1970). Halophytic plants have been collected from areas near glassmaking centers, turned into ash and analyzed chemically for comparison (Barkoudah and Henderson 2006; Henderson 2013). They have also been used in replication experiments to see if glass with similar compositions to those found in the Late Bronze Age can be produced. These methods have provided more information on plant ash sources, but have presented some challenges in the identification of plant species. In the case of ancient texts, there has been difficulty in the translation of some terms and determining which specific plant genus or species is mentioned. Because so few Late Bronze Age primary production centers have been identified, geographic locations for the halophytic plants used are unknown. In replication experiments, it is not clear if the modern plants harvested are the same as those used in antiquity.

The chemical variations in the plants themselves, even when they are harvested from the same area, make association with ancient compositions problematic. These differences can affect aspects of glass production such as the melting temperature, the temperature at which the glass softens when reheated or the time it can be worked (Henderson 2012). This inconsistency could also present itself in the composition when the glass is analyzed. Studies by Barkoudah and Henderson (2006) that investigated the composition of halophytic plant ashes collected in Syria found that the major and minor oxides were fairly consistent (10-30% variation) but the trace elements introduced more variability. This works shows that some connections could be made between modern halophytic plants found today but the connections may not be so straightforward. Although this type of research continues, the results of the several studies conducted thus far point to halophytic plants from the genus *Salicornia* and *Salsola* as likely candidates for the alkali (Shortland 2012; Henderson 2013).

3.1.2.2 Mixed-alkali glasses

As discussed in Chapter 2, at around 1200 BC a new type of glass appears in the archaeological record, the mixed alkali or LMHK glasses (Henderson 1988a). Unlike plant ash glasses, these vitreous materials have lower soda, magnesia, and lime, but elevated potash. Typical LMHK glasses have a composition containing 6-12% potash, 0.4-1.0% magnesia, 1-3.5% lime, and 4-9% soda (Table 3.1) (Henderson 1988a; Henderson 1988b; Brill 1992; Henderson et al. 2015). A variation of the LMHK glass has found that contains a higher concentration of potash (15-18%) and very low soda (0.8%), but shares similar quantities of the other glass components (Henderson 1992; Henderson et al. 2015).

Although there have been studies undertaken that have identified some of the LMHK glass raw materials (Henderson et al. 2015), information on which alkali was used is still unknown. There have been several alkali sources suggested. One is that the alkali source is based on plant ash, but the plant was processed in a way that affected the composition. Plant ash is higher in magnesia and lime, but purification of the ash could result in a reduction of these two components (Brill 1992). A coastal plant has been found in Italy that has a composition of soda and potash similar to that found in mixed alkali glasses, which is thought to be a

possible alkali source. The lime and magnesia contents are high in these particular plants but if they were purified in a similar way to the process used for some historical glasses, such as for some enamels from the Middle Ages or Murano glass in the 15th c. AD (Santopadre and Verità 2000), it might explain the composition. In these more recent examples, plant ashes were purified prior to being added to the raw materials. They were first dissolved in boiling water and the solution filtered to remove insoluble compounds, including some containing calcium and magnesium. When the solution dried, the evaporated soluble salts would then be collected and used as the alkali.

The use of an impure natron source has also been suggested as a possible alkali (Brill 1992). The traditional natron used did not contain much potassium (>1.5%), therefore the natron source used for the LMHK glasses would have to contain potassium minerals. Wadi Natrun in Egypt, the main natron source using for ancient glasses, does not contain high levels of potash. This means that another mineral evaporite source would have had to have been exploited. The final idea put forward for the alkali source is that neither plant ash nor a natron alkali was used, but instead some source rich in minerals such as saltpeter (KNO_3) and niter ($NaNO_3$) (Brill, 1992). One common source for these salts is latrines, where both are found in the waste. The use of these particular salts for making glass is known and can be found in Chinese glasses as well as later European glasses.

Table 3.1. Summary of the typical compositions for the different glass types mentioned in the text. Compositions were compiled from data published in Brill, 1992; Freestone, 2005; Henderson, 2012; Henderson et al., 2015; Nicholson, 2007; Scott and Degryse, 2014; Shortland, 2012.

	Plant Ash Glasses	Mixed Alkali Glasses	Natron Glasses
SiO_2	58-68%	67-85%	65-75%
Na_2O	15-21%	4-9%	12-19%
K_2O	1.5-4%	6-12%	>1.5%
MgO	2-6%	0.4-1%	>1.5%
CaO	4-9%	1-4.5%	5-10%
Al_2O_3	0.4-2.5%	1-3%	2-5%

3.1.2.3 Natron glasses

As early as the 10th c. BC in Egypt, glasses made with the mineral natron ($Na_2CO_3 \cdot 10H_2O$) as the alkali emerge (Henderson 2012). Although these types of glasses were not the predominant glass type made during the period the glasses in this project cover, there has been some evidence for some possible natron glasses discovered earlier. Glasses with compositional characteristics of natron glasses have been reported in Early Iron Age (11-9th c BC) Pella, Hasanlu, France and Italy which chronologically overlap in date with some of the glasses analyzed for this study (Reade et al. 2006; Stapleton 2012; Conte et al. 2016; Conte et al. 2018). Therefore, this glass composition will be briefly introduced here.

Natron is formed as water evaporates from saline lakes. Its formation is seasonal with the evaporates forming in the summer as the lake dries (Shortland et al. 2006). Other types of sodium-based minerals can be collected along with the natron such as trona ($Na_2CO_3 \cdot NaHCO_3 \cdot 2H_2O$), sodium chloride (NaCl), sodium carbonate (NaCl), and sodium bicarbonate ($NaCO_3$) (Henderson 2012). These additional minerals can sometimes be seen in the composition of natron glasses. Roman glass for example often contains 0.5-1.2% chlorine and 0.2-0.5% sulfur (SO_4) which is present due to the use of natron (Scott and Degryse 2014, 21).

The use of natron changed the major and minor oxide compositions of the glass, affecting not only the akalis used for the flux but the network stabilizers (Table 3.1). Natron glasses are characterized by low potash and low magnesia, both generally found at <1.5% (Scott and Degryse 2014). These glasses are often referred to a low magnesium (LMG) glasses (Sayre and Smith 1961). In plant ash glasses, the lime is introduced into the glass through the halophytic plant ashes; however, that is not the case with natron glasses. The lime must be added via another source, either through the selection of sands that are rich in lime, so they include shell

or limestone fragments, or through the intentional addition of lime to the glass batch. Alumina is higher in natron glasses due to the presence of feldspars in the sands used as the silica source (Henderson 2012). The average composition of natron glasses contains 15–20% soda, <1.5% potash, 5-10% lime, <1.5% magnesia and 2-5% alumina (Table 3.1). The composition of natron glasses varies based on where and when it was produced. Greater variation can be seen between the first natron glasses made and those made in the late Roman or early Byzantine period. It is clear though that despite these variations, they contain in general less silica, less potash, less magnesia, higher lime, and higher alumina than Late Bronze Age glasses.

3.1.3 Colorants and opacifiers

The final step in making glass is the addition of transition metal ions that add color to glass, opacify it or in some cases decolorize it (Henderson 2012). The color produced is influenced by several factors including the oxidation state of the colorant, how it was prepared, the firing temperature, and the furnace atmosphere. Below is a general description of colorants used in Late Bronze Age glasses that are related to the glasses analyzed for this research.

3.1.3.1 Copper blue glass

Copper blue was the most common color of glass produced in the Near East and one of the two blues commonly produced in Egypt (Shortland 2012). It is a strong colorant. It was used to produce not only blue glass but also blue-green or turquoise glass. It can color vitreous materials in concentrations as low as 0.5%. Egyptian copper blue glasses tend to have a copper content above 1% (Nicholson 2007).

The copper colorant used in the Late Bronze Age comes from two sources, either a copper mineral or the reuse of bronze scrap (Nicholson 2007). When bronze is used tin is found in the glass along with lead, if leaded bronze was used. The practice of using bronze as the copper source for coloring glasses was restricted to Egyptian made material (Shortland and Eremin 2006). In the Near East, copper mineral was used due to the lack of tin and lead found within the glass. Recent analysis has suggested that copper blue glass at Tell Atchana was colored with arsenical copper (Dardeniz 2018).

Despite the color of the glass, analytical work has found that all Late Bronze Age glasses seem to contain some traces of copper, at around 0.1% (Shortland 2012). The reason for this is not clear but it does not appear to be a deliberate addition. It is possible that the copper is entering the glass batch through the reuse of crucibles that were used to melt copper blue glass. Another possibility is that copper or bronze tools used for different glassmaking activities partially melted during glass production and contaminated the glass (Smirniou and Rehren 2011).

3.1.3.2 Cobalt blue glass

Cobalt is a very strong colorant and only about 0.1% is needed to impart a dark blue color to the glass (Shortland 2012). After copper blue, it is the next most common color of glass found, in particular within Egyptian and Mycenaean contexts (Shortland 2012; Smirniou and Rehren 2013; Worral 2020). It is the predominant color for Mycenaean glasses in particular (Nightingale 2008), with the majority of these dark blue glasses colored with cobalt or a mix of cobalt and copper (Co-Cu glasses). Cobalt was first used in the 2nd millennium BC in Egypt until the 1st millennium BC, but then disappears. Cobalt as a colorant is rarer in Near Eastern glasses. The dark color produced by the use of a cobalt colorant is thought to have been use to produce an imitation of the precious stone lapis lazuli or the dark blue color may have been connected to some religious or magical beliefs (Nightingale 1998).

The source of cobalt first used in Egypt seems to come from the Dakhla and Kharga Oases in the Western Desert (Shortland 2012). This was the predominant cobalt source used through the end of the 18th Dynasty (ca. 1292 BC). The cobalt from the Western Desert is associated with an alum source (cobaltiferous alum) and appeared yellow, pale purple or pink. The alum had to be processed in order to extract the cobalt for use as a glass colorant. The cobalt from the Western Desert is found in association with a group of trace

elements that are specific to a geological source. Glasses made with cobalt from this area contain elevated levels of alumina (2.7%), manganese (0.19%), nickel (0.09%) and zinc (0.17%). Because the trace elements within the cobalt source are incorporated into the glass made, the presence of specific transition elements and their concentrations can be used to locate the source of the cobalt. Based on the analysis of glasses from the 19th and 20th Dynasties (Ramesside Period), it appears as if a new cobaltiferous alum source is used. Cobalt glasses from sites in the Memphite region were found to contain less alumina and zinc, and more nickel, than glasses made using cobalt from the Western Desert (Abe et al. 2012). Although glasses using the previous source were still made, the overall number of cobalt glasses declines after the 18th Dynasty.

The concentration of cobalt in these glasses range from 0.09-0.37%, with some containing up to 1.3% (Shortland and Tite 2000; Tite and Shortland 2003; Nicholson 2007). Some Mycenaean glasses can contain higher concentrations of cobalt, but on average the values are similar to Egyptian cobalt glasses (Nikita and Henderson 2006; Smirniou et al. 2009; Zacharias et al. 2018a). Blue glasses have been found to be colored with a mix of copper and cobalt. In the cases where the two blue colorants are combined, the cobalt concentration tends to be lower (0.11%) compared to when cobalt is found alone (Shortland and Eremin 2006; Shortland 2012) .

Late Bronze Age cobalt glasses contain lower concentrations of potash (below 2%) (Shortland and Tite 2000). Although the levels of this alkali are lower, the levels of other components of the glass, such as magnesia, remain the same (Henderson 2012). The reason for this is unknown but several possibilities have been proposed. The use of a different plant ash alkali that is lower in potash has been suggested as the cause behind the lower alkali content (Shortland and Tite 2000). Glasses made in other colors have been found with potash levels similar to those seen in the cobalt blue glasses. Therefore, although dark blue glasses colored with cobalt seem to be low in potash, not all low potash glasses are cobalt blue (Nicholson 2007). If the low potash levels are due to a different alkali, these other glasses would have also been made using the low potash plant ash.

Another possibility is that the processing of the alum can alter the final composition. Replication experiments have found that cobaltiferous alum can be added directly to the raw materials when making glass. When this happens, the chlorides and sulfates in the alum are not miscible with the glass melt and separate out (Rehren 2001). With continued heating, temperatures are reached where all the components become incorporated into the final melt. Compounds such as aluminum and magnesium sulfates are some of the immiscible materials. If not fully incorporated into the glass after firing, it can create increases in the ratio of alumina and magnesia. This method would also require large amounts of alum to be used in order to obtain the concentrations of cobalt found in the finished products. However, if the alum is processed in a way to precipitate out the cobalt, then less alum can be used (Rehren 2001; Tite and Shortland 2003). The preparation of the alum could also precipitate aluminum and magnesium in a form that would prevent their separation during melting and keep the values in line with what is observed in the cobalt glasses. The process suggested is that an aqueous alkaline solution is used to precipitate out cobalt, aluminum, and magnesium as hydroxides. These then are added to the glass raw materials. Laboratory based experiments used an ammonium based alkaline solution for the alum processing, but natron was suggested as the alkaline used by the Egyptians (Rehren 2001). Despite this processing of the alum, there is still no evidence that the preparation of alum to form a concentrated cobalt aluminum hydroxide colorant would affect the potash content of the glass

A final suggestion is that the conditions under which the cobalt glass was made could have altered the potash concentration. Experiments conducted on plant ashes likely to have been used for making glass have shown that melting conditions can alter the potash concentrations within samples of the same species of

plant (Henderson 2012). Perhaps cobalt glasses were fired under certain conditions that affected the final potash concentration.

Based on all the possible suggestions for the low potash, it appears as if the idea of specific plant ashes selected for the production of cobalt blue glasses is the more accepted hypothesis. These plant ashes were likely located in areas near workshops that specialized in the production of this color of glass and their composition is due to their geography (Rehren 2001). These workshops also produced other colors using the same plant ash alkali, which explains why those glasses appear in the archaeological record. It is possible that with additional research into the elemental composition of halophytic plants available as the alkali source in different glassmaking regions, this question of varying potash concentrations will be answered.

3.1.3.3 Iron yellow, green, and black

Iron can produce a range of colors in glasses including blue, green, yellow, amber, brown and black (Schreurs and Brill 1984; Brill 1988). The typical iron content of Egyptian glasses is around 0.5%, which is present due to impurities in the raw materials. If no colorant is added, this amount of iron in a glass will produce a light blue or blue-green color. A piece of glass found at Amarna was colored brown with only 1.47% iron (Nicholson 2007). At high concentrations, iron can produce dark green glasses, some so dark that they appear black. Dark green, almost black beads, colored by high iron (avg. 9.7%) were found at Pella (Reade et al. 2006). Black beads from Iron Age contexts in Europe has been found to contain up to 20% iron in some cases (Reade et al. 2006; Conte et al. 2018).

The iron that is present in the glass can be found in two oxidation states, ferrous (Fe^{2+}) and ferric (Fe^{3+}). The ratio of each can affect the color produced. Ferrous ions produce a blue color and ferric a weak yellow color (Brill 1998). Other factors such as the furnace atmosphere and length of firing can alter the color with just the natural amount of iron present (Henderson 2012; Nicholson 2007; Shortland 2012). This is because an oxidizing atmosphere reduces the number of ferrous ions present and the glass becomes greener (Brill 1998). A reducing atmosphere increases the number of ferrous ions and the glass appears bluer.

Analyses of some Egyptian brown and black glasses were found to contain the same amount of iron as other colors of glass. This was the case for a group of brown glasses from Amarna (Nicholson 2007). A black glass from Lisht was analyzed and found to have no added iron (Shortland 2012). These two examples show that these brown and black glasses were colored due to a strong reducing atmosphere in the furnace, rather than the addition of colorants.

Additional ions within the glass could also influence the color produced by the iron naturally present. Glasses from Jalame, a late Roman site in Israel, were found to have their color influenced by the presence of sulfur introduced into the glass batch through the alkali (Schreurs and Brill 1984; Brill 1988). Sulfates are present in plant ashes and natron. Under strong reducing conditions within the furnace, the sulfate ions reduce to sulfides and then combine with the ferric ions present in the silica source to create a ferri-sulfide complex. This complex is amber in color. Due to a reducing furnace atmosphere, ferric ions will also reduce to ferrous ions. The mix of the amber colored ferri-sulfide and blue ferrous ions forms an olive green or olive amber colored glass. Different ratios of the ferric, ferrous and ferri-sulfide colorants combined with a reduced furnace environment is responsible for the range of colors observed in the Jalame glasses, which included yellow-green to olive green to amber.

3.1.3.1 Manganese black and purple

Manganese has been used to produce purple and black colored glasses (Nicholson 2007). It has also been used as a decolorizer to make clear glass, but this is rare before the 6th c. BC (Sayre 1963). Egyptian purple glasses can contain anywhere from 0.55-2.5 wt% manganese oxide (Shortland 2012). Black glasses from Amarna contained at least 2 wt% manganese (Nicholson 2007; Muros et al. 2017). Other colorants, such as copper and/or cobalt, were added to the black glasses from Amarna to produce a much darker glass. Three

black glass beads from the Mycenaean site of Pylos were colored with manganese (0.023-0.57 wt%) without the addition of another colorant to darken the glass (Polikreti et al. 2011)

3.1.3.2 Opaque white and blue glass

Opacified glasses are created through the formation of small, crystalline particles within the glass matrix. These particles have a different refractive index from the overall matrix they are dispersed in and reflect the light differently (Turner and Rooksby 1959). In opaque white glasses, the opacifier is calcium antimonate found as $CaSb_2O_6$, $Ca_2Sb_2O_7$, or a combination of both compounds (Shortland 2002). These white crystals form within a translucent, colorless glass matrix. The calcium antimonate crystals are small and well dispersed.

Opaque white glasses are common in Egyptian contexts and are often used to create a trailed decoration on beads or vessels (Shortland 2002). This color of glass is rarer in the Near East. The antimonate content of Egyptian opaque white glasses averages from 1-3 wt% (Mass et al. 2002; Smirniou and Rehren 2011). In later periods, the concentrations of antimony are elevated, such as in opaque white Roman glasses, averaging 4-5% (Mass et al. 2002).

Two methods have been suggested for how the calcium antimonate opacifier was produced in ancient glasses, either through the addition of synthesized calcium antimonate crystals to the glass melt or through in situ crystallization (Lahlil et al. 2008). In situ crystallization has been suggested as the method more commonly used to produce opaque glass in antiquity (Shortland 2002; Lahlil et al. 2009) In this method, antimonate compounds are added to colorless glass, either mixed in with the raw materials or put into the glass melt. The antimonate containing material combines with calcium in the glass matrix and precipitates as opaque white crystals. Another method is based on the addition of synthesized calcium antimonate crystals directly added to the melt (Lahlil et al. 2010b; Lahlil et al. 2010a). Experiments conducted to produce these crystals show that they can be made by heating calcium carbonate together with stibnite (Sb_2S_3) or antimony oxides (Lahlil et al. 2010b).

New Kingdom Egyptian glasses are thought to have been made using the in situ crystallization method (Shortland 2002). The opaque white glasses from this region and time period seem to have less lime than colorless glasses, averaging 8.1 wt% versus 8.7 wt% (Shortland 2002). When the calcium antimonate crystals precipitate, they draw lime from the glass matrix. This reduces the lime concentration of the bulk glass. If synthesized calcium antimonate crystals were added to the glass batch, the lime content would be higher. An opaque white glass from Nuzi contained 9.2% lime whereas it was 5.58 wt% in other glasses (Shortland 2012). This may indicate that calcium antimonate crystals were added to the glass and increased the overall lime content.

Work conducted by Lahlil et al. (2010b) may point to the use of synthesized calcium antimonate crystals in Egyptian glasses. Experimental work on laboratory made opaque white glasses and analysis of Egyptian glasses from the 18th Dynasty showed similar formations of particular calcium antimonate phases with the same crystal shapes. These differed from glasses made using in situ crystallization.

The exact antimonate source used in antiquity is unknown, but stibnite or roasted stibnite (Sb_2O_3, Sb_2O_4) was likely used (Lahlil et al. 2009). Experiments trying to reproduce the methods of manufacture for opaque white glass have shown that stibnite can be used to produce calcium antimonate opacified glass. There is historic evidence for the use of stibnite in other contexts. Pliny the Elder wrote that stibnite was roasted to prepare a white antimony oxide powder for medicinal purposes (Mass et al. 1997). Therefore, knowledge of this material and its preparation were known and it could have been used for glass production. A possible source for stibnite can be found in the Caucuses (Shortland 2012).

Opaque blue glasses are also opacified by calcium antimonate crystals. This glass color was common in both the Near East and Egypt where it was used to make artifacts as well as applied as trailed decoration

(Shortland 2012). Opaque copper blue and opaque cobalt blue glasses were produced. Like the opaque white glasses, opaque blue glasses have lower lime than their translucent counterpart does. Translucent copper glasses contain on average 8.7 wt% lime, whereas opaque copper glasses have 7.4 wt% lime (Shortland 2002). For translucent cobalt and opaque cobalt glasses, the concentrations of lime are 7.7% and 6.5% respectively. The lower lime content in the opacified glasses supports the use of the in situ crystallization method for opacification.

Opaque blue glasses also have higher concentrations of the colorant as opposed to their translucent versions (Shortland 2002). An opaque copper blue glass contains about 1.33 wt% copper versus 1.16 wt% detected in translucent copper glasses. For cobalt glasses, 0.19 wt% CoO is found in the opacified version, but translucent cobalt glass contains 0.11 wt%. This higher colorant concentration in the opaque blue glasses also points to the use of in situ crystallization of calcium antimonate within a blue glass. If a blue glass and a white glass were mixed together to produce the opaque glasses, the colorant content would be diluted and lower.

3.1.3.3 Opaque yellow and green glass

Opaque yellow glasses are commonly found in Egypt and the Near East during the Late Bronze Age (Shortland 2012). Like other opacified colors, it was used to make individual artifacts and as trailed decoration. The opacifying crystals are made by combining lead and antimonate compounds (Shortland 2002). The color comes from the formation of crystals of a lead antimonate compound ($Pb_2Sb_2O_7$) within a colorless glass matrix. In order to produce this color of glass, a lead mineral, likely galena (PbS) and stibnite are roasted together and then added to clear glass (Turner and Rooksby 1959; Shortland 2002). Unlike the calcium antimonate crystals that are small and well dispersed, lead antimonate crystals are found in large clumps or in streaks or swirls within the glass.

The concentration of lead in opaque yellow glasses is much higher than that of antimony. Analyses of opaque yellow glasses from Malkata and Lisht found that the maximum concentration of lead oxide was 13.2%, but the maximum concentration of antimony oxide was only 1.0% (Mass et al. 2002). The concentrations of both lead and antimony increases in areas where the yellow crystals are present, up to 58% and 42% respectively (Shortland 2002).

The way that the lead antimonate crystals are distributed within the glass matrix, as clumps in the glass, and that they are partially dissolved into the glass matrix, points to the material added as already formed lead antimonate crystals into the glass rather than as separate components (Shortland 2002). Lower temperatures would be required during the glassmaking process for the addition of lead antimonate. Therefore, it could not be mixed into the raw materials. If the temperature is too high, over 900°C, the crystals would dissolve in the glass matrix and not act as opacifiers (Shortland and Eremin 2006). Lead antimonate could have been added when the colorless glass was quite viscous and well formed (Shortland 2002; Nicholson 2007).

Research has been conducted to determine the source of the lead and antimony used to make the lead antimonate opacifier. Mass et al. (1997) proposed that the lead and antimony came from the byproducts of the cupellation of silver. Antimony rich litharge was produced in the Roman period in areas of silver smelting due to the processing of antimonial argentiferous galena, an antimony rich lead ore that contained silver. The use of this antimony rich litharge has been suggested for New Kingdom Egyptian glasses, and there is evidence these ores were imported into Egypt (Mass et al. 2002). The opaque yellow glasses contain zinc at levels higher than glasses in other colors. This element could have entered the glass through the use of a specific lead ore that contained zinc, such as galena (PbS) that contained the mineral sphalerite (ZnS) (Shortland 2002). The zinc content in these glasses is quite higher, greater than what is detected in metallic artifacts produced in this period. If litharge was used, the zinc content would be reduced because it would

volatize during smelting. Therefore, it is more likely that when higher concentrations of zinc are present in the opaque yellow glasses a zinc containing lead ore was the source.

Based on the high concentration of lead in the opaque yellow glasses, and lead rich areas around the opaque crystals, it is possible that additional lead was added to the glass along with the lead antimonate (Shortland 2002). This lead could have been introduced as lead oxide or metallic lead. Lead isotope analysis was conducted on the opaque yellow glasses to source the lead used. The isotopic signatures points to the Red Sea Coast, from Gebel Zeit, as the source of Egyptian lead. The lead used for Near Eastern opaque yellow glasses comes from a different source (Shortland 2012).

Opaque green glasses were created through a combination of copper and lead antimonate compounds (Shortland 2002; Nicholson 2007). No opaque green glasses have been found made with cobalt (Shortland 2012). Unlike opaque yellow glasses, the content of lead and antimony in opaque green glass is reduced. The lead content in opaque green generally ranges from 0.4-2.7 wt%, as opposed to opaque yellow that have up to 13 wt% lead (Mass et al. 2002; Nicholson 2007). The copper content is similar to that found in copper translucent glasses, so there is no increase in the colorant content like with the opaque blue glasses (Nicholson 2007). Opaque green glasses are rare in Egypt and not found in the Near East (Shortland, 2012). They generally contain some tin indicating that bronze scrap was used as the copper source and identifying them as made in Egypt.

The lead antimonate in opaque green glasses also present as clumps or swirls. This initially was taken to mean that the glass was made by mixing of opaque yellow and translucent blue glass (Nicholson 2007). It was also suggested that copper was added to opaque yellow glass to produce the green color. If either of these production methods were employed, then the lead and antimony content of the glass would be the same as what is found in opaque yellow glasses. Because these levels are lower in opaque green glasses, it cannot be made using an already formed yellow glass. The most probable method of manufacture is the addition of lead antimonate to copper blue glass.

3.1.1 Glass production

The production of glass was briefly described in chapter 2 in reference to the evidence for production sites in the Late Bronze Age. It will be discussed again below to add some additional information on the production processes involved.

Glass can be produced in a single stage, where all the raw materials are added together in a crucible and melted. Replication studies have tried to make copper blue glass and cobalt blue glass this way, and the resulting product was similar in composition to Egyptian glasses of these colors (Tite and Shortland 2003). However, even from the earliest discoveries of glass production sites, it has been proposed that glass was made in a two-step process. Petrie (1894) proposed this after his discovery of what he thought were glass and faience factories at Amarna. In the case of cobalt glasses, he thought that cobalt frit, which was found within technical ceramics at the site, was added to colorless glasses (Tite and Shortland 2003). Studies by Turner (1956) confirmed the two step processes put forth by Petrie could produce glass, but instead of mixing the cobalt frit with colorless glass, Turner suggested the cobalt frit itself was utilized to manufacture the glass.

Although these initial proposals for glassmaking would not have produced cobalt glass of the same composition as that found at Egyptian sites (Tite and Shortland 2003), archaeological remains, epigraphic evidence, and additional replication experiments show that glass was likely made in a multi-step process. The first stage involved taking the raw materials and placing them within a reaction vessel or crucible, lined with a lime based parting layer (Rehren 2000; Smirniou and Rehren 2016). The raw materials would be heated at a low temperature (600-800°C) to create a semi-fused glass (Smirniou and Rehren 2011). This is the process referred to as fritting. The semi-fused glass found at the sites of Amarna, Lisht, Qantir, and Tell

Atchana shows the vitreous material produced in the first stage was white in color, porous and frothy (Smirniou and Rehren 2011; Smirniou and Rehren 2016; Dardeniz 2018; Smirniou et al. 2018). The porosity and frothy appearance was due to the gasses and other volatile compounds that escaped from the glass batch during heating. No colorants were necessarily added in this first step of glass making.

In the second stage, the semi-fused glass would be removed from the reaction vessel or crucible, crushed, sorted, and washed to remove unwanted material (Rehren and Pusch 2005). The crushed glass would then be placed into a crucible, likely with some additional alkali. Colorants could be added at this point. The materials are heated to up to 1100°C to create a fully fused glass. Additional crushed glass could be added during the firing process, using funnels attached to the crucibles (Rehren and Pusch 2005). If colorants were not added to the raw materials before the second firing, they could be added in a third step mixed into the fully formed glass (Smirniou and Rehren 2011). The fully fused, colored raw glass would then be taken to be hot worked into a finished object, or traded to other workshops in the area or via long distance networks to other regions as an ingot.

3.2 FAIENCE

Faience is a vitreous material composed of a quartz core, or body, which is covered with an alkali glaze. It is made using materials similar to those used for glass: silica, an alkali flux and stabilizers, as well as mineral colorants. In the section below, these materials will be described briefly with an emphasis on the components or compositions that differ from what is used for glass. As with glass, most of the evidence for faience production technology and the raw materials used come from the analysis of Egyptian made faience. The discussion below focuses primarily on data obtained from New Kingdom faience objects (1550-1070 BC) for which much more analytical work has been conducted.

3.2.1 Silica

The silica source used for faience can be ground quartz pebbles or sand (Kaczmarczyk and Vandiver 2008). The source chosen affects the color of the quartz core and the elements detected. Ground quartz can produce a whiter and purer silica core as opposed to sand, which can introduce impurities, such as iron, that will alter the color. As observed with glasses, the use of sand as the quartz source also increases the concentration of alumina. Studies of Egyptian faience made with sand had alumina contents averaging 2.3% and iron oxide was at least 1.3% (Kaczmarczyk and Vandiver 2008). This is higher than the concentrations found in glasses made with quartz pebbles where the content of alumina and iron can be below 0.5%.

During firing, interstitial glass forms in the core that helps to hold the quartz particles together. The amount of interstitial glass determines the hardness of the core, as well as the color (Tite 1987). Cores can be found colored white, tan, blue, grey, and brown (Vandiver, 1983). The typical composition of the core of an Egyptian faience object contains about 92-95% silica, 3-5% alkali and 1-2% of the remaining components which includes lime, magnesia and the colorant (Vandiver 1983; Tite and Shortland 2008). In glassy faience where more interstitial glass and glassy phases are present within the core, the silica content drops to 80-85% and the remaining components make up 7-9% of the composition (Tite and Shortland 2008).

3.2.2 Alkalis and alkali earth metals

As with glass, high soda plant ash was used for the alkali in faience produced through the Late Bronze Age (Vandiver 1983). The plant ashes also introduced the network stabilizers magnesia and lime. Analysis of the various layers or phases formed within a faience object have shown a variation in the concentrations of these elements that differ from what is seen in glass objects of the same period.

The ratio of soda and potash is lower in faience than what is seen in glass from this period, but it can vary across the different layers (Kaczmarczyk and Vandiver 2008). The concentrations of lime and magnesia tend to be lower. This composition can still be produced using a plant ash alkali, and does not necessarily point to

the use of a different alkali or different plants ashes used for faience versus glass. The ratios of soda and potash can be influenced by the sands used as the silica source due to the introduction of feldspars in the raw materials. The processing of the plant ashes and mixing of raw materials can play a role. Kaczmarczyk and Vandiver (2008) found that if the plant ashes were put into solution prior to mixing with the quartz, some of the lime and magnesia could stay behind in the vessel. The method of producing the glaze could also affect the distribution of elements across the various layers of the faience. The different glaze production methods used for faience and their compositional differences will be discussed later in this chapter.

Similar alkalis were used to produce Near Eastern faience and some similarities between the ratios of the alkalis and alkali earth metals are observed (Bouquillon et al. 2008). Nevertheless, some regions produced faience that is even higher in potash than Egyptian faience. Faience from Egypt tends to have potash concentrations on average lower than 2 wt%, as does faience from Syria. Faience from Mesopotamia and Iran was found to have up to 5 wt% potash. At the end of the New Kingdom (ca. 1000 BC), natron is used for the production of faience and coincides with the use of this alkali in glass (Kaczmarczyk and Vandiver 2008). The use of high soda plant ashes are still used for faience production in Mesopotamia and Iran through the Islamic period (Bouquillon et al. 2008). This parallels what is observed in glass produced where plant ashes glasses are still made in regions of the Near East even after the introduction of natron glasses (Henderson, 2012).

3.2.3 Colorants

Many of the same mineral colorants are used for both faience and glass. The faience mineral colorants that are related to the faience objects analyzed for this project will be highlighted below.

3.2.3.1 Copper blue and green

Copper blue is the most common colorant used for faience objects in Egypt and the Near East. Like glass, the source of copper can be a copper mineral or can come from a copper alloy. Unlike glass objects, there does not seem to be a regional distinction between the copper sources used. Bronze scrap was added as the colorant for faience in both Egypt and the Near East, with traces of tin found in glazes from both regions (Bouquillon et al. 2008). Arsenic has been found in earlier faience (before 16th c. BC), in a concentration of about 0.01%, and it is thought that arsenical copper could have been used as the source of the copper (Kaczmarczyk and Vandiver 2008). This coincides with the production of arsenical copper in Egypt.

The copper content in faience objects can be variable. Some objects have copper oxide concentrations around 2.6-6.2% in the glaze layer, with a higher concentration in the glaze-body interaction layer (Kaczmarczyk and Vandiver 2008). In later periods, the concentration of copper could be up to 20%. The reason for a higher copper content could be to counter the lighter color of the core, which could dilute the intensity of the blue glaze. Excess copper could also function as a network stabilizer since lime and magnesia tends to be lower in these vitreous materials. For Near Eastern faience, the copper content in the glaze averages 2% (Tite and Shortland 2008).

Green colored faience could be produced due to the interaction of the copper with any chlorides in the raw materials (Kaczmarczyk and Vandiver 2008). The reduction of copper could also produce a green color (Vandiver 1983). However, it is thought that much of the green faience found is due to deterioration (Kaczmarczyk and Vandiver 2008). The blue copper color will alter, in the presence of chlorides in the burial environment, to copper chloride minerals such as atacamite ($Cu_2Cl(OH)_3$) or paratacamite ($Cu_3(OH)_6Cl_2$). The copper in the glaze can also convert to malachite ($Cu_2CO_3(OH)_2$) (Kaczmarczyk and Vandiver 2008; Moussa and Ali 2013).

3.2.3.2 Cobalt blue

The use of cobalt for the production of faience in Egypt appears at the same time as the use of this colorant for glass. The same source, the Western Desert of Egypt, is used for both vitreous materials (Vandiver 1983). At the end of the New Kingdom, the source of cobalt for Egyptian faience changes to one containing lower levels of transition elements (Kaczmarczyk and Vandiver 2008). Although the Western Desert cobalt source is still used for glass during this time, it is no longer used for faience. This shift in the cobalt source may be related to the appearance of glass in the 13th c. BC made using new Egyptian cobalt source reported by Abe et al. (2012).

Cobalt colored faience tends to have more interstitial glass than copper colored faience, which makes the body harder. This also causes the layers in the faience to not be well defined. This faience does not tend to have a light colored core, but instead is colored blue or dark blue, like the glaze color. This is due to the amount of interstitial glass that is present. Some Egyptian cobalt-colored faience has been found to contain copper, sometimes up to 6% (Kaczmarczyk and Vandiver 2008). The composition of the cobaltiferous alum used does not contain copper; therefore, any found in the faience was intentionally added, especially when present in higher concentrations.

Cobalt colored faience has been found in the Near East that was made using cobalt from the Western Desert (Bouquillon et al. 2008). These were imports based not only on the object style, but also because there has been no evidence for the export of the raw cobalt colorant to be used outside of Egypt. Analyses of several faience objects known to have been manufactured in the Near East during the Late Bronze Age do show the presence of transitional elements in concentrations that differ from the Egyptian sourced cobalt. Turkey, Iran, and the Caucuses have been cited as possible sources for the cobalt used in these artifacts. The cobalt from Iran contains high concentrations of arsenic, which can be used to provenance, that cobalt. There has not been as much research conducted on the sources of cobalt in these regions, compared to the analysis conducted on Egyptian cobalt sources. Determining the origin of the cobalt used for both faience and glass objects produced in the Near East is challenging and requires additional work.

3.2.3.3 Manganese and iron black

Analysis of black faience has found that manganese oxide is responsible for the color, in concentrations above 1% (Vandiver 1983; Kaczmarczyk and Vandiver 2008). The use of manganese as the mineral colorant for black faience continues through the Ptolemaic period when it is replaced by iron. Even in earlier periods, some iron can be found in combination with the manganese used for the colorant.

Additional colorants have been added to manganese colored faience to produce a darker color, similar to what has been observed in some black glasses. Copper was found in the glaze of two black beads from Abydos in concentrations comparable to blue faience colored with copper (Tite et al. 2007b). In that study, the authors concluded that the concentrations of copper oxide in the glaze, which were 9.20% and 14.09%, did not contribute to the color of the faience. Two beads from Lisht which appeared black on the surface were found to be colored by manganese as well (Lilyquist et al. 1993). Copper oxide was present in the glaze layer of these beads but in concentrations much lower than the Abydos beads, 0.4% and 1.6%. The glaze, which was actually grey-blue in color when viewed in a polished cross-section, was over a body that contained purple glassy phases and black grains. It seems from these examples that the copper was not added to alter the black color but it was included in the raw materials because the same raw materials were used regardless of faience color.

3.2.4 Manufacture of faience

The manufacture of faience occurs in a multi-step process (Vandiver 1983; Nicholson 2007). The first stage involves mixing the raw materials (crushed quartz or sand, alkali, colorant) and forming the object. The raw materials are mixed together and water is added to make a paste. The object is then hand formed or pressed into a mold. The paste can also be built up over a form or core. Many molds for the shaping of

faience objects have been found in the archaeological record. Since the physical remains of this industry have not preserved well in the archaeological record, molds are often some of the only evidence uncovered that signifies the production of faience.

The faience paste is thixotropic and can be difficult to work with (Vandiver 1983; Nicholson 2007). It does not hold its form well if too wet, and will crack if too dry, especially when pressed into a mold. There has been some speculation as to whether another material was incorporated to improve the working properties of the past and increase plasticity or act as a binder. Clay has been suggested and experiments have found that the addition of up to 1-3% clay improved not only the working properties but how well the paste took the impression within a mold (Nicholson 2007, 135). The addition of clay has also been used to explain the elevated alumina seen in some faience objects. However, no clear evidence for the addition of clay has been found in archaeological faience objects analyzed. The possible addition of gum as a binder to aid in working the paste was reported in some faience studies on pieces from Iran (Nicholson 2007) and in experimental work (Vandiver 1983). This binder though does not work well with all glazing methods and again there is no evidence for its addition in early faience.

The next stage of faience production involved glazing the faience object. The methods for glazing will be described in detail in the subsequent section. After glazing, the faience objects are fired. The firing temperatures ranged from 800-1000°C, temperatures much lower than what is needed to make a fully fused glass (Vandiver 1983). Because of the lower temperatures used for the production of faience, they vitreous materials could be made in smaller kilns rather than furnaces (Nicholson 2007). This allowed for more localized and smaller scale production.

3.2.4.1 Glazing methods

There are three methods used for the glazing of faience objects: efflorescence, application, and cementation (Vandiver 1983). Efflorescence is referred to as a "self glazing technique", where alkaline salts that are mixed into the body of the faience, such as sodium carbonate, move to the surface during drying and effloresce. A white salt film is formed which reacts with the lime, quartz and copper oxide in the body when fired to form the glaze. In application, a slurry of glazing material is applied to the surface of the formed faience object. The slurry can be brushed on, poured over the object, or the object can be dipped in it. Cementation is also a self-glazing technique where the dried faience body is placed in a vessel with glazing powder, which when heated melts and fuses with the object to form the glaze.

The method of glazing influences the way the glaze layer forms, the appearance of the interaction layer between the glaze and core, the amount of interstitial glass within the core, and the composition of all the layers and phases formed (Vandiver 1983; Tite and Bimson 1986; Vandiver 2008). Examination and analysis of a section through a faience object can allow for the identification of physical characteristics or compositional ones that correspond to specific glazing methods.

Faience objects glazed using the efflorescence method produce layers that are not necessarily well defined (Tite et al. 2007a). The glaze and the interaction layer tend to be thick, but the thickness of these layers can vary depending on drying time, firing time, or how the objects are positioned during drying (Vandiver 1983). The interaction layer merges into the core and there is no clear delineation between these two layers. In efflorescence, there is a large amount of the glazing mixture still within the core. This is what forms the interstitial glass that holds the quartz grains together (Tite and Bimson 1986).

Analyses of the layers within objects glazed using efflorescence showed a difference in the alkali composition across the section. The concentration of soda increases from the core to the glaze, whereas components such as calcium carbonate and magnesium carbonate are more abundant in the core (Kaczmarczyk and Vandiver 2008; Zacharias and Palamara 2016). The sodium carbonate in the raw materials is preferentially precipitated onto the surface when drying (Tite et al. 2007b). This variability in the raw

material concentrations is also observed with the colorants. Copper colored faience objects have a higher copper content in the body than in the glaze. The copper is not as soluble and does to precipitate onto the surface readily.

There are some physical characteristics that could also help identify glazing by efflorescence. In areas where the object was in contact with a surface, for example on a tray or stand when drying, efflorescence would not occur. Therefore, no glaze would form there (Vandiver 1983). Often objects made via efflorescence have no glaze on the underside.

The cementation method creates distinct layers between the glaze, interaction layer, and the body. The glaze is fairly even across the surface although there the glaze located at the bottom of the object can be thicker (Vandiver 1983). In section, the glaze layer appears quite thin (Tite and Bimson 1986). Some interstitial glass forms just below the interaction layer, but does not extend farther into the core. There is also variability seen in the composition of the layers. A decrease in alkali and copper oxide concentrations is observed from the glazed surface to the core (Tite et al. 2007b). This is likely because the glazing material is in direct contact with the surface during firing. Objects glazed using cementation do not show any drying or firing marks, and the glaze is visible over the entire surface. The cementation method has been described as being one that would allow for the glazing of many small objects at once and would be ideal for making a large number of beads (Vandiver 2008).

In the case of the application method, there are some characteristics that can be diagnostic for this glazing method, but they are not as clear as with efflorescence and cementation (Vandiver 1983). Some of the physical signs of glaze application include drips along the surface. The glaze can appear uneven because it can flow or run along the surface. The layers produced are not very distinct and the interaction layer can be quite thick (Tite and Bimson 1986). Their appearance can change based on firing conditions and composition. Under some conditions for example, a distinct glaze and core boundary can form (Vandiver 1983). There is very little interstitial glass formed with this glazing method (Tite and Bimson 1986). Most of the glassy phases are found mainly at the interface between the interaction layer and the core. Like with the cementation method, there is a decrease in alkali and copper oxide from the glaze layer to the core.

Although some of the characteristics described above that help to characterize glazing methods, visually determining which one was used is not always so clear. Factors like drying time and speed, firing temperatures, the use of multiple glazing techniques, and the condition of the faience object may impact the appearance and make visual identification of the glazing method difficult (Vandiver 1983; Vandiver 2008). In the application method, for example, if the object is fired at a low temperature (below 900°C) or if the alkali content is low (around 1-5%) a sharp boundary between the glaze and core is produced (Vandiver 1983). The core is friable because little interstitial glass has formed. However, if the firing temperature is increased, even to just 950°C, or more alkali is added, the microstructure can change (Vandiver 1983; Tite and Bimson 1986). More interstitial glass will form and the boundaries between the layers will not be very distinct. The interaction layer becomes thicker and the core much harder. This example points to the importance of keeping in mind all the factors that can influence the microstructure even if the same glazing method is used across different objects, when trying to visually identify how a faience object was made.

3.2.5 Faience variants

The color of the body of a faience object, and in some cases the glaze, was used to create a typology that is still used today to describe different types, or variants, of faience (Lucas and Harris 1962; Vandiver 1983). Seven categories were established, ordinary faience and Variants A-F. Five of those types are described below, ordinary faience and variants A, B, D, and E, since they are related to some of the beads studied. The variants were created based on the color of the faience and not necessarily related to the production method. There may be, however, some links between the structure of the body and the glaze that could give some clues to the possible glazing methods used.

3.2.5.1 Ordinary faience

Ordinary faience refers to objects that have a quartz core with a layer of glaze directly over it (Lucas and Harris 1962; Vandiver 1983). This variant is the most common form of faience found. Any of the glazing methods described above for manufacturing faience can be used to make ordinary faience.

3.2.5.2 Variant A

Variant A is described by Lucas and Harris (1962, 161) as faience with an extra layer, a white quartz layer found between the core and the glaze (Lucas and Harris 1962; Vandiver 1983). The layer varies in thickness and has been found to be about 0.5-2.5mm (Lucas and Harris 1962). The purpose of this extra layer was to improve the color of the glass. This would be particularly important when the body is different color than the glaze and would alter the appearance of the glaze. This could occur for example when sand was used as the quartz source in a copper blue glazed object. The application of white quartz layer over the core would prevent iron and other impurities in the core from migrating to the surface and altering the glaze color (Vandiver 1983). The white layer would also enhance the blue color. The white quartz layer would be applied over the core once formed and then undergo one of the glazing methods described above. This faience variant has been found to be more common in Egyptian faience than Near Eastern objects and could suggest a place of origin when examining beads made using this technique (Nicholson and Peltenburg 2000).

3.2.5.3 Variant B

Variant B refers to black colored faience which Lucas and Harris (1962, 162) describe as not being very common. In this type of faience, the core can be white, dark gray or brown. As described in the previous section on colorants, black faience can be made using iron or manganese.

3.2.5.4 Variant D

The faience described as Variant D has a core that is blue or green in color and has a “hard body” (Lucas and Harris 1962, 163). The glaze and body are usually the same color, but the body can appear a bit lighter. In order to achieve this, the glazing material was added into the core material during the mixing of the raw materials. The addition of the glazing material in the core, and the harder body due to an increase in the amount of interstitial glass, could suggest the use of the efflorescence glazing method. The hard or dense faience bodies could be formed through over firing, and therefore other glazing methods could have also been used (Vandiver 1983). In some cases cobalt colored Variant D faience has been found with cobalt core made with added glazing mixture, but the glaze contained both copper and cobalt (Kaczmarczyk and Vandiver 2008). In these cases, the object would have been glazed using the application or cementation method since no copper was found in the core.

3.2.5.5 Variant E

Variant E, also called “glassy faience”, has a fairly homogenous microstructure with no clear distinction between the core and the glaze (Lucas and Harris, 1962). Lucas and Harris stated glassy faience as being a variant of Variant D and was not considered faience (1962, 164). It has been described as being a material somewhere between faience and glass (Vandiver 2008, 55). Glassy faience contains much more glass within the core than faience does. It has a fine structure with unreacted quartz, wollastonite, and other phases similar to faience made with ground glass (Tite 1987). This faience tends to have a slightly higher alkali content (6-9% of soda and potash) as opposed to other variants of faience where it is lower (2-4%) (Kaczmarczyk and Vandiver 2008). The silica content in Variant E is lower than that found in ordinary faience and Variant D but higher than what is found in glass (Lucas and Harris 1962). Kaczmarczyk and Vandiver (2008) suggest that the bodies were formed by combining quartz with a prefritted mixture of silica, alkali, lime and a colorant. A higher concentration of interstitial glass in the body generally points to the use of the efflorescence method. In the case of glassy faience, since a glaze layer is not present, this points to the lack of any efflorescence taking place after the objects were formed (Kaczmarczyk and Vandiver 2008).

There is some debate as to whether this variant is actually a different type of faience (Kaczmarczyk and Vandiver 2008) or whether it is just a form of Variant D faience representing a "technical continuum" (Tite 1987, 33). Vandiver (2008, 55) argue that based on the lack of glaze, the higher alkali content, and the higher ratio of glass particles to quartz in the body, Egyptian glassy faience as a distinct variant.

3.2.6 Mycenaean faience

In Chapter 2, there was some discussion of the manufacture of faience beads in the Aegean, with evidence for faience production on Crete and the Greek mainland. Faience produced at Mycenaean sites seems to have a unique composition. The majority of these faience objects consist of a blue-gray core with a dark blue glaze (Panagiotaki 2008). The glaze layer does not appear to be distinct and there is no identifiable interaction layer between the glaze and the body (Maniatis et al. 2008). The body is composed of quartz grains in a continuous layer of a colored glassy matrix.

This lack of glaze, high proportion of glassy phases within the matrix, and the homogenous microstructure indicates that Mycenaean faience would be considered Variant E or "glassy faience". However, there does not seem to be a consensus on whether this is the case. Some have argued that Mycenaean faience is just a form of Variant D with a higher quantity of glazing mixture added to the quartz body making it distinct from Egyptian Variant E glassy faience (Vandiver 2008; Maniatis et al. 2008). It seems that the factor distinguishing the two variants in some of the literature is the presence of glaze or a glaze-body interaction layer, which sometimes is not so apparent due to poor preservation (Angelini 2008; Maniatis et al. 2008, 122).

Two types of faience have been found within Mycenaean contexts and differ based on their compositions. The first, Group A, is similar to Egyptian cobalt faience. Analysis of Mycenaean faience beads from this group tend to have been made using soda-rich plant ash (Tite et al. 2005; Maniatis et al. 2008; Panagiotaki 2008). The cobalt used comes from Egypt's Western Desert and contains the transition element concentrations expected for this cobalt source (high alumina, nickel, zinc, and manganese). These faience objects are thought to have been Egyptian imports, which have been found as early as the 3rd millennium BC on Crete and 2nd millennium BC on the Mycenaean mainland (Maniatis et al. 2008).

Group B Mycenaean faience has a very distinct composition. It was made using a different cobalt source and possibly a different alkali. This type of faience is characterized by an alkali that is much higher in soda than what is typically found in plant ash faience (Maniatis et al. 2008). The concentrations of alumina, manganese, and zinc are low, but iron and nickel are high. This does not fit the transition element makeup observed in cobaltiferous alum from the Western Desert. Faience manufactured with this cobalt colorant and alkali composition has been have been identified at Mycenaean sites in the Mesara plain, Psara, Thebes, and Elateia (Maniatis et al. 2008; Tite et al 2005). High concentrations of copper, lead, and antimony were also detected in this faience type. The copper is thought to have been added separately and was not part of the cobalt source. It has been suggested that the lead and antimony may be related to the cobalt source used (Maniatis et al. 2008) though it is possible that it could entered the raw materials with the copper (Tite et al. 2005).

Determining the cobalt source of Group B faience has been difficult since there has not been extensive analysis of cobalt sources located outside of Egypt. Two faience beads of a similar composition to those in the Group B type were found at the site of Poviglio in northern Italy (Santopadre and Verità 2000; Angelini et al. 2005). These beads differed from other faience beads found in Italy due to the elevated levels of iron, nickel, lead, and antimony present. They are thought to be of Aegean origin (Angelini et al. 2005). A low nickel and iron cobalt source has been identified in Greece at Laurion and Larymna and could have provided the colorant if Group B beads were made in the Aegean (Tite et al. 2005; Maniatis et al. 2008).

The source of the alkali used for the Group B faience is also unclear. Although soda-rich plant ash was used to make faience, the ratios of soda to potash (Na_2O/K_2O) and soda to magnesia (Na_2O/MgO) is greater than

those seen in objects of Egyptian origin and closely resembles the ratios seen in Roman glass (Maniatis et al. 2008). Natron has been suggested as the source of alkali for this faience type to explain the different alkali composition. This alkali, however, was not used in faience or glass production until the 1st millennium BC in Egypt or the Near East. If Group B faience was an Aegean technological innovation, natron could have been obtained from Lake Pikrolimni in northern Greece (Tite et al. 2005; Maniatis et al. 2008). Despite there being this source of natron, there is no evidence that it was known before the Roman period (Dotsika et al. 2009) or used to make glass. Additional analysis of Mycenaean Group B faience and possible sources of the alkali are needed in order to better understand how and where these vitreous materials were made.

4 MATERIALS AND ANALYTICAL METHODS

4.1 INTRODUCTION

Several examination and analytical techniques were used to characterize the beads to identify their composition and mineral colorants, to source the raw materials and identify primary production areas, and to understand the types of deterioration undergone during burial (Appendix A.1). The techniques used on each sample set was dependent on permissions granted for sampling and testing and access to analytical equipment.

4.2 MICROSCOPY

All objects and samples studied were examined using a stereo microscope (approximately 7-45x magnification). Photomicrographs were taken of the vitreous artifacts and samples using various digital means. The equipment used is outlined below.

- **Ancient Methone:** Photomicrographs of the beads were taken in the storage room of the KZ Ephorate of Pieria using a Dino-Lite USB microscope (10-200x magnification) belonging to the Ancient Methone Archaeological Project.
- **Kefalonia:** Photomicrographs of the beads were taken at the Archaeological Museum of Argostoli using an iScope 2.0 USB microscope (10x and 50x magnification) belonging to the Laboratory of Archaeometry, University of Peloponnese, Kalamata. Photomicrographs of the samples taken from the beads were taken using a Keyence VHX-1000 digital microscope (50x-200x magnification) at the Molecular and Nano Archaeology (MNA) Laboratory, Department of Material Science and Engineering, UCLA.
- **Lofkënd:** Photomicrographs of the beads were taken on site on the Lofkënd Archaeological Project using a Nikon D90 DSLR. Photomicrographs of the samples taken were done using the Nikon DSLR as well as the Keyence VHX-1000 at the MNA laboratory.

4.3 PORTABLE X-RAY FLUORESCENCE (PXRF) SPECTROMETRY

Portable x-ray fluorescence (pXRF) spectrometry was used to analyze all the vitreous beads in order to provide an initial characterization of the bulk composition. The analysis was qualitative and the presence or absence of elements was used primarily to determine the general type of glass (plant ash versus natron versus mixed alkali) and to identify mineral colorants.

4.3.1 Ancient Methone

Thirty-four beads—faience and glass—were analyzed with a Bruker Tracer SD-III pXRF spectrometer (rhodium x-ray tube with palladium slits) belonging to the UCLA/Getty Conservation Program, Cotsen Institute of Archaeology, UCLA. The analysis was conducted on site within the storage rooms of the KZ Ephorate of Pieria. An 8mm spot was analyzed on each bead. The beads were analyzed using two acquisition parameters. For the detection of higher Z elements, the beads were analyzed at 40 kiloVolts (kV) and 11 microAmps (μA) for 180 seconds in air using a Ti (1mm)-Al (12mm) filter. Analysis at 15 kV and 25 μA for 180 seconds under vacuum was used for identifying low to mid-range Z elements. Data were acquired and processed using the S1PXRF software (v. 8.3) by Bruker AXS.

4.3.2 Kefalonia

Forty-five beads—faience and glass—were analyzed with a Bruker Tracer SD-III pXRF spectrometer (rhodium x-ray tube with palladium slits) belonging to the Laboratory of Archaeometry, University of the Peloponnese, Kalamata. An 8mm spot was analyzed on each bead. The beads were analyzed using two acquisition

parameters. For the detection of higher Z elements, the beads were analyzed at 40 kV and 11 µA for 180 seconds in air using a Ti (1mm)-Al (12mm) filter. Analysis at 15 kV and 25 µA for 180 seconds under vacuum was used for identifying low to mid-range Z elements. Data were acquired and processed using the S1PXRF software (v. 8.3) by Bruker AXS. The selection of which beads to analyze were determined by the permit granted for non-destructive analysis of only select beads, as well as time constraints due to the time allotted for this work to take place in the Archaeological Museum of Argostoli.

4.3.3 Lofkënd

Eleven beads–faience and glass–were analyzed with a Bruker III-V pXRF spectrometer (rhodium x-ray tube). The beads were analyzed using three acquisition modes. To obtain an overall picture of the elements present and to include some low, mid and high-Z elements, the beads were analyzed with no filter at 40 kV and 1.6 µA under vacuum. For low Z elements, the instrument was run at 15 kV and 15 µA under vacuum with a Cu filter. For high Z elements, 40 kV and 1.6 µA with a Ti (1mm)-Al (12mm) filter was used. Spectra were acquired for five minutes and interpreted using the program S1PXRF (version 3.8.3) made by Bruker AXS.

4.4 SAMPLING

After the examination and pXRF analysis, beads were selected for sampling in order to conduct quantitative analysis on samples. The vitreous materials were sampled using small hand tools such as a scalpels and needle nose pliers. Permission was only granted for sampling of some vitreous objects from Lofkënd and Kefalonia. The samples that could be taken were determined by the permits granted by Ephorate of Prehistoric and Classical Antiquities of Kefalonia for material from Kefalonia. In the case of Lofkënd, samples were only taken from fragmentary objects. No samples were taken from the ancient Methone vitreous beads due to permission being granted only non-destructive analysis by the Ephorate of Prehistoric and Classical Antiquities of Pieria. Samples were taken from break edges or damaged areas. The only case of intact beads being sampled was a few pieces from Kefalonia.

The polished samples were prepared by first placing them in a one-inch Teflon (PTFE) ring and embedding them in Struers EpoFix resin under vacuum. The mounted samples were ground using aluminum oxide sandpaper and polished using Buehler's Metadi diamond suspensions (six and one micron) on Buehler Mastertex cloths. This work was undertaken in the Conservation Training Laboratory of the UCLA/Getty Conservation Program.

The number of beads sampled is as follows:

- **Kefalonia:** Eighteen glass beads sampled
- **Lofkënd:** Seven glass beads sampled

4.5 ELECTRON PROBE MICROANALYSIS (EPMA)

Electron probe microanalysis (EPMA) was conducted on the mounted samples taken from glass artifacts from Kefalonia and Lofkënd. The purpose of EPMA was to obtain more accurate quantitative data on the bulk composition of the samples, in particular looking at alkali concentrations. A JEOL JXA-8200 Superprobe electron microprobe analyzer with wave dispersive spectroscopy (WDS), located at the Dept. of Earth, Space and Planetary Sciences, UCLA, was used. WDS analysis was performed at an accelerating voltage of 15 kV and a current of 15 nA. Five areas on each sample, with a spot size of about 10 µm, were analyzed and an average weight percent (wt%) concentration for each oxide of interest calculated using geological standards commonly used by UCLA's Dept. of Earth, Space and Planetary Sciences. External glass standards (Corning A, B, C, D and NIST610, 612, 614) were used to check the accuracy of the results (Table 4.1, Appendix A.2). The

standards were analyzed 3 times throughout the EPMA analysis (start, middle, and end of archaeological sample analysis) with 4 areas analyzed on each standard. ZAF correction was applied to all WDS analyses.

Table 4.1. Results of EPMA analysis of glass standards and references with % error reported. The measured values are averages and given as weight % (wt%) oxide. Accepted values for Corning glass references from (Vicenzi et al. 2002). SRM610 and SRM612 reported values taken from (Pearce et al. 1997). SRM614 reported values from (Hollocher and Ruiz 1995).

Standard/Reference	SiO_2	Na_2O	K_2O	MgO	Al_2O_3	CaO	FeO	MnO	TiO_2	P_2O_5	Total
Corning A measured	66.49	13.93	3.02	2.67	0.90	5.19	0.97	1.04	0.84	0.11	95.16
Corning A reported	66.56	14.30	2.87	2.66	1.00	5.03	0.98	1.00	0.79	0.14	
% error	**0.10**	**2.56**	**5.08**	**0.50**	**10.32**	**3.14**	**0.77**	**3.52**	**6.04**	**18.15**	
Corning B measured	61.40	16.45	1.06	1.03	4.12	9.02	0.31	0.24	0.11	0.86	94.60
Corning B reported	61.55	17.00	1.00	1.03	4.36	8.56	0.31	0.82	0.09	0.82	
% error	**0.24**	**3.22**	**5.96**	**0.14**	**5.50**	**5.35**	**0.99**	**70.61**	**18.41**	**5.03**	
Corning C measured	34.99	1.09	3.00	2.48	0.78	5.18	0.32	0.02	1.14	0.11	49.11
Corning C reported	34.87	1.07	2.84	2.76	0.87	5.07	0.31	0.82	0.79	0.14	
% error	**0.35**	**1.74**	**5.48**	**10.01**	**9.89**	**2.20**	**2.45**	**97.98**	**44.87**	**21.37**	
Corning D measured	55.02	1.34	11.89	3.92	5.02	14.71	0.45	0.53	0.44	3.95	97.28
Corning D reported	55.24	1.20	11.30	3.94	5.30	14.80	0.47	0.55	0.38	3.93	
% error	**0.39**	**11.32**	**5.26**	**0.42**	**5.21**	**0.62**	**4.89**	**2.76**	**15.99**	**0.59**	
SRM 610 measured	69.95	12.90	0.07	0.08	1.92	11.48	0.07	0.06	0.10	0.14	96.76
SRM 610 reported	69.98	13.35	0.06	0.07	2.04	11.45	0.06	0.05	0.08	0.12	
% error	**0.04**	**3.42**	**13.42**	**19.62**	**5.68**	**0.23**	**27.23**	**6.48**	**36.67**	**19.86**	
SRM 612 measured	72.05	14.01	0.01	0.02	1.99	11.85	0.02	0.01	0.01	0.07	100.05
SRM 612 reported	71.90	13.98	0.01	0.00	2.11	11.93	0.02	0.01	0.01	0.01	
% error	**0.21**	**0.24**	**21.67**		**5.49**	**0.66**	**9.58**	**34.17**	**23.33**	**618.33**	
SRM 614 measured	72.37	13.96	0.02	0.02	1.98	11.84	0.01	0.01	0.01	0.06	100.27
SRM 614 reported	72.31	13.23	0.01	<0.01	2.32	12.14	0.01	0.02	<0.01	0.01	
% error	**0.08**	**5.52**	**51.67**		**14.75**	**2.48**	**9.17**	**42.08**		**518.33**	

4.6 LASER ABLATION INDUCTIVELY COUPLE MASS SPECTROMETRY (LA-ICP-MS)

Laser ablation inductively coupled plasma mass spectrometry (LA-ICP-MS) was used to quantify trace elements in the glass. The trace elements were used primarily to try to provenance the glass and attempt to determine the origin of the raw materials used such as the alkali and silica sources. For example, when looking at LBA plant ash glasses the elements lanthanum (La), zirconium (Zr), titanium (Ti) and chromium (Cr) (Shortland et al. 2007) differentiate glass made with raw materials from Egypt versus those in the Near East. Egyptian glasses are made from sources higher in Zr, as well as Ti and La (Shortland et al. 2007; Degryse et al. 2010a). Other trace elements can be used to source glass made in later periods as well. The levels of strontium (Sr) and Zr can differentiate silica sources between the Levantine coast and those in Egypt (Henderson 2012). Levantine sands tend to have low levels of Zr (45-73ppm) and high Sr (320-450ppm). Egyptian sands have higher Zr (about 160ppm) and lower Sr (100-200ppm). Finally, trace elements can be used to source mineral colorants such as cobalt (Co) through the identification of associated elements as part of the cobalt source (Shortland et al. 2007).

LA-ICP-MS was conducted on the samples analyzed via EPMA from Kefalonia and Lofkënd. The analyses were conducted at the UC Davis Interdisciplinary Center for Plasma Mass Spectrometry (UCD/ICPMS) using an Agilent 7500ad ICP-MS coupled to a New Wave UP213 laser. The ICP-MS was operated at 1550W forward

power and the frequency quintupled Nd:YAG laser (wavelength = 213 nm), was operated at 0.664 mJ to ablate 80um spots with 13.22 J/cm^2 fluence at a pulse rate of 10Hz. Helium gas was used to transport ablated material to the ICP-MS at 0.9 L/min, where Ar was added as a makeup gas at 1.2L/min. The samples were analyzed in He mode, with He used as the collision/reaction cell (CRC) gas at 2.8 mL/min. The background He/Ar gas signal was subtracted from acquired data. NIST SRM 610, 612, and 614 silicate glasses were analyzed in quintuplicate and used as external calibration standards (Table 4.2, Appendix A.3). Samples and quality control (QC) standards were analyzed in triplicate. NIST SRM 610, 612, and 614 were analyzed initially as QC to verify the calibration. NIST SRMs were also mounted with the samples and were analyzed before and after the samples to monitor instrument drift. Si was used as the internal standard to correct for instrument drift and changes in the ablation efficiency. Silicon values for samples were determined by EPMA.

Table 4.2. LA-ICP-MS data collected from glass standards (SRM 610, 612, 614) and glass references (Corning A, B, C, D) showing % error. The data is given in parts per million (ppm) and the values shown are averages based on three spots analyzed on each sample. Only selected elements are shown. The full results are available in Appendix A.3.

Standard/Reference	Li	B	Cr	Co	Ni	Cu	Zn	Sr	Zr	La
Corning A measured	49.73	600.27	20.34	1389.92	194.23	8605.74	488.67	1000.49	46.23	0.33
Corning A reported	46.00	621.00	7.00	1337.00	157.00	9347.00	353.00	846.00	37.00	---
% error	**8.10**	**3.34**	**190.64**	**3.96**	**23.71**	**7.93**	**38.43**	**18.26**	**24.95**	**---**
Corning B measured	11.66	49.22	63.62	349.75	766.20	19159.79	1930.36	157.29	189.46	0.21
Corning B reported	5.00	62.00	34.00	362.00	786.00	21250.00	1526.00	161.00	185.00	---
% error	**133.22**	**20.61**	**87.10**	**3.38**	**2.52**	**9.84**	**26.50**	**2.30**	**2.41**	**---**
Corning C measured	52.35	578.00	17.17	1458.74	165.90	8328.39	547.00	2412.40	45.28	0.25
Corning C reported	46.00	621.00	7.00	1416.00	157.00	9027.00	418.00	2452.00	37.00	---
% error	**13.80**	**6.92**	**145.25**	**3.02**	**5.67**	**7.74**	**30.86**	**1.61**	**22.37**	**---**
Corning D measured	27.59	266.51	19.04	150.15	400.45	2980.18	963.76	522.60	95.43	0.52
Corning D reported	23.00	311.00	17.00	181.00	393.00	3036.00	803.00	482.00	93.00	---
% error	**19.94**	**14.31**	**11.98**	**17.05**	**1.89**	**1.84**	**20.02**	**8.42**	**2.61**	**---**
SRM 610 measured	472.84	313.00	413.61	414.27	455.87	430.87	485.69	522.42	467.67	451.56
SRM 610 reported	468.00	350.00	408.00	410.00	458.70	441.00	460.00	515.50	448.00	440.00
% error	**1.03**	**10.57**	**1.37**	**1.04**	**0.62**	**2.30**	**5.58**	**1.34**	**4.39**	**2.63**
SRM 612 measured	41.76	2.07	38.72	36.60	41.28	48.72	36.80	77.34	36.40	35.28
SRM 612 reported	40.20	34.30	36.40	35.50	38.80	37.80	39.10	78.40	37.90	36.00
% error	**3.88**	**93.98**	**6.38**	**3.09**	**6.39**	**28.90**	**5.88**	**1.35**	**3.97**	**2.01**
SRM 614 measured	1.88	<LOD	1.31	0.71	1.06	8.62	4.00	44.82	0.82	0.73
SRM 614 reported	1.69	1.49	1.19	0.79	1.10	1.37	2.79	45.80	0.85	0.72
% error	**11.54**	**---**	**9.94**	**9.98**	**3.84**	**529.41**	**43.40**	**2.14**	**2.88**	**0.75**

4.7 ISOTOPIC ANALYSIS

The analysis of radiogenic stable isotopes has often been used for the provenance of artifacts and the sourcing of raw materials used to manufacture artifacts such as metals, stone, and ceramics. The technique has recently been applied to the sourcing of glass raw materials. Since these isotopes are not affected by melting, the sources of the various glass components such as the silica, flux (plant ash or natron) and colorants can be traced to their general geographical region of origin (Degryse et al. 2009). Two of the radiogenic isotopes that have been used in glass provenance studies have been strontium (Sr) and neodymium (Nd) since they can be used to distinguish between sources on the Eastern Mediterranean coast versus Egypt, as well as raw materials that come from the Western Mediterranean and NW Europe (Degryse

et al. 2010b). Sr enters the glass batch via the lime-bearing raw materials. This can include the addition of limestone or can be from shell found in the sand used as the silica source. In plant ash glasses, Sr can be incorporated into the glass batch from the plant ash itself where the plants have absorbed the element from the soil. Nd is introduced from the silica source used (Henderson, et al. 2010).

Egyptian sourced glass has been found to have lower ratios of $^{87}Sr/^{86}Sr$ and $^{143}Nd/^{144}Nd$ isotopes (Degryse et al. 2010a) as compared to Near Eastern sourced glass. In the study of Late Bronze Age glasses, the use of the isotopes has been able to differentiate between two Near Eastern sources of glass, those from Nuzi and those from Tell Brak (Degryse et al. 2010a). Nuzi glasses tend to have low $^{143}Nd/^{144}Nd$ and high $^{87}Sr/^{86}Sr$ ratios. Glass from Tell Brak has high $^{143}Nd/^{144}Nd$ ratios and intermediate $^{87}Sr/^{86}Sr$ ratios.

Due to the sample size requirements and cost of this technique, only eight samples from Kefalonia could be analyzed. $^{87}Sr/^{86}Sr$ and $^{143}Nd/^{144}Nd$ compositions were measured on a Nu Plasma HR (Nu Instruments, Inc.) multiple-collection, double-focusing, plasma-source mass spectrometer (MC-ICP-MS) equipped with fixed faraday detectors (amplified by a 10^{11} Ohm resistors), patented zoom optics and a high-sensitivity nickel cone interface. Samples are first dissolved and purified through a specific ion-exchange resin (Eichrom Technologies, Inc.), in a class 100 clean lab facility (PicoTrace, GmbH) After being reconstituted in ultrapure sub-boiling double-distilled 2% nitric acid, the purified samples are introduced into the Nu Plasma with a desolvating nebulizer system (DSN-100, MkII) with a 0.1mL/min uptake (33 psi with 700mm capillary) quartz MicroMist nebulizer (Glass Expansion, Inc.). Ratios include 50-60 data points and each data point integrates faraday signals for 10 seconds. The calculated data is subjected to 2SE statistics and allows/disallows outliers (~95% confidence). Baselines are measured for 30 seconds by electrostatic analyzer (ESA) deflection. NIST SRM 987 (certified strontium carbonate reference standard) and AMES Nd internal standard were run in parallel. The repeated measurements of the AMES Nd standard gave 143Nd/144Nd = 0.51190 ±0.00001 (2σ). The repeated measurements of the SRM 987 standard gave an average 87Sr/86Sr ratio of 0.710242 ±0.000018 (2σ).

4.8 Scanning Electron Microscopy-Energy Dispersive Spectroscopy (SEM-EDS)

Scanning electron microscopy coupled with energy dispersive spectroscopy (SEM-EDS) was used to both image the beads and samples, as well as obtain general quantitative information on the composition of the vitreous materials. The SEM-EDS analysis was primarily used to study deteriorated areas of the glass and compare those to intact glass. Two SEM-EDS instruments were used for the study.

4.8.1 SEM-EDS Analysis in Greece

SEM-EDS analysis undertaken in Greece was performed using a JEOL JSM-6510LV scanning electron microscope (SEM) coupled with an Oxford Instruments energy dispersive spectrometer (EDS) at the Laboratory of Archaeometry, University of Peloponnese, Kalamata. The analytical data were obtained with INKA software. The bulk analyzes were conducted at high vacuum, 20 kV accelerating voltage and with a count time of 300 sec. Each sample was measured at least five times and the concentrations averaged. All data were normalized to 100%. This instrument was used to analyze beads and samples from Ancient Methone and Lofkënd. Whole beads or bead samples/fragments were placed in the SEM chamber for analysis.

The accuracy and precision of this SEM-EDS setting has been described in detail elsewhere (Palamara et al. 2016). Generally, all the major oxides in glass represent high precision (error < 5%), with the exception of CaO which presents a deviation from the true value of approximately 10-15%. For alkali concentrations lower than 5 wt%, the precision of the analysis decreases significantly. The achieved accuracy of the analysis usually varies, with deviations from the mean value between 5 and 10% for all major oxides

4.8.2 VP-SEM-EDS Analysis at UCLA

Additional SEM-EDS analysis was conducted on the mounted samples from Kefalonia and Lofkënd at the MNA Laboratory at UCLA. A variable pressure (VP) Nova Nano SEM 230 SEM was used for imaging in secondary electron (SE) mode using a low vacuum detector (LVD). Elemental analysis was performed with a Thermo Scientific NORAN™ System 7, X-ray EDS. The spectra were processed using the NSS Spectral Imaging System software from Thermo Scientific, Inc. Three areas on each sample, measuring approximately 200 µm2, were analyzed with an accelerating voltage of 20kV, beam current of 10 nA and working distance of 5mm. Spot analysis was also performed. The concentrations obtained for the weight percent (wt%) of each oxide were averaged and normalized to 100% External glass standards (Corning A, B, C, D and NIST 610, 612) were used to check the accuracy of the EDS analysis (Table 4.3, Appendix A.4). ZAF correction was applied to all VP-SEM-EDS analyses.

Table 4.3. VP-SEM-EDS analysis of glass standards and references with % error reported. The measured values are averages and given as weight % oxide. Accepted values for Corning glass references from (Vicenzi et al. 2002). SRM610 and SRM612 reported values taken from (Pearce et al. 1997).

Standard/Reference	SiO_2	Na_2O	K_2O	MgO	Al_2O_3	CaO	FeO	MnO	TiO_2	P_2O5	CuO	BaO	PbO
Corning A measured	68.40	17.25	2.66	2.13	1.00	5.08	0.76	0.46	0.92	0.03	0.77	0.22	0.14
Corning A reported	66.56	14.30	2.87	2.66	1.00	5.03	0.98	1.00	0.79	0.14	1.17	0.56	0.12
% error	**2.77**	**20.63**	**7.25**	**19.99**	**0.03**	**0.93**	**22.17**	**53.71**	**16.68**	**75.90**	**34.50**	**60.20**	**18.89**
Corning B measured	61.99	16.72	1.17	0.39	3.53	11.34	0.45	0.01	0.10	0.91	1.89	0.00	0.48
Corning B reported	61.55	17.00	1.00	1.03	4.36	8.56	0.31	0.82	0.09	0.82	2.66	0.12	0.61
% error	**0.71**	**1.65**	**16.92**	**62.00**	**18.98**	**32.52**	**45.71**	**98.47**	**8.66**	**11.06**	**28.96**	**100.00**	**21.45**
Corning C measured	32.00	0.84	2.73	2.10	0.82	5.14	0.35	0.00	1.96	0.02	1.53	12.00	40.28
Corning C reported	34.87	1.07	2.84	2.76	0.87	5.07	0.31	0.82	0.79	0.14	1.13	11.40	36.70
% error	**8.23**	**21.59**	**3.72**	**23.82**	**5.36**	**1.35**	**13.29**	**100.00**	**148.23**	**85.64**	**35.08**	**5.28**	**9.77**
Corning D measured	53.98	1.38	12.71	3.03	4.46	17.73	0.43	0.75	0.68	4.14	0.14	0.00	0.18
Corning D reported	55.24	1.20	11.30	3.94	5.30	14.80	0.47	0.55	0.38	3.93	0.38	0.51	0.48
% error	**2.28**	**15.07**	**12.46**	**23.18**	**15.89**	**19.81**	**8.98**	**35.54**	**79.06**	**5.41**	**63.14**	**100.00**	**62.48**
SRM 610 measured	74.71	17.04	0.04	0.00	2.08	5.94	0.01	0.02	0.00	0.08	0.01	0.06	0.00
SRM 610 reported	69.98	13.35	0.06	0.07	2.04	11.45	0.06	0.05	0.08	0.12	0.05	0.05	0.04
% error	**6.77**	**27.63**	**27.82**	**100.00**	**1.95**	**48.16**	**76.79**	**63.77**	**100.00**	**32.48**	**73.84**	**31.98**	**100.00**
SRM 612 measured	69.13	17.18	0.00	0.11	1.75	11.77	0.00	0.02	0.01	0.03	0.02	0.00	0.00
SRM 612 reported	71.90	13.98	0.01	0.00	2.11	11.93	0.02	0.01	0.01	0.01	0.00	0.00	0.00
% error	**3.86**	**22.91**	**100.00**	**100.00**	**17.14**	**1.37**	**100.00**	**100.00**	**30.11**	**150.00**	**234.78**	**100.00**	**100.00**

4.9 X-RAY DIFFRACTION (XRD)

X-ray diffraction (XRD) analysis was used to identify the composition of opaque white glass decoration on four of the beads from Lofkënd. The samples were analyzed using a Rigaku R-Axis Spider X-ray diffractometer located in the lab of the UCLA/Getty Conservation Program. They were mounted on a glass spindle with Apiezon N vacuum grease. XRD spectra were recorded at 50 kV/40 mA using a Cu-Kά target for 900 seconds. The samples rotated 360° during acquisition. XRD data were processed and matched against reference spectra from the International Center for Diffraction Data (ICDD).

4.10 PRINCIPAL COMPONENT ANALYSIS (PCA)

Principal Component Analysis (PCA) was used to identify compositional groups among the various samples analyzed and to look for relationships between the vitreous materials found at each site and published

comparative samples. The EPMA data collected for major and minor compositional oxides was used. The PCA was calculated in R (v. 4.0.0) using the package `vegan' (Oksanen et al. 2017) on scaled variables in a correlation matrix without log-transformation (Baxter and Freestone 2006; Baxter 2009; Everitt and Hothorn 2011). The eigen values explaining the variation for each dataset are given in the chapters and appendices corresponding to each dataset analyzed.

5 VITREOUS MATERIALS FROM NORTHERN GREECE: ANCIENT METHONE

5.1 INTRODUCTION

The site of ancient Methone is located immediately north of the village of Nea Agathoupolis and not far from modern Methone in Pieria, northern Greece (Figure 5.1). The hilltop site sits on the Thermaic Gulf and is located at the delta of several rivers, including the Aliakmon River, which begins near the Albanian border to the west and is the longest river in Greece. The site was discovered in the 1970s by Greek archaeologists, with excavations taking place from 2003-2013 by the KZ Ephorate of Pieria (Morris et al. 2020). There is a long history of occupation at ancient Methone, beginning in the late Neolithic until 354 BC when Philip II destroyed the city (Papadopoulos 2016; Morris et al. 2020). The occupants were moved away from the area and the site was never reoccupied.

The area of the west hill has an acropolis with Late Bronze Age burials (Morris et al., 2020, p. 662). An Early Iron Age settlement (10th-8th c. BC) was built over the cemetery. Workshops from the Archaic period were found above these areas with evidence of metallurgy, bone and ivory working, and pottery production. The east hill also had evidence of industrial activity in a section described as an "agora" with public buildings (Morris et al., 2020, p. 662).

Evidence of long distance trade at ancient Methone is clear from Early Iron Age pottery found within *hypogeion* (basement) found on the east hill next to the area of the agora (Papadopoulos 2016; Kotsonas et al. 2017; Morris et al. 2020). Fragments of Phoenician amphorae and vessels from all over the Eastern Mediterranean were placed within this 11.8 m deep storage area. Geomorphological and archaeological evidence have identified a harbor at the site (Morris et al. 2020). It is here where these traded items could enter Greece from the north Aegean and then be transported via land or rivers to other parts of Greece and beyond. The harbor was still in use during the Classical period. Epigraphic evidence indicates that ancient Methone was a major provider of timber as well as pitch (Morris et al. 2020).

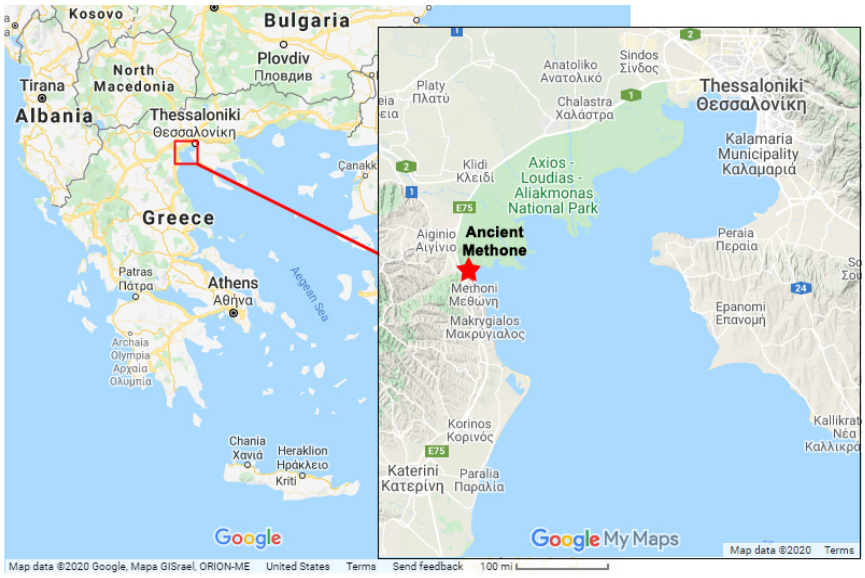

Figure 5.1. Location of ancient Methone (Maps taken from Google. Larger map: Map data ©2020 Google, Mapa GISrael, ORION-ME; Detail: Map data ©2020)

5.2 DESCRIPTION OF THE VITREOUS BEADS

5.2.1 Burial context

Between 2005-2011, archaeologists from the Ephorate of Antiquities in Pieria discovered a Late Bronze Age cemetery on the site's west hill. The graves were accelerator mass spectrometry (AMS) radiocarbon dated to the 13th c. BC.

Vitreous beads, made of faience and glass, were found in four of the burials uncovered (Table 5.1, Appendix B.1). These beads varied in the number of grave goods and the types of goods, as well as their state of preservation. Two of the graves—Tomb 245/1 and 245/3—only had one bead each, all made of glass. Tomb 245/16 had two beads. The remainder of the vitreous beads came from one grave—Tomb 245/5—where glass and faience beads were found around the head, body, and feet of the interred individual. Beads were found intact but were quite deteriorated. In Tomb 245/5, many of the beads were fragmentary. This made it difficult to determine the total number of vitreous beads discovered. An attempt was made to determine which bead fragments joined to try to get an accurate count, but in some cases due to the level of corrosion, this was not possible. The number of vitreous artifacts was roughly estimated to be 67 across the four tombs (glass=47; faience=20), though this could be an under or overestimation.

Table 5.1. Description of the tombs with vitreous beads (Papadopoulos et al. 2014a).

Tomb	Burial Type	Grave Goods
245/1	Inhumation; Adolescent (14-15 yo male?); contracted position	Ceramic vessels (hand and wheelmade) Cu alloy pin Cu alloy spiral coil beads Cu alloy spherical beads Bone bead Glass bead (MEθ 884β)
245/3	Inhumation; Child (5-6 yo)	Ceramic vessels (wheelmade) Bone pins Glass bead (MEθ 5318)
245/5	Cist grave with wooden sarcophagus; Adult, female? (<16-19 yo); supine position; infant bones in fill	Ceramic vessels (wheelmade) Cu alloy pins Cu alloy dagger Cu alloy ring Clay beads or spindle whorls Amber beads Carnelian beads Bone beads Cu alloy beads Faience beads found at skull (MEθ 889) and feet (MEθ 4164) Glass beads found at skull (MEθ 889), chest (MEθ 890) and feet (MEθ 4164)
245/16	Cist grave probably with wooden coffin; Adult, male (17-20 yo); infant (neonate)	Ceramic vessels (wheelmade) Cu alloy blade fragment Cu alloy spiral coil bead Cu alloy spherical beads Glass bead, ellipsoidal (MEθ 885α) Glass bead, spherical (MEθ 885β)

5.2.2 Glass beads

All of the glass beads at ancient Methone can be classified as simple beads (Table 5.2). Forty-six of the glass beads are short, globular beads (Beck 1928). The majority are oblate in section (rounded ends, Type I.B.1.a) (Beck 1928, 5, pl. II-III). Some are more barrel-like (flat at the perforations, Type I.B.1.b) (Beck 1928, 5, pl. II-III). One glass bead is ellipsoidal and corresponds to long beads that have a circular perimeter (Type I.D.1.a) (Beck 1928, 5, pl. II-III). All the vitreous beads have a single conical perforation (Type III) (Beck 1928, 5, pl. IV)

and were likely made using a tapered mandrel (Küçükerman 1988). The appearances of fine lines running across the beads, which are enhanced by corrosion, indicate the beads were formed by winding on a mandrel (Küçükerman 1988).

Although Mycenaean pottery and copper alloy objects were found in several of the Late Bronze Age graves (Table 5.1), including those that contained glass and faience beads, no Mycenaean relief beads were found. Relief beads were traded throughout the Aegean but few examples have been found outside the area considered the Mycenaean world (Eder 2015). In Greece, relief beads have been found only as far north as the area of Mount Olympus. Although ancient Methone is only about 60km north of Agios Demetrios, a site located on the northern slopes of Mt. Olympus where relief beads were found in cist tombs, they did not seem to travel beyond that area to be used in burial contexts. This may mark the northern border of the trade of these exclusively Mycenaean artifacts and may indicate a distinct social meaning or value placed on this bead type that restricted its movement farther north (Eder 2009) but did not restrict the movement of other object types.

5.2.3 Faience beads

Fourteen of the faience beads are a mix of disc-shaped bead types, where some have concave sides ("circular short barrel", Type I.A.1.b) and others have straighter sides ("circular short cylinder", Type I.A.2.b) (Table 5.2) (Beck 1928, 5, pl. II,III). The shapes of most of the beads are extremely common geographically, and therefore, the form or type is not indicative of a particular location for its production (Nightingale 2018).

Table 5.2. Vitreous beads found at ancient Methone

Tomb No.	Material	Quantity	Shape	Beck Type
245/1	glass	1	circular short spherical bead	I.B.1.a
245/3	glass	1	circular short spherical bead	I.B.1.a
245/5	faience	5	circular short barrel disc	I.A.1.b
245/5	faience	9	circular short cylinder disc	I.A.2.b
245/5	faience	6	fluted ("cogwheel") bead	XXIII.A.2.A
245/5	glass	31	circular short spherical bead	I.B.1.a
245/5	glass	12	circular short barrel bead	I.B.1.b
245/16	glass	1	circular long ellipsoidal bead	I.D.1.a
245/16	glass	1	circular short spherical bead	I.B.1.a

Six of the faience beads are shaped like a cogwheel and are collared, with a raised ridge around the perforation (Figure 5.2). The beads have either six or seven cogs, or ribs, which vary in shape and size. The flute depth and width, as well as the collar shape, varies. On some beads, the ribs are squared, where others have rounded or even slightly pointed ones. The spacing between the ribs is not consistent. These irregularities make it clear that the beads were hand formed and not made in a mold. Cogwheel shaped bead have been described as "notched and gadrooned beads and pendants" (Group XXIII), and Beck (1928, 25) further describes these beads as crenellated (XXIII.A.1.b). The cogwheel shaped beads found at ancient Methone are more spherical and concave in section sharing some similarities with fluted beads (XXIII.A.2.A) (Beck 1928, 11; Ingram 2005; Ingram 2014).

Cogwheel shaped beads have been found at other Bronze Age sites in Egypt, the Near East and the Greek mainland (Frankfort and Pendlebury 1933; Blegen and Pierce Blegen 1937; Oates et al. 1997; Ingram 2005; Pieniążek 2012; Ingram 2014). The shapes of these beads vary. Some are made as flat discs and others appear more convex and closer in length to a short or standard bead. In some publications beads similar to those found at ancient Methone have been described as melon beads, fluted, notched or star-shaped (Petrie 1894; Wainwright 1920; Evans 1964; Nightingale 1996; Ingram 2005; Panagiotaki 2008). Transport of this bead-shape across the Mediterranean is evident from a large group of faience cogwheel shaped beads, about 800, found in the remains of the Uluburun shipwreck (Ingram 2005; Ingram 2014). The majority of the beads were plain cogwheel shaped beads with only 17 having collars. They had six flutes and are handmade.

With finds of similar shaped beads—made of both glass and faience—and with such a broad geographic distribution, the origin of the ancient Methone beads cannot be determined based on its typology especially given that the Uluburun shipwreck was carrying vitreous cargo from Egypt, the Near East and the Aegean, both as finished objects and ingots (Ingram 2005; Jackson and Nicholson 2010; Ingram 2014, 227, fig. 1).

Figure 5.2. Faience cogwheel bead (MEΘ 889-1) which illustrates the irregular shape of the cogs, or ribs, as well as the blue gray color of the glaze.

5.2.4 Condition of the beads

Almost all the glass beads found at ancient Methone are in poor condition and show extensive deterioration. Only two glass beads show little to no surface corrosion. The remaining beads are all covered with an opaque layer of glass in shades of white, tan and yellow, as well as darkened areas due to staining or deposits from the soil (Figure 5.3). Several of the beads were completely corroded while others have some glass preserved below the opaque surface layer. In areas where intact glass remained, pitting and slight iridescence is visible on the surface.

Figure 5.3. Glass bead (MEΘ 889-4) showing the typical deterioration observed on most of the ancient Methone glass beads. The arrow points to glass preserved below the opaque corrosion layer.

The condition of the beads made determining the original color of the glass difficult. The glass colors identified in the beads examined were based on microscopic examination using a fiber optic lamp held at different angles over the bead. It is possible that many of these glasses were originally the same color, but only appear slightly different due to differences in condition or lighting that affect the color seen at the time of examination.

The faience beads were also in poor condition. The cogwheel-shaped beads were better preserved with areas of the glazed surface intact (Figure 5.2). Some dark spots or stains from the burial environment were visible, but otherwise they appeared stable. The disc shaped faience beads varied in condition (Figure 5.4-5.8). Most of the faience disc beads had lost their surface glaze and the underlying quartz core was visible. Only a few fragments were in good condition with the glazed surface well preserved. A few discs looked

white but when examined under magnification, areas of blue glaze remained on some of the beads indicating they were originally blue.

5.3 RESULTS AND DISCUSSION

Permission was not given to sample the vitreous beads and therefore all the analysis undertaken had to be non-invasive. This limited the compositional information that could be obtained from the bead. The majority of the information on colorants and manufacturing technology was obtained through microscopic examination and qualitative pXRF analysis. Twenty beads underwent surface analysis using SEM-EDS and were able to provide some quantitative information on the glass and faience beads (Appendix B.3).

5.3.1 Faience beads

5.3.1.1 Disc beads

5.3.1.1.1 Copper blue

PXRF analysis of the blue faience, which ranged in color from light blue to blue-green showed that they were colored using copper, a common mineral colorant used for faience (Table 5.3). Tin and lead were present in all the blue discs analyzed. This indicates the source of copper used as the colorant was not a copper mineral but bronze scrap (Kaczmarczyk and Vandiver 2008). Bronze was scrap was used to color faience in both Egypt and the Near East (Bouquillon et al. 2008), and therefore, the detection of tin and lead in the copper colored faience could not be used to determine the origin of the beads.

Table 5.3. Results of qualitative pXRF analysis

Bead No.	Tomb	Elements Detected
Faience		
Blue[1]		
889-9	245/5	Mg, Al, Si, S, K, Ca, Ti, Cr, Mn, Fe, Ni, Cu, Zn, Pb, Sr, Sn
4164-2	245/5	Al, Si, P, S, K, Ca, Ti, Fe, Ni, Cu, Zn, Pb, Rb, Sr, Zr, Sn
4164-3	245/5	Al, Si, P, S, K, Ca, Ti, Cr, Mn, Fe, Ni, Cu, Zn, Pb, Sr, Zr, Sn
4164-5	245/5	Al, Si, P, S, K, Ca, Ti, Cr, Mn, Fe, Ni Cu, Zn, Pb, Rb, Sr, Zr, Sn
4164-6	245/5	Al, Si, P, S, K, Ca, Ti, Cr, Mn, Fe, Ni, Cu, Zn, Pb, Rb, Sr, Zr, Sn
4164-9	245/5	Al, Si, P, S, K, Ca, Ti, Cr, Mn, Fe, Cu, Zn, Pb, Rb, Sr, Zr, Sn
4164-10	245/5	Mg, Al, Si, P, S, K, Ca, Ti, Cr, Mn, Fe, Ni, Cu, Zn, Pb, Rb, Sr, Zr, Sn
4164-11	245/5	Al, Si, S, K, Ca, Ti, Cr, Mn, Fe, Ni, Cu, Zn, Pb, Rb, Sr, Zr, Sn
4164-12	245/5	Al, Si, P, S, K, Ca, Ti, Mn, Fe, Ni, Cu, Zn, Pb, Sr, Zr, Sn
Blue-gray		
889-1	245/5	Al, Si, P, S, K, Ca, Ti, Cr, Mn, Fe, Co, Ni, Cu, Zn, Pb, Rb, Sr, Zr, Sn
889-10	245/5	Al, Si, P, S, K, Ca, Ti, Cr, Mn, Fe, Co, Ni, Cu, Zn, Pb, Rb, Sr, Zr, Sn
Black		
4164-4	245/5	Al, Si, P, S, K, Ca, Ti, Cr, Mn, Fe, Co, Ni, Cu, Zn, Pb, Rb, Sr, Zr
4164-8	245/5	Al, Si, P, S, K, Ca, Ti, Cr, Mn, Fe, Co, Ni, Cu, Zn, Pb, Rb, Sr, Zr, Sn
Glass		
Blue		
5318-1	245/3	Al, Si, P, S, K, Ca, Ti, Cr, Mn, Fe, Cu, As, Pb, Sn?, Sr
Yellow		
889-4	245/5	Al, Si, P, S, K, Ca, Ti, Cr, Mn, Fe, Ni, Cu, Zn, Pb, Rb, Sr, Sn?[2], Sb
889-5	245/5	Al, Si, P, K, Ca, Ti, Cr, Mn, Fe, Ni, Cu, Pb, Zn, Rb, Sr, Sn?, Sb
889-7	245/5	Al, Si, P, K, Ca, Ti, Cr, Mn, Fe, Ni, Cu, Zn, Pb, Rb, Sr, Sn? Sb

889-11	245/5	Al, Si, S, K, Ca, Ti, Cr, Mn, Fe, Ni, Cu, Zn, Pb, Rb, Sr, Zr, Sn, Sb
890-5	245/5	Al, Si, P, S, K, Ca, Ti, Cr, Mn, Fe, Ni, Cu, Zn, Pb, Rb, Sr, Sn?, Sb
Yellow-green		
889-3	245/5	Al, Si, P, S, K, Ca, Ti, Cr, Mn, Fe, Ni, Cu, Zn, Pb, Sr, Sn?, Sb
889-6	245/5	Mg, Al, Si, P, S, K, Ca, Ti, Cr, Mn, Fe, Ni, Cu, Pb, Zn, Rb, Sr, Sn?, Sb
890-1	245/5	Mg, Al, Si, P, S, K, Ca, Ti, Cr, Mn, Fe, Ni, Cu, Zn, Pb, Rb, Sr, Sn, Sb
4164-1	245/5	Al, Si, P, S, K, Ca, Ti, Cr, Mn, Fe, Ni, Cu, Zn, Pb, Rb, Sr, Zr, Sn, Sb
Green		
889-2	245/5	Mg, Al, Si, P, S, K, Ca, Ti, Cr, Mn, Fe, Ni, Cu, Zn, Pb, Rb, Sr, Zr, Sn, Sb
890-3	245/5	Mg, Al, Si, P, S, K, ,Ca, Ti, Cr, Mn, Fe, Ni, Cu, Zn, Pb, Sr, Sn, Sb
890-4	245/5	Al, Si, P, S, K, Ca, Ti, Cr, Mn, Fe, Ni, Cu, Zn, Pb, Rb, Sr, Sn?, Sb
Dark green		
884b-1	245/1	Mg, Al, Si, P, S, K, Ca, Ti, Cr, Mn, Fe, Ni, Cu, Zn, Pb, Sr
Opaque black/dark gray		
889-8	245/5	Al, Si, S, K, Ca, Ti, Mn, Fe, Ni, Cu, Zn, Pb, Sr
890-2	245/5	Al, Si, P, S, K, Ca, Ti, Mn, Fe, Ni, Cu, Zn, Pb, Sr
Opaque white/yellow		
885α-1	245/16	Al, Si, P, S, K, Ca, Ti, Cr, Mn, Fe, Co, Ni, Cu, Zn, Pb, Rb, Sr, Sn?, Sb
885β-2	245/16	Al Si, S, K, Ca, Ti, Cr, Mn, Fe, Ni, Cu, Pb, Sr, Zr, Sn
Opaque white/yellow and Cu alloy		
885β-1	245/16	Al, Si, P, S, K, Ca, Ti, Cr, Mn, Fe, Ni, Cu, Zn, Pb, Sr, Zr, Sn

[1]Color given is for intact glass or faience glaze observed. If no intact glass or glaze is visible general color of corroded glass or faience core is given.
[2]The peaks marked with a "?" indicate that the peak height is very small and only slightly above the background. It is unclear if the element is present.

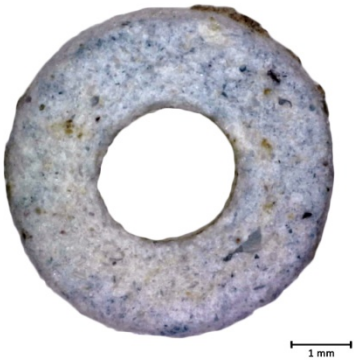

Figure 5.4. Faience disc bead (ΜΕΘ 4164-2) showing the level of deterioration of the surface and the loss of the glaze layer.

Most of the blue faience discs had lost their glazed surface revealing the quartz-rich core. This level of deterioration made determining the original composition of the glaze difficult using visual examination. For most of the beads, only small patches of glaze survived, and burial deposits and stains were visible. Some surfaces appeared fairly white while others contained areas colored blue. From microscopic examination, it was difficult to determine which layer was exposed. For example, the surface of bead ΜΕΘ 4164-2 (Figure 5.4) showed areas of what appeared to be blue interstitial glass. It is possible that this interstitial glass is in the core or within the interaction layer. If this interstitial glass is in the core, then it may indicate efflorescence was used as the glazing method.

Examination of the broken ends of some faience beads reveals that different manufacturing methods were used to produce them. One of the circular short barrel discs was composed of a tan core with a thin white layer above it and covered with blue-green glaze (Figure 5.5). The appearance of a white quartz layer

between the core and the glass corresponds to Variant A faience (Lucas and Harris, 1962). The color of the core suggests the use of sand as the quartz source rather than ground quartz pebbles that would be whiter in color due to the lack of impurities.

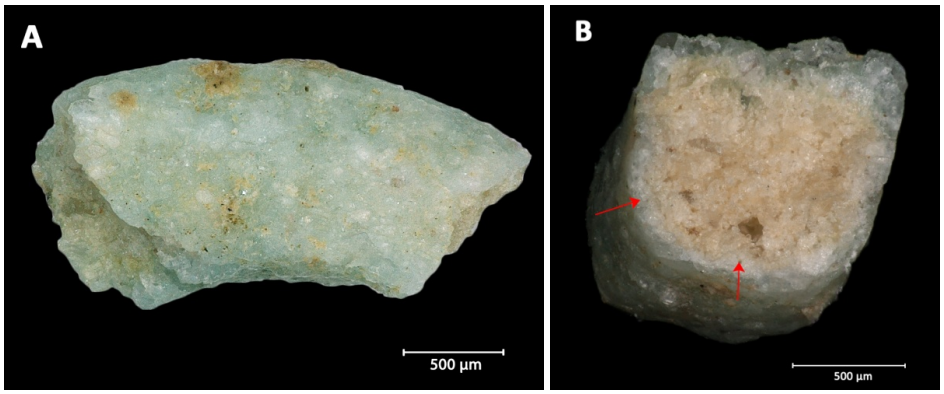

Figure 5.5. Fragment of faience disc bead (MEΘ 4164-12) from Tomb 245/5. (A) Photomicrograph showing surface of the fragment B) Photomicrograph of the break edge showing it has a tan quartz core. There appears to be a white quartz layer between the core and the glaze (red arrows) seen in Variant A faience.

Given the small size of the beads and the deterioration of the surface glaze, the identification of surface characteristics typical of the certain glazing methods was not possible. Looking at the section of the beads may provide some clues. It is important to note, however, that the same glazing method can appear different if different firing conditions or multiple glazing methods are used (Vandiver 1983; Vandiver 2008). In the case of bead MEΘ 4164-12, the layers appear somewhat distinct, but this is not uniform across the surface (Figure 5.5). The granular nature of the core could indicate that there is not much interstitial glass present. This plus a somewhat distinct glaze and core boundary in some areas could suggest cementation was used—a technique that has been suggested as ideal for glazing a large number of small items such as beads (Vandiver, 2008).

Other beads, such as MEΘ 4164-11, can be categorized as "ordinary faience", exhibiting a thin layer of glaze directly over a white quartz (Lucas and Harris 1962) (Figure 5.6). The very white core indicates that quartz pebbles were used as the silica source. There did not seem to be a clear delineation in MEΘ 4164-11 between the glaze and the core. The glaze appeared somewhat thin. These characteristics could suggest glazing using efflorescence, since this method produces poorly defined boundaries between layers (Tite et al. 2007a). The core though does seem somewhat friable. This could indicate that there is little interstitial glass formed, pointing to other methods such as cementation which produces a thin glaze layer as well. Given the condition of the bead, it is difficult to determine visually which glazing method was used for this bead since it is not clear if the thin glaze and soft core is due to manufacturing technology or deterioration.

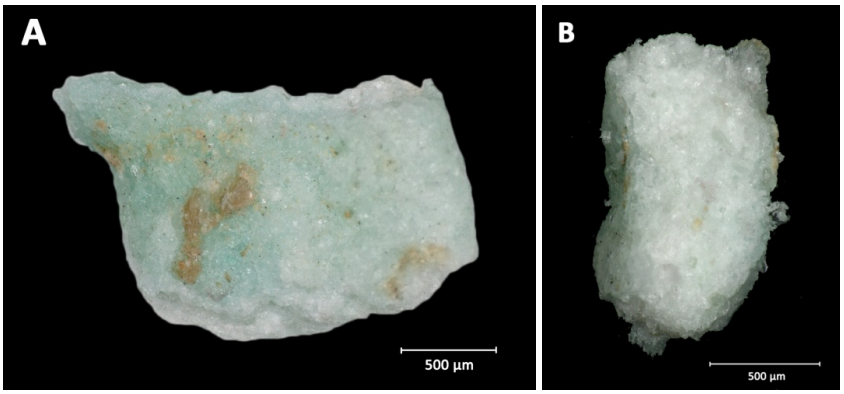

Figure 5.6. Faience disc bead (MEΘ 4164-11) from Tomb 245/5. (A) Photomicrograph showing appearance surface of the fragment. (B) Photomicrograph of the break edge showing the white quartz core.

Five blue disc beads were analyzed with EDS. Only the surface could be analyzed and this limitation, combined with the deterioration nature of the bead surfaces, meant that the original composition of the bead and various layers could not be determined (Table 5.4). The results indicated that all the beads had undergone depletion of the alkalis. Some of the insoluble components were enriched as a result, with some of the iron concentration influenced by burial deposits. The average values for soda (0.38 wt%) and potash (0.77 wt%) detected are low. In the case of two beads, soda was not detected. Some beads contained elevated concentrations of lime (1.49-9.45 wt%) and alumina (1.15-6.13 wt%). Phosphorus pentoxide values were higher than expected in the three disc beads where it was present (2.43-5.31%). Iron oxide was elevated as well on the surface of the beads (0.64-3.32 wt%). Some of these values could be due to enrichment where alkali is lost from components of the raw materials used. There could be some influence from the burial environment such as the diffusion of ions from the soil or perhaps from dissolved skeletal material since the beads come from a burial context.

Table 5.4. Results of SEM-EDS analysis conducted on the surface of selected beads. The concentrations are averages of several areas analyzed on each bead, given as weight percent oxide (wt%) and normalized to 100%.

Bead No	Na_2O	MgO	Al_2O_3	SiO_2	P_2O_5	SO_3	K_2O	CaO	TiO_2	MnO	FeO	CoO	CuO	PbO
Faience														
Blue														
889-9	n.d.	3.18	6.13	75.39	2.43	n.d.	1.40	9.43	n.d.	n.d.	2.04	n.d.	n.d.	n.d.
4164-2	0.56	0.59	2.16	92.40	n.d.	n.d.	0.20	1.49	n.d	n.d	0.64	n.d	1.96	n.d.
4164-3	0.50	1.66	3.68	77.46	5.31	n.d.	0.63	8.22	n.d.	n.d.	1.74	n.d.	0.81	n.d.
4164-5	0.08	0.60	1.15	82.63	4.55	0.92	0.68	3.89	1.61	n.d.	3.32	n.d.	0.56	n.d.
4164-6	n.d.	3.63	6.04	81.68	n.d.	n.d.	0.92	4.08	n.d.	n.d.	2.77	n.d.	0.88	n.d.
Black														
4164-4	0.84	2.00	5.83	63.31	4.40	0.88	1.19	15.56	0.70	1.38	3.89	n.d.	n.d.	n.d.
Glass														
Yellow/yellow-green/green														
889-2	0.77	4.90	2.56	83.00	n.d	0.37	1.57	4.04	0.79	n.d	1.11	n.d	0.90	n.d
889-3	n.d.	2.03	2.90	86.05	n.d.	1.29	0.73	3.71	n.d.	n.d.	3.29	n.d.	n.d.	n.d.
889-4	n.d.	1.11	2.66	87.82	n.d.	0.62	0.49	1.92	n.d.	n.d.	5.38	n.d.	n.d.	n.d.
889-5	12.39	4.58	2.40	67.81	n.d.	1.25	2.13	4.13	n.d.	n.d.	2.32	n.d.	n.d.	2.99
889-6	18.52	6.02	1.57	61.13	n.d.	1.02	3.17	4.65	n.d.	0.56	1.52	n.d.	0.61	1.22
889-7	n.d.	1.52	5.64	84.70	n.d.	0.13	0.47	2.38	n.d.	n.d.	2.68	n.d.	1.37	1.12
890-1	1.14	3.14	4.55	75.90	1.14	1.17	1.84	7.31	n.d.	n.d.	3.81	n.d.	n.d.	n.d.
890-3	2.57	1.95	5.40	77.39	n.d.	0.92	0.86	4.64	n.d.	n.d.	6.28	n.d.	n.d.	n.d.
890-4	n.d.	2.20	5.93	80.82	n.d.	n.d.	1.01	3.88	n.d.	0.76	5.40	n.d.	n.d.	n.d.
890-5	0.62	2.03	4.71	83.75	n.d.	n.d.	0.63	3.27	n.d.	n.d.	3.26	n.d.	n.d.	1.73
4164-1	1.92	1.85	4.28	80.98	n.d	0.95	0.61	3.47	n.d	n.d	3.70	n.d	n.d	2.24
Dark green														
884β	n.d.	1.33	3.84	64.17	n.d.	n.d.	0.42	3.50	n.d.	n.d.	2.97	n.d.	23.78	n.d.
Black/dark gray														
889-8	n.d.	1.97	1.73	88.17	n.d.	1.32	0.36	4.19	n.d.	2.26	n.d.	n.d.	n.d.	n.d.
Ellipsoidal bead														
885α	n.d	3.13	15.98	59.91	0.75	0.31	1.91	5.06	0.80	4.01	5.87	1.47	0.80	n.d

n.d.= Element not detected

The blue disc beads from Methone had copper oxide concentrations lower than the typical concentrations found in Egyptian or Near Eastern faience (Table 5.4). No copper oxide was detected on some of the faience surfaces. The only exception was MEΘ 4164-2, which contained 1.96 wt% copper oxide. It is difficult to know how well these low concentrations represent the original copper content given the losses to the glaze on some of the beads. Low concentrations of copper in the core and interaction layers have been found in faience made using the cementation method (Tite and Shortland 2008). However, further analysis, especially on a polished cross-section taken from a bead in good condition, would be required to support any additional conclusions drawn from this compositional analysis.

5.3.1.1.1 Black

Two of the disc beads are dark in color and appear black. Examination of the discs under magnification shows that the surface is not uniform but variable in color, with areas ranging from black to green or blue. There is loss of the glaze in areas and the presence of accretions or burial deposits (Figure 5.7). Black colored faience falls under the Variant B type established by Lucas and Harris (1962). Although neither of the two black disc beads at Methone was broken to reveal the core, small areas of white quartz were visible through losses to the glazed surface suggesting a light-colored core.

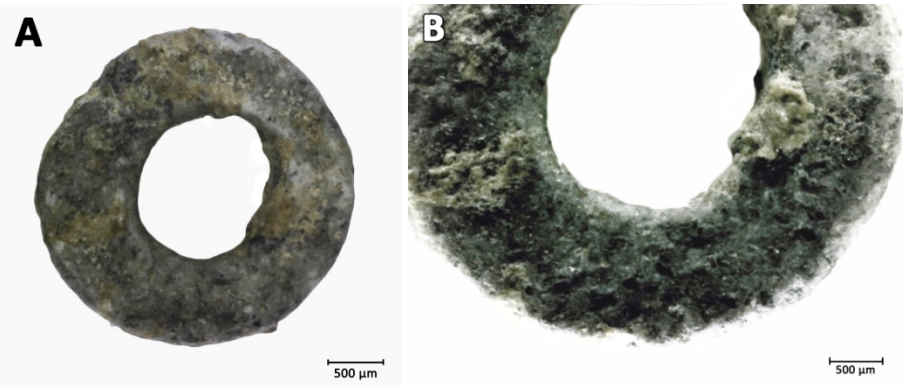

Figure 5.7. (A) Dark colored faience disc bead (MEΘ 4164-4) that appears black macroscopically. (B) Under magnification, the surface appears to be a mix of black and blue faience.

PXRF analysis of the black faience beads detected the presence of manganese, which is likely contributing to the black color. Prominent peaks for copper, cobalt, and iron were also observed. No tin or lead was found, and therefore copper ore, as opposed to bronze scraps, were used as the source of copper.

Based on published analyses of black faience, the presence of manganese, iron, and copper is not surprising in the ancient Methone beads. These three elements were found in Egyptian black faience (Lilyquist et al. 1993; Kaczmarczyk and Vandiver 2008). Most of the published examples did not seem to contain cobalt. The exception is a group of beads from Abydos that contained trace amounts of cobalt (0.01-0.02%) in different layers of the beads. The presence of copper in black faience has been attributed to the use of the same glazing mixtures used to produce both black and blue colors (Tite et al. 2007a; Kaczmarczyk and Vandiver 2008) but it is possible that the mixture of elements could have been used to produce a particular color effect. Tite, et al. (2009) conducted experiments to replicate dark colored Minoan faience and found that by varying concentrations of manganese oxide (1-3%) and up to 2% CuO in the glaze produced dark blue-violet to violet colored glaze. The presence of those oxides in the body produced a core that ranged from grey to near black.

A parallel for the intentional mixture of manganese, copper, and cobalt to create a black colored vitreous material can be found in glass from the Late Bronze Age. At the site of Amarna, a combination of manganese (2.46 wt%), copper (1.32 wt%) and cobalt (0.23 wt%) had been used to create black glass (Nicholson 2007). A Middle Bronze Age (1600-1500 BC) bead from Poviglio in Italy had a cobalt

concentration in its core of 1.6% which produced black glass (Santopadre and Verità 2000). The addition of cobalt would have made the glass appear darker, making it look black when it was actually dark blue. Another piece of black glass from Amarna housed at the Penn Museum contained 2.4 wt% MnO and 1.92 wt% CuO , but as with the piece analyzed by Nicholson (2007, p. 129), the glass was actually dark blue in areas when examined in cross-section using transmitted light (Muros et al. 2017).

The EDS analysis of the surface of the black disc bead MEΘ 889-8 showed it contained 2.26 wt% manganese oxide, a concentration higher than the other faience beads due to its presence as the colorant (Table 5.4). The iron was somewhat elevated (3.89 wt%), though it could not be determined that this was part of the manganese colorant or was present due to other factors. No cobalt or copper was detected on the surface areas analyzed. This could be due to the fact that the levels are below the detection limit of the EDS, the elements were not present in the areas analyzed, or they are located in the interaction layer or the core and not detected during surface analysis.

5.3.1.2 Cogwheel-shaped beads

Unlike the blue disc beads, the cogwheel beads are in better condition with fewer losses to the glazed surface. The glaze appears to be a pale blue to blue-gray color. In a few areas around the perforation where there is loss of glaze, the color of the body is somewhat gray in some spots. Some quartz grains are visible (Figure 5.8). Examinations of these areas of loss under magnification do not show a distinct glaze layer over the core. The cogwheel beads were initially identified as Variant D faience because of the similarities in color between the glaze and the core (Lucas and Harris 1962). The appearance of quartz grains visible in areas of glaze loss and white colored patches may indicate the color is not colored. Analysis of a section through the bead so that the glaze, interaction layer, and core can be analyzed is needed to identify the variant and understand the glazing method and manufacturing technology. PXRF analysis detected the presence of cobalt and copper both of which were used to produce the color. Tin and lead was detected, and therefore bronze scrap was likely used as the copper source. It is not clear what the distribution of cobalt and copper are across the object and whether one or both elements are present in the glaze and/or core.

Figure 5.8. Photomicrograph of a faience cogwheel bead (MEΘ 889-1). Areas where the glaze has been lost shows a core that appears in some areas to be the same blue-gray color as the glaze, though other areas appear white and quartz grains are visible

Although only qualitative pXRF was conducted, the results could provide some general information on the source of cobalt. For example, none of the beads contained arsenic which means that the cobalt source was not the high arseno-sulphide ores found in Iran (Maniatis et al. 2008). The relative peak heights of the elements manganese, nickel and zinc, and subsequent photon counts, are higher in the cogwheel beads than the blue disc beads. The higher concentration of these three elements could suggest the use of cobaltiferous alum for Egypt as the colorant (Kaczmarczyk and Hedges 1983). Trace element analysis would

be helpful to better assess the concentrations of the transition elements to help identify a possible cobalt source for the colorant.

5.3.2 Glass beads

5.3.2.1 Circular short beads

5.3.2.1.1 Copper blue

Bead MEΘ 5318-1 was the only bead found within Tomb 245/3. The bead was covered with an opaque layer of yellow-brown corrosion (Figure 5.9). No intact glass was visible due to the surface deterioration and the original color of the glass was not known.

Figure 5.9. The surface of bead MEΘ 5318-1, which had deteriorated to a yellow-brown color. The original color of the bead was unknown, but based on the presence of copper, tin, and lead it was likely blue with bronze scrap used as the copper colorant.

Qualitative pXRF analysis detected copper, lead and a very small tin peak and point to the use of leaded bronze scrap as the copper source. The bead also contained arsenic, which could be related to the bronze source where the arsenic would be present as a trace element from the ore. Based on the presence of these three elements, the bead is assumed to be blue in color; however, sampling would be required to confirm this.

5.3.2.1.2 Yellow/yellow-green/green

Twelve beads appeared to be made of yellow, yellow-green, or green glass (Figure 5.10). Under magnification, the glass appears translucent though there are areas on some beads that have opaque streaks or many small air bubbles. The beads were somewhat similar in elemental composition based on the pXRF results (Table 5.3). They all had prominent peaks for iron and lead, followed by copper and antimony. Six beads contain tin (MEΘ 889-2, 889-7, 889-11, 890-1, 890-3, 4164-1). Another six beads appear to have tin (MEΘ 889-3, 889-4, 889-5, 889-6, 890-4, 890-5) but the peak is quite small and only slightly above the background. The presence of tin points to the use of bronze scrap as the colorant. Five beads contain arsenic (MEΘ 889-3, 889-5, 889-6, 889-7, 890-4). The arsenic could be a trace element from the bronze or could be related to the antimonate compound detected (Shortland 2002). The predominance of yellow to yellow-green to green glasses could be considered somewhat unusual for Late Bronze Age glasses, especially those found on the Greek mainland, where the predominant color found is often blue (Smirniou and Rehren 2013).

The interpretation of the pXRF results and determination of the colorants used to produce the ancient Methone yellow/yellow-green/green beads is complicated by the detection of copper, lead, and antimony, in addition to iron. All of these elements could play a role in producing the colors observed. Translucent green or yellow-green glass is generally colored by iron (Shortland and Tite 2000; Nicholson 2007). The combination of copper, lead, and antimony has been used to create opaque green glass (Shortland 2002). These beads contain all four elements but are not opaque or very green.

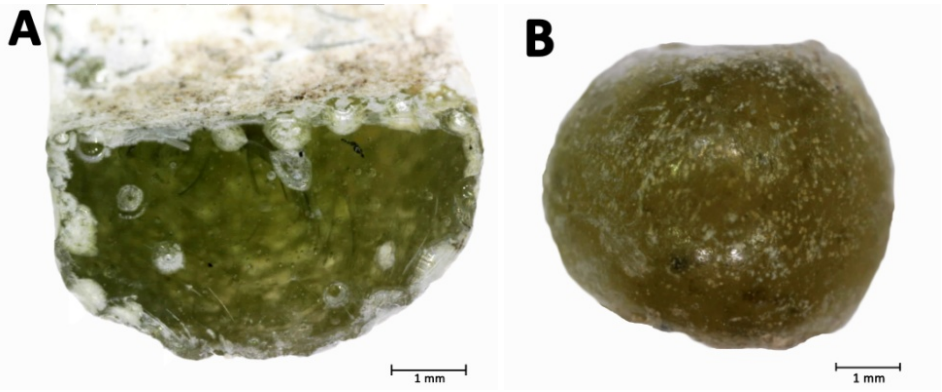

Figure 5.10. Details showing the range of colors of the glass beads. (A) Green translucent bead (MEΘ 889-2) (B) Yellow-green translucent bead (MEΘ 890-1). The qualitative pXRF results showed the two beads have similar compositions.

In the matrix of one of the glasses, MEΘ 890-1, some opaque yellow inclusions were visible under magnification, which could be the added lead antimonate opacifier (Figure 5.11). The ability to see the opacifier in lead antimonate opacified glass is common. It can be found in clumps and unevenly distributed, even appearing as swirls in the glass matrix (Shortland 2002).

One possible reason for the lack of a strong opaque color in the glass could be due to the number of particles and their distribution. If the opacifying crystals are not widely dispersed in the glass matrix and confined only to specific areas, the glass will not appear very opaque. Another possibility is that the temperature used to melt the opaque glass was too high, something that affects opacity (Sayre 1963; Shortland 2002). This is because higher temperatures, generally above 900°C, can cause the lead antimonate to dissolve into the melt or become cream colored (Shortland 2002; Shortland and Eremin 2006).

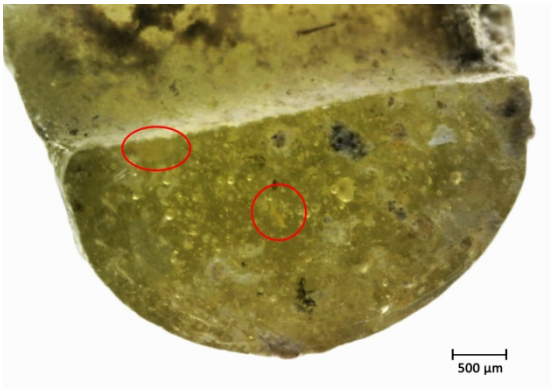

Figure 5.11. Photomicrograph of the break edge of bead MEΘ 890-1. The red circles mark areas where an opaque yellow material was visible within the glass matrix, which could be lead antimonate crystals.

When antimony is added to glass, it can work as an opacifier or decolorizer (Sayre 1963). The effect it has on the glass is dependent on what the valence state is. This has been shown through the analysis of glass opacified and decolorized by antimony where the concentration of antimony was the same in both glasses with only the valence state differing. In opaque glasses, antimony is in a pentavalent state but at high temperatures, it is reduced. This turns the antimony into a "more miscible reduced" compound which makes the glass appear clear (Sayre 1963, 272). Although antimony was not used as a decolorizer until the 1st millennium BC, the translucency of these beads could have been caused unintentionally due to the use of

a high melting temperature during manufacture, the results of the small number of lead antimonate particles present that would cause opacity, or a combination of both conditions.

Copper was detected in only two of the eight beads analyzed from this group. Bead MEΘ 889-6, the best preserved bead, has a copper concentration of 0.61 wt%. MEΘ 889-7 contains 1.37 wt% copper (Table 5.4). Analysis of blue copper colored glass from Amarna has shown that the range of copper in translucent blue glasses can vary from 0.52-3.17 wt% copper (avg. 1.5 wt%) (Nicholson 2007; Shortland 2012). The copper content of opaque green glasses from Malkata, Lisht and other early glass sites had lower concentrations of the colorant, 0.5-1.9% (Mass et al. 2002; Shortland and Eremin 2006; Shortland 2012). The concentration of copper in the two ancient Methone beads falls within the range observed for green opaque glasses.

The iron content (1.11-6.20 wt%) was relatively high for these beads in comparison to the naturally occurring iron in the raw materials used for plant ash glasses (Table 5.4). Since quartz pebbles are generally used the iron impurities are fairly low (avg. 0.5%, up to 1.5%) (Schreurs and Brill 1984; Brill 1988). Since the furnace atmosphere can be used to color the glass with the iron in the raw materials no additional iron is required. Green and amber colored glasses from Jalame contained a maximum concentration of 0.5% iron oxide. The ancient Methone beads contained a higher concentration though the source of the iron cannot be clearly identified. Since the surfaces of the beads were analyzed, it is not clear if all of the iron detected comes from the glass or the corroded surface. The less corroded beads (MEΘ 889-5 and 889-6) did contain elevated iron, 1.52 and 2.32 wt%, so it is possible these glasses do contain higher levels of iron if soil and other deposits from the burial environment are not influencing the results

Antimony was not detected using SEM-EDS, but lead was measured in five beads (MEΘ 889-5, 889-6, 889-7, 890-5, 4164-1). The concentrations ranged from 1.12-2.99 wt% PbO (Table 5.4). Although the concentration of lead in opaque yellow glasses is quite high in areas where the lead antimonate crystals are located, the lead concentration in the bulk glass is lower, from 0.6-13 wt% lead (Mass et al. 2002; Shortland and Eremin 2006; Nicholson and Jackson 2007; Shortland 2012). The lead content in ancient Methone glasses falls within this range.

Based on the results obtained it is likely that the copper, lead, and antimony present are part of the mineral colorants and opacifier used for the glasses. The role of iron, however, is unclear. It is not known whether the iron detected is due to the raw materials, such as the source of silica, if the concentrations identified are due to burial deposits or enrichment of this element on the surface, or if iron was added as a colorant. Analysis of an intact, interior surface of the glass would be needed for better characterization of the glass composition and mineral colorants used.

EDS analysis shows that the bead surfaces are depleted in alkalis and enriched in other oxides (Table 5.4). Only one bead (MEΘ 889-6) had a composition that falls within the average range expected for Late Bronze Age plant ash glass with 18.52 wt% Na_2O, 6.02 wt% MgO, 3.17 wt% K_2O, and 4.65 wt% CaO. The alumina content was slightly elevated (1.57 wt%). Bead MEΘ 889-5 seemed to have undergone some leaching. The soda concentration was slightly low, at 12.39 wt%. It is unclear if the potash concentration (avg. 2.13 wt%) measured was higher originally and has also undergone leaching or represents the actual content of this alkali.

It was not possible to use the data collected using EDS to determine the origin of these yellow, yellow-green, and green beads based on the concentrations of major and minor elements. The identification of tin in all of the beads of this color points to the glass being made in Egypt. The detection of arsenic may be related to the bronze scrap used for the colorant, if arsenic was present as a trace element in the alloy. Arsenic has also been found in antimonate opacified glass made in Egypt and is associated with the source of antimony (Shortland, 2002).

5.3.2.1.3 Copper dark green

Bead MEΘ 884β was very deteriorated and had turned opaque white. It was also fragmentary. There were a few areas within the perforation and along the break edges where a dark green glass was present (Figure 5.12). This could possibly be the original color. From what remains of the dark green glass, it appears translucent under magnification though it is difficult to be sure because of the level of deterioration.

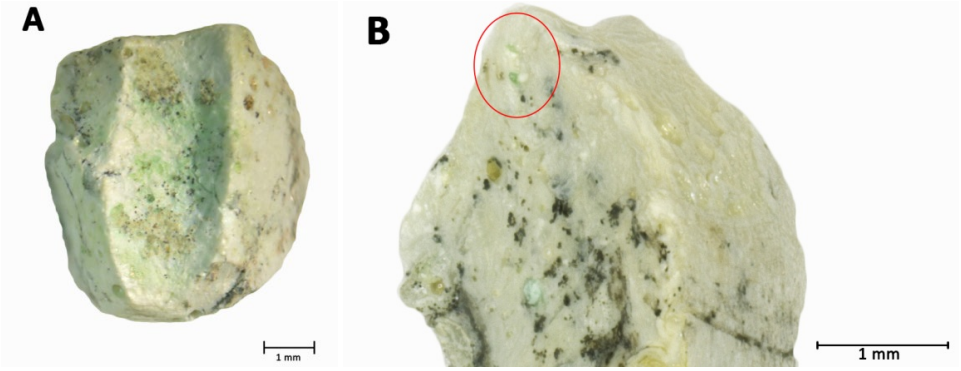

Figure 5.12. Fragments of bead MEΘ 884β. (A) Dark green glass was primarily found in areas along the perforation. (B) Some very small pieces of green glass were found in other areas (indicated by the red circle).

PXRF analysis of this bead showed a prominent peak for copper but also for iron. It is not clear if the iron is related to the colorant or to the soil and other burial deposits present on the surface. Given the burial deposits and stains on the surface (Figure 5.12), the peak heights were influenced by the iron in these areas. Lead was detected, but no tin, antimony, or arsenic was found. The lack of tin may suggest a copper ore was used as the copper colorant source rather than bronze scrap. If the lead is associated with the copper, then it is possible leaded copper could have been used.

The lack of antimony and tin indicated that different colorants were used to make this green bead than those used for the green beads discussed in the previous section. Based on the data collected thus far, the bead appears to have been colored by copper, possibly using leaded copper scrap. It is also possible that this bead was not originally colored green. Studies of blue pigments made from the copper mineral azurite, as well as copper colored faience, have found that they can alter to a green color when exposed to certain environmental conditions or processes such as moisture, alkaline solutions, chloride ions, and reduction (Vandiver 1983; Scott 2002; Moussa and Ali 2013). The bead may have originally been colored blue but altered to green due to degradation in the burial environment.

EDS analysis of the areas of green glass shows a very high concentration of copper, up to 23.78 wt% (Table 5.4). This is much higher than what is reported in the literature for copper content in translucent and opaque blue, as well as opaque green glasses. It appears that these areas have become enriched in copper due to the depletion of most of the other elements in the glass matrix or the areas analyzed could include unreacted copper-containing components of the glass. Lead was not detected used EDS and it is likely not present in the surfaces analyzed or below the detection limit in these areas.

5.3.2.1.4 Black/dark gray

Two fragmentary beads (MEθ 889-8, MEθ 890-2) that appeared black/dark gray in color were found in Tomb 245/5 (Figure 5.13). Examination showed the fragments are quite opaque and iridescent in areas. The surface color under magnification is not uniform and appears mottled, with areas also colored white and brown. The combination of the dark color of the bead fragments and the iridescence gives them an almost metallic luster. They are extremely corroded. Upon initial examination, it was not clear whether the beads were originally this color or this was due to deterioration processes and/or staining from the burial environment.

Manganese and iron were detected via pXRF analysis (Table 5.3). Lead and copper are also present. Both beads are very similar in composition. It appears that these beads may have been colored using the same combination of colorants as the black faience disc beads. No tin was detected in either bead. Copper mineral could have been used as the colorant, or if the lead is associated with the copper, then leaded copper scrap was the colorant. EDS analysis of a fragment from MEΘ 889-8 2.26 wt% MnO was detected, a concentration that falls within the range of manganese values found in black glasses (Nicholson 2007). Due to the level of deterioration of the beads, and that no intact glass was found that could be analyzed, no further information could be obtained on the glass composition.

Figure 5.13. Fragment of a dark gray/black glass bead (MEθ 889-2).

5.3.2.1.5 Glass and Cu alloy bead

Excavation of Tomb 245/16 revealed a glass bead which contained a copper alloy bead inside the perforation (MEΘ 885β) (Figure 5.14). The glass bead was extremely corroded and appeared opaque with a slight yellow or tan coloration. The copper alloy bead was spherical in shape. Other copper alloy beads were found in this tomb, mainly spiral beads, but no other spherical copper alloy beads were recovered. No examples of a copper alloy bead intentionally placed within a glass bead have been found in the literature for comparison. Initially it was thought that perhaps the copper alloy bead was not a bead at all but a fragment of a larger object the bead was attached to that has broken off, such as a copper alloy tube. However, the edges of the copper alloy bead appear finished and are not broken. It is likely that the insertion of the smaller copper alloy bead into the glass bead was accidental and was caused due to taphonomic processes within the burial.

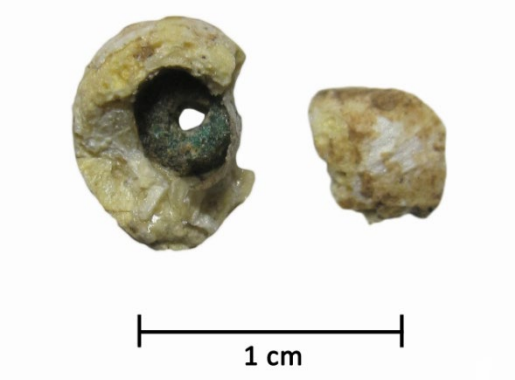

Figure 5.14. Glass bead with copper alloy bead in perforation (MEθ 885β). The copper alloy bead was likely unintentionally inserted during burial and is not originally part of the glass bead.

The glass plus copper alloy bead (MEΘ 885β-1) and the small glass fragment that had broken off the bead (MEΘ 885β-2) were analyzed with pXRF. Iron and copper were the most prominent peaks (Table 5.3). A small amount of tin was detected and trace lead was found. The peak heights for copper and tin were taller in the glass plus copper alloy bead as opposed to the glass fragment. This was to be expected since the pXRF beam would have traveled through the corroded glass and reached the copper alloy bead. The detection of

both copper and tin means the bead is made of bronze. What is interesting is that the iron and lead peak heights remained the same between the glass fragment and the glass plus copper alloy bead. This means that lead and iron are present in the glass. The glass is very corroded with no intact glass remaining. Based on the elements detected the bead appears to contain copper as a colorant, with the tin and likely also the lead, pointing to the use of bronze scrap as the colorant. No antimony was detected and therefore the lead present is likely not because of the use of lead antimonate, as was observed in the yellow, yellow-green and green glass beads.

5.3.3 Ellipsoidal bead

The only noncircular glass bead found at ancient Methone was ellipsoidal in shape (MEΘ 885α) (Figure 5.15). The bead is much larger than any of the other vitreous beads found and appears opaque black in color. The surface is very smooth. Under magnification, there are areas of loss of the dark surface that reveal that the black layer is thin and located over opaque white to pale yellow corroded glass. All the exposed glass is very deteriorated and no intact glass is visible on the surface. Since the bead is intact and there are no large areas of loss, the core of the bead could not be examined to determine whether any intact glass was preserved. The smooth, thin appearance of this black layer is quite unusual and its relationship to the underlying glass in unclear.

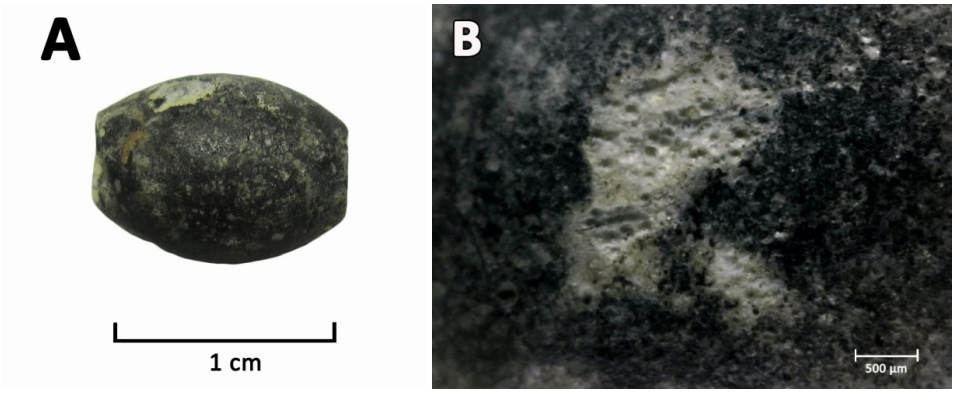

Figure 5.15. (A) Ellipsoidal bead MEΘ 885α which has a smooth, opaque black surface. (B) Under magnification areas of opaque, white, and yellow corroded glass are visible underneath the black layer.

PXRF analysis of several areas of the bead revealed the presence of manganese, iron, copper, and cobalt (Table 5.3). Small peaks for lead and antimony were also present. The presence of these elements makes determination of the colorant(s) used for the bead challenging. This is in part because these elements can be present from different sources, and even different colorants. The manganese and iron peaks are most prominent and perhaps related to the dark layer on the exterior or the surface. The presence of cobalt and copper suggests the bead could be blue and the detection of antimony would indicate the bead was opacified. A very small peak for tin was observed and if present, this would point to the use of bronze as the copper colorant. The small lead peak may be related to the antimony detected, suggesting the addition of lead antimonate to produce an opaque green bead. The lead can also be related to the copper source. If the lead peak is attributed to the copper source, the antimony could be associated with calcium and the presence of a calcium antimonate opacifier.

Areas on the black surface and the opaque white glass were analyzed using EDS (Table 5.4). No soda was detected and the potash concentration was low (1.91 wt%). This shows leaching of the alkali. The alumina content was very high, at around 15.98 wt%, and levels of manganese (4.01 wt%) and iron (5.87 wt%) were elevated. The concentrations point to enrichment of these oxides on the surface.

The average concentration of copper detected was 0.80 wt%, which falls within the range of copper colorants, found in Late Bronze Age glasses (Table 5.4). The cobalt concentration was quite elevated (1.47

wt%) and it is not clear why. Cobalt is a strong colorant and generally found in low concentrations in glasses. It can range in some Egyptian glasses up to 1.3% but is generally below 0.37% (Shortland and Tite 2000; Tite and Shortland 2003; Nicholson 2007). There were areas found on the bead where the mineral colorant levels were very high (Table 5.5). These were primarily located in areas with losses or pits where the corroded glass was quite granular in appearance. The cobalt concentrations in these spots ranged from 2.75-12.68 wt% and for copper from 2.29-8.27 wt%. When cobalt and copper were very high, so were the manganese, iron, and alumina. All other elements were very low, such as silica which was anywhere from 18-50 wt%. It is not clear what these areas represent. One possibility is that elements have been leached due to extensive corrosion, and this has left areas enriched in the less soluble components of the glass. Some of these elements could also have been enriched by diffusion from the burial environment. Another suggestion could be that some of these enriched areas may represent unreacted raw materials from the glass batch and therefore are higher in concentration because they did not completely diffuse into the glass melt during production.

With only pXRF and EDS analysis of the surface conducted, it is not possible to obtain more information on the original composition of the ellipsoidal bead or what is the relationship between the dark layer to the underlying glass. Sampling of the glass and additional analysis would be needed to be able to identify the glass components and colorants.

Table 5.5. SEM-EDS analysis of areas on bead ΜΕΘ 885α. Values given as weight percent (wt%) oxide and normalized to 100%.

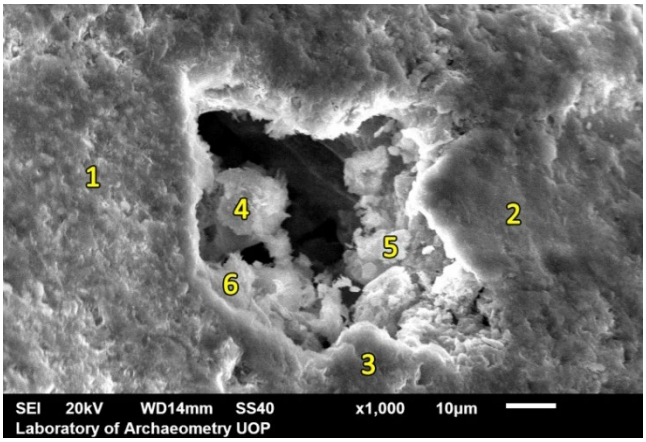

Area	Na_2O	MgO	Al_2O_3	SiO_2	SO_3	K_2O	CaO	TiO_2	MnO	FeO	CoO	CuO
1	n.d.	4.65	21.45	56	n.d.	2.93	1.67	0.68	2.58	8.2	1.42	0.41
2	n.d.	14.77	24.43	42.17	n.d.	0.55	0.77	n.d.	0.62	16.5	0.17	0.04
3	n.d.	4.44	22.14	54.94	n.d.	2.7	1.56	0.57	4.28	8.15	0.91	0.32
4	n.d.	n.d.	0.22	3.63	0.32	0.63	6.83	4.28	45.88	17.28	12.68	8.27
5	n.d.	4.72	14.23	41.21	n.d.	1.9	3.58	2.36	16.78	7.47	4.51	3.25
6	n.d.	3.28	15.38	37.37	n.d.	1.72	1.84	1.06	6.07	28.5	2.49	2.29

5.4 CHAPTER SUMMARY AND CONCLUSIONS

Sixty-seven vitreous beads were discovered within a Late Bronze Age cemetery at the site of ancient Methone that were AMS radiocarbon dated to the 13th c. BC. Forty-seven of the beads are made of glass. Almost all of them are short, circular beads, with one bead ellipsoidal in shape. The remaining beads are made of faience. Fourteen are disc shaped. Six are shaped like cogwheels and have collars around the perforation. No relief beads or Mycenaean bead forms were found, despite the presence of other types of Mycenaean objects uncovered in the graves. The site is located beyond the northernmost boundary at which relief beads were found. It is possible that ancient Methone was importing glass and faience from elsewhere that may have been arriving directly into the Thermaic Gulf directly from the north Aegean.

The faience beads are predominately blue in color. The disc beads are light blue or blue-green and colored by copper. The presence of lead and tin points to bronze scrap being used as the copper source. Among the blue disc beads, both Variant A and "ordinary faience" are represented. The cogwheel beads are blue gray in color and contain a combination of copper and cobalt. Tin and lead were also detected, therefore suggesting bronze was used as the copper source for the colorant of these beads. The other elements detected in the cogwheel beads could suggest an Egyptian source for the cobalt used, but additional analysis is required to confirm. Examination of areas of glaze loss on the cogwheel beads shows that the core may not be white and they may represent the Variant D type faience.

Two black faience discs (Variant B) contained manganese, copper, and cobalt. Manganese is commonly used for the manufacture of black faience and glass during this period and is likely the source of the dark color. The addition of copper and cobalt could have been added to affect the tone of the glaze, as is seen in some examples of black Egyptian glasses. It is also possible the blue colorants detected are present because similar base glazing materials were used regardless of the surface color to be produced. Tin and lead were detected in the black faience and point to the use of bronze scrap as the source of the copper.

The faience beads were in poor condition and many had lost areas of the glaze leaving the core exposed. Since the faience beads were not sampled to produce polished cross-sections for compositional analysis of the layers, microscopic examination was used to try to identify the glazing method used. Based on microscopic examination, and the size of the objects, it is possible that cementation and/or efflorescence methods were used. Other methods or combinations of glazing techniques could not be ruled out.

The predominant color of the glass beads ranges from translucent yellow to yellow-green to green. Only one possible blue bead was excavated from the cemetery. This color palette is not typical for Late Bronze Age sites in the Eastern Mediterranean where the predominant colors tend to be blue (or turquoise blue) and dark blue.

Yellow and green translucent glass is generally produced by iron and iron-sulfur compounds. In addition to iron, copper, lead, and antimony were also detected. It is not clear if the presence of iron is related to the color or if it was due to burial deposits and soil on the surface of the beads. Copper, lead, and antimony have been used to create opaque green glasses through a combination of copper blue glass with lead antimonate crystals added. However, these beads were not all green nor were they opaque. Some inclusions in the bead appeared to be opaque yellow, and these could represent lead antimonate crystals. The lack of a strong green color or opacity could be due to the limited number of opacifying crystals or the firing temperature of the beads. If the temperature were too high, the lead antimonate crystals would dissolve into the glass melt and would not act as an opacifier.

Other glass beads found included fragments of a dark gray-black bead likely colored with manganese. Copper and lead were also detected and could be contributing to the color. Another black bead was found which was ellipsoidal in shape, but under magnification, the smooth black surface seems to be a thin layer overlying a white to pale yellow opaque glass. The glass is very corroded and no intact glass could be observed to be able to identify the original color of the glass. This bead contained copper, cobalt, lead, and antimony, elements that contribute to an opaque green color and found in other beads at ancient Methone. High concentrations of manganese and iron were also detected. It is not clear if those elements contributed to the original color of the glass or were only present in the black layer on the surface.

Almost all of the glass beads were in poor condition and their original composition could not be determined using SEM-EDS. They all showed depletion of alkali earth elements and enrichment of other components. The exception was one bead, ΜΕΘ 889-6, which had a composition typical for plant ash glasses. Another bead, ΜΕΘ 889-5, had only undergone a small amount of leaching and contained concentrations of the alkali

and alkali earth elements close to the lower end of the range of average plant ash compositions. The exception was soda, which was low, at 12.39 wt%.

The analysis conducted thus far on the disc beads does not seem to provide information on where they were produced. Bronze scrap was used as a copper source for faience made in Egypt and the Near East. The bead shapes are ubiquitous and do not point to a regional type. Based on the prominent pXRF peaks for manganese, nickel, and zinc, the cogwheel beads may have been made in Egypt. However, quantitative analysis would be required to determine this.

The majority of the glass beads analyzed contained tin. This points to an Egyptian origin, since bronze scrap was only used in Egypt as the copper source. This however does not rule out the possibility that some of the beads may be of Near Eastern origin, especially those beads that contained a copper colorant but did not have tin, such a MEΘ 884β-1, 889-8, and 890-2. This could point to the use of a copper mineral as the colorant source, a practice that was done in the Near East.

6 VITREOUS BEAD FROM THE IONIAN ISLANDS: KEFALONIA

6.1 INTRODUCTION

The island of Kefalonia is located about 30 km off the western coast of Greece in the Ionian Sea (Figure 6.1). It is part of a group of seven islands (including Lefkada, Corfu, Ithaca, Zakynthos, Paxos, and Kythera) referred to as the Ionian Islands or the Heptanese. The Ionian Islands have a history of settlement since the Neolithic period with some islands having continuous occupation through the Late Bronze Age (Souyoudzoglou-Haywood 1999). They have been an area with evidence of trade with mainland Greece and areas farther north, east and west, as well as a place of local innovation and style.

After the Neolithic period more settlements and burials appear on the islands beginning in the Early Bronze Age (3000-2100 BC) (Souyoudzoglou-Haywood 1999). During this period, the tomb styles and grave goods show an import of goods or adoption of outside styles, but also contain characteristics unique to the Ionian Islands. In the Early Bronze Age, burials were placed in pithoi—a practice not known on mainland Greece, Crete, or the eastern Greeks islands during this period—but were similar to burial practices in the Eastern Aegean and Anatolia. Other grave types, such as tumuli, were found which have parallels in western Greece, the Balkans and Attica indicating connections with those regions. Grave goods exhibit stylistic influences from other regions as well, which links the Ionian Islands to sites on the west Peloponnese, northwest Greece, Crete, and the Cyclades. This evidence shows that by this period, sea trade routes along the western coast of Greece had been established.

Figure 6.1. Location of Kefalonia and the sites included in this study (from Google Maps; Larger map: Map data ©2020 GeoBasics-DE/BKG (©2009), Google, Inst. Geogr. Nacional, Mapa GISrael, ORION-ME; Detail: Map data ©2020)

It is not until the Late Bronze Age (1550-1050 BC) that there is a significant increase in the number of sites found across the Ionian Islands along with more evidence for larger scale trade (Souyoudzoglou-Haywood 1999). Twenty-seven sites have been found so far dating to this period, however, occupation was not uniform across all the islands. Most of the occupation during the Late Bronze Age comes from evidence found at cemeteries, caves or isolated finds. Very few settlements have been identified. During this period, Mycenaean artifacts and tomb types from the mainland appeared as part of the expansion of Mycenaean culture westward, likely from the southwest Peloponnese. These cultural materials did not arrive at the same time across the Ionian Islands, with Mycenaean cultural material first found on the island of Zakynthos. On Kefalonia, Mycenaean cultural influences were represented through the adoption of tholos and chamber tombs in the 14th c. BC (Souyoudzoglou-Haywood et al. 2017). It is not clear if these Mycenaean style artifacts and burials were introduced by a small groups of settlers arriving on the Ionian islands, by local

groups adopting characteristics of the Mycenaean culture from contact with the mainland, or a combination of both (Souyoudzoglou-Haywood et al. 2017; Voskos 2019). In addition to the appearance of Mycenaean material, this period on Kefalonia was also marked by evidence of strong trade links with other areas along the Ionian and Aegean Seas, with connections possibly farther north and west. Finds from northern Greece and Albania, amber from the Baltic, and gold and bronze objects with parallels in central and southern Italy have been discovered in most of the cemeteries on Kefalonia (Souyoudzoglou-Haywood et al. 2017). The evidence of artifacts spanning such a wide region indicates that during the Late Bronze Age, Kefalonia was likely a stop on eastern and northwestern sea trade routes.

Beginning in 1250 BC, Mycenaean sites on the Greek mainland were destroyed or abandoned (Voskos 2019) and there is a change in the centralized power of the palatial centers. This is described as the beginning of the decline of the Mycenaean civilization which resulted in its collapse at around 1100-1050 BC (Souyoudzoglou-Haywood 1999). This decline, or collapse, however was not observed on all the Ionian Islands, and in particular not on Kefalonia (Souyoudzoglou-Haywood 1999; Souyoudzoglou-Haywood et al. 2017; Voskos 2019). While populations decreased on mainland Greece, those on Kefalonia seemed to grow. Although settlements on Kefalonia remained scarce, the cemeteries that were in use during the earlier parts of the Late Bronze Age were still functioning until ca. 1100 BC (Voskos, 2019). Some cemeteries, such as at Mazarakata and Metaxata, had new tombs built (Souyoudzoglou-Haywood 1999). New local pottery styles appeared. It is not clear why this expansion and innovation occurred. Some attribute it to a new population inhabiting the island, perhaps coming from the mainland, or an emerging group of elites on the island (Voskos 2019). Continuity in occupation was observed on Kefalonia until about 1075-1050 BC when the cemeteries on the island were abandoned (Souyoudzoglou-Haywood 1999). The reason for abandonment is unknown.

6.2 Description of the Late Bronze Age Sites In Study Group

Information for the Late Bronze Age on Kefalonia comes primarily from the excavations of cemeteries since few settlements have been found on the island dating to this period (Souyoudzoglou-Haywood 1999; Souyoudzoglou-Haywood et al. 2017) The majority of the cemeteries were excavated in the early and mid-20th century and documentation on what was found is not available or is incomplete. The Late Bronze Age beads analyzed for this project come from three sites located on the Argostoli plain (Argostoli-Livatho region): Mazarakata, Metaxata, and Kokkolata-Kangelisses (also referred to as Kokkolata-Menegata) (Figure 6.1). All the beads studied are currently housed in the collection of the Archaeological Museum of Argostoli.

The three cemeteries were used from the beginning of the LH IIIA2 period through the LH IIIC (Table 6.1) (Souyoudzoglou-Haywood 1999; Voskos 2019). Mycenaean tomb types were adopted and Mycenaean artifacts were placed as grave goods. Tholos, chamber, shaft, and cist tombs were built with similar burial customs observed across the sites. Tomb architecture with characteristics unique to Kefalonia, in addition to local pottery styles found in the graves, further reinforces the idea that although aspects of Mycenaean culture were adopted, local customs were retained and new regional styles and practices were created.

6.2.1 Mazarakata

The Late Bronze Age cemetery of Mazarakata is located near the present day town of Mazarakata about 8 km south of Argostoli (Figure 6.1). Mazarakata is the largest cemetery found on the island with a total of 17 chamber tombs and a tholos (Table 6.1) (Souyoudzoglou-Haywood 1999; Voskos 2019). The earliest investigations of the burials took place in the 19th century when 16 tombs (A-Π) were discovered. These first excavations were conducted first by C.P. de Bosset in 1813 and were followed in 1899 by archaeologist P. Kavvadias (Souyoudzoglou-Haywood 1999). In 1951, the 17th chamber tomb (P) was found after a collapse in the road and subsequently excavated by archaeologist S. Marinatos. The level of documentation

for these excavations varies and sometimes includes field records and some publications. There does not seem to be a full inventory of description of all the work undertaken or the discoveries made.

Table 6.1. Chronology of the tombs found at Mazarakata, Metaxata, and Kokkolata-Menegata (after Souyoudzoglou-Haywood, 1999; Voskos, 2019). The dates given are based on the chronology of the Ionian Islands, which differs slightly for some of the same periods on the mainland.

Site	Tomb No.	Type	Relative Chronology	Approximate Dates
Mazarakata	A	chamber	LH IIIA2/IIIB, LHIIIC	1350/1300-1200/1190 BC, 1200/1190-1050/40 BC
Mazarakata	B	chamber	LH IIIB	1300-1200/1190 BC
Mazarakata	Γ	chamber	LH IIIB-IIIC	1300-1050/40 BC
Mazarakata	Δ	chamber	LH IIIC	1200/1190-1050/40 BC
Mazarakata	E	chamber	LH IIIB	1300-1200/1190 BC
Mazarakata	Z, H, Θ, I, K, Λ, M, N, Ξ, O, Π,	chamber	LH IIIC	1200/1190-1050/40 BC
Mazarakata	P	chamber	period unknown	
Mazarakata		tholos	period unknown	
Metaxata	A	chamber	LH IIIC	1200/1190-1050/40 BC
Metaxata	B	chamber	LH IIIA2-IIIC	1350-1060 BC
Metaxata	Γ	chamber	LH IIIC	1200/1190-1050/40 BC
Metaxata	Δ	chamber	LH IIIC	1200/1190-1050/40 BC
Metaxata	E	chamber	LH IIIC	1200/1190-1050/40 BC
Metaxata	ΣT	chamber	LH IIIA2-IIIC	1350-1050/40 BC
Kokkolata-Menegata	A, B	tholos	LH IIIA2/IIIB, LH IIIC?	1350/1300-1200/1190 BC, 1200/1190-1050/40 BC
Kokkolata-Menegata	B', Δ, E, Z, H	cist	MH III	1700-1550 BC
Kokkolata-Menegata	B''	cist	LH IIIC	1200/1190-1050/40 BC
Kokkolata-Menegata	Γ	shaft	LH IIIA2-IIIC?	1350-1050/40 BC?

The chamber tombs found share similarities with those seen on mainland Greece but also have a few features seen only in this area. The tombs vary in shape but in general the floor plan seem to be elliptical, rectangular or trapezoidal with a number of burial pits dug into the floor of the tombs (Souyoudzoglou-Haywood 1999). All of the tombs are preceded by a *dromos*, or passageway, that is tapered in shape, wider at the doorway (*stomion*) to the tomb than the beginning of the passageway. Variations among the stomia are found among the tombs at Mazarakata with different shaped lintels topping them (flat, rounded, triangular, and sloping). It is believed that the larger chamber tombs all had doors. A single stone slab, held in place by another slab was found at Mazarakata Π. Smaller tombs, such as Mazarakata A, may have had the doorways closed off using earth or a perishable material since no door was found. Some Mycenaean chamber tombs are found to have thresholds at the door, but at Mazarakata the end of the dromoi, the doorway and the chamber floor were all at the same height.

Ten of the tombs (A,B,Γ,E,I,K,Λ,M,N,O) are type IA tombs (Figure 6.2) (Souyoudzoglou-Haywood 1999). In these tombs, the burial pits are arranged along the dromos axis, though four tombs do not follow that convention. The roof of type IA is similar to the doorway. Larger type IA tombs at the site, such as Mazarakata N, show evidence of expansion and a new burial area was created at the side of the main chamber to accommodate the additional graves. Four tombs (Δ, H, Y, Π) are of the "cave dormitory" type (type II) with pits located on either side of a central path. These tombs have a square or rectangular plan and were never enlarged. The "cave dormitory" type seems to be limited to the Argostoli-Livatho area of the island and is unique to Kefalonia with no outside parallels. The site of Mazarakata has the earliest type II tombs suggesting it was possibly developed here and then spread to other sites.

The use of burial pits dug directly into the tomb chamber floor was a burial style unique to Kefalonia (Souyoudzoglou-Haywood 1999). Two shapes were used, either rectangular or oval. The burials represented are thought to be secondary burials where the bodies were first laid on the chamber floor and then moved into the pits. Kavvadias' notes from his excavation stated that all the grave goods were found in the pits and some had undisturbed burials, perhaps representing a single burial event (Souyoudzoglou-Haywood 1999). Some of the burial pits contained single individuals, but by the LH IIC, multiple individuals were interred within the graves.

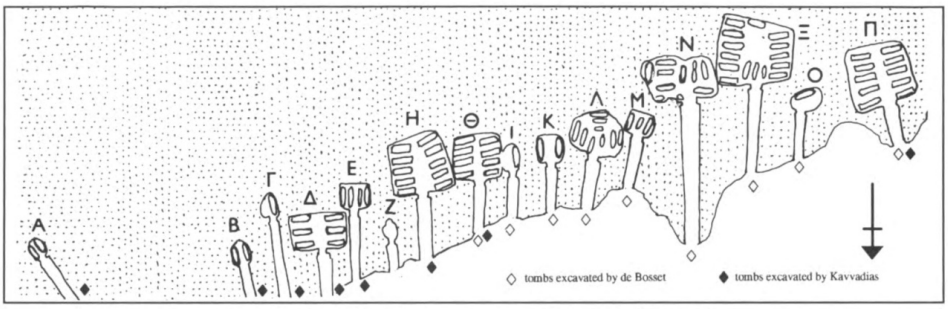

Figure 6.2. Plan of the tombs excavated at Mazarakata (from Souyoudzoglou-Haywood, 1999, p. 41, fig. 5). Not pictured is Tomb P, excavated by Marinatos in 1951.

The chamber tombs were dated using the pottery found within the graves (Souyoudzoglou-Haywood 1999). The earliest pottery dates to the LH IIIA2-B1. Vessels dating through the LH IIIC were found in all the tombs except for two (B and E) suggesting almost all the tombs were used throughout the Late Bronze Age. Other grave goods found, such as spearheads, knives, violin bow fibulas, pins, gold ornaments and bead, conuli, amber and glass beads are all representative of LBA types. Type IA tombs are thought to date earlier than the "cave dormitory" styles.

6.2.1.1 Bead types

There is some information about the vitreous beads found within the tombs though much of the detail centers on the Mycenaean style glass relief beads discovered. The vitreous finds all come from the chamber tombs since no artifacts were found within the tholoi at Mazarakata. Based on the material at the Archaeological Museum of Argostoli, various forms of both faience and glass beads were uncovered. Several types of Mycenaean relief beads were also excavated which dated to LH IIIA2-IIIC contexts (Souyoudzoglou-Haywood 1999). These bead types seem to be the ones with the most documentation and are described below.

6.2.1.1.1 Spiral

Eleven spiral relief beads of a pendant type thought to have been used in a necklace or diadem were uncovered. These bead types generally have two or three spirals with a rolled bar at one end where the perforation is located (Nightingale 2000) (Figure 6.3A). The other end is rounded. Seven of these beads were found at Mazarakata and have three spirals.

6.2.1.1.2 Single rosette

A group of single rosette beads was found all with a double perforation running along the center. In Mycenaean relief bead typology, it is referred to as Higgins type 1 (Higgins 1961; Souyoudzoglou-Haywood 1999). This is one of the more common Mycenaean relief bead types found. The rosette is represented as an eight petal flower that has a central depression and raised boss (Nightingale 2000) (Figure 6.3B).

6.2.1.1.3 Double and triple rosette

These are the most common relief bead type found on Kefalonia. The type with two rosettes and bars at either end are found at sites on mainland Greece (Nightingale 2000) (Figure 6.3C). The triple rosette relief bead, where the bead has no bars and the rosettes have six petals, is unique to Kefalonia (Figure 6.3D).

6.2.1.1.4 Bracket or curled leaf

This type corresponds to Higgins type 2 and is a common type (Higgins 1961) (Figure 6.3). It is not clear what the bead represents but it is often found with gold or glass discs attached to the bead using wires. Two of these relief bead types were found at Mazarakata (Souyoudzoglou-Haywood 1999). They are similar to beads found on mainland Greece but the Kefalonian style is much simpler. This bead type does not appear

as early in the tombs as the other relief beads and dates to the LHIIB-IIIC use of the burial chambers (Souyoudzoglou-Haywood 1999).

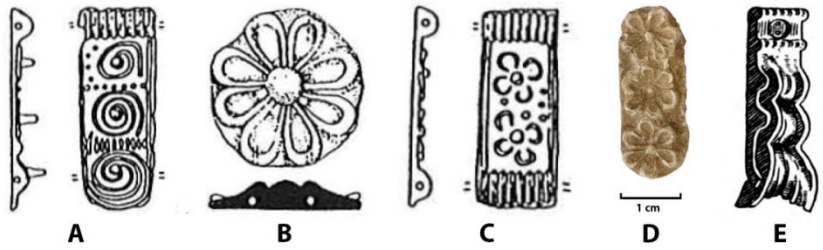

Figure 6.3. Mycenaean relief bead types found at Mazarakata: (A) Spiral (from Nightingale, 2000, p. 9, fig. 2.1); (B) Single rosette (from Nightingale, 2000, p. 8, fig. 1.1); (C) Double rosette (from Nightingale, 2000, p. 8, fig. 1.2); (D) Triple rosette (author's image-parallel from Metaxata); (E) Bracket or curled leaf (after Higgins 1961, p. 78, fig. 14d)

6.2.2 Metaxata

The site of Metaxata is located near the modern town of the same name, about 4 km southwest of Mazarakata (Figure 6.1). Six chamber tombs were found at the site through three different archaeological campaigns (Table 6.1). Marinatos excavated the site in 1933 uncovering three tombs (A,B,Γ), and then returned in 1960 where he discovered two more (Δ,E) (Souyoudzoglou-Haywood 1999). A final chamber tomb (Στ) was excavated in 1973 by the archaeologist P. Kalligas. Limited information exists on the tombs and the finds since only the first three tombs found in the 1930s were ever published.

The dates of the Metaxata tombs overlap with those at Mazarakata, ranging in date from LH IIIA2- IIIC (Souyoudzoglou-Haywood 1999; Voskos 2019). However only two of the tombs, B and Στ, had cultural material dating to this period. The other four tombs had artifacts only from the LH IIIC showing primarily a later use for this part of the cemetery. All the chamber tombs had been disturbed in antiquity, except for Γ (Souyoudzoglou-Haywood 1999).

Two different styles of chamber tombs are represented at the site (Souyoudzoglou-Haywood 1999). Like Mazarakata, Metaxata had tombs built in the "cave dormitory" style (type II) that is unique to Kefalonia. The four type II tombs (A, Δ, E, Στ) had rectangular chambers. The two other tombs, B and Γ, were of a form known as the "tholoid type" (type IB) with a circular chamber and an imitation of corbel vaulting to resemble the tholos tombs found on the mainland (Figure 6.4). As with most chamber tombs, the ones at Metaxata were all preceded by a dromos. Burials are not usually found in the dromos, but Γ had one, which was small in size suggesting a child's grave. The stomia varied in style across the tombs. Some had roughly cut entryways (B), possible doorframes (Γ) with one that may have been made of stone (A), and the remainder had straight-sided doorways.

The appearance of the different tomb types on Kefalonia has an interesting chronology and distribution. Tomb types IA and IB are found with pottery dating to the earlier portion of the Late Bronze Age, unlike type II tombs which predominately have LH IIIC pottery (Souyoudzoglou-Haywood 1999). As mentioned previously, the cave dormitory style has only been found in the Argostoli-Livatho area and all the cemeteries in this area contain this tomb type. Types IA and IB were found at other sites outside this area, however, both these tombs types were not present within the same cemetery. Souyoudzoglou-Haywood (1999) suggests that the choice of chamber tomb built exemplified different burial practices by different communities.

At the Metaxata cemetery, the individuals were buried in pits dug into the chamber floor. Like tomb type IA, IB also had rounded-shaped pits, though there is some disagreement as to whether the burials found within the pits represent secondary burials (Souyoudzoglou-Haywood 1999). Some have suggested that the

deceased were first laid on the chamber floor and then moved to the pits. Marinatos, who excavated both of the ones at Metaxata, thought the burial pits were used for primary burials. Several of the pits contained multiple individuals.

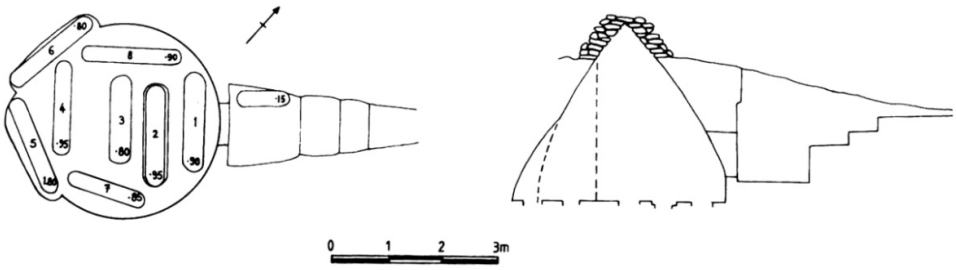

Figure 6.4. Example of a tholoid tomb (type IB). Plan and elevation drawing of Metaxata B (after Souyoudzoglou-Haywood, 1999, p. 52, fig. 8A)

Many of the pits are described in the summaries of the excavation as having dismembered remains, but this is likely due to disturbance of the pit to allow for the internment of an additional individual (Souyoudzoglou-Haywood et al. 2017). The disturbance of the graves has resulted in the mixing of grave goods, and therefore the dates and contexts of the finds are unclear in some cases. Brief summaries were written on the artifacts uncovered and it seems that they were similar to those found at Mazarakata. The excavated material includes pottery, bronze, conuli, and beads made of gold, amber, semi-precious stone, and glass (Marinatos 1933; Souyoudzoglou-Haywood 1999).

6.2.2.1 Bead types

Glass, and possibly faience, of different shapes and types were found in the chamber tombs (Marinatos 1933). Glass relief beads were also present and were found within chamber Tombs A, B, Γ with the majority of the relief beads coming from Metaxata B. The relief beads found (Souyoudzoglou-Haywood 1999) are described below.

6.2.2.1.1 Spiral

Seven relief beads with a spiral motif were found (Figure 6.3A). One was in Tomb A and the others were found in B.

6.2.2.1.2 Triple rosette

These beads were found in Tomb B and were the type with three rosettes, each with six petals, and no bar (Figure 6.3D). This type is local to Kefalonia and similar to the beads found at Mazarakata.

6.2.2.1.3 Bracket or curled leaf

Several fragments of relief beads that appear to be of this type were found (Figure 6.3E).

6.2.2.1.4 Ivy

These relief beads show two ivy leaves positioned between rolled bars located at each end (Nightingale 2008) (Figure 6.5A). Parallels to this type are found at Mycenaean sites on the mainland. The ivy beads found come from Metaxata B.

6.2.2.1.5 Waz-lily

This bead style is not a plaque but appears as a “cut out” (Souyoudzoglou-Haywood 1999, 83). The type (Higgins type 16) is common and thought to be of Egyptian origin (Higgins 1961), with examples found as early as the 17th c. BC on Crete. The motif is described as a hybrid of an Egyptian papyrus (“waz”) and a lily (Higgins 1961, 83). The ones from Metaxata were found in Tholos B.

6.2.2.1.6 Volute with bar

One of these relief beads was found in Tholos B. This type corresponds to Higgins type 3 (Higgins 1961; Souyoudzoglou-Haywood 1999). The motif is represented by a volute that is suspended from a bar (Figure 6.5C) (Nightingale 2000).

6.2.2.1.7 Double figure of eight shield

This motif, Higgins type 28, is considered to be of Minoan origin (Higgins 1961). The motif can be found as a cut out or on a plaque with rolled bars at either end that are perforated (Figure 6.5D). Only one bead, found in Tomb B, has been published (Souyoudzoglou-Haywood 1999).

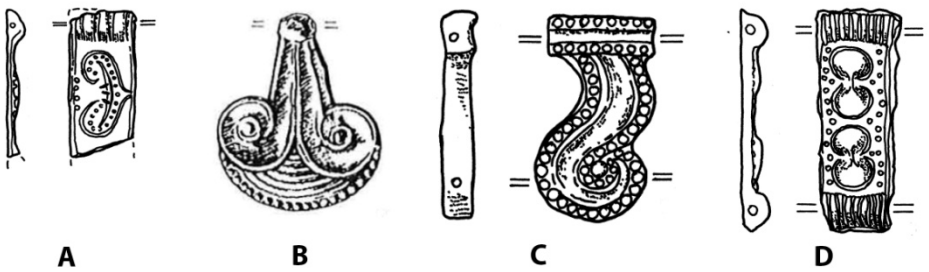

Figure 6.5. Some of the Mycenaean relief bead types found at Metaxata: (A) Ivy (after Nightingale 2008, 69, fig. 4.3.5); (B) Waz-lily (after Nightingale 2000, 8, fig. 1.5); (C) Volute with bar (after Nightingale 2008, 70, fig. 4.4.5) (D) Double figure of eight shield (from Nightingale 2008, 70, fig. 4.4.3)

6.2.3 Kokkolata-Kangelisses (Kokkolata-Menegata)

The cemetery referred to as Kokkolata-Kangelisses (Souyoudzoglou-Haywood, 1999) was found on the rocky plateau of Kangelisses across from the modern town of Kokkolata-Argostoliou. It is located about six kilometers from Argostoli and just north of Mazarakata and Metaxata (Figure 6.1). The cemetery is also referred to as Kokkolata-Menegata in the records of the Archaeological Museum of Argostoli. From here on it will be referred to with that name for consistency with the information in the museum.

Excavations at the site by Kavvadias (1913) in 1909 revealed that several burial types were found at the site, some dating back the MH III period (Table 6.1). The discovery of these 16th-13th c BC tombs makes Kokkolata-Menegata the oldest cemetery on the island. Burials continued through the LH IIIC period (Souyoudzoglou-Haywood 1999). The six MH III tombs (B', B'', Δ, E, Z, H) are slab cist-types (Figure 6.6) (Kavvadias 1913; Souyoudzoglou-Haywood 1999; Voskos 2019). They were built with large, roughly cut stones and some had covering slabs. The cist graves contained pottery as grave goods, and one grave also had a bronze knife (Kavvadias 1913; Souyoudzoglou-Haywood 1999). The number of vessels in each grave may suggest the presence of multiple burials. Two Middle Helladic settlements were discovered nearby at Kokkolata-Junction and Kokkolata-Kourapata with similar types of pottery (Souyoudzoglou-Haywood 1999). It is possible there is a connection between those in the settlements and those buried in the cemetery.

In the Late Bronze Age, the tomb forms expanded to include two tholoi and pit graves (Figure 6.6) (Kavvadias 1913; Souyoudzoglou-Haywood 1999; Voskos 2019). The tholoi were located next to each other and were free standing, unlike at Mazarakata where the tholos was carved into the rock (Souyoudzoglou-Haywood 1999). Tholos B was built over one of the earlier MHIII graves (Kavvadias 1913). Only the lowest courses of the tholoi were preserved. The style was similar to others found on the island and share similarities with those found on the mainland. Both tholoi seem to have been used during the same time period. Based on the pottery, the first burials date to the LH IIIA2-LH IIIB and internments continued through the LH IIIC period.

Tholos A had two burials (Λ, Κ) which were dug into the chamber floor (Souyoudzoglou-Haywood 1999). No details of the pits were published but only a description that the pits were "very deep". (Souyoudzoglou-Haywood 1999, 58). Grave goods included pottery, seal stones, gold and copper alloy objects, steatite

buttons, and sardonyx and glass beads. The pottery types found suggests tholos A was built during the LH IIIA2 or IIIB period and was used for some time during the LH IIIC period.

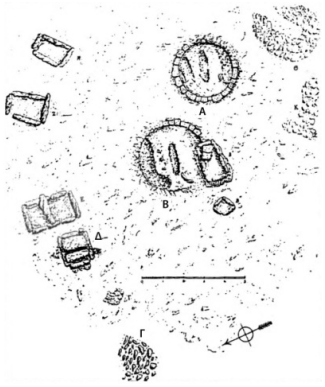

Figure 6.6. Plan of the cemetery at Kokkolata-Menegata (Kangelisses) showing the MH III cist graves, the LH III tholoi, and the LH III pit graves (after Souyoudzoglou-Haywood 1999, p. 39).

Tholos B had three burials in the chamber floor (M, P, Ψ) (Souyoudzoglou-Haywood 1999). As with tholos A, details of the pits were not published but burial Ψ was described as being shallow. Grave goods were also found within the graves. These included a large number of ceramic vessels, some that were handmade. The graves also contained seal stones, stone and clay conuli, biconical beads made of argyradmas (the mineral smaragdite), and glass beads.

Several pit graves (Γ) were found outside the tholoi in an area rocky area (Kavvadias 1913; Souyoudzoglou-Haywood 1999; Alivizatou 2017).The burials were placed within pits roughly cut into the rock or into existing crevices. The grave goods included pottery as well as a bronze knife, gold hair spirals, seals, conuli and beads of gold, stone and glass (Kavvadias 1913; Souyoudzoglou-Haywood 1999). The earliest of these graves dates to the LHIII A2. Burials continued through LH IIIC and were contemporaneous with the use of the tholoi. As to why these individuals were buried outside the tholoi is unclear. A "hierarchical explanation" between those in the tholoi and those outside has been offered (Souyoudzoglou-Haywood 1999, 58). Three cairn structures were found in the area outside the tholoi. Although the purpose is unknown, it has been suggested that they may be monuments associated with the tombs.

6.2.3.1 Bead types

Different bead forms were found within the tombs, including circular, ovoid and relief beads (Kavvadias 1913; Marinatos 1952; Alivizatou 2017). The majority of the beads were found in Tholos B (Kavvadias 1913; Souyoudzoglou-Haywood 1999). However, Kavvadias (1913, 259, 266) published glass beads from tholos A and relief beads from the pit tombs (Γ). The following are the relief beads he excavated described by Souyoudzoglou-Haywood (1999, 83-84).

6.2.3.1.1 Single rosette

Single rosette relief beads, similar to those from the Mazarakata cemetery (Figure 6.3A).

6.2.3.1.2 Bracket or curled leaf

These beads come from the pit graves and are similar to those found at Mazarakata (Figure 6.3E).

6.2.3.1.3 Beaded circle

Twenty-four of these bead types were found in Tholos B. The center of the bead is a boss surrounded by a circle or raised dots similar to granulation (Figure 6.7A). There are rolled bars at either end. The form has no exact parallels outside of Kefalonia (Souyoudzoglou-Haywood 1999). Some types of circular beads with raised dots have been found at other sites (Figure 6.7B,C), but this particular motif is rare (Nightingale 2000, 9, fig. 23, 25). The Kefalonia type beaded circle appears to have some aspects of the beaded circle relief

beads found at other sites incorporated into its form. Souyoudzoglou-Haywood (1999, 83) describes this particular type as being found only at Kokkolata-Menegata, however the beads look very similar to beads at the Archaeological Museum of Argostoli that are labeled as having been excavated from Mazarakata by Marinatos in 1951 (Appendix C.1, nos. M23-4, M23-5). The bead shape may not be unique to the site of Kokkolata-Menegata, or the beads at the museum are mislabeled.

6.2.3.1.4 Cylindrical beads

In addition to the relief plaques described above, short cylindrical beads with an incised hatched pattern were discovered (Souyoudzoglou-Haywood 1999). These were only found at Kokkolata-Menegata and no other sites on the island.

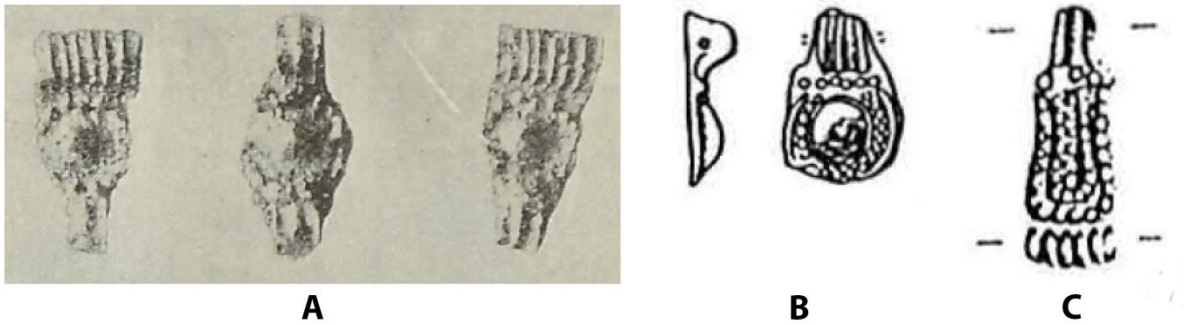

Figure 6.7. (A) Beaded circle relief beads found at Kokkolata-Menegata (after Kavvadias 1913, 262, fig. 39); Beaded circle relief bead types found at other Mycenaean sites: (B) Circular bead with granules (from Nightingale 2000, 9, fig. 2.3); (C) Bead with rib or dot pattern (from Nightingale 2000, 9, fig. 2.5)

6.3 DESCRIPTION OF THE SAMPLES

Several groups of Late Bronze Age vitreous beads from the sites of Mazarakata, Metaxata and Kokkolata-Menegata, currently housed in the collection of the Archaeological Museum of Argostoli, were made available for examination and analysis. The group analyzed represents only a portion of the vitreous beads discovered by Kavvadias and Marinatos. None of these beads have previously undergone any kind of instrumental analysis. Due to incomplete excavations records, few publications, and the loss of documentation and artifacts during an earthquake in 1953, information about the exact archaeological context of many of the beads cannot be found. Below is a general description of the collection. A detailed catalog, including some archaeological information, descriptions, and dimensions can be found in Alivizatou (2017).

6.3.1 Mazarakata

The cultural material analyzed from this site may come from Marinatos' 1951 excavations at Mazarakata. In the museum records, the boxes are annotated as “Marinatos 1951”. There are no further details regarding the context of the finds but likely come from chamber Tomb P which Marinatos excavated (Souyoudzoglou-Haywood 1999). Although Marinatos (1952, 184) did not publish images of the vitreous finds from this tomb, he does mention that glass beads of various types were found, including relief beads. No additional details on the beads are provided except that they are all given the date “LHIII” in the museum records. The artifacts include glass and faience beads, in addition to an unidentified chunk of glass (Table 6.2, Appendix C.1).

6.3.1.1 Box M18

A box containing about 18 circular beads with varied in size. Most of the beads are blue, though other colors are found. The condition of the beads varies. Pitting and iridescence are observed. Some of the beads have been repaired. Some are heavily corroded. The beads have been strung together on a modern nylon thread.

6.3.1.2 Box M23

A box containing 23 relief beads either dark blue or lighter blue in color. The beads are in varying states of preservation. Most are not complete and very pitted and deteriorated. It is difficult to make out the motif on the beads, but they appear to be spirals or rosettes. One light blue relief bead appears to have 3 rosettes. The other beads, which are darker blue in color, seem to have a single rosette or spiral with bars. The beaded circle bead type is also represented, similar in appearance to those from Kokkolata-Menegata (Figure 6.7A). A few of these beads have bars of varying widths, though it is unclear if that is intentional or due to damage.

One item in the box is of an unusual shape and not a relief bead. It is ovoid and has two rounded sides, one with some kind of raised decoration. The bead is heavier than those made of glass are and is brown in color. It did not appear to be made of glass and therefore was not included in the analysis.

6.3.1.3 Box M32

Box containing about 30 beads and bead fragments. This box contains various bead types. Simple circular beads are represented in addition to some ovoid and pendant forms. Some of the beads appear to be faience with loss of the glaze. There are three relief beads. One is a beaded circle but does not resemble the type in Box 23 or those from Kokkolata-Menegata. It is more like the examples of beaded circles from other sites shown in Figure 6.7B. The majority of these beads are blue. The beads are in various stages of preservation but most have the majority of the bead shape preserved. The beads are pitted and many are iridescent. Others have thicker corrosion layers.

6.3.1.4 Box M32R

A second box was labeled "32" and contained single rosette relief beads. Some of the beads are fragmentary so it is not clear how many there are in total, but there are at least 15. The beads are dark blue in color and have two perforations. The surfaces of the beads are pitted and most are iridescent with some being more corroded. The museum label accompanying the box says that the rosettes were floor finds, perhaps meaning they were found scattered on the floor of a grave or tomb. To differentiate between the two boxes, the beads analyzed from this box were designated as "M32R" during analysis (R for rosette).

6.3.1.5 Box M40

This box contained nine glass bead fragments. From the fragments preserved, the majority of the beads appear to be simple round beads. One bead may be a small fragment of a relief bead. It has a small piece of gilding or gold foil associated with it. Most of the beads are blue in color, of varying shades. Two of the beads are very dark in color and appear almost black. The beads are not only fragmentary but also vary in condition. Most are pitted and iridescent. Two are very corroded. Associated with this box is a chunk of translucent purple glass that has some kind of crust or corrosion on one side. It is not clear what type of artifact it is. It is possible that this is a fragment from a larger glass object. However, the altered surface is relatively flat and resembles a fragment of raw glass.

6.3.2 Metaxata

The beads analyzed possibly come from Marinatos' 1933 excavation of Metaxata. The museum records state that the beads come from Tomb B8 and that they are from the LH III period. The tomb was used from the LH IIIA2-IIIC periods, so it is not clear what the exact dates of Tomb B8 is. A published photograph of relief beads from Tomb B, with an annotation in the photos “B8” resemble those in the boxes described below (Marinatos 1933, 91, pl. 3). The study group consists of three types of relief plaques (Table 6.2, Appendix C.1). Some of the museum numbers accompanying the boxes seem to repeat which makes the context and association with the excavation information unclear.

6.3.2.1 Box 1615

This box contains 13 double ivy plaques. These plaques have separated from the other Metaxata plaques because they were on display in the museum at some point. The plaques are made of dark blue glass. They have two ivy leaves and a rolled bar at either end. The bars are perforated. The glass is covered with of layer of white opaque corrosion. Most of the plaques are complete and some are intact with very little loss. Seven show signs of previous repair. The adhesive used to join the fragments has yellowed and excess adhesive is visible on the surface. Two of them have numbers written on the back in black ink.

6.3.2.2 Box 1616

This box contains 12 triple rosette (Kefalonian type) plaques. These plaques have separated from the other Metaxata plaques because they were on display in the museum at some point. The plaques are made of a pale blue glass, which appears slightly opaque. The glass is covered by a layer of white opaque corrosion with some darker patches over that. Most of the plaques are complete and some intact with very little loss. Three of the plaques are fragmentary and have been reconstructed. The adhesive has yellowed. Three of the reconstructed plaques are missing a small section at the end. The number "1616" is written in black ink on the back of one of the plaques.

6.3.2.3 Box K13

The box contained nine relief plaques or fragments of them. Four of the relief plaques appear to be of the Kefalonia triple rosette type. Two additional fragments show a rosette with a rolled bar. The other three fragments only preserved parts of rosettes and the ends are not visible, so it is not clear which motif it is. All the plaques are corroded and covered with a layer of white glass corrosion. This box comes from drawer "K13, 1616-1618". Two of the beads have the number "1616" written on the back. It is not clear what the "1618" refers to, whether bead numbers 1616 through 1618 are represented or whether the two beads with numbers are 1616 and the other two are 1618. The only other documentation available for these beads stated they come from Grave B8 (Figure 6.4B).

6.3.3 Kokkolata-Menegata

The beads analyzed were in two boxes containing circular or ovoid vitreous beads; however, none are relief beads (Appendix C.1). The museum information accompanying the boxes dates them to the LH III. It is not clear in which tombs the beads were found. For beads 580.2, the museum records state that they come from "Tholos, Grave 1" but the label did not list which tholos. Souyoudzoglou-Haywood (1999, 40) notes a small find number, A580, in the description of the cultural material found in Tholos B, and this may include beads 580.2. A label accompanying box Σ2-K1 states the beads come from Grave Δ, which would be one of the MH III cist tombs (Figure 6.6). Souyoudzoglou-Haywood (1999, 39) mentions that the pottery from the cist tombs in the Archaeological Museum of Argostoli come from four of the tombs (A- Δ), however she states that the grave designations in the museum records do not match those in Kavvadias' publication. It is not clear if this is the same situation with the beads in box Σ2-K1. It should also be noted that in Souyoudzoglou-Haywood's (1999, 39) description of the finds from the cist tombs, and the published photos of the beads by Kavvadias (1913), there is no mention of vitreous beads from those graves. Only pottery and one bronze knife were described. (Souyoudzoglou-Haywood 1999, 39). Therefore, the context of the Σ2-K1 beads is unknown. The collection consists of simple bead forms and includes stone, glass, and possibly faience beads (Table 6.2).

6.3.3.1 Box Σ2-K1

A box containing seven beads made of stone and vitreous materials. There are two standard circular beads made of glass, one blue and one green. There are two ribbed biconical beads (Nightingale 2000, 9, fig. 2.15) that may be faience, though identification of the material visually is difficult due to the layer of white, opaque glass corrosion on the surface. There are two stone beads present. One is a translucent white color and the other an opaque white rectangular bead. The final bead is made of dark blue glass and cylindrical.

The beads are in fairly good condition but do show some signs of deterioration. The glass beads appear pitted with some slight iridescence in areas. The ribbed biconical beads are covered with a layer of corrosion. The stone beads are chipped and pitted. The rectangular bead has a slightly powdery surface. All beads show some small areas of loss and abrasions.

6.3.3.2 Box 580-2

A box containing 67 beads all strung on a modern cotton cord. The majority of the beads are small, circular beads made of blue glass. These beads show very little signs of deterioration. Three beads are different in shape and color. One is cylindrical and opaque green. It is heavily pitted and iridescent. Next to this bead is a blue one with a layer of corrosion and iridescence on the surface. The third bead is a pale green disc bead.

Table 6.2. Description of bead groups excavated from the sites of Mazarakata, Metaxata, and Kokkolata-Menegata that are housed in the collection of the Archaeological Museum of Argostoli.

Site	Inventory No.	Material	Quantity	Shape
Mazarakata	M18	glass	18	globular beads
Mazarakata	M23	glass	23	relief beads
Mazarakata	M23	iron?	1	globular bead
Mazarakata	M32	glass	10	globular beads
Mazarakata	M32	glass	5	elliptical grooved beads
Mazarakata	M32	glass	1	teardrop pendant
Mazarakata	M32	faience?	11	elliptical grooved beads
Mazarakata	M32	glass	20	single rosette relief beads
Mazarakata	M40	glass	9	globular beads
Metaxata	K13 (1616-1618)	glass	9	relief beads
Metaxata	1615	glass	13	double ivy relief beads
Metaxata	1616	glass	12	triple rosette relief beads
Kokkolata-Menegata	Σ2-K1	glass	2	globular beads
Kokkolata-Menegata	Σ2-K1	glass	1	ellipsoidal bead
Kokkolata-Menegata	Σ2-K1	stone	1	globular bead
Kokkolata-Menegata	Σ2-K1	stone	1	rectangular bead
Kokkolata-Menegata	Σ2-K1	faience	2	biconical, grooved beads
Kokkolata-Menegata	580.2	glass	66	annular beads
Kokkolata-Menegata	580.2	glass	1	disc bead

6.4 RESULTS AND DISCUSSION

6.4.1 Glass

6.4.1.1 Raw materials-Alkali flux

Thirteen of the beads analyzed are plant ash glasses with compositions typical for the Late Bronze Age (Table 6.3, Figure 6.8) (Nicholson 2007; Henderson 2012; Shortland 2012). The average composition of this group is 67.1 wt% SiO_2, 17.0 wt% Na_2O, 1.72 wt% K_2O, 3.36 wt% MgO, 1.74 wt% Al_2O_3, 6.75 wt% CaO. The purple chunk of glass, M40-P, has an overall composition that also falls within the typical values of Late Bronze Age plant ash glasses and is similar to the beads found at the three sites. Two beads, M40-1 and M40-6, are deteriorated and depleted in soda, potash, magnesia, and lime, with elevated levels of silica. The original composition of these beads could not be determined due to the level of weathering.

Six beads from Mazarakata (M23-2, M23-6, M23-7, M32-1, M32-9, M32-4R) have potash values that are at the lower end of the average concentrations expected (1.04-1.37 wt%). All these beads are blue in color, with five of them colored dark blue using a combination of cobalt and copper (Tables 6.3, 6.4). The low levels of potash in the cobalt containing glasses falls within the pattern observed for other cobalt colored glasses that contain levels of potash below 2% (Shortland and Tite 2000; Rehren 2001; Nicholson 2007).

Table 6.3. Results of EPMA analysis. The results are given as weight % (wt%) oxide and represent the average of three areas analyzed on each sample.

Sample No.	Site	Na_2O	K_2O	MgO	Al_2O_3	CaO	SiO_2	FeO	MnO	CuO	P_2O5	TiO_2	Total
Faience													
Blue, opaque													
Σ2-K1-4	Kokkolata	11.27	0.77	0.48	1.19	1.10	72.00	4.85	n.d.	3.12	0.07	0.68	95.53
Glass													
Blue													
M23-6	Mazarakata	18.18	1.04	1.95	1.38	5.32	70.15	0.48	n.d.[1]	1.01	0.09	0.08	99.69
M40-4	Mazarakata	16.64	3.22	4.68	1.25	6.66	65.18	0.34	0.03	1.15	0.17	n.d.	99.32
M40-1 blue	Mazarakata	0.08	0.08	0.19	1.51	1.07	82.19	0.67	n.d.	1.64	n.d.	0.12	87.54
M40-1 green	Mazarakata	0.06	0.05	0.19	1.47	1.20	65.61	0.72	n.d.	12.56	n.d.	0.13	81.98
M40-6 blue	Mazarakata	n.d.	n.d.	0.12	0.84	1.20	81.98	0.36	n.d.	1.53	n.d.	0.09	86.12
M40-6 green	Mazarakata	n.d.	n.d.	n.d.	0.84	0.67	84.18	0.38	n.d.	1.19	n.d	n.d.	87.39
580.2-1	Kokkolata	6.13	10.70	0.45	2.76	1.05	75.27	0.57	n.d.	2.71	0.09	0.13	99.85
580.2-2	Kokkolata	17.01	1.01	1.33	1.16	7.55	67.15	0.61	n.d.	3.20	0.16	0.07	99.24
Σ2-K1-1	Kokkolata	16.62	2.53	4.73	1.72	4.77	68.16	0.70	n.d.	n.d.	0.15	0.07	99.46
Dark blue													
M23-2	Mazarakata	17.16	1.14	3.26	2.67	7.58	66.48	0.54	0.14	0.08	0.19	0.08	99.30
M23-7	Mazarakata	17.20	1.06	3.13	2.35	6.86	67.56	0.73	0.17	n.d.	0.22	0.15	99.43
M32-1	Mazarakata	16.70	1.27	3.51	2.70	8.25	64.87	0.75	0.16	n.d.	0.22	0.16	98.59
M32-9	Mazarakata	16.61	1.23	2.93	2.18	7.93	67.30	0.48	0.12	0.14	0.22	0.11	99.24
M32-4R	Mazarakata	16.47	1.13	2.83	2.08	7.81	67.71	0.46	0.10	n.d.	0.22	0.09	98.91
580.2-3	Kokkolata	17.18	1.58	2.82	2.04	6.73	67.21	0.64	0.11	0.48	0.17	0.11	99.08
Blue, opaque													
K13-4	Metaxata	16.81	1.67	3.24	2.50	6.05	67.10	0.87	0.12	0.49	0.18	0.16	99.18
Purple/black													
M40-5	Mazarakata	19.28	2.61	3.51	0.70	6.67	64.78	0.68	0.53	n.d.	0.39	n.d.	99.14
M40-P	Mazarakata	16.24	2.15	4.15	0.61	8.09	66.83	0.35	0.26	n.d.	0.31	n.d.	99.00
Pink													
M18-3	Mazarakata	16.52	2.50	4.91	1.00	4.19	69.50	0.41	n.d.	n.d.	0.14	0.08	99.26

[1]n.d. - not detected

One bead from Kokkolata-Menegata, 580.2-1 has high potash (10.70 wt%), low soda (6.13 wt%), low magnesia (0.45 wt%), and low lime (1.05 wt%). It is a mixed alkali LMHK glass. The concentrations of potash and magnesia found are comparable to mixed-alkali glasses from Frattesina in northern Italy and the Mycenaean mixed-alkali glasses found at the site of Elateia on mainland Greece (Brill 1992; Nikita and Henderson 2006; Henderson et al. 2015). This could suggest they used the same type of alkali. Bead 580.2-1 was stored at the museum, strung on a cord with about 64 similar looking beads in color and shape (Appendix C.1). It is possible that these other beads may also be LMHK beads; however, analysis would be required to confirm this.

The mixed-alkali glasses from Elateia are some of the earliest LMHK glasses found on the Greek mainland. The majority come from LH IIIB-IIIC contexts (1340/1330-1065-60 BC), with one bead dated earlier (late 15th-early 14th c. BC) (Nikita and Henderson 2006). Early mixed-alkali glass beads from Late Bronze Age contexts (1200-1100 BC) were also found in the north Aegean, on the island of Thasos. These represent the earliest examples of this type of glass, and those found farthest east (Henderson 1992). From the Thasos group, bead 3 from the site of Theologos-Tsiganadika is similar in composition to the Kefalonia mixed-alkali bead (Henderson 1992, 805-806, table 1). No specific dates are given for the grave bead 580.2-1 found

within, but Tholos B at Kokkolata-Menegata was in use during the LH IIIA2/LH IIIB periods (ca. 1350/1330-1200/1190 BC) and possibly the LH IIIC as well (ca. 1200/1190-1050/40 BC) (Souyoudzoglou-Haywood 1999; Voskos 2019). This makes the Kefalonian LMHK bead, along with those from Elateia and the one from Thasos, some of the earliest examples of this glass technology.

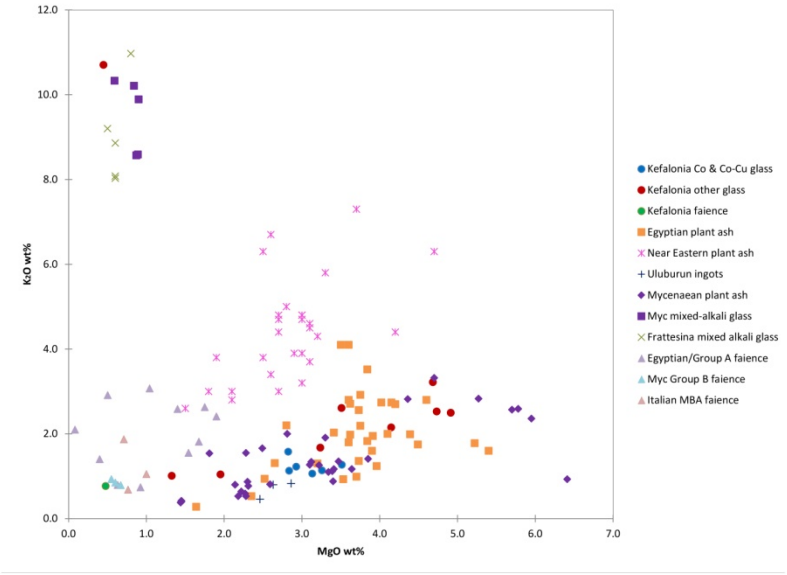

Figure 6.8. Biplot of alkali components MgO and K_2O in the Kefalonia samples compared to glass and faience from Egypt (Shortland and Eremin 2006; Tite et al. 2008; Kaczmarczyk and Vandiver 2008), the Near East (Shortland and Eremin, 2006), Mycenaean sites (Nikita and Henderson 2006; Tite et al. 2008; Smirniou and Rehren 2013), Frattesina (Henderson et al. 2015), Italian MBA faience (Tite et al. 2008) and ingots from the Uluburun shipwreck (Jackson and Nicholson, 2010).

The alkali flux used for the glasses was further investigated by looking at the values of lime and potassium pentoxide. In plant ash glasses, the magnesia and lime are contributed by the plant ash (Barkoudah and Henderson 2006), and therefore looking at these two oxides could provide additional information on whether different sources of plant ashes were used. The concentrations of magnesia and lime in the Kefalonia glasses were compared to plant ash glasses from Egypt, the Near East and Mycenaean Greece, as well as mixed alkali glasses from Mycenaean Greece and Frattesina (Figure 6.9) (Shortland and Eremin 2006; Nikita and Henderson 2006; Smirniou et al. 2009; Walton et al. 2009; Henderson et al. 2015). Two clear groups are formed between the glasses made with the plant ash alkali and the mixed alkali glasses. This is to be expected since mixed-alkali glasses are lower in lime and are made using a different alkali, possibly a mineral alkali or a purer plant ash with low magnesia and lime (Henderson 2013). The mixed alkali glasses seem to split into two groups. One group, with both lower lime and magnesia, includes the Kefalonian mixed alkali bead, 580.2-1, as well as glasses from Elateia and Frattesina. The other mixed alkali glasses are all from Elateia. The two groupings point to the use of a different source for the lime and magnesia that is contributing the composition. In the case of each mixed alkali subgroup, the clustering and the lack of variation in the concentrations could point to a very specific source used. The group that contains only mixed-alkali glasses from Elateia could point to the glasses being made as a batch using the same glass melt (Henderson 2013, 193).

In the case of the plant ash glasses, the lime and magnesia content of the Egyptian and Mycenaean glasses appear to be positively correlated. The Kefalonia cobalt and Co-Cu glasses follow a similar pattern. Several of the Mycenaean plant ash glasses have magnesia and lime values lower that most of the Egyptian plant ashes. A group with three Mycenaean plant ash glasses with the lowest magnesia (1.44-1.45 wt%) and lime concentrations (4.11-4.42 wt%) were excavated from the site of Elateia (Nikita and Henderson 2006). Another group of four glasses consisting of the next lowest concentrations of both these oxides (2.18-2.31

wt% MgO, 5.15-5.29 wt% CaO) were excavated from Thebes. The same plant ash—and the same glass batch—were likely used for the flux for each of the groups. A cluster is also formed by the Kefalonian cobalt and Co-Cu glasses, and may point to the beads being made from the same batch of raw glass or at least having been made using the same plant ash source.

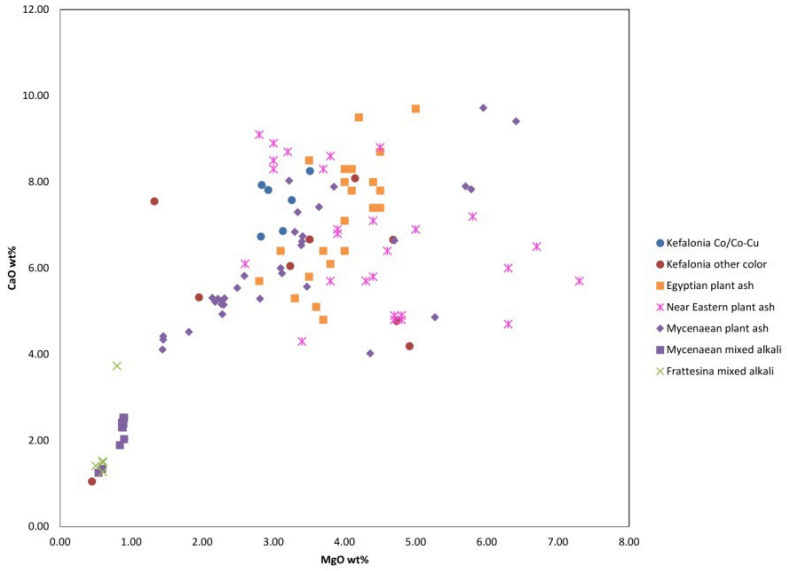

Figure 6.9. Biplot of alkali components MgO and CaO in the Kefalonia glass samples compared to glasses from Egypt (Shortland and Eremin 2006), the Near East (Shortland and Eremin, 2006), Mycenaean Greece (Nikita and Henderson 2006; Smirniou et al. 2009; Walton et al. 2009), and Frattesina (Henderson et al. 2015).

The other Mycenaean glasses overlap with Egyptian samples and so they may have used a similar type of plant ash as the flux. The non-cobalt containing Kefalonian glasses appear to have variation among the plant ashes used for the alkali. They do not follow the positive correlation as closely and have a wider range of concentrations, in particular, of magnesia. This could mean different plant ash genera or plants from different geographic areas were used in the production. The Near Eastern glasses are similar in their pattern to the non-cobalt colored Kefalonian glasses where they do not follow the correlation line. This again may point to greater variation among the plant ashes used or perhaps another source is contributing to the lime and magnesia concentrations.

The concentrations of potash and phosphorus pentoxide can also provide information on the alkali flux used. The relationship between these two oxides in the Kefalonian samples, as well as glasses from Egypt, the Near East and Mycenaean Greece, as well as mixed alkali glasses from Mycenaean Greece and Frattesina were examined (Shortland and Eremin 2006; Nikita and Henderson 2006; Smirniou et al. 2009; Walton et al. 2009; Henderson et al. 2015). Again, two distinct groups are observed, between the plant ash glasses and the mixed alkali glasses based on the concentrations of potash (Figure 6.10). The phosphorus pentoxide values for the mixed alkali glasses are in a somewhat similar range as the plant ash glasses, but they are differentiated by the potash content that is much higher in the LMHK glasses. Among the mixed-alkali glasses, there again seems to be a distinction between the glasses from Elateia. Therefore, each subgroup was likely made with a different source of alkali flux—perhaps a different type of plant harvested or from an area with a distinct soil geochemistry.

Among the plant ash glasses, there seems to be some variation among the particular plant ashes used for the Egyptian glasses that exhibit a range of phosphorus pentoxide concentrations. There is some overlap between some of the Egyptian and Mycenaean plant ash glasses but again there are some distinct groups formed. One group consists of eight samples from Thebes with 0.53-1.41 wt% K_2O and 0.14-0.28 P_2O_5 (Nikita and Henderson 2006). The plant ashes used to make this group are different from those used in Egypt

and the Near East. The similarities among the concentrations of these two oxides, as well as the lime and magnesia concentrations, support the idea that these glasses were made with the same source of plant ash, and likely the same batch of raw glass. The plant ashes are of a type or from a source that is distinct from other Mycenaean and Egyptian glasses.

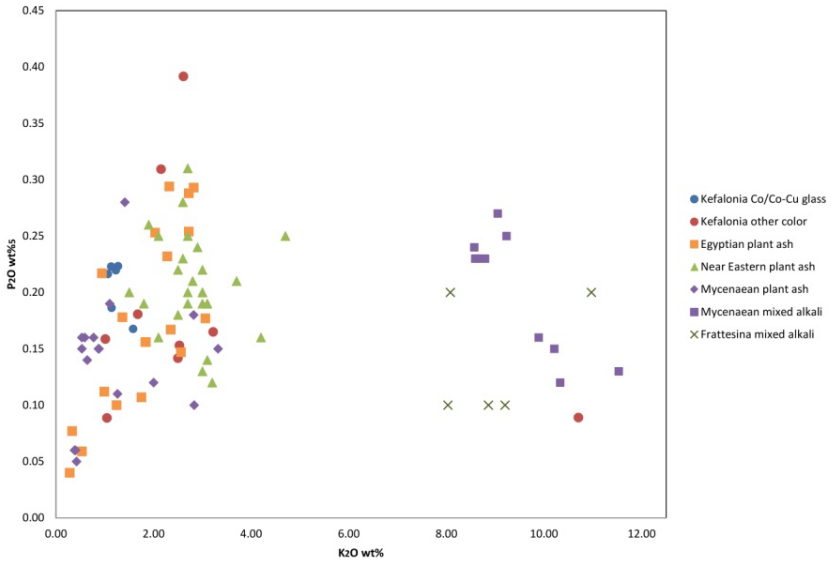

Figure 6.10. Biplot of alkali components K_2O and P_2O_5 in the Kefalonia glass samples compared to glasses from Egypt (Nicholson 2007), the Near East (Shortland and Eremin, 2006), Mycenaean Greece (Nikita and Henderson 2006), and Frattesina (Henderson et al. 2015).

A discrete group is also made by four of the relief beads from Mazarakata (M23-7, M32-1, M32-9, M32-4R). They have potash concentrations in the range of 1.06-1.27 wt% and 0.216-0.223 wt% phosphorus pentoxide (Table 6.3). The grouping of these beads point to the likely use of the same source of plant ash, and they were also possibly made as a batch. The non-cobalt colored Kefalonian glasses show more variation in the source of plant ash used in regards to these two oxides. The two samples of purple glass, M40-5 and M40-P, have the highest concentrations of phosphorus pentoxide among the Kefalonian samples. M40-5 had the highest concentration of this oxide than all the comparative samples. These glasses appear to have been made with a plant ash that was different from that used for the other Kefalonian glasses and also different for each of the purple glasses, either in the type of plant used to make the ash or its geographic location.

6.4.1.2 Raw materials-Colorants

Initial identification of the mineral colorants and any opacifiers used in the manufacture of the glass beads was determined using pXRF for a large part of the museum collection examined (Table 6.4). Only a small group of glass beads could be sampled for quantitative analysis so this group provided additional quantitative information on colorants and opacifiers. The terms used to describe the beads were based on the initial surface examination of the beads under magnification. However, for many of the beads, the surface deterioration, iridescence, or corrosion layers made identifying the actual color of the glass difficult. For beads that were sampled, the original color and opacity could be determined by examining the glass with transmitted light.

6.4.1.2.1 Copper blue

Eleven blue beads and one blue-green bead (M18-2, M18-5, M18-6, M18-7, M23-6, M40-1, M40-2, M40-3, M40-4, M40-6, 580.2-1, 580.2-2) had large peaks for copper, which is the source of their color (Table 6.4). All are globular or annular beads except for M23-6 and M40-3, which are both relief beads from Mazarakata. The motif on M23-6 is not very clear due to the level of pitting and deterioration on the surface. The

fragment of relief bead M40-3 appears to have a raised circle and a line or raised dots resembling the beaded circle relief beads from Kokkolata-Menegata (Figure 6.7A).

Table 6.4. Results of pXRF qualitative analysis.

Sample No.	Site	Elements detected
Blue[1]		
M18-2	Mazarakata	Al, Si, S, K, Ca, Ti, Mn, Fe, Ni, Cu, Zn, Pb, Rb, Sr, Zr, Sn?[2]
M18-5	Mazarakata	Al, Si, S, K, Ca, Ti, Mn, Fe, Ni, Cu, Pb, Rb, Sr, Y, Zr
M18-6	Mazarakata	Al, Si, S, K, Ca, Ti, Mn, Fe, Ni, Cu, Pb, Rb, Sr, Zr
M18-7	Mazarakata	Al, Si, S, K, Ca, Ti, Mn, Fe, Ni, Cu, Zn, Pb, Sr, Zr
M40-1	Mazarakata	Al, Si, P, S, K, Ca, Ti, Mn, Fe, Ni, Cu, Zn, Pb, Sr, Zr
M40-2	Mazarakata	Al, Si, P, S, K, Ca, Ti, Cr, Mn, Fe, Ni, Cu, Zn, Pb, Sr, Zr, Sn, Sb
M40-3	Mazarakata	Al, Si, S, K, Ca, Ti, Cr, Mn, Fe, Cu, Zn, Pb, Sr, Zr
M40-3 gold foil	Mazarakata	Cu, Au, Ag
M40-4	Mazarakata	Al, Si, S, K, Ca, Ti, Cr, Mn, Fe, Ni, Cu, Zn, Pb, Sr, Zr
M40-6	Mazarakata	Al, Si, S, K, Ca, Ti, Cr, Mn, Fe, Ni, Cu, Zn, Pb, Sr, Zr
580.2-1	Kokkolata	Al, Si, S, K, Ca, Ti, Cr, Mn, Fe, Ni, Cu, Zn, Pb, Rb, Sr, Sn
580.2-2	Kokkolata	Al, Si, S, K, Ca, Ti, Mn, Fe, Ni, Cu, Zn, Pb, Rb, Sr, Zr, Sn
Blue-green		
M23-6	Mazarakata	Al, Si, S, K, Ca, Ti, Mn, Fe, Ni, Cu, Zn, Pb, Rb, Sr, Zr, Sb, Sn, Sb
M32-6	Mazarakata	Al, Si, S, K, Ca, Ti, Mn, Fe, Co, Ni, Cu, Zn, Pb, Rb, Sr, Zr, Sn
Σ2-K1-1	Kokkolata	Al, Si, S, K, Ca, Ti, Cr, Mn, Fe, Ni, Cu, Zn, Pb, Rb, Sr
Dark blue		
M18-1	Mazarakata	Al, Si, P, S, K, Ca, Ti, Mn, Fe, Co?, Ni, Cu, Zn, Pb, Rb, Sr, Zr
M23-2	Mazarakata	Al, Si, S, K, Ca, Ti, Cr, Mn, Fe, Co?, Ni, Cu, Zn, Pb, Rb, Sr, Zr, Sn, Sb
M23-3	Mazarakata	Al, Si, S, K, Ca, Ti, Cr, Mn, Fe, Co, Ni, Cu, Zn, Pb, Rb, Sr, Zr, Sb
M23-4	Mazarakata	Al, Si, S, K, Ca, Ti, Mn, Fe, Co, Ni, Cu, Zn, Pb, Rb, Sr, Zr, Sn, Sb
M23-5	Mazarakata	Al, Si, S, K, Ca, Ti, Cr, Mn, Fe, Co, Ni, Cu, Zn, Pb, Rb, Sr, Zr, Sn, Sb
M23-7	Mazarakata	Al, Si, S, K, Ca, Ti, Cr, Mn, Fe, Co, Ni, Cu, Zn, Pb, Sr, Zr, Sn
M32-1	Mazarakata	Al, Si, P, S, K, Ca, Ti, Mn, Fe, Co, Ni, Cu, Zn, Pb, Rb, Sr, Zr, Sn, Sb
M32-2	Mazarakata	Al, Si, S, K, Ca, Ti, Cr, Mn, Fe, Co, Ni, Cu, Zn, Pb, Rb, Sr, Zr, Sn, Sb
M32-3	Mazarakata	Al, Si, S, K, Ca, Ti, Cr, Mn, Fe, Co, Ni, Cu, Zn, Pb, Rb, Sr, Zr, Sn, Sb
M32-4	Mazarakata	Al, Si, S, K, Ca, Ti, Cr, Mn, Fe, Co, Ni, Cu, Zn, Pb, Rb, Sr, Zr, Sn, Sb
M32-5	Mazarakata	Al, Si, S, K, Ca, Ti, Cr, Mn, Fe, Co, Ni, Cu, Zn, Pb, Rb, Sr, Zr, Sn
M32-7	Mazarakata	Al, Si, S, K, Ca, Ti, Cr, Mn, Fe, Co, Ni, Cu, Zn, Pb, Rb, Sr, Zr, Sn
M32-8	Mazarakata	Al, Si, S, K, Ca, Ti, Cr, Mn, Fe, Co, Ni, Cu, Zn, Pb, Rb, Sr, Zr, Sn
M32-9	Mazarakata	Al, Si, S, K, Ca, Ti, Cr, Mn, Fe, Co, Ni, Cu, Zn, Pb, Rb, Sr, Zr, Sn
M32-1R	Mazarakata	Al, Si, S, K, Ca, Ti, Mn, Fe, Co, Ni, Cu, Zn, Pb, Sr, Zr
M32-2R	Mazarakata	Al, Si, S, K, Ca, Ti, Mn, Fe, Co, Ni, Cu, Zn, Pb, Sr, Zr
M32-3R	Mazarakata	Al, Si, S, K, Ca, Ti, Mn, Fe, Co, Ni, Cu, Zn, Pb, Sr, Zr
M32-4R	Mazarakata	Al, Si, S, K, Ca, Ti, Mn, Fe, Co, Ni, Cu, Zn, Pb, Sr, Zr
1615-8	Metaxata	Al, Si, S, K, Ca, Ti, Cr, Mn, Fe, Co, Ni, Cu, Zn, Pb, Sr, Zr, Sn
1615-11	Metaxata	Al, Si, P, S, K, Ca, Ti, Mn, Fe, Co, Cu, Zn, Pb, Sr, Zr, Sn
580.2-3	Kokkolata	Al, Si, S, K, Ca, Ti, Cr, Mn, Fe, Co, Ni, Cu, Zn, Pb, Sr, Zr, Sn, Sb
Blue, opaque		
1616-9	Metaxata	Al, Si, P, S, K, Ca, Ti, Cr, Mn, Fe, Ni, Cu, Zn, Pb, Sr, Zr, Sn, Sb
K13-2	Metaxata	Al, Si, S, K, Ca, Ti, Cr, Mn, Fe, Ni, Cu, Zn, Pb, Sr, Zr, Sn, Sb
K13-3	Metaxata	Mg, Al, Si, P, S, K, Ca, Ti, Cr, Mn, Fe, Ni, Cu, Zn, Pb, Sr, Zr, Sn, Sb
K13-4	Metaxata	Al, Si, S, K, Ca, Ti, Cr, Mn, Fe, Ni, Cu, Zn, Pb, Sr, Zr, Sn, Sb
Σ2-K1-4	Kokkolata	Al, Si, S, K, Ca, Ti, Cr, Fe, Co, Ni, Cu, As, Pb, Sr, Sb
Green		
M18-4	Mazarakata	Al, Si, S, K, Ca, Ti, Mn, Fe, Ni, Cu, Zn, Pb, Rb, Sr, Zr
Σ2-K1-2	Kokkolata	Al, Si, P, S, K, Ca, Ti, Cr, Mn, Fe, Ni, Cu, Zn, Pb, Sr
Purple/black		
M40-P	Mazarakata	Al, P, S, K, Ca, Ti, Mn, Fe, Ni, Cu, Zn, Rb, Sr
M40-5	Mazarakata	Al, Si, S, K, Ca, Ti, Cr, Mn, Fe, Ni, Cu, Zn, Pb, Sr, Zr
Pink		
M18-3	Mazarakata	Al, Si, S, K, Ca, Ti, Mn, Fe, Ni, Cu, Zn, Pb, Rb, Sr, Zr

[1]Color given is for intact glass or faience glaze observed. If no intact glass or glaze is visible general color of corroded glass or

faience core is given.
[2]The peaks marked with a "?" indicate that the peak is small, slightly above background, and it is unclear if the element is present.

Bead M40-3 is unique in that it is the only bead examined for this study that is associated with gold. The dot pattern is pressed into the gold foil indicating this fragment covered the front decorated surface of the bead. It is not clear from the remains whether the entire bead was covered with gold. The gold foil is composed of gold, silver, and copper, and was likely made from the natural alloy electrum (Karydas 2007). Gold covered relief beads have been previously found in Mycenaean contexts, such as at the site of Mycenae (Nightingale 2008). These beads have been found covered using two separate pieces of gold sealed at the edges or covered completely with gold foil. There have been beads found at Mycenae which only had a strip of gold attached or pressed onto the decorated surface. One reason that has been proposed for the use of gold foil covered glass beads was to use the glass as a "cheap substitute" (Nightingale, 2008, p. 79) for a solid gold bead or a thicker piece of gold needed to create the beads. Given that glass was imported, and that in later Mycenaean periods trade was beginning to be disrupted, glass would have been a material that likely became harder to procure and not necessarily a "cheaper" alternative (Nightingale 2008).

Six of the copper-colored beads (M18-5, M18-6, M18-7, M40-1, M40-4, M40-6) use copper mineral as the source for the color. Six beads (M18-2, M23-6, M40-2, M40-3, 580.2-1, 580.2-2) contain tin which points to the use of bronze scrap as the source of the colorant and that the beads were likely made in Egypt. Four of beads, M23-6, M40-4, 580.2-1, 580.2-2, that were analyzed quantitatively contained 1.01-12.56 wt% CuO (avg. of 2.96 wt%) (Table 6.3).

Two beads from Mazarakata, M40-1 and M40-6, are heavily corroded and have an opaque green colored surface. The samples taken from both beads show that the glass has areas that are both translucent blue and green (Figure 6.11). The blue glass is likely the original color of the bead and the green coloration is due to alteration of the colorant (Vandiver 2008; Cavallo 2009; Moussa and Ali 2013). The area of green glass analyzed on sample M40-1 has a much higher concentration of copper oxide as opposed to the blue areas (12.56 wt% green, 1.65 wt% blue) (Table 6.3). The green glass has likely become enriched in copper due to leaching of more soluble components such as soda, potash, lime, and magnesia. Bead M40-6 has also become depleted in these same oxides; however, the area has not become enriched in copper.

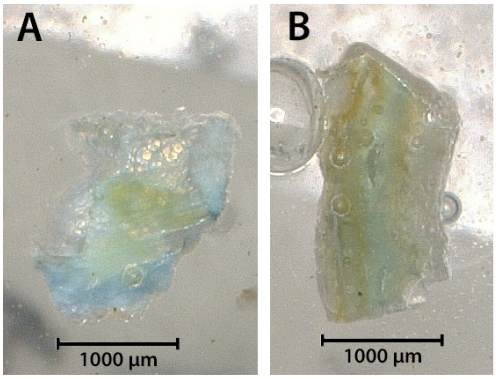

Figure 6.11. Sample M40-1 (A) and M40-6 (B) showing areas of blue and green glass. The exterior surface of the bead appeared green and somewhat opaque. The blue glass is the original color of the glass.

Two of the copper blue beads (M23-6 and M40-2) also contained antimony (Table 6.4). Bead M40-2 is covered with a layer of green and white corrosion, but blue glass is visible at the break edges. Antimony is found in copper blue glasses as the opacifier calcium antimonate, which would produce opaque blue glass. The presence of antimony in the bead was surprising since the glass does not appear opaque. M23-6 also contains antimony and is not opaque. This bead was sampled and the polished section of the glass appears translucent with no opacifying crystals visible (Figure 6.12). LA-ICP-MS analysis detected 2047 ppm of antimony (Table 6.5). This is higher than the average antimony content in Egyptian colorless glasses

(153ppm) and copper-colored translucent glasses (0.05% Sb_2O_5, or 400pm) (Shortland 2002). The level of antimony in M23-6 is still lower than the average values in opacified copper-colored blue glass (1.48% Sb_2O_5, or 11,100 ppm) and opacified white glass (8210 ppm) (Shortland 2002). This suggests that antimony was added at some stage in glass production. It is not clear what the purpose of adding antimony was. It could be that production issues occurred that resulted in less opaque glass, such as the formation of only a few calcium antimonate crystals. The temperatures used to melt the glass could have reduced the number of antimonate crystals that formed. Finally, it is possible that the antimony could be a contaminant from the reuse of a crucible or reaction vessel that was used to produce calcium antimonate opacified glass.

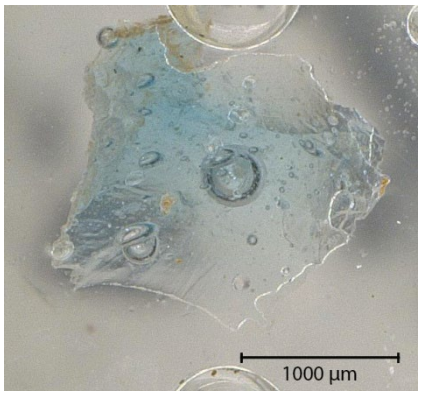

Figure 6.12. Samples taken from relief bead M23-6. Even though antimony was detected in the glass, it appears translucent.

6.4.1.2.2 Cobalt blue

The largest color group (22) includes those beads where the pXRF has detected the presence of cobalt (Table 6.4). All the beads are a dark blue color except for M32-6, which appears blue-green on the surface. All the beads also had prominent peaks for copper. Sixteen of the beads contain tin as well. The presence of cobalt and copper in the blue beads would suggest that these could be the Co-Cu glasses commonly seen in Mycenaean contexts (Smirniou and Rehren 2013). The presence of tin in the glass would indicate the source of the copper was bronze scrap as opposed to copper mineral.

Table 6.5. LA-ICP-MS results of selected elements related to the blue colorants and opacifiers used. Results are given in parts per million (ppm) and are averages of three replicates.

Sample	Mn	Co	Ni	Cu	Zn	As	Y	Sn	Sb	Pb
Blue										
M23-6	472.76	248.56	160.98	6291.50	396.42	19.12	6.70	511.26	2047.21	43.33
M40-1[1]	243.49	5.55	34.80	45386.67	146.47	1.09	6.28	4.68	11.23	58.63
M40-4	391.59	4.96	11.05	7490.69	19.29	5.41	3.67	1.76	2.66	4.90
M40-6[1]	58.63	0.70	2.44	12223.80	48.11	1.54	3.26	7.24	1.63	7.26
580.2-1	122.63	14.45	12.39	19129.88	88.07	13.69	5.81	2246.96	15.41	56.04
580.2-2	477.79	130.20	91.78	18321.03	128.43	42.30	6.76	44.74	180.64	206.98
Blue-green										
Σ2-K1-1	386.29	2.90	24.01	20.07	23.24	2.10	4.10	2.10	1.65	7.76
Dark blue										
M23-2	1169.23	409.10	300.25	512.85	587.41	2.98	10.41	16.95	207.98	4.31
M23-7	1297.69	453.38	305.10	1174.55	634.64	4.45	8.74	67.35	66.95	21.61
M32-1	1050.26	461.53	315.93	1205.44	651.18	4.81	12.63	73.85	299.01	659.33
M32-9	784.01	291.70	191.70	152.19	438.21	1.08	5.74	3.68	24.90	3.47
M32-4R	688.28	248.82	162.54	147.68	378.20	1.29	5.19	5.64	33.34	5.04
580.2-3	822.84	420.00	328.08	3249.14	661.38	20.65	12.97	147.31	565.43	50.29

Blue, opaque										
K13-4	1019.24	575.29	353.18	3257.82	733.43	19.30	8.09	115.34	930.42	252.09
Σ2-K1-4	31.48	4718.23	809.17	9855.52	20.92	223.10	0.63	10.73	2452.21	6976.67
Purple										
M40-5	3745.25	2.50	3.81	27.73	21.25	0.76	3.29	0.55	1.85	2.15
M40-P	2062.49	5.70	6.51	70.92	27.86	1.42	2.92	3.80	22.99	4.08
Pink										
M18-3	351.29	6.42	15.63	14.97	13.97	1.45	3.06	0.52	1.87	8.68

[1] Only area of blue glass was analyzed with LA-ICP-MS since it is assumed that is the original color of the glass

Looking at the concentrations of cobalt and copper in the six sampled beads from this group (M23-2, M23-7, M32-1, M32-9, M32-4R, 580.2-3), they may be not all be considered Co-Cu colored glasses (Table 6.5). Applying the definitions for Co-Cu colored glasses established by Smirniou and Rehren (2013), only samples M23-7, M32-1, and 580.2-3 have cobalt and copper concentrations high enough to have been colored using both mineral colorants (419-461 ppm Co and 1174-3249 ppm Cu). Sample M23-2 has a cobalt concentration (409 ppm) high enough to have had this mineral added as a colorant, but the copper levels are quite low (512 ppm). Therefore, it is considered cobalt colored glass. Samples M32-9 and M32-4R have cobalt and copper values below the definitions for any of the blue colored glasses (copper colored, cobalt colored, or Co-Cu colored). The samples seem to be weakly colored, though their cobalt values (248-291 ppm) are near the threshold for being considered cobalt glasses (at least 300 ppm) (Smirniou and Rehren 2013, 4732). The low concentration of cobalt is apparent in the biplot of cobalt and copper concentrations (Figure 6.13) where these two beads have the lower cobalt values than the Egyptian, Mycenaean, and mixed-alkali glasses used for comparison (Towle et al. 2001; Nikita and Henderson 2006; Smirniou and Rehren 2013; Conte et al. 2015) The Co-Cu samples from Kefalonia and most of the copper colored glass fall within the ranges for these colorants found in plant ash glasses. Sample M40-1 has very elevated levels of copper compared to all the other published glass. This was caused by the enrichment of copper due to the deterioration.

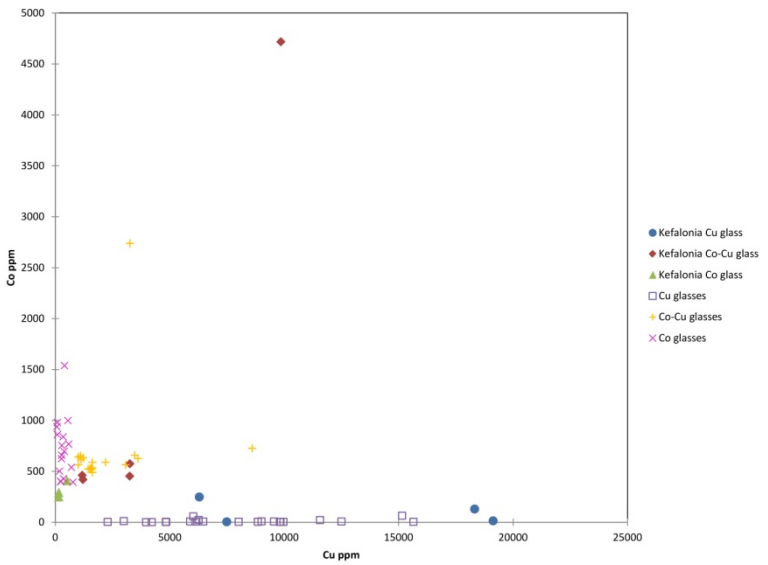

Figure 6.13. Plot of copper and cobalt values in Kefalonian copper colored, cobalt colored, and Co-Cu colored glasses compared to published examples of glasses with similar colorants. Data for plant ash glasses taken from Smirniou and Rehren 2013. Data for cobalt colored mixed alkali glass taken from Conte et al. 2019: Nikita and Henderson 2006; Towle et al. 2001.

The tin concentrations in these samples confirm the classification of the glass colors (Table 6.5). Co-Cu colored Egyptian glasses have been found to have higher tin concentrations than cobalt glasses (Smirniou

and Rehren, 2013). A study of numerous New Kingdom Egyptian samples showed on average that Co-Cu colored glass contains 68 ppm Sn as opposed to cobalt colored glass that averages 21 ppm. The three Co-Cu colored glasses M23-7, M32-1, and 580.2-3, have tin concentrations above 67 ppm. The cobalt colored glasses have lower concentrations of tin, less than 17 ppm. The presence of tin in the cobalt colored glass cannot be easily explained since it would not naturally appear in the raw materials used to make glass. The tin could be due to contamination from the use of bronze vessels during the processing of the cobaltiferous alum (Smirniou and Rehren 2013).

Nine of the beads contain antimony (Table 6.4), however the beads do not appear very opaque. It is not clear why antimony is present. Perhaps the low concentration of antimony (Table 6.5) helped to darken the tone of the blue by providing some opacity, however, when samples, the beads appeared somewhat translucent.

6.4.1.2.2.1 Source of cobalt colorant

The source of cobalt used for the Kefalonian cobalt colored and Co-Cu colored glasses seems to be the cobaltiferous alum deposits found in the Western Desert. This was determined by examining the concentrations of manganese, nickel, and zinc in the samples (Table 6.5). The concentrations of manganese (688-1297 ppm) and zinc (378-661 ppm) fit the range of values from that Egyptian source (500-1700ppm Mn, 300-13000 ppm Zn) (Smirniou and Rehren 2013). The nickel concentrations for M23-2, M23-7, M32-1 and 580.2-3 (300-328 ppm) fall within the lower end of the expected range for the Western Desert cobaltiferous alum (250-700 ppm) (Smirniou and Rehren 2013). Samples M32-9 and M32-4R have values even lower (162-191 ppm). These samples also had low concentrations of cobalt and copper, and have the lowest concentrations of manganese and zinc of the samples analyzed. The low levels of the elements associated with the cobalt source could be because the glass is weakly colored with cobalt. The cobalt and Co-Cu colored Kefalonian glasses were compared to glasses found at Egyptian and Mycenaean sites, as well as two cobalt colored ingots from the Uluburun, that were colored with cobalt from the Western Desert (Figure 6.14). There is overlap of the groups further confirming all are colored by cobalt from this same source.

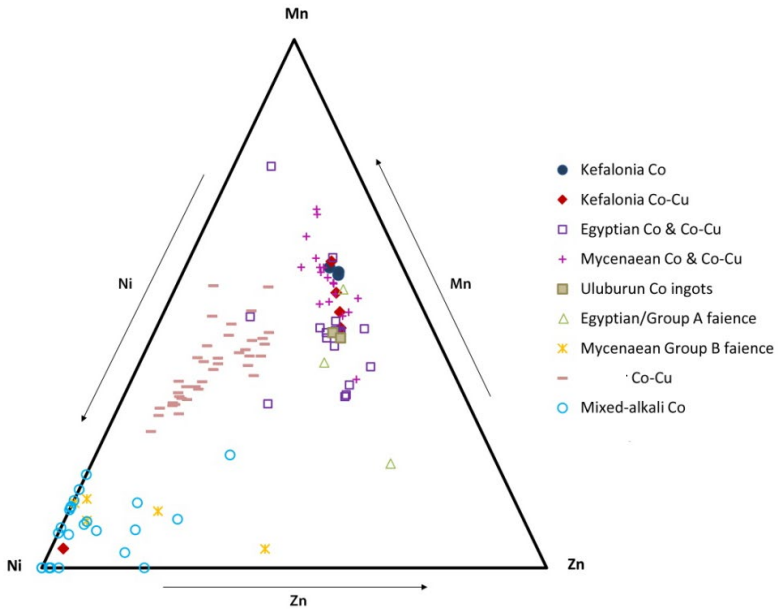

Figure 6.14. A ternary diagram comparing the concentrations of manganese, nickel and zinc in the Kefalonian cobalt colored and Co-Cu colored glasses. These glasses were compared to Egyptian and Mycenaean glasses containing cobalt from the Western Desert of Egypt (Smirniou and Rehren 2013), cobalt colored faience (Tite et al., 2008), Co-Cu glasses from Nippur (Walton et al. 2012), and mixed alkali cobalt colored glass (Conte et al. 2019: Nikita and Henderson 2006; Towle et al. 2001).

Further examination of the ternary plot shows that even though the published Egyptian and Mycenaean samples used the same source for the cobalt colorant, differences between the concentrations of the three transition elements exists. The two groups are somewhat separated based on the proportions of the three elements. Mycenaean cobalt and Co-Cu glasses seem to contain more manganese, but less nickel and zinc. The Egyptian cobalt containing glasses show the opposite, lower manganese and higher nickel and zinc. It is not clear what is causing these differences, but since the cobalt source is the same, there must be some stage of the production process, or a raw material other than the cobalt colorant such as the plant ash or alkali, that is accounting for these differences. The Kefalonia cobalt colored samples overlap with the Mycenaean samples. The Kefalonian Co-Cu colored ones mainly overlap with the Mycenaean samples but some do plot with the Egyptian samples and the Uluburun ingots. One of these samples was taken from the triple rosette bead (K13-4), the unique Kefalonian style relief bead.

6.4.1.2.3 Opaque blue

Based on the pXRF results (Table 6.4), four opaque blue relief beads from Metaxata (1616-9, K13-2, K13-3, K13-4) are colored using copper and contain antimony as the opacifier. The relief beads are of the triple rosette type unique to Kefalonia. The beads are covered with a layer of white corrosion and have some iridescence, but in areas where the underlying glass is exposed, it appears pale blue in color and slightly opaque (Figure 6.15). PXRF analysis found tin in the four samples suggesting the copper colorant comes from the use of bronze scrap rather than a Cu-containing mineral.

Figure 6.15. Triple rosette relief beads 1616-8 (left) and 1616-9 (right). Arrows point to areas where the underlying glass is visible appears to be a pale blue color that is somewhat opaque.

Although no cobalt was detected with the pXRF, cobalt was found in bead K13-4 using LA-ICP-MS (Table 6.5). The bead is a Co-Cu colored glass and contained 575 ppm Co and 3252 ppm Cu. It is possible that the other three relief beads could also be colored with a combination of cobalt and copper since they are the same type and appear to be the same color. Sampling of the other beads would be required in order to confirm they are all manufactured using the same colorants.

Antimony was detected in these relief beads, but the beads were not completely opaque. The sample taken from K13-4 appears darker and more opaque in a few areas. This opacity is not uniform across the bead and areas still appear somewhat translucent (Figure 6.16). The antimony content in the sample is 930ppm, which is higher than Egyptian copper-blue or colorless glasses, but not as high as opacified copper blue glass (Shortland 2002). These beads appear opaque under macro-examination, but the antimony levels are lower than that of M23-6, which appears translucent under transmitted light (Figure 6.12).

Figure 6.16. Sample taken from K13-4 showing an area in the center that appears darker, but the glass still appears translucent despite containing antimony.

6.4.1.2.4 Manganese purple

Two glasses, M40-5 and M40-P, are purple in color. Bead M40-5 looked black when examined but once it was sampled the light purple color of the glass was visible (Figure 6.17A). The black exterior was likely due to corrosion of the glass and possibly alteration due to burial deposits. As mentioned previously, it is not clear what type of object M40-P is. The purple glass piece is not a bead, but either a fragment from a larger artifact type or possibly is a chunk of raw glass (Figure 6.17B). The side that contains the crust or altered surface is somewhat flat. The color, texture and shape of this surface resembles that observed in some raw glass pieces and glass working debris from Amarna where this surface is thought to be the side that was against the wall of a cylindrical vessel used as a crucible (Muros 2020). The discovery of raw glass within a Late Bronze Age tomb context has not found within the literature search. There has been evidence for misshapen bead or incompletely worked beads found the tombs excavated at Archanes on Crete (Sakellarakēs and Sapouna-Sakellarakē 1997, 628, fig. 278, 279). Double and single cockleshell beads were found within the tombs, and one bead had a third cockleshell attached to it. The beads were interpreted as being unfinished, where they were still stuck to each other and had been placed in the tombs before polishing (Panagiotaki 2008, 46). The significance behind the placement of a glass chunk within the tomb is unclear and it is not clear what the connection is between these objects and the interred individuals.

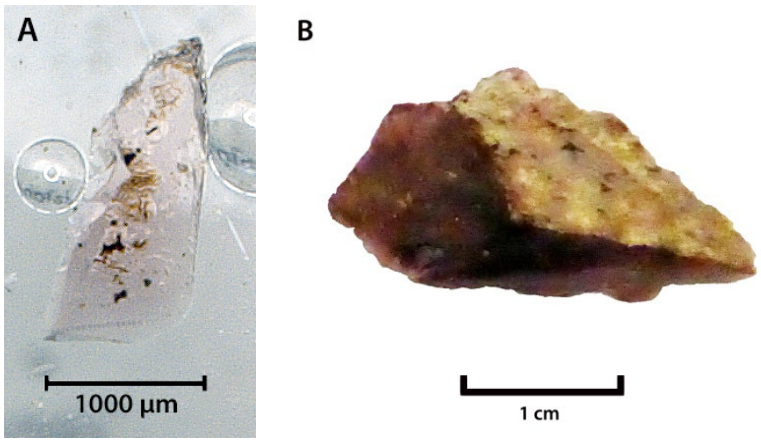

Figure 6.17. (A) Sample taken from bead M40-5 showing the bead is made from a light purple glass; (B) Image of M40-P that may be a fragment of a larger artifact or a chunk of raw glass.

Based on the analysis undertaken on samples of these two pieces, and comparison with Egyptian purple glass manganese is the likely colorant (Nicholson 2007; Shortland 2012; Henderson 2013). The concentration of manganese oxide in both M40-5 (0.53 wt%) and M40-P (0.26 wt%) are low for Egyptian manganese purple glasses (Table 6.3) (Nicholson 2007; Shortland 2012). A purple glass bead from Elateia

however, has a low concentration of manganese (Ela/17-0.22 wt%) close to that detected in the purple chunk (Nikita and Henderson 2006, 89, table 4). The tone of purple in both M40-5 and M40-P is quite light and perhaps this is due to the low amount of manganese in the glass.

6.4.1.2.5 Iron-colored pink

Bead 18-3 from Mazarakata is a pale pink color, and the colorant used to produce its shade is unclear. Reduced copper has been used to make red glass and as discussed above manganese produces purple (Shortland 2012), but neither was detected using EPMA (Table 6.3). LA-ICP-MS did detect both manganese and copper, but in low concentrations and likely not enough to impart any pink color to the glass (Table 6.5). Since iron can produce a range of colors, the addition of iron was explored. The concentration of iron in M18-3, however, is low (0.4 wt%) and within the range found naturally occurring in the raw materials. It is possible that the color was created using the iron already present in the glass through changes in the furnace atmosphere that affected the color produced (Nicholson 2007; Shortland 2012; Henderson 2013). No other beads were found in the collection that were this color and could not provide additional material for comparison or further investigation. No other oxides were present that would have produced the pink color. The colorant will tentatively be identified as iron with a particular furnace atmosphere playing a role in the color of the glass.

6.4.2 Faience

6.4.2.1 Composition and microstructure

Only one faience bead was sampled for compositional analysis, a biconical grooved bead (Σ2-K1-4) from Kokkolata-Menegata. In section, the faience is blue throughout and does not appear to have a distinct glaze layer. Whether glaze is present was difficult to determine since the bead was covered with a white, opaque corrosion layer along with some burial deposits. The composition of the bead (Table 6.3) is unlike the typical composition of Egyptian or Mycenaean Group A faience (Vandiver 1983; Tite and Shortland 2008). It is closer to the Group B Mycenaean faience type with low concentrations of potash (0.77 wt%), magnesia (0.48 wt%), alumina (1.19 wt%), and high iron (4.85 wt%) (Tite et al. 2005; Maniatis et al. 2008; Tite et al. 2008).

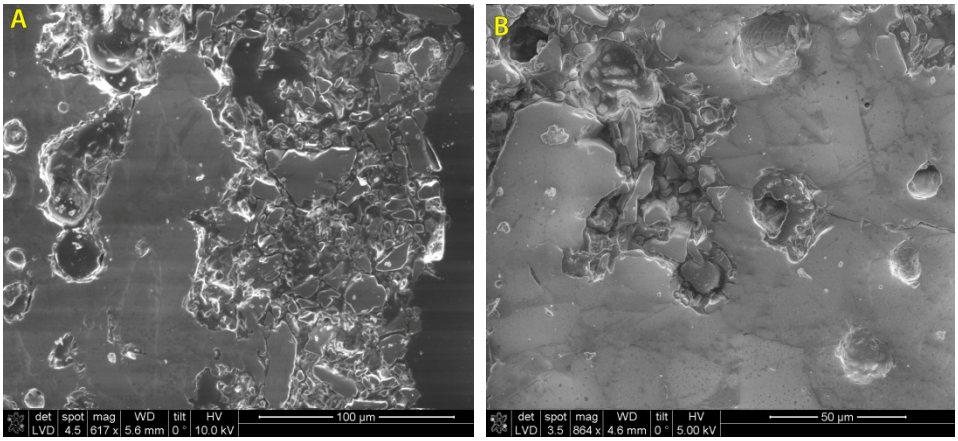

Figure 6.18. VP-SEM images of the microstructure of bead Σ2-K1-4. (A) There does not seem to be a distinct glaze layer on the surface of the bead. (B) The interior of the bead seems to be composed of grains of silica or silica-rich phases within a glassy matrix.

The microstructure of the Kefalonian faience bead was investigated to better identify the type of faience it was and the layers present. Imaging of the surface and sub-surface using the VP-SEM-EDS highlights the lack of a distinct glaze layer, in comparison to what is seen in Egyptian or Mycenaean Group A faience (Maniatis et al. 2008). An area about 50-100µ in from the surface appears to have a different structure than the core. This could be due to deterioration of the surface and not solely due to the presence of a glaze layer (Figure

6.18A). It appears as if the areas surrounding grains of silica have disappeared and the surface is breaking apart. Below that section of the surface is a more cohesive area core of the faience. The EDS analysis was conducted using a low vacuum secondary electron detector (LVD) and the contrast was not optimal for imaging. However, the interior matrix of the glass is somewhat visible in Figure 6.18B. The core appears to be made of a continuous glassy matrix with some pores. There are grains visible, some rather block-like, that are either silica grains or silica rich particles (Table 6.6). This microstructure is somewhat similar to what is observed in the Group B bead from the island of Psara (Maniatis et al. 2008, 122, fig. 6.3b).

Table 6.6. VP-SEM-EDS analysis of a sample from bead Σ2-K1-4. Values given as weight % (wt. %) oxide and normalized to 100%

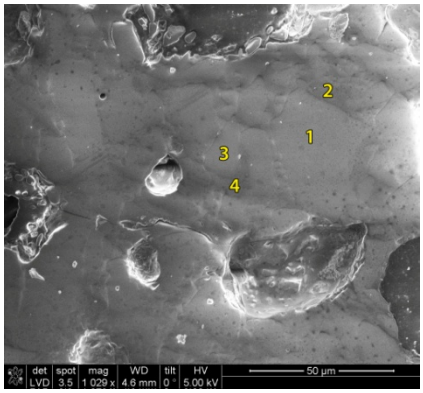

Area	Na_2O	MgO	Al_2O_3	SiO_2	P_2O_5	Cl	K_2O	CaO	MnO	FeO	CoO	CuO	PbO
1-grain	0.52	0.00	0.09	98.86	0.14	0.03	0.00	0.04	0.02	0.16	b.d.	0.14	0.00
2-glass matrix	1.40	0.14	0.12	97.81	n.d.	0.06	0.00	0.03	0.06	0.22	b.d.	0.16	0.00
3-grain	2.60	0.14	0.26	95.65	n.d.	0.12	0.15	0.26	0.02	0.53	b.d.	0.22	0.05
4-glass matrix	6.32	0.26	0.35	88.15	n.d.	0.27	0.39	0.75	0.00	1.88	0.63	0.82	0.18

6.4.2.2 Raw materials-Alkali flux

Faience objects tend to have lower concentrations of some of the alkali components compared to glass (Kaczmarczyk and Vandiver 2008). This can be seen in the biplot of glass and faience objects, where faience objects from Egyptian and Mycenaean contexts have lower magnesia and potash than most Late Bronze Age plant ash glasses (Figure 6.8). Distinctions between the values for magnesia and potash among different types of faience are also apparent. The concentrations of potash and magnesia are lower in the Kefalonian faience bead compared to Egyptian faience made with plant ash. There are similarities however with Egyptian faience samples from the site of Memphis made using natron, as well as three Mycenaean Group B faience from Greece and one from Italy, all of which have low magnesia and potash (Kaczmarczyk and Vandiver 2008; Maniatis et al. 2008; Angelini 2008).

The low concentrations of the alkali components in the biconical bead are similar to those found in faience made using natron and it is possible the Kefalonian faience bead was made using this mineral alkali. Although there is some overlap with other Group B faience beads (Figure 6.8), the nature of the alkali used for the comparative samples is somewhat unclear (Maniatis et al. 2008; Angelini 2008). The ratios of soda to potash, magnesia, or lime are often used when discussing the alkali flux for faience objects. In the case of the sample from Σ2-K1-4, the ratios are Na_2O/K_2O=14.6, Na_2O/MgO=23.5, and Na_2O/CaO=10.2. These ratios are similar to those from the Mycenaean Group B faience beads from Mesara and Psara (Na_2O/K_2O=13.0-14.5, Na_2O/MgO=17.1-22.3, Na_2O/CaO=5.7) (Maniatis et al. 2008), though the soda to lime ratio is slightly lower than the Kefalonian faience. Faience made using soda rich plant ash generally has a lower Na_2O/K_2O ratio (below 10) than those made with natron and have higher Na_2O/MgO ratios (47-103) (Kaczmarczyk and Vandiver 2008). There seems to be some variability in the Na_2O/CaO ratios of the plant ash faience but it is generally higher (8-12) than that found in natron glasses. Faience made using natron also has very low

concentrations of phosphorus pentoxide, around 0.1% (Maniatis et al. 2008). There are, however, plant ash faience objects that do not follow this typical composition. Some New Kingdom faience made using a soda rich plant ash has contained higher Na_2O/K_2O ratios. Egyptian cobalt colored faience made using plant ash has been found to have lower Na_2O/MgO and Na_2O/CaO ratios (averaging 7.5-11.7 and 7.7-8) than copper colored faience made using the same alkali due to the use of natron during the processing of the cobalt colorant (Kaczmarczyk and Vandiver 2008). In the case of the Kefalonian bead, the higher Na_2O/K_2O ratios, the lower Na_2O/MgO ratios, the low phosphorus pentoxide content (0.07 wt %), and the similarities between this biconical bead and some of the Egyptian natron faience from Memphis could point to the use of natron for its production.

6.4.2.3 Raw materials-Colorant

6.4.2.3.1 Cobalt blue

The visual identification of which beads were faience was difficult due to the level of corrosion on the surface. The white corrosion layers on many of the beads made it difficult to see morphological features that would allow for identification of the material. Five of the beads analyzed with pXRF (M32-5, M32-6, M32-7, M32-8, Σ2-K1-4) are thought to be made of faience. All the beads are some shade of blue. Copper and cobalt was detected in these beads suggesting that the faience could be Co-Cu colored (Table 6.4). Tin was found in beads M32-5, M32-56, M32-7, and M32-8 indicating that bronze was used as the copper colorant.

LA-ICP-MS analysis of the biconical faience bead (Σ2-K1-4) provided more information on the colorant of this faience bead. The bead contained 4718.23 ppm Co and 9855.52 ppm Cu making it Co-Cu colored (Table 6.5) (Smirniou and Rehren 2013). The concentration of cobalt was quite high compared to cobalt containing Kefalonian glasses as well as to Egyptian and Mycenaean cobalt and Co-Cu colored glasses (Figure 6.13).

6.4.2.3.1.1 Source of the cobalt colorant

Looking at the concentrations of the main transition elements associated with the cobalt colorant source for the Mycenaean Group B faience bead, Σ2-K1-4 (Table 6.5), it appears the cobalt was obtained from a source other than the cobaltiferous alum of the Western Desert (Tite et al. 2005; Maniatis et al. 2008; Tite et al. 2008). The biconical bead had low concentrations of zinc (20.92 ppm) and manganese (31.48 ppm) with high concentrations of nickel (809.17 ppm). The concentrations of these three elements differ from what is found in 18th Dynasty Egyptian or Mycenaean Group A faience colored using cobaltiferous alum (Tite et al. 2008). The Kefalonia faience sample has elevated cobalt and lead, both characteristics of Group B faience. When comparing Σ2-K1-4 to cobalt-containing glasses from Kefalonia to those found in Egypt and the Greek mainland made using the Western Desert cobalt, it is clear that the source is not the same (Figure 6.14).

Data from cobalt colored glass and faience, which used a source other than the cobaltiferous alum of Egypt, were also included in the plot. The concentrations of manganese, zinc, and nickel detected within the Kefalonian biconical bead is similar to that used for the Group B type, cobalt colored, faience beads from Mesara on Crete and from the island of Psara (Tite et al. 2008). These beads have higher nickel and lower manganese and zinc levels than those made with Egyptian cobalt. The values of these transition elements overlap with cobalt colored mixed alkali glasses from northern and southern Italy (Towle et al. 2001; Conte et al. 2019) and Elateia on the Greek mainland (Nikita and Henderson 2006). It appears that at least in regards to these particular three elements, the cobalt sources of these samples are somewhat similar.

Analysis of Late Bronze Age Co-Cu colored glasses from Nippur pointed to the use of a different cobalt source exploited for Near Eastern glasses (Walton et al. 2012). The concentrations of manganese, nickel, and zinc differed from the Western Desert source. The glass from Nippur also contains higher iron and cobalt concentrations. Some of these characteristics are shared by the Group B faience attribute to the Mycenaeans. Because of these similarities, the Nippur samples were included in the ternary plot (Figure

6.14) to see if they shared a similar cobalt source. The Nippur cobalt source is clearly different from the Egyptian one, and it is not similar to either the Kefalonian faience bead or the samples from Crete and Psara.

The alumina and iron oxide concentrations in cobalt colored vitreous materials can also be used to distinguish cobalt sources. Several samples of cobalt colored glasses from the Mycenaean site of Elateia, which were thought to be colored using non-cobaltiferous alum, had elevated levels of iron and alumina (Nikita and Henderson 2016). Glass from Nippur made with cobalt from a unidentified non-Egyptian source also had elevated alumina and iron concentrations (Walton et al. 2012). The Kefalonian biconical bead has elevated levels of iron oxide (4.85%) and a low concentration of alumina (1.19%) and therefore this differs from the Nippur and Elateia material (Table 6.3). The high iron and low alumina places Σ2-K1-4 in the same grouping as published Group B faience (Tite et al. 2008). Even though the biconical bead was similar in its concentrations of manganese, nickel and zinc with the mixed alkali glasses from Elateia and northern and southern Italy they differ in iron and alumina content (Figure 6.19). This further makes the case that Mycenaean Group B faience has a unique, and unidentified, cobalt source that differs from that used in other contemporaneous cobalt colored vitreous materials from Egypt and the Near East.

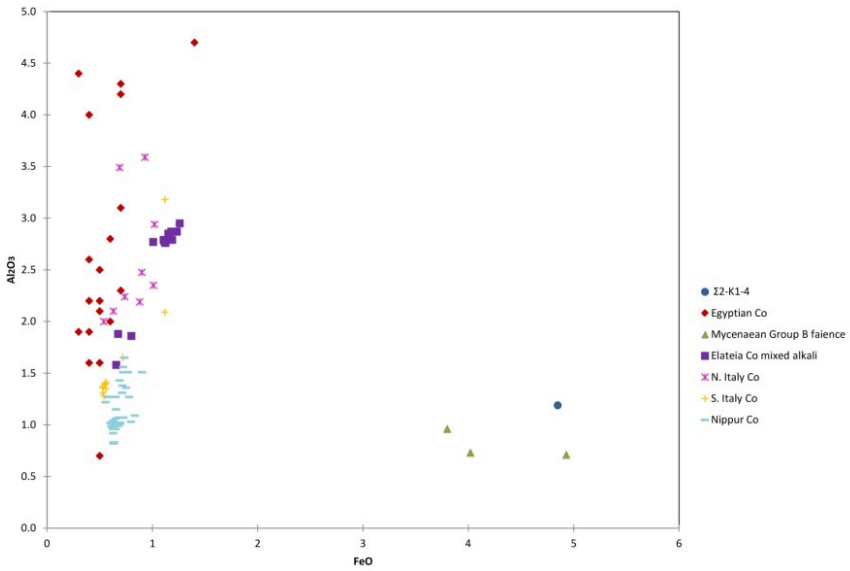

Figure 6.19. Comparison of iron oxide and alumina levels in the biconical faience bead from Kefalonia (Σ2-K1-4) compared to other cobalt colored vitreous materials made with cobalt from the Western Desert of Egypt (Shortland and Eremin, 2006) and from sources outside of that area (Brill 1992; Towle et al. 2001; Nikita and Henderson 2006; Shortland and Eremin 2006; Tite et al. 2008; Walton et al. 2012; Henderson et al. 2015; Conte et al. 2019).

6.4.3 Provenance

6.4.3.1 Principle Component Analysis (PCA)

Principal Component Analysis (PCA) was used to identify possible compositional groups among 16 Kefalonian beads sampled for quantitative analysis. The PCA was used to also look at their relationships to compositional groups of published Late Bronze Age vitreous materials and whether any information can be obtained on the primary production area (Figure 6.20) (Brill 1992; Nikita and Henderson 2006; Shortland and Eremin 2006; Smirniou et al. 2009; Jackson and Nicholson 2010). The PCA was performed on EPMA data of 11 major and minor glass composition oxides (Na_2O, K_2O, MgO, Al_2O_3, CaO, SiO_2, FeO, MnO, CuO, P_2O_5, TiO_2) (Table 6.3). The first two principal components together explain 61.1% of the variance in the data (Appendix C.3).

The results of the PCA indicate that there are positive correlations between several of the oxides. For example, there is a correlation between FeO, TiO_2, MnO, Al_2O_3, which correspond to impurities in the silica source and those found within cobalt colorant sources (Figure 6.20). Na_2O, CaO, and MgO are somewhat

correlated, all of which are related to the plant ash alkali. There is a negative correlation between phosphorus pentoxide (P_2O_5), contributed by the plant ash, and the group of elements related to cobalt sources and silica impurities. These variables, and their negative correlations, have formed two probable compositional groups among the samples from Kefalonia and the comparative samples. A group of blue glasses from Kefalonia, cobalt and Co-Cu Egyptian and Mycenaean glasses (Nikita and Henderson 2006; Shortland and Eremin 2006; Smirniou et al. 2009), and two cobalt colored glass ingots from the Uluburun shipwreck (Jackson and Nicholson 2010) have negative PC2 values and cluster near each other. These glasses are distinguished by their higher concentrations of transition elements and lower phosphorus pentoxide. A second group is composed of non-cobalt colored glasses that is higher in phosphorus pentoxide and includes Egyptian, Near Eastern and Mycenaean glasses, and one ingot from Uluburun. These glasses have negative PC1 and PC2 values. Only one sample from Kefalonia plotted along with these glasses. The separation of the group of cobalt colored glasses from the other glasses makes sense based on their composition. Cobalt colored glasses would be higher in iron, manganese, and alumina because of the cobalt colorant used. These glasses are thought to have been made with a different type of plant ash than colorless glasses or those made in other colors, and they seem to contain less phosphorus pentoxide (Rehren 2001).

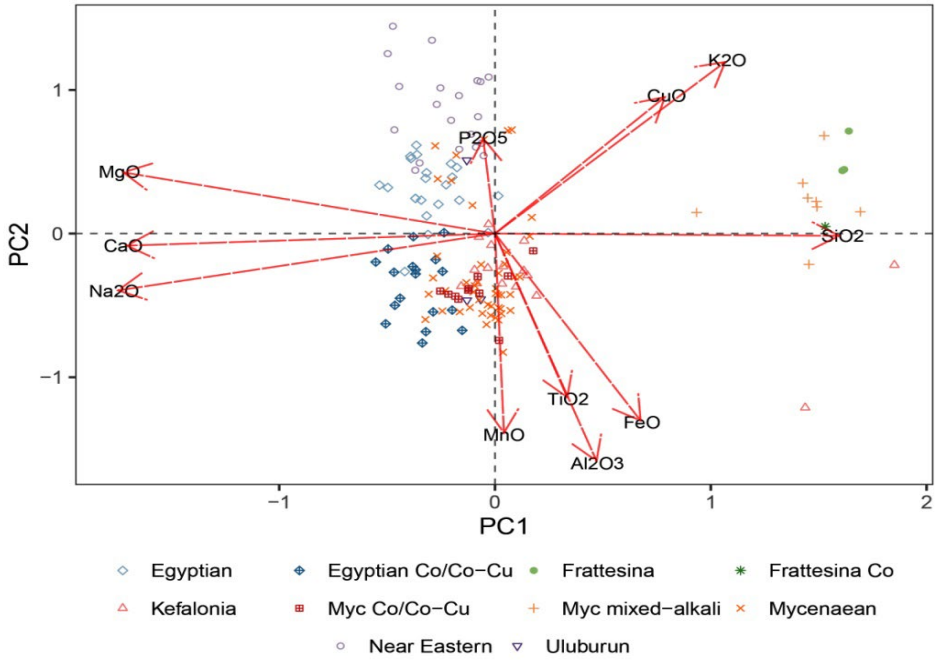

Figure 6.20. Biplot of principal components 1 (34.9% of the variance) and 2 (26.2% of the variance) calculated using EPMA data of 11 major and minor oxides from the Kefalonia samples (15 glass and one faience sample). Included in the PCA was published data from LBA vitreous materials for comparison (Brill 1992; Nikita and Henderson 2006; Shortland and Eremin 2006; Smirniou et al. 2009; Jackson and Nicholson 2010). The position of the samples is scaled proportional to the eigenvalues of each principal component (Appendix C.3) (Oksanen et al. 2017). Samples that are closer together are more similar in composition. Vectors are not scaled according to their eigenvalues. The positions of the variables show their relative positions to each other, indicating their correlation and relative influence on the elemental composition.

Taking a closer look at these two compositional groups, geographic subgroups are observed within them. In the case of the non-cobalt colored glasses, there is a separation between most of the Egyptian and Near Eastern plant ash glasses. There also appear to be subgroups among the cobalt colored glasses. There is a separation between the Egyptian cobalt glasses and the Mycenaean and Kefalonian samples. The Kefalonian samples overlap with many of the Mycenaean samples, but not with most of the Egyptian ones. The variance is driven by the elements related to the plant ash (Na_2O, CaO, and MgO). Mycenaean glass has been found to generally be lower in magnesia than Egyptian glasses (Nikita and Henderson 2006; Worral 2020) so this may be contributing to the groupings observed. The two cobalt blue Uluburun ingots that were

sourced to an Egyptian glassmaking site (Jackson and Nicholson 2010) also plot with Mycenaean and Kefalonian samples suggesting a shared compositional group. This helps to strengthen the argument that the Uluburun was setting sail to the Aegean to unload some of its cargo (Pulak 2008). The overlap of the Mycenaean and Uluburun samples may also support the idea that Mycenaean glass made at primary production sites in Egypt represent a specific composition made exclusively for export (Worral 2020). The raw glass that would be sent to the Aegean could have been made using raw materials available at a specific production site and would have differed from the raw materials used to produce glass that would be locally consumed in Egypt.

An additional compositional group is comprised of the mixed-alkali glasses from Frattesina in northern Italy (Brill 1991) and mixed-alkali glasses from Elateia (Nikita and Henderson 2006). This group is distinguished from the other glasses by their higher silica content and lower soda, lime and magnesia concentrations, variables that are negatively correlated. The mixed alkali Kefalonian bead, 580.2-1, falls within this group, as is expected. This composition of this bead is similar to a Mycenaean mixed-alkali annular bead from Elateia (Ela/37) (Nikita and Henderson, 2006, p.85, table 3, p. 94, table 4). Both the Kefalonian bead and Ela/37 have concentrations of alumina and titania that are the same (580.2-1: 2.76 wt% Al_2O_3, 0.13 wt% TiO_2; Ela/37: 2.77 wt% Al_2O_3, 0.13 wt% TiO_2) (Nikita and Henderson, 2016). Levels of other oxides such as soda, potash and silica are close as well (580.2-1: 6.13 wt% Na_2O, 10.70 wt% K_2O, 75.27 wt % SiO_2; Ela/37: 5.87 wt% Na_2O, 9.23 wt% K_2O, 73.76 wt% SiO_2) (Nikita and Henderson, 2016). The parallels in the composition between these two mixed-alkali beads may point to a similar primary production location.

An outlier is the biconical faience bead, Σ2-K1-4, which has a high positive PC1 value and high negative PC2 value. It has elevated levels of silica, as well as iron, alumina, manganese, titania and iron. The biconical bead is unique in composition and not similar to any other samples from Kefalonia or the published examples used in the PCA.

6.4.3.2 Trace elements

The concentrations of the transition elements lanthanum, chromium, zirconium, and titanium were used to determine the provenance of the 16 glass beads sampled (Table 6.7) Looking at the ratios of Cr/La and 1000Zr/Ti, there seem to be two identifiable sources for the Kefalonian materials analyzed (Figure 6.21). Twelve samples (M23-2, M23-6, M23-7, M32-1, M32-9, M32-4R, M40-4, M40-5, M40-P, K13-4, 580.2-2, 580.2-3) are similar to glasses made in Egypt, the Uluburun ingots, and Mycenaean glass of Egyptian origin (Shortland et al. 2007; Smirniou et al. 2009; Jackson and Nicholson 2010). The glasses analyzed contained 4.96-15.22 ppm Cr (avg. 9.67 ppm), 2.84-4.88 ppm La (avg. 3.86 ppm), 307.48-885.12 ppm Ti (avg. 584.56 ppm), and 26.51-67.07 ppm Zr (avg. 48.60 ppm). Beads formed from glass made at Egyptian primary production sites were found at all three Kefalonian sites. All the relief beads are in this provenance group suggesting that the glass was imported into Greece from Egypt and then worked to create this Mycenaean type bead. Relief beads produced using glass from Egypt are found at Mycenaean sites on the mainland as well (Smirniou et al. 2009).

Table 6.7. Results of LA-ICP-MS analysis of Kefalonia samples showing selected elements found in the alkali and silica sources. Concentrations are given in parts per million (ppm) and are the average of three replicates.

Sample	Cr	La	Ti	Zr	Cr/La	1000Zr/Ti	Sr	Nd
M18-3	19.79	2.77	339.54	13.61	7.15	40.07	332.20	2.56
M23-2	7.61	4.08	629.45	54.47	1.87	86.54	805.70	5.95
M23-6	10.60	4.86	708.90	56.59	2.18	79.82	496.71	4.77
M23-7	9.63	4.58	769.84	62.73	2.10	81.48	721.03	4.97
M32-1	11.75	4.88	885.12	67.07	2.41	75.77	950.87	6.88
M32-9	7.71	3.65	632.22	47.31	2.11	74.83	934.27	4.35
M32-4R	6.56	3.26	532.32	38.47	2.01	72.28	790.43	3.73

M40-4	15.22	3.54	307.48	27.12	4.30	88.21	654.33	3.28
M40-5	5.32	3.07	497.63	61.45	1.73	123.48	781.76	2.98
M40-P	4.96	2.84	357.87	26.51	1.75	74.09	732.49	2.68
K13-4	12.89	4.19	655.39	54.67	3.08	83.41	490.25	5.22
Σ2-K1-1	49.29	3.43	492.67	23.10	14.35	46.89	285.18	3.26
Σ2-K1-4	4.46	0.70	103.41	4.73	6.41	45.71	17.26	1.80
580.2-1	7.69	11.58	633.01	94.54	0.66	149.35	86.54	8.50
580.2-2	13.32	3.04	374.89	26.55	4.38	70.81	226.02	3.71
580.2-3	10.52	4.38	663.64	60.28	2.40	90.84	601.11	5.83

Two of the beads (M18-3, Σ2-K1-1) are similar to glasses made using Near Eastern raw materials (Figure 6.21). The beads were excavated from Mazarakata and Kokkolata-Menegata. Because only one bead from Metaxata was sampled, it is not known whether that site also had glasses from the Near East. The glasses analyzed contained 19.79-49.29 ppm Cr (avg. 34.54 ppm), 2.77-3.44 ppm La (avg. 3.10 ppm), 339.54-492.67 ppm Ti (avg. 416.10 ppm), and 13.61-23.10 ppm Zr (avg. 18.35 ppm) (Table 6.7). Mycenaean relief beads sourced to the Near East have been found at the site of Tiryns (LH IIIA, 1400-1300 BC) (Walton et al. 2009). At the site of Pylos, a group of globular beads excavated from older levels at the site were found to have originated in the Near East (Polikreti et al. 2011).

Sample, Σ2-K1-1, had elevated chromium levels (49.29 ppm) that exceeded most of the comparative glasses (Table 6.7). Although these chromium concentrations exceed the published concentrations from Tell Brak and Nuzi published by Shortland, et al. (2007), a few samples from Nuzi analyzed by Kirk (2011) had elevated chromium concentrations. Recent analyses by Kemp, et al. (2020) on glass from Gurob, Egypt, which are Near Eastern imports, also have elevated chromium levels. One of these high chromium glasses from Gurob and from the Nuzi samples analyzed by Kirk (2011) are in the range of bead Σ2-K1-1 (Figure 6.22). It is possible that there could be different raw materials, such as silica sources, available in the Near East that are higher in chromium impurities than the majority of the published samples from Tell Brak and Nuzi that are used for comparisons.

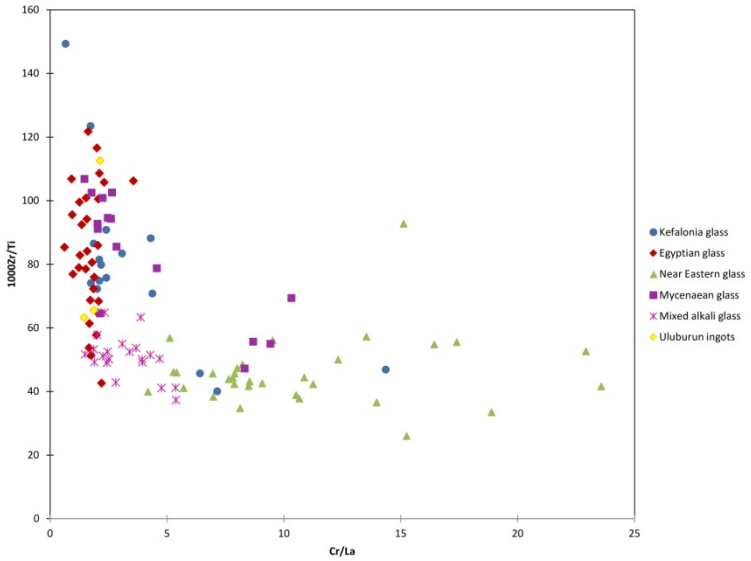

Figure 6.21. Biplot of the ratios of Cr/La and 1000Zr/Ti of the Kefalonian samples compared to glasses from glasses made using Egyptian sourced raw materials from Amarna and Malkata (Shortland et al. 2007), glasses made using Near Eastern sourced raw materials from Tell Brak, Nuzi, and Gurob (Shortland et al. 2007; Kirk 2011; Kemp et al. 2020), Mycenaean glasses of both Near Eastern and Egyptian origin (Smirniou et al. 2009; Walton et al. 2009), and ingots from the Uluburun shipwreck (Jackson and Nicholson 2010).

One glass bead, 580.2-1, did not plot near any of the other samples from Kefalonia or the glasses of Egyptian or Near Eastern origin (Figure 6.21). This was to be expected because the bead is a mixed-alkali glass and therefore likely made elsewhere. The glass is characterized by elevated levels of lanthanum (11.58 ppm) and zirconium (94.54 ppm) (Table 7.6). The bead did not overlap with mixed alkali glasses from southern Italy (Conte et al. 2019) and was not produced in the same region. Trace element data for the Frattesina mixed alkali glasses has not been published, and therefore could not be used to determine if 580.2-1 was made in northern Italy. Due to the small number of published trace element data for mixed alkali glasses, no parallels have been found as of yet that could help determine where the glass the Kefalonian LMHK bead was made.

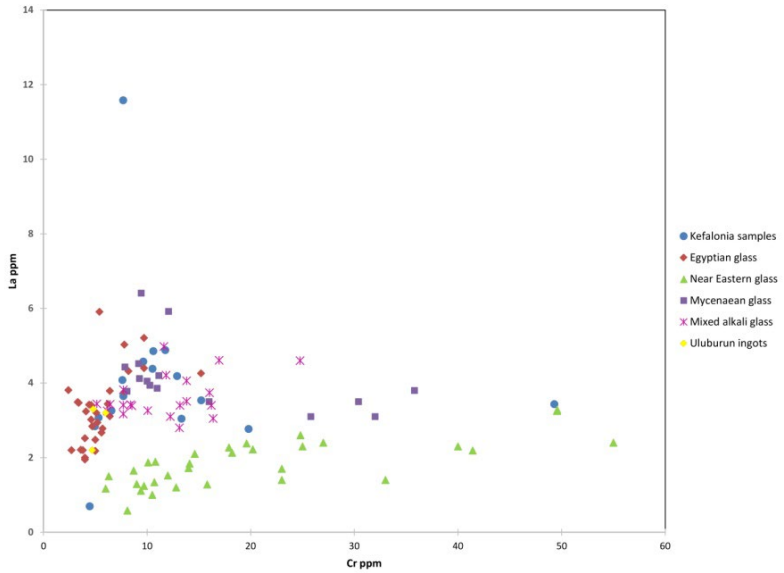

Figure 6.22. Plot of the concentrations of chromium and lanthanum in the Kefalonian samples compared to glasses of Egyptian origin (Shortland et al. 2007), Near Eastern origin, (Shortland et al. 2007; Kirk 2011; Kemp et al. 2020), Mycenaean glass of both Near Eastern and Egyptian origin (Smirniou et al. 2009; Walton et al. 2009), mixed alkali glasses from southern Italy (Conte et al. 2019), and ingots from the Uluburun shipwreck (Jackson and Nicholson 2010)

Σ2-K1-4, the Mycenaean Group B faience bead, is not of Egyptian origin based on the cobalt colorant used and the concentrations of chromium, lanthanum, zirconium, and titanium, and their ratios, confirms this (Figure 6.21, Figure 6.22). It has low concentrations of the four transition elements of interest (Table 6.7) and is similar to the alkali and silica sources used for glasses manufactured in the Near East. Trace element data was found from one published example of a glassy faience bead (PZ FP3) from Punta di Zambrone, southern Italy that was found to be similar to Mycenaean Group B faience (Conte et al. 2015). However, the southern Italian bead is not similar in these transition elements to the Kokkolata-Menegata faience bead, Σ2-K1-4. PZ FP3 has much higher concentrations of chromium (48.76 ppm), lanthanum (48.76 ppm), and zirconium (51.71 ppm) (Conte et al. 2015). The lack of published trace element data for other Mycenaean Group B faience makes interpretation of the Σ2-K1-4 data challenging. Additional Aegean examples could help determine whether this faience bead is of Near Eastern origin or produced in a different region with raw materials that are low in these particular trace elements.

The concentrations of strontium and neodymium were examined to see whether any additional information could be obtained on the provenance of those beads (Table 6.7). All the beads that had been identified as having an Egyptian origin based on the ratios of Cr/La and 1000Zr/Ti grouped with glasses from Amarna based on their strontium (226.02-950.07 ppm, avg. 682.08 ppm) and neodymium (2.68-6.88 ppm, avg. 4.53 ppm) concentrations. Bead 580.2-2 has the lowest concentration of strontium (226.02 ppm) of all the Egyptian sourced samples. The range of strontium and neodymium concentrations in the Amarna glasses

(Henderson et al. 2010; Muros 2020), those from mainland Greece (Henderson et al. 2010; Smirniou et al. 2009; Walton et al. 2009), and the Uluburun ingots (Jackson and Nicholson 2010) is quite varied, and they do not make a tight group like the Near Eastern samples (Figure 6.23).

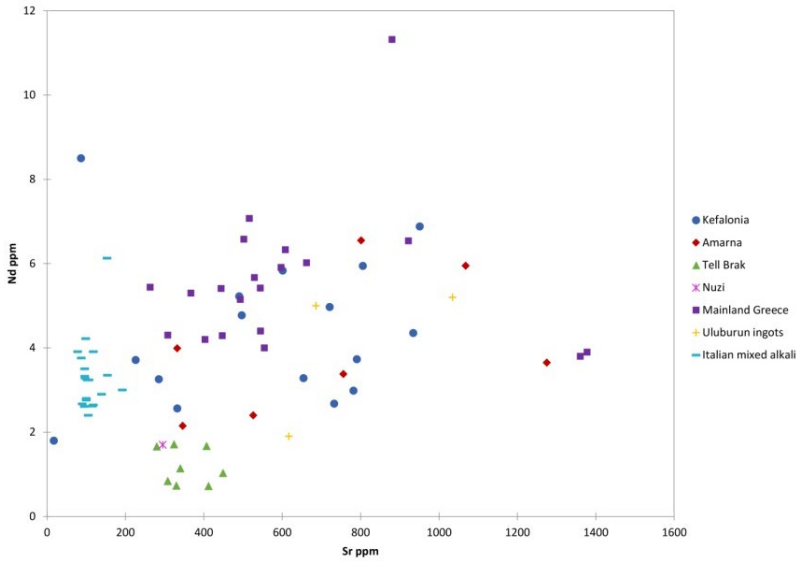

Figure 6.23. Concentrations of strontium and neodymium in the Kefalonian samples compared to samples from Egypt (Henderson et al. 2010; Muros 2020), the Near East (Henderson et al. 2015), mainland Greece (Smirniou et al. 2009; Walton et al. 2009; Henderson et al. 2010), Uluburun ingots (Jackson and Nicholson 2010), and mixed alkali glasses from Italy (Henderson et al. 2015; Conte et al. 2019).

Despite the variations seen across the Egyptian and Mycenaean samples, there seem to be some differences in the strontium and neodymium concentrations between the two groups (Figure 6.23). Most of the Mycenaean glasses appear to have higher concentrations of neodymium and the majority of glasses have strontium concentrations that fall between 300-600 ppm. This is different from what is seen in the samples from Egypt. It is not clear whether the lack of overlap between the Mycenaean and Egyptian strontium and neodymium samples is due to the small number of published data available or is related to the use of different silica sources or plant ashes used to make Mycenaean glass. Differences between the Egyptian and Mycenaean glasses, and in particular the cobalt and Co-Cu glasses, were found in the examination of the levels of impurities from the cobalt colorant, even though the source for both was cobaltiferous alum from the Western Desert (Figure 6.14). A distinction between the cobalt containing glasses from these two areas was also observed in the PCA (Figure 6.20). In light of the fact that there seem to be distinctions between the raw materials used between these sets of glasses, even when the Mycenaean glasses seem to be from raw materials of Egyptian origin, the different components of the raw materials need be investigated further to determine what is causing these distinctions in the compositions.

Sample M18-3 has concentrations of strontium (332.20 ppm) and neodymium (2.56 ppm) that plotted just above the Near Eastern group (Table 6.7). Bead 580.2-2 and Σ2-K1-1 had strontium concentrations higher than the Near Eastern group, but lower than the Egyptian, Greek, and Uluburun glasses. Based on the concentrations of chromium, lanthanum, zirconium, and titanium, 580.2-2 was similar to glasses made in Egypt. Σ2-K1-1 was closer to glasses made in the Near East, however it contained high concentrations of chromium. It is possible that these two samples represent variations within the raw materials used or the use of a raw material from a different geological source.

Two samples (Σ2-K1-4, 580.2-1) did not plot near the Amarna or Near Eastern groups (Figure 6.23). Both beads are characterized by low concentrations of strontium (11.71-86.54 ppm) (Table 6.7). Bead 580.2-1 is the mixed alkali bead whose origin is still unclear. It has a low concentration of strontium (86.54 ppm), but

very high neodymium (8.50 ppm) (Table 6.7). Since Kefalonia had evidence of southern Italian imported cultural material (Souyoudzoglou-Haywood et al. 2017), the bead was compared to mixed-alkali glasses of southern Italy (Figure 6.23) (Conte et al. 2019). The strontium values were similar but the Kefalonian bead has much more neodymium than the southern Italian glass. Northern Italian glasses from Frattesina were also included in the plot (Henderson et al. 2015), but those concentrations overlapped with the southern Italian material and not bead 580.2-1. It is clear based on many aspects of the raw materials the glass was not made with raw materials sourced to Egypt or the Near East, however, no further information on provenance is known. The biconical faience bead, Σ2-K1-4, has low concentrations of both trace elements (17.26 ppm Sr, 1.80 ppm Nd). Although the origin of Group B Mycenaean faience is unknown, some of the trace elements concentrations appear to be similar to glasses from the Near East. Without trace element analysis of additional examples of Mycenaean Group B faience, determining the provenance of these vitreous materials is difficult.

Based on the concentrations of the trace elements, the sites on Kefalonia contained glasses made from Egyptian raw materials, as well as raw glass made in the Near East. As mentioned above, beads were found at Pylos that were made in the Near East, but there were also beads analyzed that came from Egyptian primary production sites (Polikreti et al. 2011). The dates of the Pylos beads showed that the earlier beads were Near Eastern imports, while later beads Egyptian. This may provide information on changes to trade routes or connections for this type of prestige item over time into Mycenaean Greece. This geographic pattern of glass imports counters what is seen in other artifact material types where in earlier periods, such as the LH I-II, Egyptian imports dominated, but in later periods (LHIII) the origins of foreign object were more varied (Polikreti et al. 2011, 2894). On Kefalonia, the dates of many of the contexts are not known or secure, nor are the find locations for most of the beads. Based on the relative dates provided for the tombs, almost all beads date to the LH IIIA2-C period (ca. 1350-1050 BC). The exception is Σ2-K1-1 (glass bead) and Σ2-K1-4 (biconical faience bead), that may come from a MH III tomb (ca. 1700-1550 BC). Although the sample set is small, it does appear that the Kefalonian samples do follow the trends observed at Pylos, where older material seems to be originating in the Near East, with later glasses are predominately of Egyptian origin. On Kefalonia, however, mixed alkali glasses were present in LH III contexts and therefore glass imports from production sites west of Greece were also taking place. More analysis is needed of glasses from securely dated contexts to further determine these chronological trends and changes in trading partners.

6.4.3.3 Isotopic analysis

Six samples underwent radiogenic isotopic analysis to further aid in identifying the provenance of the beads using strontium and neodymium signatures from the alkali and silica used (Table 3.1). The ratios of $^{87}Sr/^{86}Sr$ and $^{143}Nd/^{144}Nd$ isotopes in the Kefalonian samples were compared to those from Egyptian (Degryse et al. 2010a; Henderson et al. 2010; Degryse et al. 2015; Muros 2020), Near Eastern (Degryse et al. 2010a; Henderson et al. 2010; Degryse et al. 2015; Shortland et al. 2018), and Mycenaean glasses from mainland Greece (Henderson et al. 2010) (Figure 6.24).

Table 6.8. Results of the strontium and neodymium isotopic analysis

Sample	$^{87}Sr/^{86}Sr$	$^{143}Nd/^{144}Nd$
M18-3	0.70844	0.51221
M23-2	0.70785	0.51212
M32-1	0.70786	no data
K13-4	0.70818	0.51215
Σ2-K1-1	0.70855	0.51225
Σ2-K1-4	0.70889	no data

No data was obtained on the neodymium isotopic ratios for the biconical faience bead, Σ2-K1-4, and the relief bead M32-1, and therefore they were not included on the biplot. The ratios show there is some variation among the source of the glasses from Kefalonia, with the isotopic data confirming some of the source interpretations made using the LA-ICP-MS data.

Two of the samples, M23-2 and K13-4, both relief beads, are likely of Egyptian origin (Figure 6.24). They contained 0.07085 -0.70818 $^{87}Sr/^{86}Sr$ and 0.51212 -0.51215 $^{143}Nd/^{144}Nd$ (Table 6.8). Both beads however did not fit neatly into the group of glasses from Amarna and Malkata in Egypt. Bead M23-2 had isotopic ratios lower than those found in Egyptian and Mycenaean glasses. It is possible that these lower values reflect a variation among the known Egyptian sources or perhaps points to a different source of Egyptian raw materials that differs from what is used to make glasses at Amarna and Malkata. The $^{87}Sr/^{86}Sr$ ratio for K13-4, the Kefalonian type triple rosette relief bead, is slightly higher than those found in Egyptian glasses. The ratio moves it closer to the strontium signatures seen in Near Eastern glasses, mainly from Nuzi, with higher $^{87}Sr/^{86}Sr$ signatures but lower $^{143}Nd/^{144}Nd$. It is not clear if this necessarily means that K13-4 is not of Egyptian origin, especially since the trace element analysis does show similarities with Egyptian sourced silica and plant ashes. Without additional published samples for comparison, it is not known whether this is just simply a variation among the strontium isotope signatures of Egyptian raw materials or has some other significance. Having additional Egyptian and Near Eastern samples to compare the Kefalonian glasses to would help improve the sourcing, in particular for K13-4 since that represents a regional style of relief bead. It would be interesting to determine if these beads did originate from another glassmaking center, whether the raw glass used to form the triple rosette bead was made with raw materials specifically chosen for this bead form, or whether it was made through the mixing of materials from different sources.

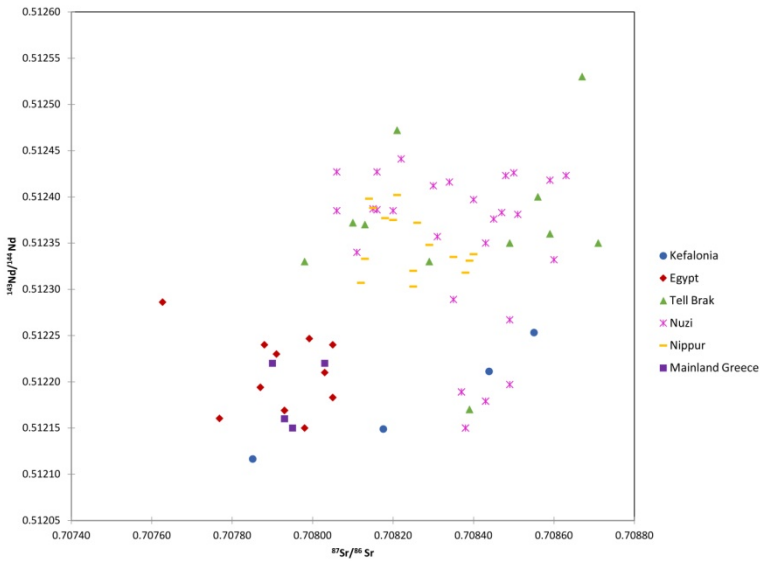

Figure 6.24. Results of $^{87}Sr/^{86}Sr$ and $^{143}Nd/^{144}Nd$ isotopic analysis of the samples from Kefalonia compared to glasses from Amarna and Malkata in Egypt (Degryse et al. 2010a; Henderson et al. 2010; Degryse et al. 2015; Muros 2020), from Tell Brak, Nuzi, and Nippur in the Near East (Degryse et al. 2010a; Henderson et al. 2010; Degryse et al. 2015), and Mycenaean glasses found on mainland Greece (Henderson et al. 2010).

Glass beads M18-3 and Σ2-K1-1 seem to have a varied range of strontium and neodymium isotopic signatures ($^{87}Sr/^{86}Sr$ 0.70844-0.70855, $^{143}Nd/^{144}Nd$ 0.51221-0.51225) (Table 6.8). The trace element data indicated the beads could be of Near Eastern origin and the isotopic data supports this. Both samples had higher ratios of $^{87}Sr/^{86}Sr$ than the Egyptian samples (Figure 6.24). M18-3, which was the pink bead, is similar in its alkali and silica source as reflected in the isotope results to a group of glasses from Nuzi and one from Tell Brak. Σ2-K1-1 has similar measurements to a multicolor bead from Nuzi (Degryse et al. 2015). The Near Eastern material, which contains the majority of the Tell Brak glasses and all of those from Nippur, has a

wider range of strontium and neodymium signatures. Therefore, it is possible that Σ2-K1-1 falls within that source group. It is also possible that the glass was made using a source of silica or plant ash different from those used for Nuzi, Tell Brak, and Nippur glasses, especially given the high concentration of chromium in the bead. Until there is more published data from Late Bronze Age glasses of known provenance, interpretation of isotopic data from these glasses will continue to be challenging.

6.5 CHAPTER SUMMARY AND CONCLUSIONS

A group of beads excavated from the sites of Mazarakata, Metaxata, and Kokkolata-Menegata on the island of Kefalonia were analyzed. The Ionian Islands, which Kefalonia belongs to, has evidence of occupation since the Neolithic period with the number of sites increasing over time until the Late Bronze Age (1200-1050 BC) when the largest number of sites were established. Few settlements have been discovered on Kefalonia and most of the archaeological information comes from cemeteries.

Beginning in the 4th millennium BC and continuing through the 11th c BC, there is evidence for the import of artifacts from various regions. Kefalonia was strategically positioned along an east-west trade route with material arriving from the Aegean/Eastern Mediterranean and the Adriatic Sea/Western Mediterranean. Objects from the Greek mainland were also abundant, in particular Mycenaean artifacts. Adoption of burial styles and tomb types from the mainland also occurred. Alongside the import of foreign material and the adoption of cultural practices from other parts of the Aegean, regional styles emerged. These were observed in the creation of cave dormitory type tombs, unique pottery styles, and in glass bead forms, such as the triple rosette and beaded circle. The relief bead forms are unique to the island and have not been found outside Kefalonia. Although the decline of the Mycenaean palatial centers and the destruction of sites begins on the mainland in the late 13th-12th century, this does not occur on Kefalonia. During this period, settlements and cemeteries continue to be used until the 11th c. BC. The number of sites increases in some areas of the island. New pottery types appear and material still seem to be imported.

The sites of Mazarakata, Metaxata, and Kokkolata-Menegata are located on the Argostoli plain. All three cemeteries were used during the Late Bronze Age, with most of the tombs dating to the LH IIIC period (ca. 1200-1040 BC), and some with earlier burials used in earlier periods (ca. 1350-1200BC, LH IIIA2-LH IIIB). The cemetery at Kokkolata-Menegata has cist tombs that were the earliest found built in the LM III period (1700-1550 BC). The beads analyzed were discovered in excavations that took place in the first half of the 20th century and are currently housed at the Archaeological Museum of Argostoli. There is some published information available on the beads, but the archaeological context for many of the beads excavated is not available.

Forty-five beads were analyzed qualitatively using pXRF and 18 were sampled for quantitative compositional analysis. The bead forms and the color palette represent typical Mycenaean glass assemblages with relief beads and the majority of the glasses are blue. The blue glasses are colored with copper, cobalt, or a combination of cobalt and copper. The copper containing glasses included those with tin where the colorant source was bronze scrap and those without tin where a copper mineral was used. Some of the blue beads contained antimony. This is generally added as an opacifier, but the beads were not opaque. The reason for the addition of antimony in the translucent beads is unclear. It is possible that it is a contaminant from perhaps reuse of a crucible or some kind of manufacturing error where the beads should have been opacified but did not turn out that way.

Other colors were represented among the glasses. One bead was pink in color. From the results of the analysis, it did not appear to contain any added mineral colorants. Iron was present in concentrations found naturally in the raw materials, and the bead could have been colored through a combination of the iron in the glass changing color due to the furnace atmosphere.

Two of the glasses were purple and colored using manganese. One of the purple glasses (M40-P) was a chunk of glass with a crust on one side. It was not clear if this object was a fragment of a larger artifact or it represented a piece of raw glass or an ingot. The crust resembled the surfaces seen on glass chunks from Amarna with the remains of the crucible interior and the glass/crucible interaction layer (Muros, 2020). Further visual examination of M40-P would be needed, as well as analysis of the crust, to determine whether it was a piece of raw glass with some of the crucible still attached.

All the glass beads analyzed, with the exception of one bead, were high soda plant ash glasses typically found in the Late Bronze Age. All the beads that contained cobalt were low in potash, something found in cobalt glasses in Egypt and Mycenaean contexts. The concentrations of the transitional elements related to the cobalt source (manganese, nickel, zinc, iron, and aluminum) all fell within the range found in glasses made using cobaltiferous alum from the Western Desert.

One bead from Kokkolata-Menegata, 580.2-1, was a mixed alkali glass (LMHK) similar in composition to mixed alkali beads from Frattesina in northern Italy and the Mycenaean site of Elateia. The date of the Kefalonian LMHK bead is unclear since a range was given for the tomb it was found in, from the 14th-11th c. BC. However, this range does place it alongside the LHMK bead from Elateia and one from the island of Thasos as some of the oldest examples of this glass compositional type in the Eastern Mediterranean.

Trace element analysis was used to determine the origin of the glasses. Two beads from Mazarakata and Kokkolata-Menegata were similar in their concentrations of chromium, lanthanum, titanium, and zirconium to glasses made in the Near East. All the other samples were similar to those made in Egypt, including one triple rosette relief bead (K13-4) and the purple chunk of glass (M40-P). Even though the design of the triple rosette was unique to Kefalonia, the glass was imported from elsewhere. The bead could have been worked locally or was produced elsewhere and exported only to the island. No evidence of glass workshops or associated materials, such as molds, has been found on Kefalonia. Therefore, the location of the glassworking site where the triple rosette relief bead was manufactured has not been identified.

Strontium and neodymium isotopic analysis was conducted on six glass samples in order to obtain more accurate information on the source of the silica and alkalis. The ratios of $^{87}Sr/^{86}Sr$ and $^{143}Nd/^{144}Nd$ in four of the beads were somewhat similar to beads made in the Near East. One bead, M18-3, groups with beads from Nuzi. The other three beads (M40-1, M40-6, Σ2-K1-1) contained higher strontium ratios and lower neodymium ones than most of the Near Eastern samples from Nuzi, Nippur, and Tell Brak they were compared to but were not of Egyptian origin. Bead M23-2 grouped close to the beads from Egypt and Mycenaean glasses from Egyptian origin, though it had lower values of both $^{87}Sr/^{86}Sr$ and $^{143}Nd/^{144}Nd$ than the comparative material.

The triple rosette relief bead (K13-4) underwent isotopic analysis to confirm whether the raw materials were of Egyptian origin, as was shown with the trace element analysis. The strontium isotope ratios fell somewhere between the values for Egyptian glasses from Amarna and Malkata and another group containing glasses from Nuzi and one from Tell Brak. It is not clear if this is just the result of variability among the raw materials in a particular regional source or if it represents the mixing of glasses imported from two different production areas. There has not been much isotopic analysis of Late Bronze Age glasses undertaken, and with limited comparative data, determining the source of the glasses that do not fall neatly within the isotopic ratio groups is challenging.

The mixed alkali bead (580.2-1) could not undergo radiogenic isotopic analysis because the sample was too small. The concentrations of strontium and neodymium in the bead obtained through LA-ICP-MS were examined to see if any additional information could be gleaned to determine the provenance of the glass. The bead did not overlap with any of the data used for comparison that included southern Italian mixed alkali glasses. The Kefalonia LMHK bead was similar to mixed alkali glasses from Frattesina and Elateia in

regards to the levels of chromium, lanthanum, titanium, and zirconium, but data was not available for the neodymium and strontium values for comparison. For now, the source of the raw materials used to make bead 580-2.1 is unknown, but it is clear that it was not made in the Near East, Egypt, or southern Italy.

One biconical faience bead (Σ2-K1-4) from Kokkolata-Menegata underwent compositional analysis. The bead was dark blue and colored with a combination of cobalt and copper. The bead has a glassy microstructure with no distinct glaze layer. It appears to be Mycenaean Group B faience. Group B has a different composition than Egyptian faience, with low potash and magnesia, and high alumina, iron, cobalt, and lead. The concentrations of the alkali flux components could point to the use of natron.

The biconical bead was low in manganese and zinc, but high in nickel. The concentrations of these elements indicate that the source of the cobalt used as the colorant is different from the cobaltiferous alum found in the Western Desert. These values were not similar to cobalt color glasses from Nippur that uses a different cobalt source. The composition of Σ2-K1-4 overall, including the elements related to the cobalt source, is similar to Mycenaean Group B beads found on Crete and the island of Psara. The cobalt source of the biconical bead was also similar to one used for some cobalt colored mixed alkali glass in northern and southern Italy and Elateia. The location of the primary production center for these beads, as well as the source of the cobalt used, is unknown.

The concentrations of chromium, lanthanum, titanium, and zirconium in the biconical bead was not similar to glasses made in Egypt but did share some similarities with glasses from the Near East, such as a low ratio of Cr/La and a high ratio of Zr/Ti. However, the ratios and the values of some of the trace elements exceed those found in the Near East. Trace element data was found for a Mycenaean Group B faience bead from southern Italy, but it was not similar to Σ2-K1-4 in that the concentrations of the four trace elements of interest were much higher. The sample taken from biconical bead could not undergo isotopic analysis, but the strontium and neodymium concentrations were examined to see whether it provided any additional information on provenance. The neodymium and strontium concentrations in the faience bead are low, though the levels of neodymium are at the higher end of those found in Near Eastern glasses. The biconical bead was an outlier in the biplot and did not overlap with any other samples. There are some similarities between biconical faience bead and the trace elements of some of the Near Eastern silica and alkali raw materials so perhaps this points to a possible origin for these glasses. Without additional trace element and isotopic analysis of Mycenaean Group B faience beads found at other sites and cobalt colorants from different regions, sourcing this particular vitreous material is not possible.

7 VITREOUS MATERIALS FROM THE BALKANS: THE TUMULUS AT LOFKËND

7.1 INTRODUCTION

The prehistoric tumulus of Lofkënd is located in the Mallakaster region of southwestern Albania, near the modern village of Lofkënd (Figure 7.1). The site was excavated from 2004-2008 through a collaborative project undertaken by the Cotsen Institute of Archaeology at the University of California, Los Angeles (UCLA), the Institute of Archaeology, Academy of Sciences, Tirana and the International Center for Albanian Archaeology (Papadopoulos et al. 2014b). Over the four seasons of excavation 100 graves were discovered containing over 150 individuals (Damiata and Southon 2014a). The tumulus was in use from ca. 14th c. BC to the late 9th c./early 8th c. BC, spanning the Late Bronze Age to Early Iron Age periods (Damiata et al. 2009). Several graves were found in the northeast section of the tumulus, which date to the 19th c. AD and are evidence for reuse of the site as a modern cemetery.

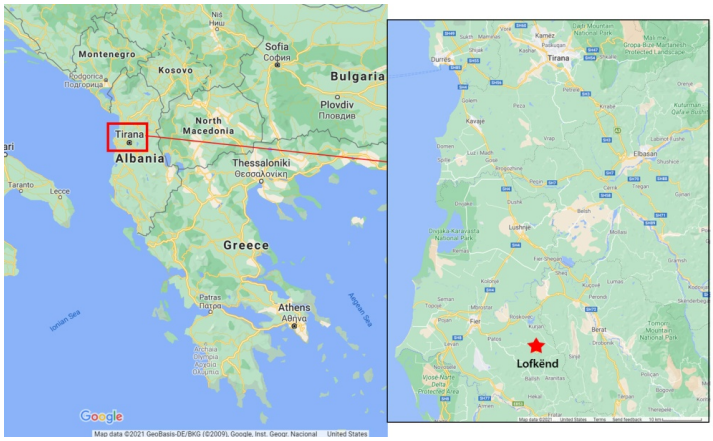

Figure 7.1. Location of Lofkënd (Maps from Google Maps. Larger map: Map data ©2020 Google, GeoBasis-DE/BKG ©2009 ; Detail: Map data ©2020)

The region known as Illyria, which encompasses the western Balkan Peninsula, was situated at a crossroads between several land and sea trade routes. Evidence for the import of foreign cultural material is found as early as the Middle Bronze Age, ca. 1650 BC (late MH period) (Bejko 2002). These early finds consist mainly of some pottery and bronze artifacts of Minoan origin. Although Mycenaean objects are not found during this period, locally made objects were discovered with characteristics from the Greek mainland. This shows contact with both Crete and mainland Greece during this period. These cultural objects are found primarily at coastal sites indicating the Adriatic was the likely route taken to transport many of these materials from the Aegean. The inland part of the country also had some of this material suggesting movement over land routes from northern Greece.

Beginning in the 15th c. BC (LH IIB) there is an increase in the number of Mycenaean finds (Bejko 2002). Unlike in earlier periods where these finds came from burial contexts, they appear in both settlements and cemeteries. The number of imports continues to increase even during the period of the destruction of the Mycenaean palaces and their centralized control (ca. 1250 BC). As was observed on Kefalonia, though Mycenaean sites were destroyed or abandoned on the mainland, the import of cultural material from the Aegean continued, and intensified, during this period. Imported finds were not limited to Mycenaean material. Evidence for cultural material from northwest Greece, the northern Balkans, southern Albania, and southern Italy are also found (Bejko 2002; Papadopoulos 2010). Amber beads have also been excavated from Late Bronze Age contexts, and therefore Albania was part of the amber route, where these beads traveled from the Baltic Coast along the Adriatic to reach coastal sites and then moved inland (Harding 1976; Kurti 2017)

7.2 DESCRIPTION OF THE TUMULUS AT LOFKËND

The tumulus at Lofkënd was formed over 600 years and was a prominent feature on the landscape (Papadopoulos et al. 2014c). Tumuli are common in Albania during the Bronze and Iron Ages (Stapleton 2014). They first appear in the 3rd millennium BC and continue to be built through the 4th c. BC. The tumuli all share common characteristics. They are generally built over a single central burial, surrounded by stones. Stones or cairns are often placed on the top of the tumulus. All the tumuli seem to have pit graves, though there is some variation in the type of grave as some have cist graves and others have wooden coffins. Inhumations, some with multiple individuals interred, seem to be common though cremations have also been found.

The tumulus at Lofkënd, measuring 20.54 m by 10.54 m was built over several phases (Papadopoulos et al. 2015). Over the period of its use the mound itself was often modified as it was reopened to add more burials (Papadopoulos et al. 2014c). Construction began with the earliest burials in 1400 BC (LH IIIA1-IIIB) positioned around a central grave (Papadopoulos 2010; Stapleton 2014). Unlike other tumuli, however, this grave was not marked by a ring of stones (Stapleton 2014). The burials during this initial phase do not have many grave goods. Some pottery is found in the tombs along with some items of personal adornment (Morris and Papadopoulos 2014).

It is during the next phase of use that the mound grew (Morris and Papadopoulos 2014). More individuals are interred in tombs with more grave goods. Multiple inhumations are found. An increase in the number of female, child, and adolescent burials is observed. These burial patterns continue until about the Early Iron Age (ca. 953 BC), marking the third phase of tumulus use.

The final phase took place during 900-800 BC where many more burials occur (Morris and Papadopoulos 2014). The use of the tumulus ends around 800 BC and it is not clear what led the abandonment of this cemetery. Settlements in neighboring areas begin to fortify signaling some kind of change. One suggestion has been that incoming groups entered the region and displaced the people who used the tumulus at Lofkënd, perhaps forcing them to move to the fortified settlements or migrate out of the region to southern Italy.

No settlement has been found near the tumulus, but the Gjanicë River valley below the tumulus is the likely location (Martin-McAuliffe 2014). Given the size of the tumulus, it would clearly have been something visible on the landscape. It has been suggested that the mound may have acted as a boundary marker for the clan-based tribes that had control of the area (Stapleton 2014).

Eighty-five of the graves date to the prehistoric period, with the remaining 13 from the period of reuse of the tumulus (Schepartz 2014; Stapleton 2014). The majority of the tombs are single inhumations, though 27 contained multiple individuals (Schepartz 2014). The preservation of skeletal material is poor, but when human remains were found, the bodies were generally laid out in a supine position with legs flexed and the arms bent over the chest (Stapleton 2014). In addition to deteriorated skeletal remains, some graves also showed signs of disturbance due to the reopening of the tumulus for burials that took place at different times. In some cases, graves cut into each other, which disturbed older remains and grave deposits. All the graves at Lofkënd were pit graves, where larger tombs had rectangular cuts and smaller ones were ovoid. Although there are some general characteristics that apply to all the graves, each one is unique in that they are all different sizes with different combinations of grave goods.

Only half of the graves contained grave goods, with female and child burials including a larger number (Stapleton 2014). The grave goods included varied materials and artifact types: local and imported pottery, metal tools or weapons, items of personal adornment such as hair ornaments, jewelry, fibulae and pains, and beads made of stone, glass and faience (Papadopoulos and Kurti 2014). As mentioned above, the range

of finds from the tumulus show contact with people outside of Illyria with artifacts arriving from northwest Greece, the Aegean, northern Balkans, central Europe, and southern Italy.

7.3 DESCRIPTION OF THE VITREOUS BEADS

Eleven vitreous beads, 10 glass and one faience, were found during the excavation of the tumulus (Table 7.1). These artifacts come from four tombs that range in date from the 12th-9th c. BC , spanning the Late Bronze Age to the Early Iron Age (Damiata and Southon 2014b). Two glass beads, 10/110 and 10/111, were found in the topsoil (Papadopoulos et al. 2014a) and are not included in this study since their context was unknown.

7.3.1 The Tombs and their Burial Context

7.3.1.1 Tomb XXI

Tomb XXI (Grave 55) was a pit tomb dating to the 12th-11th c. BC (Late Bronze Age) (Damiata and Southon 2014b; Papadopoulos et al. 2014a). The grave contained a double inhumation, an adolescent female and an adult male. The skeleton of the male was in better condition. He had been laid out in a northeast-southwest orientation with his head to the northwest. He was in a supine position with his arms crossed over his torso. The legs were disturbed and therefore their position could not be determined. Only the cranium of the adolescent female survived. Grave goods included pottery, both wheel and handmade, four bronze objects of personal adornment (fibula, ring, headband, disc or boss), tubular iron beads and coil/spirals, and a glass bead (10/114) (table 7.1). The fibula found is of the Cassibile type found in southern Italy and an import.

Table 7.1. Description of the tombs with vitreous beads

Tomb	Date	Burial Type	Grave Goods
XXI (Grave 55)	12th-11th c. BC	Inhumation; Adolescent female (15 yo ±3); adult male (20-25 yo) in supine position with arms folded across lower torso	Ceramic vessel (kantharos) Bronze fibula (Cassibile type) Bronze headband Bronze boss Bronze ring Iron sheet object Iron tubular beads Iron coil/spiral Glass bead (10/114)
XXVIII (Grave 77)	12th-11th c. BC	Inhumation; Child/infant (3 yo ±24 months)	Bronze spectacle ornament Bronze wheel pendant Bronze fibula (Cassibile type) Carnelian or sardonyx bead Glass bead (10/106) Glass bead (10/108) Glass bead (10/112) Glass bead (10/115) Glass bead (10/116) Glass bead (10/117)
LIII (Grave 63)	11th-10th c. BC	Inhumation; Adult (25-35 yo) on side with flexed knees; child (4 yo ±1.3)	Ceramic vessel Bronze disc or boss Bronze earring Bronze spectacle ornament/pendant Bronze spiral coil Carnelian or sardonyx bead Faience bead (10/105) Glass bead (10/107) Glass bead (10/109)
LV (Grave 63)	Late 10th-9th c. BC	Inhumation; child	Matt painted ceramic vessel Iron fibula Bimetallic (Fe and Cu alloy) fibula tubular iron beads Glass bead (10/113)

7.3.1.2 Tomb XXVIII

Tomb XXVIII (Grave 77) was a pit tomb containing a child or infant about 3 (±2) years old (Papadopoulos et al. 2014a). The skeletal remains were poorly preserved, with only the cranium remaining. There were no post-cranial skeletal remains but based on the position of the skull, it is possible the infant/child was oriented northeast-southwest. Visible in the stratigraphy of the tomb were bands of a dark organic materials. Wooden coffins have been found within tumuli graves in Albania (Stapleton 2014), and it is possible that this decayed organic material could be the remains of a wood coffin or some kind of covering. The majority of the finds in the grave were located on or below the cranium. The grave goods included pottery, three bronze objects, one bead made of carnelian or sardonyx, and six glass beads that were found on or around the skull (Table 7.1). This tomb also contained a Cassibile type fibula. This burial contained the largest number of glass beads. The tomb dates to the 12th-11th c. BC (Late Bronze Age) (Damiata and Southon 2014b).

7.3.1.3 Tomb LIII

Tomb LIII (Grave 63) was a pit tomb that contained two inhumations—an adult (25-35 years old) and a child (4 years old ±16 months) (Papadopoulos et al. 2014a). The skeletal remains of both individuals were poorly preserved. The adult appeared to have been laying on his/her side with flexed knees in a southeast-northwest orientation. The only remains found of the child were fragments of the cranium and teeth. Several grave goods were found in the tomb including a ceramic vessel, four bronze ornaments or items of personal adornments, a carnelian or sardonyx bead, a faience bead, and two glass beads. This tomb dates to the 11th-10th c. BC (Sub-Mycenaean period – Early Iron Age) (Damiata and Southon 2014b).

7.3.1.4 Tomb LV

Tomb LV (Grave 53) was a pit tomb that contained a single inhumation of a child aged 8 (± 1) years old (Papadopoulos et al. 2014a). The skeleton was poorly preserved, but from the remains, it was possible to determine the child had been laid out in a supine position in a southeast-northwest orientation. The grave goods were found near or around the cranium and mandible area. The items included a matt-painted vessel, an iron fibula, a bimetallic (iron and bronze) fibula, four tubular iron beads, and one glass bead. This tomb dates to the late 10th-9th c. BC (Early Iron Age) (Damiata and Southon 2014b).

7.3.2 Vitreous bead types

Although there are only 11 vitreous beads that were discovered at the site, they represent a varied range of bead shapes and decoration types (Table 7.2, Appendix D.1) (Papadopoulos and Muros 2014). No two beads are alike and several shapes and types of decoration that have not been widely published are represented.

7.3.2.1 Glass beads

Four of the glass beads (10/106, 10/108, 10/109, 10/113) are globular, a very common bead shape (Table 7.2) (Papadopoulos and Muros 2014). Bead 10/106 and 10/113 correspond to Beck's (1928, 5, pl. II-III) "circular standard beads" (Type I.C.1.a). 10/113 is slightly ovoid in shape along the perimeter and is considered a short bead based on its length ("ovoid, short circular bead", Type III.B.1.a) (Beck, 1928, p. 5, pls. II-III). 10/109 is slightly ellipsoidal in shape (Type II.C.1.a) (Beck 1928, 5, pls. II-III). All of these bead shapes are ubiquitous in the archaeological record and found in a variety of material types. Beads 10/108, 10/109, and 10/113 have the perforation preserved and the shape is conical, corresponding to Beck's perforation Type III (1928, pl. IV). The bead was formed by winding the gob of glass on a tapered mandrel (Küçükerman 1988). There are a series of fine lines running across the surface of the bead showing the direction the glass was wound on the mandrel (Figure 7.2). The perforation on bead 10/106 is damaged at one end and it is not clear if it is also conical. Based on what is preserved it appears that it may have straight sides and correspond to perforation Type IV (Beck 1928, pl. IV).

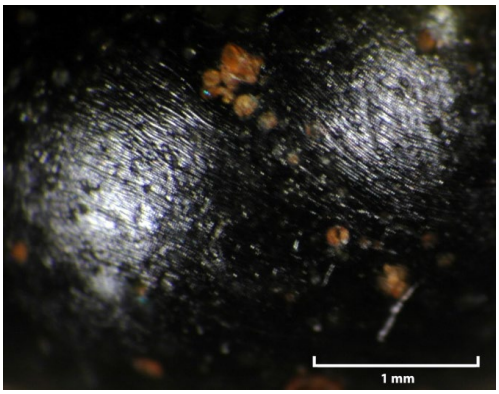

Figure 7.2. Photomicrograph of bead 10/113 showing horizontal ridges on the surface of the glass. The ridges are the result of the bead being formed through winding on a mandrel.

Table 7.2. Description of the vitreous beads examined

Bead No.	Add'l Nos.	Material	Color	Bead shape and decoration	Beck Type[1]	Perforation Type[1]
10/105	SF298/ TLIII-9	Faience	Blue-green glaze and whitish-yellow interior	Circular long barrel granulated bead	I.D.1.b/ XXV.A.5	Single cone (III)
10/106	SF342/ TXXVIII-8	Glass	Translucent dark green /Glass corroded to opaque yellow-brown	Circular standard bead	I.C.1.a	Plain (IV?)[2]
10/107	SF295/ TLIII-8	Glass	Translucent dark green/Glass corroded to opaque golden yellow	Bead shape unknown	Fragmentary	Fragmentary
10/108	SF341/ TXXVIII-7	Glass	Translucent dark green with opaque white horizontal band/ Glass corroded to opaque orange-brown	Circular standard bead/zone bead	I.C.1.a/ XLVII.A.1.a	Single cone (III)
10/109	SF294/ TLIII-6	Glass	Translucent dark green with opaque white spots and line/glass corroded to opaque reddish-brown	Ellipsoidal standard bead/simple spot eye bead	II.C.1.a/ XLVI.A.2	Single cone (III)
10/112	SF338/ TXXVIIII-4	Glass	Translucent blue-green	Fluted ellipsoidal short bead	II.B.1.a/ XXIII.A	Single cone, extra large (III/VI.a)
10/113	SF283/ TLV-8	Glass	Translucent dark green	Ovoid short circular bead	III.B.1.a	Single cone, medium large (III/VI.a)
10/114	SF258/ TXXI-8	Glass	Opaque white	Fluted ellipsoidal standard bead	XXIII.A.2.a	Single cone (III)?[3]
10/115	SF339/ TXXVIII-5	Glass	Translucent dark green with opaque white waves or chevrons	Circular flat long bead with wire-drawn chevrons	VII.D.I.a/ XLVII.A.7.a	Single cone (III)
10/116	SF344/ TXXVIII-9	Glass	Translucent dark green with opaque white spots/Glass corroded to opaque golden yellow	Spot eye bead	XLVI.A.2[4]	fragmentary
10/117	SF351/ TXXVIII-10	Glass	Translucent light blue /Glass corroded to opaque white	Bead shape unknown	fragmentary	fragmentary

[1] For the bead shape, two types are given if the bead is decorated. For the perforation, two types are given if the diameter of the perforation is particularly large.
[2]A part of the perforation of the bead is damaged and therefore the classification is only an approximation based on what is preserved
[3]The perforation is damaged towards one end and therefore the shape is an approximation based on the preserved section of the perforation.
[4]Although the bead is too fragmentary to provide a type based on shape, it could be classified according to the decoration preserved on the fragments.

Two of the beads are ellipsoidal and decorated around the perimeter by a series of flutes or ribs (Papadopoulos and Muros 2014). Bead 10/114, opaque white in color, has five ribs (Figure 7.3A). 10/112, a translucent blue-green bead, has three to four ribs (Figure 7.3B). The ribs are not very well defined on either bead, and appear quite shallow. The unevenness of the flutes points to the beads being hand formed rather than mold made. Bead 10/112 has ribs only on half of the bead. The surface of the bead is quite pitted, and

it is possible some of the ribs may have been lost due to deterioration. It is also possible that it is misshapen. The shape of the ribs on these two beads, their depth and spacing, were not similar to the examples given in Beck (1921, 25, fig. 21) for fluted or gadrooned beads. Initially the beads were initially thought to be "melon beads", a well-known bead type. However, the rib/flutes shape and spacing on melon bead seem to be closer together and well defined (Ingram 2005, 47, fig. 2.15, 184, fig. B.26). Therefore, the beads were placed in the "fluted" bead type, where flutes can be shallower and spaced wider apart (fluted ellipsoidal bead, Type XXIII.A.2.A) (Beck 1921, 24, fig. 21).

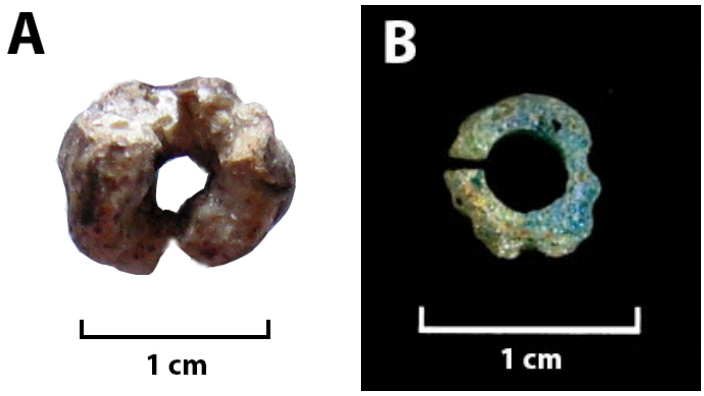

Figure 7.3. Views of the ends of beads 10/114 (A) and 10/112 (B) showing the position and spacing of the flutes, or ribs, as well as the perforation.

Four of the beads at Lofkënd (10/108, 10/109, 10/115, 10/116) were decorated with opaque white glass (Papadopoulos and Muros 2014). Beads 10/108, 10/109, and 10/106 are very corroded and appear various shades of opaque yellow to red. The glass was originally a dark green glass, almost black, similar in color to 10/115. The white decoration would have contrasted against the dark color of the beads.

The opaque white decoration on each of the beads is of a different type (Table 7.2). 10/108 is the simplest in that is has a single horizontal band of white opaque glass running across middle of the bead ("zone bead", Type XLVII.A.1.a) (Figure 7.4A) (Beck 1921, 46, fig. 35 and 68). Bead 10/116 is in poor condition but some of the fragments do preserve portions of opaque white spots. This bead is a spot or eye bead, where the white decoration is flush against the surface (Type XLVI.A.2) (Figure 7.4B) (Beck 1921, 42, fig. 34a and 57). Since the spot is a white dot without any rings, it is a simple spot bead.

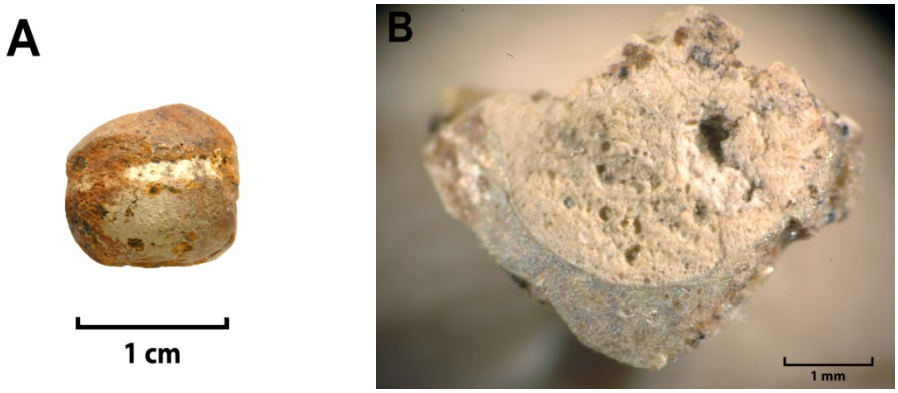

Figure 7.4. (A) Bead 10/118 decorated with a white opaque horizontal band across the center of the bead; (B) Fragment of bead 10/116 with the remains of an opaque white spot.

Although the term "eye beads" is sometimes used to refer to beads with simple spots (Beck 1921), some distinguish the two and reserve "eye beads" as a classification for beads where the decoration is a central dot in a different color than the glass matrix that has one more layers of glass around the central dot (Venclová 1983). Due to the fragmentary nature of the bead, it is not clear if the spots are arranged in some

kind of order or are random. Therefore, further classifying the bead as a glass bead with "flush definite spots" (ordered) or "with flush crumbs" is not possible (Beck 1921, 42). The decoration on these beads, whether with bands or spots, was made by applying a gob of white glass as a spot or trailing it across the surface. Since the decoration is impressed, the bead would be rolled onto a flat surface, such as a marver, to make the decoration flush with the surface (Ingram 2005; Xia 2014).

A combination of a horizontal band and spots were used to decorate bead 10/109. At one end, just below the perforation, there is what looks like a collar with a horizontal band of opaque white glass below (Figure 7.5A). Scattered across the body are small circular depressions with traces of opaque white glass (Figure 7.5B). These depressions are the remnants of a spot or eye decoration that have been lost. The loss of the spot, eye or line, which has been pressed into the surface during manufacture, leaves an imprint when it is damaged and is removed from the surface (Eisen, 1916; Ingram, 2005, 63, fig. 2.26). The decoration is poorly preserved, and the surface somewhat damaged, so it is difficult to determine whether the spots were ordered or not.

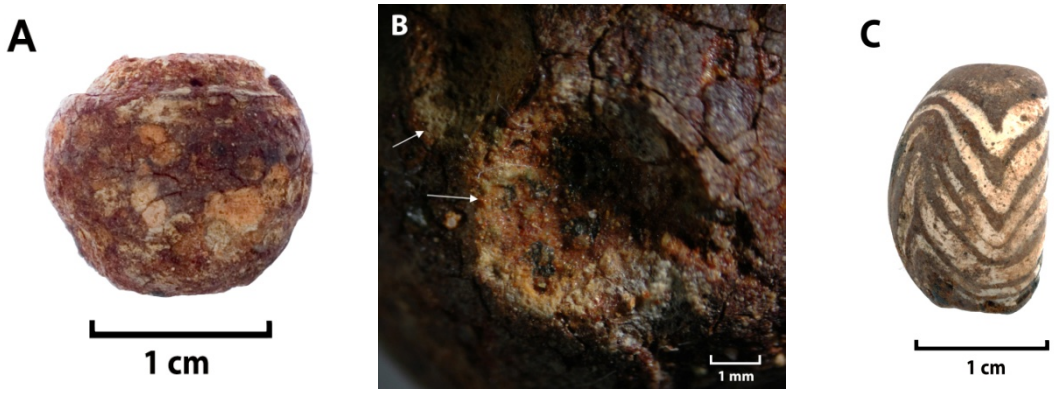

Figure 7.5. (A) Profile of bead 10/109 decorations with a horizontal recessed band near the top end. This recess contains the remains of opaque white glass. (B) Photomicrograph of bead 10/109 showing circular depressions (indicated by the white arrows) that are the result of an impressed spot decoration that has now been lost. These depressions contain some remnants of opaque white glass. (C) Profile of bead 10/115, which is decorated with a series of opaque white waves or chevrons.

The final bead decorated with opaque white glass is 10/115 (Figure 7.5C). This bead is one of the best preserved from Lofkënd with very little corrosion. It is a different shape than all the other beads found. It is an elongated bead that is flat on one side and corresponds to Beck's "circle and flat ellipsoid" bead (Type VII.D.I.a) (Beck 1921, 6, pls., I-III). It is decorated with trails of opaque white glass that resemble waves or chevrons (Type XLVII.A.7.a) (Beck 1921, 48, fig. 72). The bead would have been decorated in a method similar to how the other three beads were decorated, where a gob of white opaque glass would have been trailed around the bead. A wire would have then been drawn across the lines to make the chevron or wave pattern (Xia 2014). The bead would then have been rolled on a marver to make the pattern flush with the surface and to also flatten the underside of the bead (Ingram 2005).

Spot or eye beads, as well as beads decorated with bands, lines, spirals and waves, have a broad distribution both chronologically and geographically. Early examples of spots and eye beads are found in the Near East, Egypt, and prehistoric central Europe (Petrie et al. 1891; Eisen 1916; Mackay 1925; Beck 1928; Mackay et al. 1929; Haevernick 1981b; Venclová 1983; Ingram 2005; Ingram 2014; Xia 2014). They have been found in Late Bronze Age and Early Iron Age contexts in Greece (Haevernick 1981a; Ingram 2005; Nikita and Henderson 2006), Italy (Bellintani 2015; Conte et al. 2018) and the northern Balkans (Venclová 1978; Venclová 1983; Lazar 2006). Many of the published images or drawings of the spot or eye beads from these times periods appear to be true eye beads rather than simple spots, (Beck 1928; Eisen 1916; Haevernick 1981a; Mackay 1925; Mackay et al. 1929; Venclová 1978; Xia 2014) or unique examples such as the horn stratified eye bead

from Elateia (Nikita and Henderson 2006, 80, fig. 5). However, there are several examples from LBA/EIA contexts that have simple white spots on the surface that are not "eyes" that may be closer to those found at Lofkënd (Bellintani 2015, 17, fig. 1, no. 48; Ingram 2005, 62, fig. 2.25; Ingram 2014, 234, fig. 7).

Just like spot or eye beads, glass beads decorated with lines and waves have also been discovered in various geographic and chronological contexts (Eisen 1916; Mackay 1925; Beck 1928; Haevernick 1981b; Lazar 2006; Bellintani 2015; Conte et al. 2016; Conte et al. 2018). Many of the beads found that have multiple bands or spirals are not exactly the same as the Lofkënd beads. For example, a black long or barrel bead from the cemetery at Gurob (ca. 15th c. BC, 18th Dynasty) was found with a series of white lines (Petrie 1905, pl. XL, no. 16). The decoration appears to run at a slight angle and possibly is a spiral. No examples have been found yet with a single white horizontal band running across the center of the bead as in 10/108. Beads with waves or chevrons have been found, but again the beads are not exactly the same at 10/115. Three beads from Italy (ca. 1350-1000/950 BC) with waves or chevrons have a chronological overlap, but a closer look at the bead shape and the type of waves shows they are different (Bellintani 2015, 17, fig. 1., nos. 42, 45, 47). Some later beads from central Europe (ca. 6th-5th c. BC) have a wave or chevron design applied to a long bead. The bead shape in those examples is more tube-like and lacks a flat side (Haervernick 1981, 412, nos. 37, 38; Venclová 1978, 124, fig. 1, no. 7).

Finally, beads with both simple spots and a linear design, like on bead 10/109, do not seem to be very common. Eye beads can be found with rings around the eyes (Eisen 1916, 3, pl. I, nos. 1-4) or are decorated with an "impressed coil" across other areas of the bead between the eyes (Eisen 1916, 3, pl. I, nos. 29-34; Petrie 1891, pl. XVIII, no. 32). Another black glass bead excavated by Petrie (1904 pl. XL, no. 16) from Gurob has white colored simple spots and a band running along the center of the bead. Iron Age black beads excavated from sites in Italy are described as having eyes and bands, with the band running across the center of the bead (Conte et al. 2018). Eisen (1916, 3, pl. I, fig. 5) published a bead from his collection that has simple white spots with a short bar across the center. One example of a simple spot bead with bands at either end of the bead was also published by Eisen (1961, 3, pl. 1, fig. 8). The colors, location of the spots and the number of bands differs, but it was the only example found that had a band around the end that also had simple spot, similar to bead 10/109.

No Mycenaean relief beads were found among the glass artifacts. This fits with the distribution pattern observed of these bead types, which is primarily restricted to palatial centers on the Greek mainland and some peripheral areas (Eder, 2015). Some relief beads have been found outside of Greece, but it appears to be restricted to areas to the east, such as the Levant (Nightingale 2008; Eder 2015), the Uluburun shipwreck (Pulak 1998; Aruz et al. 2008), and Turkey (Aruz et al. 2008). Relief beads have not been found west of Greece or farther north into Europe.

7.3.2.2 Faience bead

The only faience bead found at Lofkënd, 10/105, is a long barrel bead (Type I.D.1.b) with surface decoration resembling a grid (Figure 7.6A) (Beck 1921). The bead appears to have a collar at one end. It is not clear if there was also a collar at the other end of the bead since that end is damaged. Beck (1921, 27, fig. 23) describes these beads as "granulated" and those made of faience are classified as Type XXV.A.5 (Beck 1921, 27). The faience example illustrated by Beck (1921, 27, fig. 23A.5), which is from Egypt and dates to the 23rd Dynasty, has a different bead shape and granulated decoration than 10/105. The example shown of the Egyptian etched glass bead (19th Dynasty) has a more grid-like decoration and is closer to the pattern seen on the surface of the Lofkënd faience bead (Beck 1921, 27, fig. 23A.4). The Lofkënd bead was not etched nor made in a mold like some of the examples shown. The "granulated" or gridded areas vary in size and are not regularly spaced; therefore, this decoration was added by hand.

This granulated type of faience bead does not appear to be very common and only a few published examples have been found. Like the examples published by Beck (1921, 27), beads with a granulated, notched or

cross-hatch pattern have been found in other materials, such as metal, stone, glass, faience, ivory, and bone (Wainwright 1920; Beck 1928; Brunton 1930; Brunton and Morant 1937). Some of these however, have a pattern that is more like a series of crosshatches rather than a grid. Examples of faience collared barrel beads with a crosshatch pattern were found at Mostagedda (Brunton and Morant 1937, 125, sect. 169(iv), pl. LXXVI, no. 33) and Qau (Brunton 1930, pl. XXXII, no. 27). Faience beads with a more grid-like pattern have been found at Balabish (Wainwright 1920, pl. XIII, no. 6) and Qau (Brunton 1930, pl. IV, no. 58r2, pl. XXII, no. 28). These beads though are square or rectangular in section.

The best examples of this type of granulated faience bead come from the tumuli at Barç and Pazhok in Albania (Bodinaku 1982; Papadopoulos et al. 2014a). The two beads published from Pazhok were described as being made of soft white stone with a net or mesh pattern (Bodinaku 1982, 67). The description of the material could represent a faience bead that has lost its glaze leaving the quartz core exposed. The Pazhok examples look very similar to faience bead 10/105 and is the only published image found so far that looks so similar (Figure 7.6B) (Bodinaku 1982, pl. VI, no.13, pl.XII, no. 10).

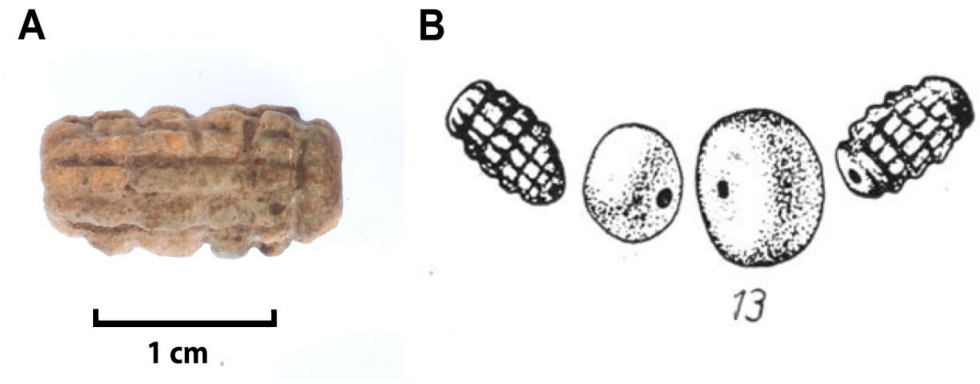

Figure 7.6. (A) Faience bead 10/105 (B) Two beads excavated from Pazhok that have a collar and a grid or granulated pattern similar to the Lofkënd bead (after Bodinaku 1982, pl. VI, no.13).

7.3.2.3 Condition of the beads

Most of the beads excavated at Lofkënd were in poor condition. Only two of the beads were better preserved, 10/113 and 10/115, though the latter did have some loss of the opaque white decoration. The blue-green fluted bead (10/112) was iridescent and had a very pitted surface. As described above, the faience bead (10/105) suffered loss of the glaze. The quartz core was extremely soft and friable.

Many of the beads had completely corroded and had little to no intact glass left. Beads 10/114 and 10/117 had corroded to an opaque white color. 10/114 was fragmentary but the fragments were somewhat stable. Bead 10/117 was extremely friable and had broken up into fragments, most which were flaky. They could not be safely separated from the soil during cleaning without further loss or damage. Beads 10/106, 10/107, 10/108, 10/115, and 10/116, were originally dark green, almost black in color, similar to the color of beads 10/113 and 10/115. These five beads are extremely corroded. They have become opaque and altered in color to be a pale yellow or a reddish-brown color. Beads 10/108 and 10/109 are complete and the entire bead shape is preserved. Beads 10/106 and 10/107 were fragmentary but could be reconstructed so that some or most of the bead shape could be determined. Bead 10/116 was in many small fragments that could not be reconstructed. Some of these yellow and reddish-brown beads retain some of the original dark colored glass within the corroded matrix, though the level of preservation varies.

7.4 Results and Discussion

The 11 Late Bronze Age to Early Iron Age vitreous beads excavated at Lofkënd underwent instrumental analysis. All the beads were analyzed using pXRF in order to identify the mineral colorants used. Seven of

the beads that had some uncorroded glass were sampled for compositional analysis. No sample was taken from 10/113 since the bead was intact and did not have damaged areas that could be easily sampled. 10/116 was also not sampled because the small fragments of black glass preserved in the matrix were too small and sample preparation for EPMA analysis was not successful.

7.4.1 Glass

7.4.1.1 Raw materials-Alkali flux

EPMA analysis of seven Lofkënd beads shows that the glasses contain 16.29-19.76 wt% (avg. 18.29 wt%) soda, 1.16-1.41 wt% (avg. 1.30 wt%) potash, 1.95-4.79 wt % (avg. 3.75 wt%) magnesia, 1.07-1.89 w% (avg. 1.45 wt%) alumina, and 2.76-6.12 wt% (avg. 4.88 wt%) lime (Table 7.3, Appendix D). This composition falls within the ranges observed for HMG glasses of the Late Bronze Age produced using a plant ash alkali, though some of the values are on the lower end of the typical ranges for these oxides (Henderson 2012; Nicholson 2010; Shortland 2012).

Table 7.3. Results of EPMA analysis. The results are given as weight % (wt%) oxide and represent the average of three areas analyzed on each sample. For some of the beads (10/106, 10/112, 10/115, 10/116), several samples had to be taken for analysis due to the small size obtained of intact glass.

Bead No.	Sample No.	Glass color	Na_2O	K_2O	MgO	Al_2O_3	CaO	SiO_2	FeO	MnO	P_2O_5	TiO_2	Total
10/106	Lof-342	Dark green	18.32	1.30	3.79	1.40	5.97	64.13	3.90	0.01	0.26	0.18	99.26
10/108	Lof-341	Dark green	19.65	1.28	3.98	1.89	2.76	61.65	8.24	0.06	0.15	0.30	99.95
10/109	Lof-294	Dark green	16.87	1.26	4.79	1.39	5.72	62.82	6.63	0.02	0.16	0.20	99.88
10/112	Lof-338	Blue-green	18.88	1.27	3.30	1.51	4.84	67.53	0.40	0.26	0.27	0.25	98.51
10/115	Lof-339	Dark green	16.29	1.40	3.69	1.07	5.14	65.00	6.96	0.01	0.12	0.14	99.82
10/116	Lof-344	Dark green	19.18	1.16	4.72	1.60	6.12	64.48	2.52	0.01	0.22	0.23	100.25
10/117	Lof-351	Light blue	18.86	1.41	1.95	1.28	3.60	70.52	0.25	0.03	0.20	0.12	98.22

All of the Lofkënd beads have concentrations of potash that are relatively low for typical plant ash glasses, below 2%, and are closer to the concentrations seen in cobalt colored glasses (Shortland and Tite 2000; Rehren 2001; Nicholson 2007). However, low potash concentrations are not restricted to cobalt containing glasses, and other colors have been found with low concentrations of this alkali (Nicholson 2007). The concentrations of these two oxides are similar to those found in Egyptian and Mycenaean glasses (Figure 7.7). The Lofkënd beads are relatively low in potash compared to Near Eastern glasses, non-cobalt containing Egyptian glasses and a group of Mycenaean glasses. They group closest with several Egyptian and Mycenaean cobalt and Co-Cu colored glasses, though the potash levels are not as low as several of the Mycenaean and Egyptian cobalt glasses or the Uluburun ingots.

One explanation given for the low potash values in cobalt glasses is the use of a different alkali in their production (Shortland and Tite 2000), and this possibility was explored with the Lofkënd glasses. Plant ash compositions are influenced by factors such as the plant genera and the geochemistry of the soil which in turn will affect the concentrations of several oxides, including phosphorus, silica, potash, and soda (Barkoudah and Henderson 2006). These varied compositions can help differentiate plant ash sources. The levels of phosphorus pentoxide and potash in the Lofkënd beads were compared to those of other Late Bronze Age glasses to look for similarities between the plant ashes used for each group of glasses (Figure 7.8) (Nikita and Henderson 2006; Shortland and Eremin 2006; Nicholson 2007; Walton et al. 2009; Jackson and Nicholson 2010; Smirniou and Rehren 2013).

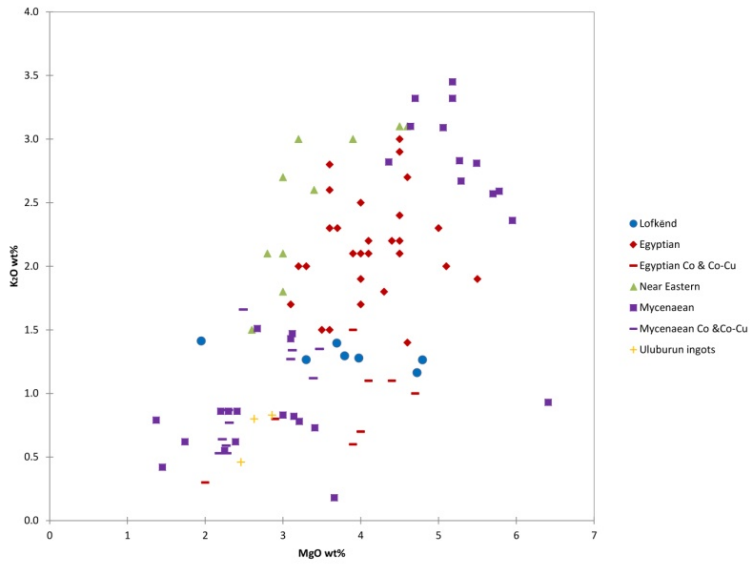

Figure 7.7. Biplot of the concentrations of MgO and K_2O in the Lofkënd beads compared to glass from Egypt (Shortland and Eremin 2006; Nicholson 2007), the Near East (Shortland and Eremin, 2006), Mycenaean sites (Nikita and Henderson 2006; Walton et al. 2009; Smirniou and Rehren 2013), and ingots from the Uluburun shipwreck (Jackson and Nicholson 2010).

Although the Lofkënd beads overlapped with several Egyptian and Mycenaean cobalt colored glasses in terms of potash and magnesia values, the groups are distinguished by their phosphorus pentoxide concentrations. Two groups of cobalt and Co-Cu colored glasses appear in the biplot (Figure 7.8). One has phosphorus levels similar to the Lofkënd beads, but with lower potash. The other group of cobalt glasses is much lower in both oxides. The Lofkënd beads form a somewhat distinct group compared to most Late Bronze Age Near Eastern and Egyptian glasses, as well as a group from Mycenaean Greece.

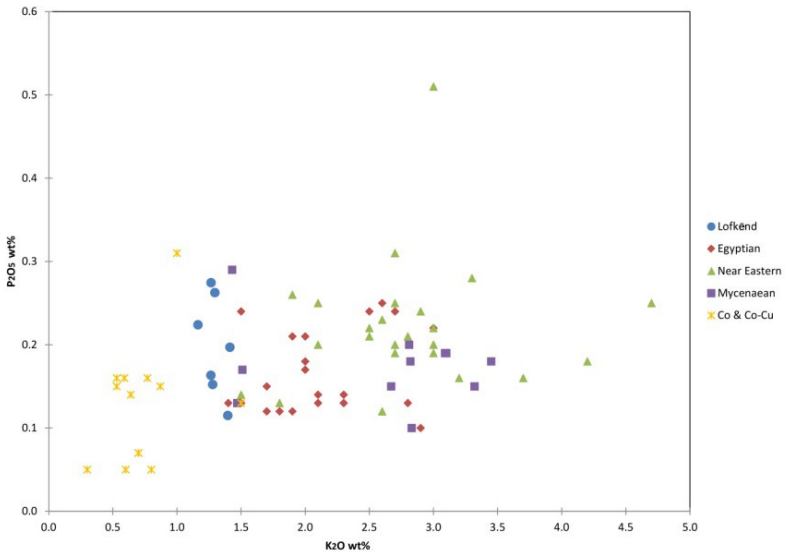

Figure 7.8. Biplot of the concentrations of K_2O and P_2O_5 in the Lofkënd samples compared to glass from Egypt (Shortland and Eremin 2006; Nicholson 2007), the Near East (Shortland and Eremin, 2006), Mycenaean sites (Nikita and Henderson 2006; Walton et al. 2009; Smirniou and Rehren 2013), and ingots from the Uluburun shipwreck (Jackson and Nicholson 2010).

Some Mycenaean beads from Elateia (Nikita and Henderson 2006), as well as a Co-Cu colored glass from Egypt (E5613/5) and a sample from Tell Brak (Shortland and Eremin 2006), are similar to some of the Lofkënd beads. It is not clear if the differences observed are related to variation within the same type of

plant ash used, a different plant ash was used (as has been suggested with cobalt glasses) (Rehren 2001), the plant ashes underwent some kind of purification prior to use which reduced levels of some of the glass components (Henderson 2013), or if another alkali was used such as one that is mineral based.

In addition to having low potash concentrations, beads 10/108 and 10/117 have low concentrations of lime (2.76 and 3.60 wt%) (Table 7.3). Typical Late Bronze Age glasses contain 4-8% lime (Nicholson 2007; Shortland 2012; Henderson 2013). 10/117 also had a higher concentration of silica (70.52 wt%) and a lower magnesia (1.95 wt%).

High silica, low lime, and low potash are characteristics typical of natron glasses. Natron glasses first appear in Egypt during the 1st millennium BC (Henderson 2013), with one of the earliest examples dated to the 10th c BC from the site of Nesikohns (Schlick-Nolte and Werthmann 2003). Although natron glasses are not that common outside of Egypt during this period, some early examples of natron glass have been found in Iron Age contexts at Pella in Jordan (1050-850 BC) (Reade et al. 2006), France, and Italy (10th-6th c BC) (Conte et al. 2016; Conte et al. 2018). There seems to be quite a bit of variability among these early natron glasses, in particular among those from the sites in Italy. This variability is attributed to early experimentation with a new alkali before a set recipe was established (Conte et al. 2018)

Several of these Early Iron Age glasses have higher levels of magnesia (up to 3-4%), though they still retain other natron glass characteristics such as high soda, low potash, low lime, and low phosphorus pentoxide (Conte et al. 2016; Conte et al. 2018). In these cases, the higher magnesia levels are attributed to the use of impure sands as the silica source that are richer in iron and magnesium containing minerals, such as amphiboles and pyroxenes, as opposed to entering the glass batch from the alkali used—like what occurs with plant ash alkalis (Conte et al. 2018). These beads are referred to by Conte et al. (2018) as high magnesium low potassium (HMLK) glasses.

Beads 10/108 (dark green) and 10/117 (blue), were both found within the same tomb (XXVIII) that was dated to the 12-11th c BC (Table 7.2). These samples are too early to fit in chronologically with the group of early natron glasses from Pella or Italy. The earliest natron bead in Europe seems to be from the 10th-9th c. BC (Conte, et al., 2018, 2015). Despite the early date, the Lofkënd glasses were compared to the Italian Iron Age natron glasses (Conte et al. 2016; Conte et al. 2018), the glasses from Pella (Reade et al. 2006), and those from Nesikohns (Schlick-Nolte and Werthmann 2003) to try to better understand the unusual composition of the Lofkënd beads.

Looking at the main alkali components, almost all of the Lofkënd glasses have higher concentrations of potash and magnesia compared to the natron glasses (Figure 7.9). The only exception is 10/117 which is similar to some of the Italian HMLK glasses (Conte et al. 2015). The biplot also shows that there are plant ash glasses, in particular Mycenaean glasses from Elateia (Nikita and Henderson 2006), that overlap with some of the Italian Iron Age natron glasses. This comparison of magnesia and potash values did not clarify which alkali was used for the Lofkënd glasses.

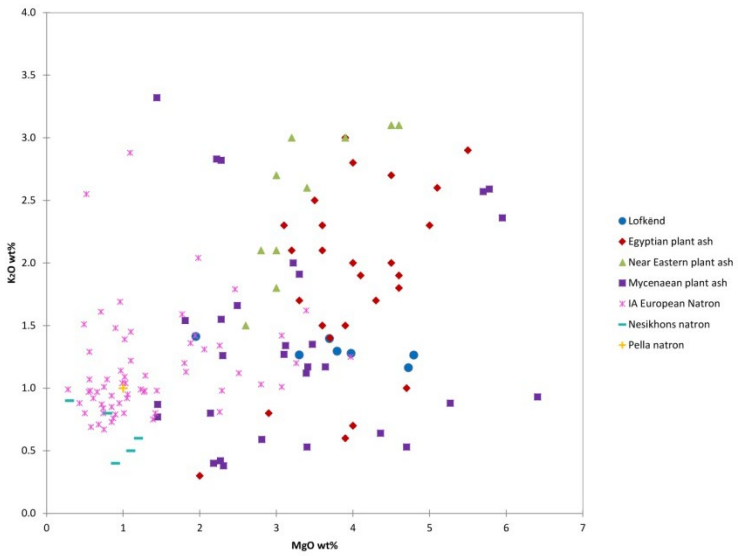

Figure 7.9. Biplot of the concentrations of alkali components (MgO and K_2O) in the Lofkënd samples compared to plant ash glasses (Nikita and Henderson 2006; Shortland and Eremin 2006; Nicholson 2007; Walton et al. 2009; Jackson and Nicholson 2010; Smirniou and Rehren 2013) and Iron Age natron glasses (Reade et al. 2006; Conte et al. 2016; Conte et al. 2018).

In regards to the concentrations of lime and potash, bead 10/117 again plots alongside some of the Italian Iron Age and the Pella natron glasses (Figure 7.10). Bead 10/108 also has low lime values compared to most plant ash glasses; though there are a few Mycenaean and Egyptian plant ash glasses with low potash and lime concentrations close to this sample. The Lofkënd beads predate the earliest Egyptian example of natron glass, so it is unlikely they were made using that alkali. It is not clear what is causing the low potash and lime values, and whether it is indicative of a particular plant ash used with these characteristics or due to some other aspect of the raw materials or manufacturing technology. More analyses of beads from the Late Bronze Age and Early Iron Age transition are needed, and in particular from these regions where this early natron glass appears, in order to better aid in the interpretation of the lime and a potash data obtained from the Lofkënd beads.

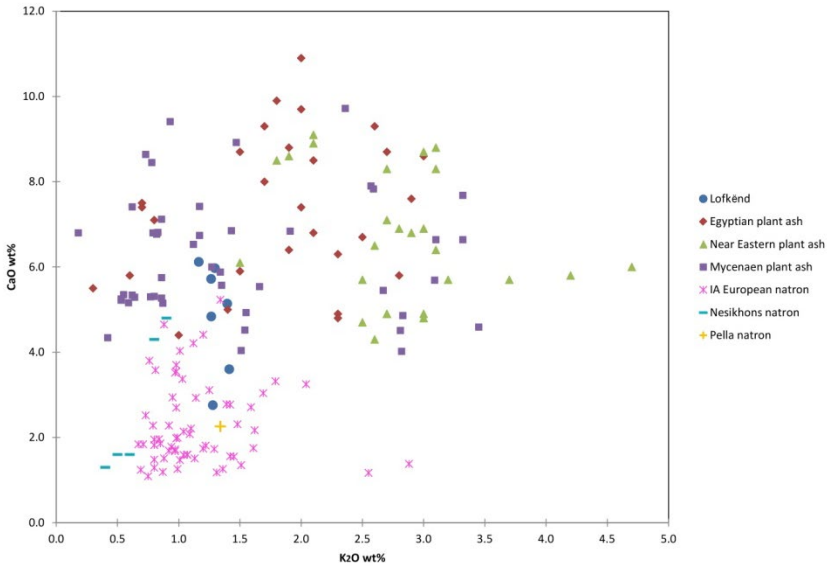

Figure 7.10. Biplot of K_2O and CaO in the Lofkënd samples compared to plant ash glasses (Nikita and Henderson 2006; Shortland and Eremin 2006; Nicholson 2007; Walton et al. 2009; Jackson and Nicholson 2010; Smirniou and Rehren 2013) and Iron Age natron glasses (Reade et al. 2006; Conte et al. 2016; Conte et al. 2018)

7.4.1.2 Raw materials-Colorants

PXRF analysis was used for the initial identification of the mineral colorants and any opacifiers used in the manufacture of 10 glass beads discovered in the tumulus (Table 7.4). This analysis took place in the field during the final field seasons of the Lofkënd project.

Table 7.4. Results of qualitative pXRF analysis.

Bead No.	Color	Elements detected
10/105	Faience with blue green glaze	Si, S, K, Ca, Ti, Cr, Mn, Fe, Ni, Cu, Zn, Pb, Sr, Zr, Sn
10/106	Opaque yellow-brown	Al, Si, S, K, Fe, Ti, Cr, Mn, Fe, Ni, Cu, Zn, Pb, Rb, Sr, Zr, Sb
10/107	Opaque golden yellow	Al, Si, S, K, Ca, Ti, Cr, Mn, Fe, Cu, Zn, As, Rb, Sr, Zr
10/108	Dark green glass with opaque white horizontal band	Al, Si, S, K, Ca, Ti, Cr, Mn, Fe, Cu, Zn, As, Rb, Sb, Zr
10/109	Dark green glass with an opaque white line and spots	Al, Si, S, K, Ca, Ti, Cr, Mn, Fe, Cu, As, Pb, Rb, Sr, Sb
10/112	Translucent blue-green	Al, Si, S, K, Ca, Ti, Cr, Mn, Fe, Ni, Cu, Zn, As, Pb, Rb, Sr, Zn, Sn
10/113	Translucent dark green glass	Al, Si, S, K, Ca, Ti, Mn, Fe, Cu, Zn, Zr
10/114	Opaque white glass	Al, Si, S, K, Ca, Ti, Cr, Mn, Fe, Cu, Zn, As?[1], Sr, Zr
10/115	Dark green glass with opaque white waves or chevrons	Si, S, K, Ca, Ti, Fe, Cu, As?, Zn, Rb, Sr, Zr, Sb
10/116	Dark green glass with opaque white spots	Al, Si, S, K, Ca, Ti, Cr, Mn, Fe, Cu, As, Pb, Rb, Sr, Zr, Sb
10/117	Translucent light blue glass	Al, Si, S, K, Ca, Ti, Cr, Mn, Fe, Cu, Pb, Sr, Zr

[1]The peaks marked with a "?" indicate that the peak is small, slightly above background, and it is unclear if the element is present

7.4.1.2.1 Copper blue

The two blue beads, 10/112 (blue-green) and 10/117 (light blue) were colored using copper (Table 7.4). Bead 10/112 also contained a peak for lead and tin indicating the copper source was bronze scrap. A very small lead peak was detected in bead 10/117, but no tin peak was present. This may indicate that leaded copper may have been used for the colorant as opposed to bronze.

LA-ICP-MS analysis allowed for quantification of the copper content in the glass (Table 7.5). Bead 10/112 contains 9167.10 ppm Cu (1.15 wt%) and 10/117 has 7753.12 ppm Cu (0.97 wt%). The values fall within the average concentrations found in copper colored Late Bronze Age glasses, which typically range from 0.5-2% CuO (above 3500 ppm Cu) (Shortland and Eremin 2006; Smirniou and Rehren 2013).

Table 7.5. LA-ICP-MS results of selected elements related to the glass colorants. The concentrations are given in parts per million (ppm) and are averages of three replicates. Some beads had additional samples taken for analysis because of the small samples size obtained due to the level of deterioration.

Bead No.	Sample No.	Fe	Cu	Sn	Sb	Pb
10/106	Lof-342	27458.96	3316.88	1.26	461.34	94.25
10/108	Lof-341	57789.84	41.35	1.26	17.10	3.02
10/109	Lof-294	51301.51	84.33	0.78	30.28	2245.52
10/112	Lof-338	3182.38	9167.10	17.34	50.25	46.69
10/115	Lof-339	53636.77	358.16	0.86	171.56	14.40
10/116	Lof-344	17504.59	88.28	0.92	599.00	156.00
10/117	Lof-351	2162.88	7753.12	1.94	4.28	3.42

The opaque white fluted bead, 10/114, was completely corroded and did not appear to have any intact glass remaining. Analysis of the bead using pXRF showed prominent peaks for iron, copper and manganese. The iron and manganese peaks were likely the result of the layer of soil and burial deposits visible on the surface of the bead (Figure 7.11A). The copper peak is due to the original colorant of the bead, which has

completely altered. Within the corroded matrix there were small green spherical inclusions (Figure 7.11B) that when analyzed had a larger copper peak than the surrounding matrix. This could be some remnants of the copper colorant. The glass was probably blue and these inclusions altered to a green color due to corrosion.

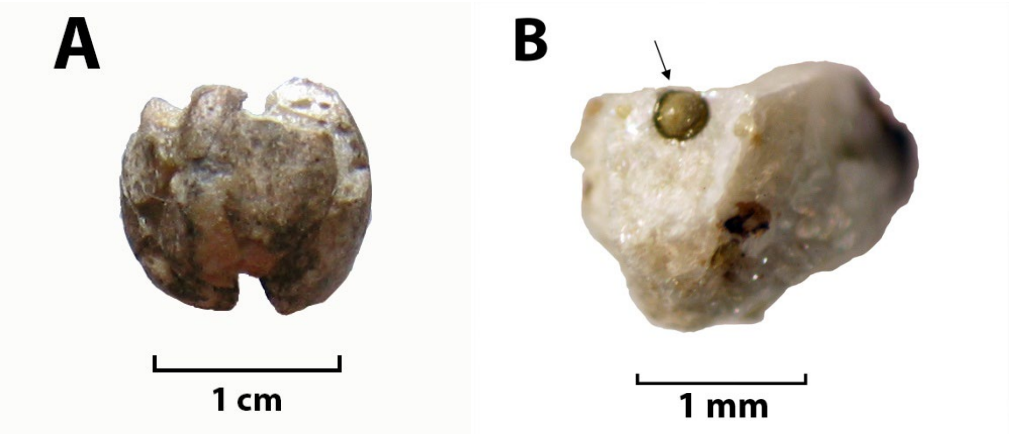

Figure 7.11. (A) Profile view of 10/114 showing brown and black soil and burial deposits on the surface of the glass. (B) Fragment of bead 10/114 showing a circular green inclusion within the corroded matrix (indicated by the arrow) that may be a component of the original glass colorant.

7.4.1.2.2 Iron dark green

Seven of the Lofkënd beads (10/106, 10/107, 10/108, 10/109, 10/113, 10/115, 10/116) were made of dark green glass that appeared almost black in color. Examination of the beads or samples using transmitted light revealed the true bead color, which was dark green and the beads are described as such. The majority of the beads found at Lofkënd were of this color (70%), a color palette not commonly reported for Late Bronze Age contexts. Many of the glasses found during this period tend to be blue in color and colored with copper, cobalt or a combination of both colors (Smirniou and Rehren 2013). The large assemblages of dark green or black glass beads described in the literature seem to date to the Early Iron Age and to later periods (Henderson and Warren 1981; Reade et al. 2006; Cosyns 2011; Cholakova and Rehren 2014; Conte et al. 2016; Conte et al. 2018). The appearance of fewer dark green or black beads in earlier periods could be due to the lack of studies or publications on the materials and not necessarily due to geographical or chronological differences in color preferences. Without more analysis of dark green or black glasses from earlier periods, it is difficult to comment on color trends.

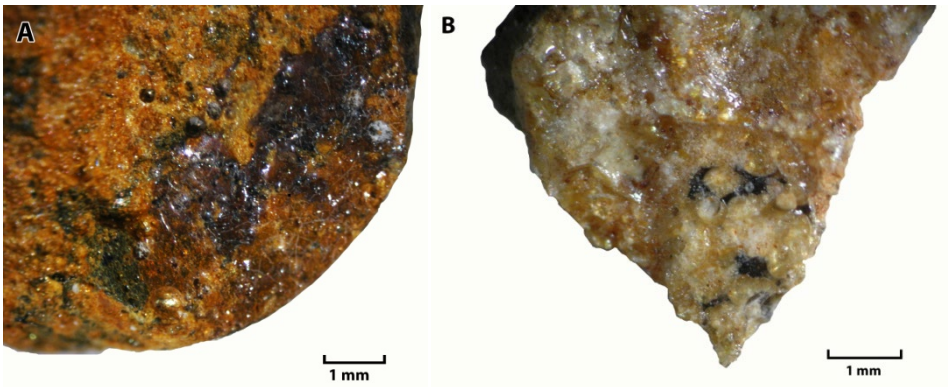

Figure 7.12. (A) Photomicrograph of the interior of bead 10/108 showing areas of dark glass preserved within the reddish-brown corroded matrix. (B) Photomicrograph of the interior of bead 10/116 showing very small pieces of dark colored glass preserved towards the lower section of the fragment. The rest of the bead has corroded to an opaque yellow or yellow-orange color.

Only two of the beads, 10/113 and 10/115, were well preserved. The other four beads were deteriorated to varying degrees. The beads had altered in color, ranging from an opaque pale yellow to a reddish-brown color. The core of bead 10/108 still retained some dark colored glass and some was visible on the surface (Figure 7.12A). For the other beads, the glass was only preserved as very small fragments within a corroded glass matrix (Figure 7.12B).

PXRF analysis conducted on all six of the beads indicated that the glass colorant was iron. From the five samples analyzed, the iron concentrations range from 2.52-8.24 wt% (avg. 5.65 wt%) (Table 7.3). Black, or dark green, glasses colored by high concentrations of iron oxide have been found at Iron Age sites in Italy, Slovakia, France, and at Pella, Jordan (Reade et al. 2006; Conte et al. 2016; Conte et al. 2018). Iron oxide dark green or black glass continued to be manufactured after this period with many examples found during the Roman period (Cosyns 2011; Cagno et al. 2014; Cholakova and Rehren 2014). The black Iron Age glasses have concentrations of iron ranging from 3-15.6%, and the iron oxide content of the Lofkënd beads falls within that range. Although some Late Bronze Age black glass has been found colored by manganese (Nicholson 2007; Polikreti et al. 2011; Muros 2020), the levels in the Lofkënd dark green beads are too low to have contributed to the color (0.01-0.06 wt%, avg. 0.02% MnO). It is interesting that the dark green Lofkënd beads also seem to have similar colorants to the black HMLK glasses from Italy and the dark green-black natron glasses from Pella, beads with which they shared similar potash and lime concentrations. There seems to be some link between these beads and their raw materials despite the chronological and geographic differences.

The high concentration of iron oxide in the glasses indicates the colorant was added to the glass and is not due to any iron naturally occurring in the raw materials. Several sources for the iron have been suggested based on analysis of Iron Age black and green-black glasses (Reade et al. 2006; Conte et al. 2016; Conte et al. 2018) as well as iron black glasses from the Roman period (Cagno et al. 2014; Cholakova and Rehren 2014). Backscatter SEM imaging of green-black glasses from Pella revealed chromium grains within the glass matrix (Reade et al., 2006). These inclusions could have entered the glass as part of an iron mineral that was rich in chromium, such as chromite. Similar chromite grains were observed in Iron Age black glasses from southern Italy (Conte et al. 2015). These minerals were thought to be present due to the use of iron-rich chromite contained sands as the silica source and colorant. In addition to high iron and chromium, the use of these sands would have produced elevated levels of other oxides, transition elements, and rare earth elements (REE) not observed in glasses made with purer silica source such as quartz pebbles. The sands contained elevated levels of titania, alumina, vanadium, zinc (23-405 ppm), and neodymium (5.4-16 ppm) (Conte et al. 2016; Conte et al. 2018).

In the Roman period, studies of some iron black glasses indicated that pure iron oxide was added as the colorant. Iron oxide particles were found within 2-3rd c. AD black glass from Bulgaria (Cholakova and Rehren 2014). The glass was discovered within a crucible, providing a glimpse into the production of this type of glass during the Roman period. A later dark green-black glass (4-5th c. AD) found in Montenegro contained iron oxide flakes, iron metallic spheres and slag inclusions added as the color source (Cholakova and Rehren 2014). The addition of iron oxide or iron metallurgical waste to the glass can be identified through the examination of the REE concentrations. If a fairly pure source of iron was used, such as magnetite, hematite or hammer scale, then there should not be an increase in these elements in the glass (Cagno et al. 2014).

Backscatter SEM imaging was not performed on the Lofkënd beads, and therefore identification of chromite, iron oxide particles, hammer scale, or slag inclusions was not possible. The concentrations of chromium in the samples were used to see if the colorant source could be identified. The chromium concentrations of the five dark green glasses range from 12.34-97.25 ppm (Table 7.6). This is similar to the concentrations found in the northern and southern Italian black glasses (5-334 ppm, though most were lower than about 21 ppm) (Conte et al. 2018. 2016) but lower than the Pella glasses which had concentrations above 400 ppm

(Reade et al., 2006). The Lofkënd blue glasses, 10/112 and 10/117 have low levels of chromium (9.70 and 13.24 respectively) but they still fall within the range found in chromite bearing sands (Brems and Degryse 2013) and iron black glasses. These levels are only slightly higher than the concentrations of chromium found in a group of Egyptian colorless glasses which were made with quartz pebbles (Smirniou and Rehren 2013) so they do not necessarily point to the presence of chromite.

There are three dark green glasses, 10/106, 10/108, and 10/116, that have chromium concentrations higher than the other Lofkënd samples (Table 7.6). These beads could have been colored by a chromite containing material, such as the iron rich sounds used for the Italian black glasses. A different colorant source may have been used for the two other dark green beads (10/109, 10/115) due to their lower chromium content.

Table 7.6. Results of LA-ICP-MS analysis of selected elements related to the glass raw materials related to the source of the iron colorant. Concentrations are given in parts per million (ppm) and are averages of three replicates.

Sample	Color	Ti	V	Cr	Ni	Zn	Sr	Y	Zr	La	Nd	Hf	Th	Cr/La	1000Zr/Ti
10/106	dk gr	1310.67	23.54	97.25	86.95	42.75	235.75	7.07	77	10.96	8.91	1.84	5.64	1.23	3065.22
10/108	dk gr	1777.71	50.14	89.35	297.14	30.73	124.2	12.1	81.1	17.15	14.14	1.87	9.3	1.21	4973.26
10/109	dk gr	1122.48	24.88	12.34	7.13	155.65	322.26	8.5	91.87	12.85	11.09	2.38	7.16	1.16	3008.40
10/112	bl gr	1404.79	15.15	13.24	16.4	15.2	222.54	9.55	97.29	13.05	10.29	2.35	6.27	1.27	2668.09
10/115	dk gr	888.75	25.3	14.42	10.34	109.59	253.83	5.29	56.92	7.98	6	1.23	3.79	1.33	3081.30
10/116	dk gr	1314.27	21.24	60	49.86	17.44	301.75	7.39	50.14	10.62	8.12	0.96	4.53	1.31	4718.75
10/117	bl	597.53	7.72	9.7	9.45	13.92	161.61	8.42	51.2	8.83	7.52	1.19	2.69	1.17	2260.50

7.4.1.2.2.1 Opaque white

Four of the dark green beads (10/108, 10/109, 10/115, 10/116) were decorated with spots and/or lines in opaque white glass. PXRF analysis of the decorated areas on all four glasses showed the presence of antimony indicating the opacifier was calcium antimonate. Beads 10/109 and 10/116 also showed prominent peaks for lead, along with antimony. The combination of lead and antimony was used to create opaque yellow glass, but there were no areas of this color found on the fragments of the bead.

A detailed compositional study was conducted on these four beads by Muros and Zacharias (2019) which involved XRD and VP-SEM-EDS analysis of the opaque white glass. The results are summarized below, along with additional results and interpretation of the data collected on 10/106 and 10/109.

XRD analysis identified several different compounds comprising the composition of the opaque white glass (Table 7.7) (Muros and Zacharias 2019). Two calcium antimonate compounds are generally found within opaque white glasses, $Ca_2Sb_2O_6$ and $Ca_2Sb_2O_7$ (Shortland 2002; Lahlil et al. 2009). These compounds were present in three of the Lofkënd decorated beads. The opaque white glass in bead 10/109 was composed of $Ca_2Sb_2O_7$. Bead 10/115 had the other form of calcium antimonate, $Ca_2Sb_2O_6$. It also contained antimony oxide (Sb_6O_{13}). Both forms of calcium antimonate were found in bead 10/116.

The identification of a particular calcium antimonate compound within the glass can provide clues as to the manufacturing technology of the glass. The identification of antimony oxide in bead 10/115 points to the use of "in situ crystallization" to produce the opacity. The antimony oxide found within the Lofkënd opaque white glass would be unreacted material that did not combine with the lime. The presence of only the $Ca_2Sb_2O_6$ form of calcium antimonate suggests that the glass was produced using higher temperatures. Based on laboratory replication experiments, this phase forms at temperatures of 927°C and is the main phase present in the glass at higher temperature (Lahlil et al. 2008; Lahlil et al. 2009). At 1000°C both forms of calcium antimonate can still be present (Lahlil et al. 2008) therefore the furnace must be heated above that temperature so that only $Ca_2Sb_2O_6$ was detected. Bead 10/116 had both forms of the calcium antimonate compounds and was likely fired at around 927-1000°C. Bead 10/109 only contained $Ca_2Sb_2O_7$,

and therefore it is possible that it was fired at a lower temperature that inhibited the formation of $Ca_2Sb_2O_6$ (Muros and Zacharias 2019).

Table 7.7. Results of the XRD analysis on the opaque white glass (after Muros and Zacharias, 2019)

Bead No.	Area Sampled	Results
10/108	Opaque white horizontal band	Brizziite, $NaSbO_3$ (PDF# 00-047-1843)
		Sodium antimony oxide, $Na_2Sb_2O_6$ (PDF# 00-052-1123)
10/109	Opaque white line	Romeite, $Ca_2Sb_2O_7$ (PDF# 01-073-1736)
10/115	Opaque white wave/chevron	Calcium antimony oxide, $CaSb_2O_6$ (PDF# 00-046-1496)
		Antimony oxide, Sb_6O_{13} (PDF# 00-033-0111)
10/116	Opaque white dot	Calcium antimony oxide, $CaSb_2O_6$ (PDF# 00-046-1496)
		Calcium antimony oxide, $Ca_2Sb_2O_7$ (PDF# 00-026-0293)
		Bindheimite, $Pb_2Sb_2O_7$ (PDF# 00-042-1355)
		Lead oxide, PbO (PDF #00-035-2482)

Two of the beads contained additional compounds within the opaque white glass (Table 7.7). XRD analysis identified two sodium antimonate compounds on bead 10/108, $NaSbO_3$ and $Na_2Sb_2O_6$ (Muros and Zacharias, 2019). These compounds were not used in antiquity to make opaque white glass, but have been found in opaque white glass tesserae and objects from the Roman period (Painter and Sax 1970; Lahlil et al. 2008; Silvestri et al. 2015; Verità and Santopadre 2015), and opaque white glaze on bricks from several sites in the Near East (7th c.- 6th c. BC) (Tite and Shortland 2004; Holakooei et al. 2017). Sodium antimonate compounds in the white glass were confirmed using VP-SEM-EDS where a crystal of sodium antimonate was identified within the glass matrix (Muros and Zacharias 2019, 1779-17780, fig. 9).

The presence of the sodium antimonate compounds is not an intentional addition. It is formed during the in situ crystallization of antimonate compounds in glasses with a low lime content where the antimony combines with some of the sodium present in the glass because there is not enough calcium available (Lahlil et al. 2008; Zacharias et al. 2018b). The dark green glass of Bead 10/108 did have one of the lowest lime contents of all the beads, 2.76 wt%.

Bead 10/116 contained two lead compounds in addition to the calcium antimonate compounds (Table 7.7): lead antimonate ($Pb_2Sb_2O_7$) and lead oxide (PbO). This was a surprising find since lead antimonate generally produces an opaque yellow glass, yet no yellow color was observed in the decorative areas. No crystals of lead antimonate or lead oxide were found in the white glass using VP-SEM-EDS. The overall composition of the white glass contained at least 7.96 wt% PbO along with 4.80 wt% CaO and 7.96% Sb_2O_3 (Muros and Zacharias 2019). Due to the level of deterioration of the samples, it is not clear what the actual composition of the opaque white glass was and whether the lead concentration is the result of enrichment.

There do not seem to be published examples of lead compounds found in Late Bronze Age opaque white glasses, but there are some instances of this occurring in 18th-21st c. AD glasses from Europe (Lahlil et al. 2008). In these cases, the base composition of the glass contained lead. Through in situ crystallization, the antimonate crystals combined with lead instead of calcium, similar in the way that sodium antimonate crystals were formed.

The addition of lead to the base glass used for bead 10/116 made in the 12th-11th c. BC would be unlikely. Leaded glass was found in China and other parts of southeast Asia as early as 400 BC and then made their way west along the Silk Road (Henderson 2012). Leaded glaze is reported to have been found on pottery in the Near East dating to the 15th c BC site of Tell Atchana in Turkey and a recipe for making this type of glaze

was found on a cuneiform tablet from a site in the area from the same time period (Singer et al. 1956). However, in western glasses prior to the Roman period, lead appears as an opaque yellow colorant, part of the copper colorant if leaded bronze scrap is used, or in the production of red opaque glasses (Freestone 1987). There are technological advantages to the addition of lead since it can improve working properties, lower the temperature at which the glass softens, reduces stress upon cooling of the glass, may aid in the precipitation of opacifying crystals and can add to the brilliance of the glass color (Henderson and Warren 1981; Freestone 1987; Mass et al. 2002; Foster and Jackson 2005; Rehren and Freestone 2015). The intentional addition of lead to the white glass on bead 10/116 could have improved the working properties of the glass making it easier to apply the decorative elements (Muros and Zacharias 2019). It is still not clear, however, why a yellow color was not produced if lead antimonate was present. It could be that the lead antimonate crystals are small and well dispersed so do not act as a strong colorant. The other possibility is that the opaque white glass was formed at a high temperature that caused the lead antimonate crystals to dissolve in the glass or turn a cream color (Shortland 2002).

Two additional Lofkënd beads contained lead, 10/106 and 10/109. PXRF analysis of bead 10/109 showed the presence of lead in areas of the opaque white decoration (Figure 7.13). XRD analysis did not detect any lead compounds, like those found in 10/116, nor was lead detected in the VP-SEM-EDS analysis (Muros and Zacharias 2019). The detection of only $Ca_2Sb_2O_7$ in the opaque white glass could perhaps indicate that it did originally contain lead. Lahlil et al. (2008) found that in Roman opaque blue and white glasses with a high quantity of lead (2-40%) only the $Ca_2Sb_2O_7$ phase was identified. The same was seen in modern glasses opacified by calcium antimonate that contained high concentrations of lead (4-25%). Present in these Roman and modern glasses were lead compounds, which are not present in 10/109. It is possible that the lead is not uniformly present in the opaque white glass or its concentration is not high enough to have been detected in the sample taken for XRD or VP-SEM-EDS analysis.

The identification of a particular calcium antimonate compound within the glass can provide clues as to the manufacturing technology of the glass. The identification of antimony oxide in bead 10/115 points to the use of “in situ crystallization” to produce the opacity. The antimony oxide found within the Lofkënd opaque white glass would be unreacted material that did not combine with the lime. The presence of only the $Ca_2Sb_2O_6$ form of calcium antimonate suggests that the glass was produced using higher temperatures. Based on laboratory replication experiments, this phase forms at temperatures of 927°C and is the main phase present in the glass at higher temperature (Lahlil et al. 2008; Lahlil et al. 2009). At 1000°C both forms of calcium antimonate can still be present (Lahlil et al. 2008) therefore the furnace must be heated above that temperature so that only $Ca_2Sb_2O_6$ was detected. Bead 10/116 had both forms of the calcium antimonate compounds and was likely fired at around 927-1000°C. Bead 10/109 only contained $Ca_2Sb_2O_7$, and therefore it is possible that it was fired at a lower temperature that inhibited the formation of $Ca_2Sb_2O_6$ (Muros and Zacharias 2019).

10/106 contained both lead and a very small peak for antimony in two areas analyzed using pXRF (Figure 7.13). There is no opaque white or yellow decoration visible on the surface of the bead. It is not clear if the bead was decorated and the added glass has been lost, similar to what occurred in areas on bead 10/109 (Figure 7.5B). No recesses that could have contained colored glass were found on the surface. The source of lead and antimony found in 10/106 are unknown.

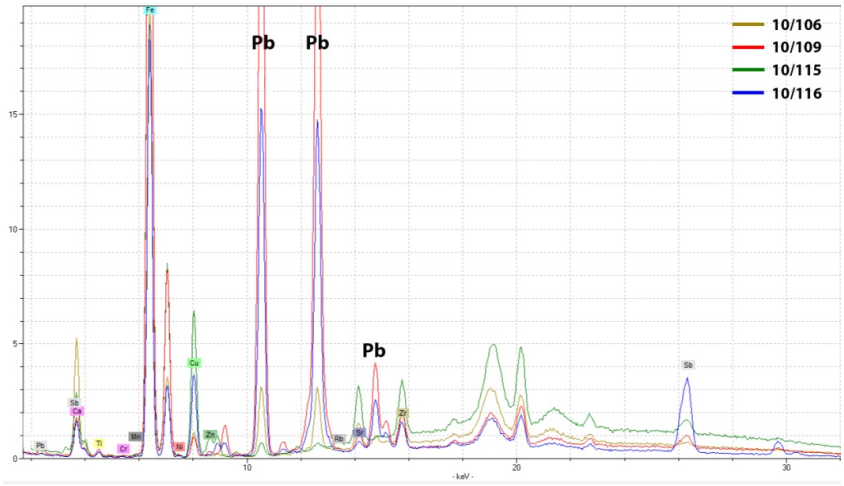

Figure 7.13. The results of pXRF analysis areas of opaque white glass on beads 10/109, 10/115, 10/116, and the surface of 10/106. Beads 10/106, 10/109, and 10/116 contain peaks for Pb in addition to a peak for Sb. Bead 10/115 is presented as a comparison since it contains and extremely small peak of lead that is just above the background, indicating it was likely not intentionally added.

7.4.1.1 Raw materials-Silica source

The investigation into the iron colorant, as well as the similarities between the Lofkënd dark green glasses and the Italian black ones led to the conclusion that the study group was likely made using sand as the silica source as opposed to quartz pebbles. Several oxides and trace elements were looked at in order to confirm whether sand was used to make the Lofkënd glasses and their origin by looking at impurities in the silica. The first impurities compared were titania and alumina, both of which would primarily enter the glass melt via the silica added and which should be higher if sands were used (Conte et al. 2018). The levels of titania and alumina in the dark green Lofkënd samples overlap those oxides in the Italian black glasses thought to have been made with Fe-rich sands and the Pella dark green glasses (Figure 7.14) (Reade et al. 2006; Conte et al. 2016; Conte et al. 2018). The concentrations of these oxides in plant ash cobalt colored Egyptian glasses (Shortland and Eremin 2006) and non-black Italian natron glasses (Conte et al. 2016; Conte et al. 2018) are much lower.

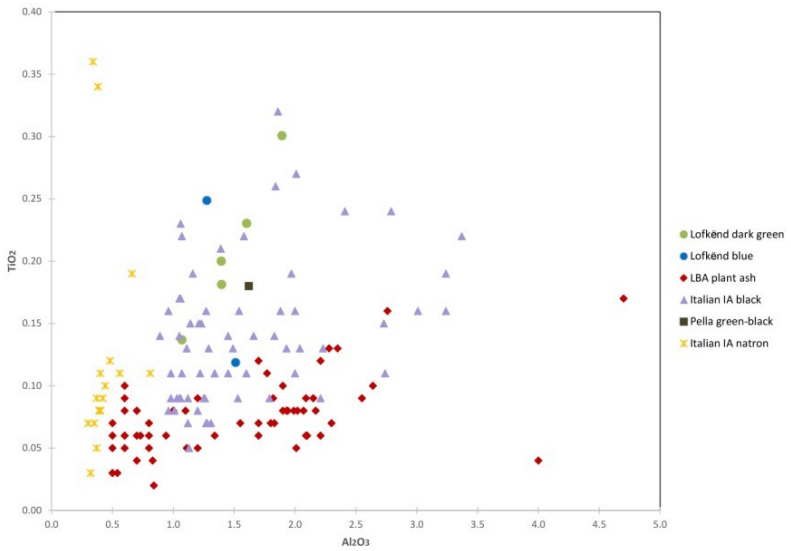

Figure 7.14. Biplot of alumina and titania concentrations in the Lofkënd glasses compared to Egyptian plant ash glasses (Shortland and Eremin 2006), Iron Age black glasses from Italy glasses (Conte et al. 2016; Conte et al. 2018), Early Iron Age dark green-black glasses from Pella (Reade et al. 2006) and Iron Age natron glasses from Italy (Conte et al., 2016).

The high alumina and titania concentrations are not limited to just the dark green Lofkënd glasses but are also found in the two blue glasses (10/112 and 10/117). Bead 10/112 has a fairly high concentration of titania, the second highest value of the beads. Since both the blue and dark green beads have these elevated levels of alumina and titania, the concentrations observed of these oxides are not specific to the colorant used but more than likely represent a sand based silica source used for all the glasses.

The relationship between the trace elements related to the silica source (vanadium, nickel, zinc, yttrium, zirconium, neodymium, hafnium and thorium) were further examined using a line graph to try and obtain more information on the silica source used to make the Lofkënd glasses (Figure 7.15). These elements were found to be elevated in the Italian black glasses and seen as indicative of iron rich sands selected as both the colorant and silica source (Conte et al. 2016; Conte et al. 2018). Strontium was included in the comparison because these levels were low in the published black glasses and also indicative of a different silica and alkali source. Although already discussed previously titanium and chromium were included as well. The values of these trace elements in the Lofkënd beads were compared to the Italian Iron Age black glasses (Conte et al. 2016; Conte et al. 2018). LBA plant ash glasses (Smirniou and Rehren, 2013) were included in the comparison to contrast these trace element concentrations when a purer silica source, like quartz pebbles is used. Egyptian and Mycenaean cobalt colored glasses were used for the Late Bronze Age comparison because few trace element analyses from this time period have been published. The transitional elements present due to the cobalt source used would influence the concentrations of some of the elements, and therefore this was taken into account when interpreting the data. Iron Age natron and plant ash glasses in colors other than black (Conte et al. 2016) were also included.

In the line graph (Figure 7.15), it is clear that the Lofkënd beads, both the dark green and the blue beads, show a marked difference in the elemental concentrations from the plant ash glasses, regardless of period. The plant ash glasses have higher zinc and strontium levels and lower titanium. The Late Bronze Age plant ash glasses have the highest nickel concentrations, possibly due to the cobalt colorant, and the lowest zirconium. The zirconium levels of the Iron Age plant ash glasses are similar to those in the Lofkënd beads.

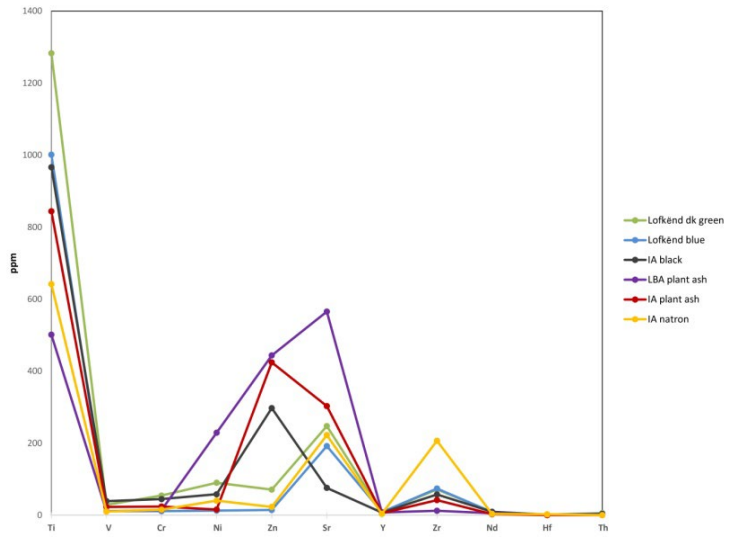

Figure 7.15. Line graph showing concentrations of certain minor and trace elements in the Lofkënd glasses compared to LBA plant ash glasses (Smirniou and Rehren 2013) and Iron Age plant ash, natron and black glasses from Italy (Conte et al. 2016; Conte et al. 2018)

Both the Lofkënd dark green and the Iron Age black glasses have the highest levels of titanium and chromium of the group (Figure 7.15). Both have nickel and zirconium concentrations that are similar as well. The Iron Age black glasses have lower strontium concentrations and higher zinc. The low strontium in the Iron Age black samples (0.3-1 ppm), and also the low lime content (2.6% avg.), was attributed to use of a low

lime sand to make the samples (Conte et al. 2016). The Lofkënd dark green beads have higher concentrations of both strontium (124.20-322.26 ppm) and lime (avg. 5.4 wt%), and therefore if sands were used they were not as low in lime (Table 7.3, Table 7.6). The strontium content of the Lofkënd beads is very similar to the Iron Age natron glasses in colors other than black (Conte et al. 2016). The Lofkënd blue glasses also have similar concentrations of strontium to both the natron glasses and the dark green Lofkënd beads. In the case of the overall concentrations of the trace elements of interest, it appears that the Lofkënd beads were made using a silica source that is closer to the Italian natron glasses in colors other than black.

Looking at the levels of these elements among the Lofkënd beads themselves, all the beads have low concentrations of vanadium, yttrium, neodymium, hafnium and thorium (Figure 7.16). As discussed earlier, three of the dark green beads—10/106, 10/108, and 10/116—have the highest concentrations of chromium while the other two dark green beads have similar chromium concentrations to the copper colored glasses (Table 7.6). The beads with elevated chromium were found within the same tomb (XXVIII) and date to the 12th-11th c. BC. These glasses also have higher nickel concentrations than the other Lofkënd glasses (49.86-297.14 ppm), with 10/108 having the highest levels of this element. 10/108 has the highest concentration of iron oxide (8.24 wt%) and it is unclear if the high nickel content is the result of the particular iron source used for the colorant. Finally, these three beads have the lowest levels of zinc of the Lofkënd group (17.44-42.75 ppm). Based on these similarities, it is likely that these three beads were made with the same raw materials and the same type of iron colorant making them distinct from the other four beads.

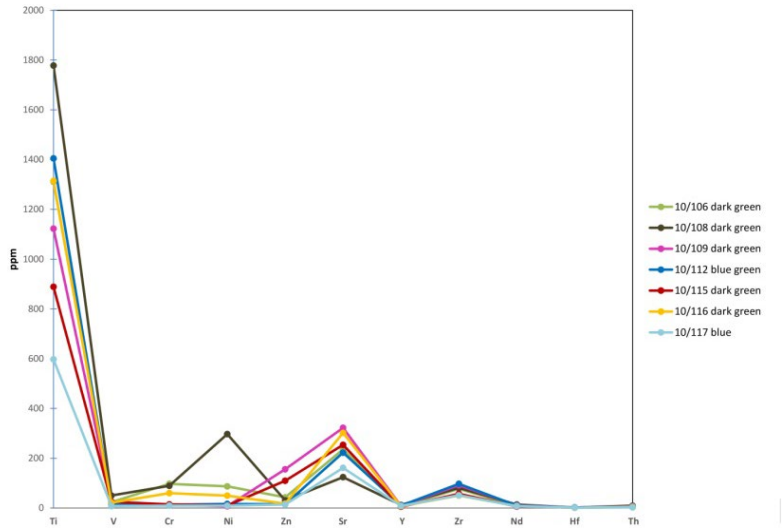

Figure 7.16. Line graph showing concentrations of certain minor and trace elements in the Lofkënd glasses.

The other two dark green beads, 10/109 and 10/115, share more similarities to the blue glasses (10/112 and 10/117) that the other dark green ones. 10/109 and 10/115 have a much higher concentration of zinc than all the other Lofkënd glasses (109.59 and 155.65 ppm). The low concentrations of the other trace elements, coupled with the high zinc and higher strontium (253.86 and 322.26 ppm), plus a higher lime content (5.14 and 5.72 wt%) suggests these two beads could have been made with similar raw materials. What is interesting is the beads are from two different tombs and time periods. 10/115 was found in the 12th-11th c. BC Tomb XXVIII. Bead 10/109 dates to the 11th-10th c. BC and comes from Tomb LIII.

7.4.2 Faience

7.4.2.1 Raw materials-Colorants

Due to the poor condition of the faience bead (10/105), only pXRF analysis was conducted. In areas where the glaze was preserved, copper was detected, along with tin and lead. This shows that bronze scrap was

used as the colorant for the glaze. The color is varied with areas, with the glaze appearing greener or paler (Figure 7.17A). The green color is likely due to the alteration of the copper blue glaze (Moussa and Ali 2013).

7.4.2.2 Production-Glazing method

Examination of the perforated end allowed for a partial section of the glazed surface and core to be examined (Figure 7.17). The core is extremely friable and is not cohesive, having the texture of sugar grains. This could be influencing the appearance of the glaze-core interface but it does appear that there is a clear boundary between the glaze and the core. The bead may have been glazed using the cementation method or via application and fired at a low temperature (Tite and Bimson 1986).The friable and granular appearance of the core of the bead could be the result of cementation glazing which produces a somewhat softer core with less interstitial glass (Tite and Bimson 1986). A faience object glazed using the application method and fired at a low temperature would also contain little interstitial glass. Due to the level of deterioration, and the fact that sampling could not be undertaking for compositional analysis or examination of the microstructure, the actual method of glazing could not be determined.

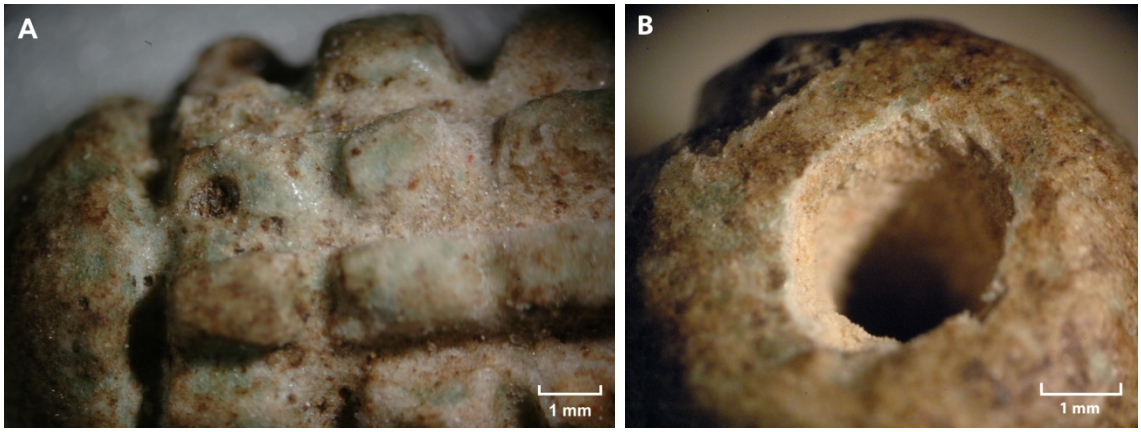

Figure 7.17. Photomicrographs of faience bead 10/105. (A) Area on the bead where the glaze is preserved (B) Area at one end of the bead showing the glaze around the perforation over the quartz core.

7.4.3 Provenance

7.4.3.1 Principal Component Analysis (PCA)

7.4.3.1.1 Major and minor oxides

Principal Component Analysis (PCA) was used to identify possible compositional groups among the seven glass beads sampled for EPMA analysis, as well as their relationships to compositional groups of published Late Bronze Age vitreous materials to provide information on the provenance of the raw materials used to make the glasses (Figure 7.18) (Brill 1992; Nikita and Henderson 2006; Shortland and Eremin 2006; Smirniou et al. 2009; Jackson and Nicholson 2010). The PCA was performed on EPMA data from 10 major and minor oxides (Na_2O, K_2O, MgO, Al_2O_3, CaO, SiO_2, FeO, MnO, P_2O_5, TiO_2) (Table 7.3, Appendix D.2). The early natron black glasses from Italy (Conte et al. 2016; Conte et al. 2018) were also included in the PCA since they were similar in some aspects of the major and minor oxides to the Lofkënd samples. The first two principal components explain 54.2% of the variance in the data (Appendix D.4).

Correlations can be found between several of the oxides. For example, there is a positive correlation between MgO and CaO, and to some extent Na_2O, oxides related to the plant ash alkali in Late Bronze Age glasses. P_2O_5 and K_2O, also elements related to the alkali, are correlated. Higher concentrations of these oxides are present in plant ash glasses. Correlations between FeO, TiO_2, Al_2O_3, MnO, and SiO_2 are also

observed. These elements are found as impurities in sands used as the silica sources, but are also present as impurities in some colorants such as cobaltiferous alum.

There seems to be two large compositional groups formed along the negative correlations between the oxides corresponding to the impurities in sand/colorants and those of the plant ash alkali. The Iron Age black natron glasses are grouped together and their variance is explained by the concentrations of FeO, the colorant, TiO_2 and SiO_2, which are contributed by the silica source. All the other glasses group along the other vectors related to the plant ash alkali found in Late Bronze Age glasses.

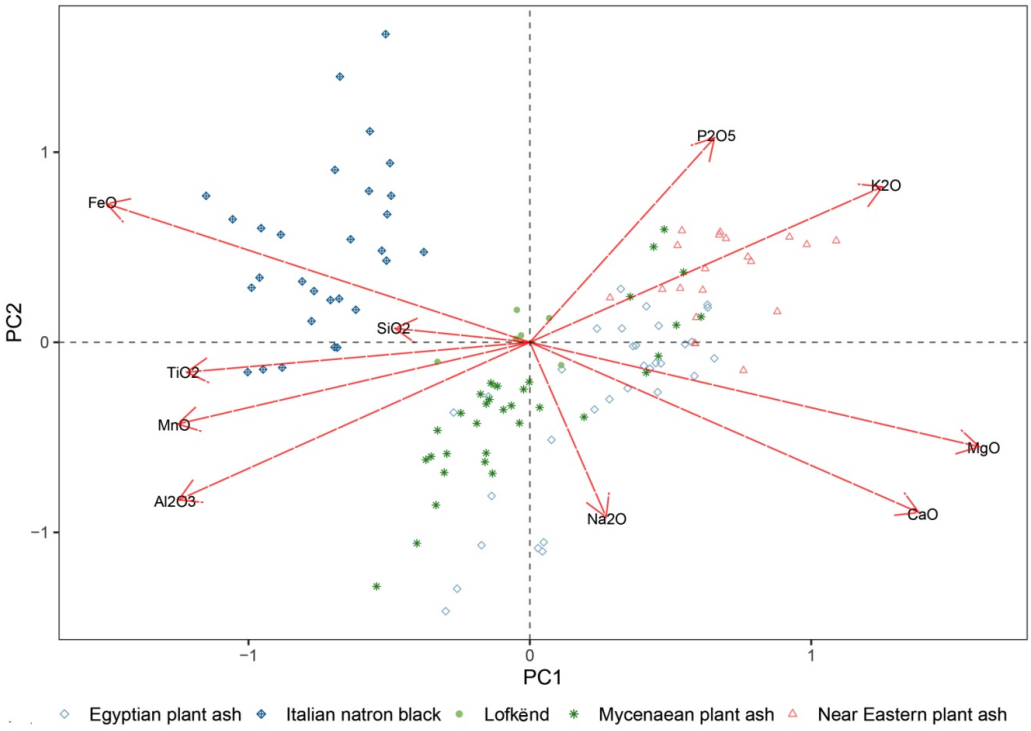

Figure 7.18. Biplot of principal components 1 (39.2% of the variance) and 2 (15.0% of the variance) calculated using EPMA data of 10 major and minor oxides from the Lofkënd glasses. Included in the PCA was published data from LBA vitreous materials for comparison (Brill 1992; Nikita and Henderson 2006; Shortland and Eremin 2006; Smirniou et al. 2009; Jackson and Nicholson 2010) and Iron Age black natron glasses (Conte et al. 2016; Conte et al. 2018). The position of the samples is scaled proportional to the eigenvalues of each principal component (Oksanen et al. 2017). Samples that are closer together are more similar in composition. Vectors are not scaled according to their eigenvalues. The positions of the variables show their relative positions to each other, indicating their correlation to each other and relative influence on the elemental composition.

Within this larger group however, there appear to be subgroups based on different compositions. The Near Eastern glasses are somewhat separate from most of the Egyptian and Mycenaean samples, with higher concentrations of potash, magnesia, and phosphorus pentoxide. There is also a distinction between the majority of Mycenaean glasses and the Egyptian ones. The variance among the Mycenaean samples is influenced more by the alumina content and to some extent soda, while the Egyptian samples have a higher content of lime, magnesia, and potash.

The Lofkënd samples seem to form their own group near the origin of PC1 and 2. One dark green bead with an opaque white band, 10/108, has the highest concentration of titania of the Lofkënd glasses (0.30 wt%) and is separate from the cluster at the origin (Table 7.3). Another dark green bead with opaque white spots, 10/116, has the highest concentration of soda (19.18 wt%) and lime (6.12%) and has plotted near an Egyptian plant ash sample with similar concentrations of those oxides. Based on the PCA of the EPMA data, it looks as if most of the Lofkënd samples are not similar in the concentrations of their major and minor

oxides to Late Bronze Age plant ash glasses and the Iron Age black natron glasses from Italy. They may belong to a different compositional group and primary production area.

7.4.3.1.2 Trace elements

Based on the similarities between the Lofkënd glass beads and the silica and colorant sources for the Italian natron glasses (Figure 7.15), Principal Component Analysis (PCA) was used to better visual the different compositions among these samples, as well as potentially provide additional information on the sources of the raw materials (Figure 7.19). The PCA was performed using LA-ICP-MS data from 11 elements (V, Cr, Ni, Zn, Sr, Y, Zr, L, Nd, Hf, Th) (Table 7.3, Appendix D.2). Data from Late Bronze Age plant ash glasses (Smirniou and Rehren 2013) along with trace element data from Italian Iron Age natron glasses of different colors. (Conte et al. 2016; Conte et al. 2018) was included for comparison. The first two principal components explain 59.6% of the variance in the data (Appendix D.4). Due to the lack of published data for the trace elements of interest for Late Bronze Age plant ash glasses and Early Iron Age non-black, natron glasses, additional samples could not be included in the PCA.

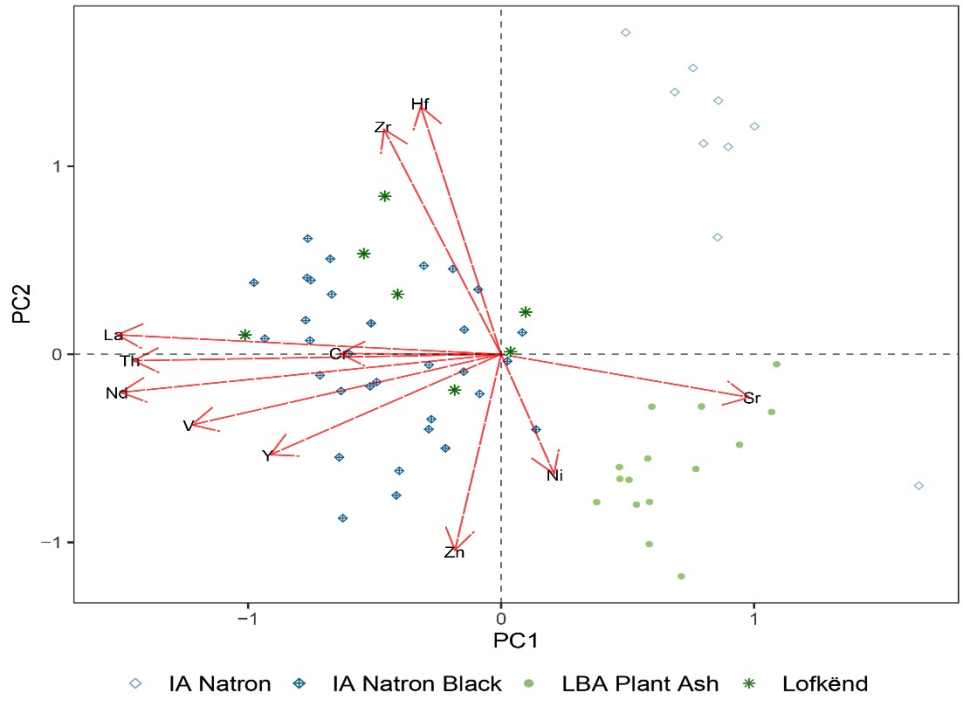

Figure 7.19. Biplot of principal components 1 (39.4% of the variance) and 2 20.1% of the variance) calculated using LA-ICP-MS data of 11 trace from the Lofkënd glasses. Included in the PCA was published data from LBA plant ash glasses (Smirniou and Rehren 2013) and Iron Age natron glasses (Conte et al. 2016; Conte et al. 2018). The position of the samples is scaled proportional to the eigenvalues of each principal component (Oksanen et al. 2017). Samples that are closer together are more similar in composition. Vectors are not scaled according to their eigenvalues. The positions of the variables show their relative positions to each other, indicating their correlation to each other and relative influence on the elemental composition.

Correlations are found among several of the trace elements. Zr and Hf are positively correlated, and negatively correlated with Ni. The elements V, Nd, Th, Cr, and La are positively correlated. This group is somewhat negatively correlated with Sr, which is related to the source of lime. Three compositional groups are visible within the PCA. One large group contains six of the Lofkënd glasses and all the black natron glasses. These samples have a negative PC1 value. Their variation is explained by a group of seven elements related to the silica source (Conte et al. 2016; Conte et al. 2018). The other two groups have a positive PC1 value, but are distinguished by PC2. One group includes almost all the non-black Iron Age natron glasses and the other is made up of the Late Bronze Age plant ash glasses. The non-black natron glasses have higher

concentrations of hafnium and strontium (Conte et al. 2016), pointing to a different silica source for these natron glasses. This would make sense since the sands used for the black glasses were high in iron and other impurities that were selected to also act as the colorant (Conte et al. 2018). The group of Late Bronze Age plant ash glasses are grouped because they use a different alkali from the natron glasses and a different silica source, which in some cases was fairly pure and free of impurities (Shortland 2012). The lime source, which would introduce strontium, would come from the plant ashes used. Not only do plant ash glasses use a different source of lime than natron glasses, but they also have a composition higher in lime (Henderson 2013).

There is quite a bit of variation among the group consisting of the black natron glasses and the Lofkënd glasses. This may point to a wider range of silica and colorant sources used, not only between these two sets of glasses, but also within the Lofkënd glasses. None of the Lofkënd glasses forms a tight group and most do not plot near each other. This may mean that the PCA is useful to distinguish the Lofkënd glasses from non-black natron and plant ash glasses, but not for an intra-site compositional comparison.

7.4.3.2 Trace elements

The concentrations of the trace elements chromium, lanthanum, titanium and zirconium in the Lofkënd beads were compared to glasses from Egypt (Shortland et al. 2007), the Near East (Shortland et al. 2007; Kirk 2011; Kemp et al. 2020), mainland Greece (Smirniou et al. 2009; Walton et al. 2009), and the Uluburun ingots (Jackson and Nicholson 2010) to determine the primary production site of the glasses.

The biplot shows that the Lofkënd glasses come from two different primary production regions (Figure 7.20). Four beads (10/109, 10/112, 10/115, 10/117), are similar to glasses manufactured in Egypt, Mycenaean beads with an Egyptian origin, and the Uluburun ingots. The four Lofkënd beads of Egyptian origin have low Cr/La ratios (0.96-1.81) and higher 1000Zr/Ti ratios (64.04-85.69) (Table 7.6). The other three beads (10/106, 10/108, 10/116) are similar to glasses made in the Near East and to Mycenaean glasses of Near Eastern origin. They have higher Cr/La ratios (5.21-9.14) and lower 1000Zr/Ti ratios (38.15-59.21). The groupings of the Lofkënd beads based on these trace element ratios are similar to the pattern observed in the line graph (Figure 7.16).

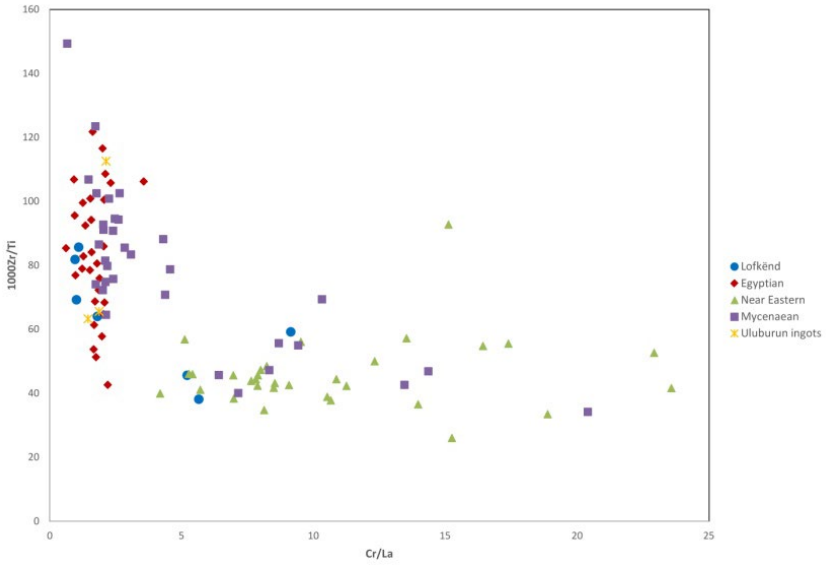

Figure 7.20. Biplot of the ratios of Cr/La and 1000Zr/Ti of the glasses from Lofkënd compared to samples of Egyptian origin (Shortland et al. 2007), Near Eastern origin (Shortland et al. 2007; Kirk 2011; Kemp et al. 2020), Mycenaean glass of both Near Eastern and Egyptian origin (Smirniou et al. 2009; Walton et al. 2009), and ingots from the Uluburun shipwreck (Jackson and Nicholson 2010).

The four Egyptian-made beads were found in two different graves from two different time periods (10/112, 10/115, 10/117-Tomb XXVIII, 12th-11th c. BC and 10/109-Tomb LIII, 11th-10th c. BC), while the three beads of Near Eastern origin all come from Tomb XXVIII. There do not seem to be any chronological trends linking the date of the beads and their origin. Since only one bead from the 11th-10th c. BC was analyzed and none from the 10th-9th c BC, there could be some differences observed over time if a larger sample group were analyzed. There also does not seem to be any link between the color of the beads and origin. Both blue and dark green beads were imported from Egypt. There does not seem to be a link between the composition of the opaque white decoration and the production area either.

A second biplot was made comparing the concentrations of chromium and lanthanum in the Lofkënd beads to the comparative samples mentioned above in addition to Italian Iron Age black glasses (Figure 7.21). The Lofkënd samples split along the same regions of production as in the biplot of the ratios (Figure 7.20). The Near Eastern Lofkënd beads have much higher concentrations of chromium than the published Late Bronze Age glasses. This is likely related to the iron colorant. These three beads, however, do not have the same iron content, nor are those levels the highest (Table 7.3). The elevated concentration of iron does not necessarily seem to increase the chromium content.

The concentrations of chromium and lanthanum do show that the Lofkënd beads overlap with the Italian Iron Age black glasses (Figure 7.21). In both sets of glasses, their chromium and lanthanum concentrations exceed the Late Bronze Age plant glasses made in Egypt and the Near East. Despite the higher values of these two trace elements found the Lofkënd and Italian glasses, they still could have been made with Egyptian or the Near Eastern raw materials. Two of the Italian black glasses included in the comparative data, which come from northern Italy near Bologna, underwent isotopic analysis to determine provenance (Conte et al. 2018). The isotopic signatures for neodymium and strontium in those two glasses were similar to those found in sandstone from Egypt and sand from Wadi Natrun, pointing to an Egyptian silica source. These two Italian black glasses are similar in their concentrations of chromium and lanthanum (Cr-16 and 18, La-9.0 and 7.6 ppm) (Conte et al. 2018, 511, table 3) to two Lofkënd beads, 10/115, a dark green bead (Cr-14.42 ppm, La-7.98 ppm), and 10/117, a blue bead (Cr-9.70, La-8.83 ppm). It is possible that these Lofkënd beads are also of Egyptian origin.

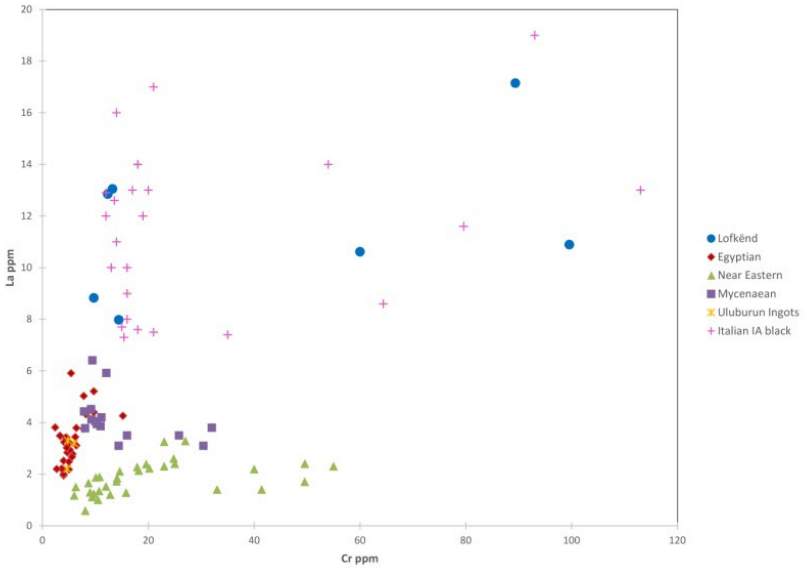

Figure 7.21. Plot of the concentrations of chromium and lanthanum in the Lofkënd samples compared to glasses of Egyptian origin (Shortland et al. 2007), Near Eastern origin, (Shortland et al. 2007; Kirk 2011; Kemp et al. 2020), Mycenaean glass of both Near Eastern and Egyptian origin (Smirniou et al. 2009; Walton et al. 2009), ingots from the Uluburun shipwreck (Jackson and Nicholson 2010), and Iron Age black glasses from Italy (Conte et al. 2016; Conte et al. 2018).

There are two group created among the Lofkënd beads from Egypt based on their lanthanum concentrations (Table 7.6). Beads 10/109 and 10/112 have very similar concentrations of chromium (12.34 and 13.24) and lanthanum (12.55 and 13.05), with levels of the latter higher than the Late Bronze Age glasses and similar to many of the Iron Age black glasses. It is interesting to note that these two beads are from different tombs and different periods, but appear to have been made with raw materials with the same concentrations of these trace elements.

Some caution should be taken when using these particular transition elements for provenancing glasses made with natron. The elements do distinguish between Late Bronze Age Near Eastern and Egyptian plant ash and silica sources (Shortland et al. 2007). However, there have been some issues when they have been used to provenance classic natron glasses. A study by Oikonomou et al. (2020, 269, fig.7) found that when 6th-8th c. AD natron glasses made at primary production sites on the Levantine coast were included in a plot to provenance glasses from Thesprotia, Greece, the Levantine glasses grouped with Egyptian Late Bronze Age plant ash glasses. Egyptian natron glasses belonging to the compositional groups Egypt I and II overlapped with Near Eastern plant ash glasses. This shows that these trace elements may not be optimal for distinguishing between silica sources for natron glasses.

It is possible though that the links between transition element concentrations and provenance still holds true for the Lofkënd samples and the Iron Age natron glasses. The PCA showed a correlation between chromium and lanthanum for the Lofkënd and Iron Age black natron glasses. Therefore, the provenance groups observed in figure 7.21, and possibly figure 7.20, may be representative of the origin of some of the raw materials. The groupings observed suggest the silica sources used for the Lofkënd glasses that are different from those used for glasses from Amarna, Malkata, and Mycenaean Greece made with raw materials from Egypt. In the case of the Near Eastern glasses, the silica source is very different from that used for samples from Tell Brak, Nuzi, Gurob, and Mycenaean glasses of Near Eastern origin. Rather than indicating the use of different raw materials within the same larger geographic area, the data could point to a different production region all together for the Lofkënd glasses. More analysis is needed, in particular isotopic analysis, to better determine the origin of the raw materials used to produce the Lofkënd glasses.

The concentrations of neodymium and strontium in the Lofkënd glasses were compared to Late Bronze Age glasses (Smirniou et al. 2009; Walton et al. 2009; Henderson et al. 2010) and the Italian black beads (Conte et al. 2016; Conte et al. 2018) in an effort to see if the origin of the raw materials used to make the Lofkënd beads could be further pinpointed. The strontium and neodymium content does differentiate some regions of glass production (Figure 7.22). The Lofkënd glasses have low strontium levels and higher neodymium concentrations separating them from the Late Bronze Age glasses from the Near East, Egypt, and mainland Greece. The Near Eastern glasses create a tight group. There is more variation among the Mycenaean glasses but they do group together. The Egyptian samples have a wider spread due to the variations in strontium levels.

The Iron Age natron glasses have both low strontium and neodymium concentrations, and therefore are different from the Lofkënd beads. There is some overlap between the Lofkënd samples and the Italian black glasses, where they both have similar strontium and neodymium concentrations. However, the Italian samples have an even lower strontium content. The concentrations of these two trace elements can distinguish larger regional and chronological groups, but the primary production area of the Lofkënd beads is not apparent. What is clear from this biplot (Figure 7.22), along with the line graphs (Figure 7.15, 7.16) and other comparisons of trace elements and oxides, is that the Lofkënd beads were made with a different alkali and silica source from that used for Late Bronze Age plant ash glasses. They share similarities to some of the Italian HMLK Iron Age black in some aspects of their composition such as the colorant, alkali and silica sources, but also overlap with the concentrations of some of the transition and rare earth elements found in Italian natron glasses of other colors. They also have compositional similarities to the Pella dark-green black

glasses considered early natron samples. It is not clear if this means the Lofkënd glasses are very early examples of natron glasses, this is evidence of experimentation with a different mineral alkali source, or if they are plant ash glasses made with a halophytic plant specific to their primary production region and sand as the silica source. More glasses dating to the Late Bronze Age and Early Iron Age from the Balkans need to be analyzed, and the raw materials sourced using radiogenic isotopes, to understand the variability observed in the beads from the Lofkënd tumulus.

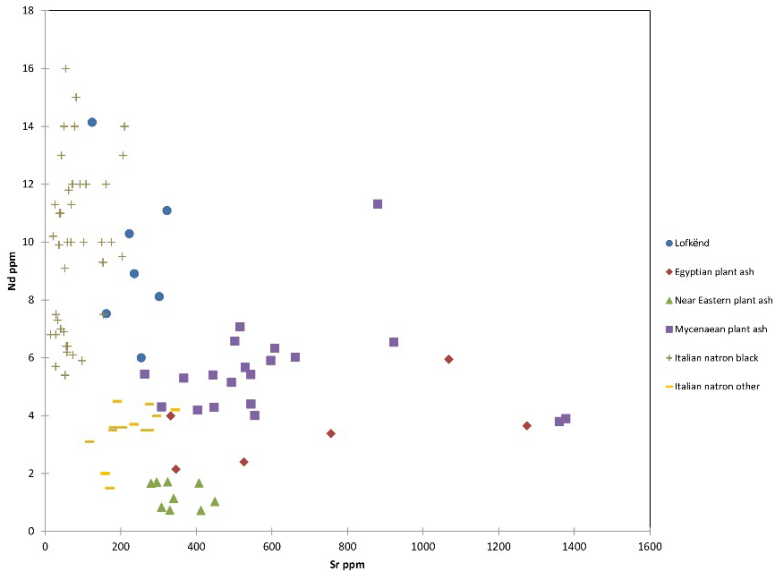

Figure 7.22. Plot of the concentrations of strontium and neodymium in the Lofkënd samples compared to samples of Egyptian origin (Henderson et al. 2010), Near Eastern origin, (Henderson et al. 2010), Mycenaean glass of both Near Eastern and Egyptian origin (Henderson and Warren 1981; Smirniou et al. 2009; Walton et al. 2009), and Iron Age natron glasses from Italy (Conte et al. 2016; Conte et al. 2018).

7.5 Chapter Summary and Conclusions

Eleven vitreous beads (10 glass and one faience) were excavated from the tumulus at Lofkënd located in southwestern Albania. The tumulus was in use from the 14th–late 9th/early 8th c. BC and contained 98 graves. The glass and faience beads were found in four of the tombs and date to the 12th-9th c. BC. The tombs contained a range of grave goods in addition to the glass beads. This included pottery and items of personal adornment such as fibulae, hair spirals, pins, and carnelian beads. The types of artifacts found represent regional and foreign styles showing that Lofkënd imported items from the Aegean, southern Italy, and the northern Balkans via sea and land routes.

The 11 beads discovered represent a color palette and decorative style that is not commonly reported for vitreous materials typically found within Late Bronze Age contexts. Two, possibly three, of the beads were blue. Two of these were fluted. The remaining glass beads were a dark green, almost black, color. Four were decorated with lines and/or spots of opaque white glass. The shape of the faience bead mimics a gridded or granulated form, which is somewhat rare.

PXRF analysis was conducted on all eleven beads to identify the mineral colorants. The blue beads are colored using copper, with only one having a peak for tin indicating the use of bronze scrap as the colorant. The color of dark green beads was due to iron. The four decorative motifs on the beads were made using antimonate compounds. The glaze of the faience bead was a copper blue color that used bronze scrap as the colorant source due to the detection of tin.

Seven of the Lofkënd beads were sampled for compositional analysis. This included two blue glass beads and five dark green beads spanning the 12th-10th c. BC. EPMA analysis showed that the Lofkënd beads have

a somewhat unusual composition compared to most Late Bronze Age plant ash glasses. They contain low concentrations of potash (avg. 1.30 wt%) and low concentrations of lime (4.8 wt%). The potash concentrations overlap with some Egyptian and Mycenaean cobalt colored glasses. The lime content of the Lofkënd beads is lower than that found in most Near Eastern and Egyptian glasses, and some Mycenaean glasses.

The Lofkënd beads share similarities in alkali and alkali earth metal concentrations with black glasses, some with opaque white decorations, from Early Iron Age sites in Italy and dark green-black glasses from Pella that also date to the same period. These glasses are also low in lime and potash, and some of the Italian glasses also have high magnesia. These Early Iron Age glasses seem to have been made using sand as the silica source and a mineral alkali, like natron, instead of plant ash. Although low lime is not characteristic of natron glasses, the mineral alkali does not contain this network stabilizer and so it must be added separately or enter the glass batch with the silica source. If the early glassmakers were experimenting with a new type of alkali and silica source for glassmaking and were not aware of the need for additional lime, this may explain the low lime content of these early natron glasses.

Bead 10/117 contains low magnesia (1.41 wt%) at levels found in natron glasses, in addition to low lime. The other Lofkënd beads have higher levels of magnesia and are similar to the high magnesium low potassium (HMLK) natron glasses discovered in Italy. The high magnesia found in the HMLK natron glasses comes from the silica source used, which is high in magnesium containing minerals.

Although the composition of the Lofkënd beads is similar to these low lime natron glasses, they do not fit the chronology of the first appearance of natron glasses. These do not appear in the archaeological record until the 10th c. BC. With six of the Lofkënd beads analyzed dating to the 12th-11th c. BC, something other than the use of natron must be influencing the composition. The low potash content could be explained by the use of a different plant ash alkali, one that is low in potassium, a similar idea proposed to explain the low potash levels of plant ash cobalt colored glasses. The particular plant ash alkali could also be low in lime. It is also possible that a different alkali all together was used to manufacture these glasses or some part of the production processes resulted in the composition revealed. The final possibility is that these glasses are actually early examples of the experimentation with natron and represent part of the transition to this new glass technology.

The source of the iron colorant in the dark green beads was explored to determine whether it was based on iron oxide or an iron metallurgical product as seen in some Roman period black glasses, or was made using iron rich sands, which worked as both the silica and iron source, used for Iron Age black glasses from Italy. The use of iron rich sands was found to increase the concentrations of chromium, titania, alumina and a group of rare earth elements (REEs). The levels of these were examined in the Lofkënd glasses. Three of the beads (10/106/ 10/108, 10/116) have high concentrations of chromium, similar to the Italian black glasses colored with iron rich sands that contained the mineral chromite. The remaining two dark green and the two blue glasses had low levels of chromium. This suggests that the three glasses with elevated chromium may have been made with a colorant from a source distinct from the one used for the other two dark green beads.

XRD analysis was used to characterize the opaque white glass decorations found on four of the dark green beads. The opaque white glasses on three of the beads contained calcium antimonate compounds. Antimony oxide was found in bead 10/115 and indicated that the opaque white glass was made using in situ crystallization. In addition to calcium antimonate compounds, bead 10/116 lead antimonate and lead oxide was also detected in the opaque white glass. It is unclear if lead was added to the white glass to improve the working properties or if it was introduced in the raw materials and combined with antimony due to a low lime content during in situ crystallization. Only sodium antimonate compounds were found in the fourth

bead (10/108). Due to the low lime content of that glass, sodium from the alkali combined with the antimonate compounds instead of calcium.

Looking at the concentrations of titanium, aluminum, and several trace elements, it was clear that the raw materials used to make Lofkënd beads are different than those used to make the plant ash glasses in the Late Bronze Age. The silica source points to the use of sand with a high level of impurities. There are some similarities between the REEs in the silica source used for the Italian black natron glasses and the Lofkënd samples, but the values for some of the elements overlap with Italian natron glasses made in other colors. The Italian black glasses were colored using a dark, iron rich soil that contained chromite, but these same sands do not appear to have been used to produce the Lofkënd beads. The two sets of beads likely come from two different primary production areas.

The concentrations of the various trace elements among the Lofkënd beads themselves, two distinct groups of raw materials are created. One group contains the chromium rich black glasses (10/106, 10/108, 10/116), all found within the same tomb and dating to the 12th-11th c. BC. These three beads appear to have been made with the same silica source. The iron content among these beads varied and the iron may have come from another source and not necessarily iron rich dark colored sands. The second group includes the other two dark green beads (10/109, 10/115) which were closer in their concentrations of REEs to the two blue Lofkënd beads (10/112,10/117). These four beads were made with a separate set of raw materials that also likely included sand as the silica source. The similarities between the silica source across the different colors means that the sand used is likely not the source of the iron colorant in this case.

The concentrations of chromium, lanthanum, titanium, and zirconium, as well as the ratios of the elements, the Lofkënd beads were used to try to source the glasses. Three of the dark green beads, 10/106/ 10/108, 10/116, are similar to glasses produced in the Near East. The other four beads 10/109, 10/112, 10/115, 10/117, two dark green and two blue, were produced in Egypt. The Egyptian made glasses come from two tomb contexts of different dates. This means that in this region of Albania, Egyptian glass was imported in the Late Bronze Age through to the start of the transition to the Early Iron Age. It is possible that the use of Egyptian glass continued into later periods. Near Eastern glass was being used in the 12-11th c. BC but could also have been a source for later glasses. Tomb XXVIII contained a mix of both Egyptian made and Near Eastern made glasses. The limited number of samples analyzed from Lofkënd did not allow for additional conclusions to be drawn on trends in regards to glass origins. Additional analysis of the Lofkënd beads, and samples from other sites in southwestern Albania, are needed to obtain more information on this aspect of trade and consumption of glass in the region.

The chromium and lanthanum concentrations of all the Lofkënd beads exceed the levels found in the plant ash glasses from the Near East, Egypt, and Mycenaean Greece. The Iron Age black glasses from Italy, however, are similar in their concentrations of these two trace elements to the Lofkënd glasses. The same pattern is seen in the levels of neodymium and strontium, which are related to the silica and alkali source. Most Lofkënd beads have lower strontium and higher neodymium values than Late Bronze Age plant ash glasses and non-black colored Iron Age glasses from Italy. They are somewhat similar in their content of strontium and neodymium to the Italian black natron glasses.

The analysis of the Lofkënd beads has seemed to raise several questions about the production technology and composition of glass in this region during the Late Bronze Age and Early Iron Age that could not be definitively answered. The glasses seem to be distinct from Late Bronze Age glasses found in Egypt, the Near East, and Mycenaean Greece in many aspects of their composition. They are somewhat similar in their alkali, silica, and colorant compositions of Iron Age black glasses from Italy that have been described as early natron glasses with low lime and high magnesia. There are some similarities as well with the dark-green black glasses from Pella that are also examples of an early natron composition. Despite their similarities to the early glasses, it appears that based on the concentrations of some of the transition elements such as

chromium and lanthanum, glasses from primary production sites in the Near East and from Egypt were deposited as grave goods at Lofkënd.

It is not clear whether the composition of the Lofkënd dark green beads is due solely to the use of particular raw materials selected near the primary production workshops in Egypt and the Near East. Something worth investigating further is whether after the ingots were imported to the Balkans, or elsewhere in Europe, regional glassworking took place that created the composition observed. This could explain the similarities between these beads from southwestern Albania to those found in Italy, while retaining shared compositional similarities to glasses made in Egypt and those from the Near East. More analysis is needed of iron-colored dark green and black glasses found in Europe that span the Late Bronze Age and Early Iron Age to look for technological trends that could help answer these outstanding questions on glass production and trade. The use of radiogenic isotopic analysis would help to address the outstanding questions regarding this unique glass composition.

8 THE DEGRADATION PATHOLOGIES OF ARCHAEOLOGICAL GLASSES

8.1 INTRODUCTION

The deterioration of archaeological glass is a complex process that is influenced by numerous factors. The burial environment can play a primarily role in the corrosion of ancient glasses, but the composition of the glass, the surface area of the object, the method of manufacture, contents of vessels, and exposure time are also important (Freestone 2001; Davison 2008; Jackson et al. 2012; Zacharias and Palamara 2016; Zacharias et al. 2020). The types of deterioration vitreous artifacts undergo impacts our understanding of this technology and in extreme cases results in loss of material creating an incomplete record of the glass industry in antiquity. The investigations into the degradation pathologies observed in archaeological glasses and deterioration mechanisms can provide information on what the burial environment was like and the taphonomic processes that have acted upon the vitreous materials in situ, in addition to providing technological information even when the glass is not well preserved.

The types of deterioration observed on the beads from ancient Methone, Kefalonia, and Lofkënd have been touched upon in the previous chapters but will now be addressed in more detail. All the beads studied have undergone some kind of deterioration. The level and the types of degradation pathologies vary even among vitreous beads found within the same burial context. Surface changes in translucency and color, staining, pitting, and iridescence were observed. Changes to the structure of the bead have also occurred leaving the vitreous material friable, flaky, or completely fragmented with little to no intact glass remaining.

8.2 DETERIORATION OF GLASS

8.2.1 Mechanisms of glass decay

There are two main mechanisms under which glass deteriorates: dealkalization (also referred to as ion exchange or leaching) and network dissolution (Freestone 2001; Davison 2008; Zacharias et al. 2020). The primary catalyst for both of these types of decay is water interacting with the surface of the glass. The source of the moisture could be in the burial environment or in the atmosphere.

In dealkalization, deterioration occurs when water enters the glass and alkalis are leached out of the structure (Jackson et al. 2012). Hydronium ions (H_3O^+) from the water attack the surface and exchange a hydrogen ion (H^+) for the alkali (Davison 2008). These alkalis are leached out of the glass into the surrounding water on the surface. The loss of the alkali creates a silica rich layer on the surface, sometimes referred to as a "gel layer" (Davison 2008, 175). Dealkalization can be expressed by the following reaction (after El-Shamy et al. 1972; Freestone 2001):

$$H_3O^+ + \equiv Si\text{-}O\text{-}M^+ \rightarrow \equiv Si\text{-}OH + H_2O + M^+$$

where "M" represents the alkali, such as Na^+ or K^+. Since the hydrogen ion is smaller than the alkali ion it is replacing, the glass network is left weakened and can contract (Freestone 2001; Davison 2008). Dealkalization begins at the surface of the glass, and the creation of the silica rich layer can create a somewhat protective layer. This silica rich layer is not as dense as the glass and ion exchange will continue to occur as long as moisture is present, just at a slower rate (Jackson et al. 2012). This layer also behaves almost as silica gel. It is hygroscopic, continuing to attract more moisture and introduce it into the weakened glass structure (Freestone 2001).

Network dissolution occurs under alkaline conditions (pH >9); therefore not only is water required but the pH of the environment also becomes a factor in the rate of deterioration (Clark and Hench 1981; Davison 2008). Under these conditions, a hydroxide ion (OH^-) enters the glass causing a break in the bonds of the oxygen that acts as a bridge between the silicon atoms (Davison 2008). Network dissolution is represented by the following reaction (Freestone 2001):

$$=Si\text{-}O\text{-}Si= + OH^- \rightarrow =Si\text{-}OH + Si\text{-}O^-$$

This reaction causes the silica network to breakdown and the silica to dissolve. The rate of degradation observed by network dissolution is much faster than with leaching (Clark and Hench 1981).

Ion exchange is the more common deterioration mechanism observed in archaeological glasses due to the burial environment (Freestone 2001). This is because ground water generally has a mid-range pH and is not very alkaline (Davison 2008). Network dissolution has been observed more often in glasses exposed to the atmosphere, such as window glass. In buried vitreous materials, the pH of the glass/water interface increases as the alkali is leached out of the glass. However, because ground water is present the built up alkalis will be washed away if the source of water is not static. This will then lower the pH in that area. In window glass, the alkalis leached from the glass sit on the surface as salts and create a consistent alkaline environment at that interface (Davison 2008). Since the alkaline salts are not removed, this sets up conditions preferential to network dissolution. Although there are mechanisms that seem be more prevalent in different environments, both ion exchange and the dissolution of silica can occur at the same time in both environments, especially if conditions change and the moisture content and pH varies (Hench and Clark 1978; Freestone 2001).

8.2.2 Surfaces produced by deteriorated glass

The mechanisms of dealkalization and network dissolution can produce various surfaces on glasses, both in appearance and composition. A series of experiments conducted by Hench and Clark (1978) have identified five types. Type I surfaces are simply hydrated, with no loss of alkali or dissolution of silica. The surface and bulk glass have the same composition. A Type II surface is what commonly occurs during dealkalization, where the alkali is leached and the surface becomes silica rich. This surface tends to form in glasses with low concentrations of alkali, so that the ratio of alkali to silica is low. The silica rich surface layer can be protective reducing continued dealkalization. The glass can remain stable if the pH is not very alkaline.

Type III surfaces are also protective and are made up of layers of different films (Hench and Clark 1978). The first layer formed is silica rich one observed in Type II surfaces due to dealkalization. In Type IIIA surfaces, a film is formed above this using alumina or phosphorus pentoxide extracted from the glass. These protective layers are comprised of alumina silicate or calcium phosphate. Having a protective layer of silica rich glass and another above of either alumina silicate or calcium phosphate makes the glass more durable across different pH ranges. Type IIIB films are composed of oxides and hydroxides over a silica rich layer (Davison 2008). They are not generally observed in archaeological or historic glasses, but are seen in glasses used for nuclear waste storage. Type III films can form through different processes such as dealkalization, precipitation from solution, or modifications to the surface structure (Hench and Clark 1978).

Type IV surfaces are similar to Type II in that they are silica rich and are the result of dealkalization (Hench and Clark 1978). However, Type IV surfaces are not as protective so dealkalization can continue to occur, allowing the glass to degrade due to network dissolution. The glasses that develop a Type IV surface tend to have an overall composition low in silica with high concentrations of alkalis so that the ratio of alkali to silica is high. The final type of surface identified by Hench and Clark (1978), known as Type V, has undergone loss of both alkali and silica in the same concentrations. The composition of the surface in the glasses is the same as the bulk composition. This surface is most often caused by network dissolution, whereas Type II, III, and IV are generally the result of dealkalization. For archaeological and historic glasses—especially soda-

lime-silicate compositions found in the Late Bronze Age and Early Iron Age—Types III, IV and V are the most common surfaces found (Hench and Clark 1978; Davison 2008). Type I is unlikely to be found on archaeological glass (Davison, 2008). Type IIIA glasses can form but requires a higher concentration of alumina and phosphorus pentoxide found in many archaeological glasses (Zacharias et al. 2020). This surface has been observed in some medieval glasses.

Hench and Clark (1978) discuss the composition of the surface types produced by deteriorated glass but do not provide many details as to their visual aspects. Images of Type II-IV surfaces on test glasses found in a publication by Clark and Hench (1981, 96, fig2) may provide some clues (Figure 8.1). A sample of a Type II surface shows what appear to be fractures or fine cracks (Figure 8.1A) (Clark and Hench 1981, 96, fig. 2A). It is possible that this is the result of the weakening and contraction that occurs due to the decrease in volume of the surface layers after dealkalization (Davison 2008). Although Clark and Hench (1981) have documented microscopic surface fractures, the surfaces overall appear to have little deterioration and can remain "quite glossy and unmarked" (Davison 2008, 196). The Type III surface was rough with linear features or scratches, though it is not clear which film this image is depicting (Clark and Hench 1981, 96, fig. 2B). The final surface depicted in the publication is Type IV, which appears uneven or rough with somewhat rounded depressions or pits (Figure 8.1B) (Clark and Hench 1981, 96, fig. 2C). A profile drawing of the Type IV surface shows that the depth of the losses can vary (Figure 8.1C) (Clark and Hench 1981, 96, fig. 2C). Type V surfaces were described by Davison (2008, 196) as developing marks due to the action of solution. Pitting can occur in areas of where alkaline solutions have created localized corrosion.

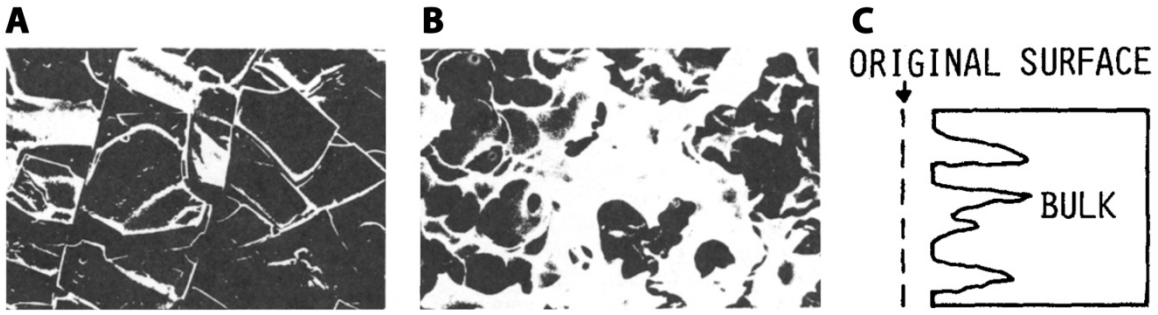

Figure 8.1. Examples of two types of surfaces found on archaeological glasses, (A) Type II and (B) Type IV. Type IV glasses can exhibit pitting of varying depths (C) (from Clark and Hench 1981, 96, fig. 2A, 2C).

8.3 Degradation Pathologies Due to the Burial Environment

As mentioned above, one of the main causes of the degradation of archaeological glasses is water in the burial environment. The pH of the groundwater is also important since alkaline solutions can promote network dissolution. Low pH can also be problematic since acidic environments have been found to cause more severe corrosion and ion diffusion (Jackson, et al. 2012). The alkalis and alkali earth ions, in particular lime when present at higher concentrations, are leached out at a faster rate at a lower pH (Clark and Hench, 1981; Jackson, et al. 2012).

8.3.1 Physical changes to glasses

The degradation pathologies of dealkalization and network dissolution create various physical changes to the surface of archaeological glasses. These physical changes to the surface are often referred to as weathering (Van Giffen 2014). Dulling of the surface is one of the first things that can be observed where the glass loses translucency and clarity (Davison 2008). In leached surfaces, a layered structure can form. The composition of the lamina can vary in their concentrations of silica and less soluble compounds. In addition to varying compositions, these layers can also appear with different morphologies such as zigzags, parallel or hemispherical structures (Cox and Ford 1993; Doménech-Carbó et al. 2006). Many of the beads examined

from all three sites have flaky or a laminar surface corrosion. In some cases, the layered surfaces were superficial and easily seen through examination under the microscope. For other beads, the laminar corrosion was more extensive and the depth of this type of deterioration could be seen using SEM imaging (Figure 8.2A)

One result of this layered deterioration is the formation of iridescence, where the surface color of the glass changes based on the angle of the light source or the angle at which its viewed (Figure 8.2B) (Corning Museum of Glass 2002). The light hitting the layers undergoes interference effects when reflected and produces the iridescence (Corning Museum of Glass 2002; Davison 2008). Iridescence, or any other laminar deterioration, can continue to develop into a thick layer that eventually flakes away. If thick enough, it can flake away completely and weaken the structure of the glass (Davison 2008).

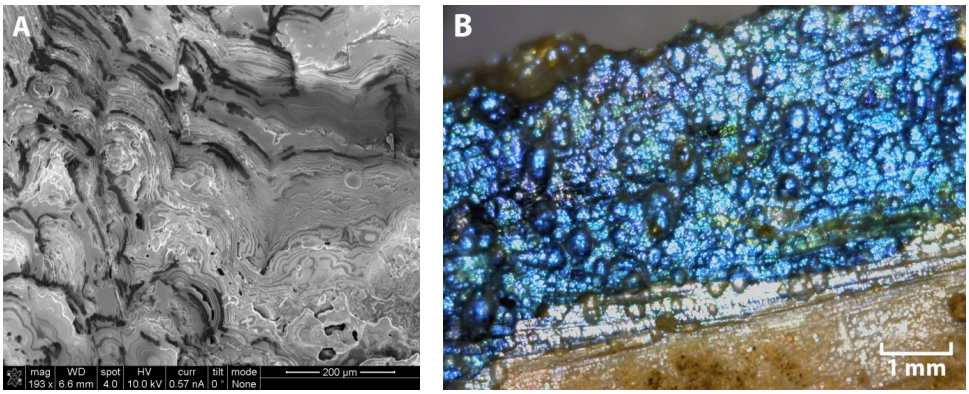

Figure 8.2. A) SEM image of bead MEΘ 890-2 from ancient Methone showing laminar corrosion layers. B) Photomicrograph of the back of a Mycenaean relief bead from Metaxata (1616-9) with iridescence.

In addition to iridescent layers, archaeological glass can also develop a layered opaque white surface. It begins as small white spots or patches and is referred to as "milky weathering" (Davison 2008, 184). The corrosion can extend into the structure of the glass and expand over the entire surface. The opaque layer can be a few microns to millimeters thick. Because of the laminar nature of the corrosion, it can flake off. As the degradation continues, it moves into the core and glass is lost, very little of the glass can remain. The overall structure of the glass becomes very weak. Most of the beads found at ancient Methone were covered with a layer of opaque white corrosion (Figures 5.3, 5.9A, Appendix B). Due to the thickness of the layer and the extent, it was likely the type of weathering known as "enamel-like weathering" (Davison 2008, 185). Some of the beads had turned completely opaque white (Figure 5.11) and were very flaky (Figure 5.13). Beads from Kefalonia (Figures 6.4D, 6.14, 8.1B, Appendix C) and Lofkënd (Figures 7.3A, 7.11A-B, Appendix D) also exhibited these thick, opaque white corrosion layers.

Pitting on the surface of archaeological glasses is a commonly observed visual sign of deterioration. As mentioned above, it has been observed in Type V surfaces and possibly Type IV surfaces. Many of the beads from all three sites show signs of pitting often with iridescence (Figures 8.2B, 8.3A-C). Pitted glass surfaces were also found below layers of "enamel-like weathering" (Figure 8.3A).

Archaeological glass beads can develop dark or black staining on the surface. Many of the beads from all three sites exhibited this discoloration. Some formed as patches or spots (Figures 5.11,7.11A), but others were linear (Figure 5.3). Staining can be caused by ions in the burial environment, primarily manganese and iron, entering the glass matrix via ion diffusion. However others have suggested that the discoloration is caused by the solubilization of these components within the glass, that then get precipitated onto the surface (Knight 1996; Watkinson et al. 2005; Davison 2008). Jackson et al. (2012) have described this staining as the result of the diffusion of components within the glass. Manganese and iron are soluble only at a low pH. They are insoluble at pH 8 or 9, which is generally the pH at the surface of a glass undergoing

dealkalization. If the burial environment is acidic, however, it is possible that manganese and iron can enter the glass.

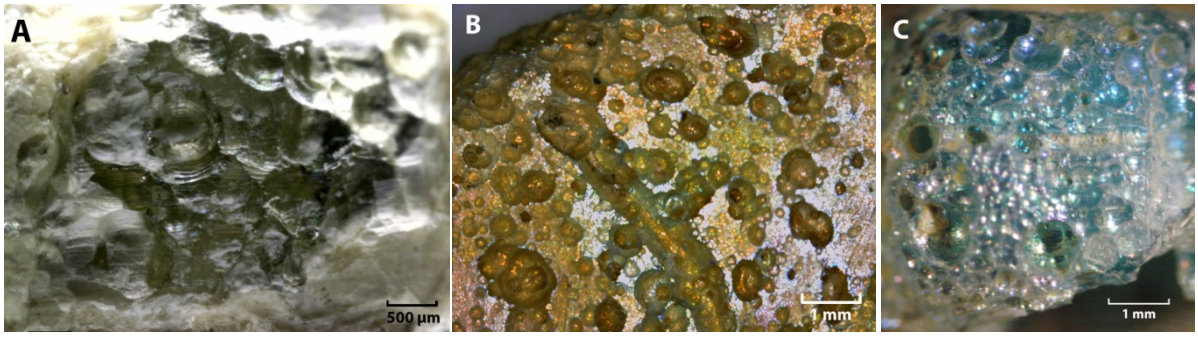

Figure 8.3. Photomicrographs showing pitting on the surface of glass beads from (A) ancient Methone (MEΘ 4164-1) (B) Metaxata (K13-2) and (C) Lofkënd (10/112)

Several of the yellow-green and green colored glasses from ancient Methone had elevated levels of iron oxide on the surface, especially beads MEΘ 889-4, MEΘ 890-3, and MEΘ 890-4 with iron oxide concentrations above 5 wt% (Table 5.4). Bead MEΘ 890-4 also had slightly elevated manganese oxide levels, as did MEΘ 889-6. It is possible that these oxides were present in the glass and became enriched or were precipitated from the glass itself. However, low pH within the burial environment that could have solubilized these elements cannot be ruled out. No information is available for what the soil pH was in the tombs at ancient Methone where the glass beads were found. Soil pH tests were conducted on samples from other areas of the West Hill, some near the area of the Late Bronze Age cemetery, showing the soil had a pH in the mid-range (6-8) (Muros and Pantages 2015; Ancient Methone Archaeological Project 2018). It is possible however, for soil pH to be localized and for acidic microenvironments to be created, even though the overall pH of the soil is more alkaline. This is especially true in burial contexts where the decomposition of the body and the metabolic byproducts of microorganisms can produce localized acidic conditions (Muros and Scott 2018). Dark brown and black staining due to manganese or iron present in the glass will be further discussed in section 8.5.

8.3.2 Composition of leached surfaces

The majority of studies on the chemical effects of glass deterioration have been conducted primarily on medieval glasses, rich in potash, and Roman natron glasses that are soda rich (Cox et al. 1979; Perez y Jorba et al. 1980; Roemich et al. 2002; Gueli et al. 2020). Not as many analyses have been performed on archaeological soda-rich plant ash glasses, nor have many deterioration experiments been conducted using lab-made model glasses of these compositions. However research into the surfaces and compositions of these earlier glasses exhibiting different degradation pathologies is increasing (Kirk 2011; Zacharias et al. 2020).

As described in the previous section, the process of dealkalization results in the loss of alkali and alkali earth metals in the glass. For Late Bronze Age and Early Iron Age glasses, this means the soda and potash that make up the alkali are leached, as well as magnesia and calcium (Perez y Jorba et al. 1980; Cox and Ford 1993; Doménech-Carbó et al. 2006). The leached areas become enriched in silica and other elements that are not as soluble, for example alumina, manganese and iron oxides. Enrichment of other insoluble components such lead, tin, and antimony can occur (Freestone 2001; Doménech-Carbó et al. 2006; Palamara et al. 2016). Enrichment of lead and antimony were detected in the Lofkënd opaque white glasses (Muros and Zacharias, 2019, table 3).

SEM-EDS analysis of the surfaces of 12 glass beads from Methone (Table 5.4) showed that these beads have very little soda remaining. The beads were also low in potash and magnesia. These 12 beads all had elevated concentrations of silica on the surface, 75.9 wt% or higher, showing it was silica rich. Two samples

from the site of Mazarakata on Kefalonia, 40-1 and 40-6, are almost completely depleted of soda, potash, and magnesia (Table 6.3). The lime concentrations are also very low. The silica concentrations above are 80 wt%.

The corrosion layers on sample 40-1 were analyzed to determine the makeup of this degraded area that had undergone dealkalization and to see if the layers varied in concentrations of silica or other insoluble glass components. The six areas analyzed had concentrations of silica above 92 wt% with depletion of most of the other oxides present in the glass (Table 8.1). Alumina (2.19-2.49 wt%) was detected in concentrations that are typical for undeteriorated LBA glasses (Nicholson 2007; Henderson 2012; Shortland 2012). The levels of the oxides detected were somewhat consistent across the layers, with only slight variations. In the case of the iron concentrations across the sample, they seemed to have the most variation with one area higher in that particular oxide.

Table 8.1. VP-SEM-EDS analysis of the laminar structure of glass bead 40-1 from Mazarakata showing depletion of all oxides within the glass except for alumina and silica, which is enriched. The concentrations are given as weight percent oxide (wt%) and normalized to 100%.

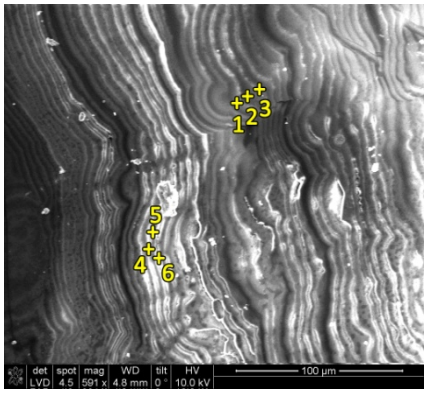

Area	Na_2O	MgO	Al_2O_3	SiO_2	SO_3	Cl	K_2O	CaO	TiO_2	MnO	FeO	CuO
1	0.43	0.09	2.49	93.51	n.d.	0.28	0.13	1.58	n.d.	n.d.	1.05	0.44
2	0.33	0.18	2.46	93.50	0.53	0.35	n.d.	1.57	n.d.	n.d.	0.60	0.48
3	0.42	0.28	2.77	92.77	0.67	0.25	n.d.	1.52	n.d.	n.d.	0.80	0.52
4	0.34	0.14	2.19	93.94	0.13	0.28	0.06	1.39	0.15	0.14	0.72	0.52
5	0.24	0.23	2.48	94.01	0.06	0.33	0.06	1.41	0.10	n.d.	0.68	0.40
6	0.16	0.19	2.31	94.63	n.d.	0.17	0.09	1.49	n.d.	n.d.	0.57	0.39

An EDS line scan was performed across the sample to visualize the changes across this section of glass (Figure 8.4). The scan shows that the layers are predominately composed of silicon (black line) and oxygen (red line), with concentrations varying across the layers. The lines for both elements rise and fall in the same pattern. All the other elements in the sample are present in very low concentrations at approximately the same levels. Alumina (yellow line) is slightly higher across the section of glass, something also seen in the EDS data (Table 8.1). There is one area where the composition changes, at about the 250 µm mark of the line scan. There is a drop in silicon and oxygen and an increase in calcium, sulfur, sodium, and magnesium. Potassium and chlorine are slightly higher here than in the rest of the sample. This is a layer in the sample that did not undergo as much leaching.

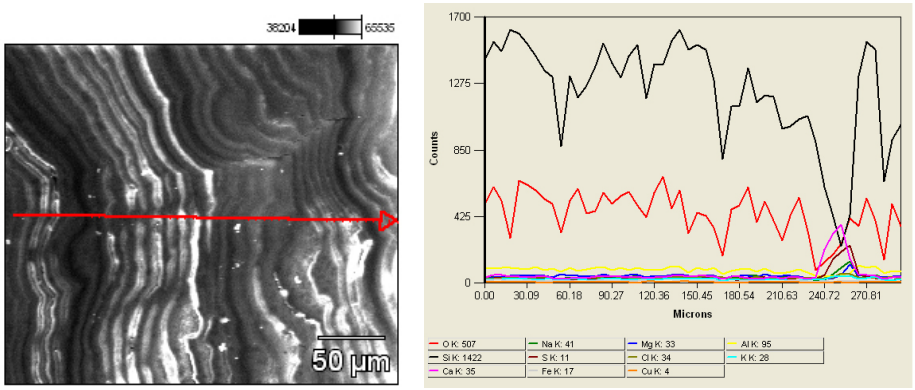

Figure 8.4. EDS line scan across a section of the sample taken from Mazarakata bead 40-1.

8.4 Degradation Pathologies Due to Microorganisms

Microorganisms can also play a role in the deterioration of glass, causing either physical or chemical damage. Most of the analytical studies conducted to understand glass biocorrosion have looked at historic glass, with many studies looking at window glass from the medieval periods or later (Perez y Jorba et al. 1980; Krumbein et al. 1991; Cox and Ford 1993; Piñar et al. 2013). However, more research is being undertaken on the effects of microorganisms on the deterioration of older archaeological glass (Krumbein et al., 1991; Palamara et al., 2016; Zacharias et al., 2020).

Biocorrosion can result in the darkening of glass or physical damage represented by pits, rings or groups of concentric circles, and linear features (Krumbein et al., 1991; Palamara et al., 2016; Perez y Jorba et al., 1980; Piñar et al., 2013; Zacharias and Palamara, 2016). These features are observed in glasses exposed to atmospheric conditions, such as window glass, and glasses found within in a burial environment. Microorganisms found on glasses, which include fungi and bacteria, can create a microenvironment conducive to glass deterioration through the formation of a biofilm (Koestler et al. 1987; Krumbein et al. 1991). It is within this biofilm that the composition of the surfaces can be altered both chemically and physically. The biofilm acts as a protective layer for the microorganisms and maintains the conditions necessary for their continued damage of the glass.

The changes to the composition of glass undergoing biocorrosion are caused primarily by the metabolic byproducts of the microorganisms present. These byproducts are sometimes acidic which can alter the pH of the glass surface in localized areas (Krumbein et al. 1991; Piñar et al. 2013). This metabolic activity can leach out particular elements or chelate particular ions. Some bacteria can cause the transport of certain ions and have them redeposited. Microorganisms can also affect the moisture content on the surface of the glass. They attract water from the environment, and some even expel water as a metabolic byproduct. This can begin the process of dealkalization or increase the rate of leaching.

Biocorrosion creates a glass composition similar to that seen in glass undergoing other decay mechanisms, such as dealkalization. Moreover, both types of deterioration can occur on the same surfaces. Microprobe analysis conducted on the surface of medieval glasses that was affected by the activity of microorganisms detected surfaces depleted in alkali, especially those made with a potash alkali (Perez y Jorba et al. 1980). Magnesia and lime were reduced and there was also migration of some lime and phosphorus pentoxide. Sulfur was found in cracks within the glass. Perez y Jorba et al. (1980) found that the composition resulting from biocorrosion was similar in many respects to the composition of stained glass corroded due to atmospheric conditions. This could mean that identifying biocorrosion just on the basis of composition alone may be difficult and that the physical signs of the activity of microorganisms need to be identified as well. Molecular analysis of the deteriorated surfaces could also be used as a tool to determine the presence of microorganisms on glass, as well as to identify which organisms are present (Piñar et al. 2013).

Since the activity of microorganisms can cause pitting and leaching of alkali and alkali earth metals from the glass, it is difficult to be certain whether the physical and chemical changes observed in the beads from ancient Methone, Kefalonia, and Lofkënd are due to microorganisms. However, several beads did have degradation patterns that were likely due to biocorrosion. For example, some beads from ancient Methone and Kefalonia, had rings or groups of concentric circles on the surface (Figure 8.5A-B). SEM imaging undertaken on samples taken from the beads showed the concentric circles could also be found inside the glass (Figure 8.5C).

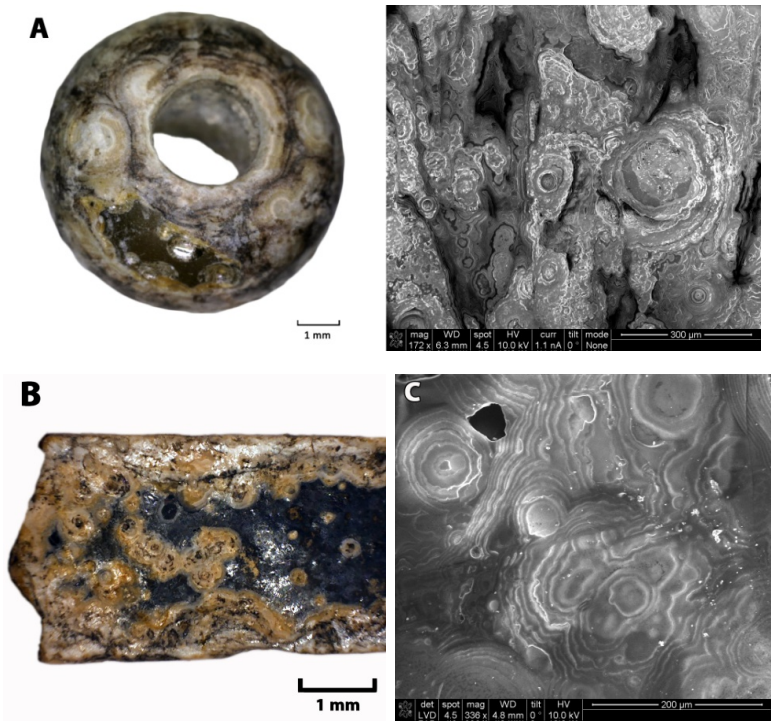

Figure 8.5. Examples of biocorrosion in the form of rings or concentric circles. A) Bead ΜΕΘ 889-3 from ancient Methone (left: photomicrograph, right: SEM image) B) Photomicrograph of the back of relief bead 1615-11 from Metaxata C) VP-SEM image of a sample from bead 40-1 from Mazarakata.

The manganese and iron stains described in the previous section could also form due to the activity of microorganisms. It is caused by the metabolic activity of specific bacteria, such as ferrobacteria, that metabolize these elements in the glass (Perez y Jorba et al. 1980; Krumbein et al. 1991; Davison 2008). They are also responsible for solubilizing and diffusing them within the glass as well. The darkening of the solubilized manganese and iron is due to the oxidation of these ions that then precipitate as insoluble oxides (Cox and Ford 1993). Because the oxidation can easily occur through an increase in oxygen within the burial environment or due to the metabolic activity of the microorganisms themselves, the staining tends to be somewhat localized (Cox and Ford 1993; Watkinson et al. 2005). This may explain why dark stains are located within ringed deterioration on the surfaces of beads that underwent biocorrosion (Figure 8.5).

An area on the interior of bead 40-1 from Mazarakata, which exhibited areas of circular or ringed deterioration, was analyzed using VP-SEM-EDS to determine whether there was an increase in the concentrations of manganese or iron in the glass. This could signify that biocorrosion had taken place due to ferrobacteria or other organisms that metabolize these elements. The area of degradation was located about 300 µm below the surface (Figure 8.6). Analysis of three spots in a ringed section (center, ring, and outer ring) showed depletion of soda, potash, magnesia, and lime (Table 8.2). The areas are silica-rich, and alumina is elevated. The concentrations of manganese are low, and there does not seem to be manganese deposited in these areas. The iron content in the two areas analyzed is slightly higher than in other areas of

the glass (Table 6.3). It is not clear if this is the results of biocorrosion or simply that the more soluble components of the glass have been leached out leaving the area enriched in iron.

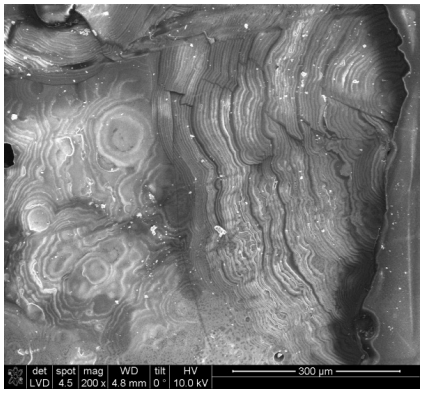

Figure 8.6. VP-SEM image of a section through bead 40-1 from Mazarakata.

The presence of sulfur in the darkened areas may indicate the metabolic activity of sulfobacteria (Perez y Jorba et al. 1980; Davison 2008). Because sulfur can be present in glasses due to the raw materials used, it could be difficult to determine whether any sulfur detected is due to microorganisms, unless it can be found within areas where biocorrosion can be clearly identified. Sulfur was detected in one of the areas analyzed on bead 40-1 within the ringed corrosion (0.29 wt%) (Table 8.2). However, sulfur was also detected in some of the laminar corrosion observed closer to the surface (0.06-0.67 wt%) (Table 8.1). It is possible that the sulfur detected is not necessarily due to the presence of bacteria. The surfaces analyzed on the ancient Methone beads also contain sulfur, as SO_3, ranging from 0.03-0.35 wt% (Table 6.3). Sulfur has been found within the raw materials used for glass, such as in the plant ash and can be present in concentrations up to 0.3% (Zacharias et al. 2020). Since the concentrations of sulfur in these beads falls within the range found in high soda plant ash alkalis, it is difficult to ascertain whether its presence is due to the raw materials used or the metabolic activity of microorganisms.

Table 8.2. VP-SEM-EDS analysis of an area of circular or ringed deterioration inside a sample from bead 40-1 from Mazarakata. Concentrations are given as weight % (wt%) and normalized to 100%

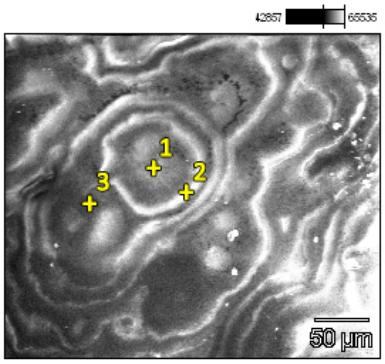

Area	Na_2O	MgO	Al_2O_3	SiO_2	P_2O_5	SO_3	Cl	K_2O	CaO	TiO_2	MnO	FeO	CuO
1	0.54	0.23	3.23	92.14	0.00	0.29	0.52	0.11	1.48	0.28	0.00	1.00	0.72
2	0.36	0.32	3.68	91.76	0.00	0.00	0.52	0.16	1.68	0.15	0.00	1.00	0.72
3	0.69	0.32	3.40	92.54	0.00	0.00	0.49	0.15	1.50	0.13	0.05	0.73	0.68

8.5 Degradation Pathologies Due to Glass Composition

In addition to the above factors, the composition of glass plays a large role in its preservation and level of deterioration. Factors such as the type of alkali used, the silica content, and the presence and concentration of alkali earth elements impact both the type and rate of degradation observed (Hench and Clark 1978; Clark and Hench 1981; Davison 2008; Jackson et al. 2012; Zacharias et al. 2020)

8.5.1 Alkali

8.5.1.1 Soda-rich and potash-rich glasses

Studies comparing the deterioration of soda-rich and potash-rich glasses exposed to different burial and atmospheric conditions have shown that the choice of alkali plays a large role in the preservation of glass and the rate of decay (Freestone, 2001; Davison 2008; Jackson et al. 2012). Analysis of archaeological samples of Roman glass (soda rich) and medieval glasses (potash rich) have shown that those with higher concentrations of potash deteriorate more quickly (Davison 2008; Jackson et al. 2012). Soda rich glasses create a more stable glass network. The sodium cation is smaller than potassium, which allows it to be more tightly bound to the silicon network and not as easily leached out (Jackson et al. 2008, 490). When the sodium cation is removed due to dealkalization, it leaves a much smaller space open within the network than if a potassium cation was removed. Therefore, not as much water can enter the network to continue the deterioration process. In potash rich glasses, the physical deterioration observed has been more severe. An increase in pitting, lamina formation, and discoloration was observed compared to natron glasses. There has been greater leaching of the alkali, as well as more damage to the glass network. The soda-rich glasses did undergo some alteration of the surface, but it was often minor with only superficial changes observed and less leaching of the alkali and alkali earth elements compared to the potash glasses.

8.5.1.2 Mixed alkali (LMHK) glasses

Mixed alkali glasses that contain both soda and potash have been found to be more durable than if the glass was made with just one alkali (Hench and Clark 1978; Rodrigues et al. 2019). The combination of alkalis creates a "mixed alkali effect" that reduces the amount of leaching (Hench and Clark 1978, 96). Studies of mixed alkali glasses have found that the combination of alkali can reduce the mobility of the alkali cations within the glass structure when exposed to water resulting in slower dealkalization (Rodrigues et al. 2019). Hench and Clark (1978) found that in experimental mixed alkali glasses with about 12% soda and 3% potash, there was less diffusion of ions. If, however the potash concentration was increased to at least 12-15% and the soda reduced to about 3%, the rate of corrosion would increase (Hench and Clark 1978; Davison 2008).

Although the mixed alkali effect does decrease the rate of degradation, these glasses can still undergo some level of leaching and alterations to the surface. Iridescence, discoloration, and the formation of laminae are observed on some mixed-alkali glasses. The changes to the surface have been considered minor or just occurring in very thin surface layers (Rodrigues et al. 2019). SEM imaging of 2nd-14th c. AD mixed alkali and natron archaeological glasses from Vincenza, Italy, demonstrated that both sets of glasses were iridescent and had developed laminar deterioration. However, the mixed-alkali sample had thicker corrosion (500 µm) than the natron glasses (>200 µm) (Silvestri et al. 2005, 1345). The experimental glasses created by Rodrigues et al. (2019) and the mixed-alkali archaeological glass analyzed by Silvestri et al. (2005) did contain more potash and less soda than the mixed alkali glasses tested by Hench and Clark (1978). This is likely the reason why more corrosion was seen in these glasses as opposed to what Hench and Clark (1978) report in their experimental samples.

Mixed alkali glasses from older archaeological contexts also show reduced corrosion due to the mixed alkali effect. At the site of Frattesina, glasses with an alkali composition of 7.83-12.8 wt% potash and 4.72-7.60 wt% soda were found to be in good condition (Brill 1992, 14, table 2). Despite the higher potash and lower soda value, these glasses still benefited from the mixed alkali effect and were better preserved. The

Frattesina beads were low in lime and should have undergone more corrosion because of the lack of the network stabilizer (Brill 1992, 17). It was the concentrations of the two akalis that made the glass more durable.

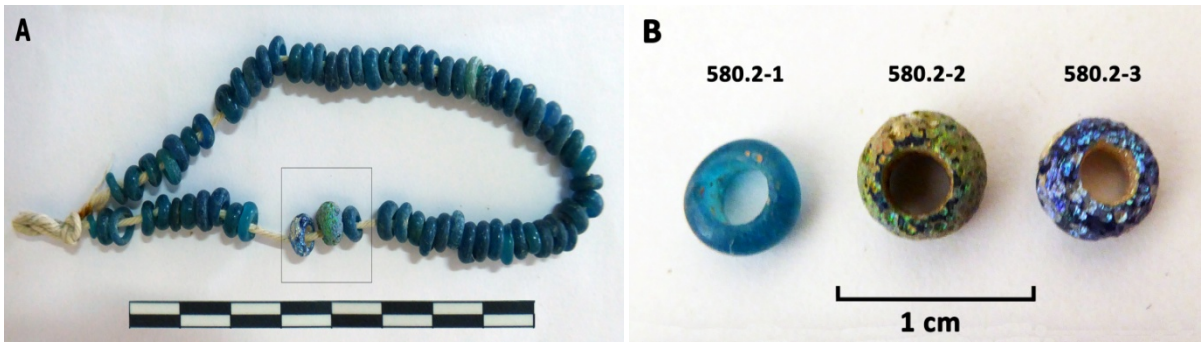

Figure 8.7. (A) Group of beads from Mazarakata found in Tholos B (580.2). (B) Detail of the three beads (indicated with a box in the left image) analyzed from this group.

At the site of Mazarakata, the mixed alkali bead from Tholos B (580.2-1) was much better preserved than two of the plant ash glasses from the same tomb (580.2-2-3). There is severe pitting and iridescence on the surface of the plant ash glasses (Figure 8.7). They are also slightly more opaque. The mixed-alkali bead on the other hand had no iridescence and only very small pits and abrasions on the surface. The bead was still very translucent. Bead 580.2-1 has a similar composition to the Frattesina beads (Table 6.3) and like those glasses, the level of preservation observed must be due to the mixed alkali effect.

8.5.1.3 Late Bronze Age plant ash glasses

Late Bronze Age glasses are made with an alkali that is high in potash, which can be up to 4%, but is also soda rich, containing on average 15-21% (Shortland 2012; Henderson 2013). The concentrations of some of these glasses are close to the "mixed alkali" concentration tested by Hench and Clark (1978) of 12% soda and 3% potash. Late Bronze Age glasses, however, do not seem to benefit from the mixed-alkali effect. These glasses do not preserve as well as natron glasses, which have even lower concentrations of potash (Freestone 2001). One of the reasons for the fewer number of Late Bronze Age glasses found could be in part because the composition still makes the glass quite unstable in most burial environments where moisture is present. Studies of glasses found at the site of Nuzi compared the condition of 2nd millennium glasses, which were plant ash based, to later glasses made using natron (Kirk 2011). The natron glasses were in considerably better condition. It appears that Late Bronze Age plant ash glasses, which contain both soda and potash, do not seem to behave the same in the burial environment as the mixed alkali glasses tested by Hench and Clark (1978). It appears that if only taking the soda and potash contents into account, the "mixed alkali" effect seems to work better with glasses of higher potash and lower soda concentrations of the range seen in the Mazarakata mixed alkali bead or the published glasses from Frattesina (Brill 1992).

8.5.2 Network stabilizers

The network modifiers can also influence the level and rate of corrosion. Oxides such as lime, magnesia and alumina increase the durability of glass, and therefore slow down dealkalization and dissolution of the silica network when the glass is exposed to moisture (Clark and Hench 1981). If the composition of the glass is low in any of these stabilizers, deterioration more readily occurs. Under certain conditions, these alkali earth metals can be solubilized within the glass matrix and precipitating out onto the surface of the glass in turn protecting it (Clark and Hench, 1981; Jackson et al. 2012). In experiments conducted on test glasses containing alumina above 5 mol% and phosphorus pentoxide above 6 mol% a Type IIIA protective surface forms (Jackson et al. 2012).

The lime within the glass is susceptible to leaching not just due to the action of water but also the pH of the environment. In acidic environments lime is more likely to be removed from the glass, but this dissolution is dependent on the concentration of lime in the glass (El-Shamy et al. 1975; Jackson et al. 2012). Glasses containing up to 6-10 mol% of lime appear to be stable (El-Shamy et al. 1975). If the lime content is higher, more than 15 mol%, then the lime is more readily leached, especially if the pH is very low. Magnesia is also lost at a faster rate in low pH increasing the potential for corrosion. The loss of the stabilizer, which also occurs along with the diffusion of the alkali, leaves a silica rich layer with an open glass network allowing for more water to enter the glass. One of the reasons for the formation of more severe corrosion on medieval glasses could be the lime content of the glass. Medieval potash glasses tend to be higher in lime (some up to 18 mol%) than Roman natron glasses (averaging around 8 mol%) (Jackson et al. 2012). The combination of the higher lime and potash accelerate the rate of dealkalization and network dissolution.

The low concentration of network stabilizers in bead 10/117 from Lofkënd may explain its poor preservation. When discovered, the bead was in six fragments with soil and other burial deposits well adhered to the surface (Figure 8.8A). The glass had turned opaque white with only two areas containing small fragments of intact glass (Figure 8.8B). The glass structure had completely degraded. The material that remained was very flaky and extremely friable when handled. The bead required conservation treatment prior to cleaning. Despite the additional strength consolidation with a resin imparted to the deteriorated fragments, they were still too fragile to completely clean (Figure 8.7A).

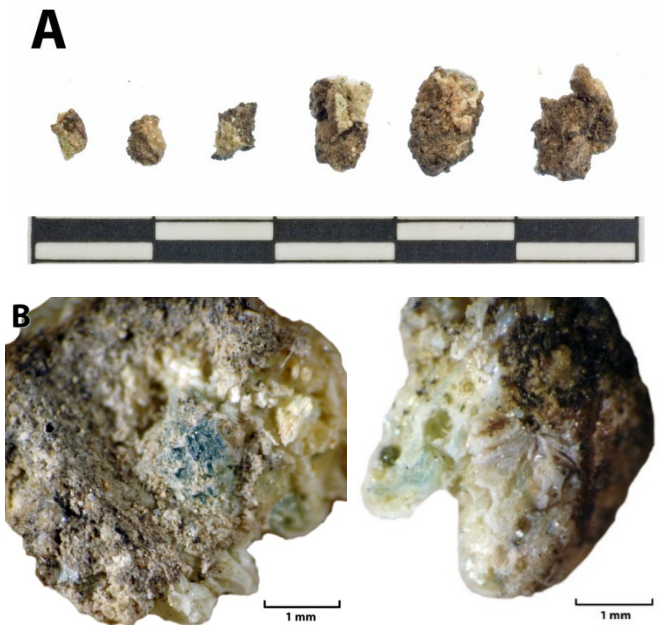

Figure 8.8 (A) Fragments of Lofkënd bead 10/117 after conservation treatment (B) Photomicrographs of two of the bead fragments showing small areas of intact glass along with the heavy corrosion and staining/burial deposits.

Analysis of an area of intact glass has low concentrations of both lime (3.60 wt%/3.95 mol%) and magnesia (1.95 wt%/2.98 mol%) for LBA plant ash glasses (Table 7.3, 8.3). Alumina (1.2 wt%/0.77 mol%) and phosphorus pentoxide (0.20 wt%/0.04 mol%) are quite low as well so a Type IIIA protective surface could not form. The low levels of alkali earth elements that could act as network stabilizers, coupled with the burial conditions, likely led to the poor preservation and the thick corrosion and structural damage observed.

The lime contents of the rest of the Lofkënd beads are also at the lower end of the concentration needed for the glass to be stable, with some even below the levels established. Three of the beads are only slightly above the 6 mol% threshold (10/109, 10/106, 10/116), but their lime content does not seem to be the main factor in their preservation. 10/106 and 10/116 are very corroded despite their lime content and the amount of magnesia present (5.71 mo% and 7.00 mol%) (Table 8.3). Bead 10/115 and 10/112 had lower

lime and magnesia concentrations but were in much better condition. The level of preservation seen across the beads from Lofkënd, as well as the level of degradation, must be due to multiple factors and does not seem to be based on any one alkali or alkali earth ion present in the glass.

Table 8.3. Composition of the Lofkënd glass beads analyzed using EPMA given as molar %.

Bead No.	Color	Na_2O	K_2O	MgO	Al_2O_3	CaO	SiO_2	FeO	MnO	P_2O_5	TiO_2
10/106	dark green	17.93	0.83	5.71	0.83	6.46	64.74	3.29	0.01	0.06	0.14
10/108	dark green	19.29	0.83	6.01	1.13	2.99	62.45	6.99	0.05	0.03	0.23
10/109	dark green	16.38	0.81	7.16	0.82	6.14	62.93	5.56	0.02	0.03	0.15
10/112	blue-green	18.59	0.82	5.00	0.91	5.27	68.60	0.34	0.22	0.06	0.19
10/115	dark green	15.91	0.90	5.55	0.64	5.55	65.46	5.87	0.01	0.02	0.10
10/116	dark green	18.46	0.74	7.00	0.94	6.51	64.03	2.10	0.01	0.05	0.17
10/117	blue	18.73	0.92	2.98	0.77	3.95	72.26	0.22	0.03	0.04	0.09

Other oxides in the glass can act as stabilizers and make the glass more durable. Iron age dark green glasses from Pella contained low concentrations of lime (avg. 2.3 wt%, with some glasses containing less than 1 wt%) (Reade et al. 2006). Such a low level of this stabilizer should have resulted in severe corrosion of the glass or complete loss of the beads, but the glasses were well preserved. It is suggested that the high iron content due to the colorant (avg. 9.7 wt%) acted as the network stabilizer. The same is suggested for a group of well preserved Iron Age black beads from Italy (Conte et al. 2018). These beads contained low lime (avg. 2.29 wt%), and high iron (avg. 11.6 wt%), as well. The preservation of the bead is attributed to the iron content of the glass. The dark green glasses from Lofkënd are high in iron but have a lower average concentration (5.65 wt%) than the Pella or Italian Iron Age beads. Because of the poor preservation of several of the Lofkënd beads, perhaps this concentration of iron is not high enough (avg. 5.4 wt%) to act as a stabilizer to compensate for the low lime concentration.

Taking a closer look at iron concentration and condition of the Lofkënd dark green beads, there does not seem to be a connection between high iron content and level of corrosion observed on the beads. For example, bead 10/115 was the best preserved of the Late Bronze Age beads analyzed with EPMA. This bead contained 6.96 wt% iron oxide (Table 7.3). 10/109 has a similar iron concentration, at 6.63 wt%. Both glasses also had similar lime contents, with 10/115 having 5.15 wt% and 10/109 with 5.72 wt%. However, their levels of preservation are very different (Figure 7.5 A, C). 10/115 has little surface corrosion and is still translucent. 10/109 has completely corroded and is an opaque reddish brown color. Both are from different graves (Table 7.2) so therefore the burial conditions, moisture, pH, or perhaps even the activity of microorganisms, is responsible for the level of degradation observed.

8.5.3 Silica content

The silica content of the glass is also important to the overall preservation of the material. Studies have found that if the silica content is low, there is more overall deterioration of the glass network (Jackson et al. 2012). Early studies conducted on various compositions of test glasses showed greater corrosion and less durability of the glass when the silica concentration was below 66.7 mol% (El-Shamy et al. 1975). Later studies though indicate that the silica content may need to be lower (62 mol%) for this instability to occur (Jackson et al. 2012). When the concentration of silica is low, each silicon atom is associated with an alkali or alkali earth atom, such as sodium, potassium, or calcium. This allows for there to be sites for the movement of ions between the solution and the glass (El-Shamy et al. 1975). When the silica concentrations are higher, the ions are not as mobile because the silicon and oxygen groups are isolated (Jackson et al 2012).

Taking a look again at the group of beads from Lofkënd, most of which shows signs of extensive corrosion, there appear to be differences in the silica content based on color. The copper blue beads have the highest silica content (Table 8.3). Both beads though have different levels of deterioration. 10/112 was pitted and

iridescent but still retained its translucency and a large amount of preserved intact glass (Figure 7.3B). 10/117, as described above, was severely corroded. The silica content alone was not enough to reduce the rate of ion diffusion and network dissolution observed, but likely was the result of the lower stabilizers in the glass.

All the dark green glasses were lower in silica, containing between 62.45-65.46 mol% (Table 8.3). These values are below the threshold observed by El-Shamy et al. (1975) for a more durable glass but still higher than the lower threshold of 62 mol% (Jackson et al. 2012). Not all the dark green glasses, however, exhibit the same levels of preservation. As was observed with the lime content in these glasses, other aspects of the composition or the burial environment influence the rate of corrosion.

8.5.4 Alteration of the iron colorant

One of the interesting aspects of the corrosion observed on the Lofkënd beads is the alteration of the glasses from dark green to a range of opaque yellow and opaque reddish brown glass. The colorant of those beads was based on iron and it is thought that alteration of the iron colorant was likely the cause of the colors observed. The mechanisms that result in the movement of iron ions in glasses and the formation of the dark brown/black coloration was looked into to see if it might explain this particular degradation pathology.

As mentioned previously, dark brown/black discoloration can occur due to the metabolic activity of microorganisms that results in mobilization of manganese and iron in the glass and precipitation on the surface. Burial conditions can also mobilize these ions and produce the dark stains. Most of the investigations into these stains have focused on manganese, but there are similarities in the way both iron and manganese dark brown/black staining form and the conditions under which they occur.

Manganese and iron are present in the glass due to the raw materials such as the silica source, but can also be present due to the choice of colorant. Looking specifically at the effect of the burial environment on these components, when leaching begins due to the presence of water, the Mn^{2+} and Fe^{2+} ions are freed from the glass network (Cox and Ford 1993; Knight 1996). When oxygen levels increase, they oxidize and precipitate onto the surface forming a dark brown or black crust. They can also precipitate within the silica rich layer. The oxidized manganese and iron are insoluble and do not travel as easy through cracks and fissures in the glass (Watkinson et al. 2005). This means the staining can often be quite localized.

In its reduced state, iron (II) (Fe^{2+}) is a blue-green in color (Knight 1996; Watkinson et al. 2005). When hydrated and oxidized it becomes iron oxyhydroxide (FeOOH) varying in color from yellow to amber to brown. Several burial conditions can create conditions that can promote this reaction or increase the rate of formation. Anaerobic burial conditions can help to make the iron ions more mobile (Cox and Ford 1993). Alkaline conditions can allow oxidation to occur rapidly (Watkinson et al. 2005). In addition to insoluble oxides, iron can also form insoluble iron sulfides under mild reducing conditions if bacteria are present. Iron sulfides are also dark in color and range from brown to black.

Formation of a brown, reddish brown, or “orangey-amber” colored weathering crust has been observed in glasses from different times periods that originally looked “black” (Brill 2008). Brill (2008) analyzed numerous beads and glasses that were originally very dark green or an olive-amber that exhibited this coloration of corrosion. The glasses were from different periods, and included ancient, medieval, and 18-19th c. objects. The colorants in these glasses were iron based, either due to ferric or ferrous ions or in some cases an iron-sulfur chromophore. The change in color of the glass occurred during dealkalization, which created a silica rich layer that still contained the iron ions. The remaining iron is hydrated and then oxidized forming brown, red and orange insoluble products. Alteration of dark green or black beads to a brown or reddish brown color has been described or is visible in images in several publications (Smithson 1968, 115, no. 78d, note 81; Brill, 1999; Henderson 1988; Conte et al. 2018, table 1).

Analysis of corroded areas on the Lofkënd dark green beads shows there is an increase of iron in some of these opaque yellow and reddish brown areas (Muros and Zacharias 2019). VP-SEM-EDS analysis of a corroded area on bead 10/106 provides a look at the composition of some of the layers and possibly what has caused their formation (Table 8.4). Area 1 is intact glass and gives a general idea of the composition including the iron content. Area 2 is the layer of corrosion directly on the surface of the glass. Dealkalization has taken place and this layer shows a decrease in soda, potash, magnesia, and lime. There is a marked increase in alumina likely due to enrichment in the spot analyzed. The silica content has also increased indicating a silica rich layer has formed. A slight increase is iron is observed. This could be due to enrichment due to the loss of other glass components or could indicate mobilization and precipitation of some iron ions.

Table 8.4. VP-SEM-EDS analysis of a corroded area on Lofkënd bead 10/106. Concentrations are given as weight % (wt%) oxide and are normalized to 100%

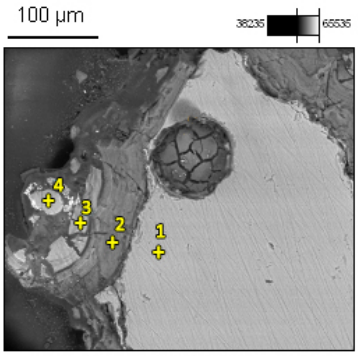

Area	Na_2O	MgO	Al_2O_3	SiO_2	P_2O_5	SO_3	Cl	K_2O	CaO	TiO_2	FeO
1	16.12	3.37	1.19	68.42	0.37	n.d.	n.d.	1.25	5.67	0.20	3.41
2	2.49	0.40	12.04	74.56	n.d.	n.d.	n.d.	0.57	4.35	0.44	5.14
3	0.11	0.36	9.19	60.23	0.57	1.48	n.d.	0.36	5.13	1.71	20.86
4	1.31	0.49	5.91	45.78	0.78	1.90	0.19	0.22	7.02	2.57	33.85

Area 3 has even less soda, magnesia and potash (Table 8.4). There is an increase in titania and phosphorus pentoxide. Lime has increased slightly. Alumina and silica have decreased in this layer. It is possible that this area may be undergoing other degradation mechanisms such as network dissolution, which may explain the decrease in silica. Some of the other oxides detected in higher concentrations could also be present due to enrichment, precipitation from inside the glass, or diffusion from the burial environment. The most noticeable change is the large increase in iron oxide. There was a 15% increase in the concentration of iron from layer two to three showing a marked mobilization of the iron out of the glass and precipitating in this area. Sulfur was also detected in area 3. It is possible that this is due to the activity of microorganisms in the burial environment. Area 4 has less alumina and silica, but has an increase in all other oxides. It is not clear why some of the alkali concentrations have increased here. The glass in the spot analyzed looks to be in slightly better condition so that may explain this change in concentrations. It is also possible that since it is near the surface it is an area where the leached alkali and alkali earth ions are being deposited. The iron is this area is much higher than in the area below, as is the sulfur.

The extensive color alteration observed with the dark green glass beads from Lofkënd may suggest that there was high mobilization of ions in the glass, both alkali and iron ions, and perhaps rapid oxidation. Although the site of Lofkënd is a terrestrial site, with aerated, alkaline soils, there may have been burial conditions that could have created a situation that increased the rate of corrosion and color change. Metallographic studies of the copper alloy objects excavated at Lofkënd, as well as corrosion studies, found the formation of a copper sulfate corrosion product, brochantite (Muros and Scott 2018). This type of

corrosion is not generally reported for archaeological bronzes, but is more commonly found on outdoor copper alloy sculpture exposed to sulfur due to atmospheric pollution. Some of the bronzes did not have any cuprite present, a copper oxide corrosion product that is the first to form in the presence of oxygen and water, which was an unusual find. The reason for these two corrosion phenomena is likely due to the activity of microorganisms in the graves and the decomposition of human remains. Because not all of the copper alloy objects within the same grave had the same type of the corrosion, these phenomena were more localized. The cause was likely due to specific microenvironments formed within the biofilm on the surface of the metal artifacts.

Similar burial conditions could explain the extensive corrosion and formation of the opaque yellow-brown and reddish-brown, iron rich layers on the beads. Anaerobic conditions created by biofilms on the glass could have increased the mobilization of iron. Decomposition of the bodies and other organic materials in the grave may have changed the pH of the area immediately surrounding the beads since they were found on or near the skull. The pH could have also been changed within the biofilms and either acidic or alkaline conditions could have been locally created. Finally, sulfur released as a metabolic byproduct from bacteria could have reacted with mobilized iron ions to produce iron-sulfur compounds that contributed to the colors observed in the weathering layers.

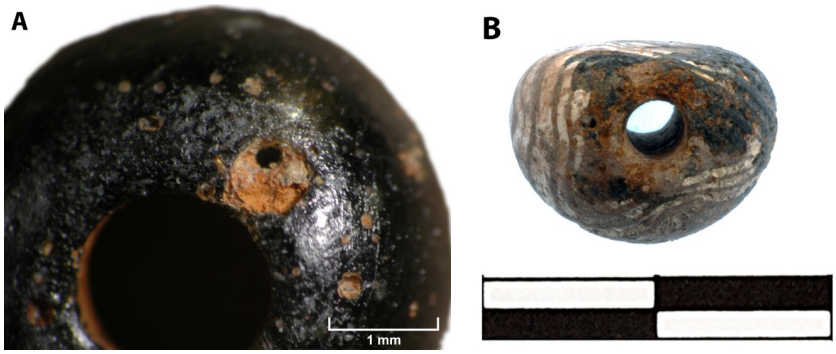

Figure 8.9. Images of bead 10/113 (A) and 10/115 (B) from Lofkënd showing areas that have discolored from dark green, almost black, glass to an orange or reddish brown degradation product.

Two of the Lofkënd beads, 10/113 and 10/115, were in good condition and still preserved their original dark green, almost black, color and translucency. However, there were areas on the surface that were pitted and contained a powdery or flaky orange or reddish brown material (Figure 8.9). The surface of the perforation on each bead also contained a thin orange or reddish brown surface layer. These are likely areas that are iron rich and are the early signs of the degradation and discoloration observed on the other beads.

8.6 Deterioration in Context: Tomb XXVIII at Lofkënd

The study of deteriorated glasses from one archaeological site can provide some insight into the mechanisms responsible for the different degradation pathologies observed. However, variations in the burial environment across the site, or across the depth of one area of the site, may not provide any correlations between these factors (Kirk 2011). At the site of Lofkënd, the glass finds from Tomb XXVIII (12-11th c. BC) may provide a more localized context within which to examine the corrosion of glass beads and compare their condition, to perhaps better understand what changes they physically and chemically underwent.

As described in the section on the burial context, six glass beads were found within the tomb. Four of the beads were originally dark green (10/106, 10/108, 10/115, 10/116) and two blue (10/112, 10/117). Although the beads were found all within the same burial context, and although five were found on the same area of the skull right next to each other, they all varied in their level of deterioration (Figure 8.10). Bead 10/115 has the least corrosion and 10/108 nearby is the next best preserved (Figure 8.11). 10/117 and

10/116, which are at either side of 10/115, are poorly preserved. They have extensive degradation and were fragmentary, especially 10/117. 10/106 was slightly separated from this group but still underwent heavy corrosion. Although bead 10/112 was found in this grave, its location was somewhat separate from the group of five beads pictured in Figure 8.11 and is not included in this discussion.

Figure 8.10. Block lifted skull and associated grave goods from Lofkënd Tomb XXVIII. Beads 10/016, 10/108, 10/115, 10/116 and 10/117 were found on the skull and were positioned next to each other. Bead 10/117 is still obscured by soil but the arrow points to its position.

Given that the beads are from the same burial context and were found right next to each other, what accounts for their varied condition? The compositions of the beads do not seem to provide a clear reason why some were more susceptible to corrosion (Tables 7.3, 8.3). In regards to the alkali, all the beads have very low concentrations of potash and high soda. The content of alkali cannot account for why some beads were more deteriorated. Looking at the network stabilizers, bead 10/115 did not have the highest concentrations of lime and magnesia despite having less corrosion. Bead 10/116 has the highest concentrations of these oxides that should mean it was more stable, but the bead underwent severe dealkalization and structural damage. Almost all the beads have a low silica content that is at or below the threshold for increased stability. 10/117 is the exception with the highest silica content. Yet this bead was one of the most corroded with not only dealkalization taking place but likely some network dissolution.

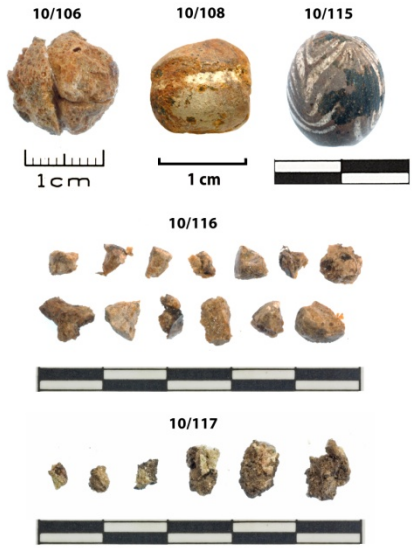

Figure 8.11. Beads found next to each other within Lofkënd Tomb XXVIII showing their various states of preservation. Image shows the beads after conservation treatment.

Moreover, the iron content of the dark green glasses does not seem to have improved preservation. Bead 10/108 has the highest iron concentration but it underwent heavy corrosion.

Examining the beads within this particular context, a single tomb, illustrates the complexity of archaeological glass deterioration in situ. No component of the composition on its own, nor several coupled together, seem to clearly point to why one bead was preserved, while the bead right next it suffered severe corrosion. Because the burial conditions within the tomb were the same, the type of degradation and its rate was likely influenced by microenvironments formed within specific areas of the. These microenvironments, which would have affected the amount of moisture, the pH, the ions nearby in the soil, and which microorganisms were present and what specific metabolic byproducts were produced. This coupled with components of the glass composition, influenced the degradation that took place within each bead and would account for the different levels of preservation observed.

8.7 Chapter Summary and Conclusions

The corrosion of archaeological glasses is a complex process influenced by many factors. These include the composition of the glass, moisture, pH, ions in the soil, and the activity of microorganisms. The deterioration of glasses is caused by two general mechanisms due to the presence of water: dealkalization and network dissolution. The glasses from ancient Methone, Kefalonia and Lofkënd were examined and analyzed to try to identify the degradation pathologies present and the determine the causes. Specific beads, or groups of beads, were highlighted to illustrate this.

All the beads showed physical signs of deterioration due to dealkalization. Glass surfaces were dull and pitted. Many had developed laminar corrosion. Some of it was superficial and resulted in iridescence. With other beads, the corrosion continued into the core and was visible when imaged using the SEM. Other beads, mainly the ones from ancient Methone, had developed “enamel like weathering” with thick layers of opaque white glass obscuring the intact glass below.

The surface analysis of the glass beads from ancient Methone showed that most underwent extensive dealkalization. Most were depleted in soda with low concentrations of potash and magnesia. The silica concentrations were elevated. There has been some discussion as to whether the laminar corrosion structure represents layers of different glass compositions. The analysis of a corroded sample from Mazarakata (40-1) showed that this is not always the case. The layers were fairly similar to each other, depleted in soda, magnesia, potash, and lime, with little variation.

The physical signs of biodeterioration were visible on several of the beads from ancient Methone, Mazarakata and Metaxata providing clear examples of concentric circles and ringed damage. These were visible on the surface of several of the beads, but as seen on a bead from Mazarakata (40-1), damage due to the activity of microorganisms also occurred farther into the glass matrix. This area with concentric circles within the glass was analyzed to look at the levels of manganese, iron, and sulfur, elements that can become enriched due to the activity of microorganisms. The concentrations, however, were very low or no higher than the levels found in the raw materials or plant ash glasses. It was visually possible to identify biocorrosion, but no chemical changes clearly linked to microorganisms were observed in the sample.

The mixed alkali bead (580.2-1) from Kokkolata-Menegata was in good condition with very little signs of deterioration on the surface. This was in contrast to two soda rich plant ash beads found with it (580.2-2 and 3) which exhibited extensive pitting, iridescence and some loss of translucency. Mixed alkali glasses tend to undergo less corrosion due to the mixed alkali effect and this explains why 580.2-1 was better preserved than the plant ash beads.

Although Late Bronze Age glasses do have a mix of two alkalis being soda rich and containing potash typically up to 4-5%, the ratio of the two alkalis does not seem to impart any protection due to the mixed alkali effect.

Soda rich plant ash glasses show greater signs of degradation than natron glasses and mixed-alkali glasses. This faster rate of corrosion may explain why many of these types of glasses are not found in the archaeological record.

Several of the Lofkënd beads had lower lime and silica concentrations than are typically found in plant ash glasses, two factors that increase the rate of corrosion and network dissolution. The low lime content of bead 10/117 (3.95 mol%) may explain the extremely degraded condition of the glass which had undergone both dealkalization and network dissolution. The low silica and lime content did not seem to produce the same results on some of the dark green beads. 10/115 for example had both low lime (5.55 mol%) and silica (65.46 mol%) concentrations, but it was one of the best preserved beads excavated from the tumulus. Studies of Iron Age black glasses colored using high concentrations of iron and having low lime have been found to undergo less corrosion due to the iron oxide present acting as a stabilizer. The same does not seem to be the case at Lofkënd where most of the dark green glasses had undergone extensive corrosion with only intact glass preserved in the core. It is possible that the iron content of the Lofkënd beads was not sufficient to stabilize the glass network.

In addition to undergoing dealkalization and in some cases possibly network dissolution, the dark green glasses underwent corrosion that which resulted in their color altering to opaque yellow brown to reddish brown. The color change is the results of several processes, likely occurring simultaneously. The alkalis in the glass were leached, as were the alkali earth elements. Enrichment of certain elements occurred, which could have included iron. Iron ions could have become mobilized due to the activity of microorganisms or a low pH. This low pH microenvironment could have occurred with the biofilms produced by microorganisms as a results of their metabolic activity or could have occurred in areas within the grave due to the decomposition of human remains. The mobilized iron ion oxidized and changed color. Sulfides may have also been released by bacteria and perhaps some ferri-sulfide compounds that are amber in color could have formed.

Finally, the glass finds from Tomb XXVIII at Lofkënd were used to look at the deterioration of beads within a single burial context. Five beads were found right next to each other in the tomb, but they varied in their level of deterioration. This tomb contained bead 10/115, which was the best preserved bead of those found. It also contained bead 10/117, which was one of the most poorly preserved. Since the beads were found next to each other on one area of the skull, it was thought that perhaps the composition of the beads influenced the rate of deterioration rather than the burial environment. After looking at various aspects of the composition, such the concentrations of the alkalis, lime, silica, and iron, the poor condition of some of the glasses could not be tied to any specific factor. It appears that even within a single grave and specific area within that grave, multiple processes acting simultaneously are responsible for whether glasses are preserved in the archaeological record.

9 CONCLUSIONS

The primary aim of this thesis was to contribute to a better understanding of the production and trade of vitreous materials in the Eastern Mediterranean during the Late Bronze Age. The work that has been presented here has added to the existing body of knowledge but has also worked to further advance the field through the three case studies chosen. Ancient Methone, Kefalonia, and Lofkënd are all located in areas where few archaeometric studies of vitreous materials have been undertaken. The results of the compositional analysis and sourcing of this collection of faience and glass beads have provided some insight into the production and consumption of vitreous materials outside of the primary areas that have been the predominant areas of focus, such as Egypt, the Near East and Mycenaean sites on the Greek mainland.

In each of the chapters, the results of the examination and analysis from each case study were discussed and some conclusions were drawn. In this chapter, the results will be discussed within the larger context of Late Bronze Age glass technology and trade, comparing the sites with each other and to the broader trends observed in the technology and production of the beads.

9.1 BEAD TYPES AND COLORS

The collection of beads studied from ancient Methone, Kefalonia, and Lofkënd differ from each other in the bead types and colors of the vitreous materials excavated from the funerary contexts. The glass and faience beads studied from Mazarakata, Metaxata, and Kokkolata-Menegata on Kefalonia represent a typical Mycenaean bead typology. The majority of the beads are blue in color regardless of the shape (Table 9.1). The shades of blue vary between lighter or more blue-green shades colored by copper and those that are dark colored by cobalt or a Co-Cu colorant. The dark blue glasses are the predominant color and this fits with what is observed in many Mycenaean bead collections (Smirniou and Rehren 2013; Worral 2020). Relief beads were found in the tombs and the motifs are typical of Mycenaean bead forms. As with the tomb types and other artifacts found in the graves, many of the beads represent the adoption of Mycenaean style burial practices and the importation of material from Mycenaean sites on the mainland.

Regional innovation was observed in tomb types and ceramic vessels on Kefalonia, and this also carries through to some of the bead types found. The triple rosette and the double bar beaded circle relief bead are unique to Kefalonia. Although these bead types have not been found at other Mycenaean sites, they do retain components of Mycenaean style relief beads. They could be interpreted as a local adaptation of an existing type rather than a completely new motif. The vitreous finds represent a strong connection to the palatial centers on the mainland. The number of relief beads found at the three sites, both mentioned in publications and from this study, show that Kefalonia was still considered to be within the boundaries of the Mycenaean world.

The vitreous finds from ancient Methone and Lofkënd represent very different assemblages. Although both sites show trade with Greece and the presence of Mycenaean objects either at the site or in the region, no typical Mycenaean bead types were found. The shapes of the beads from both sites are very common and have a wide geographical span. At ancient Methone, Mycenaean style pottery and bronzes were found within graves at the Late Bronze Age cemetery. However, no Mycenaean relief beads made its way north along with the other artifact types. The northernmost point at which relief beads were found was about 60 km south of ancient Methone (Eder 2009), and the boundary remains there for the time being. Ancient Methone is outside of the trading region for this bead type despite its proximity to Mycenaean sites to the south.

The faience beads excavated at ancient Methone were fairly typical in shape and color for this period, with both copper colored and cobalt colored faience discovered (Table 9.1). More unusual were the colors

represented by the glass beads, the majority ranging in color from yellow to green. They were also made with a mix of colorants that cannot be clearly identified and may have included an opacifier, despite the fact that the glass did not appear opaque. Since blue glasses commonly found at Mycenaean sites, and also make up a large number of glasses excavated in the Near East and Egypt (Smirniou and Rehren 2013), it is unusual that the color was not broadly represented. Less than half of the beads excavated from ancient Methone were blue, and the majority found were made of faience rather than glass.

Both light and dark blue glasses would have been extensively traded as finished objects or ingots, as illustrated by the cargo of the Uluburun shipwreck (Pulak 1998; Ingram 2005). Blue glasses were common at Mycenaean sites south of ancient Methone. Both suggest that acquiring blue glass may have been possible; therefore, other factors were at play in regards to the consumption of specific glass colors at the site. If access to a wider range of colors was not a factor, then it is possible that this color palette was preferred by the ancient Methonians. Some of the glasses excavated were very corroded. It is possible blue glasses were placed in the graves, but they have not preserved well or could not be identified due to the level of corrosion.

Table 9.1. Bead colors represented within the three geographic groups analyzed

Colors of analyzed materials	Ancient Methone	Kefalonia	Lofkënd
Cu blue faience	9	0	1
Co-Cu blue faience	2	1	0
Mn black faience	2	0	0
Cu blue glass	3	16	3
Co and Co-Cu blue glass	0	22	0
Yellow/Green glass Fe?Cu?+PbSb	13	0	0
Fe pink glass	0	1	0
Mn purple glass	0	2	0
Mn black glass	2	0	0
Fe dark green	0	0	7
Percentage of blue vitreous beads	**45.2%**	**92.9%**	**36.4%**

A similar pattern was observed at Lofkënd where the presence of less common Late Bronze Age glass colors and bead types were placed within the graves (Table 9.1). Seven out of the 10 glass beads excavated were a dark green, almost black color. Based on publications on the analysis of early glasses, black glasses do not seem to be very common. When black glass was found, such as at Amarna or Pylos, manganese was the main colorant, sometimes with copper and cobalt added to make it appear black (Nicholson 2007; Polikreti et al. 2011; Muros 2020). The Lofkënd dark green beads were colored using iron. Several of the glasses were decorated with opaque white glass, which increases their distinctiveness. Parallels for sites with mainly dark green or black, iron colored beads—some also having white decoration—were found in Europe and in Jordan, but these published examples all date to the Early Iron Age (Reade et al. 2006; Conte et al. 2018; Conte et al. 2019). The particular color palette found at Lofkënd may be influenced by its proximity to areas, such as Italy and Slovakia, where in later periods dark green or black glasses with opaque white decoration seem to occur more frequently in the archaeological record. This color of glass and decorative types may be a regional variation; however, more research is needed on collections of iron colored dark green or black glasses to better understand their distribution.

9.2 BEAD COMPOSITIONS

The majority of the glass beads analyzed are soda-rich plant ash glasses, a composition typical for the Late Bronze Age. This is the case for most of the glasses from Kefalonia. The compositions of the beads from

ancient Methone could not be fully assessed because they were not sampled for quantitative analysis. Based on the EDS surface analysis of two beads and the pXRF qualitative analysis, the assemblage appears to include plant ash glasses, though it is possible other compositions are represented.

Included in the collection of vitreous materials from Kefalonia were two additional compositional types. A mixed alkali bead and a Group B faience bead were found at Kokkolata-Menegata. Only one of each type was quantitatively analyzed and more beads like these could be present in the collection. Based on the small number of beads of this type analyzed, it is not possible to draw any conclusions specifically about the use of certain compositional types at Kokkolata-Menegata. It is possible that this type of faience and glass was also present at Mazarakata and Metaxata, though analysis of additional beads is needed. What the analysis of these two beads does show is that vitreous materials of different compositional types were imported to Kefalonia and used by the people living there.

Based on the analysis of major and minor oxides and trace elements, the mixed alkali bead (580.2-1) was produced outside of Egypt and the Near East and was similar to mixed-alkali glasses found at the site of Frattesina. These types of glasses were likely made at production sites west of Greece. This type of bead is not very common east of central Europe and the Kefalonia bead joins an assemblage from Elateia and one bead from Thasos as some of the earliest examples of this compositional type found, as well as the examples further east.

The trace element analysis of the Mycenaean Group B faience biconical bead, Σ2-K1-4, allowed for further characterization of the colorant and raw materials in an effort to determine the origin of this bead type. Very little trace element and isotopic analysis has been conducted on this type of faience, and the inclusion of that bead in this research has contributed some new data. The results indicate that the cobalt source seems to be unlike those currently known in Egypt and the Near East. The colorant is unique to the Mycenaean B faience found in Greece, with the Σ2-K1-4 sharing a cobalt source with this type of faience found on Crete and Psara. The trace element concentrations of the raw materials are close to those from glasses of a Near Eastern origin, though there were no clear overlaps with the Near Eastern comparative data. It is interesting that the published examples come from islands within the Aegean, and the presence of beads with this particular composition is found along sea trade routes in the Eastern Mediterranean. This could be coincidental and just a consequence of the lack of trace element and isotopic analysis of this type of faience or the publication of the data from these studies. As with much of the data collected from the beads analyzed for this study, the lack of sufficient comparative data from the areas where the beads were excavated, and more broadly from the regions where Late Bronze Age glasses have been excavated and produced, makes it difficult to draw definitive conclusions from the compositional data obtained.

Turning to Lofkënd, interpretation of the glass compositional types represented is more complicated. None of the seven beads analyzed quantitatively fit the typical plant ash glasses found at other Late Bronze Age sites. The glasses are all low potash glasses similar in alkali concentrations to cobalt colored glasses. The phosphorus pentoxide levels also overlap with Egyptian cobalt glasses. These characteristics could point to a different kind of plant ash used for the Lofkënd glasses, similar to what is proposed for cobalt blue glasses. The Lofkënd glasses were also low in lime, which differs from the cobalt plant ash glasses. This may point to the use of plant ash alkali that needs to be low potash and lime, or it may point to a different type of alkali entirely, such as a mineral based one. The Lofkënd beads are similar in several aspects of their composition to black glass beads from Italy and Pella dating to the Early Iron Age (Reade et al. 2006; Conte et al. 2016; Conte et al. 2018). These Iron Age beads are thought to have been made using natron as the alkali with one group that contained high magnesia (HMLK) and the other with low magnesia (LMLK).

The alumina concentration detected in the Lofkënd glasses, along with the levels of some transition and rare earth elements suggests the use of sand as the silica source. This is something also not commonly found in Late Bronze Age glasses, but more common in later periods, in particular with natron glasses. The Lofkënd

beads are too early to be natron glasses, since those do not appear until the 10th c. BC (Schlick-Nolte and Werthmann 2003). Therefore, it is not possible at this stage to identify what was used as the alkali source for the Lofkënd glasses and whether they do represent very early examples of these low lime, HMLK glasses, or some kind of experimentation with other alkalis and raw materials. The selection of a different alkali, a sand silica source, and the similarities of the Lofkënd glasses to later natron black glasses does indicate a distinct compositional type that perhaps is particular to certain region or indicative of trade with a particular production center. The lack of other examples of iron colored dark green or black glasses from the Late Bronze Age, however, does not allow for a more complete interpretation of the glass production technology represented at Lofkënd.

What the data from Lofkënd illustrates, as does the material from ancient Methone, is that sites located outside the areas of Mycenaean influence on glass consumption and trade can have a more diverse representation of glass color, decoration, and composition. This is in contrast to what has been observed from published studies of Late Bronze Age plant ash glasses commonly found in Egypt, the Near East, and Mycenaean Greece and may point to regional preferences or access to different primary and/or secondary production sites or trade routes.

9.3 Origins and Production Centers

The compositional analysis conducted helped to provide information on the origins of the glass and faience discovered at each of the sites. Due to sample size limitations, radiogenic isotope analysis could not be undertaken on all the samples. The combination of the different types of instrumental techniques applied to this study, however, offered some clues as to where the general primary production sites of the vitreous materials were located.

It is clear from the data collected that all three regions were importing glass from Egypt, either via sea trade routes that moved material from Egypt to different areas of the Eastern Mediterranean via intermediaries such as trade ships such as the Uluburun, or through the Mycenaeans on mainland Greece who were also receiving the glasses themselves. The presence of Egyptian made raw glass was confirmed through the presence of tin in the copper blue colored glasses, as well as the concentration of trace elements and ratios of strontium and neodymium isotopes related to the silica and alkali sources. Glasses made in the Near East were also found on Kefalonia and Lofkënd. It is possible that glass from the Near East was also present at ancient Methone, but because quantitative analysis could not be conducted on the glasses, it was not possible to determine this. The origin of the faience at ancient Methone bears some similarities to Egyptian faience, although again, the presence of Near Eastern faience objects cannot be ruled out.

The origins of the raw materials used to make the mixed alkali bead and the biconical faience bead from Kokkolata-Menegata are unknown. It is clear that they were not produced in the same major primary production centers that have been identified for Late Bronze Age vitreous materials in the Near East and Egypt. Aspects of the mixed alkali bead's composition were similar to the Frattesina LMHK beads, but the trace element data for the Frattesina samples has not been published so a full comparison of the elements related to the alkali and silica sources between both sets of samples was not possible. Unfortunately, the Kefalonian LMHK bead could not undergo isotopic analysis, data that does exist for the Frattesina glasses. Based on the results obtained thus far, it appears that this mixed alkali bead fits the compositional make up of other mixed alkali glasses found in Europe and likely made in that region.

The origin of the Kefalonian biconical bead is unknown. It was similar to two other Mycenaean Group B faience from two sites in Greece, therefore they likely originated from the same region. The source of the raw materials and location of primary and possibly secondary production cannot be identified without analysis of additional samples. Characterization of additional cobalt sources would also be helpful to determine where the bead was made.

Although the Lofkënd beads seem to have atypical glass compositions for the Late Bronze Age, the origin of the raw glass used to manufacture these beads seems to be from Egypt and the Near East. Both blue glasses were made with raw materials sourced to Egypt. The dark green glasses, however, came from Egypt and the Near East. There was no link between raw material source and the decoration found on the bead. Dark green glasses from both primary production regions were decorated with opaque white glass. If glasses from both regions were made with this unusual glass composition, could this be a case of workshops in two different regions using the same technology, whether due to transfer or regional innovation? Or is there secondary production taking place in another region where this glass composition and decoration is being produced using glass imported from both regions? These questions cannot be explored further due to the small sample size and the lack of comparative material. It is also possible that if the glasses are made with a natron alkali, provenancing the glass using certain trace elements may not be as reliable, and other types of analysis may be required (Oikonomou et al. 2020). The similarities between the Lofkënd beads and Early Iron Age glasses from Jordan and Europe may provide avenues for further exploration of the source of these glasses.

In regards to the location of secondary production workshops for the regions studied, additional evidence could not be provided. All of the beads come from cemetery contexts, and unless molds were interred with individuals, excavations of settlements will be needed in order to identify workshops for glassworking. The raw materials used to make the Kefalonian triple rosette bead were similar to those of glasses made in Egypt, though the isotopic ratios of strontium did show some slight variation from the raw materials in that area. The sourcing data did reveal that the glass used to make this unique bead type was imported to the Aegean from Egypt. The location of the workshop(s) where they were formed is unknown. No molds have been reported from excavations on Kefalonia, and it is unclear if this bead type was made locally or made elsewhere exclusively for export to the island.

The presence of a possible purple glass chunk or ingot fragment (M40-P) within one of the graves at Mazarakata was an unusual find. Only one published example has been found of glassworking debris present in a tomb, and this was at the site of Archanes (Panagiotaki 2008). The exact archaeological context of the Mazarakata purple glass chunk is unknown. At present, it is not clear whether it actually represents a chunk of raw glass or is a fragment of a larger unidentified object. If it is raw glass, it was imported to Kefalonia directly or indirectly from Egypt, which may point to the presence of workshops on the island. Without further analysis of the glass and examination of the fragment in order to determine what type of artifact it is, more conclusions cannot be drawn.

Finally, the appearance of the triple rosette bead found at Metaxata possibly within LH IIIC contexts, as well as the Kefalonian type of beaded circle relief beads from Kokkolata-Menegata and Mazarakata may be of importance within the larger backdrop of the destruction of the Mycenaean palaces and the collapse of the palatial system. During the postpalatial period on the mainland (ca. 1200 BC), the use of glass is greatly reduced, and some conclude that there was no production of Mycenaean faience and glass beads (Nightingale 1998, 211). It is possible that these unique Kefalonian bead forms were made earlier and kept for an extended period until they were deposited as LH IIIC grave goods. They could also have been made post-1200 BC. This would illustrate that local glass production persisted on Kefalonia even if it was not occurring on the mainland. The continued use of these bead forms until the 11th c. BC, and possibly their production, does not mirror the decline observed on the mainland but instead supports the continued growth on Kefalonia that is also observed through the expansion of cemeteries and the creation of new vessel forms.

9.4 Preservation of Vitreous Materials

The final aim of this research was to produce additional information on the types of deterioration pathologies that occur on archaeological vitreous materials. The focus of this part of the study was to provide more information on degradation processes and their physical and chemical impacts on archaeological glasses. The bulk of the research conducted in this area has focused on glasses from the Roman period onwards, and therefore more work is needed on the deterioration of earlier glasses.

The examination and documentation of glass corrosion helped to provide a visual guide for several types of degradation pathologies that are formed due to the burial environment or the activity of microorganisms. Compositional data from these deteriorated areas highlights the changes in the glass that can be detected quantitatively and point to leaching of alkalis and alkali earth elements or enrichment less soluble components. The effects of glass composition on the level of preservation were also explored. The examination of one grave at Lofkënd, Tomb XXVIII, where five glass beads were found in varying states of preservation, offered an opportunity to investigate this further by looking at a single burial event. The compositional data unfortunately did not provide a clear indication as to why some beads within the same context were more deteriorated than others. The results of this portion of the study highlighted how complex the deterioration of vitreous materials can be even within the same burial environment and that it is influenced by numerous factors and processes that can occur simultaneously. Even though no definitive causes for the types of deterioration observed on some of the beads can be given, illustrating and describing the physical signs of different degradation process, coupled with a discussion of compositional changes vitreous materials undergo, can aid cultural heritage professionals in the preservation of early vitreous materials.

9.5 Directions for Further Research

The work presented here has met the aims set out at the beginning of the thesis. Questions arose, however, during the analysis that could not be definitely answered. Therefore, there are several areas where further research can be undertaken. Due to time and budget constraints, issues with sampling permissions, or the limitations of the analytical techniques chosen, there were aspects of the composition and sourcing of the vitreous materials that could not be further explored. Some of these areas of additional research are outlined below.

Additional analysis of the beads is one of the main areas of further research that can be pursued in an effort to clarify outstanding questions on composition or sourcing. If additional sampling is allowed or funds are available for further analysis, the following lines of inquiry would be important:

- Sampling and quantitative analysis to identify the composition and sources of the ancient Methone beads. Based on the uncommon predominant color and the presence of lead antimonate in glasses that do not seem to produce the desired color or opacity, the composition and colorants should be investigated. Sampling and analysis of the faience disc beads and cogwheel beads would provide more information on their production technology and origins.
- Further study of the mixed alkali bead from Kokkolata-Menegata should be undertaken. The bead should be sampled again, at a size that would allow for isotopic analysis for sourcing. The other beads from box 580.1 should also be analyzed since those beads could represent additional examples of LMHK glasses.
- The Kefalonian type beaded circle relief bead should be sampled for compositional, trace element, and isotopic analysis. One of the mainland beaded circle types was analyzed as part of this study and can be used for comparison to identify any technological differences between this bead type from the mainland and those made locally.

- The purple chunk of glass from Mazarakata should be further investigated. Work should be undertaken to determine what the artifact type is, whether it is a piece of raw glass or whether it is a fragment of a larger object. The crust on the surface should be further analyzed to establish whether it is the results of glass being in contact with the walls of a crucible. A larger sample should be taken for isotopic analysis for further sourcing.
- Additional samples of Mycenaean Group B faience found at the Kefalonian sites should be analyzed for comparison to the biconical bead analyzed for this thesis. If the cobalt source is likely from Greece as has been proposed by some, analysis and characterization of the cobalt sources from Laurion and Larymna should be undertaken so that the chemical signature is known and can be compared to the archaeological samples. Additional cobalt sources should also be analyzed since this data is lacking for this material outside the sources known in Egypt and Iran.
- The dark green glasses from Lofkënd should undergo radiogenic isotopic analysis for further sourcing of the raw materials. In addition, the Early Iron Age dark green bead found at the site, which was not sampled, should be analyzed quantitatively. This would allow for a diachronic comparison of the dark green glasses at the site and for comparison to other dark green or black Iron Age glasses from other sites that were mentioned in this text. Since this glass color, and the composition of the Lofkënd beads, is not typical of Late Bronze Age technology, there is a need for additional investigations into the production of this compositional group.

Further research focused on degradation pathologies and the deterioration of archaeological glasses could be undertaken. Other groups of beads from this study found within a single grave context could be used as cases studies for investigating the processes involved in the level of corrosion observed. Studies using experimental glasses exposed to various burial conditions observed at the sites studies could be conducted. This could include laboratory made glasses made with Late Bronze Age plant ash compositions, but also the LMHK and HMLK glass types found at Kefalonia and Lofkënd, glass types that have not been well studied in regards to specific processes that may affect preservation in the archaeological record.

Finally, one the biggest challenges in the interpretation of the data, which was mentioned throughout the text, was the lack of comparative material from the areas of northern Greece, the Ionian Islands, and southwestern Albania dating to the Late Bronze Age and transition to the Early Iron Age. This is likely an issue encountered by many other researchers studying material from this period found in regions that have not received much attention in previous archaeometric studies. In some case, when published studies were found, the analytical data was incomplete with only averages or selected results included in the publication. One of the future goals of the analytical results presented here is to make the data collected from the ancient Methone, Kefalonia, and Lofkënd beads widely accessible to other researchers studying ancient glass. This will be done either through the publication of certain portions of this text in journals that allow for complete analytical results to be included as supplemental data, or in journals specializing in the publication of archaeological data. Creating an open access data platform with the analytical results is another option to increase accessibility. The sharing of analytical data can only benefit future studies of Late Bronze Age and Early Iron Age vitreous materials and greatly contribute to our understanding of this technology and the use and distribution of these cultural materials.

APPENDIX A – ANALYTICAL METHODS: WORKFLOW AND GLASS STANDARDS DATA

A.1. Examination and Analytical Methods Workflow

The table provides a general workflow for the examination and analysis undertaken on the glass and faience beads. The first five techniques were used for all the material studied in the order listed. The final three techniques were conducted on only selected artifacts or samples.

	Technique	Purpose/Goal	Sampling Undertaken	Limitations
1	Optical Microscopy (OM)	Surface examination, material identification, condition assessment, and sample selection.	No	Surface degradation can obscure identification of material and color.
2	Portable X-ray Fluorescence Spectrometry (pXRF)	Qualitative analysis, identification of colorants. Results were used to select beads for sampling and quantitative analysis.	No	Since it is primarily a surface analysis technique, the results are influenced by surface deposits or degradation. No quantitative analysis was possible.
3	Electron Probe Microanalysis (EPMA)	Quantitative analysis of glass composition-major and minor oxides, colorants	Yes. Sample was mounted in epoxy and polished. Also required carbon coating prior to analysis. Sample size for this analysis was 3-5mm.	Somewhat cost prohibitive which limited the amount of time spent analyzing each sample. Not all oxides could be quantified.
4	Laser Ablation Inductively Coupled Plasma Mass Spectrometry (LA-ICP-MS)	Quantitative analysis-trace elements. Used for sourcing silica, colorants, and primary production area. All samples analyzed using EPMA underwent this analysis.	Yes. Same samples used for EPMA were used for LA-ICP-MS.	Somewhat cost prohibitive limiting the number of samples that were analyzed. Not many labs have laser ablation. Loss of sample due to ablation. However, material removed is small and embedded sample can be reused for other types of analysis afterwards.
5	Radiogenic Isotopic Analysis	Quantitative analysis-Nd and Sr isotopes for provenance.	Yes. Sample required was a fragment (20-30 mg minimum but larger is better).	Cost prohibitive so only a few samples could be analyzed. Not many labs do this type of analysis. Large sample required which limited which beads could be analyzed. Could not use previously mounted samples. Not much comparative data available for Late Bronze Age glass to help with provenancing.
	Scanning Electron Microscopy-Energy Dispersive Spectroscopy (SEM-EDS)	Quantitative analysis of glass composition-major and minor oxides and colorants (conducted only on ancient Methone beads)	No, if object is small enough to fit in the SEM sample chamber	Only surface analysis could be undertaken. Due to leaching of the surface, could get not accurate compositional information
	Variable Pressure-Scanning Electron Microscopy-Energy Dispersive Spectroscopy (VP-SEM-EDS)	Quantitative analysis of deteriorated areas for study of degradation processes	No. Analysis conducted on previously mounted samples. However this technique does not require prepared samples as long as the object fits in the SEM sample chamber	Analysis conducted using a low vacuum detector (LVD) in secondary electron mode therefore limiting some of the imaging and analytical investigations.
	X-ray Diffraction (XRD)	Qualitative analysis of opaque white glass (Lofkënd dark green beads)	Yes. Small sample of opaque white glass taken. The model of powder diffractometer used only required a very small sample (a few mg)	Not many labs have an XRD that can analyze such small samples. Some difficulty analyzing glass that was in better condition because of its amorphous structure.

A.2. EPMA of Corning reference glasses (A, B, C, D) and NIST SRM 610, 612, and 614.

Results given as oxide weight % (wt%).

Standard	SiO_2	Na_2O	K_2O	MgO	Al_2O_3	CaO	FeO	MnO	TiO_2	P_2O5	SO_3	Cl	Total
CorningA-1	66.516	13.886	3.063	2.717	0.912	5.136	0.999	1.075	0.951	0.116	0.143	0.083	95.578
CorningA-1	66.462	14.184	2.971	2.592	0.904	5.203	0.958	1.029	0.795	0.113	0.144	0.093	95.427
CorningA-1	66.584	14.107	3.028	2.673	0.917	5.209	0.974	1.061	0.811	0.144	0.14	0.09	95.718
CorningA-1	66.654	13.545	2.965	2.649	0.861	5.293	0.944	1.002	0.806	0.089	0.164	0.091	95.042
CorningA-2	65.498	14.02	3.051	2.647	0.857	5.15	1.004	1.043	0.857	0.111	0.162	0.066	94.451
CorningA-2	66.534	13.912	3.068	2.734	0.941	5.185	0.928	1.003	0.903	0.125	0.109	0.089	95.511
CorningA-2	67.096	13.818	2.923	2.705	0.927	5.248	0.917	0.982	0.757	0.153	0.135	0.093	95.754
CorningA-2	66.694	13.9	3.016	2.684	0.853	5.287	0.999	1.024	0.773	0.057	0.069	0.098	95.432
CorningA-3	66.393	13.899	3.026	2.614	0.949	5.158	0.972	1.055	0.871	0.109	0.14	0.11	95.271
CorningA-3	66.04	13.769	2.98	2.674	0.868	5.094	0.989	1.08	0.792	0.122	0.142	0.083	94.645
CorningA-3	66.653	13.916	3.074	2.666	0.874	5.077	0.994	1.059	0.924	0.125	0.079	0.07	95.508
CorningA-3	66.761	14.243	3.025	2.725	0.899	5.213	0.992	1.009	0.813	0.111	0.187	0.084	96.043
CorningB-1	61.053	16.091	1.107	1.079	4.102	9.078	0.241	0.224	0.127	0.858	0.538	0.158	94.661
CorningB-1	61.671	16.305	1.101	0.979	4.129	8.795	0.305	0.233	0.043	0.884	0.57	0.163	95.217
CorningB-1	61.588	16.376	1.084	1.053	4.058	8.824	0.306	0.226	0.108	0.797	0.529	0.18	95.142
CorningB-1	61.409	16.834	1.072	1.125	4.161	9.12	0.302	0.251	0.099	0.838	0.513	0.163	95.889
CorningB-2	61.046	15.78	1.038	1.009	4.072	9.055	0.33	0.255	0.114	0.867	0.587	0.174	94.288
CorningB-2	60.865	16.441	1.066	1.022	4.053	8.86	0.26	0.266	0.197	0.876	0.619	0.188	94.671
CorningB-2	62.022	16.786	1.051	1.012	4.274	9.006	0.32	0.218	0.131	0.871	0.536	0.162	96.352
CorningB-2	61.493	16.794	0.983	1.081	4.008	9.036	0.332	0.222	0.143	0.86	0.492	0.16	95.601
CorningB-3	60.872	15.877	1.107	1.019	4.171	9.154	0.269	0.271	0.047	0.926	0.572	0.146	94.398
CorningB-3	61.253	16.655	0.987	0.988	4.062	9.166	0.339	0.241	0.114	0.886	0.545	0.145	95.348
CorningB-3	61.887	16.436	1.119	1.011	4.165	9.204	0.361	0.247	0.069	0.844	0.535	0.171	96.025
CorningB-3	61.496	16.852	1.054	1.027	4.088	8.976	0.303	0.222	0.044	0.87	0.553	0.195	95.636
CorningB-4	61.272	16.708	1.051	1.014	4.181	9.059	0.31	0.235	0.085	0.861	0.551	0.162	95.482
CorningB-5	61.707	16.413	1.014	1.021	4.161	8.916	0.319	0.263	0.171	0.82	0.619	0.16	95.548
CorningC-1	34.816	1.087	2.949	2.445	0.793	5.21	0.369	0.034	1.164	0.113	0.081	0.093	49.133
CorningC-1	34.869	1.125	3.046	2.484	0.834	5.091	0.297	0	1.102	0.095	0.056	0.088	49.126
CorningC-1	34.831	1.164	2.898	2.445	0.791	5.274	0.263	0	1.109	0.222	0.042	0.061	49.086
CorningC-1	34.784	1.135	2.96	2.534	0.731	5.246	0.407	0.031	1.187	0.076	0.032	0.059	49.169
CorningC-2	34.869	1.124	3.008	2.449	0.766	5.147	0.292	0.072	1.007	0.099	0.079	0.088	48.98
CorningC-2	35.197	1.049	3.008	2.478	0.788	5.103	0.346	0	1.243	0.141	0.048	0.098	49.537

Standard	SiO_2	Na_2O	K_2O	MgO	Al_2O_3	CaO	FeO	MnO	TiO_2	P_2O5	SO_3	Cl	Total
CorningC-2	35.066	1.025	2.916	2.471	0.74	5.173	0.31	0.06	1.183	0.125	0.035	0.063	49.153
CorningC-2	35.172	1.158	3.137	2.593	0.796	5.297	0.202	0	1.063	0.11	0.085	0.079	49.674
CorningC-3	34.997	1.097	2.98	2.567	0.779	5.136	0.329	0	1.037	0.125	0	0.102	49.126
CorningC-3	35.303	0.995	2.965	2.485	0.782	5.098	0.311	0	1.275	0.082	0.005	0.093	49.38
CorningC-3	34.874	1.065	3.056	2.42	0.788	5.202	0.301	0	1.203	0.046	0.108	0.062	49.111
CorningC-3	35.13	1.04	3.026	2.434	0.819	5.199	0.384	0.002	1.161	0.087	0.071	0.098	49.523
CorningD-1	54.711	1.308	11.951	3.852	4.933	14.67	0.46	0.606	0.47	3.991	0.211	0.141	97.272
CorningD-1	55.025	1.379	11.93	3.863	5.007	14.738	0.47	0.524	0.445	3.938	0.235	0.138	97.661
CorningD-1	55.536	1.355	11.803	3.99	5.004	14.57	0.472	0.561	0.478	3.933	0.179	0.17	98.013
CorningD-1	55.057	1.44	12.002	4.031	5.098	14.622	0.416	0.558	0.438	3.94	0.197	0.131	97.9
CorningD-2	54.405	1.324	11.891	3.915	4.927	14.892	0.409	0.48	0.389	3.915	0.222	0.158	96.912
CorningD-2	54.985	1.362	11.931	3.92	5.018	14.426	0.429	0.532	0.425	3.995	0.197	0.13	97.324
CorningD-2	54.98	1.328	11.921	3.891	5.045	14.594	0.461	0.496	0.472	3.83	0.246	0.14	97.372
CorningD-2	55.079	1.32	11.892	3.89	5.033	14.793	0.471	0.551	0.464	4.03	0.207	0.142	97.847
CorningD-3	54.751	1.344	11.854	3.852	5.071	14.847	0.406	0.526	0.462	3.976	0.199	0.149	97.403
CorningD-3	55.243	1.369	11.992	3.93	5.009	14.944	0.472	0.491	0.409	4.001	0.22	0.152	98.287
CorningD-3	55.273	1.278	11.872	3.922	5.014	14.677	0.44	0.581	0.438	3.957	0.185	0.144	97.749
CorningD-3	55.234	1.223	11.687	4.026	5.125	14.718	0.458	0.512	0.399	3.931	0.264	0.148	97.746
NIST610-1	69.254	13.704	0.066	0.079	1.942	11.512	0.067	0.067	0.016	0.189	0.126	0.041	97.054
NIST610-1	69.659	13.483	0.02	0.073	1.931	11.359	0.081	0.123	0.119	0.146	0.133	0.026	97.159
NIST610-1	69.565	13.786	0.084	0.101	1.943	11.443	0.062	0.074	0.058	0.15	0.139	0.024	97.424
NIST610-1	69.778	13.734	0.044	0.08	1.857	11.358	0.12	0.065	0.085	0.099	0.115	0.034	97.424
NIST610-2	69.777	13.417	0.065	0.083	1.887	11.412	0.051	0.073	0.048	0.209	0.15	0.047	97.208
NIST610-2	69.859	13.635	0.104	0.063	1.953	11.391	0.022	0.047	0.145	0.115	0.114	0.032	97.535
NIST610-2	69.637	13.701	0.086	0.082	1.964	11.478	0.045	0.026	0.123	0.125	0.128	0.026	97.451
NIST610-2	69.504	13.617	0.06	0.094	1.831	11.467	0.09	0.027	0.121	0.122	0.081	0.03	97.039
NIST610-3	69.603	13.598	0.068	0.069	1.892	11.394	0.027	0.036	0.168	0.14	0.107	0.031	97.168
NIST610-3	69.717	13.677	0.101	0.088	1.933	11.465	0.077	0.072	0.13	0.128	0.137	0.038	97.622
NIST610-3	73.147	4.678	0.049	0.046	1.973	11.845	0.119	0.043	0.11	0.129	0.153	0.039	92.329
NIST610-3	69.85	13.721	0.056	0.075	1.972	11.595	0.094	0.037	0.107	0.174	0.124	0.006	97.842
NIST612-1	72.019	13.76	0.007	0.011	2.029	12.122	0.011	0.031	0.022	0.092	0.071	0.012	100.184
NIST612-1	72.027	14.197	0.012	0.018	1.99	11.758	0.023	0.006	0	0.051	0.066	0.006	100.185

Standard	SiO_2	Na_2O	K_2O	MgO	Al_2O_3	CaO	FeO	MnO	TiO_2	P_2O5	SO_3	Cl	Total
NIST612-1	72.309	13.993	0.015	0.031	1.996	11.836	0.011	0.011	0.01	0.062	0.089	0.011	100.407
NIST612-1	72.108	14.173	0	0.031	1.979	11.869	0.076	0	0.036	0.088	0.077	0.001	100.476
NIST612-2	71.711	13.985	0.015	0.017	2.057	11.856	0.036	0.003	0.014	0.12	0.054	0.003	99.879
NIST612-2	71.922	13.898	0	0.033	1.966	11.684	0	0.034	0	0.081	0.076	0	99.694
NIST612-2	72.075	14.047	0.005	0.002	1.998	11.765	0	0.018	0.027	0.067	0.029	0.022	100.094
NIST612-2	71.874	13.819	0.008	0.032	1.998	12.043	0.023	0.005	0.018	0.02	0.084	0.004	99.927
NIST612-3	71.707	13.933	0	0.017	1.972	11.87	0.043	0	0	0.072	0.078	0	99.74
NIST612-3	72.506	14.085	0.003	0	1.956	11.552	0.008	0.053	0.021	0.054	0.037	0.014	100.352
NIST612-3	71.875	13.989	0	0.004	2.02	11.93	0	0	0	0.06	0.08	0.012	99.967
NIST612-3	72.453	14.28	0.029	0.002	1.968	11.926	0.032	0	0	0.095	0.092	0	100.877
NIST614-1	72.287	13.843	0.015	0.018	1.989	11.87	0.02	0	0	0.077	0.062	0.037	100.223
NIST614-1	72.483	14.137	0.028	0.032	1.999	11.793	0.026	0	0	0.094	0.08	0.011	100.681
NIST614-1	72.59	13.964	0	0.02	1.945	11.922	0	0.026	0.013	0.03	0.07	0.033	100.634
NIST614-1	72.556	13.96	0.015	0.042	1.992	11.803	0	0.011	0	0.072	0.05	0.004	100.504
NIST614-2	72.098	13.925	0.017	0.01	2.02	11.873	0.032	0.037	0.016	0.109	0.066	0.02	100.218
NIST614-2	72.195	13.866	0.004	0	1.997	11.824	0	0.016	0.006	0.033	0.053	0.006	99.999
NIST614-2	72.625	13.892	0.012	0.025	1.993	11.956	0	0.014	0	0.059	0.034	0.016	100.625
NIST614-2	72.316	14.041	0	0	1.91	11.836	0	0	0.036	0	0.063	0	100.202
NIST614-3	71.879	13.891	0.037	0.02	1.962	11.875	0.002	0	0	0.068	0.084	0.006	99.823
NIST614-3	72.478	14.017	0.021	0	1.951	11.625	0.006	0	0	0.104	0.068	0	100.283
NIST614-3	72.434	13.964	0.005	0.017	1.977	11.746	0	0.032	0	0.077	0.072	0.023	100.342
NIST614-3	72.471	14.02	0.028	0.037	1.999	11.949	0.023	0.003	0	0.019	0.086	0	100.651

A.3. LA-ICP-MS analysis of Corning references glasses (A, B, C, D) and NIST SRM 610, 612, and 614.

Results given as parts per million (ppm).

Standard	Analysis Type	7 Li	9 Be	11 B	23 Na	24 Mg	27 Al	31 P	39 K	44 Ca	45 Sc
SRM 610	Calibration Standard	442.1409	457.3204	354.9629	95440.3308	423.0476	10620.9687	444.5241	434.8640	81108.5913	463.2217
SRM 610	Calibration Standard	453.6944	477.6837	369.9642	99595.2850	454.3875	10807.3910	388.5253	458.2668	84314.6496	490.2784
SRM 610	Calibration Standard	461.0622	469.2155	338.1263	97895.6557	455.6527	10436.3004	361.0468	436.6654	81656.7290	477.0021
SRM 610	Calibration Standard	472.3788	506.3100	299.4932	98669.3614	468.7926	10759.7145	447.9975	444.0505	88560.5067	501.6682
SRM 610	Calibration Standard	435.5807	465.5881	336.9466	99215.6897	444.9218	10532.9570	422.9063	448.0145	83113.3051	470.5509
SRM 612	Calibration Standard	39.3224	36.9816	64.4536	95187.0511	66.3276	10291.6499	77.1756	72.7578	83728.1039	37.8011
SRM 612	Calibration Standard	44.0128	41.8423	44.1825	103092.6196	61.2253	10262.1611	62.3553	71.5101	78509.0734	34.3200
SRM 612	Calibration Standard	38.3836	40.2531	38.2592	96902.2752	65.3663	10269.0857	16.1051	60.6904	84090.2641	40.2557
SRM 612	Calibration Standard	44.6953	36.2054	23.9817	103839.7416	59.0795	10627.8620	48.5037	69.2552	82751.3809	38.4473
SRM 612	Calibration Standard	41.2995	32.5293	30.7766	101080.6380	62.9601	10600.8269	28.8603	61.0586	80898.7839	37.2826
SRM 614	Calibration Standard	1.0616	0.9361	-5.0978	105321.4994	30.5195	11328.7543	19.7831	31.1895	85569.8287	1.4636
SRM 614	Calibration Standard	1.6740	0.9447	3.2498	102652.6952	34.7210	10860.6418	6.1093	27.4790	90064.2829	0.9968
SRM 614	Calibration Standard	1.8671	0.5928	3.3267	104670.4912	37.3153	10809.5882	31.7285	30.2988	87781.6686	0.6387
SRM 614	Calibration Standard	1.4107	0.5600	7.6143	107602.7207	35.2353	10713.4509	-0.5793	32.1811	79769.4541	0.7122
SRM 614	Calibration Standard	2.4257	0.7313	-15.1712	102076.6617	36.8645	10434.1449	19.1994	23.7494	86426.5464	0.6159
SRM 614	Quality Control 1-1	1.5612	0.7609	-6.8943	108133.7988	35.4431	10894.2084	6.5826	30.0053	85612.9860	1.1434
SRM 614	Quality Control 1-1	1.6668	0.9757	-12.2098	106934.8787	34.6375	11356.8824	-7.6732	28.7679	86720.6010	0.2835
SRM 614	Quality Control 1-1	1.2049	1.8016	-23.6196	110568.6979	36.6584	10512.3382	21.6932	29.2401	84745.7489	1.3566
	Average	1.4776	1.1794	-14.2412	108545.7918	35.5797	10921.1430	6.8675	29.3378	85693.1120	0.9278
	Cert. Values	1.69	0.753	1.49	101634	33.8	10796	11.4	30	85049	0.74
	%Recovery	87.43	156.63	-955.79	106.80	105.27	101.16	60.24	97.79	100.76	125.38
SRM 614	Quality Control 1-2	1.8867	1.0763	-16.8916	108135.2269	37.3661	10436.2055	42.4400	65.0071	87180.1129	0.6746
SRM 614	Quality Control 1-2	3.1122	0.8861	-45.7893	109391.7522	35.5335	10824.4554	2.3737	43.0380	85640.7979	0.6408
SRM 614	Quality Control 1-2	1.8780	1.1596	-42.8094	106938.8092	33.5839	10636.6601	47.6366	43.4122	88153.2441	0.7385
	Average	2.2923	1.0407	-35.1634	108155.2627	35.4945	10632.4403	30.8168	50.4857	86991.3850	0.6846
	Cert. Values	1.69	0.753	1.49	101634	33.8	10796	11.4	30	85049	0.74
	%Recovery	135.64	138.20	-2359.96	106.42	105.01	98.48	270.32	168.29	102.28	92.52
SRM 612	Quality Control 2-1	46.0684	46.7983	29.6405	102356.3846	61.1520	10575.6026	18.6224	79.7814	90730.9476	41.3520
SRM 612	Quality Control 2-1	37.0315	40.6594	13.4684	96819.1014	58.1552	10502.6330	39.3786	64.2275	90576.1497	40.6276
SRM 612	Quality Control 2-1	39.1516	38.1035	20.7653	102246.9378	58.3742	10923.4172	16.8613	53.9746	83805.0286	36.5137
	Average	40.7505	41.8537	21.2914	100474.1412	59.2272	10667.2176	24.9541	65.9945	88370.7086	39.4978
	Cert. Values	40.2	37.5	34.3	101634	68	10743	46.6	62.3	85049	39.9
	%Recovery	101.37	111.61	62.07	98.86	87.10	99.29	53.55	105.93	103.91	98.99
SRM 612	Quality Control 2-2	44.0774	34.2630	2.2976	113727.3504	64.4214	10882.5938	55.1897	68.2881	85914.0316	38.5114
SRM 612	Quality Control 2-2	44.6233	36.7283	-4.2600	109710.9860	61.2613	10462.5367	60.4067	60.2960	85872.1496	35.7451

Standard	Analysis Type	47 Ti	51 V	52 Cr	55 Mn	56 Fe	59 Co	60 Ni	63 Cu	66 Zn	71 Ga	72 Ge
SRM 610	Calibration Standard	404.5792	439.7899	390.0976	432.6566	423.5944	392.7715	450.4854	407.8334	457.1706	398.5806	398.3895
SRM 610	Calibration Standard	458.8567	453.1479	409.9347	432.8035	424.6238	409.1739	448.5692	431.2162	470.3230	424.1816	424.2271
SRM 610	Calibration Standard	446.2519	447.4862	404.6546	446.1784	448.1016	421.9955	473.2202	467.6687	489.0259	440.7906	421.8408
SRM 610	Calibration Standard	458.0063	464.8213	407.6657	453.0606	465.7472	423.2011	476.2344	481.7867	491.5843	417.5163	429.5707
SRM 610	Calibration Standard	444.8850	437.1634	397.0906	423.5742	427.3418	402.3067	454.3085	425.1813	479.4195	426.0867	423.8411
SRM 612	Calibration Standard	55.4620	36.9055	36.2427	37.2156	60.7930	33.3357	35.5737	59.8676	35.8451	35.9781	32.7879
SRM 612	Calibration Standard	36.9442	40.0540	36.9106	42.5199	59.5346	39.6750	44.8044	55.6314	43.1864	39.2793	42.5765
SRM 612	Calibration Standard	48.7545	39.2876	37.8768	38.9782	49.8766	34.7523	37.7156	39.3719	36.2674	37.3954	37.2165
SRM 612	Calibration Standard	37.4632	39.7800	37.8223	40.2116	50.7243	36.6280	39.7411	39.0537	40.4674	40.9999	41.9943
SRM 612	Calibration Standard	41.3762	38.6434	35.9576	37.4363	51.0843	33.1577	35.3559	34.2043	31.7711	35.9427	37.2723
SRM 614	Calibration Standard	10.8180	0.9757	1.2649	1.3392	17.3939	0.7892	1.0027	1.7898	3.0154	1.1982	0.7254
SRM 614	Calibration Standard	11.4418	0.8944	1.1375	1.3531	17.5946	0.6856	1.1689	1.2653	1.9628	1.3262	0.7372
SRM 614	Calibration Standard	14.4101	1.1216	1.0577	1.7485	20.0782	0.8531	1.4060	79.4645	3.2208	1.1455	0.5879
SRM 614	Calibration Standard	12.7384	0.9642	1.2200	1.4637	18.7737	0.6761	1.0373	1.3545	3.0082	1.3137	1.1308
SRM 614	Calibration Standard	12.5217	1.0936	1.2671	1.1919	18.0174	0.9460	0.8856	1.0713	2.7801	1.5605	1.5216
SRM 614	Quality Control 1-1	12.7309	1.2459	1.1980	1.1694	21.1350	0.6749	0.8237	1.2077	3.7074	1.2719	1.6785
SRM 614	Quality Control 1-1	10.3170	1.0748	1.2549	1.9697	18.6969	0.6986	0.7830	1.3587	3.3533	0.9250	0.9038
SRM 614	Quality Control 1-1	10.9479	0.7658	1.0108	1.3812	18.8548	0.6232	1.0562	1.0891	2.8519	1.0092	0.9711
	Average	11.3319	1.0288	1.1546	1.5068	19.5622	0.6656	0.8876	1.2185	3.3042	1.0687	1.1844
	Cert. Values	3.61	1.01	1.19	1.42	18.8	0.79	1.1	1.37	2.79	1.31	0.942
	%Recovery	313.90	101.86	97.02	106.11	104.05	84.25	80.69	88.94	118.43	81.58	125.74
SRM 614	Quality Control 1-2	13.3353	1.1835	1.5639	1.7472	29.8326	0.9702	1.4195	35.9452	5.6679	1.7424	1.0564
SRM 614	Quality Control 1-2	11.4042	1.3105	1.5421	1.7152	19.2645	0.6404	1.1801	8.2811	4.0307	1.7355	0.9894
SRM 614	Quality Control 1-2	12.2561	1.2639	1.2797	1.4025	20.1437	0.6594	1.0840	3.8560	4.3938	1.4359	1.0305
	Average	12.3318	1.2526	1.4619	1.6216	23.0803	0.7567	1.2279	16.0274	4.6975	1.6379	1.0254
	Cert. Values	3.61	1.01	1.19	1.42	18.8	0.79	1.1	1.37	2.79	1.31	0.942
	%Recovery	341.60	124.02	122.85	114.20	122.77	95.78	111.63	1169.89	168.37	125.03	108.86
SRM 612	Quality Control 2-1	52.7324	42.0579	40.4981	40.6697	59.0079	38.5643	42.9349	42.9756	37.9979	40.2688	40.4009
SRM 612	Quality Control 2-1	40.8029	40.5868	37.9594	38.7205	52.2929	33.1708	37.2876	36.8698	32.0036	35.6458	34.9424
SRM 612	Quality Control 2-1	42.9675	41.3962	37.9840	36.9834	53.0454	36.0782	38.6330	43.3117	31.4600	34.5472	36.9783
	Average	45.5009	41.3469	38.8138	38.7912	54.7821	35.9378	39.6185	41.0523	33.8205	36.8206	37.4405
	Cert. Values	44	38.8	36.4	38.7	51	35.5	38.8	37.8	39.1	36.9	36.1
	%Recovery	103.41	106.56	106.63	100.24	107.42	101.23	102.11	108.60	86.50	99.78	103.71
SRM 612	Quality Control 2-2	37.6185	44.4942	39.7168	40.1726	57.4452	38.3124	43.4146	46.7640	33.0041	38.1238	41.1218
SRM 612	Quality Control 2-2	37.2945	40.4921	38.2196	38.6788	54.4559	36.6978	40.8120	39.0968	36.3543	36.7012	39.2363

Standard	Analysis Type	75 As	82 Se	85 Rb	88 Sr	89 Y	90 Zr	93 Nb	95 Mo	103 Rh	105 Pd	107 Ag	111 Cd
SRM 610	Calibration Standard	323.6453	127.0544	393.7715	502.1488	455.1438	440.4809	451.4148	406.4288	1.2937	0.9319	334.2399	262.5885
SRM 610	Calibration Standard	326.5484	148.6224	416.9784	524.2191	480.7983	461.2072	473.1824	427.0347	1.1592	1.0766	298.1914	273.0933
SRM 610	Calibration Standard	334.4113	125.9324	420.4274	533.3798	483.4334	465.1690	487.3085	427.0841	1.1391	0.9217	228.2922	266.9359
SRM 610	Calibration Standard	275.8121	132.5624	434.3812	526.7402	492.1782	469.9482	485.7121	424.0742	1.1196	1.2256	305.9367	282.0665
SRM 610	Calibration Standard	326.2980	155.8284	400.2273	508.5377	461.1728	451.7878	456.4980	405.4557	1.1748	1.0716	222.4783	262.2972
SRM 612	Calibration Standard	30.7999	15.0512	29.1017	69.8915	33.5266	34.2237	35.0565	32.9591	0.8658	1.3087	142.1093	27.3988
SRM 612	Calibration Standard	39.7591	22.7680	33.7097	82.3531	39.6777	39.0485	41.7500	42.8623	0.9727	1.5896	191.2349	32.9076
SRM 612	Calibration Standard	34.5000	14.0067	33.2702	78.4290	36.7310	37.1546	38.1442	37.0769	0.9296	1.2655	24.6925	27.6015
SRM 612	Calibration Standard	37.2696	13.7232	34.1116	83.0326	39.1147	39.8172	40.9834	39.1126	1.0870	1.0731	28.2475	27.3657
SRM 612	Calibration Standard	34.9511	15.9510	31.5526	72.4533	37.1495	35.0589	36.0818	34.5247	0.8063	1.0732	17.6300	25.5464
SRM 614	Calibration Standard	0.4573	0.9472	0.8187	44.1102	0.8320	0.8288	0.6691	0.7829	1.5692	2.0705	15.0060	0.6203
SRM 614	Calibration Standard	0.7025	1.5605	0.7410	45.8332	0.8493	0.8050	0.8853	1.0455	1.6623	2.2550	0.3273	0.5154
SRM 614	Calibration Standard	0.7672	5.8352	0.7828	47.8080	0.7348	0.9745	0.7570	0.6996	1.7950	2.1069	0.4900	0.5693
SRM 614	Calibration Standard	1.0877	-1.8298	0.9725	46.8770	0.8120	0.9188	0.8958	0.8822	1.6106	2.2908	1.9481	0.7562
SRM 614	Calibration Standard	0.6858	1.9889	0.9568	46.2264	0.7240	0.7149	0.9138	0.5900	1.5473	1.9046	0.4411	0.3387
SRM 614	Quality Control 1-1	0.8393	0.4979	1.0418	44.6669	0.8518	0.9055	0.7651	0.9042	1.4937	1.7961	0.4857	0.8691
SRM 614	Quality Control 1-1	0.9768	4.6999	0.8606	45.9599	0.6730	0.6402	1.0746	1.2310	1.6455	2.2421	0.4472	0.6511
SRM 614	Quality Control 1-1	0.7286	3.5414	0.8096	42.6463	0.7935	0.7137	0.6551	0.9952	1.6022	1.9202	0.3088	0.5372
	Average	0.8483	2.9131	0.9040	44.4244	0.7727	0.7531	0.8316	1.0435	1.5804	1.9861	0.4139	0.6858
	Cert. Values	0.74	0.4	0.85	45.8	0.79	0.848	0.824	0.8	1.54	2.05	0.42	0.56
	%Recovery	114.63	728.27	106.35	97.00	97.82	88.81	100.93	130.44	102.63	96.88	98.55	122.46
SRM 614	Quality Control 1-2	1.3660	2.3212	0.7846	43.5102	0.8024	0.9782	0.7409	0.7650	1.6183	2.0299	251.0149	0.6644
SRM 614	Quality Control 1-2	1.1414	6.8470	0.8945	46.6057	0.7291	0.7883	0.8861	1.0948	1.7017	1.9614	46.9151	0.7020
SRM 614	Quality Control 1-2	0.4064	5.7021	1.0328	45.5244	0.7414	0.9156	0.8092	0.6301	1.5263	1.9502	33.3767	0.5812
	Average	0.9713	4.9568	0.9040	45.2135	0.7576	0.8940	0.8121	0.8300	1.6154	1.9805	110.4355	0.6492
	Cert. Values	0.74	0.4	0.85	45.8	0.79	0.848	0.824	0.8	1.54	2.05	0.42	0.56
	%Recovery	131.26	1239.19	106.35	98.72	95.90	105.43	98.55	103.75	104.90	96.61	26294.18	115.93
SRM 612	Quality Control 2-1	43.0509	20.8297	36.2771	85.0747	41.9089	40.5481	40.4596	39.0055	1.0427	0.9705	53.6500	31.5042
SRM 612	Quality Control 2-1	34.2086	9.5892	32.0947	74.1706	36.1424	36.0792	36.3957	37.6875	0.9043	1.1391	66.2656	26.8414
SRM 612	Quality Control 2-1	33.2870	14.4203	30.7353	77.5962	36.3532	38.0482	38.1006	34.5554	0.9577	1.1901	31.3764	27.5141
	Average	36.8488	14.9464	33.0357	78.9472	38.1348	38.2252	38.3186	37.0828	0.9682	1.0999	50.4307	28.6199
	Cert. Values	35.7	16.3	31.4	78.4	38.3	37.9	38.9	37.4	0.91	1.05	22	28.1
	%Recovery	103.22	91.70	105.21	100.70	99.57	100.86	98.51	99.15	106.40	104.75	229.23	101.85
SRM 612	Quality Control 2-2	37.5558	10.2716	34.1320	79.0874	36.4396	38.1294	39.5703	42.3721	0.9901	1.2408	65.2587	26.0829
SRM 612	Quality Control 2-2	36.4458	14.7199	30.6915	71.4577	33.2408	33.8366	36.4499	39.2115	0.9213	1.1130	29.1086	28.6327

Standard	Analysis Type	115 In	118 Sn	121 Sb	133 Cs	137 Ba	139 La	140 Ce	141 Pr	146 Nd	147 Sm	153 Eu
SRM 610	Calibration Standard	419.6543	415.9007	382.6098	346.1227	425.0401	419.6900	423.7662	426.6198	411.9388	437.6002	430.3927
SRM 610	Calibration Standard	450.6558	441.6449	399.9075	365.9960	460.1199	455.9598	452.2627	453.5793	444.5088	472.6119	461.6277
SRM 610	Calibration Standard	445.0504	431.2821	393.5071	356.2488	447.2598	443.6196	450.7881	456.8325	439.1756	469.4557	454.4845
SRM 610	Calibration Standard	453.4367	444.5591	412.6005	364.1973	450.6942	445.8741	451.2713	452.1888	433.9838	468.4671	461.4272
SRM 610	Calibration Standard	432.9252	417.5633	382.3920	354.9289	436.5360	436.2171	433.8668	442.4919	429.3565	461.8386	451.0825
SRM 612	Calibration Standard	35.7654	39.0809	34.8525	43.9961	40.1599	35.2424	38.9747	37.4648	35.1020	37.3215	34.0949
SRM 612	Calibration Standard	42.9089	42.3562	36.1890	44.8934	41.0346	37.8425	41.5469	40.3600	36.0356	36.7515	36.2992
SRM 612	Calibration Standard	37.7104	37.4117	34.2294	43.6148	42.0081	35.5545	39.3822	37.9738	36.1222	38.5803	36.6257
SRM 612	Calibration Standard	40.3089	39.6438	36.1903	44.4315	41.6266	36.9295	39.2254	38.4755	36.1905	37.9585	36.0131
SRM 612	Calibration Standard	34.9095	34.4186	32.8427	41.5925	35.4631	34.3178	37.4563	35.9402	33.2950	34.0753	33.0156
SRM 614	Calibration Standard	0.7997	1.7706	0.7436	0.6270	3.1329	0.7422	0.7118	0.7565	0.6398	0.6185	0.7798
SRM 614	Calibration Standard	0.8252	1.6827	0.8419	0.6140	3.4710	0.6064	0.8501	0.7135	0.7181	0.7022	0.7385
SRM 614	Calibration Standard	0.7592	1.5531	0.8304	0.6424	3.0063	0.7952	0.9246	0.8504	0.8440	0.7545	0.7983
SRM 614	Calibration Standard	0.7847	1.9273	0.7694	0.7290	3.6490	0.7500	0.7843	0.7810	0.7993	0.9432	0.8250
SRM 614	Calibration Standard	0.7823	1.4664	0.7643	0.7066	2.7177	0.7063	0.7922	0.7384	0.7591	0.7531	0.7092
SRM 614	Quality Control 1-1	0.7962	1.9241	0.6873	0.6863	3.8101	0.7057	0.7217	0.7386	0.7523	0.6102	0.7122
SRM 614	Quality Control 1-1	0.8354	1.7086	0.8156	0.6896	3.3853	0.6872	0.7155	0.6993	0.7461	0.6896	0.6618
SRM 614	Quality Control 1-1	0.8167	1.8507	0.9130	0.7558	3.0322	0.7060	0.7734	0.6935	0.6747	0.5350	0.7464
	Average	0.8161	1.8278	0.8053	0.7106	3.4092	0.6996	0.7369	0.7105	0.7244	0.6116	0.7068
	Cert. Values	0.79	1.68	0.79	0.664	3.2	0.72	0.813	0.768	0.752	0.754	0.77
	%Recovery	103.31	108.80	101.94	107.01	106.54	97.17	90.63	92.51	96.33	81.11	91.79
SRM 614	Quality Control 1-2	0.7749	2.3353	1.1375	0.6310	2.9724	0.7597	0.8309	0.7964	0.9618	0.6376	0.7289
SRM 614	Quality Control 1-2	0.6478	1.6627	0.9096	0.7389	3.6879	0.7372	0.7793	0.7803	0.6872	0.6679	0.8084
SRM 614	Quality Control 1-2	0.8335	2.1177	0.7792	0.7316	3.3533	0.7568	0.7970	0.7544	0.6969	0.6236	0.7546
	Average	0.7521	2.0386	0.9421	0.7005	3.3379	0.7512	0.8024	0.7770	0.7820	0.6430	0.7640
	Cert. Values	0.79	1.68	0.79	0.664	3.2	0.72	0.813	0.768	0.752	0.754	0.77
	%Recovery	95.20	121.34	119.25	105.50	104.31	104.34	98.69	101.18	103.99	85.28	99.22
SRM 612	Quality Control 2-1	41.1472	41.1279	38.3510	47.5886	43.6417	39.3336	42.0288	41.2929	37.3194	37.8124	36.6938
SRM 612	Quality Control 2-1	36.0985	37.0059	32.6816	40.7666	38.9529	33.9503	36.3799	36.3602	33.6218	36.1755	34.2138
SRM 612	Quality Control 2-1	36.4833	37.3018	34.7675	41.2264	39.5825	35.2157	38.2353	38.2496	34.2920	36.5463	35.4475
	Average	37.9096	38.4785	35.2667	43.1939	40.7257	36.1665	38.8813	38.6342	35.0777	36.8447	35.4517
	Cert. Values	38.9	38.6	34.7	42.7	39.3	36	38.4	37.9	35.5	37.7	35.6
	%Recovery	97.45	99.69	101.63	101.16	103.63	100.46	101.25	101.94	98.81	97.73	99.58
SRM 612	Quality Control 2-2	40.9386	41.7894	36.7135	46.4001	39.3164	35.4511	40.0157	37.8056	35.2506	36.9561	34.4868
SRM 612	Quality Control 2-2	39.9694	40.7389	35.3280	43.9598	39.1730	33.4622	39.5530	37.4557	34.8885	37.2604	35.0273

Standard	Analysis Type	157 Gd	159 Tb	163 Dy	165 Ho	166 Er	169 Tm	172 Yb	175 Lu	178 Hf	181 Ta	182 W
SRM 614	Calibration Standard	0.6837	0.7198	0.7453	0.6685	0.7356	0.6788	0.7519	0.7443	0.6556	0.7931	0.8183
SRM 614	Calibration Standard	0.9306	0.7566	0.7535	0.7511	0.7297	0.7352	0.8276	0.6789	0.6947	0.7842	0.7418
SRM 614	Calibration Standard	0.7070	0.7476	0.7400	0.7923	0.6992	0.7457	0.7643	0.7404	0.8200	0.8543	0.8996
SRM 614	Calibration Standard	0.8981	0.8129	0.8325	0.8361	0.8353	0.7896	0.8382	0.7820	0.7001	0.8431	0.7820
SRM 614	Calibration Standard	0.5970	0.6569	0.6606	0.6956	0.7022	0.7090	0.7064	0.7168	0.6863	0.7633	0.7878
SRM 612	Calibration Standard	35.1711	37.0054	32.5371	36.5578	33.2026	35.0233	34.4755	32.8832	32.8900	35.5195	34.8658
SRM 612	Calibration Standard	37.5306	39.4640	35.8628	40.3271	38.6987	39.8831	39.9226	37.4639	36.5965	40.0301	39.9555
SRM 612	Calibration Standard	38.0429	39.8128	35.8117	40.5258	38.1980	39.4033	38.7836	37.0590	37.5599	40.1431	39.6281
SRM 612	Calibration Standard	37.4336	39.4506	36.4838	40.6432	38.2429	38.5703	38.0026	36.4521	37.2124	40.0780	40.1418
SRM 612	Calibration Standard	34.5949	35.9621	32.0734	37.2153	35.7795	35.9923	35.4093	34.3359	34.1503	36.9249	36.9217
SRM 610	Calibration Standard	439.2022	416.1314	431.0396	422.5590	452.2924	404.1278	456.3365	437.3021	432.0027	422.1493	430.6989
SRM 610	Calibration Standard	469.2528	436.5565	458.1669	446.2948	474.3587	432.7436	480.0968	462.5119	453.4036	439.4016	445.2575
SRM 610	Calibration Standard	462.6328	427.0071	449.2017	438.6957	469.7871	428.6083	474.4268	463.5095	452.5730	443.2769	446.0243
SRM 610	Calibration Standard	460.5685	436.0708	453.1376	449.6637	474.2594	426.7053	473.9073	454.9856	445.1627	431.7684	439.0105
SRM 610	Calibration Standard	457.3628	427.0628	450.5681	444.3910	473.4295	426.2708	471.2574	455.9775	451.1284	438.8048	441.6751
SRM 614	Quality Control 1-1	0.6677	0.7559	0.6890	0.7541	0.7172	0.6445	0.7485	0.6566	0.6706	0.7795	0.7721
SRM 614	Quality Control 1-1	0.7832	0.7502	0.7054	0.7939	0.6960	0.7290	0.7362	0.7520	0.7271	0.8001	0.8582
SRM 614	Quality Control 1-1	0.7460	0.6618	0.7184	0.7218	0.6468	0.6372	0.6891	0.6509	0.4589	0.6502	0.7033
	Avgerage	0.7323	0.7227	0.7043	0.7566	0.6867	0.6702	0.7246	0.6865	0.6189	0.7433	0.7779
	Cert. Values	0.763	0.739	0.746	0.749	0.74	0.732	0.777	0.732	0.711	0.808	0.806
	%Recovery	95.98	97.79	94.41	101.02	92.79	91.56	93.25	93.79	87.04	91.99	96.51
SRM 614	Quality Control 1-2	0.7726	0.8410	0.7792	0.7900	0.8664	0.7388	0.7614	0.8019	0.7139	0.9129	0.8692
SRM 614	Quality Control 1-2	0.7702	0.7501	0.7318	0.8613	0.7282	0.7417	0.7116	0.6590	0.7274	0.8639	0.8311
SRM 614	Quality Control 1-2	0.5980	0.7482	0.6028	0.7379	0.7739	0.7121	0.7219	0.7088	0.6656	0.8656	0.7592
	Avgerage	0.7136	0.7798	0.7046	0.7964	0.7895	0.7309	0.7316	0.7232	0.7023	0.8808	0.8198
	Cert. Values	0.763	0.739	0.746	0.749	0.74	0.732	0.777	0.732	0.711	0.808	0.806
	%Recovery	93.53	105.52	94.45	106.33	106.69	99.85	94.16	98.80	98.78	109.01	101.71
SRM 612	Quality Control 2-1	36.6352	40.0558	36.5884	40.7097	40.0345	39.8088	38.6434	37.0926	37.0182	39.0908	38.6807
SRM 612	Quality Control 2-1	36.3760	38.6552	35.9786	40.3043	38.7375	39.3453	38.4065	36.8563	36.5483	39.0211	39.5469
SRM 612	Quality Control 2-1	36.7891	39.6537	36.0291	39.7887	38.3940	38.6521	38.4312	35.8045	35.4931	39.3038	38.7742
	Avgerage	36.6001	39.4549	36.1987	40.2676	39.0553	39.2687	38.4937	36.5845	36.3532	39.1386	39.0006
	Cert. Values	37.3	37.6	35.5	38.3	38	36.8	39.2	37	36.7	37.6	38
	%Recovery	98.12	104.93	101.97	105.14	102.78	106.71	98.20	98.88	99.06	104.09	102.63
SRM 612	Quality Control 2-2	36.8813	36.7403	32.9103	37.9872	35.8386	36.1301	36.9857	33.1656	34.6889	37.0930	40.1732
SRM 612	Quality Control 2-2	34.5329	36.1562	32.8140	37.0691	35.2854	36.0468	36.1321	33.3629	33.7053	37.0729	41.4663

Standard	Analysis Type	185 Re	195 Pt	197 Au	205 Tl	208 Pb	209 Bi	232 Th	238 U
SRM 614	Calibration Standard	0.1653	2.7412	0.4907	0.2473	2.2206	0.5530	0.7952	0.7737
SRM 614	Calibration Standard	0.1901	2.4391	0.4127	0.2698	2.2276	0.4598	0.7395	0.6682
SRM 614	Calibration Standard	0.1931	2.3001	0.4950	0.2516	2.4434	0.7354	0.8088	0.8257
SRM 614	Calibration Standard	0.1537	2.6245	0.5645	0.3169	2.5036	0.6375	0.7354	1.0906
SRM 614	Calibration Standard	0.1474	2.4688	0.4498	0.2782	2.1915	0.5148	0.6594	0.7509
SRM 612	Calibration Standard	6.0999	2.1400	57.9069	17.5070	36.3112	30.6862	35.6638	37.7794
SRM 612	Calibration Standard	7.1252	2.4409	34.6075	19.8685	41.2883	34.7583	40.1897	41.4973
SRM 612	Calibration Standard	7.0920	2.4818	5.0504	20.1703	40.4403	32.8779	38.1425	38.3281
SRM 612	Calibration Standard	6.9277	2.3958	3.5032	20.6119	43.2311	35.7841	42.3655	44.1985
SRM 612	Calibration Standard	6.5273	2.0011	4.2107	16.8195	35.5846	30.1329	36.9187	37.9556
SRM 610	Calibration Standard	47.6388	2.9960	25.5906	55.1565	401.7426	339.9005	427.2682	407.3965
SRM 610	Calibration Standard	48.6772	3.3874	27.3229	56.3341	416.5073	352.9354	445.8492	432.4451
SRM 610	Calibration Standard	49.6562	3.1908	17.4467	56.1798	423.4349	349.9318	454.4583	442.0532
SRM 610	Calibration Standard	41.1219	3.1239	25.2046	56.5064	429.3305	360.1490	458.1536	441.3194
SRM 610	Calibration Standard	49.0504	3.2344	23.3024	55.9669	417.1777	351.7300	448.8349	428.7462
SRM 614	Quality Control 1-1	0.1741	2.3890	0.4466	0.2412	2.2468	0.3158	0.6907	0.7449
SRM 614	Quality Control 1-1	0.1484	2.0982	0.4820	0.2839	2.4634	0.3527	0.6865	0.7242
SRM 614	Quality Control 1-1	0.1596	2.4082	0.4107	0.2551	2.1538	0.2807	0.5743	0.6790
	Avgerage	0.1607	2.2985	0.4464	0.2601	2.2880	0.3164	0.6505	0.7161
	Cert. Values	0.17	2.36	0.48	0.273	2.32	0.581	0.748	0.823
	%Recovery	94.54	97.39	93.01	95.26	98.62	54.45	86.97	87.01
SRM 614	Quality Control 1-2	0.1809	2.4261	30.3832	0.3495	2.7786	0.3789	0.7835	0.8045
SRM 614	Quality Control 1-2	0.1800	2.7545	3.6441	0.3685	2.4076	-0.0578	0.7525	0.8064
SRM 614	Quality Control 1-2	0.1733	2.3369	4.0884	0.2611	2.4494	-0.0906	0.7497	0.8627
	Avgerage	0.1781	2.5058	12.7053	0.3264	2.5452	0.0768	0.7619	0.8245
	Cert. Values	0.17	2.36	0.48	0.273	2.32	0.581	0.748	0.823
	%Recovery	104.74	106.18	2646.93	119.54	109.71	13.22	101.86	100.19
SRM 612	Quality Control 2-1	6.3835	2.6523	7.3568	19.7442	38.3258	31.8317	38.2303	39.9637
SRM 612	Quality Control 2-1	6.4429	2.2104	11.4802	19.7285	39.1218	31.0723	37.1469	37.2276
SRM 612	Quality Control 2-1	6.6795	2.1853	5.1578	19.0657	37.9709	31.2059	38.2830	37.9439
	Avgerage	6.5020	2.3494	7.9983	19.5128	38.4729	31.3699	37.8867	38.3784
	Cert. Values	6.63	2.51	4.77	14.9	38.57	30.2	37.79	37.38
	%Recovery	98.07	93.60	167.68	130.96	99.75	103.87	100.26	102.67
SRM 612	Quality Control 2-2	6.8653	2.5053	5.5876	19.2064	39.4760	31.3115	35.7452	39.4023
SRM 612	Quality Control 2-2	7.2519	2.3806	3.2274	19.0890	39.0265	30.8274	34.6043	40.1796

Standard	Analysis Type	7 Li	9 Be	11 B	23 Na	24 Mg	27 Al	31 P	39 K	44 Ca	45 Sc
SRM 612	Quality Control 2-2	42.8896	32.8981	-3.5115	111997.1882	59.9166	10493.1663	23.6828	68.9623	84334.5564	37.0636
	Average	43.8634	34.6298	-1.8247	111811.8415	61.8665	10612.7656	46.4264	65.8488	85373.5792	37.1067
	Cert. Values	40.2	37.5	34.3	101634	68	10743	46.6	62.3	85049	39.9
	%Recovery	109.11	92.35	-5.32	110.01	90.98	98.79	99.63	105.70	100.38	93.00
SRM 612	Quality Control 2-3	42.1881	37.5606	-14.3876	103581.6228	91.8569	10292.1656	109.1003	181.5342	92534.7306	43.6167
SRM 612	Quality Control 2-3	38.7396	35.2543	-8.8310	108851.0698	74.6350	10561.5429	125.2876	147.8328	84260.9631	37.2588
SRM 612	Quality Control 2-3	41.0720	35.8946	-16.5946	105929.9499	66.0555	10665.2238	27.5024	94.3072	84647.4412	37.8602
	Average	40.6666	36.2365	-13.2710	106120.8808	77.5158	10506.3108	87.2967	141.2248	87147.7116	39.5786
	Cert. Values	40.2	37.5	34.3	101634	68	10743	46.6	62.3	85049	39.9
	%Recovery	101.16	96.63	-38.69	104.41	113.99	97.80	187.33	226.69	102.47	99.19
SRM 612	Quality Control 2-4	46.3947	37.3120	-19.1326	107704.4810	59.4960	10960.3458	30.3973	82.2009	86646.6301	37.5753
SRM 612	Quality Control 2-4	44.7133	39.5716	-18.0713	103488.4316	61.5515	10693.7928	21.7678	69.5028	86393.5168	38.8276
SRM 612	Quality Control 2-4	40.7123	32.0970	-23.0096	102736.8285	60.8876	10847.6145	46.8282	65.1020	82904.3043	37.6966
	Average	43.9401	36.3269	-20.0712	104643.2470	60.6450	10833.9177	32.9978	72.2686	85314.8170	38.0332
	Cert. Values	40.2	37.5	34.3	101634	68	10743	46.6	62.3	85049	39.9
	%Recovery	109.30	96.87	-58.52	102.96	89.18	100.85	70.81	116.00	100.31	95.32
SRM 610	Quality Control 3-1	470.8312	457.7803	319.3399	99078.1086	467.3223	11154.2321	293.4657	452.3223	84704.6330	491.5945
SRM 610	Quality Control 3-1	458.6731	458.2487	360.7596	97820.2211	469.0890	10950.5519	482.6408	434.8187	86850.5286	509.9473
SRM 610	Quality Control 3-1	473.5883	496.8127	349.3799	100975.7360	452.2482	11098.4279	336.0683	451.3012	85907.8694	514.3670
	Average	467.6975	470.9472	343.1598	99291.3553	462.8865	11067.7373	370.7249	446.1474	85821.0103	505.3030
	Cert. Values	468	476	350	99408	432	10320	413	464	81475	455
	%Recovery	99.94	98.94	98.05	99.88	107.15	107.25	89.76	96.15	105.33	111.06
SRM 610	Quality Control 3-2	485.1324	440.7353	284.4998	101026.6006	458.9465	10763.2563	428.6748	463.3081	85658.9224	482.8358
SRM 610	Quality Control 3-2	466.9917	413.0441	291.0849	99963.0250	426.2621	10482.8788	400.2245	448.6595	83280.4654	492.1277
SRM 610	Quality Control 3-2	481.7997	458.7276	272.9147	100828.9849	461.1738	10650.9752	379.7561	444.9294	86516.6234	498.8915
	Average	477.9746	437.5023	282.8331	100606.2035	448.7941	10632.3701	402.8851	452.2990	85152.0038	491.2850
	Cert. Values	468	476	350	99408	432	10320	413	464	81475	455
	%Recovery	102.13	91.91	80.81	101.21	103.89	103.03	97.55	97.48	104.51	107.97
Corning A	Quality Control A-1	48.1424	0.3607	564.5948	108990.4967	14396.9246	5204.8756	422.6258	23652.9552	40079.8138	0.2203
Corning A	Quality Control A-1	50.5045	0.1562	607.4617	110062.1207	14680.5394	5482.1396	342.7677	23184.5473	39152.8560	0.1540
Corning A	Quality Control A-1	50.5300	0.1562	628.7627	111547.7919	14970.7061	5578.2213	433.5789	24021.8128	40544.5128	0.1561
	Average	49.7256	0.2244	600.2731	110200.1365	14682.7234	5421.7455	399.6574	23619.7718	39925.7275	0.1768
	Cert. Values	46	---	621	106085	16042	5292	567	23825	35949	---
	%Recovery	108.10	---	96.66	103.88	91.53	102.45	70.49	99.14	111.06	---

Standard	Analysis Type	47 Ti	51 V	52 Cr	55 Mn	56 Fe	59 Co	60 Ni	63 Cu	66 Zn	71 Ga	72 Ge
SRM 612	Quality Control 2-2	38.0359	41.7368	39.7843	37.4709	53.4922	36.6244	40.9481	44.1215	42.5802	39.3558	41.0436
	Average	37.6496	42.2410	39.2402	38.7741	55.1311	37.2115	41.7249	43.3274	37.3129	38.0603	40.4672
	Cert. Values	44	38.8	36.4	38.7	51	35.5	38.8	37.8	39.1	36.9	36.1
	%Recovery	85.57	108.87	107.80	100.19	108.10	104.82	107.54	114.62	95.43	103.14	112.10
SRM 612	Quality Control 2-3	40.9793	46.0285	40.5741	46.8701	58.7059	35.8864	45.6768	84.7988	43.2084	33.8036	37.7529
SRM 612	Quality Control 2-3	36.8903	38.9848	37.3973	46.1960	61.9414	37.3506	42.0960	54.2270	37.2206	38.4382	43.0834
SRM 612	Quality Control 2-3	49.9876	39.5248	36.3649	40.1338	116.9496	36.6893	39.7130	46.3379	37.3852	35.5395	43.3052
	Average	42.6191	41.5127	38.1121	44.4000	79.1990	36.6421	42.4952	61.7879	39.2714	35.9271	41.3805
	Cert. Values	44	38.8	36.4	38.7	51	35.5	38.8	37.8	39.1	36.9	36.1
	%Recovery	96.86	106.99	104.70	114.73	155.29	103.22	109.52	163.46	100.44	97.36	114.63
SRM 612	Quality Control 2-4	41.6304	41.0814	36.4608	39.2025	54.8970	35.7347	35.2109	50.1786	39.1138	36.3893	40.8939
SRM 612	Quality Control 2-4	53.7531	40.2267	38.7713	40.0900	52.8483	36.5965	36.7261	38.1205	39.0752	34.7948	37.6473
SRM 612	Quality Control 2-4	44.4857	41.0715	35.3306	37.1321	51.3172	34.0941	40.0508	36.9418	38.0656	34.8705	33.6919
	Average	46.6231	40.7932	36.8542	38.8082	53.0208	35.4751	37.3293	41.7470	38.7515	35.3516	37.4110
	Cert. Values	44	38.8	36.4	38.7	51	35.5	38.8	37.8	39.1	36.9	36.1
	%Recovery	105.96	105.14	101.25	100.28	103.96	99.93	96.21	110.44	99.11	95.80	103.63
SRM 610	Quality Control 3-1	452.4480	454.4983	406.2018	438.0930	436.0765	415.3423	461.4109	459.6152	486.7520	425.2236	430.5484
SRM 610	Quality Control 3-1	435.8752	459.9753	411.1773	442.0828	443.8839	419.2015	465.3314	433.0713	494.3919	434.4632	419.6655
SRM 610	Quality Control 3-1	444.6297	470.9878	423.9449	455.3576	459.5223	433.3692	474.4028	428.1197	508.0034	429.0014	435.4783
	Average	444.3176	461.8205	413.7747	445.1778	446.4942	422.6377	467.0484	440.2688	496.3824	429.5627	428.5641
	Cert. Values	452	450	408	444	458	410	458.7	441	460	433	447
	%Recovery	98.30	102.63	101.42	100.27	97.49	103.08	101.82	99.83	107.91	99.21	95.88
SRM 610	Quality Control 3-2	435.9855	462.5847	406.2408	430.8924	431.2937	399.8935	433.7167	409.9962	474.9340	411.7902	410.1689
SRM 610	Quality Control 3-2	498.5014	464.8539	414.2178	440.6644	446.7741	404.0338	453.4397	421.5807	463.5069	423.8481	420.6357
SRM 610	Quality Control 3-2	436.2127	477.4641	419.8541	444.0348	444.6559	413.7682	446.9252	432.8079	486.5574	409.1245	418.0510
	Average	456.8998	468.3009	413.4375	438.5305	440.9079	405.8985	444.6939	421.4616	474.9994	414.9209	416.2852
	Cert. Values	452	450	408	444	458	410	458.7	441	460	433	447
	%Recovery	101.08	104.07	101.33	98.77	96.27	99.00	96.95	95.57	103.26	95.82	93.13
Corning A	Quality Control A-1	4431.6632	35.9837	20.6477	7066.9093	6029.9048	1377.3150	192.1128	8573.6185	482.4877	0.5597	-0.1531
Corning A	Quality Control A-1	4405.6684	37.5586	19.4329	7096.3433	5925.8551	1366.3325	192.0041	8399.5187	471.9348	0.7116	0.0868
Corning A	Quality Control A-1	4607.7691	38.9299	20.9529	7179.3523	6135.5373	1426.1246	198.5786	8844.0798	511.5798	0.9179	0.0300
	Average	4481.7002	37.4907	20.3445	7114.2017	6030.4324	1389.9241	194.2318	8605.7390	488.6675	0.7297	-0.0121
	Cert. Values	4735	34	7	7745	7624	1337	157	9347	353	---	---
	%Recovery	94.65	110.27	290.64	91.86	79.10	103.96	123.71	92.07	138.43	---	---

Standard	Analysis Type	115 In	118 Sn	121 Sb	133 Cs	137 Ba	139 La	140 Ce	141 Pr	146 Nd	147 Sm	153 Eu
SRM 612	Quality Control 2-2	39.9192	41.3935	36.5832	45.4438	39.2769	34.2803	40.8765	37.6590	34.3030	36.1874	34.5995
	Average	40.2757	41.3073	36.2082	45.2679	39.2554	34.3979	40.1484	37.6401	34.8140	36.8013	34.7045
	Cert. Values	38.9	38.6	34.7	42.7	39.3	36	38.4	37.9	35.5	37.7	35.6
	%Recovery	103.54	107.01	104.35	106.01	99.89	95.55	104.55	99.31	98.07	97.62	97.48
SRM 612	Quality Control 2-3	39.3194	41.4315	51.4136	41.6184	46.5387	34.9588	38.7700	36.8030	34.8843	36.1236	34.1856
SRM 612	Quality Control 2-3	39.4123	41.9038	49.5039	43.3180	43.9979	34.7930	39.4295	38.3763	34.7458	36.3898	36.4054
SRM 612	Quality Control 2-3	40.5189	42.1768	46.7326	44.3927	53.0732	36.0412	40.3045	39.0821	32.7986	39.1315	35.8181
	Average	39.7502	41.8374	49.2167	43.1097	47.8699	35.2643	39.5013	38.0871	34.1429	37.2150	35.4697
	Cert. Values	38.9	38.6	34.7	42.7	39.3	36	38.4	37.9	35.5	37.7	35.6
	%Recovery	102.19	108.39	141.83	100.96	121.81	97.96	102.87	100.49	96.18	98.71	99.63
SRM 612	Quality Control 2-4	37.9790	37.4585	37.4907	43.8733	42.6087	37.1750	40.1041	38.2893	34.9833	36.7560	34.7046
SRM 612	Quality Control 2-4	38.9306	38.8759	36.1490	43.1259	39.6440	37.2562	39.4467	38.6083	34.4919	38.3815	36.2942
SRM 612	Quality Control 2-4	36.5961	36.9964	34.2760	42.9741	39.6349	34.5148	37.1624	36.4010	32.3442	35.0382	34.0386
	Average	37.8352	37.7769	35.9719	43.3244	40.6292	36.3153	38.9044	37.7662	33.9398	36.7253	35.0125
	Cert. Values	38.9	38.6	34.7	42.7	39.3	36	38.4	37.9	35.5	37.7	35.6
	%Recovery	97.26	97.87	103.67	101.46	103.38	100.88	101.31	99.65	95.61	97.41	98.35
SRM 610	Quality Control 3-1	449.3709	433.3983	395.9368	363.4549	445.5892	450.1124	452.4054	457.4296	438.7582	469.5113	459.8285
SRM 610	Quality Control 3-1	447.5534	441.0981	403.1640	372.5334	457.8219	466.0549	458.2620	455.5345	448.9751	485.7547	473.5261
SRM 610	Quality Control 3-1	455.8658	449.9452	409.2198	377.2375	459.0741	459.6703	452.4755	453.7875	448.9625	480.8621	468.6563
	Average	450.9300	441.4805	402.7735	371.0752	454.1617	458.6125	454.3810	455.5839	445.5652	478.7094	467.3370
	Cert. Values	434	430	396	366	452	440	453	448	430	453	447
	%Recovery	103.90	102.67	101.71	101.39	100.48	104.23	100.30	101.69	103.62	105.68	104.55
SRM 610	Quality Control 3-2	433.9967	425.2791	400.3829	363.7662	463.6580	443.9247	461.0591	454.5096	436.7228	468.9277	454.1523
SRM 610	Quality Control 3-2	437.8478	443.8482	408.3343	372.8223	457.6034	444.1245	448.5826	443.1934	427.6454	458.1100	447.5178
SRM 610	Quality Control 3-2	451.7709	452.2175	406.4389	368.9897	452.2580	445.5011	454.2972	450.7605	438.2862	469.9359	457.9557
	Average	441.2051	440.4482	405.0520	368.5261	457.8398	444.5168	454.6463	449.4878	434.2181	465.6578	453.2086
	Cert. Values	434	430	396	366	452	440	453	448	430	453	447
	%Recovery	101.66	102.43	102.29	100.69	101.29	101.03	100.36	100.33	100.98	102.79	101.39
Corning A	Quality Control A-1	7.2708	1543.9951	11718.3868	0.2684	4603.0763	0.3415	0.3014	0.0098	0.1903	-0.0735	0.0016
Corning A	Quality Control A-1	7.0002	1556.3846	11661.4757	0.2175	4713.7472	0.3194	0.2060	0.0057	0.1505	-0.1073	-0.0097
Corning A	Quality Control A-1	7.1822	1586.5399	11941.1276	0.2743	4921.4691	0.3434	0.3026	-0.0025	0.0971	-0.0849	0.0012
	Average	7.1511	1562.3066	11773.6634	0.2534	4746.0976	0.3348	0.2700	0.0044	0.1460	-0.0886	-0.0023
	Cert. Values	---	1497	13174	---	5016	---	---	---	---	---	---
	%Recovery	---	104.36	89.37	---	94.62	---	---	---	---	---	---

Standard	Analysis Type	157 Gd	159 Tb	163 Dy	165 Ho	166 Er	169 Tm	172 Yb	175 Lu	178 Hf	181 Ta	182 W
SRM 612	Quality Control 2-2	34.7495	36.8231	32.9514	36.9473	35.1731	35.9492	35.3101	32.2341	33.3594	36.7100	40.1840
	Avgerage	35.3879	36.5732	32.8919	37.3345	35.4324	36.0421	36.1426	32.9209	33.9179	36.9586	40.6078
	Cert. Values	37.3	37.6	35.5	38.3	38	36.8	39.2	37	36.7	37.6	38
	%Recovery	94.87	97.27	92.65	97.48	93.24	97.94	92.20	88.98	92.42	98.29	106.86
SRM 612	Quality Control 2-3	34.7058	37.5851	33.1342	39.0541	37.2962	37.7546	38.7714	35.9409	36.0650	39.2275	41.3094
SRM 612	Quality Control 2-3	37.5093	37.7263	33.6219	38.9806	37.8007	37.5929	37.5667	35.7679	35.1689	39.0097	40.4550
SRM 612	Quality Control 2-3	37.5160	37.9449	34.8517	38.7835	36.6351	37.3357	36.4027	34.5607	34.6274	38.1661	40.3590
	Avgerage	36.5770	37.7521	33.8693	38.9394	37.2440	37.5611	37.5803	35.4232	35.2871	38.8011	40.7078
	Cert. Values	37.3	37.6	35.5	38.3	38	36.8	39.2	37	36.7	37.6	38
	%Recovery	98.06	100.40	95.41	101.67	98.01	102.07	95.87	95.74	96.15	103.19	107.13
SRM 612	Quality Control 2-4	38.1321	39.5397	36.1493	40.6894	38.2777	38.7608	38.6196	36.9299	37.6727	40.1503	39.8120
SRM 612	Quality Control 2-4	38.1960	39.2324	34.9551	39.1969	37.9058	39.2886	39.2640	37.2670	37.7177	40.2920	40.3946
SRM 612	Quality Control 2-4	35.4393	36.2756	33.1286	36.9481	36.0726	36.4556	35.2911	34.4023	33.7647	37.2590	38.0353
	Avgerage	37.2558	38.3493	34.7443	38.9448	37.4187	38.1684	37.7249	36.1998	36.3850	39.2338	39.4140
	Cert. Values	37.3	37.6	35.5	38.3	38	36.8	39.2	37	36.7	37.6	38
	%Recovery	99.88	101.99	97.87	101.68	98.47	103.72	96.24	97.84	99.14	104.35	103.72
SRM 610	Quality Control 3-1	464.8314	433.1528	456.1315	448.4771	487.3616	436.3624	481.2987	469.5091	465.3096	450.0203	458.9842
SRM 610	Quality Control 3-1	482.7623	439.2561	472.2444	455.1651	490.7682	439.1754	488.6047	469.3058	468.5636	454.9762	450.7245
SRM 610	Quality Control 3-1	479.8944	442.6571	473.8482	461.4469	505.7589	451.4039	502.2129	471.9687	470.9958	458.4338	457.5362
	Avgerage	475.8294	438.3553	467.4081	455.0297	494.6296	442.3139	490.7054	470.2612	468.2897	454.4768	455.7483
	Cert. Values	449	437	437	449	455	435	450	439	435	446	444
	%Recovery	105.98	100.31	106.96	101.34	108.71	101.68	109.05	107.12	107.65	101.90	102.65
SRM 610	Quality Control 3-2	468.2810	474.5496	452.2476	484.4039	467.2680	450.5045	465.2829	452.5928	446.7291	435.2884	438.7984
SRM 610	Quality Control 3-2	453.3060	462.9270	436.8078	468.9646	461.3975	438.1332	461.1796	449.0854	439.8279	432.1025	441.3033
SRM 610	Quality Control 3-2	461.2702	471.7310	447.5524	483.1569	465.7581	433.8986	467.8836	457.3117	453.1282	448.5342	463.9183
	Avgerage	460.9524	469.7359	445.5359	478.8418	464.8079	440.8454	464.7820	452.9966	446.5618	438.6417	448.0067
	Cert. Values	449	437	437	449	455	435	450	439	435	446	444
	%Recovery	102.66	107.49	101.95	106.65	102.16	101.34	103.28	103.19	102.66	98.35	100.90
Corning A	Quality Control A-1	0.0214	-0.0316	0.0353	-0.0199	0.0073	-0.0461	0.0086	-0.0009	0.9791	0.1117	0.0604
Corning A	Quality Control A-1	0.0208	-0.0369	0.0449	-0.0175	0.0177	-0.0451	0.0131	0.0053	1.1444	0.1286	0.0458
Corning A	Quality Control A-1	0.0291	-0.0383	0.0504	-0.0213	0.0108	-0.0450	0.0331	0.0006	1.1372	0.1409	0.0553
	Avgerage	0.0237	-0.0356	0.0435	-0.0196	0.0119	-0.0454	0.0183	0.0017	1.0869	0.1270	0.0538
	Cert. Values	---	---	---	---	---	---	---	---	---	---	---
	%Recovery	---	---	---	---	---	---	---	---	---	---	---

Standard	Analysis Type	7 Li	9 Be	11 B	23 Na	24 Mg	27 Al	31 P	39 K	44 Ca	45 Sc
Corning B	Quality Control B-1	11.8495	0.3649	55.9003	131234.9700	5681.4262	24631.1931	3050.9519	8262.9331	66455.3801	0.0975
Corning B	Quality Control B-1	11.6173	0.1562	49.1936	131667.7947	5744.6016	24649.7486	3276.3316	8227.5340	64694.3720	0.3409
Corning B	Quality Control B-1	11.5156	0.1562	42.5645	127640.7014	5580.6875	24703.0235	3011.5790	8376.8822	66335.4876	0.6274
	Average	11.6608	0.2258	49.2195	130181.1554	5668.9051	24661.3217	3112.9542	8289.1164	65828.4132	0.3553
	Cert. Values	5	---	62	126115	6212	23074	3578	8301	61178	---
	%Recovery	233.22	---	79.39	103.22	91.26	106.88	87.00	99.86	107.60	---
Corning C	Quality Control C-1	52.1872	0.3672	587.4912	10308.7686	15163.8205	4883.5573	410.0652	21868.1218	44786.1703	0.0342
Corning C	Quality Control C-1	50.5632	0.1562	560.8243	9500.9327	15133.5759	4971.7897	409.0326	21148.0652	44889.1313	0.1280
Corning C	Quality Control C-1	54.2998	0.1562	585.6773	9606.9842	15307.7095	4922.9858	370.0833	22944.4762	45556.2431	0.1033
	Average	52.3501	0.2265	577.9976	9805.5619	15201.7020	4926.1109	396.3937	21986.8877	45077.1815	0.0885
	Cert. Values	46	---	621	7938	16645	4604	611	23576	36235	---
	%Recovery	113.80	---	93.08	123.53	91.33	107.00	64.88	93.26	124.40	---
Corning D	Quality Control D-1	26.5345	0.1562	274.2983	11317.1297	22406.4530	28952.1258	15127.0596	78177.1354	113908.4371	0.2867
Corning D	Quality Control D-1	28.3221	0.1562	252.1625	10950.9155	22041.8519	28779.6877	15067.5617	77436.7859	113055.6197	0.2092
Corning D	Quality Control D-1	27.9014	0.1562	273.0654	11463.7890	22294.5349	29918.0298	16085.9131	80226.6448	117042.4006	0.0308
	Average	27.5860	0.1562	266.5087	11243.9447	22247.6133	29216.6144	15426.8448	78613.5221	114668.8191	0.1756
	Cert. Values	23	---	311	8902	23761	28049	17150	93807	105775	---
	%Recovery	119.94	---	85.69	126.31	93.63	104.16	89.95	83.80	108.41	---

Standard	Analysis Type	47 Ti	51 V	52 Cr	55 Mn	56 Fe	59 Co	60 Ni	63 Cu	66 Zn	71 Ga	72 Ge
Corning B	Quality Control B-1	611.4548	201.5423	65.1320	1860.8941	2257.1937	353.7643	786.4425	19162.8115	1944.8857	3.0430	0.1672
Corning B	Quality Control B-1	596.3191	193.6011	61.0294	1795.6193	2182.1550	343.3278	753.2130	19135.6696	1935.7833	2.4721	0.2121
Corning B	Quality Control B-1	614.2520	197.5236	64.6837	1828.1987	2225.0035	352.1636	758.9361	19180.8836	1910.4139	2.3949	0.5485
	Average	607.3420	197.5557	63.6150	1828.2374	2221.4507	349.7519	766.1972	19159.7882	1930.3610	2.6367	0.3093
	Cert. Values	533	168	34	1936	2378	362	786	21250	1526	---	---
	%Recovery	113.95	117.59	187.10	94.43	93.42	96.62	97.48	90.16	126.50	---	---
Corning C	Quality Control C-1	4586.0809	40.5828	17.2719	10.6676	2055.9016	1458.4712	168.3999	8317.3700	554.1057	0.6338	-0.1792
Corning C	Quality Control C-1	4611.0850	42.9104	16.8832	10.1587	2079.4403	1449.0733	163.5719	8262.2984	535.8488	0.6865	-0.2451
Corning C	Quality Control C-1	4788.5329	44.2441	17.3469	11.2867	2103.0208	1468.6814	165.7401	8405.4997	551.0387	0.5840	-0.1407
	Average	4661.8996	42.5791	17.1673	10.7043	2079.4542	1458.7420	165.9040	8328.3894	546.9977	0.6347	-0.1884
	Cert. Values	4735	34	7	6351	2378	1416	157	9027	418	---	---
	%Recovery	98.46	125.23	245.25	0.17	87.45	103.02	105.67	92.26	130.86	---	---
Corning D	Quality Control D-1	2165.1570	103.5264	19.3479	4193.5256	3360.2651	146.5528	392.4238	2960.4197	959.3942	2.4056	0.0374
Corning D	Quality Control D-1	2181.2960	105.8081	18.5034	4163.0464	3288.2370	150.7074	392.1753	2911.0250	943.5306	3.2106	-0.1021
Corning D	Quality Control D-1	2241.9110	107.1897	19.2577	4405.9411	3427.5861	153.1851	416.7399	3069.0917	988.3648	2.7649	0.0852
	Average	2196.1214	105.5081	19.0363	4254.1710	3358.6960	150.1485	400.4463	2980.1788	963.7632	2.7937	0.0068
	Cert. Values	2278	84	17	4260	3637	181	393	3036	803	---	---
	%Recovery	96.41	125.60	111.98	99.86	92.35	82.95	101.89	98.16	120.02	---	---

Standard	Analysis Type	75 As	82 Se	85 Rb	88 Sr	89 Y	90 Zr	93 Nb	95 Mo	103 Rh	105 Pd	107 Ag	111 Cd
Corning B	Quality Control B-1	17.5890	4.8423	11.4825	155.5884	0.5231	186.9499	0.1595	1.3762	0.3849	0.2724	86.7910	0.8402
Corning B	Quality Control B-1	21.3512	2.8391	11.4150	157.6417	0.3576	188.8184	0.1258	1.4968	0.3586	0.2716	52.2352	0.8708
Corning B	Quality Control B-1	21.3465	0.9498	11.9385	158.6508	0.3934	192.6081	0.2351	1.5825	0.3996	0.2707	55.7135	0.5654
	Average	20.0956	2.8770	11.6120	157.2936	0.4247	189.4588	0.1735	1.4852	0.3811	0.2716	64.9132	0.7588
	Cert. Values	---	---	9	161	---	185	---	---	---	---	93	---
	%Recovery	---	---	129.02	97.70	---	102.41	---	---	---	---	69.80	---
Corning C	Quality Control C-1	2.8099	-0.2533	89.7513	2419.8493	0.1662	45.0735	0.6783	3.4285	5.8838	0.3336	85.5767	1.2078
Corning C	Quality Control C-1	1.8074	0.8876	86.1012	2376.9939	0.1926	45.8848	0.6070	2.6222	5.7880	0.3716	17.0994	0.7157
Corning C	Quality Control C-1	2.8354	0.1553	88.9003	2440.3676	0.1852	44.8696	0.6108	3.0479	5.6641	0.3366	36.8885	1.2485
	Average	2.4842	0.2632	88.2509	2412.4036	0.1813	45.2760	0.6320	3.0329	5.7786	0.3473	46.5215	1.0573
	Cert. Values	---	---	91	2452	---	37	---	---	---	---	19	---
	%Recovery	---	---	96.98	98.39	---	122.37	---	---	---	---	244.85	---
Corning D	Quality Control D-1	261.7906	-0.0066	42.5030	516.4229	0.2478	94.6810	0.5844	2.9872	0.3775	0.3385	117.9140	0.5404
Corning D	Quality Control D-1	265.9303	0.3921	41.7969	513.8452	0.3061	91.6867	0.4858	3.2553	0.4716	0.2457	49.6881	0.1790
Corning D	Quality Control D-1	274.2623	1.0463	43.3752	537.5223	0.2312	99.9256	0.6751	3.4227	0.4670	0.3097	66.0923	0.3525
	Average	267.3277	0.4773	42.5584	522.5968	0.2617	95.4311	0.5818	3.2217	0.4387	0.2980	77.8981	0.3573
	Cert. Values	---	---	46	482	---	93	---	---	---	---	47	---
	%Recovery	---	---	92.52	108.42	---	102.61	---	---	---	---	165.74	---

Standard	Analysis Type	115 In	118 Sn	121 Sb	133 Cs	137 Ba	139 La	140 Ce	141 Pr	146 Nd	147 Sm	153 Eu
Corning B	Quality Control B-1	1.0109	210.4406	3454.1087	0.0429	748.8571	0.1817	0.1493	0.0000	0.0620	-0.1183	-0.0428
Corning B	Quality Control B-1	1.1165	207.6296	3466.6274	0.0532	743.1201	0.2216	0.1442	-0.0026	0.0876	-0.0962	-0.0406
Corning B	Quality Control B-1	0.8667	210.1777	3365.2795	0.0224	742.5624	0.2145	0.1269	-0.0167	0.0671	-0.1076	-0.0360
	Average	0.9981	209.4160	3428.6719	0.0395	744.8465	0.2060	0.1401	-0.0064	0.0722	-0.1073	-0.0398
	Cert. Values	---	315	3463	---	1075	---	---	---	---	---	---
	%Recovery	---	66.48	99.01	---	69.29	---	---	---	---	---	---
Corning C	Quality Control C-1	7.3355	1630.9321	2.0475	0.2126	99999.8141	0.2416	0.0446	-0.0255	0.0340	-0.0663	0.9580
Corning C	Quality Control C-1	7.0867	1586.1682	1.5573	0.1824	98439.8999	0.2510	0.0528	-0.0230	0.0288	-0.1013	0.9473
Corning C	Quality Control C-1	7.1678	1604.4051	1.8979	0.2364	99424.2933	0.2604	0.0337	-0.0218	0.0104	-0.0585	0.9896
	Average	7.1967	1607.1684	1.8342	0.2105	99288.0024	0.2510	0.0437	-0.0234	0.0244	-0.0754	0.9650
	Cert. Values	---	1497	226	---	102102	---	---	---	---	---	---
	%Recovery	---	107.36	0.81	---	97.24	---	---	---	---	---	---
Corning D	Quality Control D-1	3.2982	757.0443	6318.9217	0.1571	2952.8477	0.5220	0.2589	0.0033	0.0990	-0.0616	-0.0137
Corning D	Quality Control D-1	3.3783	731.4753	6167.7220	0.0908	2871.7623	0.4915	0.2790	0.0065	0.1114	-0.0969	-0.0309
Corning D	Quality Control D-1	3.5354	747.3806	6263.6433	0.1878	2947.4875	0.5495	0.2516	0.0157	0.1048	-0.0854	-0.0099
	Average	3.4039	745.3001	6250.0957	0.1452	2924.0325	0.5210	0.2632	0.0085	0.1051	-0.0813	-0.0182
	Cert. Values	---	788	7302	---	4568	---	---	---	---	---	---
	%Recovery	---	94.58	85.59	---	64.01	---	---	---	---	---	---

Standard	Analysis Type	185 Re	195 Pt	197 Au	205 Tl	208 Pb	209 Bi	232 Th	238 U
Corning B	Quality Control B-1	-0.0200	0.8423	1.3748	-0.0650	4364.8056	38.3428	0.9128	0.1190
Corning B	Quality Control B-1	-0.0200	0.8965	0.4687	-0.0797	4246.7283	36.8669	0.8415	0.1327
Corning B	Quality Control B-1	-0.0200	0.8754	1.1136	-0.0716	4251.0392	36.7028	0.8396	0.1059
	Avgerage	-0.0200	0.8714	0.9857	-0.0721	4287.5244	37.3042	0.8647	0.1192
	Cert. Values	---	---	---	---	5663	45	---	---
	%Recovery	---	---	---	---	75.71	82.90	---	---
Corning C	Quality Control C-1	-0.0187	5.6637	3.3630	0.1836	340168.1957	41.1394	0.1603	-0.0472
Corning C	Quality Control C-1	-0.0200	5.7592	0.7049	0.1836	358886.8030	43.6401	0.1955	-0.0402
Corning C	Quality Control C-1	-0.0186	5.9031	2.3431	0.1749	359305.0493	43.4747	0.1805	-0.0367
	Avgerage	-0.0191	5.7753	2.1370	0.1807	352786.6827	42.7514	0.1788	-0.0414
	Cert. Values	---	---	---	---	340692	9	---	---
	%Recovery	---	---	---	---	103.55	475.02	---	---
Corning D	Quality Control D-1	-0.0200	0.5823	3.8793	-0.0293	2076.3810	9.9301	0.6298	0.0565
Corning D	Quality Control D-1	-0.0175	0.4256	2.3234	-0.0665	2014.1364	9.6941	0.6557	0.0840
Corning D	Quality Control D-1	-0.0149	0.4708	3.1641	-0.0694	2146.0685	10.3896	0.7285	0.0618
	Avgerage	-0.0175	0.4929	3.1223	-0.0551	2078.8619	10.0046	0.6714	0.0675
	Cert. Values	---	---	---	---	4456	22	---	---
	%Recovery	---	---	---	---	46.65	45.48	---	---

LA-ICP-MS Detection Limits

Mass	Analyte	DL's (ppm)	DL's (ppb)	BEC (ppm)	BEC/30 (ppm)
7	Li	0.07330	73.30	0.05539	0.00185
9	Be	0.18696	186.96	-0.12834	-0.00428
11	B	0.81780	817.80	78.47619	2.61587
23	Na	4.31134	4311.34	0.00000	0.00000
24	Mg	0.00000*	0.00	-2.08778	-0.06959
25	Mg	0.00000	0.00	-4.89174	-0.16306
27	Al	0.00000	0.00	0.00000	0.00000
31	P	39.61081	39610.81	54.07748	1.80258
39	K	1.27231	1272.31	48.38371	1.61279
43	Ca	212.23040	212230.40	0.00000	0.00000
44	Ca	16.58447	16584.47	0.00000	0.00000
45	Sc	0.00000	0.00	0.31995	0.01066
47	Ti	0.00000	0.00	-10.43312	-0.34777
49	Ti	0.00000	0.00	-14.30533	-0.47684
51	V	0.00000	0.00	0.01740	0.00058
52	Cr	0.32123	321.23	-0.03887	-0.00130
55	Mn	0.12254	122.54	0.25910	0.00864
56	Fe	0.36748	367.48	-3.50134	-0.11671
57	Fe	0.00000	0.00	-3.31443	-0.11048
59	Co	0.02128	21.28	0.06817	0.00227
60	Ni	0.00000	0.00	-0.06199	-0.00207
63	Cu	0.08618	86.18	-0.01507	-0.00050
65	Cu	0.09954	99.54	-0.15059	-0.00502
66	Zn	0.00000	0.00	-0.35521	-0.01184
71	Ga	0.00000	0.00	-0.05185	-0.00173
72	Ge	0.39729	397.29	0.55797	0.01860
75	As	0.00000	0.00	0.16203	0.00540
77	Se	0.00000	0.00	-6.94805	-0.23160
78	Se	11.66147	11661.47	13.03104	0.43437
82	Se	5.14214	5142.14	0.33867	0.01129
85	Rb	0.00000	0.00	0.03726	0.00124
86	Sr	1.14892	1148.92	-0.53005	-0.01767
88	Sr	0.00000	0.00	-2.83908	-0.09464
89	Y	0.00000	0.00	0.00369	0.00012
90	Zr	0.00000	0.00	-0.00048	-0.00002
93	Nb	0.00000	0.00	0.06949	0.00232
95	Mo	0.00000	0.00	0.13182	0.00439
97	Mo	0.00000	0.00	0.17349	0.00578
103	Rh	0.00000	0.00	-0.23470	-0.00782

Mass	Analyte	DL's (ppm)	DL's (ppb)	BEC (ppm)	BEC/30 (ppm)
105	Pd	0.00000	0.00	-0.43703	-0.01457
107	Ag	0.05623	56.23	0.24618	0.00821
109	Ag	0.21859	218.59	0.17413	0.00580
111	Cd	0.00000	0.00	0.02567	0.00086
115	In	0.02191	21.91	0.00938	0.00031
118	Sn	0.04192	41.92	-0.13979	-0.00466
121	Sb	0.07046	70.46	0.06219	0.00207
123	Sb	0.04990	49.90	-0.06347	-0.00212
133	Cs	0.03697	36.97	0.05785	0.00193
137	Ba	0.00000	0.00	-0.13891	-0.00463
139	La	0.00000	0.00	0.03309	0.00110
140	Ce	0.00000	0.00	-0.00282	-0.00009
141	Pr	0.00000	0.00	0.05115	0.00170
146	Nd	0.00000	0.00	0.01816	0.00061
147	Sm	0.00000	0.00	0.01969	0.00066
153	Eu	0.00000	0.00	0.02454	0.00082
157	Gd	0.00000	0.00	-0.02468	-0.00082
159	Tb	0.00000	0.00	0.09291	0.00310
163	Dy	0.00000	0.00	0.02695	0.00090
165	Ho	0.00000	0.00	0.08862	0.00295
166	Er	0.00000	0.00	0.02361	0.00079
169	Tm	0.00000	0.00	0.02729	0.00091
172	Yb	0.00000	0.00	0.00251	0.00008
175	Lu	0.00000	0.00	0.01796	0.00060
178	Hf	0.00000	0.00	0.04931	0.00164
181	Ta	0.00000	0.00	0.03434	0.00114
182	W	0.00000	0.00	0.02888	0.00096
185	Re	0.00000	0.00	0.01418	0.00047
195	Pt	0.00696	6.96	-0.98907	-0.03297
197	Au	0.04652	46.52	0.14965	0.00499
205	Tl	0.01208	12.08	0.05685	0.00190
206	Pb	0.01680	16.80	0.08330	0.00278
207	Pb	0.00928	9.28	-0.02339	-0.00078
208	Pb	0.00380	3.80	0.06867	0.00229
208	Pb	0.00408	4.08	0.05198	0.00173
209	Bi	0.01132	11.32	1.26576	0.04219
232	Th	0.00000	0.00	0.09575	0.00319
238	U	0.00000	0.00	0.12375	0.00413

DL approximation = BEC/30

The DL = 0 happens when the isotope has the same CPS for all three replicates of the calibration blank (in most of these cases the blank reps are all 0 CPS). In these cases the standard deviation is 0, so the DL is 0 since DL = 3(std dev of cal blank replicates)/sensitivity factor (the sensitivity factor is the slope of the calibration equation).
http://www.spectroscopyonline.com/spectral-background-radiation-and-background-equivalent-concentration-elemental-spectrochemistry?id=&sk=&date=&pageID=3 uses an approximation for the DL based on the background equivalent concentration (BEC). In this case DL~BEC/30. This may be a way to replace the DL = 0 values, but you should make it explicit that this is what you are doing. There are some cases where the DL = 0 and the BEC/30 is negative - perhaps DL = 0 is the only option in those cases.

A.4. VP-SEM-EDS Analysis of Corning reference glasses (A, B, C, D) and NIST SRM 610, 612.

Results given as oxide weight percent (wt%) and normalized to 100%

Standard	SiO_2	Na_2O	K2O	MgO	Al_2O_3	CaO	MnO	FeO	TiO2	P_2O_5	CuO	BaO	PbO	SO_3	Cl
Corning A	69.04	17.46	2.72	2.06	1.12	5.19	0.00	0.59	1.13	0.00	0.50	0.00	0.00	0.02	0.17
Corning A	68.84	17.64	2.48	2.28	1.20	4.82	0.00	0.65	1.01	0.00	0.60	0.00	0.00	0.32	0.16
Corning A	68.13	16.89	2.73	2.05	0.87	5.19	0.94	0.90	0.92	0.13	0.93	0.32	0.00	0.00	0.00
Corning A	67.60	17.01	2.71	2.12	0.81	5.11	0.91	0.92	0.63	0.00	1.03	0.57	0.57	0.00	0.00
Corning B	60.72	15.86	1.15	0.41	3.38	12.02	0.00	0.52	0.00	0.85	3.65	0.00	0.38	0.82	0.22
Corning B	62.47	19.65	1.00	0.41	3.83	8.66	0.02	0.24	0.15	0.97	1.12	0.00	0.54	0.71	0.22
Corning B	63.39	15.46	1.36	0.33	3.50	12.50	0.03	0.51	0.24	0.95	0.08	0.00	0.61	0.77	0.26
Corning B	61.35	15.92	1.17	0.41	3.41	12.20	0.00	0.53	0.00	0.86	2.70	0.00	0.38	0.83	0.22
Corning C	29.59	1.15	2.82	1.70	0.86	5.63	0.00	0.44	1.26	0.04	1.92	14.29	40.04	0.00	0.26
Corning C	34.41	0.53	2.64	2.51	0.78	4.65	0.00	0.26	2.67	0.00	1.13	9.72	40.53	0.00	0.17
Corning D	56.09	1.65	11.57	3.43	4.82	15.76	0.55	0.30	0.57	4.40	0.28	0.00	0.18	0.20	0.20
Corning D	51.87	1.11	13.85	2.62	4.09	19.70	0.94	0.56	0.79	3.88	0.00	0.00	0.18	0.19	0.21
NIST 610	70.06	15.63	0.09	0.00	2.00	11.87	0.04	0.03	0.00	0.16	0.00	0.12	0.00	0.00	0.00
NIST 610	79.37	18.45	0.00	0.00	2.15	0.00	0.00	0.00	0.00	0.00	0.03	0.00	0.00	0.00	0.00
NIST 612	70.38	15.29	0.00	0.07	2.03	12.18	0.00	0.00	0.01	0.00	0.03	0.00	0.00	0.00	0.00
NIST 612	67.87	19.07	0.00	0.15	1.47	11.35	0.04	0.00	0.00	0.05	0.00	0.00	0.00	0.00	0.00

APPENDIX B - VITREOUS BEADS FROM METHONE: IMAGES AND DATA

B.1. Macrophotographs of Beads and Tomb Assemblages

Tomb 245/1
ΜΕΘΟΝΗ 2005
25/8/2005
ΑΓΡΟΤ. 245
#245/001020, #245/013, 2
ΜΕ 116

Assemblage of beads found in Tomb 245/1 near the right wrist of the interred individual. Five fragments of the glass bead ΜΕΘ 884β are visible between the larger bone bead in the upper left and the top rows of Cu alloy beads. Photo credit: Ian Coyle/Myles Chykerda (left). Detail of ΜΕΘ 884β (right).

Tomb 245/3
ΜΕΘΟΝΗ 2005
ΑΓΡΟΤ. 245
#245/002, 3
ΜΕΘ 5318

Glass bead found in Tomb 245/3 during flotation/water sieving. Photo credit: Jeff Vanderpool

Tomb 245/5
ΜΕΘΟΝΗ 2005
13/9/2005
ΑΓΡΟΤ. 245
#245/013013, 3
ΜΕ 123

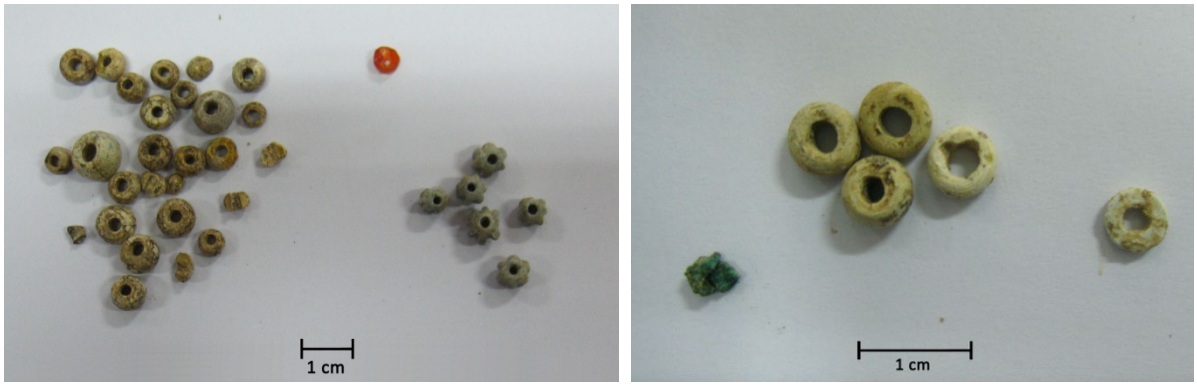

Vitreous beads found in the area of the skull of the individual in Tomb 245/5. These beads are designated as ΜΕΘ 889 and were stored in two different bags. The beads on the left were found during excavation and include glass beads (group of beads in the left part of the image), one carnelian bead (top, center of image) and cogwheel faience beads (right side of image). The image on the right shows material found during water sieving soil collected from the area around the skull. One fragment of a copper alloy was found (left side of image) along with 4 glass beads (center of image) and one faience disc bead (right side of image)

Vitreous beads found in the chest area of the individual in Tomb 245/ 5. These beads are designated as ΜΕΘ 890. There is a mix of material types for these beads. Fragments of an amber bead (left side of image). A group of glass beads (central group in image). A red carnelian bead (right side of image). Fragment of copper alloy (right side of image)

Vitreous beads found at the feet of the individual in Tomb 245/5. These beads are designated as ΜΕΘ 4164. The beads in the image on the right were found during excavation. They consist of beads made of Cu alloy glass faience and bone. A group of these beads was strung on a cord, but it does not represent how they were found in the tomb. Photo credit: Jeff Vanderpool (left). The beads on the right were found during water sieving of the soil recovered from around the feet. This group is made of faience discs as one shell fragment (on the right).

Tomb 245/16
ΜΕΘΟΝΗ 2005
ΑΓΡΟΤ. 245
#245/013028, 5
ΜΕ 190

Vitreous beads found in Tomb 245/16. Glass ellipsoidal bead ΜΕΘ 885α (left). Glass bead with a copper alloy bead within the perforation (ΜΕΘ 885β) (right).

B.2. Photomicrographs of beads analyzed using pXRF and SEM-EDS

Object No.	Sample No.		Bead Dimensions[1]
ΜΕΘ 884β	884β-1		H: 6.44mm W/D: 9mm PD: 3.2mm Wt: 0.2g
ΜΕΘ 885α	885α-1		H: 11.4mm W/D: 8.4mm PD: 3.1mm Wt: 0.5g
ΜΕΘ 885β	885β-1		H: 11.4mm W/D: 8.4mm PD: 3.1mm Wt: 0.2g
ΜΕΘ 885β	885β-2	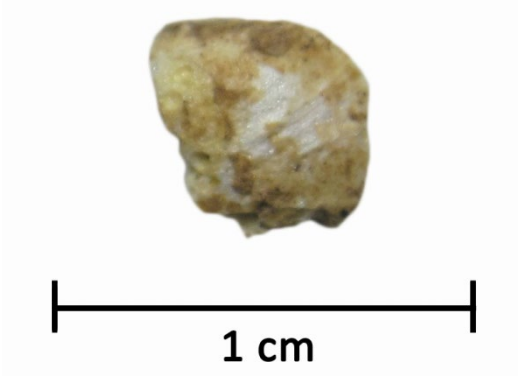	H: 11.4mm W/D: 3.2mm PD: 3.1mm Wt: >1g

ΜΕΘ 889	889-1		H: 5.9mm W/D: 6.7mm PD: 2.0mm Wt: 0.2g
ΜΕΘ 889	889-2		H: 7.1mm W/D: 10.02mm PD: 4.0mm Wt: 0.8g
ΜΕΘ 889	889-3		H:4.2mm W/D: 7.0mm PD: 2.5mm Wt: 0.5g
ΜΕΘ 889	889-4		H: 4.6mm W/D: 7.1mm PD: 2.7mm Wt: 0.5g

ΜΕΘ 889	889-5		H: 3.4mm W/D: 6.5mm PD: 2.8mm Wt: >0.1g
ΜΕΘ 889	889-6		H: 4.1mm W: 5.5mm PD: 2.6mm Wt: >0.1g
ΜΕΘ 889	889-7		H: 2.9mm W/D: 4.9mm PD: 2.7mm Wt: >0.1g
ΜΕΘ 889	889-8	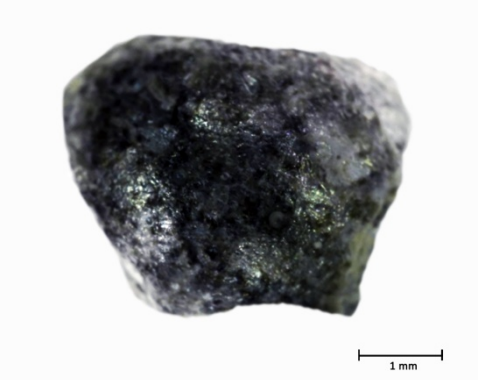	H: 3mm W: 3.8mm PD: 2.2mm Wt: >0.1g

ΜΕΘ 889	889-9		H: 1.4mm W: 5.6mm PD: 2.6mm Wt: >0.1g
ΜΕΘ 889	889-10	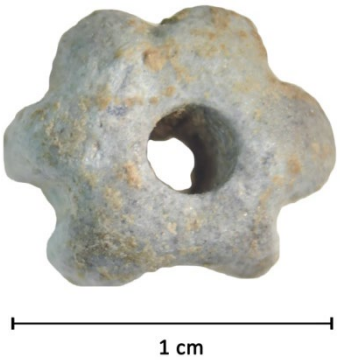	H: 5.9mm W/D: 7.5mm PD: 2mm Wt: 0.2g
ΜΕΘ 889	889-11		H: 3.mm W/D: 8.5mm PD: 2.5mm Wt: 0.1g
ΜΕΘ 890	890-1		H: 4.2mm W/D: 5.1mm PD: 1.9mm Wt: 0.1g

ΜΕΘ 890	890-2	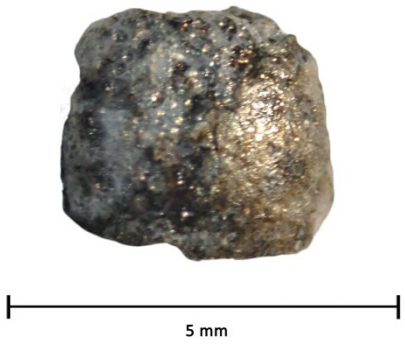	H: 3.3mm W/D: 8.8mm PD: 2.3mm Wt: >0.1g
ΜΕΘ 890	890-3		H: 3.8mm W: 3.7mm PD: 2.2mm Wt: >0.1g
ΜΕΘ 890	890-4		H: 2.9mm W: 5.6mm PD: 2.7mm Wt: >0.1g
ΜΕΘ 890	890-5		H: 4.1mm W: 5.5mm PD: 2.3mm Wt: >0.1g

ΜΕΘ 4164	4164-1		H: 4.8mm W: 8.5mm PD: 3mm Wt: >0.1g
ΜΕΘ 4164	4164-2	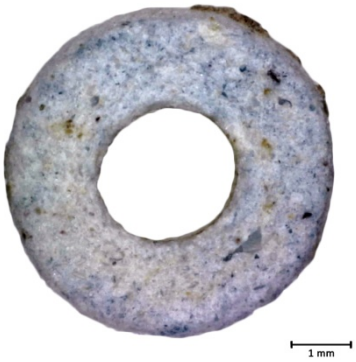	H: 1.4mm W: 4.8mm PD: 1.7mm Wt: >0.1g
ΜΕΘ 4164	4164-3		H: 1.2mm W: 5.8mm PD: 2.7mm Wt: >0.1g
ΜΕΘ 4164	4164-4		H: 1.4mm W: 4.2mm PD: 2.2mm Wt: >0.1g

ΜΕΘ 4164	4164-5	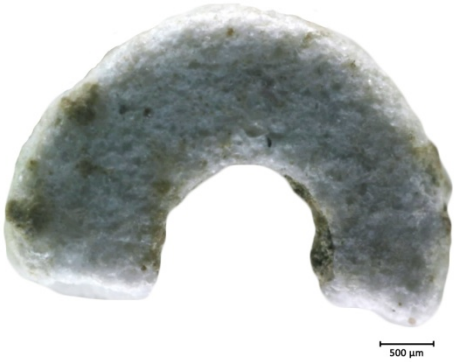	H: 1.4mm W: 4.3mm PD: 1.8mm Wt: >0.1g
ΜΕΘ 4164	4164-6		H: 1mm W/D: 5.4mm PD: 1.8mm Wt: >0.1g
ΜΕΘ 4164	4164-8	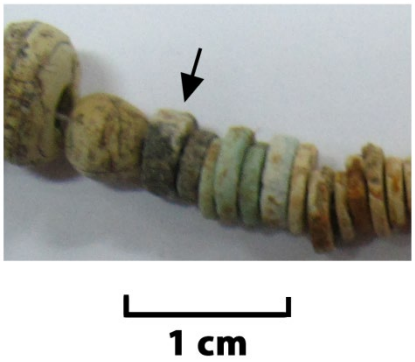	H: 2.1mm W/D: 5.5mm PD: 1.8mm Wt: >0.1g
ΜΕΘ 4164	4164-9		H: 1mm W/D: 4.3mm PD: 1.8mm Wt: >0.1g

ΜΕΘ 4164	4164-10	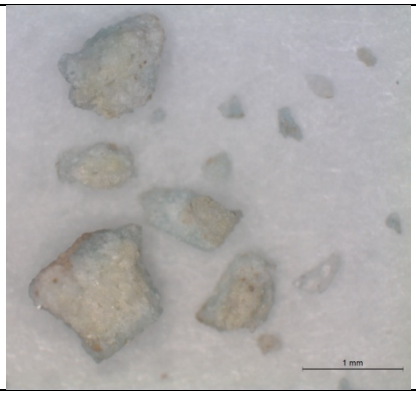	Too fragmentary to measure Wt: >0.1g
ΜΕΘ 4164	4164-11		H: 1mm W/D: 1.4mm Wt: >0.1g
ΜΕΘ 4164	4164-12		H: 1.4mm W/D: 1.6mm Wt: >0.1g
ΜΕΘ 5318	5318-1		H: 6.5mm W/D: 3.5mm PD: 2.4mm Wt: >0.1g

[1]H=Height, W/D=Width/Diameter, PD=Perforation Diameter, Wt=Weight

B.3. SEM-EDS Data

Data given weight % (wt%) and normalized to 100%

Bead 884b-1	Na_2O	MgO	Al_2O_3	SiO_2	P_2O_5	SO_3	K_2O	CaO	TiO_2	MnO	FeO	CoO	CuO	PbO
Area 1	n.d	0.76	4.18	81.85	n.d	n.d	n.d	2.58	n.d	n.d	4.45	n.d	6.20	n.d
Area 1	n.d	1.92	3.91	60.21	n.d	n.d	n.d	4.12	n.d	n.d	1.97	n.d	27.87	n.d
Area 1	n.d	n.d.	3.51	51.86	n.d	n.d	0.42	3.87	n.d	n.d	2.55	n.d	37.78	n.d
Bead 885a-1														
Area 1	n.d	2.54	14.40	61.96	1.53	n.d	1.70	9.83	n.d	2.78	5.26	n.d	n.d	n.d
Area 2	n.d	1.74	11.98	70.24	0.00	n.d	0.99	5.73	n.d	6.50	3.80	n.d	n.d	n.d
Area 3	n.d	3.91	17.71	57.46	n.d	n.d	2.22	3.53	0.95	4.58	6.83	1.59	1.22	n.d
Area 4	n.d	4.65	21.45	56.00	n.d	0.32	2.93	1.67	0.68	2.58	8.20	1.42	0.41	n.d
Bead 889-2														
Area 1	1.02	4.30	3.12	82.74	n.d	0.17	2.09	4.37	n.d	n.d	1.28	n.d	0.93	n.d
Area 2	n.d	6.28	n.d	90.04	n.d	n.d	n.d	3.68	n.d	n.d	n.d	n.d	n.d	n.d
Area 3	0.41	5.25	1.88	83.94	n.d	0.59	1.61	4.40	n.d	n.d	1.50	n.d	n.d	n.d
Area 4	0.94	4.38	2.91	85.72	n.d	n.d	1.17	4.22	0.81	n.d	0.65	n.d	n.d	n.d
Bead 889-3														
Area 1	n.d	2.01	2.30	86.97	n.d	0.97	0.65	3.45	n.d	n.d	3.64	n.d	n.d	n.d
Area 2	n.d	2.05	3.48	84.72	n.d	1.60	0.81	3.95	n.d	n.d	2.92	n.d	n.d	n.d
Bead 889-4														
Area 1	n.d	n.d	n.d	90.65	n.d	n.d	n.d	n.d	n.d	n.d	9.35	n.d	n.d	n.d
Area 2	n.d	1.51	2.75	89.28	n.d	0.64	0.50	1.67	n.d	n.d	3.65	n.d	n.d	n.d
Area 3	n.d	0.78	2.71	90.66	n.d	n.d	n.d	2.27	n.d	n.d	3.59	n.d	n.d	n.d
Bead 889-5														
Area 1	10.84	4.27	3.13	72.54	n.d	1.28	1.98	3.69	n.d	n.d	2.28	n.d	n.d	n.d
Area 2	14.48	5.08	1.78	66.02	n.d	n.d	2.37	4.75	n.d	n.d	2.46	n.d	n.d	3.06
Bead 889-7														
Area 1	n.d	n.d	3.06	57.77	n.d	n.d	n.d	1.54	n.d	n.d	1.93	n.d	n.d	n.d
Area 2	n.d	n.d	6.21	89.31	n.d	n.d	0.36	1.92	n.d	n.d	2.21	n.d	n.d	n.d
Area 3	n.d	1.05	5.71	86.03	n.d	n.d	0.53	2.76	n.d	n.d	2.62	n.d	1.29	n.d
Area 4	n.d	1.80	6.25	85.46	n.d	0.12	n.d	2.72	n.d	n.d	3.31	n.d	n.d	1.05
Bead 889-8														
Area 1	n.d	0.86	0.86	94.74	n.d	0.92	n.d	0.92	n.d	1.70	n.d	n.d	n.d	n.d
Area 2	n.d	0.50	0.35	98.49	n.d	n.d	n.d	0.67	n.d	2.93	n.d	n.d	n.d	n.d
Area 3	n.d	4.69	4.11	77.76	n.d	1.78	0.37	11.29	n.d	n.d	n.d	n.d	n.d	n.d
Bead 889-9														
Area 1	n.d	5.65	7.32	26.38	n.d	n.d	1.78	56.63	n.d	n.d	2.23	n.d	n.d	n.d
Area 2	n.d	2.87	6.53	54.82	n.d	n.d	0.98	33.32	n.d	n.d	1.47	n.d	n.d	n.d
Area 3	n.d	4.01	8.62	43.98	2.63	n.d	1.80	36.69	n.d	n.d	2.28	n.d	n.d	n.d
Area 4	n.d	1.24	4.09	81.63	n.d	n.d	n.d	10.21	n.d	n.d	2.84	n.d	n.d	n.d
Bead 890-1														
Area 1	1.16	3.59	4.33	76.58	n.d	1.19	2.00	6.66	n.d	n.d	4.50	n.d	n.d	n.d
Area 2	1.62	2.84	4.67	73.97	1.16	n.d	1.98	9.59	n.d	n.d	4.16	n.d	n.d	n.d
Area 3	0.68	3.15	4.85	80.72	n.d	n.d	1.64	6.02	n.d	n.d	2.94	n.d	n.d	n.d

Bead 890-3	**Na_2O**	**MgO**	**Al_2O_3**	**SiO_2**	**P_2O_5**	**SO_3**	**K_2O**	**CaO**	**TiO_2**	**MnO**	**FeO**	**CoO**	**CuO**	**PbO**
Area 1	n.d	1.28	5.50	86.16	n.d	n.d	n.d	3.31	n.d	n.d	3.75	n.d	n.d	n.d
Area 2	2.64	3.07	4.89	75.44	n.d	0.55	0.96	4.95	n.d	n.d	7.51	n.d	n.d	n.d
Area 3	2.61	2.09	6.46	74.38	n.d	1.33	0.79	5.28	n.d	n.d	7.06	n.d	n.d	n.d
Area 4	n.d	1.54	5.23	80.45	n.d	n.d	n.d	5.44	n.d	n.d	7.34	n.d	n.d	n.d
Bead 890-4														
Area 1	n.d	2.92	3.54	83.73	n.d	n.d	1.10	3.99	n.d	0.77	3.95	n.d	n.d	n.d
Area 2	n.d	2.37	5.90	77.47	n.d	n.d	0.89	3.67	n.d	n.d	10.59	n.d	n.d	n.d
Area 3	n.d	1.38	8.56	84.09	n.d	n.d	1.08	4.12	n.d	n.d	1.86	n.d	n.d	n.d
Bead 890-5														
Area 1	0.60	2.48	4.52	83.98	n.d	n.d	0.62	3.04	n.d	n.d	4.76	n.d	n.d	n.d
Area 2	0.67	2.10	4.95	86.08	n.d	n.d	0.72	2.34	n.d	n.d	3.81	n.d	n.d	n.d
Area 3	n.d	1.61	3.81	84.15	n.d	n.d	0.58	5.71	n.d	n.d	1.79	n.d	n.d	2.35
Area 4	n.d	2.05	5.89	86.57	n.d	n.d	n.d	2.23	n.d	n.d	2.90	n.d	n.d	1.16
Bead 890-6														
Area 1	17.51	5.60	1.70	62.35	n.d	n.d	3.45	5.87	n.d	n.d	1.75	n.d	n.d	1.76
Area 2	22.06	6.63	n.d	63.07	n.d	n.d	2.59	3.96	n.d	n.d	1.07	n.d	0.63	n.d
Area 3	18.69	5.92	1.63	62.34	n.d	n.d	3.49	4.79	n.d	n.d	1.58	n.d	n.d	1.56
Area 4	20.28	7.36	n.d	63.33	n.d	1.05	3.19	3.69	n.d	n.d	0.79	n.d	n.d	0.32
Area 5	16.65	5.44	1.52	63.21	n.d	n.d	3.57	5.62	n.d	0.58	2.60	n.d	n.d	1.39
Bead 4164-1														
Area 1	1.24	1.33	5.64	82.59	n.d	n.d	0.42	2.61	n.d	n.d	6.17	n.d	n.d	n.d
Area 2	0.71	1.77	3.76	88.21	n.d	n.d	0.44	2.51	n.d	n.d	2.59	n.d	n.d	n.d
Area 3	3.93	2.16	3.57	78.98	n.d	n.d	0.69	4.39	n.d	n.d	3.57	n.d	n.d	2.70
Area 4	1.96	2.31	4.50	80.96	n.d	0.97	0.96	4.65	n.d	n.d	2.78	n.d	n.d	1.88
Bead 4164-2														
Area 1	0.58	0.92	3.93	89.92	n.d	n.d	0.25	1.73	n.d	n.d	0.66	n.d	2.02	n.d
Area 2	n.d	n.d	2.20	96.90	n.d	n.d	n.d	0.90	n.d	n.d	n.d	n.d	n.d	n.d
Area 3	n.d	n.d	1.40	97.03	n.d	n.d	n.d	1.57	n.d	n.d	n.d	n.d	n.d	n.d
Area 4	n.d	n.d	1.77	96.29	n.d	n.d	0.17	1.77	n.d	n.d	n.d	n.d	n.d	n.d
Area 5	n.d	0.29	1.81	96.20	n.d	n.d	n.d	1.70	n.d	n.d	n.d	n.d	n.d	n.d
Bead 4164-3														
Area 1	n.d	1.36	3.79	65.22	5.57	n.d	0.49	21.37	n.d	n.d	2.20	n.d	n.d	n.d
Area 2	n.d	1.25	2.41	89.76	n.d	n.d	0.40	3.67	n.d	n.d	1.38	n.d	1.14	n.d
Area 3	0.52	2.15	4.34	86.43	n.d	n.d	0.91	3.13	n.d	n.d	1.95	n.d	0.56	n.d
Area 4	n.d	2.21	4.92	83.90	n.d	n.d	0.84	6.36	n.d	n.d	1.77	n.d		n.d
Bead 4164-4														
Area 1	n.d	2.18	5.49	59.66	7.21	n.d	1.26	20.39	n.d	n.d	3.81	n.d	n.d	n.d
Area 2	0.89	2.08	5.27	61.84	2.07	n.d	0.95	23.41	n.d	2.66	3.50	n.d	n.d	n.d
Area 3	0.89	1.77	8.05	71.38	n.d	n.d	1.12	12.56	n.d	0.39	4.24	n.d	n.d	n.d
Area 4	n.d	2.42	5.79	74.04	n.d	0.93	1.69	9.25	0.74	1.31	4.86	n.d	n.d	n.d
Bead 4164-5														
*Area 1	n.d	0.81	0.65	95.69	1.91	1.02	0.57	1.84	1.79	n.d	5.93	n.d	0.62	n.d
Area 2	n.d	0.52	1.34	96.41	n.d	n.d	1.35	1.73	n.d	n.d	n.d	n.d	n.d	n.d
Area 3	n.d	n.d	n.d	98.98	n.d	n.d	0.34	1.02	n.d	n.d	n.d	n.d	n.d	n.d
Area 4	0.09	n.d	1.84	75.74	8.20	n.d	n.d	12.70	n.d	n.d	1.44	n.d	n.d	n.d

Bead 4164-6	Na_2O	MgO	Al_2O_3	SiO_2	P_2O_5	SO_3	K_2O	CaO	TiO_2	MnO	FeO	CoO	CuO	PbO
Area 1	n.d	2.07	4.12	88.78	n.d	n.d	n.d	2.87	n.d	n.d	2.16	n.d	n.d	n.d
Area 2	n.d	3.17	7.19	81.81	n.d	n.d	1.00	5.03	n.d	n.d	1.79	n.d	n.d	n.d
Area 3	n.d	2.62	4.80	88.95	n.d	n.d	n.d	0.84	n.d	n.d	1.32	n.d	0.79	n.d
Area 4	n.d	6.78	8.22	69.56	n.d	n.d	0.85	7.71	n.d	n.d	5.89	n.d	0.98	n.d

APPENDIX C - VITREOUS BEADS FROM KEFALONIA: IMAGES AND DATA

C.1. Macrophotographs of beads analyzed

Mazarakata

Box 18

Box 23

Box 32

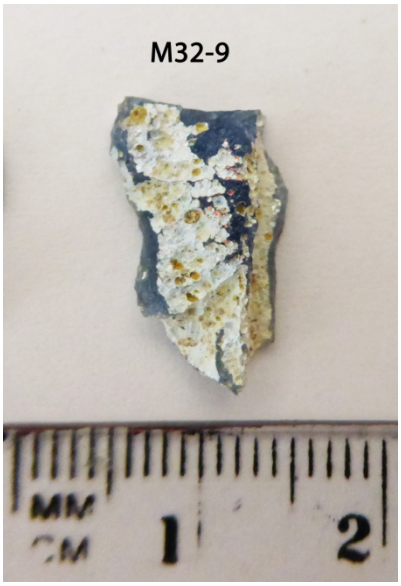

Box 32R

Box 40

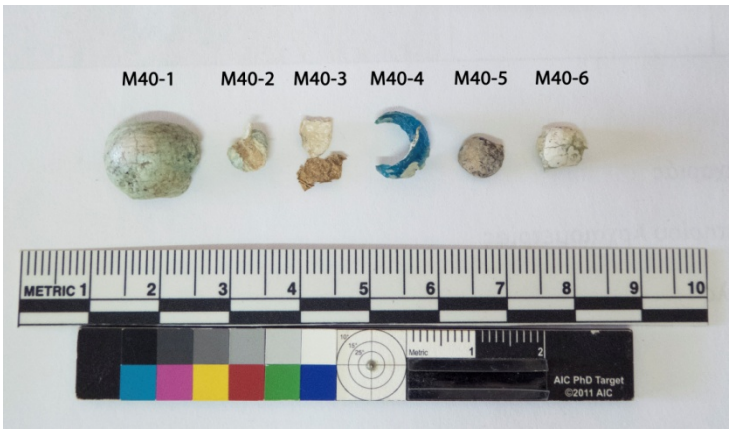

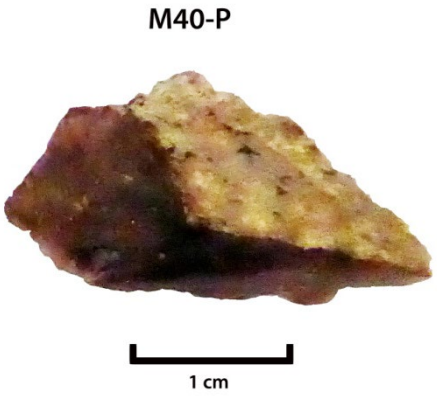

Metaxata

Box K13

Box 1615

Box 1616

Kokkolata-Menegata

Box 580.2

Box Σ2-K1

C.2. EPMA results

Data is given as weight percent (wt%) oxide

Sample No.	Na_2O	K_2O	MgO	Al_2O_3	CaO	SiO_2	FeO	MnO	CuO	P_2O_5	TiO_2	Total
M18-3	16.67	2.48	4.92	1.02	4.27	69.76	0.38	0.02	0.05	0.09	0.07	99.72
M18-3	16.55	2.50	4.93	0.97	4.18	69.27	0.44	0.01	0.02	0.16	0.06	99.10
M18-3	16.35	2.52	4.88	1.02	4.12	69.46	0.42	0.05	n.d.	0.17	0.08	99.07
M23-2	17.14	1.14	3.26	2.67	7.65	66.49	0.53	0.13	0.11	0.20	0.14	99.46
M23-2	17.31	1.17	3.18	2.66	7.52	66.40	0.51	0.14	n.d.	0.18	n.d.	99.19
M23-2	17.04	1.10	3.33	2.68	7.57	66.54	0.57	0.15	0.12	0.18	0.11	99.38
M23-6	18.07	1.10	1.90	1.28	5.27	70.28	0.43	n.d.	1.08	0.11	0.11	99.67
M23-6	18.17	0.98	1.71	1.05	5.01	71.24	0.42	n.d.	1.08	n.d.	n.d.	99.82
M23-6	18.29	1.04	2.24	1.81	5.68	68.93	0.61	n.d.	0.89	0.15	0.14	99.81
M23-7	17.10	1.02	3.11	2.36	7.02	67.19	0.75	0.17	0.09	0.21	0.15	99.15
M23-7	17.37	1.08	3.16	2.34	6.67	68.02	0.71	0.17	0.21	0.22	0.14	100.10
M23-7	17.14	1.08	3.13	2.35	6.90	67.47	0.71	0.18	0.21	0.22	0.15	99.54
M32-1	16.80	1.25	3.54	2.60	8.36	64.94	0.74	0.18	0.14	0.19	0.17	98.91
M32-1	16.65	1.27	3.49	2.70	8.18	64.89	64.89	0.17	0.08	0.25	0.19	98.62
M32-1	16.64	1.29	3.51	2.80	8.22	64.77	0.76	0.12	0.16	0.23	0.12	98.62
M32-9	16.70	1.17	2.97	2.26	7.97	66.98	0.48	0.13	0.04	0.21	0.07	98.99
M32-9	16.48	1.42	2.86	2.07	7.76	67.44	0.48	0.11	0.14	0.22	0.11	99.10
M32-9	16.66	1.08	2.95	2.20	8.06	67.48	0.47	0.13	0.04	0.23	0.06	99.36
M32-4R	16.19	1.10	2.76	2.00	7.52	68.43	0.42	0.08	0.03	0.22	n.d.	98.79
M32-4R	16.72	1.19	2.84	2.01	7.90	67.58	0.50	0.10	0.03	0.21	0.13	99.20
M32-4R	16.51	1.10	2.91	2.23	8.03	67.11	0.46	0.12	n.d.	0.25	0.13	98.85
M40-1 blue	0.08	0.08	0.14	1.95	1.00	75.19	0.77	n.d.	1.29	n.d.	0.12	80.61
M40-1 blue	n.d.	n.d.	0.19	1.30	1.09	86.60	0.67	n.d.	1.78	n.d.	n.d.	91.83
M40-1 blue	n.d.	n.d.	0.23	1.27	1.11	84.78	0.57	n.d.	1.85	n.d.	n.d.	89.89
M40-1 green	0.06	0.05	0.12	1.37	1.17	83.08	0.68	0.01	2.11	0.01	0.10	88.75
M40-1 green	0.06	0.03	0.15	1.45	1.28	54.85	0.75	0.03	19.58	n.d.	0.13	78.30
M40-1 green	0.05	0.07	0.29	1.59	1.16	58.91	0.75	0.06	15.98	0.04	0.16	79.03
M40-4	16.33	3.25	4.64	1.30	6.58	65.68	0.36	n.d.	1.09	0.19	0.04	99.48
M40-4	16.59	3.23	4.61	1.27	6.74	65.16	0.37	0.08	1.16	0.17	0.03	99.40
M40-4	17.02	3.18	4.80	1.19	6.66	64.71	0.29	n.d.	1.19	0.15	0.04	99.23
M40-5	19.29	2.59	3.52	0.69	6.60	64.72	0.70	0.56	0.01	0.40	0.08	99.15
M40-5	19.42	2.64	3.45	0.70	6.68	64.85	0.67	0.52	0.01	0.37	0.05	99.33
M40-5	19.13	2.60	3.56	0.72	6.73	64.78	0.67	0.50	n.d.	0.41	0.08	99.17
M40-6	0.01	n.d.	0.09	0.84	1.19	82.39	0.36	0.01	1.31	n.d.	0.05	86.25
M40-6	0.03	0.01	0.17	0.86	1.17	81.53	0.33	0.02	1.80	n.d.	0.06	85.97
M40-6	0.05	0.03	0.11	0.82	1.25	82.02	0.39	0.01	1.49	n.d.	0.09	86.24
M40-P	16.24	2.19	4.15	0.60	8.08	66.90	0.36	0.22	0.04	0.38	0.05	99.20
M40-P	16.23	2.08	4.15	0.64	8.12	66.72	0.34	0.31	0.00	0.27	0.06	98.91
M40-P	16.26	2.19	4.15	0.60	8.06	66.89	0.35	0.26	n.d.	0.28	0.05	99.09
K13-4	16.66	1.68	3.26	3.32	5.94	66.14	1.14	0.11	0.48	0.17	0.21	99.12
K13-4	17.03	1.60	3.22	2.09	6.12	67.53	0.78	0.13	0.50	0.15	0.14	99.31
K13-4	16.73	1.74	3.23	2.09	6.09	67.62	0.68	0.12	0.49	0.22	0.15	99.13
580.2-1	6.10	10.79	0.47	2.74	1.03	74.92	0.52	0.02	2.64	0.14	0.14	99.51
580.2-1	6.20	10.52	0.44	2.78	1.08	75.25	0.61	0.01	2.80	0.12	0.12	99.92
580.2-1	6.08	10.80	0.44	2.75	1.04	75.65	0.59	0.01	2.69	n.d.	0.11	100.24
580.2-2	17.17	0.98	1.35	1.17	7.66	67.20	0.59	0.06	3.28	0.17	n.d.	99.71
580.2-2	16.96	1.02	1.30	1.15	7.50	67.16	0.62	0.05	3.11	0.19	0.09	99.15
580.2-2	16.89	1.04	1.33	1.17	7.49	67.10	0.61	0.06	3.19	0.11	0.11	99.11
580.2-3	17.13	1.54	2.78	1.97	6.68	67.17	0.64	0.11	0.38	0.16	0.06	98.62
580.2-3	17.23	1.60	2.85	2.10	6.75	67.23	0.65	0.11	0.62	0.22	0.11	99.46
580.2-3	17.19	1.60	2.84	2.07	6.77	67.22	0.63	n.d.	0.45	0.13	0.08	99.05
Σ2-K1-1	16.66	2.54	4.70	1.78	4.76	68.14	0.71	0.02	0.00	0.17	0.09	99.59
Σ2-K1-1	16.55	2.48	4.78	1.45	4.87	68.15	0.70	0.05	n.d.	0.18	n.d.	99.25
Σ2-K1-1	16.63	2.56	4.71	1.93	4.68	68.19	0.70	0.04	0.04	0.11	0.13	99.73
Σ2-K1-4	11.90	0.74	0.43	0.34	1.16	69.73	6.48	0.02	3.18	0.05	0.06	94.08
Σ2-K1-4	12.98	0.89	0.55	1.33	1.46	67.18	4.88	n.d.	3.81	0.04	0.03	93.15
Σ2-K1-4	8.93	0.67	0.45	1.90	0.68	79.10	3.19	0.05	2.38	0.13	0.68	98.14

C.3. LA-ICP-MS Data

Data is given as parts per million (ppm)

Sample	Replicate	7 Li	9 Be	11 B	23 Na	24 Mg	27 Al	31 P	39 K	44 Ca	45 Sc	47 Ti
M18-3	1	26.098	0.270	107.944	133130.121	28323.395	5703.498	426.049	20288.352	34091.846	1.079	335.871
M18-3	2	27.730	0.375	114.657	130171.591	28055.512	5974.045	506.504	20562.180	34223.667	0.998	335.915
M18-3	3	25.484	0.374	100.776	131550.139	28252.861	5798.538	504.000	20753.722	34748.586	1.047	346.821
M23-2	1	11.335	2.507	69.692	130049.375	17753.876	14791.239	493.840	8975.370	62406.580	1.803	676.917
M23-2	2	9.941	3.695	68.127	132570.399	17884.547	15585.024	500.093	9110.024	60630.911	2.213	612.873
M23-2	3	9.699	3.729	71.514	134752.406	17805.680	14942.474	551.437	8884.187	60435.898	2.182	598.572
M23-6	1	15.025	0.497	91.682	142344.883	10647.294	7972.430	478.517	9972.773	46870.348	1.344	600.953
M23-6	2	12.371	0.708	106.972	145844.913	9806.566	7294.768	319.691	8662.404	40547.473	2.039	592.173
M23-6	3	13.359	1.209	93.698	135572.361	15947.483	18351.059	591.551	13300.859	67851.103	2.789	933.585
M23-7	1	11.286	1.672	124.340	135401.847	17040.903	13138.811	534.946	8586.500	52035.088	0.899	764.558
M23-7	2	10.244	0.799	112.135	128365.585	16282.332	12798.652	458.489	8324.927	52477.734	1.429	744.483
M23-7	3	11.641	1.587	136.685	130145.351	16618.687	12937.330	475.465	8278.168	53366.790	1.708	800.487
M32-1	1	10.831	1.635	80.956	122822.571	18343.974	14564.762	741.401	9839.959	62348.519	1.600	911.014
M32-1	2	10.520	1.471	87.282	125440.142	18659.328	14563.448	741.966	9939.477	62460.223	1.756	837.952
M32-1	3	12.334	1.286	96.597	125881.936	18472.353	14701.777	703.319	10042.867	63240.469	1.643	906.397
M32-9	1	9.715	1.484	65.793	129119.853	16127.566	11838.600	509.496	8955.153	64164.417	0.527	640.013
M32-9	2	8.952	1.293	70.083	128291.948	15473.476	11873.698	615.298	8747.170	64502.851	1.269	619.972
M32-9	3	8.379	1.705	74.349	129115.382	15570.319	11619.189	626.224	9452.323	66665.621	1.606	636.675
M32-4R	1	9.558	2.567	72.807	130055.632	16357.477	12281.862	621.462	8763.079	64530.672	1.443	647.415
M32-4R	2	9.272	3.205	73.215	130585.218	16180.712	11896.729	562.601	8822.205	65228.437	1.358	624.037
M32-4R	3	5.918	0.844	10.257	83001.210	9666.708	6315.417	434.303	5996.229	36393.282	0.685	325.493
M40-1	1	0.189	0.479	-77.375	846.742	618.649	15183.396	-29.803	225.195	13072.987	2.067	784.328
M40-1	2	0.208	0.829	-67.764	923.665	1012.684	17212.624	92.195	299.239	14685.072	4.262	1156.606
M40-1	3	0.191	0.662	-54.283	820.383	982.686	14364.971	60.896	258.999	17605.218	4.688	1789.360
M40-4	1	23.123	0.495	126.140	127172.564	26423.913	7106.760	521.984	24953.974	51253.039	0.762	317.257
M40-4	2	23.560	0.161	124.182	127809.932	26779.742	7042.139	643.344	24777.039	52897.757	0.595	305.474
M40-4	3	25.833	0.161	118.391	131026.185	27156.791	7250.188	380.608	25275.160	52294.340	1.103	299.710
M40-5	1	6.372	0.485	48.677	141196.102	18402.595	3752.310	1596.467	19986.785	50920.231	0.509	515.889
M40-5	2	6.931	0.273	45.616	144712.739	18928.550	3759.330	1377.605	20533.019	52159.511	0.535	469.581
M40-5	3	7.503	0.161	45.113	145386.129	18834.878	3844.799	1634.950	20635.360	52404.729	0.416	507.426
M40-6	1	0.078	0.389	-77.448	482.334	665.972	4899.701	-32.018	11.520	8814.820	0.730	316.767
M40-6	2	0.114	0.366	-84.716	255.649	563.594	4938.261	-36.930	5.322	10797.935	0.681	324.358
M40-6	3	0.033	0.355	-82.411	377.249	1124.146	5002.693	-46.024	9.445	11869.714	1.432	345.586
M40-P	1	7.908	0.275	23.031	119427.235	23534.140	3381.049	902.166	16584.738	65419.197	0.608	363.342
M40-P	2	6.610	0.161	15.468	116443.351	22983.076	3377.427	951.911	16814.247	64713.252	0.647	370.487
M40-P	3	8.002	0.271	27.142	119992.534	23590.768	3326.562	1010.135	16726.067	61928.410	0.637	339.768
K13-4	1	23.649	1.418	97.241	133423.929	17109.138	11428.932	523.120	13249.549	45425.952	0.909	625.578

Sample	Replicate	51 V	52 Cr	55 Mn	56 Fe	59 Co	60 Ni	63 Cu	66 Zn	71 Ga	72 Ge	75 As	82 Se	85 Rb
M18-3	1	10.522	20.498	355.046	3360.265	8.698	15.772	21.380	13.510	1.341	0.550	1.046	-0.103	10.605
M18-3	2	10.056	20.604	348.437	3441.579	7.543	15.371	14.432	14.342	1.567	0.656	1.529	-0.185	11.075
M18-3	3	10.384	18.272	350.375	3355.397	3.004	15.745	9.107	14.067	1.354	0.588	1.774	-0.203	10.972
M23-2	1	11.404	8.148	1212.940	4093.897	413.412	299.793	488.094	578.307	1.937	0.576	3.190	0.550	6.656
M23-2	2	10.733	6.983	1163.126	3887.817	406.296	301.165	520.059	578.349	1.528	0.532	2.545	-1.746	6.699
M23-2	3	9.642	7.713	1131.621	3749.280	407.575	299.785	530.396	605.583	1.710	0.415	3.211	-0.664	6.328
M23-6	1	11.869	8.476	312.574	4229.527	124.056	85.581	7419.984	201.281	1.851	0.249	20.521	1.645	10.173
M23-6	2	9.900	7.262	242.257	3632.250	89.749	66.725	6160.997	156.399	1.514	0.360	18.500	2.042	8.120
M23-6	3	22.747	16.055	863.456	6660.596	531.885	330.631	5293.531	831.570	2.917	1.371	18.337	0.755	16.372
M23-7	1	13.489	9.933	1290.934	5028.557	453.567	305.523	1259.970	650.361	2.671	0.730	4.736	-1.725	6.788
M23-7	2	14.029	9.500	1303.135	5029.146	452.525	303.440	1155.949	625.578	1.683	0.962	3.532	2.387	6.968
M23-7	3	13.976	9.460	1298.991	4980.039	454.037	306.343	1107.743	627.973	1.775	0.556	5.074	-0.077	6.917
M32-1	1	14.445	11.612	1024.498	5277.830	451.528	307.967	1187.201	646.967	2.271	0.258	4.310	2.280	8.462
M32-1	2	14.854	11.229	1058.875	5123.740	456.472	311.331	1213.971	634.669	2.234	0.424	5.310	-0.628	8.573
M32-1	3	15.161	12.414	1067.409	5395.447	476.602	328.483	1215.146	671.912	2.429	0.253	4.807	1.680	8.080
M32-9	1	10.508	7.902	793.112	3772.552	286.721	187.260	146.849	430.066	1.356	0.368	1.190	3.176	6.703
M32-9	2	11.373	6.921	752.060	3667.091	286.842	188.578	148.445	431.854	1.513	0.433	0.981	-2.852	5.916
M32-9	3	11.777	8.303	806.848	3833.270	301.547	199.268	161.265	452.717	1.442	0.627	1.060	1.025	6.397
M32-4R	1	12.492	8.272	804.570	3912.474	292.867	192.114	172.416	426.496	1.405	0.603	1.648	-1.562	5.941
M32-4R	2	11.139	7.409	767.820	3611.618	277.315	181.262	158.166	424.481	1.559	0.585	1.753	-1.607	5.352
M32-4R	3	6.221	3.995	492.434	2164.525	176.282	114.246	112.454	283.636	1.136	1.014	0.462	0.399	4.166
M40-1	1	1.436	65.136	123.356	7564.365	2.393	11.141	9034.389	77.605	2.524	-0.193	0.544	1.854	0.330
M40-1	2	2.565	95.280	194.460	10941.310	4.817	26.483	18334.793	100.643	2.363	0.180	1.071	-0.011	0.283
M40-1	3	8.366	121.165	412.664	10307.768	9.446	66.786	108790.835	261.173	4.748	0.115	1.664	1.023	0.256
M40-4	1	9.567	16.092	387.944	2470.653	4.883	10.928	7328.544	21.101	2.013	0.831	6.458	-1.104	15.259
M40-4	2	8.980	15.055	390.857	2483.445	4.809	12.014	7682.147	19.175	2.241	1.101	5.041	0.550	13.737
M40-4	3	9.463	14.511	395.957	2442.768	5.180	10.201	7461.379	17.581	1.967	0.764	4.743	4.851	14.148
M40-5	1	12.393	5.883	3744.526	4954.864	2.381	3.382	33.591	21.906	1.202	0.665	0.268	-0.676	9.486
M40-5	2	12.141	5.132	3823.071	4995.127	2.561	4.256	23.972	20.693	0.632	0.899	0.939	-0.010	10.621
M40-5	3	12.258	4.946	3668.152	4958.142	2.560	3.777	25.627	21.149	1.189	0.307	1.065	1.048	10.429
M40-6	1	1.460	33.002	41.151	2931.613	0.573	2.473	10666.326	52.002	1.443	-0.272	3.933	1.209	0.110
M40-6	2	1.839	30.957	49.362	2910.032	0.535	1.621	12053.892	38.836	1.506	-0.052	0.006	0.641	0.045
M40-6	3	1.367	35.100	85.370	3122.357	1.003	3.235	13951.198	53.492	1.283	-0.074	0.689	-1.042	0.043
M40-P	1	7.005	3.817	2120.051	2505.815	4.871	6.002	120.776	28.570	1.392	0.259	1.362	0.627	7.318
M40-P	2	8.087	6.421	2149.920	2734.248	7.728	7.153	53.999	30.124	0.890	0.374	1.331	-1.647	7.320
M40-P	3	6.243	4.649	1917.485	2328.090	4.503	6.369	37.993	24.885	1.095	0.300	1.575	-0.068	7.876
K13-4	1	12.273	13.028	991.727	4990.554	563.801	354.340	3232.528	723.662	2.423	0.667	21.115	1.779	11.543

Sample	Replicate	88 Sr	89 Y	90 Zr	93 Nb	95 Mo	103 Rh	105 Pd	107 Ag	111 Cd	115 In	118 Sn	121 Sb	133 Cs	137 Ba
M18-3	1	325.197	2.919	13.802	1.222	0.618	-0.075	0.323	36.611	0.483	0.069	0.611	2.914	0.346	43.328
M18-3	2	333.683	3.136	13.621	1.234	0.790	-0.075	0.338	5.149	0.338	0.050	0.479	1.539	0.394	45.172
M18-3	3	337.718	3.123	13.393	1.174	0.707	-0.075	0.323	-0.110	0.000	0.040	0.478	1.158	0.360	43.247
M23-2	1	830.056	10.230	54.014	1.940	0.137	-0.075	0.339	52.681	0.212	0.120	17.922	197.436	0.104	54.546
M23-2	2	778.733	9.938	54.318	1.852	-0.005	-0.072	0.369	38.344	0.136	0.126	16.852	211.382	0.127	58.781
M23-2	3	808.311	11.060	55.084	1.932	-0.031	-0.075	0.385	18.835	0.205	0.079	16.075	215.115	0.077	58.216
M23-6	1	451.916	5.242	51.111	2.011	0.387	-0.064	0.339	14.947	0.212	2.573	580.380	1893.668	0.181	70.416
M23-6	2	428.655	4.646	48.554	1.865	0.159	-0.075	0.401	2.359	0.277	2.835	653.097	1930.912	0.087	57.839
M23-6	3	609.571	10.205	70.090	3.188	0.233	-0.068	0.323	21.414	0.737	1.364	300.290	2317.040	0.396	99.496
M23-7	1	710.805	8.413	63.740	2.229	0.236	-0.068	0.415	89.149	0.068	0.400	68.790	67.665	0.156	63.802
M23-7	2	716.761	8.902	59.909	2.456	0.153	-0.075	0.353	41.249	0.202	0.304	63.504	65.522	0.098	62.700
M23-7	3	735.525	8.901	64.533	2.446	0.160	-0.072	0.339	55.743	0.347	0.274	69.759	67.670	0.106	64.145
M32-1	1	950.674	12.133	66.919	2.439	0.253	-0.075	0.355	95.546	0.718	0.408	76.602	312.851	0.130	71.403
M32-1	2	938.321	12.220	66.591	2.585	0.159	-0.065	0.385	49.984	0.415	0.360	73.556	288.052	0.073	66.794
M32-1	3	963.600	13.541	67.691	2.612	0.111	-0.064	0.371	63.586	0.570	0.340	71.401	296.120	0.124	66.563
M32-9	1	956.839	5.387	47.357	1.995	0.189	-0.075	0.354	9.216	0.070	0.080	3.846	24.512	0.083	60.179
M32-9	2	914.729	5.770	46.143	1.733	0.324	-0.075	0.352	-0.041	0.065	0.063	2.938	21.745	0.067	58.711
M32-9	3	931.246	6.071	48.435	2.116	0.079	-0.072	0.354	50.642	0.070	0.075	4.249	28.441	0.055	61.867
M32-4R	1	934.809	6.344	47.996	1.925	0.001	-0.075	0.372	156.869	0.943	0.077	7.734	36.419	0.107	61.306
M32-4R	2	933.586	6.178	46.135	2.022	0.111	-0.068	0.339	86.369	0.857	0.071	5.537	30.907	0.125	58.350
M32-4R	3	502.881	3.048	21.288	0.985	0.012	-0.075	0.365	62.263	0.679	0.065	3.653	32.681	0.058	33.336
M40-1	1	28.027	2.723	40.205	2.121	-0.065	-0.067	0.357	31.266	0.252	0.084	3.640	6.975	0.003	6.838
M40-1	2	33.152	4.486	46.535	2.491	-0.085	-0.068	0.355	9.296	0.071	0.125	5.629	8.469	0.007	9.847
M40-1	3	32.182	11.635	40.843	3.923	-0.085	-0.015	0.437	6.146	0.508	0.093	4.777	18.232	-0.017	8.417
M40-4	1	640.232	3.341	28.309	1.670	0.411	-0.050	0.339	71.839	0.774	0.100	1.656	2.510	0.358	65.415
M40-4	2	652.902	3.811	25.734	1.648	0.386	-0.068	0.387	54.307	0.495	0.100	1.809	2.904	0.379	63.934
M40-4	3	669.862	3.867	27.325	1.535	0.576	-0.061	0.339	28.250	0.000	0.090	1.798	2.576	0.276	66.664
M40-5	1	759.657	3.260	61.868	1.527	0.824	-0.072	0.338	86.941	0.137	0.059	0.579	2.014	0.095	124.471
M40-5	2	791.411	3.349	63.046	1.597	0.551	-0.075	0.339	1.784	0.141	0.046	0.548	1.787	0.108	127.068
M40-5	3	794.202	3.258	59.431	1.381	0.877	-0.075	0.339	3.397	0.070	0.055	0.532	1.763	0.112	126.371
M40-6	1	11.228	2.921	14.002	1.234	0.170	-0.064	0.323	59.969	0.289	0.542	7.433	2.692	-0.012	1.029
M40-6	2	11.669	3.404	14.093	0.873	-0.085	-0.069	0.352	30.077	0.259	0.049	6.578	1.062	-0.004	0.876
M40-6	3	12.240	3.460	13.977	1.036	-0.085	-0.066	0.337	8.523	0.615	0.108	7.718	1.127	-0.009	1.186
M40-P	1	798.069	2.953	24.261	1.286	0.506	-0.075	0.323	70.912	0.216	0.071	4.174	23.246	0.170	37.968
M40-P	2	708.185	2.691	30.290	1.208	0.466	-0.075	0.323	0.013	0.000	0.055	3.543	22.267	0.113	37.233
M40-P	3	691.213	3.114	24.990	1.213	0.052	-0.075	0.354	0.117	0.000	0.070	3.691	23.445	0.088	37.704
K13-4	1	478.593	8.174	53.510	2.180	0.907	-0.071	0.372	54.045	0.072	0.726	115.076	923.176	0.186	66.247

Sample	Replicate	139 La	140 Ce	141 Pr	146 Nd	147 Sm	153 Eu	157 Gd	159 Tb	163 Dy	165 Ho	166 Er	169 Tm	172 Yb
M18-3	1	2.816	6.072	0.705	2.639	0.651	0.189	0.796	0.055	0.583	0.075	0.328	0.056	0.363
M18-3	2	2.839	5.679	0.575	2.420	0.651	0.177	0.636	0.035	0.547	0.100	0.235	0.071	0.270
M18-3	3	2.651	5.568	0.571	2.630	0.560	0.173	0.515	0.037	0.473	0.089	0.303	0.053	0.211
M23-2	1	3.884	8.854	1.369	5.983	1.381	0.310	1.816	0.185	1.640	0.267	0.848	0.133	0.809
M23-2	2	4.293	9.489	1.187	5.914	1.375	0.339	1.752	0.179	1.536	0.271	0.892	0.137	0.730
M23-2	3	4.064	9.393	1.396	5.939	1.414	0.364	1.612	0.179	1.497	0.268	0.826	0.134	0.778
M23-6	1	4.012	8.177	1.034	4.127	0.985	0.213	1.054	0.115	0.805	0.149	0.504	0.098	0.445
M23-6	2	3.827	7.388	0.832	3.904	0.846	0.202	0.928	0.094	0.787	0.099	0.533	0.075	0.471
M23-6	3	6.728	13.751	1.663	6.289	1.576	0.466	1.879	0.257	1.676	0.362	0.921	0.171	0.924
M23-7	1	4.586	9.863	1.350	4.801	1.207	0.357	1.581	0.152	1.263	0.227	0.789	0.120	0.724
M23-7	2	4.606	9.898	1.238	4.982	1.655	0.313	1.540	0.208	1.400	0.269	0.873	0.124	0.806
M23-7	3	4.535	9.765	1.265	5.127	1.122	0.338	1.661	0.185	1.166	0.238	0.935	0.155	0.860
M32-1	1	5.076	11.259	1.516	7.452	1.710	0.470	1.957	0.288	1.868	0.368	0.952	0.175	0.950
M32-1	2	4.711	10.517	1.392	6.330	1.570	0.401	2.279	0.268	1.898	0.337	1.069	0.172	0.904
M32-1	3	4.861	10.869	1.482	6.863	1.510	0.419	1.942	0.271	1.898	0.380	1.023	0.168	0.912
M32-9	1	3.749	7.964	1.117	4.536	1.024	0.256	1.058	0.113	1.023	0.168	0.546	0.091	0.589
M32-9	2	3.521	7.796	1.018	4.277	0.786	0.237	1.107	0.118	1.072	0.187	0.536	0.097	0.552
M32-9	3	3.678	8.195	1.016	4.245	0.959	0.266	1.078	0.103	0.918	0.184	0.560	0.097	0.511
M32-4R	1	3.838	8.260	1.263	4.567	0.968	0.240	1.196	0.121	0.825	0.183	0.614	0.113	0.555
M32-4R	2	3.659	8.000	0.998	4.339	0.833	0.221	1.062	0.092	0.951	0.141	0.559	0.097	0.454
M32-4R	3	2.281	4.587	0.509	2.286	0.434	0.146	0.469	0.055	0.517	0.075	0.267	0.061	0.265
M40-1	1	2.027	7.238	0.568	2.362	0.734	0.207	0.672	0.065	0.590	0.091	0.246	0.050	0.310
M40-1	2	3.448	15.264	0.971	4.339	1.218	0.309	1.211	0.138	0.983	0.194	0.466	0.079	0.473
M40-1	3	8.326	33.769	2.592	11.547	3.616	0.979	3.158	0.451	2.640	0.465	1.336	0.192	1.139
M40-4	1	3.476	6.669	0.870	3.248	0.663	0.168	0.772	0.071	0.625	0.096	0.384	0.085	0.466
M40-4	2	3.648	6.865	0.840	3.299	0.720	0.181	0.853	0.077	0.691	0.116	0.368	0.086	0.299
M40-4	3	3.485	6.969	0.806	3.298	0.715	0.171	0.715	0.081	0.605	0.114	0.379	0.062	0.405
M40-5	1	2.913	5.914	0.697	2.929	0.605	0.151	0.742	0.026	0.570	0.098	0.347	0.067	0.371
M40-5	2	3.102	6.074	0.718	3.211	0.612	0.146	0.755	0.049	0.532	0.070	0.344	0.134	0.292
M40-5	3	3.201	5.783	0.684	2.813	0.661	0.136	0.553	0.074	0.667	0.090	0.365	0.079	0.375
M40-6	1	2.167	4.784	0.549	2.199	0.653	0.143	0.548	0.044	0.680	0.071	0.324	0.075	0.273
M40-6	2	2.422	4.992	0.607	2.542	0.516	0.173	0.752	0.070	0.548	0.081	0.280	0.058	0.327
M40-6	3	2.775	6.393	0.638	2.735	0.627	0.176	0.625	0.056	0.608	0.063	0.325	0.064	0.333
M40-P	1	2.978	5.421	0.684	2.669	0.717	0.165	0.671	0.056	0.446	0.067	0.295	0.074	0.309
M40-P	2	2.886	5.669	0.653	2.657	0.531	0.115	0.564	0.051	0.556	0.063	0.321	0.047	0.357
M40-P	3	2.662	5.237	0.583	2.703	0.539	0.114	0.671	0.015	0.544	0.057	0.313	0.060	0.288
K13-4	1	4.173	9.109	1.218	5.107	0.925	0.339	1.398	0.125	1.273	0.205	0.775	0.104	0.665

Sample	Replicate	175 Lu	178 Hf	181 Ta	182 W	185 Re	195 Pt	197 Au	205 Tl	208 Pb	209 Bi	232 Th	238 U
M18-3	1	0.080	0.379	0.108	0.126	0.002	0.642	8.220	0.039	13.293	-0.314	0.672	0.497
M18-3	2	0.057	0.333	0.107	0.049	0.015	0.642	0.292	-0.027	8.073	-0.505	0.607	0.211
M18-3	3	0.055	0.346	0.093	0.089	0.009	0.637	-0.134	-0.026	4.661	-0.446	0.695	0.159
M23-2	1	0.143	1.380	0.179	0.046	-0.001	0.647	105.371	-0.007	4.792	-0.306	1.107	0.650
M23-2	2	0.112	1.130	0.156	0.049	-0.004	0.647	42.901	-0.027	4.028	-0.377	1.086	0.695
M23-2	3	0.122	1.373	0.121	0.065	0.005	0.662	6.602	-0.035	4.108	-0.411	1.125	0.641
M23-6	1	0.091	1.335	0.167	0.103	-0.004	0.637	64.788	-0.009	30.142	-0.329	1.246	0.717
M23-6	2	0.092	1.075	0.137	0.106	-0.001	0.637	9.461	-0.029	25.583	-0.361	1.090	0.639
M23-6	3	0.172	1.829	0.264	0.221	-0.004	0.642	77.515	-0.016	74.262	-0.217	2.208	0.972
M23-7	1	0.144	1.699	0.154	0.045	-0.004	0.652	61.174	-0.023	21.203	-0.303	1.107	0.657
M23-7	2	0.128	1.626	0.202	0.039	0.002	0.656	36.597	-0.033	21.692	-0.399	1.150	0.621
M23-7	3	0.152	1.526	0.216	0.071	-0.004	0.657	56.544	-0.021	21.944	-0.365	1.097	0.730
M32-1	1	0.182	1.526	0.203	0.110	-0.001	0.652	53.720	-0.005	666.973	-0.065	1.235	0.610
M32-1	2	0.153	1.807	0.207	0.060	-0.004	0.642	57.764	-0.014	629.812	-0.152	1.124	0.510
M32-1	3	0.165	1.650	0.179	0.046	0.002	0.637	22.627	-0.031	681.212	-0.289	1.207	0.590
M32-9	1	0.081	1.178	0.155	0.071	0.006	0.642	2.785	-0.033	3.977	-0.342	1.045	0.455
M32-9	2	0.080	1.150	0.154	0.048	-0.001	0.637	-0.136	-0.030	2.941	-0.387	1.070	0.460
M32-9	3	0.090	1.218	0.152	0.061	-0.001	0.647	2.721	-0.023	3.477	-0.390	1.262	0.412
M32-4R	1	0.105	1.215	0.163	0.046	-0.001	0.647	147.609	0.014	5.973	0.036	0.998	0.461
M32-4R	2	0.096	1.135	0.185	0.041	-0.004	0.647	101.505	0.001	5.313	-0.097	1.006	0.445
M32-4R	3	0.065	0.486	0.085	0.019	0.001	0.637	69.509	-0.004	3.837	-0.182	0.535	0.216
M40-1	1	0.061	0.907	0.182	0.025	-0.004	0.648	46.648	-0.027	22.924	-0.416	1.384	-0.008
M40-1	2	0.085	1.170	0.227	0.019	-0.004	0.647	10.720	-0.015	36.168	-0.058	2.011	0.014
M40-1	3	0.187	1.016	0.175	0.038	-0.004	0.637	9.274	-0.023	116.801	0.308	3.323	0.757
M40-4	1	0.064	0.675	0.216	0.108	0.006	0.657	53.589	0.001	4.933	-0.081	1.307	0.364
M40-4	2	0.076	0.734	0.241	0.124	0.006	0.652	61.758	-0.007	4.884	-0.193	1.382	0.325
M40-4	3	0.074	0.803	0.218	0.108	0.002	0.642	14.596	-0.021	4.869	-0.212	1.423	0.362
M40-5	1	0.061	1.490	0.113	0.044	-0.001	0.642	25.074	-0.022	2.731	-0.295	0.799	0.397
M40-5	2	0.076	1.490	0.125	0.066	0.002	0.642	16.310	-0.029	1.848	-0.188	0.754	0.401
M40-5	3	0.070	1.477	0.104	0.076	-0.001	0.637	16.206	-0.027	1.881	4.015	0.790	0.375
M40-6	1	0.067	0.331	0.099	0.121	-0.004	0.658	73.727	-0.010	7.452	-0.202	0.593	1.509
M40-6	2	0.057	0.424	0.100	0.019	-0.004	0.646	50.706	-0.019	7.024	-0.340	0.561	2.529
M40-6	3	0.070	0.358	0.077	0.023	-0.004	0.646	27.765	-0.026	7.299	-0.402	0.561	1.454
M40-P	1	0.081	0.624	0.111	0.057	0.023	0.642	92.664	-0.017	4.421	-0.320	0.640	0.228
M40-P	2	0.072	0.765	0.114	0.045	0.016	0.647	-0.078	-0.017	3.868	-0.354	0.656	0.246
M40-P	3	0.062	0.643	0.119	0.045	0.019	0.637	3.499	-0.017	3.936	-0.338	0.559	0.266
K13-4	1	0.103	1.560	0.148	0.191	0.030	0.642	15.860	-0.019	254.011	-0.335	1.062	0.659

Sample	Replicate	7 Li	9 Be	11 B	23 Na	24 Mg	27 Al	31 P	39 K	44 Ca	45 Sc	47 Ti
K13-4	2	24.448	0.834	76.088	132174.532	17518.540	11771.712	425.208	12919.375	45246.686	1.523	661.835
K13-4	3	23.328	1.148	84.411	133507.337	17872.567	11871.391	467.599	13650.182	48558.170	1.482	678.745
ΣK1-1	1	26.988	0.277	109.626	125615.135	24883.085	11058.898	647.255	19477.155	33964.363	3.022	505.586
ΣK1-1	2	30.397	0.496	88.649	120715.278	24643.974	7992.028	548.129	19276.205	36057.691	2.318	453.354
ΣK1-1	3	27.526	0.392	86.380	124851.935	24688.192	9386.675	624.835	20135.198	37076.928	1.748	519.076
ΣK1-4	1	11.297	0.161	287.541	33241.243	936.968	1159.657	67.546	2004.491	3091.583	-0.066	83.897
ΣK1-4	2	11.366	0.161	326.157	38154.673	1040.663	1503.067	88.645	2412.801	4125.323	0.040	102.144
ΣK1-4	3	11.032	0.272	325.878	34469.717	1057.698	1129.563	51.960	2059.179	3866.684	0.073	124.176
580.2-1	1	42.169	1.003	-11.835	47359.137	2938.250	16894.880	664.340	74443.057	8751.889	1.341	633.916
580.2-1	2	43.678	0.733	-33.098	46326.367	2798.980	16618.895	596.181	73058.929	8067.374	1.441	602.220
580.2-1	3	41.431	1.462	-30.668	45555.259	2887.741	16872.589	568.339	73919.212	8881.862	1.351	662.886
580.2-2	1	22.580	0.497	319.945	127864.363	6871.824	6187.331	384.386	7835.702	55389.144	1.345	361.358
580.2-2	2	16.902	0.732	225.244	95801.393	5295.505	25008.505	184.873	7612.518	51838.789	2.024	409.436
580.2-2	3	22.761	1.163	293.505	130974.849	7026.935	6395.611	389.662	8376.260	57244.410	1.164	353.865
580.2-3	1	50.441	2.533	125.191	131513.830	15042.680	11429.426	412.314	13012.624	53427.496	1.564	632.690
580.2-3	2	52.714	0.960	126.451	130087.723	14911.161	11205.139	425.555	12427.695	52390.291	1.905	713.634
580.2-3	3	46.040	1.903	102.973	130225.958	14766.506	11393.402	563.341	12096.972	49267.303	1.750	644.587
Σ2-K1-1	1	26.988	0.277	109.626	125615.135	24883.085	11058.898	647.255	19477.155	33964.363	3.022	505.586
Σ2-K1-1	2	30.397	0.496	88.649	120715.278	24643.974	7992.028	548.129	19276.205	36057.691	2.318	453.354
Σ2-K1-1	3	27.526	0.392	86.380	124851.935	24688.192	9386.675	624.835	20135.198	37076.928	1.748	519.076
Σ2-K1-4	1	11.297	0.161	287.541	33241.243	936.968	1159.657	67.546	2004.491	3091.583	-0.066	83.897
Σ2-K1-4	2	11.366	0.161	326.157	38154.673	1040.663	1503.067	88.645	2412.801	4125.323	0.040	102.144
Σ2-K1-4	3	11.032	0.272	325.878	34469.717	1057.698	1129.563	51.960	2059.179	3866.684	0.073	124.176

Sample	Replicate	51 V	52 Cr	55 Mn	56 Fe	59 Co	60 Ni	63 Cu	66 Zn	71 Ga	72 Ge	75 As	82 Se	85 Rb
K13-4	2	12.371	12.771	1011.667	5228.098	571.875	348.883	3224.560	747.673	2.032	0.514	19.134	-1.073	10.071
K13-4	3	12.603	12.875	1054.337	5183.250	590.180	356.306	3316.380	728.941	2.328	0.685	17.653	0.993	10.206
ΣK1-1	1	17.749	51.000	376.213	5320.871	2.739	24.529	20.499	23.449	2.279	0.685	2.496	1.877	10.546
ΣK1-1	2	15.137	46.796	398.805	4900.745	3.062	24.394	24.581	22.210	1.848	0.902	1.866	-1.091	11.466
ΣK1-1	3	16.608	50.087	383.863	4999.342	2.912	23.104	15.113	24.071	2.485	0.946	1.929	1.262	12.679
ΣK1-4	1	2.721	4.611	25.457	9002.076	4705.083	813.397	10211.821	17.636	0.521	1.605	205.439	2.045	2.542
ΣK1-4	2	3.080	4.591	29.565	11584.948	4840.223	829.033	10127.062	17.626	0.439	1.427	216.919	2.082	3.398
ΣK1-4	3	2.681	4.176	39.430	9621.060	4609.391	785.085	9227.670	27.482	0.457	1.795	246.945	2.650	2.955
580.2-1	1	8.206	7.460	122.840	4526.565	14.373	13.137	19216.047	91.171	4.551	1.079	13.253	2.096	133.726
580.2-1	2	7.928	7.764	119.656	4420.054	14.564	10.828	18978.731	87.255	4.381	1.272	11.254	0.109	131.538
580.2-1	3	7.958	7.850	125.384	4602.470	14.416	13.202	19194.872	85.786	4.705	0.926	16.558	0.404	128.494
580.2-2	1	10.549	12.412	530.772	4525.969	153.586	103.825	20101.715	139.671	1.200	0.446	45.023	3.288	8.098
580.2-2	2	8.143	16.525	381.589	5408.000	97.844	70.161	14965.335	109.185	1.931	0.063	34.181	0.098	13.328
580.2-2	3	11.265	11.021	521.017	4311.911	139.167	101.364	19896.050	136.417	1.021	0.441	47.671	-0.014	9.577
580.2-3	1	11.278	9.691	811.400	4487.657	412.057	324.081	3287.694	661.450	1.680	0.640	23.600	3.168	15.517
580.2-3	2	12.622	10.207	854.620	4638.459	435.419	339.335	3350.045	660.052	1.399	1.401	21.207	-1.018	15.503
580.2-3	3	11.468	11.667	802.489	4577.670	412.511	320.833	3109.671	662.624	1.805	0.485	17.141	2.018	16.707
Σ2-K1-1	1	17.749	51.000	376.213	5320.871	2.739	24.529	20.499	23.449	2.279	0.685	2.496	1.877	10.546
Σ2-K1-1	2	15.137	46.796	398.805	4900.745	3.062	24.394	24.581	22.210	1.848	0.902	1.866	-1.091	11.466
Σ2-K1-1	3	16.608	50.087	383.863	4999.342	2.912	23.104	15.113	24.071	2.485	0.946	1.929	1.262	12.679
Σ2-K1-4	1	2.721	4.611	25.457	9002.076	4705.083	813.397	10211.821	17.636	0.521	1.605	205.439	2.045	2.542
Σ2-K1-4	2	3.080	4.591	29.565	11584.948	4840.223	829.033	10127.062	17.626	0.439	1.427	216.919	2.082	3.398
Σ2-K1-4	3	2.681	4.176	39.430	9621.060	4609.391	785.085	9227.670	27.482	0.457	1.795	246.945	2.650	2.955

Sample	Replicate	88 Sr	89 Y	90 Zr	93 Nb	95 Mo	103 Rh	105 Pd	107 Ag	111 Cd	115 In	118 Sn	121 Sb	133 Cs	137 Ba
K13-4	2	494.751	8.229	54.895	2.204	0.778	-0.075	0.339	2.083	0.426	0.678	117.046	942.871	0.177	66.895
K13-4	3	497.414	7.869	55.595	2.003	0.513	-0.072	0.370	1.473	0.069	0.634	113.905	925.215	0.173	65.776
ΣK1-1	1	285.022	4.065	26.480	1.984	0.952	-0.075	0.373	90.083	1.250	0.082	2.745	1.952	0.305	63.612
ΣK1-1	2	280.506	3.917	19.375	1.410	0.856	-0.075	0.339	123.006	1.060	0.065	2.024	1.594	0.340	62.507
ΣK1-1	3	289.999	4.315	23.449	1.626	1.115	-0.075	0.323	66.172	1.677	0.051	1.499	1.399	0.272	65.379
ΣK1-4	1	15.462	0.544	3.429	0.206	0.468	0.058	0.342	62.184	0.000	9.371	9.657	2392.587	0.063	11.520
ΣK1-4	2	18.680	0.777	5.458	0.350	0.629	0.077	0.340	65.126	0.000	9.305	11.492	2478.911	0.056	14.851
ΣK1-4	3	17.644	0.564	5.293	0.308	0.545	0.061	0.339	22.920	0.000	9.239	11.058	2485.133	0.050	14.583
580.2-1	1	89.472	5.782	100.217	11.124	0.154	-0.067	0.340	126.308	0.076	12.596	2219.058	14.910	0.997	115.410
580.2-1	2	85.603	5.523		10.423	0.114	-0.046	0.356	39.962	0.000	12.721	2271.131	15.025	0.690	110.052
580.2-1	3	84.551	6.129	92.248	10.782	0.184	-0.065	0.323	17.854	0.069	12.759	2250.693	16.296	0.930	114.029
580.2-2	1	239.315	7.265	21.398	1.089	0.415	-0.068	0.339	75.689	0.142	0.254	30.489	204.796	0.370	49.461
580.2-2	2	187.611	5.895	34.209	1.514	0.057	-0.075	0.323	22.092	0.072	0.492	67.517	147.893	0.220	61.858
580.2-2	3	251.149	7.133	24.029	1.108	0.109	-0.064	0.355	21.430	0.282	0.307	36.201	189.233	0.387	51.700
580.2-3	1	630.839	13.693	63.933	2.243	0.239	-0.064	0.340	67.517	0.901	0.810	149.101	569.728	0.276	67.962
580.2-3	2	580.854	12.568	58.079	1.812	0.085	-0.075	0.339	19.550	0.217	0.846	145.791	562.375	0.220	65.312
580.2-3	3	591.643	12.651	58.839	2.050	0.185	-0.072	0.338	4.449	0.345	0.717	147.025	564.194	0.270	66.598
Σ2-K1-1	1	285.022	4.065	26.480	1.984	0.952	-0.075	0.373	90.083	1.250	0.082	2.745	1.952	0.305	63.612
Σ2-K1-1	2	280.506	3.917	19.375	1.410	0.856	-0.075	0.339	123.006	1.060	0.065	2.024	1.594	0.340	62.507
Σ2-K1-1	3	289.999	4.315	23.449	1.626	1.115	-0.075	0.323	66.172	1.677	0.051	1.499	1.399	0.272	65.379
Σ2-K1-4	1	15.462	0.544	3.429	0.206	0.468	0.058	0.342	62.184	0.000	9.371	9.657	2392.587	0.063	11.520
Σ2-K1-4	2	18.680	0.777	5.458	0.350	0.629	0.077	0.340	65.126	0.000	9.305	11.492	2478.911	0.056	14.851
Σ2-K1-4	3	17.644	0.564	5.293	0.308	0.545	0.061	0.339	22.920	0.000	9.239	11.058	2485.133	0.050	14.583

Sample	Replicate	139 La	140 Ce	141 Pr	146 Nd	147 Sm	153 Eu	157 Gd	159 Tb	163 Dy	165 Ho	166 Er	169 Tm	172 Yb
K13-4	2	4.299	9.525	1.177	5.665	1.267	0.305	1.258	0.187	1.205	0.188	0.843	0.116	0.568
K13-4	3	4.088	9.490	1.200	4.899	1.239	0.332	1.549	0.148	1.172	0.264	0.842	0.122	0.628
ΣK1-1	1	3.421	6.733	0.803	3.028	0.857	0.165	0.923	0.075	0.764	0.119	0.363	0.095	0.347
ΣK1-1	2	3.369	6.561	0.810	3.240	0.838	0.212	0.842	0.088	0.628	0.115	0.367	0.099	0.407
ΣK1-1	3	3.512	6.916	0.934	3.501	0.864	0.225	0.759	0.074	0.835	0.101	0.463	0.087	0.494
ΣK1-4	1	0.696	1.104	0.189	0.615	0.142	0.052	0.184	-0.024	0.130	-0.014	0.078	0.041	0.108
ΣK1-4	2	0.648	1.241	0.147	0.588	0.146	0.069	0.194	-0.033	0.154	-0.013	0.102	0.019	0.115
ΣK1-4	3	0.742	1.513	0.137	4.190	0.162	0.049	0.203	-0.032	0.137	-0.022	0.063	0.023	0.085
580.2-1	1	11.499	18.059	2.260	8.495	1.727	0.389	1.415	0.144	1.135	0.229	0.707	0.111	0.613
580.2-1	2	11.209	17.100	2.296	8.266	1.807	0.381	1.223	0.163	1.248	0.160	0.627	0.103	0.616
580.2-1	3	12.034	17.372	2.389	8.741	1.520	0.331	1.551	0.155	1.293	0.157	0.582	0.125	0.597
580.2-2	1	3.154	5.330	0.740	3.788	1.078	0.367	1.322	0.207	1.334	0.231	0.654	0.113	0.475
580.2-2	2	2.679	4.542	0.722	3.560	1.005	0.300	1.249	0.209	1.316	0.177	0.653	0.072	0.447
580.2-2	3	3.297	5.793	0.886	3.789	1.323	0.321	1.780	0.263	1.709	0.250	0.646	0.096	0.558
580.2-3	1	4.552	9.734	1.246	6.104	1.353	0.381	1.863	0.263	1.874	0.421	1.184	0.151	0.779
580.2-3	2	4.337	9.143	1.179	5.389	1.221	0.357	1.804	0.256	1.719	0.423	1.116	0.181	0.881
580.2-3	3	4.258	9.184	1.348	6.012	1.256	0.375	1.956	0.237	1.898	0.320	1.021	0.148	0.979
Σ2-K1-1	1	3.421	6.733	0.803	3.028	0.857	0.165	0.923	0.075	0.764	0.119	0.363	0.095	0.347
Σ2-K1-1	2	3.369	6.561	0.810	3.240	0.838	0.212	0.842	0.088	0.628	0.115	0.367	0.099	0.407
Σ2-K1-1	3	3.512	6.916	0.934	3.501	0.864	0.225	0.759	0.074	0.835	0.101	0.463	0.087	0.494
Σ2-K1-4	1	0.696	1.104	0.189	0.615	0.142	0.052	0.184	-0.024	0.130	-0.014	0.078	0.041	0.108
Σ2-K1-4	2	0.648	1.241	0.147	0.588	0.146	0.069	0.194	-0.033	0.154	-0.013	0.102	0.019	0.115
Σ2-K1-4	3	0.742	1.513	0.137	4.190	0.162	0.049	0.203	-0.032	0.137	-0.022	0.063	0.023	0.085

Sample	Replicate	175 Lu	178 Hf	181 Ta	182 W	185 Re	195 Pt	197 Au	205 Tl	208 Pb	209 Bi	232 Th	238 U
K13-4	2	0.088	1.365	0.166	0.109	-0.001	0.637	0.901	-0.027	250.961	-0.387	1.249	0.665
K13-4	3	0.135	1.456	0.145	0.147	-0.001	0.637	1.842	-0.031	251.290	-0.406	1.238	0.637
ΣK1-1	1	0.108	0.675	0.157	0.188	0.013	0.648	166.904	0.064	9.219	-0.148	1.252	0.324
ΣK1-1	2	0.105	0.533	0.177	0.119	0.016	0.652	115.061	0.056	7.189	-0.288	0.947	0.251
ΣK1-1	3	0.078	0.684	0.146	0.160	0.010	0.647	160.251	0.031	6.862	-0.255	1.093	0.308
ΣK1-4	1	0.023	0.041	0.044	0.180	-0.004	0.649	26.609	-0.035	6831.780	-0.077	0.144	0.135
ΣK1-4	2	0.039	0.166	0.034	0.199	-0.004	0.659	10.802	-0.024	7054.335	-0.305	0.142	0.141
ΣK1-4	3	0.024	0.127	0.044	0.112	-0.001	0.652	17.394	-0.031	7043.885	-0.450	0.085	0.092
580.2-1	1	0.101	2.347	0.779	0.318	-0.004	0.642	46.208	-0.009	53.294	2.277	3.008	0.662
580.2-1	2	0.117	2.207	0.730	0.389	-0.004	0.642	28.190	0.000	43.822	2.209	3.019	0.662
580.2-1	3	0.087	2.251	0.789	0.308	-0.004	0.652	27.790	-0.002	71.009	2.209	2.977	0.661
580.2-2	1	0.070	0.549	0.103	0.119	-0.004	0.647	74.212	-0.021	213.691	-0.175	0.746	1.165
580.2-2	2	0.087	0.995	0.175	0.100	0.003	0.642	10.206	-0.013	203.460	-0.224	1.196	0.836
580.2-2	3	0.095	0.576	0.113	0.155	0.006	0.637	4.232	-0.021	203.779	-0.195	0.779	1.256
580.2-3	1	0.193	1.513	0.156	0.036	-0.004	0.637	168.890	0.010	51.517	-0.129	1.081	0.710
580.2-3	2	0.155	1.598	0.176	0.068	-0.004	0.653	92.954	0.000	50.990	-0.187	1.152	0.692
580.2-3	3	0.172	1.583	0.153	0.121	-0.004	0.642	18.527	-0.006	48.374	-0.207	1.088	0.677
Σ2-K1-1	1	0.108	0.675	0.157	0.188	0.013	0.648	166.904	0.064	9.219	-0.148	1.252	0.324
Σ2-K1-1	2	0.105	0.533	0.177	0.119	0.016	0.652	115.061	0.056	7.189	-0.288	0.947	0.251
Σ2-K1-1	3	0.078	0.684	0.146	0.160	0.010	0.647	160.251	0.031	6.862	-0.255	1.093	0.308
Σ2-K1-4	1	0.023	0.041	0.044	0.180	-0.004	0.649	26.609	-0.035	6831.780	-0.077	0.144	0.135
Σ2-K1-4	2	0.039	0.166	0.034	0.199	-0.004	0.659	10.802	-0.024	7054.335	-0.305	0.142	0.141
Σ2-K1-4	3	0.024	0.127	0.044	0.112	-0.001	0.652	17.394	-0.031	7043.885	-0.450	0.085	0.092

C.4. Principle Component Analysis - Eigen values and their contributions to the correlations

	PC1	PC2	PC3	PC4	PC5	PC6	PC7	PC8	PC9	PC10	PC11
Eigenvalue	3.835	2.882	1.2412	0.75595	0.62609	0.5621	0.38486	0.3081	0.19545	0.13431	0.075043
Proportion Explained	0.3486	0.262	0.1128	0.06872	0.05692	0.0511	0.03499	0.02801	0.01777	0.01221	0.006822
Cumulative Proportion	0.3486	0.6106	0.7235	0.79219	0.84911	0.9002	0.93519	0.9632	0.98097	0.99318	1

APPENDIX D - VITREOUS BEADS FROM LOFKËND: IMAGES AND DATA

D.1. Macrophotographs of beads analyzed

Catalog No.	Additional Nos.		Bead Dimensions[1]
10/113	SF283/ TLV-8		H: 3.32 mm W/D: 5.5 mm PD: 1.88 mm Wt: >0.1 g
10/114	SF258/ TXXI-8		H: 11.2 mm W/D: 11.56 mm PD: 3.32 mm Wt: 0.6 g
10/109	SF294/ TLIII-6		H: 12.76 mm W/D: 14.33 mm PD: 3.48 mm Wt: 1.6 g
10/107	SF295/ TLIII-8		too fragmentary Wt: 0.5 g

10/105	SF298/ TLIII-9		H: 17.26 mm W/D: 8.92mm PD: 1.86 mm Wt: 1.2g
10/112	SF338/ TXXVIIII-4		H: 5.41 mm W/D: 7.16 mm PD: 4.12 mm Wt: 0.2 g
10/115	SF339/ TXXVIII-5		H:16.52mm W: 14.56 mm D: 10.40 mm PD: 2.5mm Wt: 3.4 g
10/108	SF341/ TXXVIII-7		H: 10.20 mm W/D: 10.51mm PD: 3.9 mm Wt: 1.5g

10/106	SF342/ TXXVIII-8		H: 14.10 mm W/D: 13.12 mm PD: 4.46 mm Wt: 1.5g
10/116	SF344/ TXXVIII-9	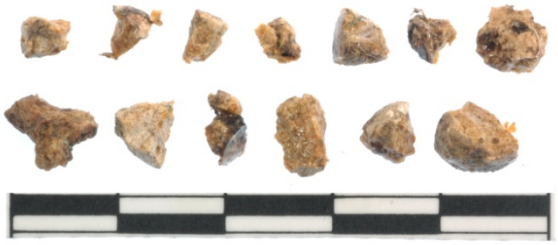	too fragmentary Wt: 0.6 g
10/117	SF351/ TXXVIII-10	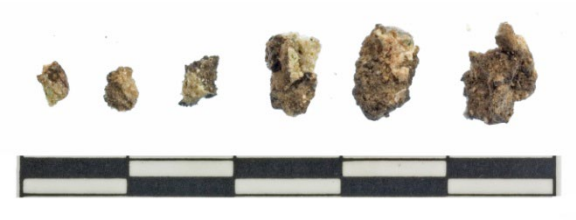	too fragmentary Wt: 0.4 g

[1]H=Height, W/D=Width/Diameter, PD=Perforation Diameter, Wt=Weight

D.2. EPMA Results

Data given as weight percent (wt%) oxides

Sample No.	Catalog No.	Area	Na2O	K2O	MgO	Al2O3	CaO	SiO2	FeO	MnO	P2O5	TiO2	Total
Lof-294-1	10/109	1	16.81	1.27	4.85	1.41	5.65	63.05	6.66	n.d.	0.19	0.26	100.15
Lof-294-1	10/109	2	16.92	1.26	4.70	1.37	5.76	62.85	6.50	0.02	0.15	0.20	99.72
Lof-294-1	10/109	3	16.89	1.26	4.83	1.40	5.76	62.57	6.74	0.04	0.16	0.14	99.79
Lof-338-1	10/112	1	18.94	1.36	3.23	1.45	4.94	67.21	0.35	0.27	0.25	0.23	98.24
Lof-338-1	10/112	2	18.93	1.20	3.26	1.58	4.82	67.66	0.41	0.25	0.32	0.32	98.77
Lof-338-1	10/112	3	18.97	1.30	3.33	1.47	4.77	67.75	0.43	0.26	0.28	0.20	98.76
Lof-338-2	10/112	1	18.85	1.24	3.22	1.50	4.98	67.64	0.42	0.27	0.25	0.23	98.59
Lof-338-2	10/112	2	18.69	1.20	3.29	1.53	4.87	67.39	0.40	0.25	0.27	0.19	98.06
Lof-338-2	10/112	3	18.91	1.30	3.46	1.54	4.65	67.55	0.40	0.27	0.27	0.33	98.66
Lof-339-1	10/115	1	16.43	1.43	3.70	1.08	5.06	64.78	7.03	n.d.	0.12	0.14	99.76
Lof-339-1	10/115	2	16.40	1.32	3.73	1.05	5.04	64.97	6.94	n.d.	0.03	0.12	99.61
Lof-339-1	10/115	3	16.45	1.40	3.74	0.99	5.06	64.80	6.94	n.d.	0.08	0.14	99.60
Lof-339-2	10/115	1	16.38	1.46	3.69	1.03	5.16	64.93	7.00	0.00	0.12	0.16	99.92
Lof-339-2	10/115	2	16.56	1.44	3.74	1.05	5.28	64.96	7.02	0.03	0.10	0.12	100.29
Lof-339-2	10/115	3	16.15	1.33	3.72	1.00	4.97	64.59	6.94	0.02	0.16	0.16	99.04
Lof-339-3	10/115	1	16.09	1.44	3.60	1.15	5.16	65.28	6.87	0.06	0.12	0.13	99.89
Lof-339-3	10/115	2	16.00	1.47	3.65	1.18	5.17	65.14	7.04	0.01	0.16	0.13	99.94
Lof-339-3	10/115	3	16.19	1.29	3.66	1.11	5.36	65.56	6.87	n.d.	0.14	0.14	100.32
Lof-341-1	10/108	1	19.38	1.31	3.99	1.87	2.80	61.59	8.29	0.03	0.15	0.29	99.70
Lof-341-1	10/108	2	19.79	1.28	3.93	1.91	2.78	61.70	8.22	0.09	0.17	0.36	100.23
Lof-341-1	10/108	3	19.77	1.25	4.00	1.89	2.70	61.66	8.22	0.06	0.13	0.25	99.94
Lof-342-1	10/106	1	18.96	1.31	4.02	1.48	5.65	64.81	3.50	n.d.	0.30	0.17	100.21
Lof-342-1	10/106	2	19.17	1.32	4.02	1.35	5.51	64.53	3.28	0.01	0.21	0.17	99.57
Lof-342-1	10/106	3	18.92	1.32	4.09	1.39	5.68	65.11	3.32	0.01	0.22	0.17	100.22
Lof-342-5	10/106	1	17.72	1.32	3.40	1.27	5.44	64.09	4.05	n.d.	0.28	0.22	97.80
Lof-342-5	10/106	2	17.70	1.29	3.64	1.33	5.39	64.13	4.05	0.03	0.30	0.17	98.03
Lof-342-5	10/106	3	17.75	1.31	3.56	1.34	5.49	64.42	4.09	n.d.	0.30	0.28	98.53
Lof-342-6	10/106	1	18.96	1.39	4.11	1.39	5.67	64.71	3.35	0.05	0.21	0.18	100.01
Lof-342-6	10/106	2	18.72	1.19	4.16	1.34	5.74	64.76	3.73	n.d.	0.25	0.17	100.06
Lof-342-6	10/106	3	18.74	1.33	4.09	1.43	5.66	64.66	3.25	n.d.	0.23	0.21	99.60
Lof-344-3	10/116	1	19.53	1.12	4.70	1.58	5.85	64.30	2.49	n.d.	0.22	0.23	100.03
Lof-344-3	10/116	2	19.52	1.20	4.70	1.63	5.80	64.80	2.46	0.01	0.18	0.12	100.40
Lof-344-3	10/116	3	19.17	1.08	4.75	1.60	6.49	63.82	2.58	0.03	0.25	0.22	99.99
Lof-351-1	10/117	1	18.71	1.46	1.98	1.26	3.61	70.50	0.25	0.04	0.21	0.08	98.10
Lof-351-1	10/117	2	18.71	1.43	1.91	1.27	3.58	70.56	0.26	0.02	0.20	0.09	98.02
Lof-351-1	10/117	3	19.15	1.36	1.95	1.30	3.62	70.51	0.25	0.04	0.18	0.19	98.53

D.3. LA-ICP-MS Results

Data given in parts per million (ppm)

Sample No.	Replicate	7 Li	9 Be	11 B	23 Na	25 Mg	27 Al
Lof-294-1	1	112.6449	0.4757	1596.9157	121415.6511	22624.7130	7815.6046
Lof-294-1	2	119.4164	0.4466	1534.5958	123476.2126	22879.1114	7611.6145
Lof-294-1	3	117.8609	0.1763	1576.2944	123888.8826	24266.9642	7338.1768
Lof-338-1	1	69.9011	0.3207	1173.7187	143773.6770	15845.0111	8144.2845
Lof-338-1	2	67.4297	0.3657	1208.2755	144130.9686	15664.2753	9980.5806
Lof-338-1	3	71.6776	0.2487	1247.2285	149098.5176	16216.7475	8162.0553
Lof-338-2	1	71.2744	0.3185	1210.4965	145704.6258	15793.8166	7921.0015
Lof-338-2	2	75.7500	0.1709	1164.6062	144998.0728	15628.2189	8044.1974
Lof-338-2	3	71.8519	0.2805	1207.1358	144739.0563	15320.1411	11486.6002
Lof-339-1	1	90.4980	0.0386	1233.8143	123287.4070	17942.6702	5663.5675
Lof-339-1	2	86.2112	0.1688	1202.6725	115336.9512	16932.8497	9101.4272
Lof-339-1	3	93.7986	0.1288	1240.4978	120781.7683	18238.7919	5889.3488
Lof-339-2	1	87.8058	0.1616	1229.7059	119657.1487	18200.0017	6975.5957
Lof-339-2	2	95.8389	0.0216	1269.3638	124182.9451	18051.9322	6946.6842
Lof-339-2	3	83.3992	0.1141	1193.6003	114860.0667	17015.4345	7107.8912
Lof-339-3	1	91.8974	0.1741	1184.8557	118523.3505	17857.7956	5971.9411
Lof-339-3	2	85.2816	0.0307	1226.9251	122634.9026	18600.7384	6290.1841
Lof-339-3	3	89.1761	0.2426	1200.7541	118249.4266	17282.7094	7983.5041
Lof-341-1	1	137.9829	0.4956	1217.4185	142581.2431	17407.1814	9942.1805
Lof-341-1	2	124.6589	0.3640	1276.1974	147261.1801	17982.9156	9875.3698
Lof-341-1	3	135.0750	0.5492	1311.5017	148486.1956	17983.7022	10533.9384
Lof-342-1	1	79.8060	0.1628	1451.6608	130804.6347	17920.4451	10086.9917
Lof-342-1	2-bad ablation						
Lof-342-1	3	72.2553	0.2746	1247.9545	112313.6762	16067.3545	18080.2981
Lof-342-2	1	86.5619	0.1092	1494.7961	141799.1892	19668.7837	7364.5564
Lof-342-2	2	82.1998	0.2149	1596.8094	144751.4837	19646.6790	6985.5124
Lof-342-2	3-bad ablation						
Lof-342-2	3	71.9681	0.2431	1288.6436	119312.1099	16715.1533	16275.8319
Lof-342-5	1	80.7283	0.0362	1359.8363	135493.6197	17152.5654	7007.6255
Lof-342-5	2	79.3627	0.2187	1453.0098	140467.5526	17926.9245	7268.5888
Lof-342-5	3	82.7471	0.2618	1354.5722	131997.0980	17365.9234	7151.7026
Lof-342-6	1	83.4567	-0.0117	1464.3491	140155.9376	19476.3534	7273.1516
Lof-342-6	2	91.6323	0.1674	1500.9071	143676.7823	19776.9362	8796.3606
Lof-342-6	3	84.0594	0.0242	1437.9320	136374.7305	19028.3493	7414.4370
Lof-344-1	1	93.5086	0.3609	1378.8216	141862.0566	22214.2407	8546.0709
Lof-344-1	2	84.3338	0.3780	1291.1219	140501.7534	21653.0771	8536.3126
Lof-344-1	3	96.1172	0.5738	1385.9122	145395.0743	22883.9291	8595.6422
Lof-344-2	1	85.1223	0.1052	1444.4657	145127.8629	21809.1878	8482.8665
Lof-344-2	2	94.1376	0.1808	1341.3838	144915.6896	22149.0841	8436.1779
Lof-344-2	3	88.3987	0.0752	1327.9331	142928.6921	22070.6841	8430.9262
Lof-344-3	1	91.8504	0.2929	1295.5484	140318.4576	21723.0739	8053.4790
Lof-344-3	2	91.8439	0.2459	1345.3949	145059.3931	22439.7779	8652.7936
Lof-344-3	3	98.5167	0.1624	1378.2441	146506.9760	22286.0762	8439.8979
Lof-351-1	1	59.6776	0.1720	1105.8419	143708.5074	8938.0227	6433.7429
Lof-351-1	2	64.9995	0.0985	1179.6798	145224.3285	9111.9991	6874.3610
Lof-351-1	3	69.7571	0.1610	1242.6553	151121.5856	9520.1019	6819.4360

Sample No.	Replicate	31 P	39 K	43 Ca	45 Sc	47 Ti	51 V	52 Cr
Lof-294-1	1	1316.4825	10153.3230	42584.4147	-35.6007	1279.7815	28.3817	12.8478
Lof-294-1	2	1095.9859	10894.0119	41423.3572	-35.3725	1065.7747	24.1323	11.7981
Lof-294-1	3	661.2848	10354.4683	44298.9642	-34.8373	1021.8707	22.1298	12.3729
Lof-338-1	1	1096.7584	10251.0128	34045.6562	-32.5104	1371.8320	14.4484	11.9808
Lof-338-1	2	1156.2786	10139.3097	34998.8427	-34.5551	1447.7212	17.4776	16.1906
Lof-338-1	3	1131.8154	10261.6662	33262.3943	-31.6399	1402.4116	14.9552	11.5540
Lof-338-2	1	1094.3834	9857.0421	33857.6513	-34.4013	1367.2325	14.7736	11.9508
Lof-338-2	2	1056.6483	9914.2216	34584.0077	-31.5350	1520.1417	15.8760	12.4119
Lof-338-2	3	1015.9501	9559.0870	34794.5264	-34.9423	1319.3828	13.3696	15.3336
Lof-339-1	1	463.6407	10756.9952	37296.5289	-36.3555	790.5342	24.3943	10.3964
Lof-339-1	2	881.8302	10412.0610	39556.4659	-33.6170	988.7953	26.8957	30.2868
Lof-339-1	3	511.8450	11265.0317	37041.5317	-34.9432	818.1693	25.1799	11.6383
Lof-339-2	1	540.8891	11267.1923	39961.3721	-35.5142	883.9739	25.9224	12.5465
Lof-339-2	2	621.0162	11392.9932	38384.8572	-36.6823	894.7492	26.2564	12.6443
Lof-339-2	3	667.3233	10820.0960	38582.4795	-37.1317	912.9234	24.7658	12.1377
Lof-339-3	1	506.2469	12244.2771	39510.9225	-36.4406	865.5716	24.2665	11.6250
Lof-339-3	2	448.0604	11848.9535	37864.6846	-38.3313	779.6482	23.0089	11.4783
Lof-339-3	3	751.0401	11582.0708	42569.3824	-37.4957	1064.4135	27.0499	17.0328
Lof-341-1	1	610.0712	10687.5786	19557.0806	-37.2753	1786.3205	50.6946	90.0683
Lof-341-1	2	623.3102	10075.1581	18935.3856	-37.7707	1701.3642	47.1128	82.4604
Lof-341-1	3	608.7731	10597.4715	18668.4869	-38.0261	1845.4445	52.6231	95.5145
Lof-342-1	1	897.3169	10121.6653	41589.7586	-36.3894	1365.3154	21.2086	89.6584
Lof-342-1	2-bad ablation							
Lof-342-1	3	856.9205	8412.0747	43006.8693	-35.9087	1950.3995	22.9495	312.1703
Lof-342-2	1	975.5874	10663.4453	40615.0017	-35.9728	1201.1333	21.1229	74.4161
Lof-342-2	2	943.0484	10655.8037	38866.7589	-36.3825	1237.5653	20.4885	69.4224
Lof-342-2	3-bad ablation							
Lof-342-2	3	802.7504	9205.2767	43777.6830	-35.5615	1660.1317	22.0267	112.3136
Lof-342-5	1	1203.4852	10565.1026	38743.4974	-37.6135	1097.5369	28.4604	60.0166
Lof-342-5	2	1167.2415	10546.1194	38253.5666	-38.2429	1068.7894	26.5324	56.8118
Lof-342-5	3	1225.7004	10682.4862	39567.5488	-38.5327	1077.9317	27.0950	56.6245
Lof-342-6	1	931.7553	10886.2085	40106.4623	-38.2283	1193.6659	21.1783	72.8274
Lof-342-6	2	931.2863	11131.2316	40162.7618	-37.0738	1333.6229	25.8746	91.2234
Lof-342-6	3	839.5039	10471.0266	40368.3616	-39.1073	1231.2815	22.0104	74.2927
Lof-344-1	1	839.3072	9333.1468	42042.4745	-37.4596	1336.4323	21.6398	63.7894
Lof-344-1	2	839.1876	9276.1228	42666.5088	-36.5752	1314.2729	20.6386	56.8750
Lof-344-1	3	844.5874	9389.0157	43116.1423	-35.5904	1413.0725	24.1240	68.5493
Lof-344-2	1	962.9959	9935.7346	41457.2302	-38.0249	1211.4228	20.0961	56.8780
Lof-344-2	2	842.5260	10256.3474	43245.0717	-36.9135	1303.8480	22.4467	64.3007
Lof-344-2	3	845.5111	10170.6543	42246.3486	-36.7388	1328.9100	21.0204	57.6905
Lof-344-3	1	810.2215	9401.9472	42200.9689	-40.2837	1209.7826	18.9414	51.8041
Lof-344-3	2	827.0744	9755.8026	45155.8159	-38.6937	1304.6563	20.6431	58.7994
Lof-344-3	3	877.7632	9578.6273	43332.4643	-38.8329	1406.0576	21.5821	61.2985
Lof-351-1	1	907.0425	11228.4580	24078.5026	-37.5963	573.5786	7.3546	7.9629
Lof-351-1	2	864.5899	11399.6195	26391.7131	-36.8761	611.8598	7.8793	8.6422
Lof-351-1	3	862.2886	11804.0409	26710.2606	-37.4435	607.1438	7.9252	12.4935

Sample No.	Replicate	55 Mn	56 Fe	59 Co	60 Ni	63 Cu	66 Zn	71 Ga
Lof-294-1	1	113.6932	54306.0664	1.4197	7.0013	95.3624	156.2123	2.5908
Lof-294-1	2	114.7752	51444.6035	1.2512	6.5042	86.7929	156.1062	3.0192
Lof-294-1	3	116.1025	48153.8736	1.2346	7.8935	70.8375	154.6195	2.9179
Lof-338-1	1	1959.8486	3204.0972	6.7549	17.9276	10142.1788	16.0774	3.2269
Lof-338-1	2	1811.4804	4004.8598	5.6393	16.0895	8804.7564	16.0375	2.9904
Lof-338-1	3	1915.2189	2917.3944	5.7826	14.1493	8295.7371	17.0202	2.6199
Lof-338-2	1	1819.5044	2848.2192	5.9177	15.6096	8828.9720	13.4786	2.7219
Lof-338-2	2	2019.9613	3128.4616	6.6043	15.8556	9700.8177	15.5270	3.0935
Lof-338-2	3	1718.9570	2991.2763	6.0507	18.7428	9230.1413	13.0343	2.7144
Lof-339-1	1	71.3955	49650.1825	1.0522	6.9942	101.8323	138.1277	2.2004
Lof-339-1	2	94.5847	58916.2241	1.3118	28.1946	944.9299	74.2866	1.8588
Lof-339-1	3	83.5367	49577.1212	1.1515	8.2272	122.3977	138.1537	2.2155
Lof-339-2	1	78.4792	54727.8486	1.3779	8.9486	242.3398	76.3175	2.1642
Lof-339-2	2	72.7211	54621.0814	1.1478	7.3310	339.1511	132.0781	2.1175
Lof-339-2	3	67.6119	54568.3690	1.0108	7.4664	534.7473	115.2647	2.1827
Lof-339-3	1	78.3592	52560.8514	1.3944	8.8378	77.6207	136.4513	2.1369
Lof-339-3	2	70.2253	46009.5868	1.2528	9.2512	69.6829	105.3586	1.9356
Lof-339-3	3	66.1691	62099.6368	1.0231	7.8507	790.7192	70.2371	2.3952
Lof-341-1	1	354.6376	56428.3960	12.0303	299.6080	46.0539	32.0853	3.6284
Lof-341-1	2	339.2470	53720.4899	11.6699	272.6694	32.8266	28.2488	3.1254
Lof-341-1	3	394.6590	63220.6422	13.1299	319.1450	45.1796	31.8642	3.5949
Lof-342-1	1	65.8377	27329.2115	3.8631	73.0621	211.2235	13.5278	2.4203
Lof-342-1	2-bad ablation							
Lof-342-1	3	75.2313	39622.1910	4.5235	223.2300	277.4008	8.4191	2.6192
Lof-342-2	1	64.5129	23325.4736	4.0937	75.7936	123.7647	14.8839	2.0403
Lof-342-2	2	61.7871	22269.6054	3.6443	70.2953	150.9064	13.0456	1.9628
Lof-342-2	3-bad ablation							
Lof-342-2	3	67.1374	32378.0504	3.7606	66.4566	240.6423	14.6722	2.4885
Lof-342-5	1	88.3173	28977.5090	12.9679	78.5402	13142.0609	127.2486	2.1445
Lof-342-5	2	87.7092	28455.0730	12.2305	74.0894	11211.6009	113.8167	2.0454
Lof-342-5	3	87.0065	28304.9061	11.8005	70.7814	10527.4107	115.7854	1.8601
Lof-342-6	1	70.2796	22355.6517	3.9743	72.8414	177.2919	17.0277	2.1739
Lof-342-6	2	88.5469	25234.0491	4.8523	79.7081	158.9533	18.0821	2.3446
Lof-342-6	3	73.8053	23796.8863	4.3112	71.6205	264.4686	13.7464	1.8927
Lof-344-1	1	77.1509	17103.4680	4.1225	49.1053	109.5398	14.8603	2.6285
Lof-344-1	2	68.5047	15422.0143	3.4428	41.4789	75.2446	14.3551	2.4271
Lof-344-1	3	83.9683	20518.7146	4.5280	54.3715	102.7035	17.1918	2.8110
Lof-344-2	1	70.6427	16386.2857	4.1286	48.9792	88.5831	22.2285	2.6376
Lof-344-2	2	85.0211	20072.4811	4.6386	57.0847	84.3538	24.1537	2.9694
Lof-344-2	3	69.2844	16291.2692	4.5134	51.8033	97.2928	18.1443	2.6125
Lof-344-3	1	68.7483	17145.8185	4.1686	48.8048	83.5482	14.8201	2.4881
Lof-344-3	2	71.4251	16958.2574	4.0269	46.7252	75.8935	15.3321	2.5772
Lof-344-3	3	75.9871	17642.9783	4.3431	50.3507	77.3541	15.8627	2.8819
Lof-351-1	1	120.8231	2195.1113	3.9078	9.9452	7697.7534	13.1299	1.7095
Lof-351-1	2	130.6586	2106.2996	3.7515	8.8968	7908.1562	14.9628	2.4845
Lof-351-1	3	131.3316	2187.2218	4.1052	9.5153	7653.4652	13.6782	1.9368

Sample No.	Replicate	75 As	78 Se	85 Rb	88 Sr	89 Y	90 Zr	93 Nb	107 Ag
Lof-294-1	1	39.0913	-2.7623	17.7669	296.5550	8.8714	95.4299	5.9418	0.1174
Lof-294-1	2	35.4045	-1.8634	21.0603	353.9151	9.1914	98.3798	5.4515	0.0002
Lof-294-1	3	26.8611	-1.0875	19.0889	316.3044	7.4504	81.8085	4.4933	-0.0173
Lof-338-1	1	316.0172	2.3581	20.2430	226.5322	9.7347	95.4751	5.5218	3.3130
Lof-338-1	2	274.5067	-2.6774	19.2048	215.4518	9.2168	94.2070	5.8002	3.0505
Lof-338-1	3	303.2784	-1.9392	18.9558	213.7026	9.4067	91.2556	5.1432	3.1196
Lof-338-2	1	318.5819	0.0071	19.4825	217.7209	9.6370	95.0295	5.5257	3.1822
Lof-338-2	2	337.3860	-0.3183	21.4190	239.1851	9.9871	98.9596	5.9388	3.4535
Lof-338-2	3	286.2711	0.5846	19.4805	222.6269	9.3100	108.7934	5.6843	3.2485
Lof-339-1	1	13.2917	-0.6433	17.5773	258.6888	5.0200	52.7194	3.1795	-0.0058
Lof-339-1	2	54.5395	-3.1166	15.3920	231.5958	4.9091	54.0395	3.6256	0.1038
Lof-339-1	3	38.0245	-0.6835	19.3171	271.8394	5.4469	55.1962	3.4519	0.0345
Lof-339-2	1	52.7962	-0.2238	20.1978	279.8988	5.4175	58.6845	3.4035	-0.0222
Lof-339-2	2	41.7530	-1.0965	19.2934	280.0981	5.6767	62.0582	3.9427	-0.0320
Lof-339-2	3	47.5897	-0.2383	16.7333	229.9533	4.9914	53.8004	3.5229	-0.0320
Lof-339-3	1	57.3546	-5.0278	21.0753	272.8385	5.7446	59.0969	3.4117	-0.0343
Lof-339-3	2	60.0442	-3.0855	17.8130	232.3758	5.2257	52.2954	2.9841	-0.0083
Lof-339-3	3	93.9133	-2.2911	17.0156	227.1943	5.1884	64.3452	3.4197	23.0277
Lof-341-1	1	21.8748	-5.9473	22.1096	128.7342	13.2568	89.3763	8.1889	-0.0489
Lof-341-1	2	13.5310	-2.8688	20.2544	120.0516	11.3808	70.2272	7.3772	-0.0740
Lof-341-1	3	16.5041	-1.6495	20.8265	123.8240	11.6704	83.7008	7.9735	-0.0463
Lof-342-1	1	59.5032	1.3555	16.9164	247.6428	6.8938	77.4066	4.7530	0.1281
Lof-342-1	2-bad ablation								
Lof-342-1	3	59.6998	-2.6579	12.8124	232.8552	7.5427	113.1691	6.1471	0.2588
Lof-342-2	1	49.7811	-0.5301	15.0069	228.0250	6.3069	67.4879	4.4209	-0.0238
Lof-342-2	2	45.1869	-2.9710	15.9331	235.2117	5.7347	52.2731	3.7345	0.0458
Lof-342-2	3-bad ablation								
Lof-342-2	3	63.9836	1.8617	13.5678	208.2743	6.7024	98.2659	5.0456	0.1176
Lof-342-5	1	219.9383	-0.1105	18.1929	248.5021	8.4992	72.8353	3.9545	4.9477
Lof-342-5	2	203.0034	-2.3273	17.7286	232.7864	8.3927	68.6602	3.5968	3.1753
Lof-342-5	3	200.7192	-3.8598	16.8245	230.7478	8.0617	67.9662	3.7624	2.8744
Lof-342-6	1	49.2409	-1.1175	16.5237	241.9726	6.2603	85.8704	4.3757	0.0558
Lof-342-6	2	60.7507	1.9195	17.9716	253.4337	7.1927	76.8447	4.3914	-0.0265
Lof-342-6	3	57.5016	-0.2039	15.8184	233.8136	6.1848	66.1931	4.1780	-0.0402
Lof-344-1	1	182.2435	1.5952	17.5432	300.8260	7.2673	50.2343	5.1609	-0.0795
Lof-344-1	2	159.7507	-0.6462	15.8744	268.0244	6.9103	45.8506	4.6970	-0.0806
Lof-344-1	3	177.5002	-4.2347	19.2973	332.4487	8.1919	55.0200	5.5726	-0.0198
Lof-344-2	1	257.3862	0.0220	17.4956	286.9335	6.8356	50.5939	5.0524	0.0589
Lof-344-2	2	247.5286	-3.1021	19.4967	312.1931	8.0391	53.8277	5.1591	-0.0798
Lof-344-2	3	174.1049	-5.8093	18.0192	302.0380	7.6787	48.5194	4.8476	-0.0637
Lof-344-3	1	143.1896	-0.1215	16.3051	283.4616	6.5632	44.1776	4.7396	-0.0562
Lof-344-3	2	162.9673	-2.8922	18.7363	308.7392	7.5533	50.0870	5.3244	0.0063
Lof-344-3	3	161.7947	-2.2933	18.2162	321.0924	7.4483	52.9667	5.5055	-0.0897
Lof-351-1	1	8.8975	-6.2681	16.5373	150.3417	8.1738	45.3295	2.7593	2.4603
Lof-351-1	2	9.1823	-3.7347	18.4155	172.6188	8.9604	57.5805	2.8585	2.5074
Lof-351-1	3	8.3154	-2.7117	17.6322	161.8764	8.1385	50.7028	2.8430	2.7431

Sample No.	Replicate	118 Sn	121 Sb	133 Cs	137 Ba	139 La	140 Ce	141 Pr	146 Nd
Lof-294-1	1	0.9216	36.6926	0.2784	69.3420	13.9038	28.0618	3.2255	11.4309
Lof-294-1	2	0.7576	31.7459	0.7411	73.7318	13.4296	26.4778	3.2152	12.5714
Lof-294-1	3	0.6586	22.3893	0.4134	59.7623	11.2148	22.3410	2.5176	9.2713
Lof-338-1	1	17.5575	51.7626	0.5787	82.2397	13.9764	27.2609	2.6996	10.9433
Lof-338-1	2	16.4346	46.8467	0.3235	66.3860	12.0963	23.9423	2.4452	9.2142
Lof-338-1	3	16.7265	48.1733	0.5020	75.1663	12.6198	26.4169	2.7025	10.4669
Lof-338-2	1	15.8665	47.9780	0.5944	75.5375	12.9140	27.0596	3.0012	9.9300
Lof-338-2	2	18.2630	58.1249	0.6763	83.1371	13.9805	27.9601	3.1954	10.6320
Lof-338-2	3	19.1954	48.6439	0.4860	112.6744	12.7191	25.2194	2.6806	10.5638
Lof-339-1	1	0.6712	13.8556	0.2486	42.4092	7.6011	15.6632	1.5097	5.7544
Lof-339-1	2	0.9363	57.4524	0.2550	73.2718	7.8005	15.6810	1.8192	5.4965
Lof-339-1	3	0.6681	135.8964	0.3628	44.2792	7.9214	16.6914	1.5958	5.8620
Lof-339-2	1	0.9344	222.5918	0.3209	49.3221	8.3756	16.6873	1.6030	6.4641
Lof-339-2	2	0.9034	148.6299	0.3796	59.4489	8.7990	18.0678	1.8242	6.8827
Lof-339-2	3	0.6974	110.0608	0.3648	65.5511	7.3097	15.3434	1.7015	6.0546
Lof-339-3	1	0.9317	321.5341	0.4521	47.7371	8.5169	17.8284	1.7096	6.3309
Lof-339-3	2	0.7640	309.7921	0.2985	46.1962	7.9233	15.4409	1.6328	5.8663
Lof-339-3	3	1.2564	224.2527	0.4356	69.9597	7.5730	15.1499	1.5862	5.3164
Lof-341-1	1	1.4181	29.8180	0.4395	146.2923	17.5166	33.7945	3.6667	13.7155
Lof-341-1	2	1.1101	5.2076	0.4837	142.7792	15.9879	32.2067	3.5447	14.0587
Lof-341-1	3	1.2396	16.2809	0.4491	144.5649	17.9405	33.7482	3.6466	14.6540
Lof-342-1	1	1.0487	370.4185	0.1739	72.0179	11.5579	22.0244	2.6067	8.9495
Lof-342-1	2-bad ablation								
Lof-342-1	3	1.7513	291.6385	0.3137	137.1266	12.8560	28.4853	3.0933	10.8663
Lof-342-2	1	0.7718	396.9238	0.3386	46.0701	10.5656	21.3739	2.3992	9.0780
Lof-342-2	2	0.4574	304.7252	0.2534	46.0879	10.4511	21.1592	2.0847	6.9237
Lof-342-2	3-bad ablation								
Lof-342-2	3	1.6161	260.4350	0.3579	102.7175	11.5475	22.5226	2.7049	9.4259
Lof-342-5	1	1.6171	869.6960	0.2438	50.5503	9.8811	19.5458	2.0893	7.7185
Lof-342-5	2	2.4129	803.9113	0.4473	47.4862	9.1180	19.7347	2.1653	8.0569
Lof-342-5	3	1.8838	781.1136	0.4640	42.9186	9.0135	17.9863	1.9442	7.0045
Lof-342-6	1	0.6670	301.3754	0.5124	50.9738	11.1592	22.4018	2.5172	9.9360
Lof-342-6	2	0.8879	397.9634	0.2011	52.7877	12.7790	25.0795	2.7929	10.1584
Lof-342-6	3	0.7070	296.5819	0.4519	49.8350	11.6533	22.9028	2.4531	9.9176
Lof-344-1	1	1.1192	370.8466	0.3717	41.9142	11.0253	20.3278	2.3253	7.3804
Lof-344-1	2	0.8483	352.0261	0.3971	37.6216	10.2095	20.0853	2.2086	7.6753
Lof-344-1	3	0.8461	373.8451	0.4161	43.8835	10.8612	21.8313	2.6611	7.7773
Lof-344-2	1	0.8382	1205.7812	0.4578	36.8888	9.1294	19.0609	2.0597	7.0493
Lof-344-2	2	0.7438	1370.1914	0.3960	42.0731	10.4679	21.1391	2.2663	9.7768
Lof-344-2	3	0.9565	666.0995	0.2291	42.3247	10.9730	21.5003	2.4317	8.4110
Lof-344-3	1	0.5405	319.7297	0.3727	38.1682	10.5197	19.3934	2.2236	8.2033
Lof-344-3	2	1.3341	370.1580	0.4731	39.9876	11.2429	21.9491	2.3126	8.5751
Lof-344-3	3	1.0348	362.2882	0.3104	42.3700	11.1173	22.9725	2.6528	8.2244
Lof-351-1	1	1.6640	4.9886	0.2832	34.9850	7.9344	16.4041	1.9016	6.6328
Lof-351-1	2	2.2066	3.7950	0.2595	41.6861	9.1476	17.5718	1.9908	7.6049
Lof-351-1	3	1.9450	4.0497	0.4202	40.8945	9.4045	19.8954	2.5075	8.3361

Sample No.	Replicate	147 Sm	153 Eu	157 Gd	159 Tb	163 Dy	165 Ho	166 Er	169 Tm
Lof-294-1	1	2.6755	0.3365	1.5511	0.2786	1.9195	0.3675	1.1824	0.1547
Lof-294-1	2	1.9284	0.2920	1.9557	0.2855	1.4321	0.1995	0.8318	0.0816
Lof-294-1	3	1.5291	0.2162	1.7000	0.1845	0.9792	0.2478	0.5679	0.0828
Lof-338-1	1	2.2741	0.2328	1.6704	0.2736	2.0081	0.3887	0.9049	0.0938
Lof-338-1	2	1.7847	0.1476	2.4696	0.2385	1.3245	0.3591	0.8398	0.0361
Lof-338-1	3	1.9061	0.1915	1.9412	0.3104	1.5612	0.2245	0.7613	0.1043
Lof-338-2	1	1.9000	0.0939	2.1031	0.2346	1.6650	0.3003	0.9458	0.0716
Lof-338-2	2	1.7788	0.1924	1.8314	0.2522	1.7479	0.2537	1.1529	0.0901
Lof-338-2	3	1.8026	0.2457	1.9584	0.1863	1.5163	0.3288	0.8048	0.0698
Lof-339-1	1	1.1424	0.1606	1.0049	0.1104	0.9412	0.1005	0.4362	0.0100
Lof-339-1	2	0.6631	0.1093	0.9985	0.1168	0.8927	0.1367	0.2783	0.0390
Lof-339-1	3	0.7821	0.1482	0.9930	0.1119	0.9777	0.1297	0.2935	-0.0130
Lof-339-2	1	1.0687	0.0918	0.6998	0.1358	0.8416	0.1462	0.3382	-0.0035
Lof-339-2	2	1.1464	0.1436	1.0596	0.2529	1.2178	0.1702	0.3720	0.0246
Lof-339-2	3	1.0188	0.1027	1.2082	0.1543	0.9487	0.1562	0.4410	0.0024
Lof-339-3	1	1.2630	0.1346	0.7570	0.1392	1.1550	0.1764	0.6292	-0.0016
Lof-339-3	2	1.0161	0.1050	1.0745	0.1275	0.9053	0.1319	0.4707	-0.0021
Lof-339-3	3	1.1616	0.1640	0.9774	0.1482	0.7091	0.2055	0.3540	0.0558
Lof-341-1	1	2.1937	0.2881	2.8131	0.3320	2.0315	0.3991	1.0839	0.1033
Lof-341-1	2	2.3098	0.2809	2.1495	0.3024	1.9381	0.3719	0.9220	0.0479
Lof-341-1	3	3.2874	0.1882	2.3401	0.2495	2.3197	0.3313	0.9583	0.0904
Lof-342-1	1	1.5393	0.2109	1.4885	0.1858	1.1501	0.2473	0.7487	0.0773
Lof-342-1	2-bad ablation								
Lof-342-1	3	2.2224	0.3599	1.9564	0.1971	1.4910	0.2899	0.6646	0.1099
Lof-342-2	1	1.7880	0.0898	1.2974	0.1282	0.8781	0.1591	0.3315	0.0286
Lof-342-2	2	1.7338	0.0990	1.8331	0.1983	1.0332	0.1019	0.4172	0.0495
Lof-342-2	3-bad ablation								
Lof-342-2	3	1.9063	0.1995	1.6600	0.2066	1.3363	0.2466	0.5222	0.0398
Lof-342-5	1	1.9784	0.3473	1.5957	0.2045	1.4947	0.2847	0.5905	0.0508
Lof-342-5	2	1.6530	0.2769	1.5081	0.2117	1.2948	0.3209	0.6126	0.0309
Lof-342-5	3	1.5535	0.2296	1.7347	0.1518	1.3926	0.1706	0.4517	0.0272
Lof-342-6	1	1.1072	0.2731	1.3630	0.2029	1.3448	0.1848	0.6290	0.0023
Lof-342-6	2	1.9306	0.1580	1.3542	0.1799	1.6552	0.1810	0.4164	0.0481
Lof-342-6	3	1.1280	0.1508	1.7589	0.2278	1.1347	0.2434	0.6642	0.0233
Lof-344-1	1	1.4283	0.1101	1.4336	0.1542	1.1338	0.2231	0.5630	0.0258
Lof-344-1	2	1.1837	0.2285	1.3566	0.1811	1.1702	0.1763	0.6406	0.0297
Lof-344-1	3	1.4588	0.1191	1.6988	0.1540	1.1796	0.2120	0.5086	0.0474
Lof-344-2	1	1.4502	0.1290	1.5268	0.1694	0.9900	0.1926	0.5194	-0.0110
Lof-344-2	2	1.5568	0.2081	2.1728	0.2576	1.1972	0.2049	0.5019	0.0493
Lof-344-2	3	1.7654	0.1709	1.4298	0.2135	1.0083	0.1855	0.6646	0.0345
Lof-344-3	1	1.3730	0.2316	1.5862	0.1342	1.3151	0.2190	0.6816	0.0322
Lof-344-3	2	1.2407	0.1792	1.2522	0.2657	1.2719	0.1793	0.5842	0.0440
Lof-344-3	3	1.2902	0.2650	1.7260	0.1757	0.9096	0.2392	0.6378	0.0958
Lof-351-1	1	1.4758	0.1700	1.8266	0.2033	1.3977	0.2700	0.7322	0.1156
Lof-351-1	2	1.9307	0.2485	1.8544	0.2065	1.6080	0.2834	0.6900	0.0512
Lof-351-1	3	2.0888	0.3183	1.8079	0.3019	1.5828	0.3069	0.7863	0.0826

Sample No.	Replicate	172 Yb	175 Lu	178 Hf	182 W	208 Pb	209 Bi	232 Th	238 U
Lof-294-1	1	0.9792	0.1074	2.8698	0.8515	4941.9632	-0.2640	9.1749	2.6010
Lof-294-1	2	1.0250	0.0611	2.3694	0.8499	1773.6262	-0.1890	6.7446	2.6997
Lof-294-1	3	0.8375	0.1105	1.8869	0.9261	20.9817	-0.1591	5.5562	2.8351
Lof-338-1	1	1.0576	0.0827	2.3181	1.2907	48.5769	-0.1052	6.1518	1.3207
Lof-338-1	2	0.8580	0.0013	2.0988	1.1146	42.6616	-0.1103	5.6050	1.5097
Lof-338-1	3	0.6779	0.0765	2.0398	0.8277	45.5184	-0.2100	5.6974	1.5267
Lof-338-2	1	1.0126	0.0565	2.4248	0.9585	48.4547	-0.1038	6.5354	1.5592
Lof-338-2	2	0.6430	0.1070	2.3534	1.2541	50.7106	-0.2986	6.6337	1.7049
Lof-338-2	3	0.9079	0.0267	2.8901	1.1372	44.2463	0.1793	6.9929	1.8090
Lof-339-1	1	0.6226	-0.0177	1.0446	0.9854	1.8879	-0.3288	3.3662	2.0928
Lof-339-1	2	0.4171	-0.0081	1.2559	0.9302	38.2129	-0.1821	4.2383	1.8642
Lof-339-1	3	0.2487	-0.0308	1.0399	0.8885	3.9446	-0.2058	3.3943	2.6413
Lof-339-2	1	0.5505	0.0157	1.0784	0.8137	9.0643	-0.1355	3.9365	2.3598
Lof-339-2	2	0.7441	0.0871	1.6354	0.7323	13.7590	-0.2328	4.1136	2.5019
Lof-339-2	3	0.6647	-0.0070	1.3054	0.6512	19.7010	-0.2585	4.4242	2.4529
Lof-339-3	1	0.6676	0.0207	1.1917	0.9908	6.6451	-0.2597	3.7236	2.8852
Lof-339-3	2	0.4079	-0.0071	0.9145	0.8302	3.7856	-0.3395	3.4893	2.1270
Lof-339-3	3	0.5547	-0.0768	1.5624	0.6876	32.6121	-0.2289	3.4688	2.0011
Lof-341-1	1	1.1476	0.1493	2.0672	0.7643	3.0389	-0.3516	9.4779	1.8030
Lof-341-1	2	1.3184	0.1002	1.4618	0.7932	2.7435	-0.3581	8.7531	1.6927
Lof-341-1	3	1.3420	0.0963	2.0953	0.6741	3.2767	-0.3425	9.6719	1.8006
Lof-342-1	1	0.5492	0.0852	2.1459	0.9642	175.6932	-0.1758	6.5563	1.7507
Lof-342-1	2-bad ablation								
Lof-342-1	3	0.7307	0.0714	2.4928	1.1474	295.3459	-0.1494	9.7882	1.3669
Lof-342-2	1	0.8939	0.0345	1.5501	0.7499	47.5083	-0.3477	5.6430	1.9082
Lof-342-2	2	0.6258	0.0122	1.1515	1.0334	29.7708	-0.3179	5.2869	1.7122
Lof-342-2	3-bad ablation								
Lof-342-2	3	0.9505	0.0587	2.5448	0.9830	238.9150	-0.2071	8.3071	1.8410
Lof-342-5	1	0.8975	0.0713	1.7070	0.7465	24.9365	-0.2477	3.7202	2.0173
Lof-342-5	2	0.8206	0.1026	1.2981	0.8647	24.7197	-0.2444	3.4439	1.7698
Lof-342-5	3	0.8146	0.0301	1.6117	0.9344	25.0104	-0.3956	3.5207	2.1901
Lof-342-6	1	0.7018	0.0028	2.0879	1.0877	56.1044	-0.3022	5.1064	1.6275
Lof-342-6	2	0.8326	0.0476	2.2878	0.9824	60.2397	-0.3433	5.9016	1.9740
Lof-342-6	3	0.6327	-0.0019	1.3398	0.7605	58.4529	-0.2139	4.7500	1.6122
Lof-344-1	1	0.6313	0.0759	1.0630	1.0192	163.5425	-0.3617	4.7708	2.2182
Lof-344-1	2	0.8029	0.0070	1.1089	0.9471	147.2684	-0.2836	4.5237	2.0335
Lof-344-1	3	0.7596	0.0827	1.4196	0.7686	156.8876	-0.3314	4.8758	1.9380
Lof-344-2	1	0.7483	-0.0245	0.8717	0.6374	169.5332	-0.2944	4.3268	1.9724
Lof-344-2	2	0.7710	0.0629	1.1198	0.7803	164.3266	-0.4327	3.9024	2.3780
Lof-344-2	3	0.7427	0.0246	0.7768	1.1583	160.1593	-0.4430	4.8148	2.0290
Lof-344-3	1	0.6286	0.0001	0.7112	0.7838	130.1535	-0.3281	3.9234	1.8411
Lof-344-3	2	0.6728	0.0519	0.8346	1.1531	148.9493	-0.2009	4.7788	2.0321
Lof-344-3	3	0.8365	0.1015	0.7404	0.8167	163.2228	-0.3389	4.8974	2.1394
Lof-351-1	1	0.7735	0.0747	1.1877	0.6784	2.9866	-0.2793	2.7279	1.1148
Lof-351-1	2	0.5255	-0.0168	1.2541	0.7399	3.7489	-0.2976	2.8035	1.0442
Lof-351-1	3	0.5683	0.0787	1.1366	0.6396	3.5154	-0.3808	2.5279	0.9929

D.4. Principle Component Analysis - Eigen values and their contributions to the correlations

EPMA-Major and Minor Oxides

	PC1	PC2	PC3	PC4	PC5	PC6	PC7	PC8	PC9	PC10
Eigenvalue	3.921	1.4972	1.407	0.87591	0.63322	0.59832	0.48222	0.35366	0.14077	0.0907
Proportion Explained	0.3921	0.1497	0.1407	0.08759	0.06332	0.05983	0.04822	0.03537	0.01408	0.00907
Cumulative Proportion	0.3921	0.5418	0.6825	0.77011	0.83343	0.89326	0.94149	0.97685	0.99093	1

LA-ICP-MS-Trace elements

	PC1	PC2	PC3	PC4	PC5	PC6	PC7	PC8	PC9	PC10
Eigenvalue	4.3385	2.2128	1.5987	1.195	0.5544	0.35881	0.28867	0.25012	0.109748	4.3385
Proportion Explained	0.3944	0.2012	0.1453	0.1086	0.0504	0.03262	0.02624	0.02274	0.009977	0.3944
Cumulative Proportion	0.3944	0.5956	0.7409	0.8495	0.8999	0.93257	0.95881	0.98155	0.991525	0.3944

REFERENCES

Abe, Y., Harimoto, R., Kikugawa, T., Yazawa, K., Nishisaka, A., Kawai, N., Yoshimura, S., and Nakai, I., 2012, Transition in the use of cobalt-blue colorant in the New Kingdom of Egypt, *Journal of Archaeological Science*, **39**(6), 1793–808.

Alivizatou, A., 2017, Τυπολογία και χαρακτηρισμός υαλωδών αντικειμένων από μυκηναϊκά νεκροταφεία της Κεφαλονιάς, Master's Thesis, University of Peloponnese, Kalamata, Greece.

Ancient Methone Archaeological Project, 2018, Methone Conservation Database, University of California, Los Angeles.

Angelini, I., Artioli, G., Bellintani, P., Diella, V., Gemmi, M., Polla, A., and Rossi, A., 2004, Chemical analyses of Bronze Age glasses from Frattesina di Rovigo, Northern Italy, *Journal of Archaeological Science*, **31**(8), 1175–84.

Angelini, I., Artioli, G., Bellintani, P., and Polla, Y., 2005, Protohistoric vitreous materials from Italy: Faience to Final Bronze Age glasses, In *Annales du 16e Congrès de l'Association Internationale pour l'Histoire du Verre* (ed. M.-D. Nenna), 32–6, AIHV, Nottingham, UK.

Angelini, I., 2008, Faience production in Northern and Western Europe, In *Production Technology of Faience and Related Early Vitreous Materials* (M. S. Tite, and A. J. Shortland), Oxford University School of Archaeology, Oxford, UK.

Angelini, I., Polla, A., Giussani, B., Bellintani, P., and Artioli, G., 2009, Final Bronze Age glass in northern and central Italy: Is Frattesina the only glass production centre?, In *Proceedings Actes ISA 2006* (eds. J.-F. Moreau, R. Auger, J. Chabot, and A. Herzog), 329–36, 36th International Symposium on Archaeometry. 2-6 May 2006, Quebec City , Canada, CELAT, Université Laval, Quebec City, Canada.

Aruz, J., Benzel, K., and Evans, J. M., 2008, *Beyond Babylon: Art, Trade, and Diplomacy in the Second Millennium B.C.*, Metropolitan Museum of Art, New York, NY.

Bachhuber, C., 2006, Aegean interest on the Uluburun ship, *American Journal of Archaeology*, **110**(3), 345–63.

Barkoudah, Y., and Henderson, J., 2006, Plant ashes from Syria and the manufacture of ancient glass: ethnographic and scientific aspects, *Journal of Glass Studies*, **48**, 297–321.

Baxter, M., 2009, Archaeological data analysis and fuzzy clustering, *Archaeometry*, **51**(6), 1035–54.

Baxter, M. J., and Freestone, I. C., 2006, Log-ratio compositional data analysis in archaeometry, *Archaeometry*, **48**(3), 511–31.

Beck, H., 1928, *Classification and Nomenclature of Beads and Pendants* Reprint 1981 ed., George Shumway Pub, York, PA.

Bejko, L., 2002, Mycenaean presence and influence in Albania, In *Grčki utjecaj na istočnoj obali Jadrana. Greek influence along the East Adriatic Coast. Zbornik radova sa znanstvenog skupa održanog 24. do 26. rujna 1998. godine u Splitu. Proceedings of the International Conference held at Split from September 24th to 26th 1998.* (eds. N. Cambi, S. Čače, and B. Kirigan), 9–24, Književni Krug, Split, Croatia.

Bellintani, P., 2015, Bronze Age vitreous materials in Italy, In *Annales du 19e Congrès de l'Association Internationale pour l'Histoire du Verre, Piran, 17th – 21st September 2012* (ed. I. Lazar), 15–21, AIHV, Thessaloniki, Greece.

Blegen, C. W., and Pierce Blegen, E., 1937, *Prosymna: The Helladic Settlement Preceding the Argive Heraeum*, Cambridge University Press, Cambridge.

Bodinaku, N., 1982, Varreza tumulare e Pazhokut (Gërmime të vitit 1973) / La nécropole tumulaire de Pazhok (Fouilles de 1973), *Iliria*, **12**(1), 49–101.

Bouquillon, A., Kaczmarczyk, A., and Vandiver, P. B., 2008, Faience production in the Near East and the Indus River Valley, In *Production Technology of Faience and Related Early Vitreous Materials* (eds. M. S. Tite, and A. J. Shortland), 93–110, Oxbow Books, Oxford, UK.

Brems, D., and Degryse, P., 2013, Trace element analysis in provenancing Roman glass-making, *Archaeometry*, **56**(1), 116–36.

Brill, R. H., 1970, Some chemical observations on the glass making texts, In *Glass and Glassmaking in Ancient Mesopotamia: An Edition of the Cuneiform Texts which Contain Instructions for Glassmakers with a Catalogue of Surviving Objects* (eds. A. L. Oppenheim, R. H. Brill, D. Barag, and A. von Saldern), 329–35, Corning Museum of Glass, Corning, NY.

Brill, R. H., 1988, Scientific investigations of the Jalame glass and related finds, In *Excavations at Jalame: Site of a Glass Factory in Late Roman Palestine* (ed. G. D. Weinberg), 257–94, University of Missouri Press, Columbia Missouri.

Brill, R. H., 1992, Chemical analyses of some glasses from Frattesina, *Journal of Glass Studies*, **34**, 11–22.

Brill, R. H., 1999, *Chemical Analyses of Early Glasses*, 2 vols., Corning Museum of Glass, Corning, NY.

Brill, R. H., 2008, Personal communication.

Brunton, G., 1930, *Qau and Badari III*, British School of Archaeology in Egypt, London, UK.

Brunton, G., and Morant, G. M., 1937, *Mostagedda and the Tasian culture*, B. Quaritch Ltd., London.

Cagno, S., Cosyns, P., Izmer, A., Vanhaecke, F., Nys, K., and Janssens, K., 2014, Deeply colored and black-appearing Roman glass: A continued research, *Journal of Archaeological Science*, **42**, 128–39.

Cavallo, G., 2009, Alteration of azurite into paratacamite at the St. Alessandro Church (Lasnigo, Italy), *Conservar Património*, **9**, 5–11.

Cholakova, A., and Rehren, T., 2014, Producing black glass during the Roman period – notes on a crucible fragment from Serdica, Bulgaria, In *Proceedings of the 39th International Symposium for Archaeometry, 28 May-1 June 2012, Leuven, Belgium*, 261–7, Center for Archaeological Sciences, Leuven, Belgium.

Clark, D. E., and Hench, L. L., 1981, An overview of the physical characterization of leached surfaces, *Nuclear and Chemical Waste Management*, Leachability of Radioactive Solids, **2**(2), 93–101.

Conte, S., Matarese, I., Quartieri, S., Arletti, R., Jung, R., Pacciarelli, M., and Gratuze, B., 2015, Bronze Age vitreous materials from Punta di Zambrone (southern Italy), *European Journal of Mineralogy*, **27**(3), 337–51.

Conte, S., Arletti, R., Mermati, F., and Gratuze, B., 2016, Unravelling the Iron Age glass trade in southern Italy: The first trace-element analyses, *European Journal of Mineralogy*, **28**(2), 409–33.

Conte, S., Arletti, R., Henderson, J., Degryse, P., and Blomme, A., 2018, Different glassmaking technologies in the production of Iron Age black glass from Italy and Slovakia, *Archaeological and Anthropological Sciences*, **10**(3), 503–21.

Conte, S., Matarese, I., Vezzalini, G., Pacciarelli, M., Scarano, T., Vanzetti, A., Gratuze, B., and Arletti, R., 2019, How much is known about glassy materials in Bronze and Iron Age Italy? New data and general overview, *Archaeological and Anthropological Sciences*, **11**(5), 1813–41.

Corning Museum of Glass, 2002, Iridescence, *Glass Dictionary*, URL: https://www.cmog.org/glass-dictionary/iridescence.

Cosyns, P., 2011, The Production, Distribution and Consumption of Black Glass in the Roman Empire During the 1st - 5th century AD: An Archaeological, Archaeometric and Historical Approach, PhD Thesis, Vrije Universiteit Brussel, Brussels, Belgium.

Cox, G. A., Heavens, O. S., Newton, R. G., and Pollard, A. M., 1979, A study of weathering behavior of medieval glass from York Minster, *Journal of Glass Studies*, **21**, 54–75.

Cox, G. A., and Ford, B. A., 1993, The long-term corrosion of glass by ground-water, *Journal of Materials Science*, **28**(20), 5637–47.

Damiata, B. N., Papadopoulos, J. K., Amore, M. G., Morris, S. P., Bejko, L., Marston, J. M., and Southon, J., 2009, Towards an absolute chronology of Albanian archaeology: AMS radiocarbon dates from Apollonia and Lofkënd, *Illyria*, **33**, 166–86.

Damiata, B. N., and Southon, J., 2014a, The absolute chronology of the tumulus: Results of AMS dating of human bone and charcoal samples from the Lofkënd tumulus, In *The Excavation of the Prehistoric Burial Tumulus at Lofkënd, Albania* (eds. J. K. Papadopoulos, S. P. Morris, L. Bejko, and L. Schepartz), Vol. 1, 2 vols., 112–6, Cotsen Institute of Archaeology Press, Los Angeles, CA.

Damiata, B. N., and Southon, J., 2014b, The relative and absolute chronology of the tumulus, In *The Excavation of the Prehistoric Burial Tumulus at Lofkënd, Albania* (eds. J. K. Papadopoulos, S. P. Morris, L. Bejko, and L. A. Schepartz), Vol. 1, 2 vols., 109–21, Cotsen Institute of Archaeology Press, Los Angeles, CA.

Dardeniz, G., 2018, The preliminary archaeological and scientific evidence for glass making at Tell Atchana/Alalakh, Hatay (Turkey), *Anatolian Archaeological Studies*, **21**, 95–110.

Davison, S., 2008, *Conservation and Restoration of Glass* 2nd ed., Routledge, London, UK.

Degryse, P., Henderson, J., and Hodgins, G., 2009, Isotopes in vitreous materials, a state-of-the-art perspective, In *Isotopes in Vitreous Materials* (eds. P. Degryse, J. Henderson, and G. Hodgins), 15–30, Studies in Archaeological Sciences, Leuven University Press, Leuven, Belgium.

Degryse, P., Boyce, A., Erb-Satullo, N., Eremin, K., Kirk, S., Scott, R., Shortland, A. J., Schneider, J., and Walton, M. S., 2010a, Isotopic discriminants between Late Bronze Age glasses from Egypt and the Near East, *Archaeometry*, **52**(3), 380–8.

Degryse, P., Freestone, I., Jennings, S., and Schneider, J., 2010b, Technology and provenance study of Levantine plant ash glass using Sr-Nd isotope analysis, In *Glass in Byzantium – Production, Usage,*

Analyses (eds. J. Drauke, and D. Keller), 83–91, Romisch-Germanischen Zentralmuseums, Mainz, Germany.

Degryse, P., Lobo, L., Shortland, A. J., Vanhaecke, F., Blomme, A., Painter, J., Gimeno, D., Eremin, K., Greene, J., Kirk, S., and Walton, M. S., 2015, Isotopic investigation into the raw materials of Late Bronze Age glass making, *Journal of Archaeological Science*, **62**, 153–60.

Doménech-Carbó, M.-T., Doménech-Carbó, A., Osete-Cortina, L., and Saurí-Peris, M.-C., 2006, A study on corrosion processes of archaeological glass from the Valencian region (Spain) and its consolidation treatment, *Microchimica Acta*, **154**(1–2), 123–42.

Dotsika, E., Poutoukis, D., Tzavidopoulos, I., Maniatis, Y., Ignatiadou, D., and Raco, B., 2009, A natron source at Pikrolimni Lake in Greece? Geochemical evidence, *Journal of Geochemical Exploration*, **103**(2–3), 133–43.

Eder, B., 2009, The northern frontier of the Mycenaean world, In *2° Αρχαιολογικό Έργο Θεσσαλίας και Στερεάς Ελλάδας, Πρακτικά επιστημονικής συνάντησης, Βόλος* (eds. A. Mazarakis Ainian, and A. Doulgeri-Intzesiloglou), 113–31, Volos, Greece.

Eder, B., 2015, Stone and glass: The ideological transformation of imported materials and their geographic distribution in Mycenaean Greece, In *Political Systems and Modes of Interaction in the Aegean and the Near East in the 2nd Millennium BCE, Proceedings of the International Symposium at the University of Freiburg Institute for Archaeological Studies, 30th May - 2nd June 2012* (eds. B. Eder, and R. Prusinsxzky), 221–42, Austrian Academy of Sciences Press, Vienna, Austria.

Eisen, G. A., 1916, The characteristics of eye beads from the earliest times to the present, *American Journal of Archaeology*, **20**(1), 1–27.

El-Shamy, T. M., Lewins, J., and Douglas, R. W., 1972, The dependence on the pH of the decomposition of glasses by aqueous solutions, *Glass Technology*, **13**(3), 81–7.

El-Shamy, T. M., Morsi, S. E., Taki-Eldin, H. D., and Ahmed, A. A., 1975, Chemical durability of Na2O-CaO-SiO2 glasses in acid solutions, *Journal of Non-Crystalline Solids*, **19**, 241–50.

Evans, A. J., 1964, *The Palace of Minos: A Comparative Account of the Successive Stages of the Early Cretan Civilization as Illustrated by the Discoveries at Knossos*, Vol. I, Biblio and Tannen, New York, NY.

Everitt, B., and Hothorn, T., 2011, *An Introduction to Applied Multivariate Analysis with R*, Springer Science & Business Media.

Foster, H. E., and Jackson, C. M., 2005, "A whiter shade of pale"? Chemical and experimental investigation of opaque white Roman glass gaming counters, *Glass Technology*, **46**(5), 327–33.

Foster, K. P., 1979, *Aegean Faience of the Bronze Age.*, Yale University Press, New Haven.

Frankfort, H., and Pendlebury, J. D. S., 1933, *The City of Akhenaton, Part II, The North Suburb and the Desert Altars. The Excavations at Tell El Amarna During the Seasons 1926-1932.*, The Egypt Exploration Society. Memoirs 40, Egyptian Exploration Society, London, UK.

Freestone, I., 1987, Composition and microstructure of early opaque red glasses, In *Early Vitreous Materials* (M. Bimson, and I. Freestone), 173–91, British Museum Press, London.

Freestone, I., 2001, Post-depositional changes in archaeological ceramics and glasses, In *Handbook of Archaeological Sciences* (eds. D. R. Brothwell, and A. M. Pollard), 615–25, John Wiley, Chichester.

Freestone, I. C., 2005, The provenance of ancient glass through compositional analysis, In *Materials Issues in Art and Archaeology VII* (eds. P. Vandiver, J. L. Mass, and A. Murray), 195–208, Materials Research Society symposium, Materials Research Society, Warrendale.

Gueli, A. M., Pasquale, S., Tanasi, D., Hassam, S., Lemasson, Q., Moignard, B., Pacheco, C., Pichon, L., Stella, G., and Politi, G., 2020, Weathering and deterioration of archeological glasses from late Roman Sicily, *International Journal of Applied Glass Science*, **11**(1), 215–25.

Haevernick, T. E., 1981a, Ausgrabungen in Tiryns 1977, In *Beiträge zur Glasforschung :die wichtigsten Aufsätze von 1938 bis 1981*, 404–10, P. von Zabern, Mainz am Rhein, Germany.

Haevernick, T. E., 1981b, Die Glasperlen der Býčí skála-Höhle, In *Beiträge zur Glasforschung :die wichtigsten Aufsätze von 1938 bis 1981 /*, 411–6, Mainz am Rhein, Germany.

Harding, A., 1976, Illyrians, Italians and Mycenaeans : Trans-Adriatic contacts during the Late Bronze Age, *Iliria*, **4**(1), 157–62.

Hench, L. L., and Clark, D. E., 1978, Physical chemistry of glass surfaces, *Journal of Non-Crystalline Solids*, **28**(1), 83–105.

Henderson, J., and Warren, S. E., 1981, X-Ray fluorescence analyses of Iron Age glass: Beads from Meare and Glastonbury Lake Villages, *Archaeometry*, **23**(1), 83–94.

Henderson, J., 1988a, Electron probe microanalysis of mixed-alkali glasses, *Archaeometry*, **30**(1), 77–91.

Henderson, J., 1988b, Glass production and Bronze Age Europe, *Antiquity*, **62**(236), 435–51.

Henderson, J., 1992, The scientific analysis of vitreous materials from Kentria and Theologos-Tsiganadika tombs, In *Prōtoïstorikē Thasos: ta nekrotapheia tou oikismou Kastri* (C. Koukoulē-Chrysanthakē), 804–6, Ekdosē tou Tameiou Archaiologikōn Porōn kai Apallotriōseōn, Athens, Greece.

Henderson, J., Evans, J., and Nikita, K., 2010, Isotopic evidence for the primary production, provenance and trade of Late Bronze Age glass in the Mediterranean, *Mediterranean Archaeology and Archaeometry*, **10**(1), 1–24.

Henderson, J., 2013, *Ancient glass : An Interdisciplinary Exploration*, Cambridge University Press, New York.

Henderson, J., Evans, J., Bellintani, P., and Bietti-Sestieri, A.-M., 2015, Production, mixing and provenance of Late Bronze Age mixed alkali glasses from northern Italy: An isotopic approach, *Journal of Archaeological Science*, **55**, 1–8.

Higgins, R., 1961, *Greek and Roman Jewellery*, Methuen, London.

Hodgkinson, A., 2014, Royal Cities of the New Kingdom: A Spatial Analysis of Production and Socio-economics in Late Bronze Age Egypt, PhD Thesis, University of Liverpool, Liverpool, UK.

Holakooei, P., Ahmadi, M., Volpe, L., and Vaccaro, C., 2017, Early opacifiers in the glaze industry of first millenniumBC Persia: Persepolis And Tepe Rabat, *Archaeometry*, **59**(2), 239–54.

Hollocher, K., and Ruiz, J., 1995, Major and trace element determinations on NIST glass standard reference materials 611, 612, 614 and 1834 by inductively coupled plasma-mass spectrometry, *Geostandards Newsletter*, **19**(1), 27–34.

Ingram, R., 2014, Vitreous beads from the Uluburun shipwreck, In *Beyond ornamentation. Jewelry as an Aspect of Material Culture in the Ancient Near East* (eds. A. Golani, and Z. Wygnanska), 225–46, Polish Archaeology in the Mediterranean Special Studies: 23/2, Polish Centre of Mediterranean Archaeology, University of Warsaw, Warzaw, Poland.

Ingram, R. S., 2005, Faience and Glass Beads from the Late Bronze Age Shipwreck at Uluburun, Master's Thesis, Texas A&M University, College Station, TX.

Jackson, C. M., and Wager, E. C. (eds.), 2008, *Vitreous materials in the late Bronze Age Aegean*, Sheffield Studies in Aegean Archaeology 9, Oxbow Books, Oxford.

Jackson, C. M., and Nicholson, P. T., 2010, The provenance of some glass ingots from the Uluburun shipwreck, *Journal of Archaeological Science*, **37**(2), 295–301.

Jackson, C. M., Greenfield, D., and Howie, L. A., 2012, An assessment of compositional and morphological changes in model archaeological glasses in an acid burial matrix, *Archaeometry*, **54**(3), 489–507.

Kaczmarczyk, A., and Hedges, R., 1983, *Ancient Egyptian Faience: An Analytical Survey of Egyptian Faience from Predynastic to Roman Times*, Aris & Philips, Warminster.

Kaczmarczyk, A., and Vandiver, P. B., 2008, Faience production in Egypt, In *Production Technology of Faience and Related Early Vitreous Materials* (eds. M. S. Tite, and A. J. Shortland), 57–92, Oxford University School of Archaeology.

Karydas, A. G., 2007, Application of a portable XRF spectrometer for the non-invasive analysis of museum metal artefacts, *Annali di Chimica*, **97**(7), 419–32.

Kavvadias, P., 1913, Περί των εν Κεφαλληνία Ανασκαφών, *Πρακτικά της εν Αθήναις Αρχαιολογικής Εταιρείας του έτους 1912*, 247–62.

Keller, C. A., 1983, Problems in dating glass industries of the Eyptian New Kingdom: Examples from Malkata and Lisht, *Journal of Glass Studies*, **25**, 19–28.

Kemp, V., McDonald, A., Brock, F., and Shortland, A. J., 2020, LA-ICP-MS analysis of Late Bronze Age blue glass beads from Gurob, Egypt, *Archaeometry*, **62**(1), 42–53.

Kirk, S., 2011, The vitreous materials from the 2nd millennium BC city of Nuzi : Their Preservation, Technology and Distribution, PhD Thesis, Cranfield University, Bedford, UK.

Knight, B., 1996, Excavated window glass: A neglected resource?, *Studies in Conservation*, **41**(sup1), 99–104.

Koestler, R. J., Santoro, E. D., Ransick, L., Brill, R. H., and Lynn, M., 1987, Preliminary SEM study of microbiologically induced deterioration of high alkali-low lime glass, In *Biodeterioration Research I* (eds. G. C. Llewellyn, and C. E. O'Rear), 295–307, Plenum, New York.

Kotsonas, A., Kiriatzi, E., Charalambidou, X., Roumpou, M., Müller, N. S., and Bessios, M., 2017, Transport amphorae from Methone: An interdisciplinary study of production and trade ca. 700 BC, In *Panhellenes at Methone: Graphê in Late Geometric and Protoarchaic Methone, Macedonia (ca 700 BCE)* (eds. J. Strauss Clay, I. Malkin, and Y. Z. Tzifopoulos), 9–19, de Gruyter, Berlin, Germany.

Krumbein, W. E., Urzì, C. E., and Gehrmann, C., 1991, Biocorrosion and biodeterioration of antique and medieval glass, *Geomicrobiology Journal*, **9**(2–3), 139–60.

Küçükerman, Ö., 1988, *Glass Beads. Anatolian Glass Bead Making : The Final Traces of Three Millennia of Glass Making in the Mediterranean Region*, Turkish Touring and Automobile Association, Istanbul, Turkey.

Kurti, R., 2017, Carnelian and amber beads as evidence of Late Bronze Age contacts between the present territory of Albania and the Aegean, In *ΕΣΠΕΡΟΣ / HESPEROS. The Aegean Seen From the West, 16th International Aegean Conference, Ioannina 2016* (eds. M. Fotiadis, R. Laffineur, Y. Lolos, and A. Vlachopoulos), 287–98, Aegaeum 16, Peeters, Leuven-Liege, Belgium.

Lahlil, S., Biron, I., Galoisy, L., and Morin, G., 2008, Rediscovering ancient glass technologies through the examination of opacifier crystals, *Applied Physics A*, **92**(1), 109–16.

Lahlil, S., Biron, I., Galoisy, L., and Morin, G., 2009, Technological processes to produce antimonite opacified glass throughout history, In *Annales Du 17e Congrès D'Associationi Internationale Pour L'histoire Du Verre*, 571–8, University Press Antwerp, Antwerp, Belgium.

Lahlil, S., Biron, I., Cotte, M., and Susini, J., 2010a, New insight on the in situ crystallization of calcium antimonate opacified glass during the Roman period, *Applied Physics A*, **100**(3), 683–92.

Lahlil, S., Biron, I., Cotte, M., Susini, J., and Menguy, N., 2010b, Synthesis of calcium antimonate nano-crystals by the 18th dynasty Egyptian glassmakers, *Applied Physics A*, **98**(1), 1–8.

Lazar, I., 2006, Glass finds in Slovenia and neighbouring areas, *Journal of Roman Archaeology*, **19**, 329–42.

Lilyquist, C., Brill, R. H., and Wypyski, M. T., 1993, Part I. Glass Materials, In *Studies in early Egyptian glass* (eds. C. Lilyquist, and R. H. Brill), 5–22, Metropolitan Museum of Art, New York.

Lucas, A., and Harris, J. R., 1962, *Ancient Egyptian Materials and Industries*, E. Arnold, London.

Mackay, E. J. H., 1925, Report on the excavation of the "A" cemetery at Kish, Mesopotamia: Part I, *Anthropology, Memoirs*, **1**(1), 1–63.

Mackay, E. J. H., Langdon, S., and Laufer, B., 1929, *A Sumerian Palace and the "A" Cemetery at Kish, Mesopotamia, Part II*, Field Museum Press, Chicago, Illinois.

Maniatis, Y., Panagiotaki, M., and Kaczmarczyk, A., 2008, Faience production in the Eastern Mediterranean, In *Production Technology of Faience and Related Early Vitreous Materials* (eds. M. S. Tite, and A. J. Shortland), 111–28, Oxford University School of Archaeology, Oxford, UK.

Marinatos, S., 1933, Αι ανασκαφαί Goekoop εν Κεφαλληνία, *Αρχαιολογική εφημερίς : εκδιδομένη υπό της εν Αθήναις Αρχαιολογικής Εταιρίας*, 68–100.

Marinatos, S., 1952, Ανασκαφαί εν Κεφαλληνία, *Πρακτικά της Εν Αθήναις Αρχαιολογικής Εταιρείας 1951*, 184–6.

Martin-McAuliffe, S. L., 2014, Lofkënd as a cultivated place, In *Excavations at the Prehistoric Burial Tumulus at Lofkënd, Albania* (eds. J. K. Papadopoulos, S. P. Morris, L. Bejko, and L. A. Shepartz), 2 vols., 537–53, Cotsen Institute of Archaeology Press, Los Angeles, CA.

Mass, J. L., Stone, R. E., and Wypyski, M. T., 1997, An investigation of the antimony-containing minerals used by the Romans to prepare opaque colored glasses, In *Material Issues in Art and Archaeology V*, Vol. 462, 193–204, Materials Research Society, Warrendale.

Mass, J. L., Wypiski, M., and Stone, R. E., 2002, Malkata and Lisht glassmaking technologies: Towards a specific link between second millennium BC metallurgists and glassmakers, *Archaeometry*, **44**(1), 67–82.

Mirtsou, E., Vavelidis, M., Ignatiadou, D., and Pappa, M., 1996, Faience beads of P.E.Ch. from Agios Mamas Chalkidiki, In *Archaeometry Issues in Greek Prehistory and Antiquity. Proceedings of 3rd Symposium of the Hellenic Society of Archaeometry* (eds. Y. Bassiakos, E. Aloupi, and Y. Fakorellis), 309–16, Hellenic Society of Archaeometry, Athens, Greece.

Moorey, P. R. S., 1994, *Ancient Mesopotamian Materials and Industries: The Archaeological Evidence*, Clarendon Press, Oxford.

Morris, S., Papadopoulos, J. K., Bessios, M., Athanassiadou, A., and Noulas, K., 2020, The Ancient Methone archaeological project: A preliminary report on fieldwork, 2014–2017, *Hesperia*, **89**(4), 659–723.

Morris, S. P., and Papadopoulos, J. K., 2014, From the Stone Age to the Recent Past: The Cultural Bioigraphy of a Landscape of an Ilyrian Tumulus, In *The Excavation of the Prehistoric Burial Tumulus at Lofkënd, Albania* (eds. J. K. Papadopoulos, S. P. Morris, L. Bejko, and L. A. Shepartz), Vol. 1, 2 vols., 371–5, Cotsen Institute Press, Los Angeles, CA.

Moussa, A., and Ali, M. F., 2013, Color alteration of Ancient Egyptian blue faience, *International Journal of Architectural Heritage*, **7**(3), 261–74.

Muros, V., and Pantages, C., 2015, Methone Archaeological Project 2015 Conservation Report, University of California, Los Angeles, Ancient Methone Archaeological Project.

Muros, V., Little, N., Lin, Y., and Boehnke, P., 2017, Down in the dumps: Analysis of glass production debris from Petrie's excavations at Amarna, In *Engaging Conservation: Collaboration Across Disciplines* (eds. N. Owczarek, M. Gleeson, and L. Grant), 231–6, Archetype, London, UK.

Muros, V., and Scott, D. A., 2018, The occurrence of brochantite on archaeological bronzes: A case study from Lofkënd, Albania, *Studies in Conservation*, **63**(2), 113–25.

Muros, V., and Zacharias, N., 2019, Lines, spots and trails: a microscopic and mineralogical study of antimonate-opacified glass beads from Lofkënd, Albania, *Archaeological and Anthropological Sciences*, **11**.

Muros, V., 2020, Analysis of glass production debris from Petrie's excavations at Amarna (unpublished report), The University of Pennsylvania Museum of Archaeology and Anthropology.

Nicholson, P., 2007, *Brilliant Things for Akhenaten: The Production of Glass, Vitreous Materials and Pottery at Amarna Site O45.1*, Excavation Memoirs, Egyptian Exploration Society Book 80, Oxbow Books Ltd., Oxford.

Nicholson, P., and Jackson, C., 2018, Identifying the characteristics of the earliest glass works from excavations, *Anatolian Archaeological Studies*, **21**, 85–94.

Nicholson, P. T., Jackson, C. M., and Trott, K. M., 1997, The Ulu Burun glass ingots, cylindrical vessels and Egyptian glass, *The Journal of Egyptian Archaeology*, **83**, 143–53.

Nicholson, P. T., and Peltenburg, E., 2000, Egyptian faience, In *Ancient Egyptian Materials and Technology* (eds. P. T. Nicholson, and I. Shaw), 177–94, Cambridge : Cambridge University Press.

Nicholson, P. T., and Hart, R., 2007, Excavations at site 045.1, In *Brilliant Things for Akhenaten: The Production of Glass, Vitreous Materials and Pottery at Amarna Site O45.1*, 27–81, Excavation Memoirs, Egyptian Exploration Society Book 80, Oxbow Books Ltd., Oxford.

Nicholson, P. T., and Jackson, C. M., 2007, The furnace experiment, In *Brilliant Things for Akhenaten: The Production of Glass, Vitreous Materials and Pottery at Amarna Site O45.1*, 83–99, Excavation Memoirs, Egyptian Exploration Society Book 80, Oxbow Books Ltd., Oxford.

Nightingale, G., 1996, Perlen aus Glas und Fayence aus der mykenischen Nekropole Elateia-Alonaki, In *Akten des 6. Österreichischen Archäologentages: 3.-5. Februar 1994, Universität Graz* (eds. T. Lorenze, G. Erath, M. Lehner, and G. Scwarz), 141–8, Phoibos Verlag, Vienna, Austria.

Nightingale, G., 1998, Glass and the Mycenaean Palaces of the Mediterranean, In *Prehistory and History of Glassmaking Technology. Papers from the 99th Annual Meeting of the American Ceramic Society, Cincinnati, Ohio (1997)* (eds. P. McCray, and D. Kingery), 205–26, American Ceramic Society, Ohio.

Nightingale, G., 2000, Mycenaean glass beads: Jewellery and design, In *Annales du 14e congrès de l' Association internationale pour l'histoire du verre, Italia/Venezia – Milano 1998*, 6–10, Lochem, The Netherlands.

Nightingale, G., 2002, Aegean glass and faience beads: An attempted reconstruction of a palatial Mycenaean high-tech Industry, In *Hyalos, Vitrum, Glass. 1st International Conference: History, Technology and Conservation of Glass and Vitreous Materials in the Hellenic World, Athens 2002* (ed. G. Kordas), 47–54, Panepistimiakes Ekdoseis Thessalias, Volos, Greece.

Nightingale, G., 2008, Tiny, fragile, common, precious. Mycenaean glass and faience, beads and other objects, In *Vitreous Materials in the Late Bronze Age Aegean* (eds. C. M. Jackson, and E. C. Wager), 64–104, Oxbow Books, Oxford, UK.

Nightingale, G., 2018, Glass of the Mycenaeans, In *Aspects of Late Bronze Age glass in the Mediterranean. Proceedings of JIAA Late Bronze Age Glass Workshop held at 27th - 28th September, 2014 in Kaman, Turkey.* (eds. J. Henderson, and M. Matsumura), 30–60, Anatolian Archaeological Studies XXI, Japanese Institute of Anatolian Studies, Tokyo, Japan.

Nikita, K., and Henderson, J., 2006, Glass analyses from Mycenaean Thebes and Elateia: Compositional evidence for a Mycenaean glass industry, *Journal of Glass Studies*, **48**, 71–120.

Nikita, K., Nightingale, G., and Chenery, S., 2017, Mixed-alkali glass beads from Elateia-Alonaki: Tracing the routes of an alien glass technology in the periphery of post-palatial Mycenaean Greece, In *Hesperos. The Aegean Seen from the West. Proceedings of the 16th International Aegean Conference*, 515–24, Aegaeum (Annales d'archéologie égéenne de l'Université de Liège et UT-PASP), Peeters, Leuven.

Oates, D., Oates, J., and McDonald, H., 1997, *Excavations at Tell Brak. v. 1: The Mitanni and Old Babylonian periods*, McDonald Institute Monographs, British School of Archaeology in Iraq, London.

Oikonomou, A., Henderson, J., and Chenery, S., 2020, Provenance and technology of fourth–second century BC glass from three sites in ancient Thesprotia, Greece, *Archaeological and Anthropological Sciences*, **12**(11), 269.

Oksanen, J., Blanchet, F. G., Friendly, M., Kindt, R., Legendre, P., McGlinn, D., Minchin, P. R., O'Hara, R. B., Simpson, G. L., Solymos, P., Stevens, M. H. H., Szoecs, E., and Wagner, H., 2017, *Vegan: community ecology package*.

Oppenheim, A. L., Brill, R. H., Barang, C., Barang, D., and von Saldern, A., 1970, *Glass and Glassmaking in Ancient Mesopotamia: An Edition of the Cuneiform Texts which Contain Instructions for Glassmakers with a Catalogue of Surviving Objects*, Corning Museum of Glass, Corning, NY.

Painter, K., and Sax, M., 1970, The British Museum collection of Roman head-stud brooches, *The British Museum Quarterly*, **34**(3/4), 153–74.

Palamara, E., Zacharias, N., Papakosta, L., Palles, D., Kamitsos, E. I., and Pérez-Arantegui, J., 2016, Studying a funerary Roman vessel glass collection from Patras, Greece: An interdisciplinary characterisation and use study, *STAR: Science & Technology of Archaeological Research*, **2**, 1–14.

Panagiotaki, M., 1999, Minoan faience and glass – making: Techniques and origins, In *Meletemata : studies in Aegean archaeology presented to Malcolm H. Wiener as he enters his 65th year.*, 617–23, Aegaeum 20, Université de Liège, Histoire de l'art et archéologie de la Grèce antique, Liege.

Panagiotaki, M., Papazoglou-Manioudaki, L., Chatzi-Spiliopoulou, G., Andreopoulou-Mangou, E., Maniatis, Y., Tite, M., and Shortland, A., 2005, A glass workshop at the Mycenaean citadel of Tiryns in Greece, In *Annales du 16e Congrès de l'Association Internationale pour l'Histoire du Verre* (ed. M.-D. Nenna), 14–8, AIHV, Nottingham, UK.

Panagiotaki, M., 2008, The technological development of Aegean vitreous materials in the Bronze Age, In *Vitreous Materials in the Late Bronze Age Aegean* (eds. C. M. Jackson, and E. C. Wager), 34–63, Sheffield Studies in Aegean Archaeology 9, Oxbow Books, Oxford.

Papadopoulos, J. K., 2010, A new type of Early Iron Age fibula from Albania and northwest Greece, *Hesperia*, **79**(2), 233–52.

Papadopoulos, J. K., and Muros, V., 2014, Beads of faience and glass, In *The Excavation of the Prehistoric Burial Tumulus at Lofkënd, Albania* (eds. J. K. Papadopoulos, S. P. Morris, L. Bejko, and L. A. Shepartz), Vol. 1, 2 vols., 371–5, Cotsen Institute Press, Los Angeles, CA.

Papadopoulos, J. K., Morris, S. P., and Bejko, L., 2014a, Catalogue of the prehistoric tombs and their contents, In *Excavations at the Prehistoric Burial Tumulus at Lofkënd, Albania* (J. Papadopoulos, S. Morris, L. Bejko, and L. A. Shepartz), Vol. 1, 2 vols., 16–28, Cotsen Institute of Archaeology Press, Los Angeles, CA.

Papadopoulos, J. K., Morris, S. P., Bejko, L., and Shepartz, L. A. (eds.), 2014b, *Excavations at the Prehistoric Burial Tumulus at Lofkënd, Albania*, 2 vols., Cotsen Institute of Archaeology Press, Los Angeles, CA.

Papadopoulos, J. K., and Kurti, R., 2014, Objects of terracotta, metal (gold/electrum, bronze, iron and bimetallic), semi-precious stone, faience, glass, and worked bone, In *Excavations at the Prehistoric Burial Tumulus at Lofkënd, Albania* (J. Papadopoulos, S. Morris, L. Bejko, and L. A. Shepartz), Vol. 1, 2 vols., 325–83, Cotsen Institute of Archaeology Press, Los Angeles, CA.

Papadopoulos, J. K., Bejko, L., and Morris, S. P., 2014c, The excavation and stratigraphy of the tumulus, In *Excavations at the Prehistoric Burial Tumulus at Lofkënd, Albania* (J. Papadopoulos, S. Morris, L. Bejko, and L. A. Shepartz), Vol. 1, 2 vols., 16–28, Cotsen Institute of Archaeology Press, Los Angeles, CA.

Papadopoulos, J. K., Bejko, L., and Morris, S. P., 2015, Reconstructing the prehistoric burial tumulus of Lofkënd in Albania, *Antiquity*, **82**(317), 686–701.

Papadopoulos, J. K., 2016, The early history of the Greek alphabet: new evidence from Eretria and Methone, *Antiquity*, **90**(353), 1238–54.

Pearce, N. J. G., Perkins, W. T., Westgate, J. A., Gorton, M. P., Jackson, S. E., Neal, C. R., and Chenery, S. P., 1997, A compilation of new and published major and trace element data for NIST SRM 610 and NIST SRM 612 glass reference materials, *Geostandards Newsletter*, **21**(1), 115–44.

Perez y Jorba, M., Dallas, J. P., Bauer, C., Bahezre, C., and Martin, J. C., 1980, Deterioration of stained glass by atmospheric corrosion and micro-organisms, *Journal of Materials Science*, **15**(7), 1640–7.

Petrie, W. M. F., Sayce, A. H., and Griffith, F. L., 1891, *Illahun, Kahun and Gurob : 1889-1890*, D. Nutt, London, UK.

Petrie, W. M. F., 1894, *Tell el-Amarna*, Methuen and Co., London, UK.

Petrie, W. M. F., 1905, *Ehnasya: 1904*, London, UK.

Pieniążek, M., 2012, Luxury and prestige on the edge of the Mediterranean World. Jewellery from Troia and the northern Aegean in the 2nd Millennium B.C. and its context, In *Kosmos, Jewellery, Adornment and Textiles in the Aegean Bronze Age. Aegaeum 33* (eds. M.-L. Nosch, and R. Laffineur), 501–8, Peeters, Leuven, Belgium.

Piñar, G., Garcia-Valles, M., Gimeno-Torrente, D., Fernandez-Turiel, J. L., Ettenauer, J., and Sterflinger, K., 2013, Microscopic, chemical, and molecular-biological investigation of the decayed medieval stained window glasses of two Catalonian churches, *International Biodeterioration & Biodegradation*, **84**, 388–400.

Polikreti, K., Murphy, J. M. A., Kantarelou, V., and Karydas, A. G., 2011, XRF analysis of glass beads from the Mycenaean palace of Nestor at Pylos, Peloponnesus, Greece: New insight into the LBA glass trade, *Journal of Archaeological Science*, **38**(11), 2889–96.

Pulak, C., 1998, The Uluburun shipwreck: An overview, *International Journal of Nautical Archaeology*, **27**(3), 188–224.

Pulak, C., 2008, The Uluburun shipwreck and Bronze Age trade, In *Beyond Babylon: Art, Trade, and Diplomacy in the Second Millennium B.C.* (eds. J. Aruz, K. Benzel, and J. M. Evans), 289–385, Metropolitan Museum of Art, New York.

Reade, W., Freestone, I., and Bourke, S., 2006, Innovation and continuity in Bronze and Iron Age glass from Pella in Jordan (eds. K. Janssens, P. Degryse, P. Cosyns, J. Caen, and L. Van't Dack), 47–54, Annales du 17eme Congres de l'Association Internationale pour l'Histoire du Verre, University Press Antwerp, Antwerp, Belgium.

Rehren, T., and Pusch, E. B., 1997, New Kingdom glass-melting crucibles from Qantir-Piramesses, *The Journal of Egyptian Archaeology*, **83**, 127–41.

Rehren, T., 1997, Ramesside glass-colouring crucibles, *Archaeometry*, **39**(2), 355–68.

Rehren, T., 2000, New aspects of ancient Egyptian glassmaking, *Journal of Glass Studies*, **42**, 13–24.

Rehren, T., 2001, Aspects of the production of cobalt-blue glass in Egypt, *Archaeometry*, **43**(4), 483–9.

Rehren, T., and Pusch, E. B., 2005, Late Bronze Age glass production at Qantir-Piramesses, Egypt, *Science*, **308**(5729), 1756–8.

Rehren, T., and Freestone, I. C., 2015, Ancient glass: From kaleidoscope to crystal ball, *Journal of Archaeological Science*, Scoping the Future of Archaeological Science: Papers in Honour of Richard Klein, **56**, 233–41.

Rodrigues, A., Fearn, S., and Vilarigues, M., 2019, Mixed reactions: Glass durability and the mixed-alkali effect, *Journal of the American Ceramic Society*, **102**(12), 7278–87.

Roemich, H., Gerlach, S., Mottner, P., Mees, F., Jacobs, P., Dyck, D. van, and Doménech Carbó, T., 2002, Results from burial experiments with simulated medieval glasses, *MRS Online Proceedings Library*, **757**, null-null.

Sakellarakēs, G., and Sapouna-Sakellarakē, E., 1997, *Archanes: Minoan Crete in a New Light*, 2 vols., Ammos Publications, Athens, Greece.

Santopadre, P., and Verità, M., 2000, Analyses of the production technologies of vitreous materials of the Bronze Age, *Journal of Glass Studies*, **42**, 25–40.

Sayre, E. V., and Smith, R. W., 1961, Compositional Categories of Ancient Glass, *Science*, **133**(3467), 1824–6.

Sayre, E. V., 1963, The intentional use of antimony and manganese in ancient glasses, In *Advances in Glass Technology: Additional Papers from the Sixth International Congress on Glass, held July 8-14, 1962, at Washington, D.C.* (eds. F. R. Matson, and G. E. Rindone), 263–82, Plenum Press, New York.

Schepartz, L. A., 2014, Bioarchaeology of the Lofkënd tumulus, In *The Excavation of the Prehistoric Burial Tumulus at Lofkënd, Albania* (eds. J. K. Papadopoulos, S. P. Morris, L. Bejko, and L. A. Shepartz), Vol. 1, 2 vols., 139–82, Cotsen Institute of Archaeology Press, Los Angeles, CA.

Schlick-Nolte, B., and Werthmann, R., 2003, Glass vessels from the burial of Nesikhons, *Journal of Glass Studies*, **45**, 11–34.

Schreurs, J. W. H., and Brill, R. H., 1984, Iron and sulfur related colors in ancient glasses, *Archaeometry*, **26**(2), 199–209.

Scott, D. A., 2002, *Copper and Bronze in Art: Corrosion, Colorants, Conservation*, Getty Conservation Institute, Los Angeles.

Scott, R. B., and Degryse, P., 2014, The archaeology and archaeometry of natron glass making, In *Glass Making in the Greco-Roman World* (ed. P. Degryse), 15–26, Leuven University Press, Leuven, Belgium.

Shelley, W. L., 2016, Biocorrosion of Archaeological Glass, Master's Thesis, University of California, Los Angeles, Los Angeles, CA.

Shortland, A. J., and Tite, M. S., 2000, Raw materials of glass from Amarna and implications for the origins of Egyptian glass, *Archaeometry*, **42**(1), 141–51.

Shortland, A. J., 2002, The use and origin of antimonate colorants in early Egyptian glass, *Archaeometry*, **44**(4), 517–30.

Shortland, A. J., and Eremin, K., 2006, The analysis of second millennium glass from Egypt and Mesopotamia, part 1: New WDS analyses, *Archaeometry*, **48**(4), 581–603.

Shortland, A. J., Schachner, L., Freestone, I., and Tite, M., 2006, Natron as a flux in the early vitreous materials industry: sources, beginnings and reasons for decline, *Journal of Archaeological Science*, **33**(4), 521–30.

Shortland, A. J., Rogers, N., and Eremin, K., 2007, Trace element discriminants between Egyptian and Mesopotamian Late Bronze Age glasses, *Journal of Archaeological Science*, **34**(5), 781–9.

Shortland, A. J., 2012, *Lapis Lazuli from the Kiln: Glass and Glassmaking in the Late Bronze Age*, Studies in Archaeological Sciences, Leuven University Press, Leuven.

Shortland, A. J., Kirk, S., Eremin, K., Degryse, P., and Walton, M., 2018, The Analysis of Late Bronze Age Glass from Nuzi and the Question of the Origin of Glass-Making, *Archaeometry*, **60**(4), 764–83.

Silvestri, A., Molin, G., and Salviulo, G., 2005, Archaeological glass alteration products in marine and land-based environments: morphological, chemical and microtextural characterization, *Journal of Non-Crystalline Solids*, **16–17**(351), 1338–49.

Silvestri, A., Tonietto, S., Molin, G., and Guerriero, P., 2015, Multi-methodological study of palaeo-Christian glass mosaic tesserae of St. Maria Mater Domini (Vicenza, Italy), *European Journal of Mineralogy*, **27**, 225–45.

Singer, C. J., Holmyard, E. J., Hall, A. R., and Williams, T. I. (eds.), 1956, *A History of Technology, II. The Mediterrranean Civilizations and the Middle Ages c. 700 B.C. to A.D. 1500*, Oxford University Press, New York.

Smirniou, M., Rehren, T., Adrymi-Sismani, V., Asderaki, E., and Gratuze, B., 2009, Mycenaean beads from Kazanaki, Volos: A further node in the LBA glass network, In *Annales du 18e Congrès de l'AIHV, Thessaloniki* (eds. D. Ignatiadou, and A. Antonaras), 11–8, ZITI Publisher, Thessaloniki.

Smirniou, M., and Rehren, Th., 2011, Direct evidence of primary glass production in Late Bronze Age Amarna, Egypt, *Archaeometry*, **53**(1), 58–80.

Smirniou, M., and Rehren, T., 2013, Shades of blue – cobalt-copper coloured blue glass from New Kingdom Egypt and the Mycenaean world: a matter of production or colourant source?, *Journal of Archaeological Science*, **40**(12), 4731–43.

Smirniou, M., and Rehren, T., 2016, The use of technical ceramics in early Egyptian glass-making, *Journal of Archaeological Science*, **67**, 52–63.

Smirniou, M., Rehren, T., and Gratuze, B., 2018, Lisht as a new kingdom glass-making site with its own chemical signature, *Archaeometry*, **60**(3), 502–16.

Smithson, E. L., 1968, The tomb of a rich Athenian lady, ca. 850 B.C., *Hesperia*, **37**(1), 77–116.

Souyoudzoglou-Haywood, C., 1999, *The Ionian Islands in the Bronze Age and Early Iron Age, 3000-800 BC*, Liverpool University Press.

Souyoudzoglou-Haywood, C., Sotiriou, A., and Papafloratou, E., 2017, Living on the edge. SW Kephalonia: An island region of the western Aegean world in the post palatial period., In *ΕΣΠΕΡΟΣ / HESPEROS. The Aegean Seen From the West, 16th International Aegean Conference, Ioannina 2016* (eds. M. Fotiadis, R. Laffineur, Y. Lolos, and A. Vlachopoulos), 383–96, Aegaeum, Peeters, Leuven-Liege.

Stapleton, C. P., 2012, Glass and glaze analysis and technology from Hasanlu, Period IVB, In *Peoples and Crafts in Period IVB at Hasanlu, Iran* (ed. M. de Schauensee), 87–102, University of Pennsylvania Press, Philadelphia, PA.

Stapleton, L., 2014, The prehistoric burial customs, In *Excavations at the Prehistoric Burial Tumulus at Lofkënd, Albania* (J. K. Papadopoulos, S. P. Morris, L. Bejko, and L. A. Shepartz), Vol. 1, 2 vols., 193–226, Cotsen Institute of Archaeology Press, Los Angeles, CA.

Tite, M. S., and Bimson, M., 1986, Faience: An investigation of the microstructures associated with the different methods of glazing, *Archaeometry*, **28**(1), 69–78.

Tite, M. S., 1987, Characterisation of early vitreous materials, *Archaeometry*, **29**(1), 21–34.

Tite, M. S., and Shortland, A. J., 2003, Production technology for copper- and cobalt-blue vitreous materials from the New Kingdom site of Amarna—A reappraisal, *Archaeometry*, **45**(2), 285–312.

Tite, M. S., and Shortland, A. J., 2004, Report on the scientific examination of a glazed brick from Susa: glazes, In *Persiens antike Pracht: Bergbau, Handwerk, Archäologie: Katalog der Ausstellung des Deutschen Bergbau-Museums Bochum vom 28. November 2004 bis 29. Mai 2005—Band 2* (T. Stöllner, R. Slotta, and A. Vatandoust), 388–90, Deutschen Bergbau-Museums Bochum, Bochum, Germany.

Tite, M. S., Hatton, G. D., Shortland, A. J., Maniatis, Y., Kavoussanaki, D., and Panagiotaki, M., 2005, Raw materials used to produce Aegean Bronze Age glass and related vitreous materials, In *Annales du 16e Congrès de l'Association Internationale pour l'Histoire du Verre* (ed. M.-D. Nenna), 10–3, AIHV, Nottingham, UK.

Tite, M. S., Freestone, I., and Bimson, M., 2007a, Egyptian faience: An investigation of the methods of production, *Archaeometry*, **25**, 17–27.

Tite, M. S., Manti, P., and Shortland, A. J., 2007b, A technological study of ancient faience from Egypt, *Journal of Archaeological Science*, **34**(10), 1568–83.

Tite, M. S., and Shortland, A. J., 2008, *Production Technology of Faience and Related Early Vitreous Materials*, Oxford University School of Archaeology, Oxford, UK.

Tite, M. S., Shortland, A. J., Hatton, G. D., Maniatis, Y., Kavoussanaki, D., Pyrli, M., and Panagoptaki, M., 2008, The scientific examination of Aegean vitreous materials – Problems and potential, In *Vitreous Materials in the Late Bronze Age Aegean*, 105–25, Oxbow Books, Oxford, UK.

Tite, M. S., Maniatis, Y., Kavoussanaki, D., Panagiotaki, M., Shortland, A. J., and Kirk, S. F., 2009, Colour in Minoan faience, *Journal of Archaeological Science*, **36**(2), 370–8.

Towle, A., Henderson, J., Bellintani, P., and Gambacurta, G., 2001, Frattesina and Adria: Report of scientific analyses of early glass from the Veneto, *Padusa*, **37**, 7–68.

Towle, A. C., 2002, A Scientific and Archaeological Investigation of Prehistoric Glasses from Italy, PhD Thesis, University of Nottingham, Nottingham, UK.

Triantafyllidis, P., and Karatasios, I., 2012, Late Bronze Age glass production on Rhodes, Greece, *Journal of Glass Studies*, **54**, 25–32.

Turner, W. E. S., 1954, Studies in ancient glass and glassmaking processes, Part I: Crucibles and melting temperatures employed in ancient Egypt at about 1370 B.C., *Journal of the Society of Glass Technology*, **38**, 436–44.

Turner, W. E. S., 1956, Studies in ancient glasses and glassmaking processes. Part IV: The chemical composition of ancient glasses, *Journal of the Society of Glass Technology*, **40**, 162–86.

Turner, W. E. S., and Rooksby, H. P., 1959, A study of the opalising agents in ancient glasses throughout three thousand four hundred years, In *Glastechnische Berichte Heft 8, 1959, Sonderband: V. Internationaler Glaskongress*, Vol. 32K: 7, 17–28, Verlag der Deutschen Glastechnischen Gesellschaft, Frankfurt, Germany.

Van Giffen, A., 2014, Weathered archaeological glass, *All About Glass | Corning Museum of Glass*, URL: https://www.cmog.org/article/weathered-archaeological-glass.

Vandiver, P. B., 1983, Appendix A: The manufacture of faience, In *Ancient Egyptian faience: An analytical survey of Egyptian faience from predynastic to Roman times* (eds. A. Kaczmarczyk, and R. Hedges), A1–143, Aris & Philips, Warminster.

Vandiver, P. B., 2008, Raw materials and fabrication methods used in the production of faience, In *Production Technology of Faience and Related Early Vitreous Materials* (eds. M. S. Tite, and A. J. Shortland), 37–56, Oxford University School of Archaeology, Oxford, UK.

Varberg, J., Gratuze, B., and Kaul, F., 2015, Between Egypt, Mesopotamia and Scandinavia: Late Bronze Age glass beads found in Denmark, *Journal of Archaeological Science*, **54**, 168–81.

Venclová, N., 1978, The origin of La Tene glassware in Bohemia, In *Annales du d'Etude 7e Congres International Historique du Verre Berlin-Leipzig, 15-21 aout 1977*, 123–8, AIHV, Liege, Belgium.

Venclová, N., 1983, Prehistoric eye beads in Central Europe, *Journal of Glass Studies*, **25**, 11–7.

Verità, M., and Santopadre, P., 2015, Unusual glass tesserae from a third-century mosaic in Rome, *Journal of Glass Studies*, **57**, 287–92.

Vicenzi, E. P., Eggins, S., Logan, A., and Wysoczanski, R., 2002, Microbeam characterization of Corning archeological reference glasses: New additions to the Smithsonian microbeam standard collection, *Journal of Research of the National Institute of Standards and Technology*, **107**(6), 719–27.

Voskos, I., 2019, Constructing 'traditions': Aspects of identity formation in the southern Ionian Islands during the Late Helladic period and the Iron Age, *Journal of Mediterranean Archaeology*, **32**(1), 88–113.

Wainwright, G. A., 1920, *Balabish*, Thirty Seventh Memoir of the Egyptian Exploration Society, George Allen & Unwin, Ltd., London, UK.

Walton, M. S., Shortland, A., Kirk, S., and Degryse, P., 2009, Evidence for the trade of Mesopotamian and Egyptian glass to Mycenaean Greece, *Journal of Archaeological Science*, **36**(7), 1496–503.

Walton, M. S., Eremin, K., Shortland, A. J., Degryse, P., and Kirk, S., 2012, Analysis of Late Bronze Age glass axes from Nippur—A new cobalt colourant, *Archaeometry*, **54**(5), 835–52.

Watkinson, D., Weber, L., and Anheuser, K., 2005, Staining of archaeological glass from manganese-rich environments, *Archaeometry*, **47**(1), 69–82.

Worral, I., 2020, Decoding the Network of Glass Production: A Meta-Analysis of Bronze Age Glass, MResThesis, University of Nottingham, Nottingham, UK.

Xia, N., 2014, *Ancient Egyptian Beads*, Springer-Verlag, Berlin Heidelberg, Germany.

Zacharias, N., and Palamara, E., 2016, Glass corrosion: Issues and approaches for archaeological science, In *Recent Advances in the Scientific Research on Ancient Glass and Glaze* (eds. F. Gan, Q. Li, and J. Henderson), Vol. Volume 2, 0 vols., 233–47, Series on Archaeology and History of Science in China Volume 2, World Scientific Publishing Co. Pte Ltd., Singapore.

Zacharias, N., Kaparou, N., Oikonomou, A., and Kasztovszky, Z., 2018a, Mycenaean glass from the Argolid, Peloponnese, Greece: A technological and provenance study, *Microchemical Journal*, **41**, 404–17.

Zacharias, N., Karavassili, F., Das, P., Nicolopoulos, S., Oikonomou, A., Galanis, A., Rauch, E., Arenal, R., Portillo, J., Roque, J., Casablanca, J., and Margiolaki, I., 2018b, A novelty for cultural heritage material analysis: Transmission Electron Microscope (TEM) 3D electron diffraction tomography applied to Roman glass tesserae, *Microchemical Journal*, **138**, 19–25.

Zacharias, N., Palamara, E., Kordali, R., and Muros, V., 2020, Archaeological glass corrosion studies: Composition, environment and content, *Scientific Culture*, **6**(3), 53–68.